ISSN 1916-6117 (online)
ISBN 978-1-4868-7449-1 (PDF)

ISSN 0826-9580 (print)
ISBN 978-1-4868-7448-4 (print)

THESE TERMS GOVERN YOUR USE OF THIS DOCUMENT

Your use of this Ontario Geological Survey document (the "Content") is governed by the terms set out on this page ("Terms of Use"). By downloading this Content, you (the "User") have accepted, and have agreed to be bound by, the Terms of Use.

Content: This Content is offered by the Province of Ontario's *Ministry of Mines* (MINES, or the Ministry) as a public service, on an "as-is" basis. Recommendations and statements of opinion expressed in the Content are those of the author or authors and are not to be construed as statement of government policy. You are solely responsible for your use of the Content. You should not rely on the Content for legal advice nor as authoritative in your particular circumstances. Users should verify the accuracy and applicability of any Content before acting on it. The Ministry does not guarantee, or make any warranty express or implied, that the Content is current, accurate, complete or reliable. The Ministry is not responsible for any damage however caused, which results, directly or indirectly, from your use of the Content. The Ministry assumes no legal liability or responsibility for the Content whatsoever.

Links to Other Web Sites: This Content may contain links, to Web sites that are not operated by MINES. Linked Web sites may not be available in French. The Ministry neither endorses nor assumes any responsibility for the safety, accuracy or availability of linked Web sites or the information contained on them. The linked Web sites, their operation and content are the responsibility of the person or entity for which they were created or maintained (the "Owner"). Both your use of a linked Web site, and your right to use or reproduce information or materials from a linked Web site, are subject to the terms of use governing that particular Web site. Any comments or inquiries regarding a linked Web site must be directed to its Owner.

Copyright: Canadian and international intellectual property laws protect the Content. Unless otherwise indicated, copyright is held by the King's Printer for Ontario.

It is recommended that reference to the Content be made in the following form:

Ontario Geological Survey 2023. Summary of Field Work and Other Activities, 2023; Ontario Geological Survey, Open File Report 6405, 390p.

or, for partial Content

Hechler, J.H. 2023. Ontario Geological Survey: Update of strategic perspective for 2023–2024; *in* Summary of Field Work and Other Activities, 2023, Ontario Geological Survey, Open File Report 6405, p.1-1 to 1-7.

Use and Reproduction of Content: The Content may be used and reproduced only in accordance with applicable intellectual property laws. *Non-commercial* use of unsubstantial excerpts of the Content is permitted provided that appropriate credit is given and Crown copyright is acknowledged. Any substantial reproduction of the Content or any *commercial* use of all or part of the Content is prohibited without the prior written permission of MINES. Substantial reproduction includes the reproduction of any illustration or figure, such as, but not limited to graphs, charts and maps. Commercial use includes commercial distribution of the Content, the reproduction of multiple copies of the Content for any purpose whether or not commercial, use of the Content in commercial publications, and the creation of value-added products using the Content.

Contact:

FOR FURTHER INFORMATION ON	PLEASE CONTACT:	BY TELEPHONE:	BY E-MAIL:
The Reproduction of the EIP or Content	MINES Publication Services	Local: (705) 670-5691 Toll-Free: 1-888-415-9845, ext. 5691 (inside Canada, United States)	Pubsales.ndm@ontario.ca
The Purchase of MINES Publications	MINES Publication Sales	Local: (705) 670-5691 Toll-Free: 1-888-415-9845, ext. 5691 (inside Canada, United States)	Pubsales.ndm@ontario.ca
Crown Copyright	King's Printer	Local: (416) 326-2678 Toll-Free: 1-800-668-9938 (inside Canada, United States)	Copyright@ontario.ca

Ontario

Ontario Geological Survey
Open File Report 6405

Summary of Field Work and Other Activities, 2023

2023

Ontario

ONTARIO GEOLOGICAL SURVEY

Open File Report 6405

Summary of Field Work and Other Activities, 2023

by

Ontario Geological Survey

Edited by R.M. Easton, M. Duguet, S. Préfontaine, O.M. Burnham, C. Gao, R.P.M. Mulligan, C. Béland Otis, K.E. Hahn, F.R. Brunton, A.K. Burt and C.E. Beckett-Brown

2023

Parts of this publication may be quoted if credit is given. It is recommended that reference to this publication be made in the following form:

Hechler, J.H. 2023. Ontario Geological Survey: Update of strategic perspective for 2023–2024; *in* Summary of Field Work and Other Activities, 2023, Ontario Geological Survey, Open File Report 6405, p.1-1 to 1-7.

Users of OGS products should be aware that Indigenous communities may have Aboriginal or treaty rights or other interests that overlap with areas of mineral potential and exploration.

© King's Printer for Ontario, 2023

© King's Printer for Ontario, 2023
ISBN 978-1-4868-7448-4 (print)
ISBN 978-1-4868-7449-1 (PDF)

Open File Reports of the Ontario Geological Survey are available for viewing at the John B. Gammon Geoscience Library in Sudbury and at the regional Mines and Minerals office whose district includes the area covered by the report (see below).

Copies can be purchased at Publication Sales and the office whose district includes the area covered by the report. Although a particular report may not be in stock at locations other than the Publication Sales office in Sudbury, they can generally be obtained within 3 working days. All telephone, fax, mail and e-mail orders should be directed to the Publication Sales office in Sudbury. Purchases may be made using cash, debit card, VISA, MasterCard, cheque or money order. Cheques or money orders should be made payable to the *Minister of Finance*.

John B. Gammon Geoscience Library 933 Ramsey Lake Road, Level B2 Sudbury, Ontario P3E 6B5	Tel:	(705) 670-5614
Publication Sales 933 Ramsey Lake Rd., Level B2 Sudbury, Ontario P3E 6B5	Tel: Toll-free: Fax: E-mail:	(705) 670-5691 (local) 1-888-415-9845 ext. 5691 (705) 670-5770 pubsales.ndm@ontario.ca

Regional Mines and Minerals Offices:

Kenora – Suite 104, 810 Robertson St., Kenora P9N 4J2

Kirkland Lake – 1451 Hwy. 66, P.O. Box 40, Swastika P0K 1T0

Red Lake – 227 Howey Street, P.O. Box 324, Red Lake P0V 2M0

Sault Ste. Marie – 740 Great Northern Rd., Sault Ste. Marie P6A 5M1

Southern Ontario – 126 Old Troy Rd., Tweed K0K 3J0

Sudbury – 933 Ramsey Lake Rd., Level B2, Sudbury P3E 6B5

Thunder Bay – Suite B002, 435 James St. S., Thunder Bay P7E 6S7

Timmins – Ontario Government Complex, P.O. Bag 3060, 5520 Hwy. 101 East, South Porcupine P0N 1H0

Every possible effort has been made to ensure the accuracy of the information contained in this report; however, the Ontario Ministry of Mines does not assume liability for errors that may occur. Source references are included in the report and users are urged to verify critical information.

If you wish to reproduce any of the text, tables or illustrations in this report, please write for permission to the Manager, Publication Services, Ministry of Mines, 933 Ramsey Lake Road, Level A3, Sudbury, Ontario P3E 6B5.

Cette publication est disponible en anglais seulement.

Parts of this report may be quoted if credit is given. It is recommended that reference be made in the following form:

Hechler, J.H. 2023. Ontario Geological Survey: Update of strategic perspective for 2023–2024; *in* Summary of Field Work and Other Activities, 2023, Ontario Geological Survey, Open File Report 6405, p.1-1 to 1-7.

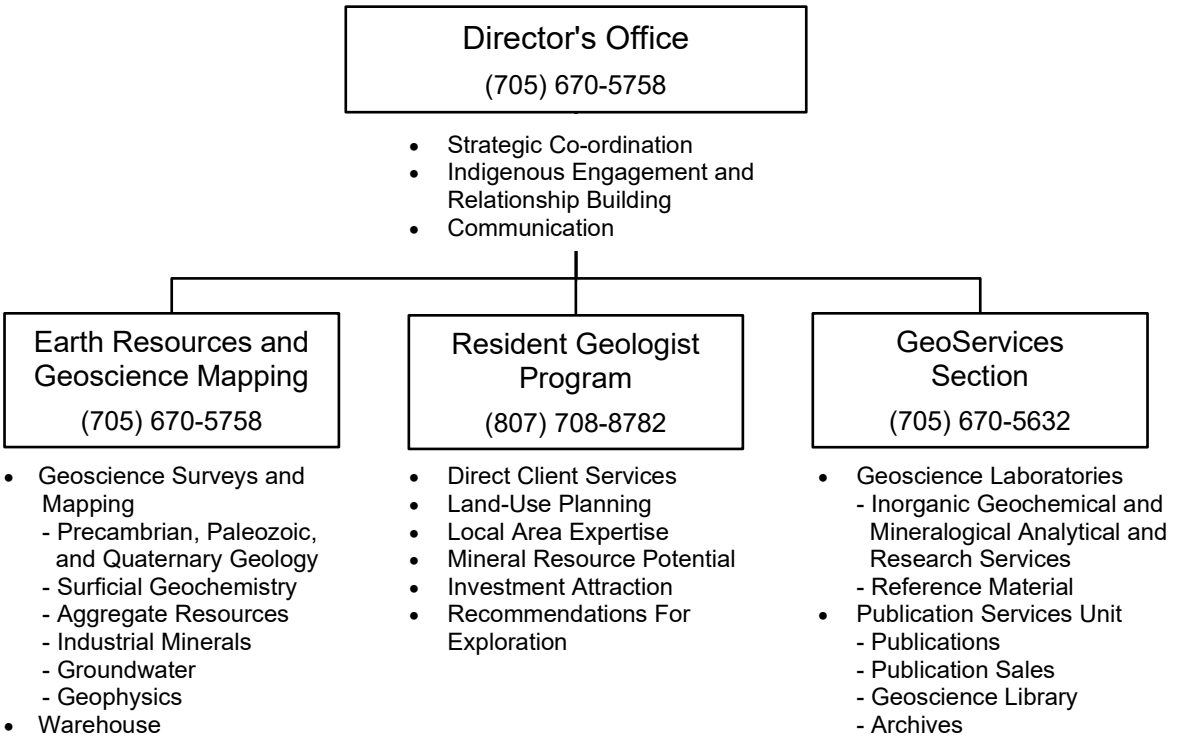


Mines and Minerals Division Regional and District Offices

CITY	ADDRESS	OFFICE(S)	TELEPHONE	FAX
Kenora	Suite 104, 810 Robertson St., Kenora P9N 4J2	○ ■	(807) 456-1780	(807) 468-2930
Red Lake	227 Howey Street, P.O. Box 324, Red Lake P0V 2M0	● ■	(807) 464-3934	(807) 727-3553
Thunder Bay – North Thunder Bay – South	Suite B002, 435 James St. S., Thunder Bay P7E 6S7	● ■ ▼	(807) 475-1332	(807) 475-1112
Sault Ste. Marie	740 Great Northern Road, Sault Ste. Marie P6A 5M1	○ ■	(705) 943-2219	
Timmins	Ontario Government Complex, P.O. Bag 3060, 5520 Hwy 101 East, South Porcupine P0N 1H0	● ■ ▼	(705) 235-1615	(705) 235-1620
Kirkland Lake	1451 Hwy. 66, P.O. Box 40 Swastika P0K 1T0	● ■	(705) 718-8735	
Sudbury	Willet Green Miller Centre, Level A3, 933 Ramsey Lake Rd., Sudbury P3E 6B5	○ ★	(705) 670-5733 (705) 670-5742 *Toll-Free (Canada, USA):* (888) 415-9845	(705) 670-5770 (705) 670-5681 *Toll-Free (Canada, USA):* (877) 670-1444
Tweed (Southern Ontario)	126 Old Troy Rd., Tweed K0K 3J0	● ■ ▼	(613) 243-0739	(613) 478-2873

Ministry of Mines

Ontario Geological Survey Branch



For all OGS general enquiries, contact us at OGS@ontario.ca

Contents

Office of the Director, Ontario Geological Survey

1. Ontario Geological Survey: Update of Strategic Perspective for 2023–2024 *J.H. Hechler*
2. Ontario Geological Survey: Measuring Success *K.J.J. Kalmo*
3. Activities of the Indigenous Geoscience Liaisons in 2022–2023 *M.D. Levesque and D.J. Bennett*

Earth Resources and Geoscience Mapping Section

4. Earth Resources and Geoscience Mapping Section: 2023–2024 Program and Projects Overview *J.H. Hechler, R.M. Easton, S. Préfontaine, M. Duguet, L. Robichaud and R. Cormier*

Precambrian Geology – Northeastern Ontario

5. Project NE-19-004. Preliminary Uranium-Lead Ages from the Ramsey–Algoma Granitoid Complex and Surrounding Area, Northeastern Ontario *S. Préfontaine and S.L. Kamo*
6. Project NE-23-004. Preliminary Geology of Riggs and Glasgow Townships, Michipicoten Greenstone Belt, Northeastern Ontario *L.E.D. Vice, S. Perrouty and S.G. Pelletier*
7. Project NE-23-002. Preliminary Geology and Mineral Potential of Cunningham Township and Part of Garnet Township, Swayze Area, Abitibi Greenstone Belt, Northeastern Ontario *T.P. Gemmell and J.R.H. Creppin*
8. Project NE-23-003. Reconnaissance Bedrock Geological Mapping in Haultain, Van Hise and Nicol Townships, Abitibi Greenstone Belt, Northeastern Ontario *J. Walker*
9. Project NE-23-001. Geology of Strathy Township, Temagami Greenstone Belt, Northeastern Ontario *P.J. MacDonald*

Precambrian Geology – Northwestern Ontario

10. Project NW-21-001. Geochronology of the LP Zone Volcanic Rocks, Red Lake Area, Uchi Subprovince, Northwestern Ontario *P.J. MacDonald, S.L. Kamo and P.M. Malegus*
11. Project NW-19-001. Precambrian Bedrock Geology Mapping in the Onion Lake and Sunshine Areas, Quetico and Wawa Subprovinces, Northwestern Ontario *G. Launay and R.T. Metsaranta*
12. Project NW-19-003. Archean Geology of the Georgia Lake Area, Quetico Subprovince, Northwestern Ontario *M. Duguet*
13. Project NW-19-003. Structural Control of the Georgia Lake Lithium-Cesium-Tantalum-type Pegmatite Field, Northwestern Ontario: Preliminary Results of Lineament Analyses *M. Duguet and G. Launay*

Precambrian Geology – Proterozoic

14. New Mafic Sill Complex Identified in the Lower Huronian Supergroup Succession: The May Township Sills *W. Bleeker, S.L. Kamo, R.M. Easton and D.W. Davis*
15. Project AS-19-002. A Study of Why Some Fine-Grained Sedimentary Rocks of the Gowganda Formation in Northeastern Ontario are Magnetic *R.M. Easton*

16. Project NE-22-001. Occurrences of Critical Minerals in Hyman Township, Southern Province, Northeastern Ontario *C.A. Gordon*

17. Project NE-22-004. Geochronological Study of a Saprolite Atop the Grenvillian Mulock Pluton near Redbridge, Northeastern Ontario *R.M. Easton, A.S. Marich and C.J. Wall*

18. Project SO-22-003. Geology of the Grenville Front Tectonic Zone near Sudbury, Northeastern Ontario: An Update *R.M. Easton*

Precambrian Geology – Pan-Provincial

19. Project ON-22-002. An Overview of the Critical Minerals in Gold Deposits Project *E.C.G. Hastie, P.M. Malegus, D.A. Campbell, O.M. Burnham and P.J. MacDonald*

Geophysics

20. Summary of Geophysical Projects and Activities *J. Evangelatos and S. Biswas*

Surficial Mapping and Sampling

21. Project ON-23-004. Determination of Indicator Minerals in Archived Fine-Fraction Non-Magnetic Heavy Mineral Concentrate Samples Using Scanning Electron Microscope Energy Dispersive Spectrometry *C. Gao, G.W. Hagedorn, D.C. Crabtree, S.A. Clarke, E.C.G. Hastie, G. Launay and C.E. Beckett-Brown*

22. Project NE-23-007. Quaternary Geological Mapping of the Eastern Part of the Lake Nipissing Basin, Northeastern Ontario: An Update Half a Century in the Making *A.S. Marich*

23. Project NW-23-002. Till Sampling and Surficial Mapping in the Georgia Lake Area, Northwestern Ontario *G.W. Hagedorn and C.E. Beckett-Brown*

Paleozoic Geology and Energy Studies

24. Project SO-23-001. Paleozoic Geology of Eastern Ontario: Hawkesbury and Alexandria Areas *C. Béland Otis*

25. Project SO-21-002. Stratigraphy and Sedimentology of Upper Ordovician Strata, Southern Ontario and Manitoulin Island *D. Atasiei, C.J. Tsujita, F.R. Brunton, J. Jin and K.H. Yeung*

26. Project SO-22-004. Revisiting the Cambrian Stratigraphy of Southwestern Ontario: Next Steps *A.R. Phillips, F.R. Brunton and K.H. Yeung*

27. Project SO-22-001. Paleozoic Geology of Eastern South-Central Ontario: Tweed–Kaladar and Belleville–Wellington Areas *K.E. Hahn*

Groundwater Studies

28. Project ON-21-005. Keeping it Simple: Geological Information on Water Well Records *A.K. Burt, K.H. Yeung, D. Grant and R.P.M. Mulligan*

29. Project ON-23-005. A Unified Stratigraphic Framework for the Provincial Groundwater Monitoring Network *R.P.M. Mulligan, A.K. Burt, K.H. Yeung and F.R. Brunton*

30. Project SO-23-002. Ambient Groundwater Geochemistry Project: Six Nations of the Grand River *L.M. Colgrove and K.M. Dell*

Aggregate Studies

31. Project NE-23-006. Aggregate Resources Inventory of the North Bay Area, Central Nipissing District, Northeastern Ontario *L.A. Handley*

Geoscience Laboratories

32. Revised Methods for the Multi-Element Analysis of Vegetation by Acid-Digestion and Inductively Coupled Plasma Mass Spectrometry at the Geoscience Laboratories *O.M. Burnham and E.G. Amyotte*

33. Characterization of New In-House Quality Control Materials for Tellurium Analysis: Results of a Round Robin Study *O.M. Burnham and E.C.G. Hastie*

34. Summary of Quality Control Data for the Geoscience Laboratories Methods IML-100, IML-101, LOI-2ST, LOI-3ST and LOI-4ST *V.L. Hingst*

35. Revision of the Calibration for Major Element Analysis of Geological Samples by Wavelength Dispersive X-ray Fluorescence at the Geoscience Laboratories *G.L. Keating*

Resident Geologist Program

36. Geochemical Data from the Critical Minerals Mine Waste Sampling Project *G.F. Paju*

37. Geology and Mineral Potential of the Eastern English River Subprovince, Northwestern Ontario: Project Introduction *S.V. Churchley*

38. Characterizing the Geochemistry and Nickel-Copper-Platinum Group Elements Potential of Mafic and Ultramafic Intrusions in Northwestern Ontario *J.R.B. Jonsson, P.M. Malegus, S.V. Churchley and R.L. Price*

39. Investigation of Biogeochemical Exploration Techniques to Aid in the Exploration for Lithium-Cesium-Tantalum Pegmatite Dikes: Preliminary Results *E.G. Amyotte*

Index of Authors

Metric Conversion Table

This page left blank intentionally

Office of the Director, Ontario Geological Survey

1. Ontario Geological Survey: Update of Strategic Perspective for 2023–2024



J.H. Hechler[1]

[1]Director's Office, Ontario Geological Survey

INTRODUCTION

This article provides an update on the strategic direction of the Ontario Geological Survey (OGS) based on activities during the 2023–2024 fiscal year.

These strategic priorities include the delivery of relevant, accurate, up-to-date public geoscience data and information about Ontario in order to

- identify economic opportunities;
- safeguard public health and safety related to natural geological factors; and
- inform environmental and land-use planning decisions.

As part of delivering on the strategic plan, the OGS continues to address government priorities and provides public geoscience to the general public, stakeholders and Indigenous partners. This is done to inform and guide decision making in the areas of mineral investment attraction and Earth resources management, land-use planning, healthy communities and energy supply.

THE ONTARIO GEOLOGICAL SURVEY

The OGS is the principal provincial government organization responsible for the collection, interpretation, documentation and dissemination of public geoscience data and information. The geoscience expertise of the OGS focusses on the description of Ontario's bedrock geology, surficial geology, the geological processes that shaped the landscape, and the Earth resources (groundwater, minerals, metals, aggregates, hydrocarbons) that occur within the geological framework. This public geoscience information is used to support and inform decisions related to

- environmental geochemical baseline;
- identification and description of naturally occurring geological hazards that may pose a threat to public health and safety;
- engineering infrastructure factors related to aggregates and terrain;
- changing climate impact and mitigation considerations;
- land-use planning and Earth resources management from a geological perspective;
- biodiversity and habitat as they relate to geology; and
- economic development and stewardship related to groundwater, energy, aggregates, metals and minerals.

Summary of Field Work and Other Activities, 2023,
Ontario Geological Survey, Open File Report 6405, p.1-1 to 1-13.

© King's Printer for Ontario, 2023

The OGS continues to generate world-class geoscience information, products and services, including the 39 articles in this volume and numerous other publications released by OGS staff. The Resident Geologist Program (RGP) continued to provide information and support to the exploration sector and are on target to release *Recommendations for Exploration 2023–2024* in late January 2024. The Geoscience Laboratories continued to function throughout 2023, providing valuable, high-quality geoanalytical data to the Ontario Geological Survey.

VISION, MISSION AND MANDATE OF THE ONTARIO GEOLOGICAL SURVEY

The OGS vision, mission and mandate statements are as follows:

Vision: The OGS is "a leading provider of reliable, credible, accessible public geoscience data, information and expert knowledge for the public good".

Mission: The OGS sustains and supports Ontario's quality of life, economic prosperity, environmental quality and public safety by providing Ontario's citizens, institutions and Indigenous Peoples with public geoscience data, information and expert knowledge to inform decision making.

Mandate: The OGS collects and disseminates public geoscience data and information and provides expert knowledge to attract and guide mineral sector investment, as well as inform a broad range of government policy priorities, including mineral investment attraction, land use planning, healthy communities, and energy supply.

ONTARIO GEOLOGICAL SURVEY: DELIVERING GLOBALLY SIGNIFICANT PUBLIC GEOSCIENCE

The OGS has maintained an international reputation for independent, credible, public geoscience expertise. The following examples highlight recent achievements of OGS technical professionals:

- launch of the new online GeologyOntario portal at the 2023 Prospectors and Developers Association of Canada (PDAC) convention on March 7. The redesigned portal features new geospatial and text search tools making it easier to search for, discover, and download Ontario's Geoscience data and information;
- publication of geochemistry and soil gas hydrocarbon data from a peat sampling transect over the Eagle's Nest nickel-copper and Blackbird chromium deposits, McFaulds Lake ("Ring of Fire") area, northern Ontario (Miscellaneous Release—Data 399);
- publication of the Precambrian geology of the North Caribou–Wachusk Lakes area, North Caribou greenstone belt, northwestern Ontario (Preliminary Map P.3463);
- publication of the regional-scale groundwater geoscience in southern Ontario 2023 Open House program and abstracts (Open File Report 6387);
- publication of the Precambrian geology of the Renfrew area, Grenville Province, southern Ontario (Preliminary Map P.3850), with accompanying geological, geochemical and geophysical data (Miscellaneous Release—Data 398);
- publication of indicator mineral and bulk geochemistry data of the till and other surficial samples collected in the Pickle Lake–Cat Lake area, northern Ontario (Miscellaneous Release—Data 388);
- publication of indicator mineral and geochemistry data of till and other surficial samples in the Sandy Lake area, northwestern Ontario (Miscellaneous Release—Data 400);

- publication of Ambient Groundwater Geochemistry Project field methods and procedures (Groundwater Resources Study 21);
- publication of new geochronological data from the eastern Ramsey–Algoma granitoid complex, northeastern Ontario (this volume, Article 5);
- publication of the preliminary geology of Riggs and Glasgow townships, northeastern Michipicoten greenstone belt, northeastern Ontario (this volume, Article 6);
- publication of the preliminary geology of Cunningham and Garnet townships, Swayze area, Abitibi greenstone belt, northeastern Ontario (this volume, Article 7);
- publication of the preliminary geology of Van Hise, Haultain and Nicol townships, Abitibi greenstone belt, northeastern Ontario (this volume, Article 8);
- publication of the preliminary geology of Strathy Township, Temagami greenstone belt, northeastern Ontario (this volume, Article 9);
- publication of new geochronological data from the metavolcanic rocks of the LP fault in the Red Lake area, Uchi Subprovince, northwestern Ontario (this volume, Article 10);
- publication of the preliminary geology of the Onion Lake and Sunshine areas in the southern Quetico Subprovince and the Shebandowan greenstone belt in the northern Wawa Subprovince, northwestern Ontario (this volume, Article 11);
- publication of the preliminary geology of the Georgia Lake area, Quetico Subprovince northwestern Ontario, with an emphasis on exploration for, and structural controls on, lithium-cesium-tantalum pegmatite units (this volume, Articles 12 and 13);
- publication of new geochronological data from the mafic intrusions in the Massey area, Southern Province, northeastern Ontario (this volume, Article 14);
- publication of preliminary results from a study of why fine-grained metasedimentary rocks of the Gowganda Formation, Huronian Supergroup are magnetic, Southern Province, northeastern Ontario (this volume, Article 15);
- publication of critical mineral occurrences in Hyman Township, Southern Province, northeastern Ontario (this volume, Article 16);
- publication of new geochronological data from a saprolite atop a granite intrusion in the Redbridge area, Grenville Province, northeastern Ontario (this volume, Article 17);
- publication of the geology of the Grenville Front tectonic zone near Sudbury, northeastern Ontario (this volume, Article 18);
- publication of an overview of the Critical Minerals in Gold Deposits Project (this volume, Article 19);
- publication of the project description and preliminary observations from a scanning-electron microscope study of indicator minerals in fine fraction non-magnetic heavy mineral concentrate samples archived at the OGS (this volume, Article 21)
- publication of Quaternary geological mapping of the Lake Nipissing Basin, northeastern Ontario (this volume, Article 22);
- publication of preliminary results from till sampling and surficial mapping in the Georgia Lake area, northwestern Ontario (this volume, Article 23);
- publication of the Paleozoic geology of the Hawkesbury and Alexandria areas (this volume, Article 24) and the Tweed–Kaladar and Belleville–Wellington areas, eastern south-central Ontario (this volume, Article 27);

- publication of Upper Ordovician stratigraphy and sedimentology of the Collingwood and Rouge River members, southern Ontario and Manitoulin Island (this volume, Article 25);
- publication of the Cambrian stratigraphy in southwestern Ontario (this volume, Article 26);
- publication of a project description and status report related to updating the geological information collected for water well records in Ontario (this volume, Article 28);
- publication of a project description and status report related to creating a unified stratigraphic framework for the Provincial Groundwater Network Program (this volume, Article 29);
- publication of preliminary results from the Ambient Groundwater Geochemistry Project sampling on the Six Nations of the Grand River, southwestern Ontario (this volume, Article 30);
- publication of preliminary results from an aggregate resources inventory study of the District of North Bay (this volume, Article 31);
- publication of articles on method development and the geochemical results from a project investigating biogeochemistry exploration techniques to aid in the exploration for lithium-cesium-tantalum pegmatite units (this volume, Articles 32 and 39, respectively);
- publication of geochemical results from 5 sites as part of the project investigating mine waste sampling for critical minerals (this volume, Article 36);
- publication of a project description for evaluating the rare-element and lithium-cesium-tantalum pegmatites potential of the eastern English River Subprovince, northwestern Ontario (this volume, Article 37);
- publication of a project description for the characterization of the geochemistry and nickel-copper-platinum group elements potential of selected mafic to ultramafic intrusions in northwestern Ontario (this volume, Article 38);
- publication of *Recommendations for Exploration 2002–2023*;
- the inaugural 2022 OGS Virtual Showcase was held October 25 to 27, and was a free, public, 3-day event held via Zoom® Webinar that highlighted OGS activities and projects. Presentations from this event were available online until October 31, 2023;
- introduction of the Ontario Geological Survey Geoscience Video publication series, with the first video of the series, the *Geology of the Sudbury Impact Structure*, being available online since January 2023;
- ongoing delivery of airborne and ground-based geophysical data and ongoing support to the Earth Resources and Geoscience Mapping Section (ERGMS) bedrock geology mapping and groundwater programs, as well as to the Resident Geologist Program (RGP) (this volume, Article 20)
- ongoing delivery of the services of a world-class inorganic geochemical laboratory, which supports the OGS geochemical program (*see also* this volume, Articles 32, 33, 34 and 35);
- publication of 10 geological field trip guidebooks for northeastern Ontario prepared in conjunction with the Geological Association of Canada–Mineralogical Association of Canada–Society for Geology Applied to Mineral Deposits Annual Meeting held on the Laurentian University campus in Sudbury in May 2023; and
- ongoing delivery of the Resident Geologist Program (RGP), which delivers local expert geoscience knowledge and front-line service to clients, stakeholders, Indigenous Peoples and the general public across Ontario.

To date, the active OGS public geoscience information holdings include 10 636 maps, 3508 reports, 751 data releases and 2 video releases. To date, in the period November 1, 2022 to October 31, 2023, the OGS published 18 new reports, 2 new maps, 5 new data releases and 2 video products.

From November 1, 2022, to October 31, 2023, numerous publications and data files were downloaded or accessed:

- downloaded from our GeologyOntario (former and new) Web sites:
  - in excess of 103 165 maps and reports in portable document format (*.pdf*) and image (*.jpg*) format
  - 16 372 compressed (*.zip*) files
- downloaded from our OGSEarth Web site:
  - 34 845 master *.kml* and/or *.kmz* files, and 582 compressed (*.zip*) files
  - Resident Geologist Program databases and recommendations
    - Ontario Mineral Inventory (OMI) 550 *.zip* files
      - Ontario Mineral Inventory (OMI) Critical Minerals 715 *.kmz* files
    - Ontario Assessment File Database (OAFD) 367 *.zip* files
    - Ontario Drill Hole Database (ODHD) 474 *.zip* files
      - OGSFocus (quantifies data from OMI, OAFD and ODHD) 272 *.kml* files and 162 *.zip* files
    - *Recommendations for Exploration* 1117 *.pdf* files, including the *Special Edition: Critical Minerals Compilation*.
      The current *2022–2023 Recommendations for Exploration* was 483 (43.2%), 2005–2022 was 599 (53.6%), the *Special Edition: Critical Minerals Compilation* was 13 (1.2%) and the *Introduction to Ontario's Critical Minerals* was 22 (2.0%).
- downloaded, viewed and accessed from our OGSEarth RGP Activity Reports—Mineral Exploration (AR—ME), compiled by the district offices:
  - AR—ME *.kml* file on OGSEarth Web page downloaded 1095 times
  - AR—ME Web page list, including individual pages for the district offices accessed 4352 times (through the AR—ME Web page list)

CURRENT TRENDS THAT WILL SHAPE THE FUTURE OF THE ONTARIO GEOLOGICAL SURVEY

Trends that continue to influence the OGS geoscience program include the following:

- Long-term global growth, largely driven by the need for mineral resources: having up-to-date inventories of Ontario's geology and Earth resources is a key aspect of attracting and fulfilling this investment potential.
- Mineral resource exploration and development continue to push geographic and technological frontiers: the Far North, "deep search" for mineral resources, potential for renewable and non-renewable energy sources, and quality and quantity of groundwater resources.
- Expectations for governments to provide robust guidance on management, mitigation and adaptation to the challenges of a changing climate require geoscience to help frame and inform some of those decisions, including drought mitigation and the identification and protection of vulnerable groundwater aquifers.
- Population growth across southern Ontario, which requires geoscience for land-use planning and the identification of groundwater aquifers and aggregate construction materials.

- Emphasis on evidence-based decision making requiring the inclusion of geoscience to fully assess risk and to support decision making.
- Increasing societal need to understand, identify and reduce disaster risks posed by natural geological features and, in a geological context, protect Ontario's natural environments. For each action, the OGS has a vital role to play in ensuring Ontario is well positioned to face these challenges through the provision of geological data and information.
- Standards and expectations for environmental responsibility continue to grow. A sound understanding of the geological features of the Earth is critical to ensuring a geochemical baseline is in place, that the material to be sampled for geochemical analysis is understood, and that the "geological container" that holds the Earth resources, such as groundwater, is described.
- Land-use planning across the Far North and municipalities elsewhere in Ontario will continue; that process requires the consideration of geology in order to assess health, safety, infrastructure, geochemical baseline, source water protection and economic potential options.
- Expectations for rapid, evidence-based policy analysis and user-friendly data discovery, access and handling will continue to grow through an "open spatial data" climate.
- Engagement, relationship-building, collaboration and notification of Indigenous Peoples and citizens of Ontario related to the delivery of OGS geoscience project activities is an essential part of operating with a social licence and is an integral part of the operations of the OGS geoscience program where a multi-year presence on the land is required.
- Jurisdictions across the globe have started assessing not only the vulnerability of their respective economies to the supply of critical minerals, but also to the availability within their borders. The OGS is positioned to provide the geoscience knowledge, data and information to support exploration and understanding of critical minerals in Ontario.
- Ontario's Critical Minerals Strategy, launched in March 2022, provides an opportunity for the continued role by the OGS in enhancing geoscience information and supporting critical minerals exploration in the province.

ONTARIO GEOLOGICAL SURVEY CLIENTS, STAKEHOLDERS AND PARTNERS

The OGS works closely with Indigenous Peoples in anticipated and planned geoscience project areas to engage, to build meaningful relationships and to discuss potential impacts and implications of OGS projects. The OGS practice is to work collaboratively with Indigenous communities on topics of mutual interest that can be the basis of a collaboration and/or partnership related to a geoscience project. This practice has matured since the OGS implemented changes in 1999 to its Indigenous engagement practices. In 2016, the OGS Director's Office recruited 2 Indigenous Geoscience Liaison positions based in Sudbury and Thunder Bay. A summary of the activities of the Indigenous Geoscience Liaisons during 2022–2023 are described by Levesque and Bennett (this volume, Article 3).

The OGS also has clients who formulate and implement policy and who are regulators in provincial, municipal and local governments. In fiscal 2022–2023, the OGS continued to support the application of geoscience information into broader government decision making by guiding other provincial ministries in applying public geoscience to help inform their decisions. The OGS continues the ongoing strengthening of collaboration and communication among government geoscientists and users of geoscience, through co-ordinated cross-ministry efforts that support the exchange of information, and at expanding the knowledge and expertise with respect to the application of geoscience in government.

In addition, public geoscience data, information and knowledge are used by municipalities, academia and a variety of private sector organizations to inform business-related decisions. The OGS conducts annual client surveys (*see* Kalmo, this volume, Article 2) to measure 6 performance indicators including the percentage of decision makers who state that their use of OGS products and services increased their decision-making efficiency and effectiveness by focussing their efforts on areas of interest identified by public geoscience. The performance and effectiveness of the OGS geoscience program, based on client input, is measured and tracked from year to year (*see* Kalmo, this volume, Article 2).

CURRENT STRATEGIC PRIORITIES

Four strategic priorities continue to be the focus of the OGS for the fiscal year out to 2024.

What Will the OGS Do Strategically?

- **Priority 1** Establish a geoscience baseline for all of Ontario in order to identify economic opportunities, safeguard public health and safety, and inform environmental and land-use planning decisions.
- **Priority 2** Contribute to the maintenance and enhancement of Indigenous relations.
- **Priority 3** Contribute to mineral development investment attraction.
- **Priority 4** Inform users about the value and relevance of OGS goods and services.

Results to Date

PRIORITY 1

Priority 1. Establish a geoscience baseline for Ontario in order to identify economic opportunities, safeguard public health and safety, and inform environmental and land-use planning decisions.

Strategic Objective: Provide modern, independent and credible geoscience data, information and knowledge to support decision making by government, Indigenous communities, citizens and industry.

Ontario Geological Survey public geoscience goods and services provide support for economic, social and environmental public policy decisions in a variety of areas:

- Economy: metal, mineral (including aggregate), water (groundwater) and energy resources;
- Environment: inorganic geochemical baseline, geological habitat that influences biodiversity, waste management and climate change mitigation and adaptation;
- Public health and safety: groundwater quality; geological hazards (e.g., landslides, karst, geochemical, gas, radioactivity); and
- Community: infrastructure planning, land-use planning, resource stewardship.

Multi-year priorities are established and reviewed annually during the OGS project planning process. The Geological Survey of Canada (Natural Resources Canada–Lands and Minerals Sector) is also an important part of the annual geoscience priority planning. These inputs are in addition to geoscience needs that are identified by public and private stakeholders and clients. The resulting geoscience projects are distributed across all of Ontario (*see* Hechler et al., this volume, Article 4).

Results

To deliver on the strategic priorities, different roles and responsibilities are distributed across the OGS Branch (Table 1.1). Some notable results of the key technical mapping commitments are the following:

- two- and three-dimensional geological mapping projects continued in various regions across Ontario to attract mineral investment, to inform land-use planning related to Indigenous communities and municipalities in northern and southern Ontario, to assess mineral, energy and groundwater resource potential and to support resource and infrastructure development decisions;
- published geochemical survey data, including groundwater characterization, to continue to assist in the identification of natural factors in the environment, water-quality issues and geohazards;

Table 1.1. Summary of OGS strategic objectives for public geoscience.

Strategic Objectives – Public Geoscience Information				
Outcomes	**Strategic Objectives**	**Activities**	**How?**	**Who? ***
Ontario geoscience portfolio recognized as a relevant resource to inform economic opportunities, health and safety, environmental and land-use planning decisions Land-use and environmental decisions informed by public geoscience Mineral investment decisions informed by public geoscience Enhanced efficiency and effectiveness and reduced risk of economic investment decisions and land-use and environmental decisions Public awareness about the value and relevance of public geoscience	Establish a geoscience baseline for Ontario to identify economic opportunity	Establish geoscience priorities based on public policy direction and input from stakeholders and clients	Gap analysis meetings with external clients, stakeholders, and with OGS staff who serve as proxy for external clients	Director's Office, ERGMS, RGP
			Project planning	ERGMS, RGP, GeoServices
	Establish a geoscience baseline for Ontario to safeguard public health and safety	Collect, analyze, advise and archive geoscience information	Mapping (OGS and collaborative projects with external collaborators or other governments)	ERGMS, GeoServices, RGP
			Property or site visits: mineral and aggregates	RGP
			Geochemistry	ERGMS, RGP, GeoServices
			Geophysics	ERGMS
			Receive third-party geoscience information	RGP, ERGMS
			Geoscience Library	GeoServices
	Establish a geoscience baseline for Ontario to inform environmental and land-use planning decisions	Provide access to OGS geoscience goods and services in a form that meets client needs	Geoscience Library	GeoServices
			GeologyOntario, OGSEarth and OGS Geoscience Atlas	GeoServices, RGP, ERGMS
			OGS expert technical staff participation in third-party technical meetings	ERGMS, RGP, GeoServices
		Inform users about the value and relevance of OGS goods and services and facilitate application of public geoscience to address priority issues faced by government, industry, and citizens	Multi-ministry committees	Director's Office, ERGMS, GeoServices, RGP, other MINES business units
			Provide geoscience information at technical meetings, symposia, workshops, and through direct client visits	ERGMS, RGP, GeoServices

***Abbreviations:** MINES = Ministry of Mines; ERGMS = Earth Resources and Geoscience Mapping Section; GeoServices = GeoServices Section; OGS = Ontario Geological Survey; RGP = Resident Geologist Program.*

- continuing updates to the Ontario Mineral Inventory (OMI) and its online database;
- a ground-based geophysical survey conducted in southern Ontario;
- continuing updates to the Aggregate Resources of Ontario (ARO) database; and
- continuing updates to the Geochronology Inventory of Ontario (GeochrON) database.

A number of technical initiatives are achieving these results (*see* Hechler et al., this volume, Article 4).

PRIORITY 2

Priority 2. Contribute to building collaborative relationships with Indigenous communities.

Strategic Objective: Continue to maintain and build meaningful and respectful relationships with Indigenous Peoples and organizations as a foundation for OGS geoscience program activities.

Within the Ministry of Mines, Mines and Minerals Division, the OGS contributes to the Divisional and Ministry goal to engagement and relationship-building with Indigenous Peoples, at a community level, and with organizations (Table 1.2).

Results

Focus during the 2023–2024 fiscal year was to continue collaborations and relationship building with Algonquins of Ontario, Anishinabek Nation, Atikmaneksheng Aninshinabek First Nation, Beausoleil First Nation, Chapleau Cree First Nation, Grand Council Treaty #3, Marten Falls First Nation, Matachewan First Nation, Mattagami First Nation, Métis Nation of Ontario, Missanabie Cree First Nation, Mississaugi First Nation, Mohawks of the Bay of Quinte, Nipissing First Nation, Red Sky Métis Independent Nation, Sheshegwaning First Nation, Six Nations of the Grand River First Nation, Temagami First Nation, Timiskaming First Nation, Whitefish River First Nation, and Wiikwekoong First Nation (*see* Levesque and Bennett, this volume, Article 3).

The Director's Office includes 2 Indigenous Geoscience liaison positions based in Sudbury and Thunder Bay. These positions report to the Director and engage, build and maintain relationships with Indigenous Peoples in remote and non-remote communities across Ontario.

Table 1.2. Strategic objectives for Indigenous relations.

Strategic Objectives – Indigenous Relations				
Outcomes	**Strategic Objectives**	**Activities**	**How?**	**Who? ***
Strong and meaningful relationships between Mines and Indigenous Peoples and organizations	Continue to maintain and build meaningful and respectful relationships with Indigenous Peoples and organizations as a foundation for OGS geoscience program activities	Engagement and relationship-building with Indigenous Peoples, at a community level, and with organizations	Seek social licence for OGS geoscience projects through engagement and relationship-building Offer OGS geoscience topic area expertise Raise awareness about geoscience and its application to Indigenous interests Help build capacity related to geoscience and mineral industry-related careers Serve as a bridge between Indigenous Peoples and government and non-government topic experts	Director's Office, ERGMS, RGP

***Abbreviations:** Mines = Ministry of Mines; ERGMS = Earth Resources and Geoscience Mapping Section; OGS = Ontario Geological Survey; RGP = Resident Geologist Program.*

PRIORITY 3

Priority 3. Contribute to mineral development investment attraction.

Strategic Objective: The OGS contributes to 2 mineral investment-related objectives that are the primary responsibility of the Mines and Minerals Division (MMD), Strategic Services Branch:

- promoting the products and services of Mines and Minerals Division, as well as promoting Ontario's geology through educational and/or informational tools;
- monitoring Ontario's exploration and mining industries and providing information and/or data and analysis on Ontario's mineral sector.

The OGS participates in the promotion of mineral development opportunities in Ontario by promoting the geology and mineral potential of the province, as well as the public geoscience data and information resources. The OGS brings geoscience data, information and expert knowledge to the investment attraction and promotional activities led by the Strategic Services Branch (Table 1.3). In addition, OGS technical experts support the investment attraction efforts by providing

- geoscience knowledge of available mineral properties in a region;
- knowledge of Ontario geology and the potential for different types of mineral resource opportunities across all of Ontario (for example, regional geochemical maps that highlight areas of enhanced mineral potential); and
- knowledge of key players in the mineral industry and facilitating relationships between interested clients.

Results

The staff of the OGS participated in-person at the Association for Mineral Exploration (AME) Annual Mineral Exploration Roundup 2023; the Prospectors and Developers Association of Canada (PDAC) 2023 Annual Convention; and co-hosted the 2023 Ontario Geological Survey, Geological Survey of Canada, and Conservation Ontario Geoscientists Open House. Staff were involved also in the Geological Association of Canada–Mineralogical Association of Canada–Society for Geology Applied to Mineral Deposits Annual Meeting held on the Laurentian University campus in Sudbury in May 2023, including leading or co-leading 4 geological field trips, and editing and publishing all 10 Field Trip Guidebook volumes associated with the meeting. Staff also participated in-person at the 2023 Institute on Lake Superior Geology Conference; the Canadian Mining Expo 2023 Big Event; the Central Canada Resource Expo 2023; the 2023 Northeastern Ontario Mines and Minerals Symposium; the Geological Society of America Connects 2023 annual conference; and the Quebec Mineral Exploration Association Convention Xplor 2023.

Table 1.3. Strategic objectives for mineral development investment and opportunities.

Strategic Objectives – Mineral Development Investment and Opportunities				
Outcomes	**Strategic Objectives**	**Activities**	**How?**	**Who? ***
Identification of investment opportunities and/or advantages that maximize mineral resource potential for Ontario's economic development Sustain and increase investment in Ontario's mineral sector	Promote the products and services of Mines and Minerals Division and Ontario's geology Monitor Ontario's exploration and mining industries Provide data and analysis on the mineral sector	Identify, assess, and promote mineral investment opportunities to industry (and local governments, conservation authorities, and groundwater-related interest groups)	Participate in provincial, national and international marketing and promotional events	RGP, ERGMS, GeoServices, Director's Office

****Abbreviations:** ERGMS = Earth Resources and Geoscience Mapping Section; GeoServices = GeoServices Section; RGP = Resident Geologist Program.*

PRIORITY 4

Priority 4. Inform users about the value and relevance of OGS goods and services.

Strategic Objective: The objective is to raise awareness and understanding about the relevance, value and application of OGS public geoscience to inform decision-making for government, clients, stakeholders, Indigenous Peoples and the public.

The OGS role is to communicate the existence, relevance and application of public geoscience and provide a broad range of products and services to deliver geoscience information to users, including two- and three-dimensional geological maps, reports, data sets and databases, technical posters, technical presentations, and expert knowledge and advice.

All geoscience publications are available for free download through the new GeologyOntario Hub site (www.hub.geologyontario.mines.gov.on.ca). In addition, the redesigned Hub site features new geospatial and text search tools, making it easier to search for, discover and download Ontario's geoscience data and information. Some key data sets, searchable using the expanded geospatial search tool on the new GeologyOntario Hub site, are also available through OGSEarth (www.geologyontario.mndm.gov.on.ca/ogsearth.html), which uses the Google Earth™ mapping service (with *.kml* files) to view public geoscience data and information in a geographic context. The Resident Geologist Program (RGP) has also enhanced access to data using both the new GeologyOntario Hub site and OGSEarth by adding mineral deposit and assessment file information, as well as increasing online accessibility to non-assessment geoscience information in the RGP offices.

Results

The OGS continued to use a variety of communication channels to deliver its products, raise awareness about geoscience and improve access to data, including

- "social media", such as X (formerly Twitter®), Facebook®, and Linkedln® professional networking service, and internal communication channels;
- formal public presentations that describe the value, relevance and application of geoscience;
- launch of the new GeologyOntario portal featuring a new spatial search tool and a redesigned text search tool to improve and enhance usability, accessibility and searchability of OGS geoscience data;
- improving the Ontario Mineral Exploration Information System, which is an internal process to improve and streamline processing and uploading of assessment files, drill-hole data and other geoscience information; and
- hosting the 2023 OGS Virtual Showcase in November 2023, a free, public, 3-day event held via Microsoft Teams to highlight OGS activities and projects from this year.

Priorities Linked to Ontario's Critical Minerals Strategy

Ontario's Critical Minerals Strategy, which is a five-year strategy, comprises 6 pillars that will solidify Ontario's position as a global leader of responsibly sourced critical minerals. The OGS plays a foundational role in "Pillar 1: Enhancing geoscience information and supporting critical minerals exploration". To date, 9 OGS activities have been initiated or completed in support of Ontario's Critical Minerals Strategy (Table 1.4).

Table 1.4. OGS activities in support of Ontario's Critical Minerals Strategy.

Goal	Geoscience Activity	Status
Releasing innovative, new geospatial data products that provide quicker, easier access to OGS geoscience data	Release of new Critical Mineral Ontario Mineral Inventory geospatial products	Completed
	Release of OGSFocus and OGS GeoData Listing through OGSEarth	Completed
Introduce a modernized digital platform for mineral exploration companies to access Ontario's critical minerals geoscience information from anywhere in the world	The Ontario Geological Survey (OGS) and the Information and Lands Branch (ILB) are collaborating to develop a new GeologyOntario application	Completed
Introduce new products that improve compilation and interpretation of existing OGS data, combined with digitizing archival information	Introduction to Ontario's Critical Minerals publication	Completed
	Release of OGSFocus and OGS GeoData Listing through OGSEarth	Completed
Reassessing historical geoscience information to better identify critical minerals deposits	Publish *Recommendations for Exploration Special Edition: Critical Minerals Compilation 2000–2022*	Completed
Undertake new geoscience initiatives that target underexplored areas of Ontario in partnership with Indigenous communities where potential partnership opportunities may exist	New bedrock mapping projects, airborne geophysics, lake sediment surveys in underexplored areas of Ontario with high critical mineral potential, as well as laboratory method development studies for the measurement of critical minerals	Ongoing (this volume, Articles 11, 12, 13, 18, 19, 20, 21, 32, 33, 36, 37, 38 and 39)
	Recommendations for Exploration published	Completed annually
Initiate a mine waste sampling project to help identify critical mineral content in tailings and waste rock, to support redevelopment of historic deposits	An introduction to the critical minerals mine waste sampling project	Ongoing (this volume, Articles 36, 19)

THE FUTURE

Building on the work initiated in 2018–2019, the OGS management team continues implementing the OGS five-year strategic plan.

The OGS continues to:

- implement a geoscience program based on accurate, modern, credible, public geoscience data, information and knowledge to help inform decision making;
- identify naturally occurring geological features and phenomena relevant to public health and safety;
- publish and promote information about Ontario's Earth resources, including its mineral, energy and water resource endowments;
- develop new geoscience products that help present our complex geoscience data in a form that is understood by non-geoscience users, including the development of products that broaden the access and awareness of OGS geoscience goods and services to both traditional and non-traditional users;
- utilize social media.

The OGS public geoscience goods and services play an important role in helping support public-policy decision makers, investors and other users. Societal needs are increasingly complex and require a sound and objective understanding of geoscience to help assess and frame the complex options available. Geoscience is an essential element of social, environmental, and resource management decision-making processes.

STAFFING CHANGES IN THE DIRECTOR'S OFFICE

In March 2023, Lesley McAdam permanently secured the position of Administrative Assistant position in the Director's Office. In April 2023, Kayla Kalmo permanently secured the position of Project and Results Management Coordinator in the Director's Office. In June 2023, John Hechler permanently secured the position of Director Ontario Geological Survey.

2. Ontario Geological Survey: Measuring Success



K.J.J. Kalmo[1]

[1]Director's Office, Ontario Geological Survey

INTRODUCTION

The Ontario Geological Survey (OGS) Branch has 3 program outcomes:

- Short-Term Outcome: Clients, stakeholders and Indigenous communities have awareness of the value, relevance and application of available geoscience information;
- Intermediate Outcome: Geoscience knowledge and information are valued and used to inform decisions related to economic, environmental and social priorities;
- Long-Term Outcome: People and communities in Ontario benefit from the informed use of Ontario's land and Earth resources.

To help achieve these outcomes, as well as to measure program success, the OGS has 6 performance indicators that it measures and tracks.

1. Percentage of decision makers who state that their use of OGS products and services increased their decision-making efficiency and effectiveness by focussing their efforts on areas of interest identified by OGS geoscience.
2. Percentage of decision makers who used OGS products and services to support their mineral investments or environmental decisions.
3. Percentage of decision makers who were satisfied with OGS products and services to support their decision making.
4. Indigenous communities who were satisfied with OGS products and services.
5. Percentage of clients and stakeholders satisfied with value-added OGS geoscience information (e.g., laboratory services, publication services, prospecting courses, groundwater meetings).
6. Annual number of square kilometres mapped by OGS based on results of OGS project proposal evaluation process.

The OGS conducts a large annual client survey by e-mail to measure each of the performance indicators. Performance is also measured by surveying participants who attend OGS presentations and information sessions; documenting the completion of major project milestones; and documenting testimonials from Indigenous communities. All of these data are collected, tracked and monitored to ensure that the OGS is providing high-quality, relevant geoscience products and services to its clients, stakeholders, Indigenous Peoples and the general public.

Summary of Field Work and Other Activities, 2023,
Ontario Geological Survey, Open File Report 6405, p.2-1 to 2-9.

© King's Printer for Ontario, 2023

VALUE-ADDED PRODUCTS AND SERVICES

Historically, the Resident Geologist Program (RGP) of the OGS conducted client surveys specific to its program area. Between 2016 and 2020, the RGP distributed hard-copy surveys at regional offices and at various tradeshows and conferences they attended. However, because of the COVID-19 pandemic throughout 2020, 2021, and partially in 2022, the RGP did not have the opportunity to distribute these surveys and, therefore, did not collect any data for those years (*see* Table 2.1 for past results). In 2023, the Annual OGS Client Survey (detailed in the following section) was deemed to be an acceptable method of gathering client feedback specific to the RGP's products and expert advisory services, moving forward.

The GeoServices Section of the OGS conducts an annual client survey specific to its program area using SurveyMonkey® software to create and distribute the survey and collect results (*see* Table 2.1).

The OGS, in collaboration with the Geological Survey of Canada and Conservation Ontario (representing the 36 Conservation Authorities in Ontario), conducts an annual Regional-Scale Groundwater Geoscience Open House in southern Ontario. Participants are surveyed on their overall satisfaction with the event, using SurveyMonkey®, and results are recorded (*see* Table 2.1).

In October 2022, the OGS hosted its inaugural Virtual Showcase, an event aimed at sharing OGS geoscience data, products and services to its clients, stakeholders, partners and the public to facilitate, disseminate and advance geoscience in Ontario. Participants were surveyed on their overall satisfaction with the event, using SurveyMonkey®, and results have been recorded (*see* Table 2.1). The OGS hosted the Virtual Showcase again in 2023 and will continue to monitor and document success metrics from such initiatives.

Table 2.1. Client survey results from the Resident Geologist Program, GeoServices Section and the Groundwater Open House.

Survey Question	Program Area	2015–2016	2016–2017	2017–2018	2018–2019	2019–2020	2020–2021	2021–2022	2022–2023
How satisfied are you with the RGP products and services	Resident Geologist Program	n/a	79%	94%	96%	100%*	n/a	n/a	n/a **
How satisfied are you with the analyses and services provided by the Geoscience Laboratories	GeoServices Section	84%	n/a	83%	97%	99%	100%*	87%*	82%*
Please rate your overall satisfaction with the Groundwater Open House	Groundwater Open House	n/a	94%	93%	99%	100%	93%	92%	95%
Please rate your overall satisfaction with the OGS Virtual Showcase.	OGS Showcase	n/a	n/a	n/a	n/a	n/a	n/a	n/a	95%

n/a = no data available.
** Less than 40 respondents.*
*** This metric is now collected via the Annual OGS Client Survey (*see *results in Tables 2.3 and 2.4).*

ANNUAL CLIENT SURVEY

Method

The 2022–2023 OGS Client Survey was conducted from April 3 to May 19, 2023. A database of 753 clients was compiled by OGS staff, with 664 of these clients having valid contact information. The survey was conducted using SurveyMonkey®, an online survey platform that is used to create and distribute

surveys and to collect and analyze results. This approach involved sending electronic invitations through the software to respondents, who had e-mail addresses provided for them, to complete the survey online. A total of 6 follow-up reminders were then sent to those who did not complete the survey.

A total of 270 responses were captured, resulting in a 41% response rate. This response was a 3% decrease from the 2022 rate and remains consistent with those of previous years (lowest to highest: 40–53%). Another factor to consider is the sample size being the largest within the 10 years that the survey has been completed.

Survey Results

Ten questions were asked of 2 major OGS client groups: 1) mineral or other resource exploration and/or development; and 2) land-use planning, groundwater or environmental. These clients were further separated into A) product users and B) service users. It should be noted that this was the fifth year since clients have been divided into these categories; therefore, the results may be skewed in the representation to years previous to 2019. Also note that clients were able to identify as solely using products, solely using services, or a user of both products and services—this separation began in 2019 as well. The results of each category are noted in Table 2.2 for questions asked of all clients, Table 2.3 for questions asked of clients who identified as product users, and Table 2.4 for those clients who identified as service users.

Table 2.2. Ontario Geological Survey 2022–2023 client survey questions and summary of results for OGS clients.

Survey Question	Mineral / Resource / Exploration								
	2014–2015	2015–2016	2016–2017	2017–2018	2018–2019	2019–2020	2020–2021	2021–2022	2022–2023
What category best describes the majority of work that you conduct?	66%	65%	72%	77%	80%	72%	84%	83%	84%
How would you rate your overall satisfaction with the OGS?	85%	80%	85%	73%	81%	86%	83%	84%	89%

Survey Question	Land-Use Planning / Groundwater / Environmental								
	2014–2015	2015–2016	2016–2017	2017–2018	2018–2019	2019–2020	2020–2021	2021–2022	2022–2023
What category best describes the majority of work that you conduct?	34%	35%	28%	23%	20%	28%	16%	17%	16%
How would you rate your overall satisfaction with the OGS?	95%	94%	93%	96%	90%	96%	86%	95%	91%

SUCCESSES WITH PRODUCTS AND SERVICES

The OGS measures its success with products and services by monitoring exploration companies working in Ontario that reference OGS data to make an informed decision. The OGS recorded 49 total mineral sector activities between September 2022 and August 2023 where OGS data had had an impact and/or was referenced. Recent significant successes are described as follows.

1. September 2022—Angold Resources Ltd. announced it has commenced its first field season at the Uchi project in the Red Lake mining district (covering 6868 ha). The news release states that the property's 340 claims were first staked in 2019 and 2020, referencing the OGS–RGP's Report of Activities (Paterson et al. 2020; Lichtblau et al. 2018), as well as historical mapping (Lemkow et al. 2006) and sampling (Parker and Atkinson 1992) conducted by the OGS.
   (Angold Resources Ltd., news release, September 13, 2022)

Table 2.3. Ontario Geological Survey 2022–2023 client survey questions and summary of results for OGS product users.

Survey Question	Mineral / Resource / Exploration								
	2014–2015	**2015–2016**	**2016–2017**	**2017–2018**	**2018–2019**	**2019–2020**	**2020–2021**	**2021–2022**	**2022–2023**
Percentage of clients who used OGS products within the past 12 months?	90%	94%	90%	89%	94%	92%	84%	93%	92%
Overall satisfaction with the quality of OGS products	n/a	n/a	88%	79%	80%	85%	86%	90%	92%
Percentage of clients who used OGS products to make a decision	69%	80%	68%	54%	57%	50%	62%	63%	57% [1]
Did OGS products allow clients to focus their efforts on areas of higher potential and/or interest?	74%	76%	73%	50%	62%	77%	76%	74%	70% [2]
Did OGS products reduce the time and cost to advance to the next stage of exploration or decision making?	61%	65%	50%	38%	32%	33%	32%	38%	42% [2]
Did the use of OGS products improve clients' exploration models or strategies?	80%	76%	55%	46%	40%	46%	51%	54%	47% [3]
Did the use of OGS products reduce clients' decision risks?	74%	65%	60%	39%	28%	34%	36%	33%	38% [3]
Did the use of OGS products/services provide evidence of the presence or absence of critical features, target deposit type or topic of interest?	72%	57%	59%	41%	43%	48%	46%	51%	50% [3]

Survey Question	Land-Use Planning / Groundwater / Environmental								
	2014–2015	**2015–2016**	**2016–2017**	**2017–2018**	**2018–2019**	**2019–2020**	**2020–2021**	**2021–2022**	**2022–2023**
Percentage of clients who used OGS products within the past 12 months?	85%	94%	91%	89%	90%	89%	86%	93%	90%
Overall satisfaction with the quality of OGS products	n/a	n/a	91%	97%	89%	95%	94%	88%	97%
Percentage of clients who used OGS products to make a decision	90%	91%	78%	77%	77%	71%	74%	83%	76% [1]
Did OGS products allow clients to focus their efforts on areas of higher potential and/or interest?	83%	58%	83%	57%	64%	66%	63%	71%	79% [2]
Did OGS products reduce the time and cost to advance to the next stage of exploration or decision making?	83%	58%	56%	60%	55%	54%	66%	58%	59% [2]
Did the use of OGS products improve clients' exploration models or strategies?	80%	58%	50%	69%	64%	86%	77%	71%	59% [3]
Did the use of OGS products reduce clients' decision risks?	78%	36%	50%	60%	34%	36%	42%	37%	59% [3]
Did the use of OGS products/services provide evidence of the presence or absence of critical features, target deposit type or topic of interest?	83%	53%	64%	74%	45%	52%	45%	53%	48% [3]

[1] An open-ended question asking respondents if there was a specific reason why they did not use OGS products to make a decision. Mineral/resource/exploration clients: 28% had no specific reason why; 28% said the information was used for other purposes than decision-making (i.e., academic, educational, etc.). Land-use/groundwater/environmental clients: 43% had no specific reason why; 29% said the information was used for other purposes than decision-making.

[2] Option for respondents to select "Other" where they could provide further comments on how products increased the efficiency of their decision-making: 20% of mineral/resource/exploration clients and 14% of land-use clients responded.

[3] Option for respondents to select "Other" where they could provide further comments on how products increased the effectiveness of their decision-making: 16% of mineral/resource/exploration clients and 10% of land-use clients responded.

n/a = no data available.

Table 2.4. Ontario Geological Survey 2022–2023 client survey questions and summary of results for OGS service users.

Survey Question	Mineral / Resource / Exploration								
	2014–2015	**2015–2016**	**2016–2017**	**2017–2018**	**2018–2019**	**2019–2020**	**2020–2021**	**2021–2022**	**2022–2023**
Percentage of clients who used OGS services within the past 12 months?	n/a	n/a	96%	85%	53%	54%	42%	44%	52%
Overall satisfaction with the quality of OGS services	n/a	n/a	91%	82%	84%	81%	80%	85%	91%
Percentage of clients who used OGS services to make a decision	69%	80%	68%	54%	48%	32%	35%	46%	47% [4]
Did OGS services allow clients to focus their efforts on areas of potential and/or interest?	74%	76%	73%	50%	50%	75%	76%	71%	67% [5]
Did OGS services reduce the time and cost to advance to the next stage of exploration or decision making?	61%	65%	50%	38%	32%	34%	33%	39%	32% [5]
Did the use of OGS services improve clients' exploration models or strategies?	80%	76%	55%	46%	46%	56%	53%	53%	50% [6]
Did the use of OGS services reduce clients' decision risks?	74%	65%	60%	39%	25%	32%	32%	40%	32% [6]
Did the use of OGS products/services provide evidence of the presence or absence of critical features, target deposit type or topic of interest?	72%	57%	59%	41%	37%	50%	41%	38%	37% [6]

Survey Question	Land-Use Planning / Groundwater / Environmental								
	2014–2015	**2015–2016**	**2016–2017**	**2017–2018**	**2018–2019**	**2019–2020**	**2020–2021**	**2021–2022**	**2022–2023**
Percentage of clients who used OGS services within the past 12 months?	n/a	n/a	100%	97%	75%	68%	48%	39%	52%
Overall satisfaction with the quality of OGS services	n/a	n/a	91%	97%	87%	100%	89%	100%	89%
Percentage of clients who used OGS services to make a decision	90%	91%	78%	77%	77%	74%	47%	86%	69% [4]
Did OGS services allow clients to focus their efforts on areas of potential and/or interest?	83%	58%	83%	57%	67%	90%	58%	73%	58% [5]
Did OGS services reduce the time and cost to advance to the next stage of exploration or decision making?	83%	58%	56%	60%	56%	52%	75%	60%	53% [5]
Did the use of OGS services improve clients' exploration models or strategies?	80%	58%	50%	69%	59%	83%	75%	71%	58% [6]
Did the use of OGS services reduce clients' decision risks?	78%	36%	50%	60%	23%	40%	44%	29%	53% [6]
Did the use of OGS products/services provide evidence of the presence or absence of critical features, target deposit type or topic of interest?	83%	53%	64%	74%	44%	50%	56%	43%	26% [6]

[4] An open-ended question was asked to respondents if there was a specific reason why they did not use OGS services to make a decision. Mineral/resource/exploration clients: 41% said that the information was used for other purposes than decision-making (i.e., academic, educational, etc.); 17% had no specific reason why. Land-use/groundwater/environmental clients: 50% had no specific reason why; 50% said that the information was used for other purposes than decision-making.

[5] Option for respondents to select "Other" where they could provide further comments on how services increased the efficiency of their decision-making: 14% of mineral/resource/exploration clients and 5% of land-use clients responded.

[6] Option for respondents to select "Other" where they could provide further comments on how services increased the effectiveness of their decision-making: 13% of mineral/resource/exploration clients and 5% of land-use clients responded.

n/a = no data available.

2. September and December 2022—Tearlach Resources Ltd. acquired 2 claim groups east of Red Lake: the Wesley lithium project (comprising 7 claims covering 3250 ha) and the Harth lithium project (6 claims, 2350 ha); as well as 2 projects north of Red Lake: the Pakwan lithium project (51 claims, 1271 ha) and the Margot Lake lithium project (102 claims, 2706 ha). The company credits historical OGS mapping for identifying the pegmatites and pegmatitic dikes in the area (Stone, Crawford and Lange 1994; Wood 1977), as well as numerous OGS publications and Ontario Mineral Inventory data for providing evidence of high potential for lithium-bearing pegmatites.
   (Tearlach Resources Ltd., news releases, September 26 and 28, and December 5, 2022)

3. October 2022—Westmount Minerals Corp., acquired 2 properties (Otatakan and East Pilot) to explore for lithium-cesium- tantalum (LCT) pegmatites, covering an area of 5002 ha. The company credits OGS mapping for identifying geological features in the area with high potential for hosting rare-element pegmatites.
   (Westmount Minerals Corp., news release, October 12, 2022)

4. December 2022—Platinex Inc. announced the acquisition of the Muskrat Dam critical minerals project that comprises 6 property blocks covering a total of 109 km^2 in northwestern Ontario based on historical OGS mapping (Ayres 1969) and OGS–RGP *Recommendations for Exploration 2019–2020* (Lewis and Paterson 2020).
   (Platinex Inc., news release, December 14, 2022)

5. January 2023—Patriot Lithium Ltd. acquired 3 lithium prospective land packages (Gorman, Forest and Birkett projects) in northwestern Ontario, covering 909 km^2. The news release credits an OGS publication (Breaks, Selway and Tindle 2003) for identifying the district as an exploration target for rare-element mineralization.
   (Patriot Lithium Ltd., ASX Announcement, January 9, 2023)

6. February 2023—Midas Minerals Ltd. signed an option to acquire the Greenbush lithium project in northwestern Ontario (covering 102 km^2) and credited the OGS for the discovery and sampling of the known pegmatite outcrop in the area (Goodwin 1965).
   (Midas Minerals Ltd., ASX Announcement, February 13, March 28, and July 13, 2023)

7. February 2023—Bastion Minerals Ltd. acquired the Pakwan East lithium property (covering 17 km^2) and announced that, upon review of OGS maps and geological data, the company will be prioritizing the mapping and sampling pegmatite clusters identified by historical OGS mapping (Wood 1977).
   (Bastion Minerals, ASX Announcements, February 20, 27, and 28, 2023)

8. February to July 2023—Sky Gold Corp. acquired 3 properties in the Shebandowan–Greenwater lakes region in northwestern Ontario. The properties are in an area that was recommended for nickel-copper-cobalt-platinum group elements exploration by the OGS–RGP in the *Recommendations for Exploration 2022–2023* (Campbell 2023). In news releases, the company credits an OGS till sampling program conducted in the Shebandowan greenstone belt (Bajc 2000) for identifying clusters of nickel-copper-cobalt-chromium-platinum-palladium in-till anomalies in the area.
   (Sky Gold Corp., news releases, February 7, March 23, and July 12, 2023)

9. March and May 2023—Newpath Resources Inc. announced the staking of a total of 586 new claims as part of its Alpha/Bravo claim group in northwestern Ontario (comprising 2974 claim units covering 631 km^2). The company states in news releases that the decision to acquire these additional properties (and the original claim group) is based on data from a regional compilation of lake sediment surveys completed by the OGS (2020) and recent OGS mapping work (Metsaranta and Walker 2019; Metsaranta 2022) that identified a potential fertile parent granite.
   (Newpath Resources, news releases, March 28, and May 30, 2022)

10. May 2023—Blaze Minerals Ltd. acquired the North Spirit lithium project (comprising 1698 claims covering 340 km^2) based on OGS mapping work (Préfontaine and Buse 2009). As announced in July 2023, Blaze Minerals commenced initial field activities, targeting two-mica granite pegmatites that were defined by OGS data.
    (Blaze Minerals Ltd., ASX Announcements, May 26, June 9, and July 26, 2023)
11. July 2023—Collective Metals Inc. acquired the lithium Whitemud project in northwestern Ontario (comprising 381 claims, 7775 ha). The company credits OGS mapping (Fenwick 1966) for identifying several outcrops of pegmatites and a lake sediment survey completed in 2000 (OGS 2002) that yielded anomalous values for cesium, niobium, lithium, tin, beryllium, mercury and thallium in the project area.
    (Collective Metals Inc., news releases, July 12 and 20, 2023)
12. August 2023—Pegmatite One Lithium and Gold Corp. announced the discovery of spodumene mineralization on its Frazier Lake Mound property in northwestern Ontario as a result of the exploration program conducted by the company in July. Based on this discovery, the company acquired an additional 79 mining claims in the vicinity of the property and decided to extend field activities in 2023. The discovery occurs in an area that was recommended for lithium exploration by the Thunder Bay South Resident Geologist in the OGS–RGP *Recommendations for Exploration 2018–2019* (Puumala and Campbell 2019) which was based on earlier OGS mapping (Hart 2005) that identified a potential fertile granite near Mound Lake.
    (Pegmatite One Lithium and Gold Corp., news releases, July 24, August 2 and 10 (×2), 2023)

SUCCESSES WITH INDIGENOUS COMMUNITIES

The OGS measures its success with Indigenous communities through qualitative data collection (e.g., collaborations, blessings, testimonials). Between October 2022 and September 2023, the OGS collaborated with many Indigenous communities, gave 17 presentations to communities, held a total of 10 days of field mapping with local community members, and were invited to host a booth and participate in 8 major community events. The following successes were documented (for full summary about OGS community engagement activities in 2022–2023, *see also* Levesque and Bennett (this volume, Article 3).

1. An in-community, formal prospector training course was held by the OGS Indigenous Geoscience Liaisons (IGL) and staff of the Kirkland Lake RGP Office in Temagami First Nation on October 19–20, 2022. A total of 11 participants from the community attended.
2. Since 2019, the OGS has worked in collaboration and partnership with Mississaugi First Nation on the Mississaugi bedrock mapping project (Project SO-19-001). In May 2023, Evan Hastie, Precambrian Geoscientist, was gifted an eagle feather from Traditional Knowledge Keeper Roger Daybutch in recognition of his work and accomplishments as project lead. For a detailed summary of this event, *see* Levesque and Bennett (this volume, Article 3).
3. In July 2023, OGS staff hosted the Mineral Development Advisors (MDA) and lands and resources staff from Grand Council Treaty #3 for a full-day session of presentations, discussions, and field trips at the RGP office in Kenora. This session was developed in collaboration with the community upon their request to learn more about their local geology. For a detailed summary of this event, *see* Levesque and Bennett (this volume, Article 3).
4. The OGS was invited to collaborate with Water First through participation in their Indigenous Schools Water Program: a summer school program that provides youth an opportunity to complete a high school credit. Staff of the RGP and the IGLs attended 2 events in July 2023, with Beausoleil First Nation and Sheshegwaning First Nation, to provide an educational session on the local geology.
    (Water First Education & Training Inc., news article, September 18, 2023)

5. In July 2023, the IGLs collaborated with the MDA for Missinabie Cree First Nation to deliver a technical session about critical minerals targeted to community staff and members.
6. In August 2023, Mohawks of the Bay of Quinte First Nation granted a Band Council Resolution to the OGS that allowed mapping to proceed on their traditional land use area and federal reserve lands (Project SO-22-001; *see also* Hahn, this volume, Article 27). The First Nation hosted the OGS field crew for a day of mapping and knowledge sharing.
7. On August 8, 2023, Lands and Resource staff of Temagami First Nation accompanied the Indigenous Geoscience Liaisons, Peter MacDonald and crew for a day of collaborative field mapping (Project NE-23-001; *see also* MacDonald, this volume, Article 9).
8. The OGS collaborated with Six Nations of the Grand River First Nation on a groundwater mapping program in southern Ontario (Project SO-23-002, *see also* Colgrove and Dell, this volume, Article 30). In September 2023, staff of the OGS and from the Six Nations Environmental Task Force sampled wells on reserve lands to help address gaps in the groundwater geochemistry in the area.

NEXT STEPS

The OGS will continue to

- collect performance measures data that include baseline values, target values and actual values;
- take steps to address gaps and downward trends and to continually improve products and services;
- communicate the value and relevance of public geoscience information;
- improve the integration of geoscience information into broader government and public decision-making; and
- build strong and successful collaborations and relationships with Indigenous communities.

REFERENCES

Ayres, L.D. 1969. Axe Lake sheet, Kenora District; Ontario Geological Survey, Map 2164, scale 1:63 360.

Bajc, A.F. 2000. Till compositional database, western part of the Shebandowan greenstone belt, northwestern Ontario; Ontario Geological Survey, Miscellaneous Release—Data 50.

Breaks, F.W., Selway, J.B. and Tindle, A.G. 2003. Fertile peraluminous granites and related rare-element mineralization in pegmatites, Superior Province, northwest and northeast Ontario: Operation Treasure Hunt; Ontario Geological Survey, Open File Report 6099, 179p.

Campbell, D.A. 2023. Nickel-copper-cobalt-PGE potential in the Shebandowan–Greenwater lakes area; *in* Ontario Geological Survey, Resident Geologist Program, Recommendations for Exploration 2022–2023, p.34-40.

Fenwick, K.G. 1967. Whitemud Lake area (Fredart–Whitemud lakes area), District of Kenora (Patricia Portion); Ontario Geological Survey, Preliminary Map 412, scale 1:15 840.

Goodwin, A.M. 1965. Geology of the Pashkokogan Lake–eastern Lake St. Joseph area, districts of Thunder Bay and Kenora; Ontario Department of Mines, Report 42, 58p.

Hart, T.R. 2005. Precambrian geology of the southern Black Sturgeon River and Seagull Lake area, Nipigon Embayment, northwestern Ontario; Ontario Geological Survey, Open File Report 6165, 63p.

Lemkow, D.R., Sanborn-Barrie, M., Bailes, A.H., Percival, J.A., Rogers, N., Skulski, T., Anderson, S.D., Tomlinson, K.Y., McNicoll, V., Parker, J.R., Whalen, J.B., Hollings, P. and Young, M. 2006. GIS compilation of geology and tectonostratigraphic assemblages, western Uchi Subprovince, western Superior Province, Ontario and Manitoba; Geological Survey of Canada, Open File 5269, (also Manitoba Geological Survey, Open File Report 2006-30; also Ontario Geological Survey, Miscellaneous Release—Data 203).

Lewis, S.[O.] and Paterson, W.[P.E.] 2020. Exploration potential for Rottenfish R. and Muskrat Dam L. greenstone belts; *in* Ontario Geological Survey, Resident Geologist Program, Recommendations for Exploration 2019–2020, p.91-96.

Lichtblau, A.F., Paterson, W., Ravnaas, C., Tuomi, R.D., Pettigrew, T.K., Lewis, S. and Wiebe, K. 2018. Report of Activities 2017, Resident Geologist Program, Red Lake Regional Resident Geologist Report: Red Lake and Kenora Districts; Ontario Geological Survey, Open File Report 6336, 100p.

Metsaranta, R.T. 2022. Highlights of bedrock geology mapping in the Quetico Subprovince, north of Thunder Bay, northwestern Ontario; *in* Summary of Field Work and Other Activities, 2022, Ontario Geological Survey, Open File Report 6390, p. 9-1 to 9-9.

Metsaranta, R.T. and Walker, J.A. 2019. Precambrian geology of western McGregor Township and adjacent areas, northeast of Thunder Bay; *in* Summary of Field Work and Other Activities, 2019, Ontario Geological Survey, Open File Report 6360, p.11-1 to 11-10.

Ontario Geological Survey 2002. Perrault Falls area high density regional lake sediment geochemical survey, northwestern Ontario: Operation Treasure Hunt; Ontario Geological Survey, Open File Report 6092, 84p.

——— 2020. Lake geochemistry of Ontario—2019; Ontario Geological Survey, Lake Geochemistry of Ontario, database.

Parker, J.R. and Atkinson, B.T. 1992. Gold occurrences, prospects and past-producing mines of the Birch–Confederation lakes area; Ontario Geological Survey, Open File Report 5835, 332p.

Paterson, W.P.E., Ravnaas, C., Lewis, S.O., Paju, G.F., Fudge, S.P., Daniels, C.M. and Pettigrew, T.K. 2020. Report of Activities 2019, Resident Geologist Program, Red Lake Regional Resident Geologist Report: Red Lake and Kenora Districts; Ontario Geological Survey, Open File Report 6363, 112p.

Préfontaine, S. and Buse, S. 2009. Geological, geochemical and geochronological data from the North Spirit Lake area, North Spirit Lake greenstone belt, North Caribou terrane, northwestern Ontario; Ontario Geological Survey, Miscellaneous Release—Data 238.

Puumala, M.[A.] and Campbell, D.[A.] 2019. Exploration potential in the Nipigon Embayment north of Dorion; *in* Ontario Geological Survey, Resident Geologist Program, Recommendations for Exploration 2018–2019, p.32-37.

Stone, D., Crawford J. and Lange, M. 1994. Precambrian geology, Margot Lake area; Ontario Geological Survey, Preliminary Map 3283, scale 1:50 000.

Wood, J. 1977. North Spirit Lake, Kenora District; Ontario Geological Survey, Map 2362, scale 1:31 680.

3. Activities of the Indigenous Geoscience Liaisons in 2022–2023



M.D. Levesque[1] and D.J. Bennett[1]

[1] Director's Office, Ontario Geological Survey

INTRODUCTION

The Ontario Geological Survey (OGS) is committed to building meaningful, collaborative and long-term relationships with Indigenous communities for anticipated and ongoing geoscience project areas. One of the current OGS mandates is to "encourage and facilitate Indigenous participation in Ontario's economy in a way that recognizes and is respectful of Indigenous rights and culture" and our work within Indigenous communities aims to meet and exceed this mandate. Since 2016, the OGS Indigenous Geoscience Liaisons (IGL) have been focussed on engaging, building and maintaining strong, respectful relationships with First Nations and Métis communities across Ontario that have measurable and realistic outcomes. One of the key responsibilities of the IGL position is to engage with our treaty partners in co-development, co-design and implementation of geoscience projects, and to discuss the application and potential impacts of OGS geoscience project work and results. Additionally, we function as pivotal liaisons, hearing the directions and priorities of First Nations and Métis communities and translating those priorities to ministry employees to ensure projects and participation is developed and facilitated in a way that is appropriate to each individual community. The further diminishing restrictions associated with the COVID pandemic resulted in the notifications of 15 OGS projects that commenced in the 2023 field season. As a result of these projects, over 50 individual Indigenous communities were consulted. The following article outlines some of these key interactions, with timelines, results and future objectives.

INDIGENOUS ENGAGEMENT BY THE INDIGENOUS GEOSCIENCE LIAISONS

Table 3.1. Indigenous Community engagements by the OGS Indigenous Geoscience Liaisons.

Community	Visit(s)	Description
Anishinabek Nation Lake Huron Regional Table	September 13, 2022 June 20, 2023	Quarterly regional roundtable meeting to provide OGS updates and maintain positive relationships. IGL staff focussed on listening and gaining a greater understanding of the participating Indigenous communities' priorities and directions.
Anishinabek Nation Northern Superior Regional Table	September 20, 2022 January 18, 2023 May 31, 2023	Quarterly regional roundtable meeting to provide OGS updates and maintain positive relationships. IGL staff focussed on listening and gaining a greater understanding of the participating Indigenous communities' priorities and directions.
Anishinabek Nation Southeast and Southwest Regional Table	September 22, 2022 May 10, 2023 July 12, 2023	Quarterly regional roundtable meeting to provide OGS updates and maintain positive relationships. IGL staff focussed on listening and gaining a greater understanding of the participating Indigenous communities' priorities and directions.

Summary of Field Work and Other Activities, 2023,
Ontario Geological Survey, Open File Report 6405, p.3-1 to 3-8.

© King's Printer for Ontario, 2023

Community	Visit(s)	Description
Algonquins of Ontario	October 4, 2022	Geology and prospecting presentation: Algonquins of Ontario requested the OGS complete a surficial geology mapping project that would target a significant gap within their traditional land use area. We met and discussed the goals of this project and ways that we could work together to meet mutual targets.
Temagami First Nation	October 12, 2022	Introductory presentation to staff and community members about their local geology and prospecting prior to in-community prospector training.
Temagami First Nation	October 19–20, 2022	Two-day in-community formal prospector training for 11 community and staff members. Training was done by the IGL staff, and Kirkland Lake RGP staff. Temagami staff and community members reported they enjoyed the session and learned a lot. Accommodations and meals were provided by the community for OGS staff.
Mineral Development Advisor and Community Consultation Liaison Officer information session	November 16, 2022	IGL staff provided "minerals in our lives" presentation and OGS products and services presentations to ~20 community staff from Indigenous communities across Ontario.
Anishinabek Nation Joint Advisory Committee	December 7, 2022 March 9, 2023 June 27, 2023	Quarterly meeting to provide OGS updates and maintain relationships. IGL staff focussed on listening and gaining a greater understanding of the participating Indigenous communities' priorities and directions.
Marten Falls First Nation	January 19, 2023	In-community OGS booth set up featuring "minerals in our lives" display and other resources. Focussed on elementary students.
Southern Mineral Development Advisor and Community Consultation Liaison Officer training	January 23, 2023	IGL staff provided "minerals in our lives" presentation and OGS products and services presentations to MDAs and CCLOs from across southern Ontario.
Anishinabek Nation GIS information session	January 26, 2023	Meeting to discuss Anishinabek Nation recently developed geoportal project and how we can help incorporate OGS data.
Formal proposed OGS geological mapping projects notification letters	February 2023	Formal notifications were emailed for 15 OGS ERGMS geological mapping projects. OGS staff contacted more than 50 Indigenous communities notifying them of proposed projects in their traditional land use area and offering a presentation. IGL staff presented to many individual Indigenous communities sharing information about these mapping projects in their traditional land use area along with informal conversations.
GAC–MAC–SGA notifications	February 2023	Sent notifications to our Indigenous mapping partners regarding field trips in their area with the offer to join the trip if there was interest. These field trips were held in conjunction with the joint annual meeting of the GAC–MAC–SGA in Sudbury in May 2023.
Anishinabek Nation Great Lakes Strategy information session	February 9, 2023	Attended presentation to learn about the initiative and see where OGS can contribute.
Anishinabek Nation Lands – resources and economic development forum 2023	February 14–16, 2023	Booth set up with ERGMS and RGP over 2 days of the conference. The conference had community members from ~1/3 of Indigenous communities across Ontario and we had great conversations and participants were provided the opportunity to meet OGS staff mapping the area.
Sheshegwanning First Nation	February 17, 2023	Aggregate information request: Community member requested to learn about local aggregate information and its potential uses. This meeting stemmed from a conversation at the Anishinabek Nation lands and resources forum between a community member and ERGMS staff.
Métis Nation of Ontario Mineral Development Advisor training	February 22, 2023	IGL staff provided "minerals in our lives" presentation and OGS products and services presentations.

Community	Visit(s)	Description
Wiikwemkoong First Nation	March 1, 2023	Geophysical meeting: Virtual meeting with staff to explain our geophysical survey in their traditional land use area. First Nation requested to increase survey boundaries to include Federal Reserve Lands as a result of our notifications and this meeting.
Nipissing First Nation	March 23, 2023	Meeting to explain a geological mapping project in Nipissing First Nation traditional land use area. Input and project participation was provided and requested by Nipissing. Plans for collaboration in the 2024 field season are underway.
Temagami First Nation	April 12, 2023	Mapping presentation: Meeting with Temagami First Nation land and resources staff, and community members to talk about upcoming geological mapping in their traditional land use area. A record number of attendees (over 30) were present at this virtual talk and asked many questions about mapping and mining activity in the area. This meeting resulted in plans to provide a field trip to any interested members, which was planned for late summer.
Chapleau Cree First Nation	April 14, 2023	Mapping presentation: Meeting to explain geological mapping project in Chapleau Cree First Nation traditional land use area.
Six Nations of the Grand River First Nation	April 26, 2023	Met with Six Nations of the Grand River Environmental Task Force to present information on the regional ground water project and potential collaborations, as well as to discuss the potential for drilling a few monitoring wells on Six Nations reserve lands to address gaps in knowledge of a potential transition zone in the subsurface of their reserve.
PDAC Student–Industry Mineral Exploration Workshop (S-IMEW) presentation	May 4, 2023	IGL staff presented the OGS consultation approach and collaborations throughout the years to students in the PDAC S-IMEW program. Benefits included providing insight into Indigenous relations in the mining sector in government and industry when the students enter their chosen field.
Timiskaming First Nation	May 5, 2023	Geophysical survey presentation: IGL and ERGMS staff presented information about a proposed geophysical survey to the MDA of Timiskaming First Nation. It was our first interaction with this community in many years and was a successful and well-received presentation.
Nipissing First Nation	May 9, 2023	OGS staff presented to Nipissing First Nation lands and resources staff regarding upcoming proposed geophysical surveys in their traditional land use area. Nipissing was supportive and recognized ways to utilize this information to address some of their own research gaps.
Red Sky Métis Independent Nation	May 24, 2023	ERGMS geoscientists presented 3 proposed geological mapping projects. Lands and Resource staff member requested to join an OGS geoscientist for a day of mapping. IGL staff followed up with OGS maps and resources.
GAC–MAC–SGA Mississaugi First Nation presentation at the special Indigenous session	May 26, 2023	IGL staff collaborated with the GAC–MAC–SGA meeting organizing committee to create an agenda for their special Indigenous session at the GAC–MAC–SGA Sudbury conference. IGL staff were able to secure a traditional knowledge keeper to provide opening and closing ceremonies. That traditional knowledge keeper also agreed to participate in the IGL staff presentation about our approach to engagement and consultation. Our presentation focussed on the very successful collaboration between Mississaugi First Nation and the OGS Mississaugi bedrock geology mapping project. *See* "Mississaugi First Nation Collaboration with OGS Bedrock Geology Mapping Project".
Critical Minerals Presentation at Big Mining Event Indigenous Partnerships Forum	June 7, 2023	IGL staff presented the OGS approach to consultation at the Critical Minerals and Indigenous Partnerships forum at the "Big Mining Event" in Timmins, Ontario. The presentation was well received and resulted in discussions to participate in field trips, community events and community visits.

Community	Visit(s)	Description
Whitefish River First Nation	June 9, 2023	OGS staff were invited to set up a booth at the Whitefish River First Nation family fun day. Staff from the OGS Director's Office, ERGMS and RGP attended the event and interacted with community members throughout the day.
Atikameksheng Anishinabek First Nation	June 29, 2023	Staff from ERGMS, RGP and the OGS Director's Office attended a consultation day held by Atikameksheng Anishinabek First Nation to allow OGS staff to talk about their mapping projects and the regional geology with staff and community members.
Beausoleil First Nation	July 5, 2023	RGP and IGL staff were invited to collaborate with the organization Water First on a summer school program that provides youth living on reserve with the opportunity to complete a high school credit on reserve during the summer. RGP staff attended the event and provided a day-long session on geology, with a focus on local information. The day included both in-class and outdoor activities.
Grand Council Treaty #3	July 11, 2023	A dozen Mineral Development Advisors from the Grand Council Treaty #3 area visited the OGS Kenora office. The visit included presentations, discussions and in-the-field training. Attendees enjoyed the opportunity to learn more about their local geology around the Kenora area. Discussions are taking place to turn this into a yearly event. *See* "Grand Council Treaty #3 Geology Session".
Sheshegwaning First Nation	July 14, 2023	RGP and IGL staff were invited to collaborate with the organization Water First on a summer school program that provides youth living on reserve with the opportunity to complete a high school credit in their community during the summer. RGP staff attended the event and provided a half-day long session on geology, with a focus on local information. The day included both in-class and outdoor activities.
Missanabie Cree First Nation	July 19, 2023	Critical Minerals evening session: IGL staff held a critical minerals session for Missanabie Cree First Nation community members. The session included a collaboration with the community MDA, to create a targeted and relevant presentation for staff and community members. Our relationship with Missinabie Cree was strengthened and knowledge was shared about our future attendance at their community gathering.
Mohawks of the Bay of Quinte / Tyendinaga Mohawk Territory First Nation	August 10, 2023	Reserve mapping: ERGMS geoscientists conducting field work near Mohawks of the Bay of Quinte submitted a request to map outcrops on reserve. The First Nation were happy to host the geoscientists for a day on reserve, and provided a band council resolution, as well as a summer student. Knowledge sharing between geoscientists and the summer student made the experience beneficial for all in attendance.
Missanabie Cree First Nation	August 16, 2023	Annual gathering: OGS staff were invited for a second year to set up a booth at the Missanabie Cree annual gathering. IGL staff and ERGMS geoscientists working in the area attended the event and interacted with community members throughout the day.
Algonquins of Ontario	August 24, 2023	Meeting to discuss local surficial geology mapping requests, as well as developing a presentation for Algonquins of Ontario staff to learn about local geology.
Six Nations of the Grand River First Nation	September 6–13, 2023	Groundwater mapping: ERGMS geoscientists, Six Nations staff, and IGL staff completed a groundwater sampling project on reserve. This program included collaborations throughout the spring and summer with Six Nations Environmental Task Force staff and culminated in over a week of sampling wells across the reserve to help address gaps in the groundwater geochemistry across the area. The project provides valuable information to the OGS and also provides important water quality information to residents who participated.

***Abbreviations**: CCLO, Community Consultation Liaison Officer; ERGMS, OGS Earth Resources and Geoscience Mapping Section; GAC–MAC–SGA, Geological Association of Canada, the Mineralogical Association of Canada and the Society for Geology Applied to Mineral Deposits; IGL, OGS Indigenous Geoscience Liaison; MDA, Mineral Development Advisor; OGS, Ontario Geological Survey; PDAC, Prospectors and Developers Association of Canada; RGP, OGS Resident Geologist Program.*

MONTHLY INDIGENOUS LEARNING ACTIVITIES

During monthly OGS section staff meetings, the IGLs have presented Indigenous learning activities. Presentations have covered topics, such as the following:

- Introductions to Indigenous groups across Ontario
- Missing and murdered Indigenous women and children
- Indigenous literature
- Colonization
- Cultural events

These short presentations and/or activities help introduce staff to various Indigenous topics and aim to promote awareness of different cultures and increase inclusivity. These 15-minute monthly presentations are enjoyed by staff, and IGLs often receive positive feedback and follow-up conversations on each respective topic. During each session, staff are encouraged to do their own follow-up research, contact IGLs for more information and resources and to participate in one of the learning activities if they have something to contribute. These activities are planned to continue in the fall and winter of 2023–2024 with input from staff on topics they are interested in learning more about.

WOODLAND ART PRESENTATIONS

Throughout the year, the IGL (senior author) has given presentations on Indigenous woodland art. This year, presentations have been given to government staff at the Ministry of Attorney General, and also included a presentation to the Rainbow District School Board as a annual event. The presentation focusses on introducing woodland art and demonstrating the multiple ways of interpreting the art using paintings from the IGL's personal collection. Woodland art is used as an avenue to share Indigenous history and customs and to explain why the IGL role is essential to the organization.

INFORMAL NOTIFICATIONS AND VIRTUAL PRESENTATIONS

For the 2023 field season, the IGLs continued with our process of "informal notifications" for communities with geological mapping projects occurring on their traditional land use area. These informal notifications are personalized emails to community contacts, and provide communities advance notice of projects, with opportunities for them to provide input, ask questions or request specific information about projects before field work for the OGS projects start. This initiative continued to be highly successful in that the IGL's received more than 10 separate requests for presentations, opportunities to participate in field trips, extensions of mapping areas, and collaborations. Many of the meetings from this year and last year led to invitations to community events.

The IGLs worked very closely with ERGMS staff to develop the presentations about their projects, to design and deliver imaginative and targeted field trips, to extend project boundaries, and to plan collaborations. The ERGMS staff brought their knowledge and passion about geology across Ontario, and the IGLs helped ensure that staff knowledge and passion were targeted, relevant and relatable. Our efforts over the past 2 years have led to incredible achievements in relationship building with Indigenous communities across Ontario. These strengthening relationships are evidenced through the requests for participation in field trips, project extensions, community visits and reserve mapping. We all worked very hard on tight timelines to make the entire process successful and send our kudos to all staff members for adeptly incorporating and growing this process while juggling other competing tasks! Miigwech to each of you!

MISSISSAUGI FIRST NATION COLLABORATION WITH OGS BEDROCK GEOLOGY MAPPING PROJECT

In May 2023, the Geological Association of Canada–Mineralogical Association of Canada (GAC–MAC), with the Society for Geology Applied to Mineral Deposits (SGA), held its annual conference in Sudbury. Ontario Geological Survey (OGS) staff were busy for months preparing oral and poster presentations and field trips, and planning for the event. The Indigenous Geoscience Liaisons (IGLs) were also involved in GAC–MAC this time around.

In early winter, we were contacted about being on a planning committee for the first-ever Indigenous session to be held at GAC–MAC. Similar to many participating OGS geologists, we helped plan, organize and suggest speakers for the event, along with presenting on OGS engagement with Indigenous communities.

A key part of our 20-minute oral presentation was the Mississaugi bedrock geology mapping project, which was a collaborative project that included staff and community members from Mississaugi First Nation. Central to the project was the ongoing involvement of traditional knowledge keeper Roger Daybutch. Traditional knowledge keeper Daybutch honoured us with his presence at the Indigenous session, which also included speaking during the OGS presentation. Although it is customary for a local elder or traditional knowledge keeper to provide an opening and closing ceremony to start and end the session in a good way, the elder who was supposed to provide this service was indisposed, and traditional knowledge keeper Roger stepped up and graciously provided this service for the session. We were extremely grateful for his presence and willingness to step in when needed. The session included talks from various levels of government, Industry, Chief and Councils, and community members, who all shared their experiences working with First Nations communities toward a common goal, with respect and a willingness to listen and learn.

The session was well received and went over time. One of the highlights of the session was a very special gift to Evan Hastie from traditional knowledge keeper Roger. Evan Hastie, lead geoscientist for the Mississaugi bedrock geology mapping project, developed a relationship with traditional knowledge keeper Roger throughout the years he worked there. Evan had welcomed Roger to his home for dinner, Evan was invited and attended a few eagle ceremonies during the field seasons and attended a Mississaugi First Nations pow wow. Despite their close working relationship, Evan was taken by surprise when, at the conclusion of the IGL talk, traditional knowledge keeper Roger gifted him an eagle feather. Eagle feathers are of extreme importance to Indigenous communities and community members obtain them through gifting practices that signify important and noteworthy accomplishments from the receiver.

The gift of the eagle's feather speaks volumes to the level of engagement and commitment Evan showed to the community, and how appreciated it was. Evan went above and beyond, as a geoscientist, a member of the public sector, and as a human, to establish and create an amazing relationship and partnership with Mississaugi First Nation. Evan Hastie shared the following about the experience.

> "It has been my honour and privilege to work alongside Mississaugi First Nations mapping the north shore of Lake Huron between Iron Bridge and Blind River. To have experienced many teachings by traditional knowledge keepers such as Roger Daybutch has been a highlight of my career in Earth Sciences and given me much perspective to the story of the rocks we live on. Reminiscing about this collaboration at GAC–MAC 2023 during a presentation at the Indigenous learning session brought the whole experience back into focus. To then be honoured at this session with a gift from Roger left me speechless, humbled and I will treasure this moment always during my journey to understand the rocks we live on."
>
> *Evan Hastie,*
> *Geoscientist, Ontario Geological Survey, Earth Resources and Geoscience Mapping Section*

In attendance were other members of the Ministry of Mines, including staff from our Indigenous Collaborations and Partnerships Branch (ICPB). Bob Jefferies shared the following about the session.

> "GAC–MAC Indigenous Partnerships Session highlighted the benefit and importance of increasing focus on training of geologists to meaningfully engage the Indigenous community before, during and after their work regardless of the nature of the project. Recognizing that all projects have a link to one or many Indigenous communities and meaningful engagement deepens the value of a project. The session also alerted participants to the need to increase training and make connection to look at how to better equip professional geologists."
>
> *Bob Jefferies,*
> *Senior Advisor, Ministry of Mines, Indigenous Collaborations and Partnerships Branch*

We were honored to be part of the first Indigenous session at a GAC-–MAC annual meeting and the projects that we were able to share with meeting participants. We look forward to many more successful collaborations with Indigenous Nations in Ontario.

GRAND COUNCIL TREATY #3 GEOLOGY SESSION

In July, Ethan Amyotte (District Geologist) and Kristen Wiebe (District Geological Assistant), of the RGP Kenora office, and Mathieu Levesque (Indigenous Geoscience Liaison) hosted a dozen Mineral Development Advisors (MDA), along with lands and resource staff from Grand Council Treaty #3, for a session focussed on local Kenora geology. This event was developed in collaboration with MDA staff who wanted to learn more about exploration and their local geology. This one-day, three-part session featured a review of OGS products and services, presentations on local geology and advanced exploration projects using OGSEarth and GeologyOntario, a barbecue lunch and a field trip.

The day started with a visit to the Kenora RGP office, where participants examined polished samples. Learning about the different minerals within lithium pegmatites was high on the agenda. Ethan helped explained how geophysics is used for the differentiation of rock types and for mineral exploration; examples were provided throughout the day. They were also shown the general library and the assessment file library at the office.

The day continued by getting together in a boardroom where Ethan used OGSEarth to explain the different subprovinces of the Superior Craton. He highlighted areas of key resource potential by familiarizing the group with the Ontario Mineral Inventory (OMI), the Ontario Drill Hole Database and the Ontario Assessment File Database. Ethan also reviewed some of the advanced exploration projects in the Kenora area, clarifying some points of concern.

During the lunch break, the group enjoyed the barbecue lunch and a tour of the Kenora core library. Because geology does not stop in the classroom, we spent the afternoon visiting several locations around Kenora that highlight the geological differences between the Winnipeg River and Wabigoon subprovinces. Stop two demonstrated how mineralization is focussed in areas of structural change and fluid flow. Ethan's offer to collect samples for multi-element and gold analysis at the OGS Geoscience Laboratories, and to report back to the group with his interpretation, was well received.

The day generated good conversations and participants appreciated having training tailored to the locations they work in. The event was a great way to highlight OGS products and services, explain our non-regulatory work and make new contacts with our Treaty 3 partners. Kenora RGP–OGS staff will be following up on numerous requests as a result of this meeting, including providing OMI locations for pipestone (soapstone) occurrences, providing prospector training and accompanying MDA staff in the field. With continued communication and collaboration, it is likely that this can become an annual event

that will grow in capacity for knowledge sharing. The knowledge sharing goes both ways in these types of events—Treaty 3 members taught us about local flora, such as *Mentha canadensis*, a species of mint native to North America that was identified while in the field. Members also shared cultural stories about the rocks in their area, and some of the challenges they face in preserving heritage sites and nature from mining, exploration and development activities. Additionally, meeting contacts from over a dozen Indigenous communities at the same time is extremely valuable for gaining and maintaining OGS social license.

This page left blank intentionally

Earth Resources and Geoscience Mapping Section

4. Earth Resources and Geoscience Mapping Section: 2023–2024 Program and Projects Overview



J.H. Hechler[1], R.M. Easton[1], S. Préfontaine[1], M. Duguet[1], L. Robichaud[1] and R. Cormier[1]

[1]Earth Resources and Geoscience Mapping Section, Ontario Geological Survey

GOAL AND RESPONSIBILITY OF THE SECTION

The goal of the Ontario Geological Survey's (OGS) Earth Resources and Geoscience Mapping Section (ERGMS) is to improve the understanding of the geology, geochemistry and Earth resources of the province and to convey this knowledge to the public through multi-year, multi-disciplinary geoscience projects that address key geoscience problems. These studies may be delivered as part of the ERGMS geoscience mapping function or through collaborative geoscience projects or initiatives.

The ERGMS is responsible for

- mapping Ontario's Precambrian and Phanerozoic bedrock geology and assessing its inherent resources at a regional scale;
- mapping and sampling of Quaternary sediments for the purpose of mineral resource assessment, land-use planning, aggregate delineation, geotechnical applications, etc.;
- three-dimensional (3-D) mapping of Quaternary and Phanerozoic hydrostratigraphic units and their contained groundwater resources at a regional scale. Determining the relationship between aquifer composition and regional groundwater geochemistry;
- collecting regional ground and airborne geophysical data and producing derivative products in support of bedrock geology and groundwater mapping projects, mineral exploration and land-use planning;
- collecting regional surficial geochemistry data from water and other surficial media (e.g., lake and stream sediments, peat, etc.) to support mineral exploration, mapping of bedrock and sediments, land-use planning, assessment of watershed quality and the establishment of natural baseline databases;
- mapping aggregate and industrial minerals to provide up-to-date inventories and quality assessments of potential aggregate and industrial mineral resources; and
- mapping bedrock that hosts traditional and unconventional non-renewable energy resources to identify new energy sources and opportunities for carbon storage.

The program direction and strategies of the ERGMS address the strategic objectives and core business of the Ontario Geological Survey Branch, which, in turn, are linked to those of the Mines and Minerals Division of the Ministry of Mines. Ministry and Government priorities are achieved through specific ERGMS strategies and initiatives that consist of one or more projects. Staff of the OGS conducts an annual, project planning exercise, including project proposals development, evaluation and selection.

Summary of Field Work and Other Activities, 2023,
Ontario Geological Survey, Open File Report 6405, p.4-1 to 4-21.

© King's Printer for Ontario, 2023

This project planning exercise is designed to achieve alignment of individual projects with higher level Divisional, Ministry and Government priorities. This article reports on the current activities of the ERGMS.

The ERGMS supported 77 active projects during the 2023–2024 fiscal year, which includes 59 active core projects and 18 active collaborative projects (Table 4.1). The collaborative projects include 1 project with other provincial ministries; 2 projects with the City of Ottawa; 1 project in collaboration with the Mineral Exploration Research Centre (MERC) at Laurentian University, Metal Earth and the Royal Ontario Museum (ROM); and 12 graduate thesis projects with universities. Locations of projects for which there are corresponding articles in this volume are depicted in Figure 4.1.

From December 2022 to December 2023, inclusive, ERGMS produced 4 Open File Reports, 2 Preliminary Maps, 3 Miscellaneous Releases—Data (MRD), 1 Groundwater Resources Study and 1 Ontario Geoscience Video (*see* "List of Publications" in this article for a complete listing of these publications). The ERGMS has several online databases, including the Aggregate Resources of Ontario (ARO) compilation, the Lake Geochemistry of Ontario (LakeGeochemON) compilation, and the Geochronology Inventory of Ontario (GeochrON), which are available for download through GeologyOntario and for viewing in the Google Earth™ mapping service by downloading the appropriate *.kml* file through the OGSEarth Web site. The ERGMS staff presented several technical talks and posters at various geoscience forums and meetings, including virtual geoscience meetings, throughout the year.

ERGMS STRATEGIES AND OBJECTIVES

The Earth Resources and Geoscience Mapping Section (ERGMS) strategies and objectives are derived from OGS strategic priorities, which stem from the Mines and Minerals Division Strategic Framework and Ministry business goals.

The purpose of ERGMS strategies and objectives is to focus staff and resources in key geological areas or geoscience themes, over a period of 3 to 5 years, to contribute to

- expanding the geoscience database of Ontario;
- supporting sustainable development and effective land-use planning;
- providing the geoscience framework for groundwater use and source water protection, public health and safety and the public good; and
- supporting and attracting new mineral investment.

To successfully deliver these strategies, ERGMS is fully engaged in building new and strengthening existing collaborations with Indigenous communities, the private sector, academia, federal agencies and other provincial ministries on initiatives of mutual interest.

The ERGMS main strategies consist of applying geoscience techniques

- to assess Earth resource potential to meet societal and government priorities;
- in areas of environmental priority to identify natural hazards related to geology;
- in areas of aggregate resource priority to meet societal and government priorities; and
- in areas of groundwater priority to meet societal and government priorities.

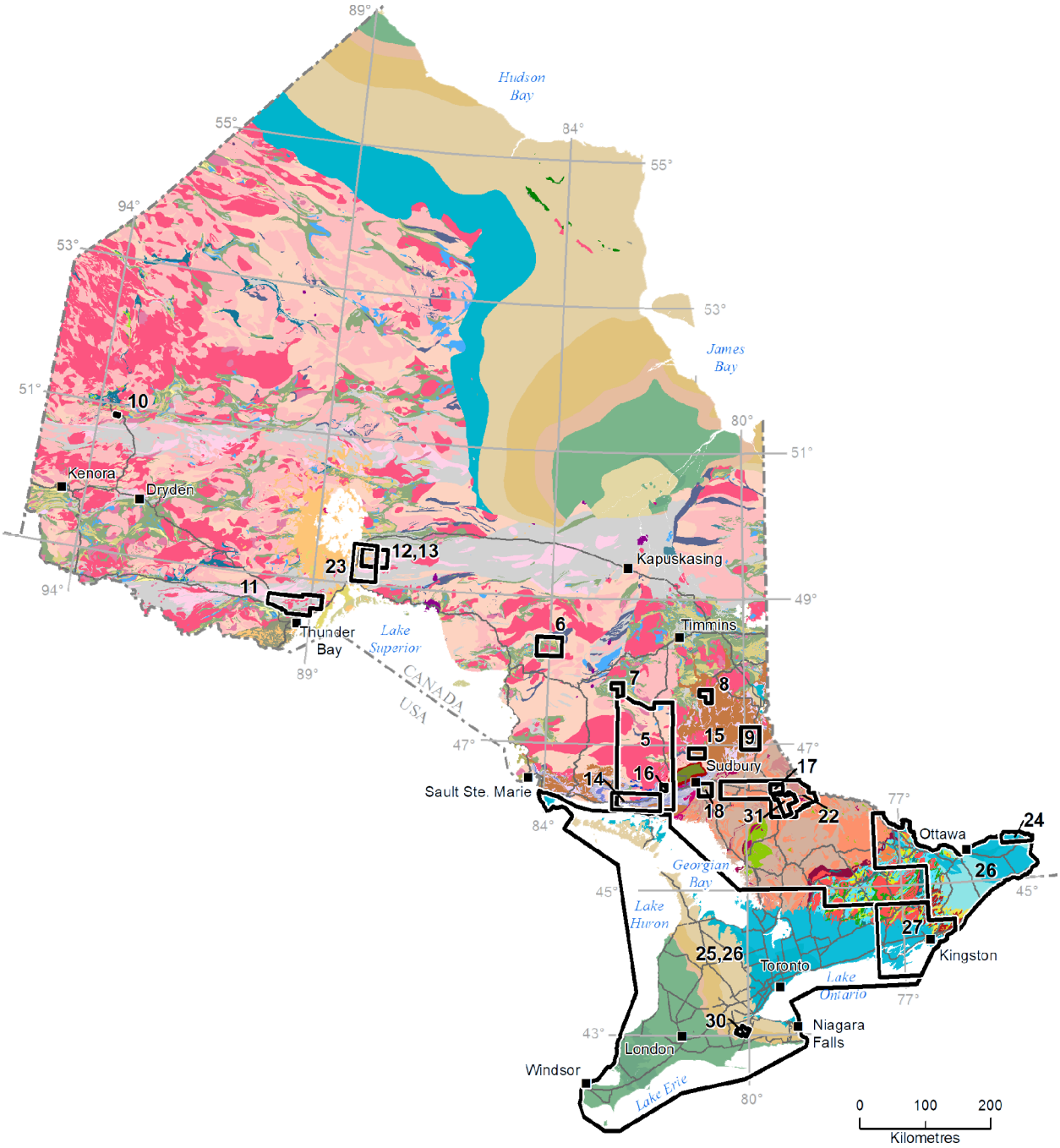


Figure 4.1. Locations of the Earth Resources and Geoscience Mapping Section projects in Ontario as described in *Summary of Field Work and Other Activities, 2023*. Numbers correspond to article numbers; note articles 19, 20, 21, 28, 29 are provincial in scope and are not indicated on the figure. Bedrock geology *from* Ontario Geological Survey (2011).

Table 4.1. Earth Resources and Geoscience Mapping Section collaborative initiatives and projects, 2023–2024.

Initiative	Project	ERGMS Core Program / Project Collaborator(s)	Project Progress
Geophysical Techniques in Support of Bedrock Geology Mapping Initiative	Ground geophysical survey ➤ Collect gravity data in support of the three-dimensional (3-D) sediment mapping project in the Guelph area	ERGMS Core Program	New project – data acquired in August to September 2023, data analysis in progress ➤ *Summary of Field Work* (this volume, Article 20)
	Magnetic data interpretation ▸ Investigate why parts of the Gowganda Formation, Huronian Supergroup, are magnetic; a follow-up study from the Sturgeon River aeromagnetic survey	ERGMS Core Program	New subproject – sampling in 2023, data analysis in progress ▸ *Summary of Field Work* (this volume, Article 15)
	Airborne gravity and magnetic surveys, Manitouwadge and Hornepayne areas, north-central Ontario ▸ Reprocessing and/or reformatting of donated survey data	ERGMS Core Program (data donated by Nuclear Waste Management Organization)	Ongoing – Geophysical Data Sets and maps being prepared for publication in 2024
Far North Land Use Planning Initiative	Bedrock geological compilation of the Obabigan–Neawagank lakes area, North Caribou greenstone belt ▸ 1:50 000 scale	ERGMS Core Program	Ongoing – compilation in progress
	Bedrock geological compilation of the Opapimiskan Lake area, North Caribou greenstone belt ▸ 1:50 000 scale	ERGMS Core Program	Ongoing – compilation in progress
	Far North terrain mapping project ▸ remote predictive mapping, field checking; Quaternary mapping ▸ Sandy Lake area ▸ Pickle Lake–Cat Lake area	ERGMS Core Program	Ongoing – predictive Quaternary geology mapping in the Sandy Lake area in 2018, preliminary maps in progress ▸ *Summary of Field Work* articles published in 2017, 2018 Ongoing – predictive Quaternary geology mapping in the Pickle Lake–Cat Lake area in 2019 ▸ *Summary of Field Work* articles published in 2019, 2020
Surficial Geochemistry of Northern Ontario Initiative	Till sampling and surficial mapping in the Georgia Lake area, northwestern Ontario	ERGMS Core Program	New project – field work in 2023 ▸ *Summary of Field Work* (this volume, Article 23)
	Marathon region sediment and water sampling project high-density lake sediment and water geochemistry survey	ERGMS Core Program	Ongoing – MRD in progress
	Surficial geochemistry sampling over the Borden Lake area and Kapuskasing Structural Zone	ERGMS Core Program	Ongoing – OFRs and MRDs in preparation ▸ *Summary of Field Work* article published in 2016

Abbreviations: *MRD, Miscellaneous Release—Data; OFR, Open File Report.*

Table 4.1, *continued.*

Initiative	Project	ERGMS Core Program / Project Collaborator(s)	Project Progress
Surficial Mapping of Northern Ontario Initiative	Highway 17 mapping and sampling project	ERGMS Core Program	Ongoing – field work in 2023 and 2022 ▸ *Summary of Field Work* (this volume, Articles 22, 17) and article published in 2022
Proterozoic Initiative	Hyman Township bedrock geology mapping project ▸ 1:20 000 scale bedrock geology mapping	ERGMS Core Program	Ongoing – field work in 2023 and 2022 ▸ *Summary of Field Work* (this volume, Article 16) and article published in 2022
	Southwest Sudbury Structure bedrock geology mapping project ▸ 1:20 000 scale bedrock geology mapping	ERGMS Core Program	Ongoing – Preliminary Map, OFR and MRD for Denison Township in progress ▸ *Summary of Field Work* articles published in 2016, 2017, 2018 ▸ Preliminary Map, OFR and MRD published in 2018 for Drury Township
	Geology and mineral potential of the Grenville Front tectonic zone near Sudbury ▸ 1:50 000 scale bedrock geology mapping	ERGMS Core Program	Ongoing – field work in 2023, 2022 and 2021; analyses in progress ▸ *Summary of Field Work* (this volume, Article 18) ▸ *Field trip guidebook:* Easton (2022)
	Proterozoic mafic intrusions of the Sudbury area ▸ Compilation and characterization project	ERGMS Core Program	Ongoing – compilation and database construction
	Geology and mineral potential of Scarfe, Cobden, Thomson and Patton townships, Blind River area, Southern Province ▸ 1:20 000 scale bedrock geology mapping	ERGMS Core Program	Ongoing – field work completed ▸ *Summary of Field Work* articles published in 2019, 2022 ▸ Preliminary Map and MRD in progress
	Geology of the Brudenell area, Grenville Province ▸ multi-year 1:50 000 bedrock geology and compilation mapping project	ERGMS Core Program	Ongoing – field work completed ▸ Preliminary Map, OFR and MRD in progress
	Geology of the Cobden area, Grenville Province ▸ multi-year 1:50 000 scale bedrock geology and compilation mapping project	ERGMS Core Program	Ongoing – field work completed; OFR and MRD published in 2017 ▸ Preliminary Map and OFR in progress
	Geology of the Perth area, Grenville Province ▸ multi-year 1:50 000 scale bedrock geology and compilation mapping project	ERGMS Core Program	Ongoing – field work completed; OFR published in 2017; MRD published in 2019 ▸ Preliminary Map and OFR in progress
	Geology of Carleton Place area, Grenville Province ▸ multi-year 1:50 000 scale bedrock geology and compilation mapping	ERGMS Core Program	Ongoing – field work completed ▸ *Summary of Field Work* articles published in 2017, 2018, 2019 ▸ Preliminary Map, OFR and MRD in progress

Abbreviations: *MRD, Miscellaneous Release—Data; OFR, Open File Report.*

Table 4.1, *continued*.

Initiative	Project	ERGMS Core Program / Project Collaborator(s)	Project Progress
Geology of Northeastern Ontario Initiative	Southern Swayze area (Abitibi greenstone belt) bedrock geology mapping project ▸ 1:20 000 scale bedrock geology mapping	ERGMS Core Program	Ongoing – field work in Cunningham Township and part of Garnet Township in 2023; field work in Swayze, Dore and part of Garnet townships in 2022 ▸ *Summary of Field Work* (this volume, Article 7), and published in 2015, 2016, 2017, 2018, 2019, 2022 ▸ Preliminary Map and MRD published in 2019 and 2020 for Mallard, Marion and part of Genoa townships ▸ Preliminary Map and MRD published in 2018 for Osway and Huffman townships and parts of Eric, Fingal and Arbutus townships ▸ Preliminary Map and MRD for Yeo and Chester townships area published in 2017 and 2018
	Swayze area (Abitibi greenstone belt) metavolcanic evolution study ▸ regional and detailed bedrock geology mapping and detailed geochemistry and volcanology	ERGMS Core Program PhD thesis (T.P. Gemmell) Laurentian University–MERC (Metal Earth)	Ongoing – field work completed in 2021; analyses in progress ▸ *Summary of Field Work* articles published in 2017, 2021
	Structural and tectonic study of the Swayze area of the Abitibi greenstone belt	PhD thesis (Q. Wu) University of Waterloo	Ongoing – field work completed ▸ *Summary of Field Work* articles published in 2015, 2016
	Northern Swayze area (Abitibi greenstone belt) bedrock geology mapping project ▸ 1:20 000 scale bedrock geology mapping and 1:50 000 scale bedrock compilation	ERGMS Core Program	Ongoing – field work completed; OFR and compilation map in progress ▸ *Summary of Field Work* articles published in 2018, 2019 ▸ Preliminary Map and MRD of Reeves and Sewell townships published in January 2021 ▸ Preliminary Map and MRD of Penhorwood Township published in December 2020
	Northeast Michipicoten greenstone belt bedrock geology mapping ▸ 1:20 000 scale bedrock geology mapping	ERGMS Core Program	Ongoing – field work in Riggs and Glasgow townships in 2023; field work in Meath Township in 2022 ▸ *Summary of Field Work* (this volume, Article 6) and articles published in 2016, 2017, 2018, 2019, 2021, 2022 ▸ Preliminary Map for Stover Township published in 2019 ▸ Preliminary Maps and MRDs for Copenace and Bruyere townships published in 2018
	Northeastern Michipicoten greenstone belt geochronological and structural study	ERGMS Core Program PhD thesis (L.E.D. Vice) Laurentian University–MERC (Metal Earth)	Ongoing – field work in 2022, 2023 ▸ *Summary of Field Work* article published in 2022

Abbreviations: *MERC, Mineral Exploration Research Centre; MRD, Miscellaneous Release—Data; OFR, Open File Report.*

Table 4.1, ***continued****.*

Initiative	Project	ERGMS Core Program / Project Collaborator(s)	Project Progress
Geology of Northeastern Ontario Initiative, *continued*	Temagami greenstone belt bedrock mapping project ▸ 1:20 000 scale bedrock geology mapping	ERGMS Core Program	Ongoing – field work in 2023, reconnaissance work in 2019 ▸ *Summary of Field Work* (this volume, Article 9) and articles published in 2019, 2021
	Bedrock geology mapping of Van Hise, Haultain and Nicol townships, Abitibi greenstone belt ▸ 1:20 000 scale bedrock geology mapping	ERGMS Core Program	New project – field work in 2023 ▸ *Summary of Field Work* (this volume, Article 8)
	Bedrock geology and compilation of the Ramsey–Algoma intrusive complex and surrounding rocks ▸ multi-year bedrock geology mapping and compilation at 1:100 000 scale	ERGMS Core Program	Ongoing – field work in 2023, reconnaissance work in 2019 ▸ *Summary of Field Work* (this volume, Article 5) and articles published in 2019, 2020
	The Rundle intrusive complex: investigating oxidation processes related to gold mineralization in an Archean alkalic intrusive setting	MSc thesis (C. Small) Laurentian University–MERC (Metal Earth)	Ongoing – field work completed ▸ *Summary of Field Work* article published in 2018
Geology of Northwestern Ontario Initiative	Bedrock geology mapping of Marks and Conmee townships ▸ 1:20 000 scale bedrock geology mapping	ERGMS Core Program	Ongoing – field work completed ▸ Preliminary Map for Conmee Township and MRD in progress ▸ *Summary of Field Work* articles published in 2017, 2018
	Bedrock geology mapping of the Straw Lake–Esox Lake area, Rowan–Kakagi greenstone belt ▸ 1:20 000 scale bedrock geology mapping	ERGMS Core Program	Ongoing – field work in 2022 ▸ *Summary of Field Work* article published in 2022
	Bedrock geology mapping and rare-element potential in the central Quetico Subprovince, Georgia Lake area ▸ 1:20 000 scale bedrock geology mapping	ERGMS Core Program	Ongoing – field work in 2023 and 2019 ▸ *Summary of Field Work* (this volume, Articles 12, 13) and articles published in 2019, 2020
	Rowan–Kakagi lakes area bedrock geology mapping project ▸ 1:50 000 scale bedrock geology mapping	ERGMS Core Program	Ongoing – field work completed ▸ Preliminary Maps and MRD in progress ▸ *Summary of Field Work* articles published in 2016, 2017
	Compilation and reconnaissance bedrock geology mapping of the Animikie Basin and Midcontinent Rift southeast of Thunder Bay ▸ 1:50 000 scale bedrock geology mapping	ERGMS Core Program	Ongoing – field work in 2023 and 2022 ▸ *Summary of Field Work* article published in 2022
	Bedrock geology mapping of the Quetico Subprovince and related Proterozoic rocks northwest of Thunder Bay ▸ 1:50 000 scale bedrock geology mapping	ERGMS Core Program	Ongoing – field work in 2023 and 2022 ▸ *Summary of Field Work* (this volume, Article 11) and articles published in 2019, 2020, 2022

Abbreviations: *MERC, Mineral Exploration Research Centre; MRD, Miscellaneous Release—Data; OFR, Open File Report.*

Table 4.1, *continued*.

Initiative	Project	ERGMS Core Program / Project Collaborator(s)	Project Progress
Geology of Northwestern Ontario Initiative, *continued*	Geological compilation of the Red Lake greenstone belt, Uchi Subprovince	ERGMS Core Program	Ongoing – field work in 2023 and 2022; compilation in progress ▸ Summary *of Field Work* article (this volume, Article 10) and article published in 2021
	Petrology and geochemistry of mafic to ultramafic rocks of the Nakina area, English River Subprovince, northwestern Ontario	MSc thesis (S. Killins) Lakehead University	Ongoing – geochemical study of drill core donated to the Resident Geologist Program in Thunder Bay; sampling in fall 2020
2-D and 3-D Surficial Sediment Groundwater Mapping Initiative	Three-dimensional (3-D) mapping of Quaternary geology in central Simcoe County ▸ multi-year project to generate geologic model for groundwater assessment; Quaternary mapping and drilling	ERGMS Core Program PhD thesis (R.P.M. Mulligan) McMaster University	Ongoing – drilling in Quaternary sediments in 2015, 2016, 2017 and 2018 ▸ Preliminary Maps published in 2017; other Preliminary Maps in progress; MRD and GRS in progress; 4 external papers published; 2 external papers in progress; PhD completed in 2019 ▸ *Summary of Field Work* articles published in 2016, 2017, 2018, 2019
	Three-dimensional (3-D) mapping of Quaternary deposits in the Niagara Peninsula ▸ multi-year project to generate geologic model for groundwater assessment; Quaternary mapping and drilling	ERGMS Core Program	Ongoing – field work completed ▸ GRS in progress ▸ *Summary of Field Work* articles published in 2013, 2014, 2015 (2), 2016, 2017 ▸ MRDs published in 2017, 2020 ▸ Geophysical survey with GSC (published in 2019)
	Regional groundwater systems mapping in the County of Simcoe, southern Ontario	ERGMS Core Program	Ongoing – groundwater sampling in 2018 and 2019 ▸ *Summary of Field Work* articles published in 2018, 2019
	Various groundwater geoscience projects (groundwater data mining, chemostratigraphic framework; 3-D model of surficial geology) in southern Ontario as part of the Federal groundwater program	Geological Survey of Canada (GSC)	Ongoing – OGS input into 3-D sediment model of southern Ontario ▸ GSC Summary Report published in 2020 (Russell and Kjarsgaard 2020) summarizes projects
	Surficial and subsurface sediment mapping in the City of Ottawa, eastern Ontario	ERGMS Core Program	Ongoing ▸ *Summary of Field Work* articles published in 2019, 2022

Abbreviations: *GRS, Groundwater Resources Study; MRD, Miscellaneous Release—Data.*

Table 4.1, *continued*.

Initiative	Project	ERGMS Core Program / Project Collaborator(s)	Project Progress
Aggregate Resources Initiative	District of North Bay Aggregate Resources Inventory	ERGMS Core Program	New project – field work in 2023 ▸ *Summary of Field Work* (this volume, Article 31)
	Renfrew County Aggregate Resources Inventory	ERGMS Core Program	Ongoing – Sand and gravel and selected bedrock areas mapping have been published in the ARO online database ▸ ARIP in progress
	Elgin County Aggregate Resources Inventory	ERGMS Core Program	Ongoing – field work completed ▸ ARIP in progress
	Regional Municipality of Niagara Aggregate Resources Inventory	ERGMS Core Program	Ongoing – field work completed ▸ ARIP in progress
	Haldimand County Aggregate Resources Inventory	ERGMS Core Program	Ongoing – field work completed in 2019 ▸ *Summary of Field Work* article published in 2019
	Identification and mapping of alkali–carbonate reactive layers in the Gull River Formation, near Kingston, Ontario (pilot project)	ERGMS Core Program	Ongoing – field work completed ▸ *Summary of Field Work* article published in 2018 ▸ OFR in progress
2-D and 3-D Paleozoic Bedrock Geology Groundwater Mapping Initiative	Bedrock aquifer, karst and Early Silurian sequence stratigraphic mapping project	ERGMS Core Program	Ongoing – field work completed in 2018 ▸ GRS 13 published 2020
	Porosity and permeability analysis of deep subsurface Lockport Group ▸ project included compilation of 11 759 core analysis data sets from 150 wells and an update of more than 15 000 formational rank contacts	ERGMS Core Program and collaboration with GSC and OGSRL, NWMO and Mitacs (University of Western Ontario)	Ongoing – subsurface mapping completed 2021 ▸ GSC Open File published (Sun et al. 2023) ▸ GSC Open File in review
	Upper Ordovician stratigraphy, sedimentology and isotope geochemistry of Upper Trenton Group Cobourg Formation (Collingwood Member) and basal Blue Mountain Formation (Rouge River Member) strata, southwestern Ontario	ERGMS Core Program and collaboration with OGSRL and Mitacs (University of Western Ontario), MSc thesis (D. Atasiei), University of Western Ontario	Ongoing – in wrap-up stage ▸ *Summary of Field Work* (this volume, Article 25) and articles published in 2021, 2022
	Cambrian mapping initiative ▸ Phase 1 involves update of stratigraphy and sedimentology of basal mixed siliciclastic and carbonate strata across southern Ontario	ERGMS Core Program and collaboration with MNRF, OGSRL and University of Western Ontario researchers	Ongoing – additional data gathering in 2023 and data analysis ▸ *Summary of Field Work* (this volume, Article 26) and article published in 2022

Abbreviations: *ARIP, Aggregates Resources Inventory Paper; ARO, Aggregate Resources of Ontario; GRS, Groundwater Resources Study; GSC, Geological Survey of Canada; MNRF; Ministry of Natural Resources and Forestry; NWMO, Nuclear Waste Management Organization; OFR, Open File Report; OGSRL, Oil, Gas and Salt Resources Library.*

Table 4.1, *continued*.

Initiative	Project	ERGMS Core Program / Project Collaborator(s)	Project Progress
2-D and 3-D Paleozoic Bedrock Geology Groundwater Mapping Initiative *continued*	Update karst map for southern Ontario	ERGMS Core Program	Ongoing – mapping and sampling in 2019 ▸ *Summary of Field Work* article published in 2019
	Various groundwater geoscience projects (3-D geological model of Paleozoic bedrock) in southern Ontario as part of the Federal groundwater program	ERGMS Core Program and Geological Survey of Canada (GSC)	Ongoing – 3-D model version 2 and report published in 2021 (Carter et al. 2021) ▸ *Summary of Field Work* articles published in 2017, 2018
Paleozoic Initiative	Paleozoic geology of eastern Ontario ▸ 1:50 000 bedrock geology mapping; establish stratigraphic framework for the area	ERGMS Core Program	Ongoing – field work in 2023 ▸ *Summary of Field Work* (this volume, Article 24) and articles published in 2017, 2018, 2019, 2022
	South Niagara Peninsula bedrock geology mapping project	ERGMS Core Program	Ongoing – field work completed ▸ Preliminary Maps published in 2017 and 2018; 1 Preliminary Map in progress
	Paleozoic geology of eastern south-central Ontario ▸ 1:50 000 scale bedrock geology mapping	ERGMS Core Program	Ongoing – field work in 2023 and 2022 ▸ *Summary of Field Work* (this volume, Article 27) and article published in 2022
	3-D Leapfrog® – updating Paleozoic digital map legend and lexicon for southern Ontario ▸ Phase 1 involves updates to Cambrian and Lower to Upper Ordovician succession of eastern and south-central Ontario	ERGMS Core Program	Ongoing – desktop study: work in progress ▸ *Summary of Field Work* article published in 2021

Table 4.1, *continued*.

Initiative	Project	ERGMS Core Program / Project Collaborator(s)	Project Progress
Ambient Groundwater Geochemistry Mapping Groundwater Initiative	Ambient Groundwater Geochemistry projects, southern Ontario ▸ data interpretation	ERGMS Core Program	Ongoing ▸ update of MRD 283 (MRD 283—Revision 2) published December 2021
	Ambient Groundwater Geochemistry project, eastern Ontario (east Ottawa–Champlain Township)	ERGMS Core Program City of Ottawa	Ongoing – field work completed ▸ *Summary of Field Work* article published in 2017; data incorporated into update of MRD 283 (MRD 283—Revision 2) published December 2021
	Ambient Groundwater Geochemistry project, eastern Ontario (west Ottawa groundwater study)	ERGMS Core Program City of Ottawa	Ongoing – field work completed ▸ *Summary of Field Work* article published in 2019; data incorporated into update of MRD 283 (MRD 283—Revision 2) published December 2021
	Ambient Groundwater Geochemistry project, eastern Ontario (south Ottawa groundwater study)	ERGMS Core Program City of Ottawa	Ongoing – field work completed; analyses in progress ▸ *Summary of Field Work* article published in 2022
	Ambient Groundwater Geochemistry project, northeastern Ontario (North Bay)	ERGMS Core Program	Ongoing – North Bay area field work completed in 2018 ▸ data to be incorporated into new northern Ontario ambient groundwater geochemistry MRD ▸ *Summary of Field Work* article published in 2018
	Ambient Groundwater Geochemistry project, northeastern Ontario (Manitoulin and North Shore)	ERGMS Core Program	Ongoing – Manitoulin Island and North Shore areas completed in 2017 ▸ Data to be incorporated into new northern Ontario ambient groundwater geochemistry MRD
	Ambient Groundwater Geochemistry project, northeastern Ontario (Sudbury)	ERGMS Core Program	Ongoing – Sudbury area completed in 2016 ▸ Data to be incorporated into new northern Ontario ambient groundwater geochemistry MRD
	Ambient Groundwater Geochemistry project, southwestern Ontario (Six Nations First Nation)	ERGMS Core Program	New project – field work completed; analyses in progress ▸ *Summary of Field Work* (this volume, Article 30)
	Characterizing the controls on groundwater chemistry in north-central Ontario	ERGMS Core Program MSc thesis (K.M. Dell) Queen's University	Ongoing – field work completed; analyses in progress ▸ OFR and northern Ontario ambient groundwater geochemistry MRD in progress ▸ *Summary of Field Work* article in 2020
	Characterization of groundwater chemistry, bedrock topography, marine sediment thickness and their inter-relationships along the south bank of the Ottawa River between Ottawa and Hawkesbury, eastern Ontario	MSc thesis (S. Foubister) University of Ottawa	Completed – thesis defended in April 2023 ▸ Foubister (2023)

Abbreviations: *MRD, Miscellaneous Release—Data; OFR, Open File Report.*

Table 4.1, *continued*.

Initiative	Project	ERGMS Core Program / Project Collaborator(s)	Project Progress
Provincial-Scale Compilation Initiative	Geochronology Inventory of Ontario (GeochrON) ▸ update current geochronology database and convert it to a Microsoft® Access® database and GIS format	ERGMS Core Program	Ongoing – inaugural publication (beta version) released in 2019; update planned for 2023–2024
	Aggregate Resources of Ontario (ARO) compilation	ERGMS Core Program	Ongoing – inaugural publication released in 2015, with updates published in 2019, 2020 and 2021
	Lake Geochemistry of Ontario (LakeGeochemON) compilation	ERGMS Core Program	Inaugural publication (beta version) released in March 2020
	Improving the records in the Ontario Water Well Information System (WWIS) database	ERGMS Core Program, Ministry of Environment, Conservation and Parks, collaboration with industry	Ongoing – phase 1 nearing completion, industry consultation ongoing ▸ *Summary of Field Work* (this volume, Article 28) and article published in 2021
	Unified stratigraphic framework for the Provincial Groundwater Monitoring Network (PGMN)	ERGMS Core Program, Ministry of Environment, Conservation and Parks	New project – overview completed, multi-year study ▸ *Summary of Field Work* (this volume, Article 29)
	Determination of indicator minerals in the archived fine fraction non-magnetic heavy mineral concentrate (HMC) samples	ERGMS Core Program	New project – first year of multi-year study ▸ *Summary of Field Work* (this volume, Article 21)
	Gold Fingerprinting: Major and trace elements associated with native gold working toward an open-source database	ERGMS Core Program Metal Earth, MERC–Laurentian University, Royal Ontario Museum	Ongoing – laboratory and desktop study; data acquisition and analysis in progress ▸ *Summary of Field Work* articles published in 2020, 2021, 2022 ▸ MSc thesis by J.D. Melo-Gómez, Laurentian University defended on October 12, 2023
	Critical Minerals in Gold Deposits	ERGMS Core Program; collaboration with industry	New project – sampling began in 2023; data acquisition and analysis in progress ▸ *Summary of Field Wo*rk (this volume, Article 19)

Abbreviations: *MERC, Mineral Exploration Research Centre.*

The ERGMS program is organized into 5 objectives based on the collection, interpretation, synthesis and distribution/communication of geoscience data and information as follows:

- provide the geological framework to support Earth resource exploration (minerals, metals, groundwater, aggregates, industrial minerals and energy), land-use planning, economic and infrastructure development and provide a geoscience baseline to help assess cumulative impacts of development;
- provide the geologic context to assess energy potential in the south and Far North;
- provide the geologic context to identify and interpret natural hazards to the environment and public health and safety;
- provide the geoscience framework to identify and inventory aggregate and industrial mineral resources for land-use planning, and resource and infrastructure development; and
- provide the geoscience framework to identify and inventory groundwater resources for use, protection and planning.

CORE GEOSCIENCE PROGRAM

The ERGMS strategies and objectives are addressed through its core geoscience program, which consists of a series of initiatives built upon one or more projects (*see* Table 4.1). In addition, the ERGMS participates in several collaborative projects to complement existing staff skills and capacity and to expand the amount of geoscience data available for the province. Collaborative projects are an important means to extend government resources and to capitalize on resources and expertise available in other organizations.

Initiatives

The ERGMS initiatives are based on geographic or functional groupings and are made up of

- team initiatives (i.e., Geology of Northeastern Ontario Initiative) consisting of individual projects that are designed to meet an overall goal; and
- individual, focussed projects.

The major initiatives of the ERGMS are subdivided into 6 broad categories outlined below and in Table 4.1.

➤ Initiatives involving geoscience mapping projects and the identification of Earth resources based on geographic area or geological region (note that all of these initiatives take into account Ontario's Critical Mineral Strategy (Ontario 2022));

- Far North Land Use Planning;
- "Ring of Fire";
- Geology of Northeastern Ontario;
- Geology of Northwestern Ontario;
- Proterozoic initiative;
- Paleozoic initiative;
- Surficial Geochemistry of Northern Ontario;

- Surficial Mapping of Northern Ontario;
- Surficial Geochemistry of Southern Ontario;
- Surficial Mapping of Southern Ontario.

➢ Initiatives involving identification of overburden and bedrock hydrostratigraphic units and contained groundwater resources at a regional scale; and understanding the geochemical effects of surface and groundwater interactions with rock and surficial media:

- two- and three-dimensional surficial sediment groundwater mapping;
- two- and three-dimensional Paleozoic bedrock geology groundwater mapping;
- ambient groundwater geochemistry.

➢ Initiatives involving aggregate and industrial mineral resource compilation and inventory studies:

- documentation and inventory of potential aggregate resources;
- documentation and inventory of potential industrial mineral resources, including those that are considered Critical Minerals (e.g., fluorspar, graphite).

➢ Initiatives involving geophysical projects:

- application of geophysical techniques in support of bedrock geology mapping;
- geophysics and rock properties data compilation;
- application of geophysical techniques in support of surficial sediment mapping.

➢ Initiatives involving provincial-scale mineral resource compilation and inventory studies:

- documentation of specific types of mineralization, including Ontario's Critical Mineral resources;
- developing inventories of various tectonic settings relevant to mineral exploration, with a focus on developing inventories of Ontario's Critical Mineral resources;
- ongoing maintenance of a database of geochronology work conducted in Ontario.

➢ Initiatives that involve collaborative project agreements with the GSC:

- participating in the bedrock and surficial geology working groups as part of the Canada-3D geological map compilation project for Canada.

To successfully develop and deliver on these initiatives, the ERGMS is engaged in numerous activities to develop, maintain and manage client, stakeholder and Indigenous relationships. The ERGMS is dedicated to maintaining relationships and exchanging technical information with partners, clients, stakeholders, regional prospector and land-owner associations and Indigenous communities. The ERGMS is also part of a number of external and internal committees to ensure these relationships are respectful, strong, long lasting and mutually beneficial.

OVERVIEW OF CURRENT COLLABORATIVE INITIATIVES AND PROJECTS

The ERGMS participates in several collaborative initiatives and projects (*see* Table 4.1). These collaborations are critical to maximizing individual organization resources and delivering the highest quality geoscience to all ERGMS clients and stakeholders.

Collaborations with Mineral Exploration Research Centre (MERC), Harquail School of Earth Sciences, Laurentian University

In the fall of 2016, Laurentian University was awarded $104 million for "Metal Earth" by the Canada First Research Excellence Fund (CFREF). The Fund's objective is to help Canadian postsecondary institutions excel globally in research areas that create long-term economic advantages for Canada. The premise of the Metal Earth project is to explain why some Archean greenstone terranes are rich in mineral deposits, whereas other, similar terranes are much less endowed despite broadly similar geology at surface. The multi-year Metal Earth project is beginning to wind down, but a limited field season was conducted in the summer 2023; details on these activities can be found on the Metal Earth Web site at https://merc.laurentian.ca/research/metal-earth [last accessed October 17, 2023]. Presentations reporting on some of the results of the Metal Earth program were made in several technical sessions at the Geological Association of Canada–Mineralogical Association of Canada–Society for Geology Applied to Mineral Deposits (GAC–MAC–SGA) meeting in Sudbury in May 2023. Abstracts for the meeting can be found in Geological Association of Canada (2023).

Collaborative Initiatives with the Geological Survey of Canada

In 2021, the federal government launched phase 6 of the Targeted Geoscience Initiative (TGI-6). The Targeted Geoscience Initiative (TGI) is a Government of Canada led, collaborative geoscience research program directed toward providing next generation knowledge and methods that will facilitate more effective targeting of buried mineral deposits. Several TGI-6 projects are being led by GSC geoscientists in Ontario and some ERGMS geoscientists have shared information and knowledge to support these various projects over the last year. As part of these activities, new geochronological data from the Southern Province in the Massey area are reported by Bleeker et al. (this volume, Article 14).

The ERGMS is also collaborating with the GSC as part of the Lands and Minerals Sector (LMS) of Natural Resources Canada (NRCan) Canada–3D digital geological map of Canada project. The Canada–3D project is a national collaboration involving the provincial and territorial geological surveys and the Geological Survey of Canada, operating under the auspices of the National Geological Surveys Committee (NGSC). The goal of this project is to develop the next generation of products to enhance the representation of Canada's subsurface geology.

Other Collaborative Projects

As mentioned previously, the ERGMS is involved with numerous governmental and academic partnerships to maximize geoscience resources and to augment the depth of geoscience projects in Ontario. The ERGMS also supported and/or participated in several collaborative projects with academic partners in 2023 (*see* Table 4.1).

Since 2013, the OGS has partnered with local municipalities in eastern Ontario to support the development of an Aquifer Capability Screening Tool (ACST). This support continued in 2023–2024 with the City of Ottawa.

The OGS provided factual reviews for 2 geological reports on behalf of the Nuclear Waste Management Organization (NWMO): the first report related to activities at the Ignace site in northwestern Ontario, and the second report related to the South Bruce site in southwestern Ontario.

The OGS has been involved in discussions with the geological surveys of Saskatchewan and Manitoba regarding a proposed lithodemic nomenclature proposal, especially as it applies to Precambrian rocks. It is anticipated that a draft document will be published in 2024.

INTERJURISDICTIONAL AND COMMITTEE REPRESENTATION

Staff of the ERGMS represented the Ministry of Mines, the OGS and other geoscience organizations on several interjurisdictional committees, internal committees and associations during the 2023–2024 fiscal year, which are summarized as follows:

- North American Commission on Stratigraphic Nomenclature (representing the Geological Association of Canada, and as a commissioner-at-large)
- International Subcommission on Stratigraphic Classification (ISSC)
- Paleontology Division of the Geological Association of Canada
- Great Lakes Geologic Mapping Coalition
- CAMIRO Geochemical Expert Committee
- Conservation Authorities Geosciences Committee
- Far North Information and Knowledge Management Working Group
- Growing the Green Belt to Protect Water Interministerial Team
- OPS Land Information Ontario (LIO) Imagery Group
- OPS Elevation Coordination & Consultation Committee (EC3)
- NDM Information Technology–Information Management (IT/IM) Strategy Committee
- Geoscience Laboratories (Geo Labs)–ERGMS Working Group
- Willet Green Miller Centre (WGMC) Joint Health and Safety Committee
- GIS in the Ontario Public Service (OPS) License Management Task Force
- Southern Ontario Stream Sediment Geochemistry Project Steering Committee
- Canadian Working Group on Regional Groundwater Flow Systems of the International Association of Hydrogeologists
- International Joint Commission (IJC) Great Lakes Science Advisory Board
- thesis committees and adjunct professorships at universities (Laurentian University, Carleton University, Ohio State University, University of Western Ontario, University of Toronto, Chinese Academy of Sciences)
- Geological Association of Canada–Mineralogical Association of Canada–Society for Geology Applied to Mineral Deposits, Annual Meeting, held in Sudbury, Ontario, May 25–27, 2023

(editing and publication of field trip guidebooks for the meeting; staff involvement on the organizing committee)

- Geological Association of Canada–Mineralogical Association of Canada–Society for Geology Applied to Mineral Deposits, Annual Meeting, held in Sudbury, Ontario, May 25–27, 2023 (staff participation)
- Prospectors and Developers Association of Canada (PDAC) Health and Safety Committee (representing the Committee of Provincial and Territorial Geological Surveys)
- Prospectors and Developers Association of Canada (PDAC) Student–Industry Mineral Exploration Workshop (S-IMEW)

STAFFING CHANGES IN THE SECTION

Two staff members, Victoria Lee and Brandon Portelance, have left the ERGMS over the past year. Several current and new staff have accepted positions in ERGMS, and include Lise Robichaud, Senior Manager, ERGMS; Jeremy Creppin, Geological Assistant; Nicholas Szumylo, Geological Assistant; Christopher Beckett-Brown, Surficial Geochemist; and Laura Colgrove, Hydrogeologist.

LIST OF PUBLICATIONS[2]

Amyotte, E.G., Kurucz, S.V., Paju, G.F., Jonsson, J.R.B. and Kurcinka, C.E. 2022. Investigation of biogeochemical exploration techniques to aid in the exploration for lithium-cesium-tantalum pegmatite dikes: Project description and preliminary observations; *in* Summary of Field Work and Other Activities, 2022, Ontario Geological Survey, Open File Report 6390, p.31-1 to 31-7.

Atasiei, D., Tsujita, C.J., Brunton, F.R., Jin, J. and Yeung, K.H. 2022. Stratigraphy and sedimentology of Upper Ordovician strata, with emphasis on the Collingwood and Rouge River members, southern Ontario and Manitoulin Island; *in* Summary of Field Work and Other Activities, 2022, Ontario Geological Survey, Open File Report 6390, p.20-1 to 20-6.

Béland Otis, C. 2022. Paleozoic geology of eastern Ontario: Russell–Thurso area; *in* Summary of Field Work and Other Activities, 2022, Ontario Geological Survey, Open File Report 6390, p.23-1 to 23-8.

Beneteau, S.B. 2022. Ontario Geological Survey: Update of Strategic Perspective for 2022–2023; *in* Summary of Field Work and Other Activities, 2022, Ontario Geological Survey, Open File Report 6390, p.1-1 to 1-12.

Bennett, D.J. 2022. Catching it by the tailings: An introduction to the Ontario Geological Survey critical minerals mine waste sampling project; *in* Summary of Field Work and Other Activities, 2022, Ontario Geological Survey, Open File Report 6390, p.32-1 to 32-6.

Biswas, S. and Evangelatos, J. 2022. Summary of geophysical projects and activities; *in* Summary of Field Work and Other Activities, 2022, Ontario Geological Survey, Open File Report 6390, p.16-1 to 16-6.

Bocking, C.N., Hamilton, S.M. and Dell, K.M. 2023. Ambient groundwater geochemistry field methods and procedures; Ontario Geological Survey, Groundwater Resources Study 21.

[2] *This list provides references for publications produced by ERGMS, during the period from December 2022 to December 2023, inclusive, comprising 4 Open File Reports, 2 Preliminary Maps, 3 Miscellaneous Releases—Data (MRD), 1 Groundwater Resources Study and 1 Ontario Geoscience Video.*

Brunton, F.R., Hahn, K.E., Béland Otis, C. and Julig, P.J. 2023. Paleozoic geology of Manitoulin Island and adjacent North Channel Islands, northeastern Ontario: A geological guidebook; Geological Association of Canada–Mineralogical Association of Canada–Society for Geology Applied to Mineral Deposits, Joint Annual Meeting, Sudbury, Ontario, May 25–27, 2023, Field Trip FT04, Ontario Geological Survey, Open File Report 6388, 62p.

Burnham, O.M. 2022. Osmium analysis at the Geoscience Laboratories by nickel sulphide fire assay with inductively coupled mass spectrometric finish; *in* Summary of Field Work and Other Activities, 2022, Ontario Geological Survey, Open File Report 6390, p.26-1 to 26-9.

——— 2022. Expansion of the capabilities of the Geoscience Laboratories methods for the analysis of trace elements important to Ontario's Critical Minerals Strategy; *in* Summary of Field Work and Other Activities, 2022, Ontario Geological Survey, Open File Report 6390, p.27-1 to 27-11.

Burt, A.K., Ford, D., Holysh, S., Kalmo, K.J.J. and Russell, H.A.J. 2023. Regional-scale groundwater geoscience in southern Ontario: The 2023 Ontario Geological Survey, Geological Survey of Canada, and Conservation Ontario Geoscientists Open House; Ontario Geological Survey, Open File Report 6387, 61p.

Burt, A.K. and Hagedorn, G.W. 2022. From mighty moraines to dramatic drumlins: Introducing the Guelph three-dimensional sediment mapping project; *in* Summary of Field Work and Other Activities, 2022, Ontario Geological Survey, Open File Report 6390, p.24-1 to 24-10.

Cundari, R.M. 2022. Identification of fertile parent granitoid units in the Superior Province of Ontario: Project description; *in* Summary of Field Work and Other Activities, 2022, Ontario Geological Survey, Open File Report 6390, p.30-1 to 30-5.

Di Iorio, T., Foubister, S. and Bocking, C.N. 2022. South Ottawa Groundwater Study, Eastern Ontario; *in* Summary of Field Work and Other Activities, 2022, Ontario Geological Survey, Open File Report 6390, p.25-1 to 25-9.

Duguet, M. 2023a. Precambrian geology of the Renfrew area, Grenville Province, southern Ontario; Ontario Geological Survey, Preliminary Map P.3850, scale 1:50 000.

——— 2023b. Geological, geochemical and geophysical data related to the Renfrew area, Grenville Province, southern Ontario; Ontario Geological Survey, Miscellaneous Release—Data 398.

Easton, R.M. 2022. Geology of the Grenville Front tectonic zone near Sudbury, northeastern Ontario; *in* Summary of Field Work and Other Activities, 2022, Ontario Geological Survey, Open File Report 6390, p.12-1 to 12-15.

——— 2023. Critical Mineral potential in cataclastic rocks of the Grenville Front tectonic zone, southeast of Sudbury, Ontario; *in* Report of Activities 2022, Resident Geologist Program, Kirkland Lake Regional Resident Geologist Report: Sudbury District, Open File Report 6403, p 102-109.

Ferguson, S.A. 2022. Precambrian geology of the North Caribou–Wachusk lakes area, North Caribou greenstone belt, northwestern Ontario; Ontario Geological Survey, Preliminary Map P.3463, scale 1:50 000.

Gao, C., Crabtree, D.C., Clarke, S.A. and Yeung, K.H. 2023. Indicator mineral and bulk geochemistry data of the till and other surficial samples collected in the Pickle Lake–Cat Lake area, northern Ontario; Ontario Geological Survey, Miscellaneous Release—Data 388.

Gao, C. and Yeung, K.H. 2023. Indicator mineral and geochemistry data of till and other surficial samples in the Sandy Lake area, northwestern Ontario; Ontario Geological Survey, Miscellaneous Release—Data 400.

Gemmell, T.P. and Buyers, A. 2022. Preliminary geology and mineral potential of Dore and Swayze townships and part of Garnet Township, Swayze area, Abitibi greenstone belt; *in* Summary of Field Work and Other Activities, 2022, Ontario Geological Survey, Open File Report 6390, p.6-1 to 6-11.

Gibson, H.L., Gemmell, T.P., Jørgensen, T.R.C., Hastie, E.C.G., Schofield, M.D., Haugaard, R., Smith, A.R., McKinley, B., Rees, M.I., Lafrance, B., Sherlock, R.L. and Chapon, B. 2023. Exploring differential metal endowment: A comparison of the western (Swayze) and eastern (Rouyn-Noranda) Abitibi greenstone belt: A geological guidebook; Geological Association of Canada–Mineralogical Association of Canada–Society for Geology Applied to Mineral Deposits, Joint Annual Meeting, Sudbury, Ontario, May 25–27, 2023, Field Trip FT07, Ontario Geological Survey, Open File Report 6395, 100p.

Gordon, C.A. 2022. Preliminary geology of Hyman Township, Southern and Superior provinces, Sudbury District, northeastern Ontario; *in* Summary of Field Work and Other Activities, 2022, Ontario Geological Survey, Open File Report 6390, p.13-1 to 13-10.

Gordon, C.A., Péloquin, A.S., and Gervais, P.A. 2023. Ontario Geological Survey Virtual Field Trip: Geology of the Sudbury Impact Structure; Ontario Geological Survey, Ontario Geoscience Video 1.

Hahn, K.E. 2022. Paleozoic geology of the Kingston area, eastern Ontario; *in* Summary of Field Work and Other Activities, 2022, Ontario Geological Survey, Open File Report 6390, p.22-1 to 22-10.

Hargreaves, J.C. 2022. Summary of quality-control data for the Geoscience Laboratories methods IMC-100, IMO-100 and IMP-101; *in* Summary of Field Work and Other Activities, 2022, Ontario Geological Survey, Open File Report 6390, p.28-1 to 28-12.

Hastie, E.C.G., MacDonald, P.J. and Duguet, M. 2022. Preliminary geology of Patton and Thompson townships, Iron Bridge area, Southern Province, northeastern Ontario; *in* Summary of Field Work and Other Activities, 2022, Ontario Geological Survey, Open File Report 6390, p.14-1 to 14-7.

Hechler, J.H., Easton, R.M., Préfontaine, S., Duguet, M., Robichaud, L. and Cormier, R. 2022. Earth Resources and Geoscience Mapping Section: 2022–2023 Program and Projects Overview; *in* Summary of Field Work and Other Activities, 2022, Ontario Geological Survey, Open File Report 6390, p.4-1 to 4-18.

Kalmo, K.J.J. 2022. Ontario Geological Survey: Measuring success; *in* Summary of Field Work and Other Activities, 2022, Ontario Geological Survey, Open File Report 6390, p.2-1 to 2-8.

Keating, G.L. 2022. Revision of the calibration for trace element analysis of geological samples by wavelength dispersive X-Ray fluorescence at the Geoscience Laboratories; *in* Summary of Field Work and Other Activities, 2022, Ontario Geological Survey, Open File Report 6390, p.29-1 to 29-7.

Levesque, M.D. and Bennett, D.J. 2022. Activities of the Indigenous Geoscience Liaisons in 2021–2022; *in* Summary of Field Work and Other Activities, 2022, Ontario Geological Survey, Open File Report 6390, p.3-1 to 3-6.

Ma, C., Vice, L.E.D., Nagy, C., Adam, Z.V., Shirriff, D., Lafrance, B. and Robichaud, L. 2023. Orogenic and intrusion-related gold deposits of the Michipicoten and Mishibishu greenstone belts in the Wawa region, with an emphasis on their structural timing and setting: A geological guidebook; Geological Association of Canada–Mineralogical Association of Canada–Society for Geology Applied to Mineral Deposits, Joint Annual Meeting, Sudbury, Ontario, May 25–27, 2023, Field Trip FT10, Ontario Geological Survey, Open File Report 6398, 57p.

MacDonald, P.J. and Kamo, S.L. 2022. New geochronological data from the Hollinger Mine, Timmins area, Abitibi greenstone belt, northeastern Ontario; *in* Summary of Field Work and Other Activities, 2022, Ontario Geological Survey, Open File Report 6390, p.5-1 to 5-11.

Marich, A.S. 2022. Quaternary geological mapping of the Lake Nipissing Basin, Highway 17 corridor, northeastern Ontario; *in* Summary of Field Work and Other Activities, 2022, Ontario Geological Survey, Open File Report 6390, p.17-1 to 17-9.

Meade, S.R. 2022. Precambrian geology of the Straw Lake–Esox Lake area, western Wabigoon Subprovince, northwestern Ontario; *in* Summary of Field Work and Other Activities, 2022, Ontario Geological Survey, Open File Report 6390, p.10-1 to 10-6.

Melo-Gómez, J.D., Hastie, E.C.G., Gibson, H.L., Tait, K.T. and Petrus, J.A. 2022. Trace element content of gold across Ontario: An update on the Gold Fingerprinting Project; *in* Summary of Field Work and Other Activities, 2022, Ontario Geological Survey, Open File Report 6390, p.15-1 to 15-11.

Metsaranta, R.T. 2022. Highlights of bedrock geology mapping in the Quetico Subprovince, north of Thunder Bay, northwestern Ontario; *in* Summary of Field Work and Other Activities, 2022, Ontario Geological Survey, Open File Report 6390, p.9-1 to 9-9.

Metsaranta, R.T. and Kurcinka, C.E. 2022. Reconnaissance bedrock geology mapping of the Animikie Basin and spatially associated Midcontinent Rift–related igneous rocks, Thunder Bay area, northwestern Ontario: A project introduction; *in* Summary of Field Work and Other Activities, 2022, Ontario Geological Survey, Open File Report 6390, p.11-1 to 11-23.

Mulligan, R.P.M. 2022. Sediment mapping in the City of Ottawa, southeastern Ontario; *in* Summary of Field Work and Other Activities, 2022, Ontario Geological Survey, Open File Report 6390, p.18-1 to 18-7.

Mulligan, R.P.M., Burt, A.K., Hagedorn, G.W. and Marich, A.S. 2023. Ice on the rocks: The Quaternary geology of Sudbury and surrounding region: A geological guidebook; Geological Association of Canada–Mineralogical Association of Canada–Society for Geology Applied to Mineral Deposits, Joint Annual Meeting, Sudbury, Ontario, May 25–27, 2023, Field Trip FT05, Ontario Geological Survey, Open File Report 6389, 49p.

Ontario Geological Survey 2022. Summary of Field Work and Other Activities, 2022; Ontario Geological Survey, Open File Report 6390, 308p.

Paterson, R.H., Brunton, F.R., Jin, J., Phillips, A.R. and Yeung, K.H. 2022. Subsurface stratigraphy of Early Silurian Medina Group mixed siliciclastic–carbonate strata, southwestern Ontario: Final update; *in* Summary of Field Work and Other Activities, 2022, Ontario Geological Survey, Open File Report 6390, p.19-1 to 19-9.

Peters, D., Baurier Aymat, S., Péloquin, A.S., Gordon, C.A. and Lesher, C.M. 2023. Geological traverse of the Sudbury impact structure and evolution of the impact melt: A geological guidebook; Geological Association of Canada–Mineralogical Association of Canada–Society for Geology Applied to Mineral Deposits, Joint Annual Meeting, Sudbury, Ontario, May 25–27, 2023, Field Trip FT03, Ontario Geological Survey, Open File Report 6393, 67p.

Phillips, A.R., Brunton, F.R. and Yeung, K.H. 2022. Revisiting the Cambrian stratigraphy of southwestern Ontario; *in* Summary of Field Work and Other Activities, 2022, Ontario Geological Survey, Open File Report 6390, p.21-1 to 21-7.

van Hees, E.H., Clarke, S.A., Crabtree, D.C., Péloquin, A.S. and Azadbakht, Z. 2022. Geology, geochemistry and mineralogy of the Enid Creek cobalt-copper-nickel-palladium-platinum prospect, Loveland township, northwest of Timmins, Ontario; *in* Summary of Field Work and Other Activities, 2022, Ontario Geological Survey, Open File Report 6390, p.33-1 to 33-7.

Vice, L.E.D. 2022. Preliminary geology of Meath Township, northeastern Michipicoten greenstone belt, northeastern Ontario; *in* Summary of Field Work and Other Activities, 2022, Ontario Geological Survey, Open File Report 6390, p.7-1 to 7-10.

Vice, L.E.D., Perrouty, S. and Robichaud, L. 2022. Introduction to a geochronological and structural study of supracrustal assemblages in the northeastern Michipicoten greenstone belt; *in* Summary of Field Work and Other Activities, 2022, Ontario Geological Survey, Open File Report 6390, p.8-1 to 8-8.

REFERENCES

Carter, T.R., Logan, C.E., Clark, J.K., Russell, H.A.J., Brunton, F.R., Cachunjua, A., D'Arienzo, M., Freckelton, C., Rzyszczak, H., Sun, S. and Yeung, K.H. 2021. A three-dimensional geological model of the Paleozoic bedrock of southern Ontario (version 2); Geological Survey of Canada, Open File 8795, 103p.

Easton, R.M. 2022. Field Trip 2 – Geology of the Grenville Front and the Grenville Front tectonic zone in the Sudbury area; *in* 68th Institute on Lake Superior Geology, Sudbury, Ontario, Proceedings, v.68, part 2, p.102-146.

Foubister, S. 2023. Characterization of bedrock topography, overburden thickness and groundwater geochemistry in eastern Ontario; unpublished MSc thesis, University of Ottawa; Ottawa, Ontario, 59p.

Geological Association of Canada 2023. Abstracts; Geological Association of Canada–Mineralogical Association of Canada–Society for Geology Applied to Mineral Deposits, Annual Meeting, Sudbury, Ontario, May 25–27, Abstracts, v.46, Geoscience Canada, v.50, p.105-237. doi.org/10.12789/geocanj.2023.50.200

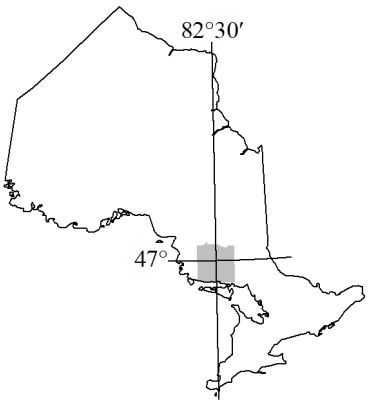
Ontario 2022. Ontario's Critical Mineral Strategy: Unlocking the potential to drive economic recovery and prosperity; Ministry of Northern Development, Mines, Natural Resources and Forestry, 53p., www.ontario.ca/page/ontarios-critical-minerals-strategy-2022-2027-unlocking-potential-drive-economic-recovery-prosperity, also available to download: select "Download English PDF". [accessed October 16, 2023]

Ontario Geological Survey 2011. 1:250 000 scale bedrock geology of Ontario; Ontario Geological Survey, Miscellaneous Release—Data 126–Revision 1.

Russell, H.A.J. and Kjarsgaard, B.A., editors. 2020. Southern Ontario groundwater project 2014–2019: Summary report; Geological Survey of Canada, Open File 8536, 245p.

Sun, S., Brunton, F.R., Carter, T.R., Clarke, J.R., Russell, H.A.J., Yeung, K.[H.], Cachunjua, A. and Jin, J. 2023. Porosity and permeability variations in the Silurian Lockport Group and A-1 carbonate unit, southwestern Ontario; Geological Survey of Canada, Open File 8977, 46p.

5. Project NE-19-004. Preliminary Uranium-Lead Ages from the Ramsey–Algoma Granitoid Complex and Surrounding Area, Northeastern Ontario



S. Préfontaine[1] and S.L. Kamo[2]

[1]Earth Resources and Geoscience Mapping Section, Ontario Geological Survey, Sudbury, Ontario P3E 6B5
[2]Jack Satterly Geochronology Laboratory, Department of Earth Sciences, University of Toronto, Toronto, Ontario M5S 3B1

INTRODUCTION

In 2018, the Ontario Geological Survey (OGS) identified the area from Sudbury to Sault Ste. Marie, south of the Swayze area of the Abitibi greenstone belt, as a major knowledge gap. In an effort to improve knowledge of this area, a 1:100 000 scale compilation and mapping project was undertaken (Préfontaine and Rainsford 2019; Préfontaine 2020). As part of this project, 16 samples for geochronology were collected in 2019 to better constrain the timing of emplacement of the main units in the study area (Figure 5.1; Table 5.1). Most of these geochronology samples are from Archean granitoids and supracrustal rocks within the Ramsey–Algoma granitoid complex (Préfontaine 2020); 1 sample from a Proterozoic unit was also collected. The use of the OGS geophysical survey data flown in 2018 and published in 2019 (Ontario Geological Survey 2019a, 2019b), coupled with historical and reconnaissance mapping, as well as the OGS Geochronology database ("GeochrON": Ontario Geological Survey 2019c) help to refine the boundaries between the different phases of granitoids within the Ramsey–Algoma granitoid complex and were useful tools in assessing where gaps in the geochronological record exist to better determine the location of the 16 sample sites reported herein. It should be noted that for the purpose of brevity, this article only provides a summary of the age data obtained as part of this study. Publication of the full geochronology data set, including data tables and concordia diagrams, will be presented in a future publication.

METHODS

Rock samples were crushed and milled using standard methods (jaw crusher and Bico disk mill, respectively). Heavy mineral concentrates were achieved by reprocessing on the Wilfley table until a significantly reduced sample size of approximately 5 to 10 g (from rock samples weighing ~8–12 kg) was produced. This was followed by magnetic separation and methylene iodide methods.

Uranium–Lead Chemical Abrasion Isotope Dilution Thermal Ionization Mass Spectrometry Analytical Method

Uranium-lead analysis for samples was done by isotope dilution thermal ionization mass spectrometry methods (ID-TIMS). Prior to analysis, zircon crystals were thermally annealed and chemically etched (chemical abrasion (CA)), which removes alteration zones where lead loss has occurred and typically improves concordance (Mattinson 2005). These alteration zones correlate with

Summary of Field Work and Other Activities, 2023,
Ontario Geological Survey, Open File Report 6405, p.5-1 to 5-11.

© King's Printer for Ontario, 2023

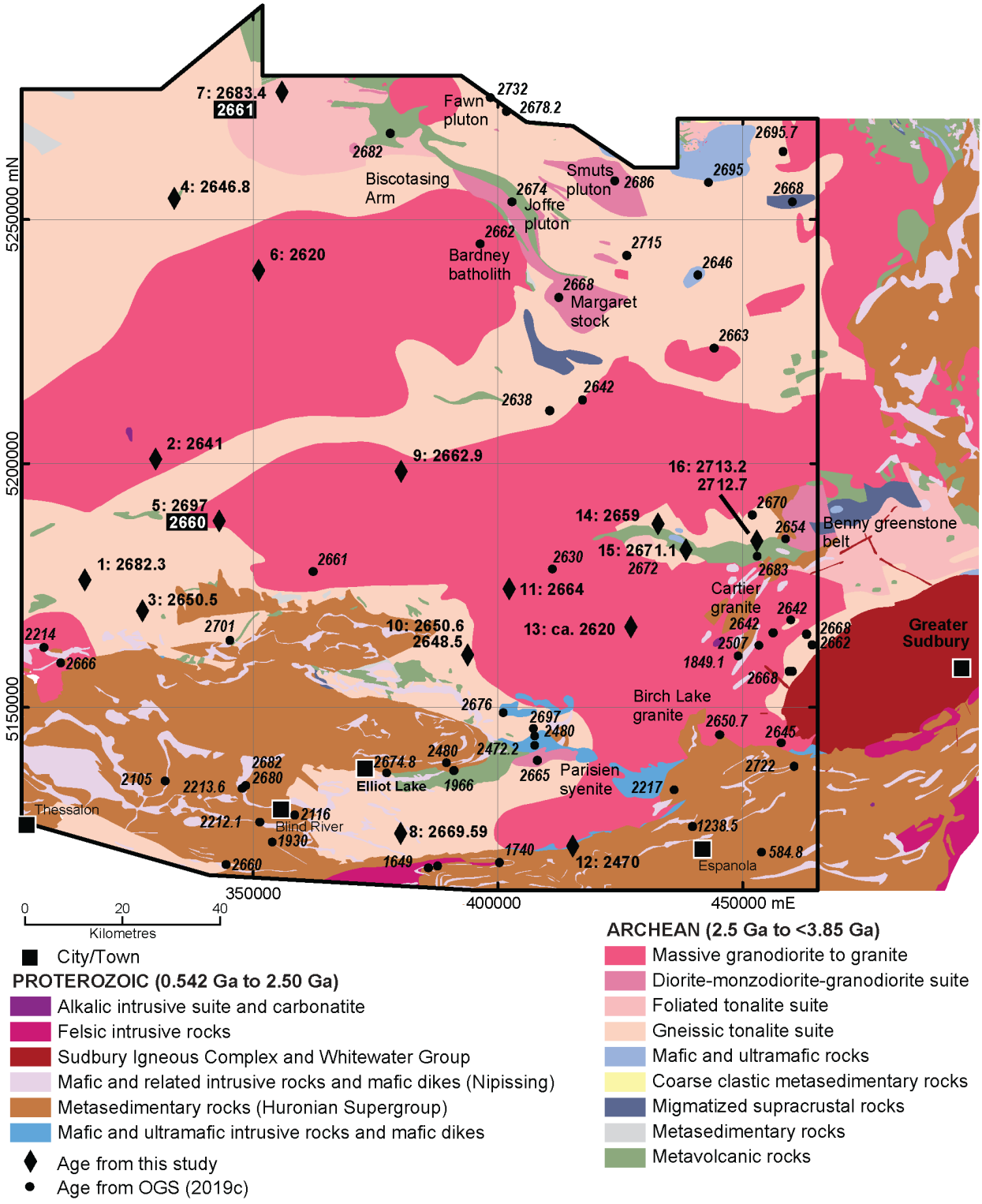


Figure 5.1. Simplified geological map of the Ramsey–Algoma granitoid complex and surrounding area, with U/Pb ages on zircon, baddeleyite or monazite (shown in black text) from intrusive and supracrustal rocks from this study and *from* Ontario Geological Survey (2019c; shown in italics). Numbers 1 to 16 correspond to ages listed in Table 5.1. Ages from this study from titanite (shown in white text in black boxes) are interpreted as thermal overprinting. Detrital zircon ages are not shown on this figure. Errors on ages are not shown for clarity. Location information provided as Universal Transverse Mercator (UTM) co-ordinates using North American Datum 1983 (NAD83) in Zone 17. Geology *modified from* Ontario Geological Survey (2011).

Table 5.1. New geochronology ages, listed from oldest to youngest, from the Ramsey–Algoma granitoid complex and surrounding area. Numbers 1 to 16 correspond to locations on Figure 5.1.

No. on Figure 5.1	Sample No.	Age (Ma)	Age Interpretation	Mineral	Method	No. of Analyses	MSWD	Note(s)	Rock Type	Reference	Easting[a]	Northing[a]
16	19SP263A	2713.2±1.2	Time of emplacement (cautious)	Zircon	CA-ID-TIMS	3	1.8		Tonalite	Kamo (2020)	452703	5184300
		2712.7±1.0	Time of emplacement	Titanite	CA-ID-TIMS	2	1.7		Tonalite	Kamo (2020)	452703	5184300
5	19SP220A	2697±4	Age of emplacement	Zircon	LA-ICP–MS	47	2.2		Granodiorite gneiss	Sutcliffe (2021)	342686	5188412
		2714.0±3.6	Time of emplacement (tentative)	Zircon	CA-ID-TIMS	4	0.12	Upper intercept; a less probable interpretation is a minimum age defined by the $^{207}Pb/^{206}Pb$ average of z1-2 at **2695±3 Ma**	Granodiorite gneiss	Kamo (2020)	342686	5188412
		ca. 1585		Zircon	CA-ID-TIMS	4		Lower intercept	Granodiorite gneiss	Kamo (2020)	342686	5188412
		2675.4±1.1	Age of emplacement	Zircon	CA-ID-TIMS	2	3.3	Weighted mean	Granodiorite	Kamo (2020)	342686	5188412
		2660±9	Thermal overprinting	Titanite	CA-ID-TIMS	2	0.27		Granodiorite gneiss	Kamo (2020)	342686	5188412
7	19SP252A	2683.4±1.1	Time of emplacement	Zircon	CA-ID-TIMS	3	0.57	Weighted mean	Granodiorite	Kamo (2020)	355535	5276189
		2661±3	Thermal overprinting	Titanite	CA-ID-TIMS	3	2.1	Mean	Granodiorite	Kamo (2020)	355535	5276189
1	19SP246A	2682.3±1.3	Time of emplacement	Zircon	CA-ID-TIMS	4	2.1	Weighted mean	Granodiorite	Kamo (2020)	315133	5176361
15	19SP243A	2672.0±1.3	Maximum age of deposition	Zircon	CA-ID-TIMS	3	0.69	Weighted mean	Intermediate tuff	Kamo (2020)	438248	5182466
		2671.1±2.5	Maximum age of deposition	Zircon	CA-ID-TIMS	youngest	n/a	Inheritance: 2695.3±1.6 Ma; 2682.4±1.2 Ma	Intermediate tuff	Kamo (2020)	438248	5182466
8	19SP264A	2669.59±0.95	Time of emplacement	Zircon	CA-ID-TIMS	3	1.1	Weighted mean	Granodiorite	Kamo (2020)	379803	5124427
11	19SP239A	2664±10	Maximum age of emplacement	Zircon	LA-ICP–MS	6	0.34		Granite	Sutcliffe (2020)	402089	5174505
9	19SP221A	2662.9±1.1	Time of emplacement	Zircon	CA-ID-TIMS	3	0.5	Weighted mean age	Granite	Kamo (2020)	379948	5198588

No. on Figure 5.1	Sample No.	Age (Ma)	Age Interpretation	Mineral	Method	No. of Analyses	MSWD	Note(s)	Rock Type	Reference	Easting[a]	Northing[a]
14	19SP240A	2659±4	Time of emplacement	Zircon	LA-ICP–MS	37	0.9	Inheritance: 2726–2767	Granite	Sutcliffe (2020)	432546	5187761
		2644–2648	Maximum age (cautious)	Zircon	CA-ID-TIMS			Youngest at 2644-2648 Ma (1.8% discordant). Age range based on assumption of Pb loss at 0 Ma to 500 Ma, respectively; inheritance: 2671 Ma (2.7% discordant), 2660 Ma (1.4% discordant)	Granite	Kamo (2020)	432546	5187761
3	19SP245A	2651.0±1.1	Time of emplacement	Zircon	CA-ID-TIMS	2	0.005		Granite	Kamo (2020)	326959	5169976
		2650.5±1.2	Time of emplacement	Zircon	CA-ID-TIMS	2	1.09		Granite	Kamo (2020)	326959	5169976
10	19SP237A	2650.6±1.6	Minimum age of emplacement	Zircon	CA-ID-TIMS	youngest	n/a	Inheritance: 2666±2 Ma; 2660±1.6 Ma?	Granite	Kamo (2020)	393577	5160960
		2648.5±1.3	Minimum age of emplacement	Monazite	ID-TIMS	youngest	n/a		Granite	Kamo (2020)	393577	5160960
4	19SP250A	2646.8±1.0	Maximum age	Monazite	ID-TIMS	3	1.5		Granite	Kamo (2020)	333450	5254406
		2646.6±1.2	Maximum age (cautious)	Zircon	CA-ID-TIMS	2	0.5	Inheritance: 2686±3 Ma; 2667±2 Ma	Granite	Kamo (2020)	333450	5254406
2	19SP247A	2641±5	Maximum age of emplacement	Zircon	LA-ICP–MS	14	0.87	Inheritance: 2664–2723 Ma	Feldspar porphyritic granite	Sutcliffe (2020)	329626	5201075
6	19SP251A	2620±4	Maximum age of emplacement	Zircon	LA-ICP–MS	51	1.3	Inheritance: 2658–2723 Ma	Granite	Sutcliffe (2020)	350716	5239715
13	19SP049A	*ca*. 2620 (2580–2646)	Maximum age of emplacement	Zircon	LA-ICP–MS	12	n/a	Precise age could not be determined on sample because of its high degree of alteration	Granite	Sutcliffe (2020)	426968	5166664
12	19SP201A	2470±10	Maximum age of emplacement	Zircon	LA-ICP–MS	11	0.44	Inheritance: 2676–2843 Ma	Gabbro	Sutcliffe (2020)	415049	5121809

[a]*Locations provided as UTM co-ordinates in NAD83, Zone 17.*

Note: *text in* **bold** *indicates age attributed to the intrusion.*

Abbreviations*: CA-ID-TIMS, chemical abrasion, isotope dilution, thermal ionization mass spectrometry; ID-TIMS, isotope dilution, thermal ionization mass spectrometry; LA-ICP–MS, laser ablation inductively coupled plasma mass spectrometry; MSWD, mean square weighted deviation; n/a, not available; No., number.*

high uranium zones that have suffered radiation damage prior to alteration. The pretreatment involved placing zircon grains in a muffle furnace at ~900°C for ~48 hours to repair radiation damage and anneal the crystal lattice, followed by a modified single-step partial dissolution procedure in ~0.10 mL of ~50% HF and 0.020 mL 7N HNO_3 in Teflon™ dissolution vessels at 200°C for 2 to 12 hours. Zircon, baddeleyite and rutile were rinsed in 7N HNO_3 at room temperature prior to dissolution. A $^{205}Pb/^{235}U$ spike was added to the Teflon™ dissolution capsules during sample loading.

The minerals were dissolved using ~0.10 mL of concentrated HF acid and ~0.02 mL of 7N HNO_3 at 200°C for 3 to 5 days. Titanite and monazite were dissolved in Savillex capsules on a hot plate at ~80°C in a mixture of HF and HNO_3 (titanite) and 6N HCl (monazite) for 3 to 5 days. All samples were dried to a precipitate and redissolved in ~0.15 mL of 3N HCl overnight (Krogh 1973). Uranium and lead were isolated from the zircon using miniaturized ~50 µL anion exchange columns using HCl for zircon, baddeleyite and monazite and using HBr for titanite. Once isolated, uranium and lead were deposited onto outgassed rhenium filaments with silica gel (Gerstenberger and Haase 1997) and analyzed with a VG354 mass spectrometer using either a Daly detector in pulse counting mode, or multiple Faraday collectors in static mode. Corrections to the $^{206}Pb/^{238}U$ ages for initial ^{230}Th disequilibrium in the zircon have been made assuming a Th/U ratio in the magma of 4.2. All common lead was assigned to procedural lead blank for zircon, baddeleyite and monazite. For titanite, initial lead was corrected using the model of Stacey and Kramers (1975). Deadtime of the measuring system for lead and uranium was 16 and 14 ns, respectively. The mass discrimination correction for the Daly detector is constant at 0.05% per atomic mass unit. Amplifier gains and Daly characteristics were monitored using the SRM 982 lead standard. Thermal mass discrimination corrections are 0.10% per atomic mass unit for both lead and uranium. Decay constants are those of Jaffey et al. (1971). All age errors are given at the 95% confidence interval. VG Sector software was used for data acquisition. In-house data reduction software in Visual Basic by D.W. Davis was used. Plotting and age calculations were done using Isoplot 3.00 (Ludwig 2003).

Uranium–Lead Laser Ablation Inductively Coupled Plasma Mass Spectrometry Analytical Method

Following crushing, pulverization and separation, the final grain selection for geochronology was completed by hand picking under a microscope, choosing the freshest, least cracked grains. Grains from all samples were mounted in epoxy and polished. Grains were imaged with backscattered electrons (BSE) using a JEOL JSM6610-Lv scanning electron microscope in order to detect phases of growth that may have different ages.

Imaged grains were partially ablated using a 193 nm New Wave Research Inc. excimer laser and an Agilent Technologies Inc. 7900 inductively coupled plasma mass spectrometer (ICP–MS). The laser was generally operated at 5 Hz and approximately 5 J/cm^2 fluence with a typical beam diameter of 20, 25 or 40 µm, depending on the sample. Data were collected on ^{88}Sr (10 ms), ^{206}Pb (30 ms), ^{207}Pb (70 ms), ^{232}Th (10 ms) and ^{238}U (20 ms). Prior to analyses, spots were pre-ablated with a larger beam diameter for 1 s (5 pulses) to clean the surface. Following a 10 s period of baseline accumulation, the laser sampling beam was turned on and data were collected for 25 s followed by a washout period. Approximately 150 measurement cycles per sample were produced and ablation pits were approximately 15 µm deep.

Data were edited and reduced using custom VBA software (UtilLAZ program) written by D.W. Davis. The $^{206}Pb/^{238}U$ values showed increasing fractionation throughout the zircon analyses, which was caused by loss of refractory uranium with increasing penetration depth, whereas the $^{207}Pb/^{206}Pb$ profile was usually flat. No corrections were made for common lead, because the ^{204}Pb peak was too small to be measured precisely. Common lead (^{204}Pb) is usually present in insignificant amounts in unaltered Precambrian zircon and monazite. If present, then common lead would have the effect of pushing data to

the right, away from the concordia curve along a shallow mixing line with slope determined by the isotopic composition of the common lead contaminant. Isotope ^{88}Sr was monitored from zircon in order to detect the intersection of the beam with zones of alteration or inclusions; data showing high strontium or irregular time resolved profiles were either averaged over restricted strontium-free time windows or rejected.

The Th/U value of zircon can be a useful petrogenetic indicator and was also measured, although these measurements are only an estimate because the Th/U ratio in the standard was not constant. Low Th/U (<0.1) is characteristic of metamorphic and hydrothermal zircon, whereas most zircon crystallized from felsic melts has Th/U in the range of 0.1 to 1.0. Two zircon standards were used: DD85-17, a quartz diorite from the Marmion batholith in northwestern Ontario, which previously gave an age of 3002±2 Ma by ID-TIMS (Tomlinson et al. 2003) and DD91-1, a monzodiorite from the Pontiac Province of Quebec with an age of 2682±1 Ma (Davis 2002). The monazite standard was DD90-26A, a sample of the Lac LaCroix granite in the western Superior Province of Minnesota, which previously gave an age of 2671±2 Ma (Sutcliffe 2020, 2021). Sets of 4 sample measurements were bracketed by measurements on standards. Differences between standards were time interpolated to correct sample measurements.

RAMSEY–ALGOMA GRANITOID COMPLEX

Based on Jenks natural break classification method (clusters) (Jenks 1967) of the over 100 geochronology ages taken from GeochrON (Ontario Geological Survey 2019c; *see* Figure 5.1), it is possible to divide the Ramsey–Algoma granitoid complex into 4 age groups: 2715–2695 Ma, 2686–2674 Ma, 2670–2654 Ma and 2650–2620 Ma.

Age Group 2715–2696 Ma

The oldest group of ages tend to be from tonalite to granodiorite intrusions, commonly foliated to gneissic. Spatially, they are located near greenstone belts (*see* Figure 5.1). During this study, 2 new ages were added to this group. The first sample is a foliated tonalite located north of the Benny greenstone belt (sample 16: *see* Table 5.1 and Figure 5.1). It had both zircon and titanite that yielded ages of 2713.2±1.2 Ma (mean square weighted deviation (MSWD)=1.8) and 2712.7±1.0 Ma (MSWD=1.7), respectively. Several previously determined ages are available for the Benny greenstone belt (*circa* 2670–2701 Ma, Ontario Geological Survey 2019c), all of which are younger than 2713 Ma. This suggests that the intrusion *circa* 2713 Ma may be the basement on which the Benny greenstone belt was formed.

The second sample of this age group, a gneissic granodiorite, located in Winkler Township near a sliver of supracrustal rocks (sample 5: *see* Table 5.1 and Figure 5.1), is more problematic. Several attempts were made using CA-ID-TIMS to get a precise age on this sample; however, the data were scattered having an upper intercept at 2714.0±3.6 Ma (MSWD=0.12) and a lower intercept at *circa* 1585 Ma, with minimum $^{207}Pb/^{206}Pb$ ages of 2695±3 Ma (average) and 2675.4±1.1 Ma (weighted mean, MSWD=3.3). In an attempt to clarify the difference in ages, the sample was also analyzed by LA-ICP–MS, yielding an age of 2697±4 Ma (MSWD=2.2). Considering both the LA-ICP–MS and CA-ID-TIMS methods yielded ages of *circa* 2696 Ma, this age is interpreted cautiously to be the age of emplacement of the unit.

Age Group 2686–2676 Ma

This slightly younger group of ages occurs dominantly in granodiorite plutons that are commonly foliated. Previously identified intrusions belonging to this age group are the Smuts pluton (<2686±1 Ma: van Breemen, Heather and Ayer 2006) and Fawn pluton (2678.2±1.1 Ma (MSWD=0.083): Kamo and

Hamilton 2018), located south of the Swayze area (Abitibi greenstone belt); as well as the Joffre pluton (2674±1 Ma (MSWD=0.92): van Breemen, Heather and Ayer 2006) in the Biscotasing arm (*see* Figure 5.1). To this group, 2 new ages were added. Similar to the older group, they are located in the northern and southern portions of the study area near greenstone belts.

The oldest sample, a foliated granodiorite (sample 7: *see* Table 5.1 and Figure 5.1), located south of the Swayze area of the Abitibi greenstone belt, yielded an age 2683.4±1.1 Ma (MSWD=0.57). This age is in accordance with the age of 2682±2 Ma (youngest grain, Kamo 2015) obtained from a tonalite located in the Biscotasing arm (Shipley Township) of the Swayze area (Abitibi greenstone belt), approximately 23 km to the southeast.

The second sample added to this age group is a granodiorite with an age of 2682.3±1.3 Ma (MSWD=2.1; sample 1: *see* Table 5.1 and Figure 5.1) located in Dagle Township. Because there are no detailed maps of the area, little is known about its geology. More investigation is needed to place this age into context because several of the surrounding ages are younger.

Age Group 2670–2654 Ma

This age group is composed mainly of granites and granodiorites that are most commonly massive, although a few are foliated or gneissic. This group also includes the Parisien syenite (2665 $^{+1.6}/_{-1.4}$ Ma: Krogh, Davis and Corfu 1984), the Margaret stock (2668±1 Ma (MSWD=0.76): van Breemen, Heather and Ayer 2006) and the Bardney batholith (2662±4 Ma: van Breemen, Heather and Ayer 2006) southwest of the Biscotasing arm (*see* Figure 5.1). Several diorites are also thought to have been emplaced during this period. To this age group, 4 new ages were added.

The oldest new age in this group is 2669.59±0.95 Ma (sample 8: *see* Table 5.1 and Figure 5.1) from a foliated granodiorite located in Lewis Township. A relatively similar age is present in the southern part of the study area: a poorly constrained age of *circa* 2660 Ma (Sutcliffe 2020) from a granitoid in the southern portion of Cobden Township near Blind River. The proximity of the 2 samples, and their relatively similar ages suggest that much of the basement under the Huronian Supergroup in the southern part of the area is similar in age (i.e., *circa* 2670–2660 Ma). The Parisien syenite, located approximately 30 km northeast, has a similar age of 2665 $^{+1.6}/_{-1.4}$ Ma (Krogh, Davis and Corfu 1984).

Samples 11, 9 and 14 (*see* Table 5.1; *see* Figure 5.1) yielded ages of 2664±10 Ma (MSWD=0.34), 2662.9±1.1 Ma (MSWD=0.5) and 2659±4 Ma, respectively. All 3 plutons are located in the central portion of the study area, with sample 14 located near the Benny greenstone belt. They are in proximity to previously studied plutons of similar age and thus constrain the age of that portion of the Ramsey–Algoma granitoid complex relatively well to *circa* 2670–2654 Ma.

Age Group 2650–2620 Ma

The youngest age group of the Ramsey–Algoma granitoid complex are all units described as granites. This group includes the Cartier (*circa* 2642 Ma: Meldrum et al. 1997) and Birch Lake (2650.7±1.4 Ma: Kamo 2006; 2657.3±1.4 Ma: Kamo 2023) granites located north and west of the Sudbury Basin, respectively (*see* Figure 5.1). To this younger group, 6 new ages were added.

Of the 6 new ages, 3 are granites that yielded ages *circa* 2650 Ma (samples 3, 10 and 4: *see* Table 5.1 and Figure 5.1). These granites occur throughout the Ramsey–Algoma granitoid complex, with 2 being located north of the Huronian Supergroup north of Elliot Lake (samples 3 and 10). The third (sample 4) is located in the north part of the study area southwest of the Swayze area (Abitibi greenstone belt). These

3 samples have ages similar to the Birch Lake granite located just west of the Sudbury Basin. More work is needed to have a better understanding of these ages and their relationship with each other.

Similarly, a fourth sample, sample 2, yielded an age of 2641±5 Ma from a granite located in Rollins Township (*see* Table 5.1; *see* Figure 5.1). This is similar to the age of the Cartier granite (*circa* 2642 Ma: Meldrum et al. 1997). However, it is located approximately 130 km to the west of the Cartier batholith and is a separate intrusion.

The youngest Archean ages of *circa* 2620 Ma are from 2 massive granites (samples 6 and 13: *see* Table 5.1 and Figure 5.1). Based on their geophysical radiometric and magnetic response, both of these ages were obtained from the central portion of large intrusions. However, sample 13 was too altered to give a precise age. The U/Pb analyses from sample 13 range from 2580 to 2646 Ma, with most analyses scattering outside the error of the average age of *circa* 2620 Ma.

Thermal Overprint

Titanites from 2 samples were analysed (sample 5 and 7: *see* Table 5.1 and Figure 5.1) and yielded ages of 2660±9 Ma and 2661±3 Ma. These ages are interpreted as a thermal overprint of perhaps regional scale.

SUPRACRUSTAL ROCK

One sample of intermediate tuff was collected in the Benny greenstone belt and yielded an age of 2672.0±1.3 Ma (sample 15: *see* Table 5.1 and Figure 5.1). This would correspond to volcanism found in the dominantly sedimentary Timiskaming assemblage or episode (2676–2670 Ma) of the Abitibi greenstone belt. To this day, the oldest rock identified in the Benny greenstone belt is 2701.6±2.9 Ma in Rhodes Township (Ontario Geological Survey 2019c), which corresponds to the youngest volcanic assemblage or episode of the Abitibi greenstone belt (Blake River assemblage or episode).

PROTEROZOIC INTRUSION

One gabbro sample (sample 12: *see* Table 5.1 and Figure 5.1) was collected in Salter Township at the contact between the Huronian Supergroup and the Ramsey–Algoma granitoid complex. This sample yielded an age of 2470±10 Ma. This corresponds to the ages associated with the East Bull Lake intrusive suite at 2472.2±0.8 Ma (Clough and Hamilton 2017). This suggests that the intrusions found at the border of the Huronian Supergroup and the Archean granitoid in Salter, May, Shakespeare and possibly extending to Drury townships are part of the East Bull Lake intrusive suite. Alternatively, they could belong to the associated Matachewan dike swarm event at 2460±2 Ma (Bleeker et al. 2015).

CONCLUSIONS

- This study expanded the geochronological database of the southern Abitibi Subprovince, particularly for the Ramsey–Algoma granitoid complex, by approximately 20%.
- In the study area, the Ramsey–Algoma granitoid complex ranges in age from 2715 to 2620 Ma. The older rock units are generally tonalites to granodiorites located near the greenstone belts, whereas the youngest granites are located in the central part of large intrusive complexes.
- The new Ramsey–Algoma granitoid complex ages of *circa* 2715 to 2620 Ma are consistent with the detrital zircon populations present within the various formations of the Huronian

Supergroup, which typically are dominated by ages of less than 2680 Ma, especially in the lowermost Huronian Supergroup (Easton 2019).

- The 2 new titanite ages of *circa* 2660 Ma suggest a thermal overprinting, possibly on a regional scale.
- One new age from the Benny greenstone belt confirms that it is a relatively young Archean greenstone belt.
- A Proterozoic age (2470 Ma) was obtained from a mafic intrusion located at the contact between the Huronian Supergroup and the Ramsey–Algoma granitoid complex. This age may correspond to the East Bull Lake intrusive suite or an early phase of the Matachewan dike swarm.

ACKNOWLEDGMENTS

Nick Szumylo, Joe Walker, Julie Chartrand and Shannon Evers are thanked for their assistance in the field as well as in the office. This project has benefited from several discussions with several colleagues at the Ontario Geological Survey, in particular, Michael Easton, Caroline Gordon and Manuel Duguet focussing on the Precambrian rocks and Desmond Rainsford (retired) for the geophysical data. Sandra L. Kamo would like to acknowledge the staff of the Jack Satterly Geochronology Laboratory for their ongoing support. Darla Bennett and Mathieu Levesque are thanked for their work with the First Nations communities located within the boundaries of this project. We would like to thank Mattagami First Nation, Brunswick House First Nation, Flying Post First Nation, Matachewan First Nation, Mississauga First Nation, Serpent River First Nation, Sagamok Anishnawbek First Nation, Whitefish River First Nation, Atikameksheng Anishnawbek, Wahnapitae First Nation, Thessalon First Nation, Wiikwemkoong Unceded Territory First Nation, Chapleau Cree, Métis Nation of Ontario Region 5 and Métis Nation of Ontario Region 3-Abitibi Inland Historic Métis Community for allowing us to map on their traditional territory. Pat Gervais is recognized for drafting the figure for this report.

REFERENCES

Bleeker, W., Kamo, S.L., Ames, D.E. and Davis, D. 2015. New field observations and U-Pb ages in the Sudbury area: Toward a detailed cross-section through the deformed Sudbury Structure; *in* Targeted Geoscience Initiative 4: Canadian Nickel-Copper-Platinum Group Elements-Chromium Ore Systems — Fertility, Pathfinders, New and Revised Models, Geological Survey of Canada, Open File 7856, p.151-166.

Clough, C.E. and Hamilton, M.A. 2017. Matachewan LIP revisited: A revised, high-resolution U-Pb age for the East Bull Lake intrusion and associated units; Geological Association of Canada–Mineralogical Association of Canada, Abstracts, v.40, p.65.

Davis, D.W. 2002. U-Pb geochronology of Archean metasediments in the Pontiac and Abitibi subprovinces, Quebec, constraints on timing, provenance and regional tectonics; Precambrian Research, v.115, p.97-117.

Easton, R.M. 2019. What do detrital zircon studies of the Huronian Supergroup tell us? An analysis of all published data; abstract *in* 65th Institute on Lake Superior Geology, Proceedings, v.65, pt.1, p.38-39.

Gerstenberger, H. and Haase, G. 1997. A highly effective emitter substance for mass spectrometric Pb isotope ratio determinations; Chemical Geology, v.136, p.309-312.

Jaffey, A.H., Flynn, K.F., Glendenin, L.E., Bentley, W.C. and Essling, A.M., 1971. Precision measurement of half-lives and specific activities of ^{235}U and ^{238}U; Physical Review, v.4, p.1889-1906.

Jenks, G.F. 1967. The Data Model concept in statistical mapping; International Yearbook of Cartography, v.7, p.186–190.

Kamo, S.L. 2006. Report on U-Pb geochronological data from the southern Abitibi Subprovince, Bannockburn–Montrose and Vernon townships, and the Grenville Front region, Thistle–Sisk townships, Ontario; internal report for the Ontario Geological Survey, Jack Satterly Geochronology Laboratory, Department of Geology, University of Toronto, Toronto, Ontario, 20p.

——— 2015. Report on the U-Pb ID-TIMS geochronology on volcanic and plutonic rocks, Superior and Grenville Provinces, Ontario; internal report for the Ontario Geological Survey, Jack Satterly Geochronology Laboratory, University of Toronto, Toronto, Ontario, 48p.

——— 2020. Part A: Report on U-Pb ID-TIMS geochronology for the Ontario Geological Survey: Bedrock Mapping Projects, Ontario, Year 5: 2019-2020; internal report for the Ontario Geological Survey, Jack Satterly Geochronology Laboratory, University of Toronto, Toronto, Ontario, 55p.

——— 2023. Report on U-Pb ID-TIMS geochronology for the Ontario Geological Survey: Bedrock Mapping Projects, Ontario 2022-2023; internal report for the Ontario Geological Survey, Jack Satterly Geochronology Laboratory, University of Toronto, Toronto, Ontario, 22p.

Kamo, S.L. and Hamilton, M.A. 2018. Part A: Report on U-Pb ID-TIMS geochronology for the Ontario Geological Survey: Bedrock mapping projects, Ontario, Year 3: 2017–2018; internal report for the Ontario Geological Survey, Jack Satterly Geochronology Laboratory, University of Toronto, Toronto, Ontario, 44p.

Krogh, T.E. 1973. A low contamination method for hydrothermal decomposition of zircon and extraction of U and Pb for isotopic age determinations; Geochimica et Cosmochimica Acta, v.37, p.485-494.

Krogh, T.E., Davis, D.W. and Corfu, F. 1984: Precise U-Pb zircon and baddeleyite ages for the Sudbury Structure; *in* Geology and Ore Deposits of the Sudbury Structure, Ontario Geological Survey, Special Volume 1, p.431-446.

Ludwig, K.R. 2003. User's manual for Isoplot 3.00: A geochronological toolkit for Microsoft® Excel®; Berkeley Geochronology Center, Special Publication No. 4, 71p.

Mattinson, J.M. 2005. Zircon U-Pb chemical abrasion ("CA-TIMS") method: combined annealing and multi-step partial dissolution analysis for improved precision and accuracy of zircon ages; Chemical Geology, v.220, p.47-66.

Meldrum, A., Abdel-Rahman, A-F.M., Martin, R.F. and Wodicka, N. 1997. The nature, age and petrogenesis of the Cartier Batholith, northern flank of the Sudbury Structure, Ontario, Canada; Precambrian Research, v.82, p.265-285.

Ontario Geological Survey 2011. 1:250 000 scale bedrock geology of Ontario; Ontario Geological Survey, Miscellaneous Release—Data 126 – Revision 1.

——— 2019a. Ontario airborne geophysical surveys, magnetic gradiometer and gamma-ray spectrometric data, grid and profile data (ASCII format) and vector data, Ramsey–Algoma area; Ontario Geological Survey, Geophysical Data Set 1086a.

——— 2019b. Ontario airborne geophysical surveys, magnetic gradiometer and gamma-ray spectrometric data, grid and profile data (Geosoft® format) and vector data, Ramsey–Algoma area; Ontario Geological Survey, Geophysical Data Set 1086b.

——— 2019c. Geochronology Inventory of Ontario—2019; Ontario Geological Survey, Geochronology Inventory of Ontario—2019 (online database).

Préfontaine, S. 2020. Summary of 2019 field activity, Ramsey–Algoma compilation project, Superior and Southern provinces; *in* Summary of Field Work and Other Activities, 2020, Ontario Geological Survey, Open File Report 6370, p.5-1 to 5-12.

Préfontaine, S. and Rainsford, D.R.B. 2019. Geological compilation project: Ramsey–Algoma granitoid complex and surrounding rocks, Superior and Southern provinces; *in* Summary of Field Work and Other Activities, 2019, Ontario Geological Survey, Open File Report 6360, p.5-1 to 5-9.

Stacey, J. and Kramers, J. 1975, Approximation of terrestrial lead isotope evolution by a two-stage model; Earth and Planetary Science Letters, v.26, p.207-221.

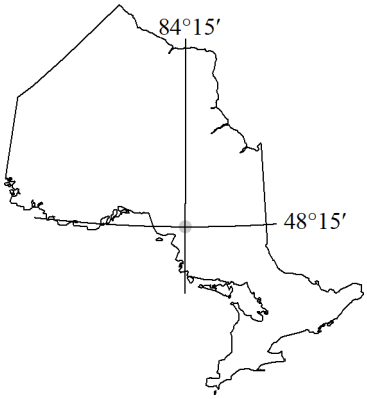
Sutcliffe, C.N. 2020. U-Pb geochronology report for samples from northern Ontario by LA-ICPMS; internal report for the Ontario Geological Survey, Jack Satterly Geochronology Laboratory, University of Toronto, Toronto, Ontario, 31p.

——— 2021. U-Pb geochronology report for samples from Ontario by LA-ICPMS; internal report for the Ontario Geological Survey, Jack Satterly Geochronology Laboratory, University of Toronto, Toronto, Ontario, 75p.

Tomlinson, K.Y., Davis, D.W., Stone, D. and Hart, T.R. 2003. U-Pb age and Nd isotopic evidence for crustal recycling and Archean terrane development in the south-central Wabigoon Subprovince, Canada; Contributions to Mineralogy and Petrology, v.144, p.684-702.

van Breemen, O., Heather, K.B. and Ayer, J.A. 2006. U-Pb geochronology of the Neoarchean Swayze sector of the southern Abitibi greenstone belt; Geological Survey of Canada, Current Research 2006-F1, p.1-32.

6. Project NE-23-004. Preliminary Geology of Riggs and Glasgow Townships, Michipicoten Greenstone Belt, Northeastern Ontario



L.E.D. Vice[1,2], S. Perrouty[2] and S.G. Pelletier[1]

[1]Earth Resources and Geoscience Mapping Section, Ontario Geological Survey, Sudbury, Ontario P3E 6B5
[2]Mineral Exploration Research Centre (Metal Earth), Harquail School of Earth Sciences, Laurentian University, Sudbury, Ontario P3E 2C6

INTRODUCTION

This multi-year project in the eastern Michipicoten greenstone belt was initiated to update and re-examine the bedrock geology, to characterize the major rock units and stratigraphy and to evaluate the mineral potential of the area. During the summer of 2023, detailed bedrock geology mapping was completed in Riggs Township and parts of Glasgow Township (Figure 6.1). Stratigraphically and structurally significant locations were also visited throughout the belt as part of the complementary doctoral thesis project in the region (Project NE-22-002; Vice, Perrouty and Robichaud 2022). The preliminary geology of previously mapped townships related to this project is presented in Robichaud (2013), Robichaud and McDivitt (2014), Robichaud, McDivitt and Trevisan (2015), Robichaud et al. (2016), Walker and Robichaud (2016), Walker (2017), Walker and Robichaud (2018) and Vice (2022).

REGIONAL GEOLOGY

The Michipicoten greenstone belt consists of successions of Archean metavolcanic and metasedimentary rocks intruded by Archean metagranitic rocks (Turek, Smith and Van Schmus 1982) and younger Proterozoic mafic dikes. The supracrustal rocks of the belt have previously been subdivided into 3 distinct volcanic cycles: 2900 Ma, 2750 Ma and 2700 Ma (Sage and Heather 1991; Heather and Arias 1992; Turek, Smith and Van Schmus 1982, 1984; Turek, Van Schmus and Sage 1988) overlain by the <2680 Ma Dore metasedimentary rocks (Corfu and Sage 1992). Geochronological data from the current mapping project suggest that volcanism is more continuous than previously interpreted with volcanic rock ages ranging from 2731 to 2704 Ma (Vice, Perrouty and Robichaud 2022, and references therein).

GEOLOGY OF RIGGS AND GLASGOW TOWNSHIPS

The Archean bedrock geology of Riggs and Glasgow townships includes supracrustal rocks and intrusive bodies that are bounded to the north by the "Wabatongushi Lake granitoid complex" (Turek et al. 1996). Proterozoic mafic intrusions crosscut all Archean rocks (Figure 6.2).

Summary of Field Work and Other Activities, 2023,
Ontario Geological Survey, Open File Report 6405, p.6-1 to 6-10.

© King's Printer for Ontario, 2023

Supracrustal Rocks

Supracrustal rocks within Riggs and Glasgow townships include mafic to intermediate and intermediate to felsic metavolcanic rocks, as well as clastic and chemical metasedimentary rocks (*see* Figure 6.2). Metamorphism of the supracrustal rocks is primarily greenschist facies, with increasing metamorphic grade to upper amphibolite facies in proximity to granitoid bodies.

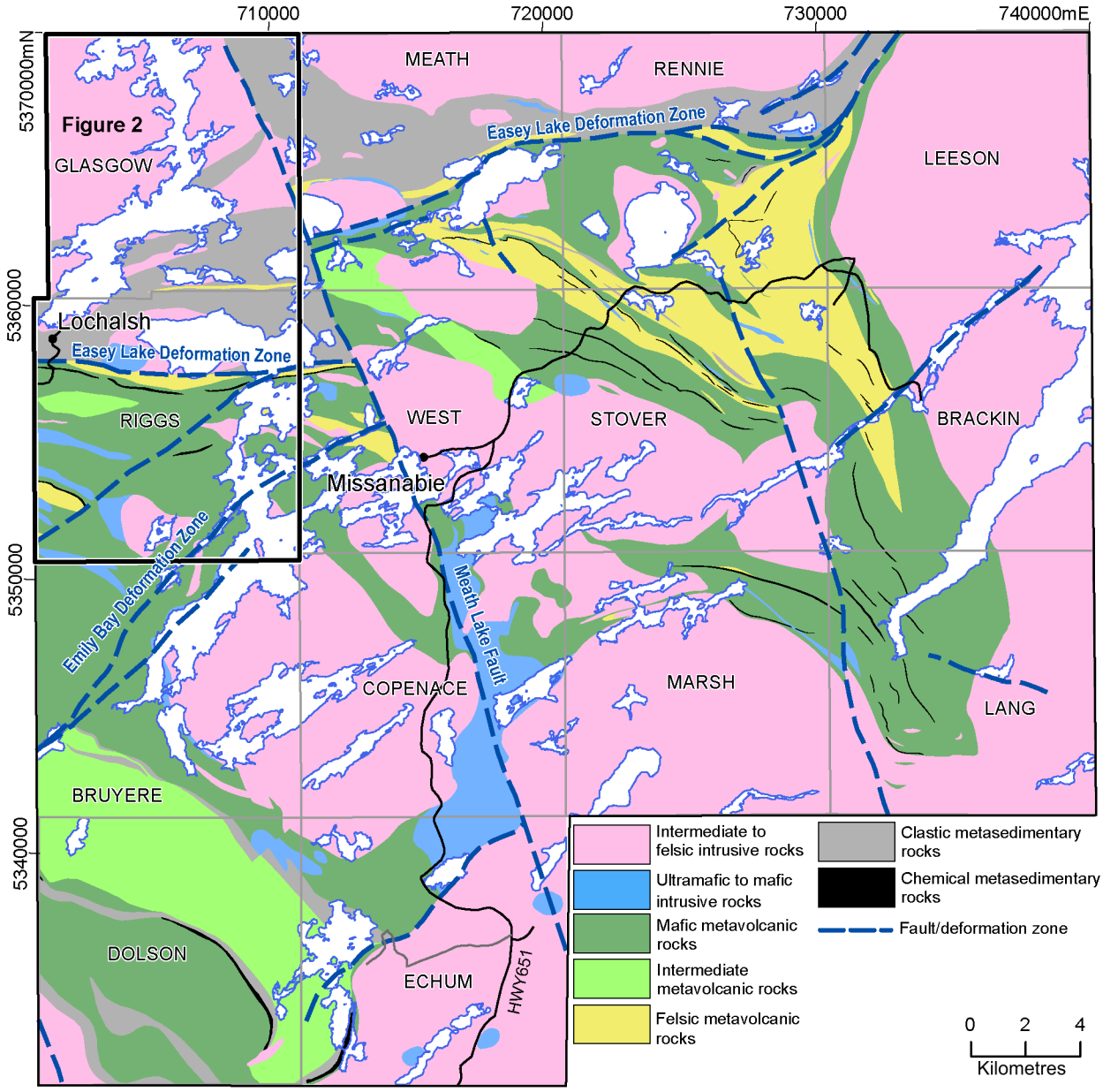


Figure 6.1. Simplified geological map of the eastern Michipicoten greenstone belt showing the location of Riggs and Glasgow townships (outlined in black). Location information provided as Universal Transverse Mercator (UTM) co-ordinates using North American Datum 1983 (NAD83) in Zone 16.

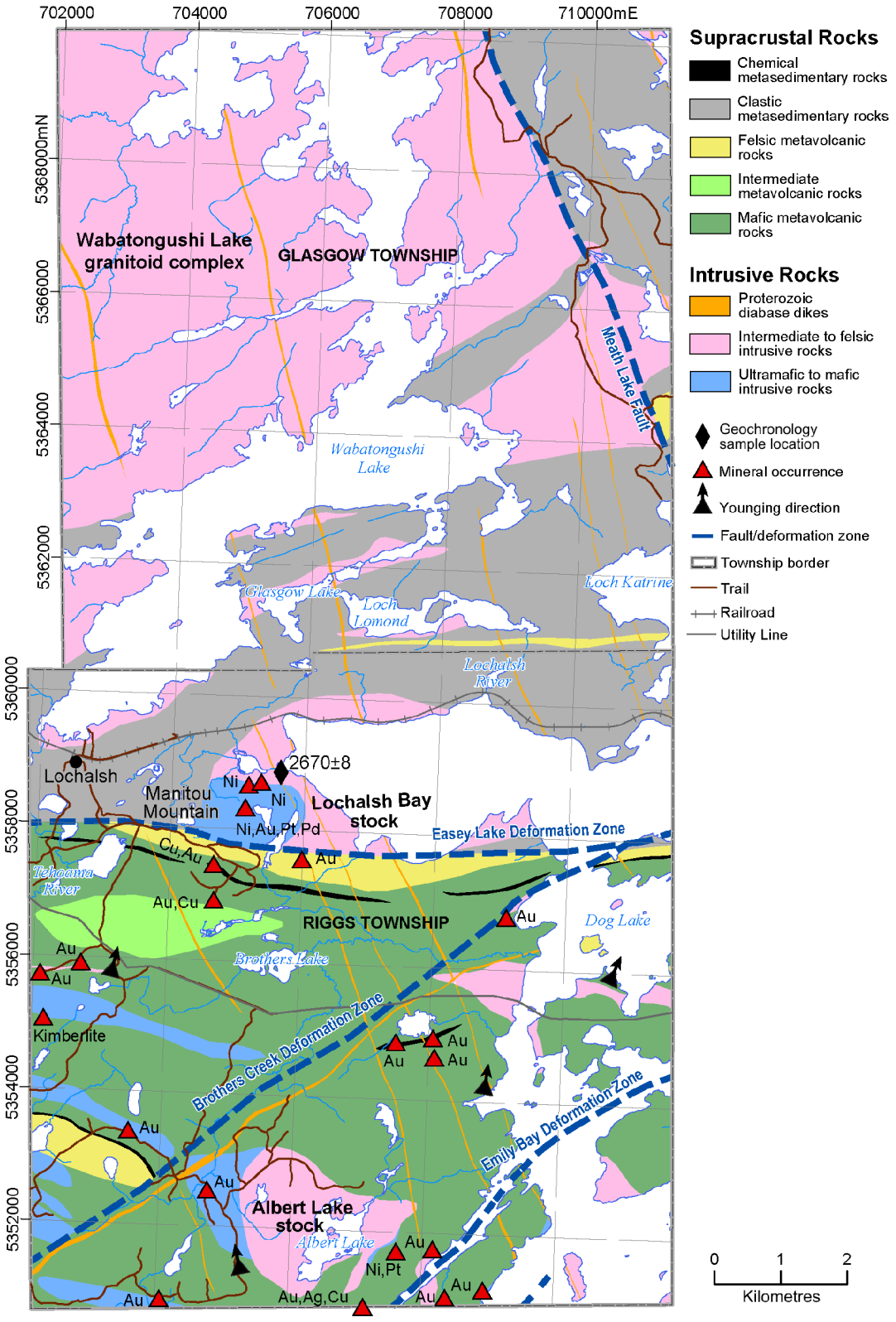


Figure 6.2. Preliminary geological map of Riggs and Glasgow townships. Ontario Mineral Inventory (OMI) occurrences and prospects (Ontario Geological Survey 2023) indicate documented primary commodities. Abbreviations used: Ag, silver; Au, gold; Cu, copper; Ni, nickel; Pd, palladium; Pt, platinum. Geochronology sample age and location *from* Turek et al. (1996). Location information provided as UTM co-ordinates using NAD83 in Zone 16.

MAFIC TO INTERMEDIATE METAVOLCANIC ROCKS

Mafic metavolcanic rocks are primarily observed in Riggs Township (*see* Figure 6.2) and consist of massive to pillowed chloritized flows. Least deformed pillows range from 20 to 50 cm long and 10 to 20 cm wide with selvages and interpillow material ranging from 1 to 2 cm in thickness (Photo 6.1A). Pillows consistently indicate approximate younging direction toward the north-northeast within the study area, with few exceptions that young to the northwest in southwest Riggs Township (*see* Figure 6.2). Contacts between mafic metavolcanic rocks and Archean gabbroic rocks in southwest Riggs Township (*see* Figure 6.2) are often sheared with increased carbonate and sulphide alteration. Additionally, mafic metavolcanic rocks are strongly deformed and carbonate altered along structural zones, such as the Emily Bay deformation zone (Photo 6.2A). Stratigraphically, this unit overlies the felsic metavolcanic rocks (2741–2728 Ma) that host the Island Gold Mine approximately 12 km west of the study area (Turek, Sage and Van Schmus 1992). Geochronological samples collected this summer will provide ages to better constrain the timing of emplacement for these rocks.

INTERMEDIATE TO FELSIC METAVOLCANIC ROCKS

Intermediate to felsic metavolcanic rocks in Riggs and Glasgow townships are relatively thin packages of chlorite-bearing massive tuff, lapilli tuff and tuff breccia (*see* Figure 6.2; Photo 6.1B). Locally, lapilli tuffs contain magnetite-rich bands. Contacts between these rocks and other supracrustal units appear to accommodate high amounts of strain with associated carbonate and sulphide alteration. Along the Easey Lake deformation zone, exposed along Dog Lake, the tuffaceous layers have varying textures from massive and undeformed to high-strain to brecciated. Tuff breccia units contain polymictic rounded 1 to 4 cm clasts of felsic intrusive rock, intermediate and mafic volcanic rocks within a foliated chloritic matrix. Where it is least affected by the deformation zone, the contact between the intermediate to felsic volcaniclastic material and the overlying clastic metasedimentary rocks appears to be gradational changing from massive tuff to tuff breccia to volcano-sedimentary rocks and, finally, to clastic metasedimentary rocks.

CLASTIC METASEDIMENTARY ROCKS

Clastic metasedimentary rocks are found to the north of the Easey Lake deformation zone in a 3 to 5 km thick package of thinly to thickly laminated turbiditic stratigraphy composed of predominantly greenschist-facies buff to dark grey siltstone and wacke (*see* Figure 6.2; Photo 6.1C). Along a corridor south of Loch Lomond, toward the southwest corner of Wabatongushi Lake, thin horizons of both mafic and felsic metavolcanic rocks are interlayered within the sedimentary package. In northern and central Glasgow Township, both east and west of the Meath Lake fault, the metasedimentary rocks are gneissic and locally migmatitic and have undergone metamorphism up to upper amphibolite facies. Adjacent to the Meath Lake fault, the contact with orthogneisses is gradational and, near the contact, the high-grade gneissic rocks contain layers of both orthogneiss and paragneiss (Photo 6.1D). This gradational contact was not observed on the shore of Wabatongushi Lake where the contacts between gneissic intrusive rocks and metasedimentary rocks have been intruded by moderately to undeformed granodioritic to granitic rocks.

Polymictic clast- and matrix-supported conglomerates have been observed in beds between 1 and 25 m thick on the southern shores of Lochalsh Bay on Dog Lake and Wabatongushi Lake (Photo 6.1E). Clast compositions include intermediate and felsic intrusive rocks, as well as mafic volcanic rock, with proportions of each clast type varying between beds. Conglomerates are locally deformed along high-strain zones, such as the Easey Lake deformation zone (Photo 6.2B), with clasts that are rounded to subrounded, ranging in size from 3 cm to up to 20 cm with more abundant clasts within the 3 to 10 cm range. Compositions of clasts include mafic to intermediate metavolcanic, tonalitic to granodioritic intrusive and gabbroic intrusive rocks.

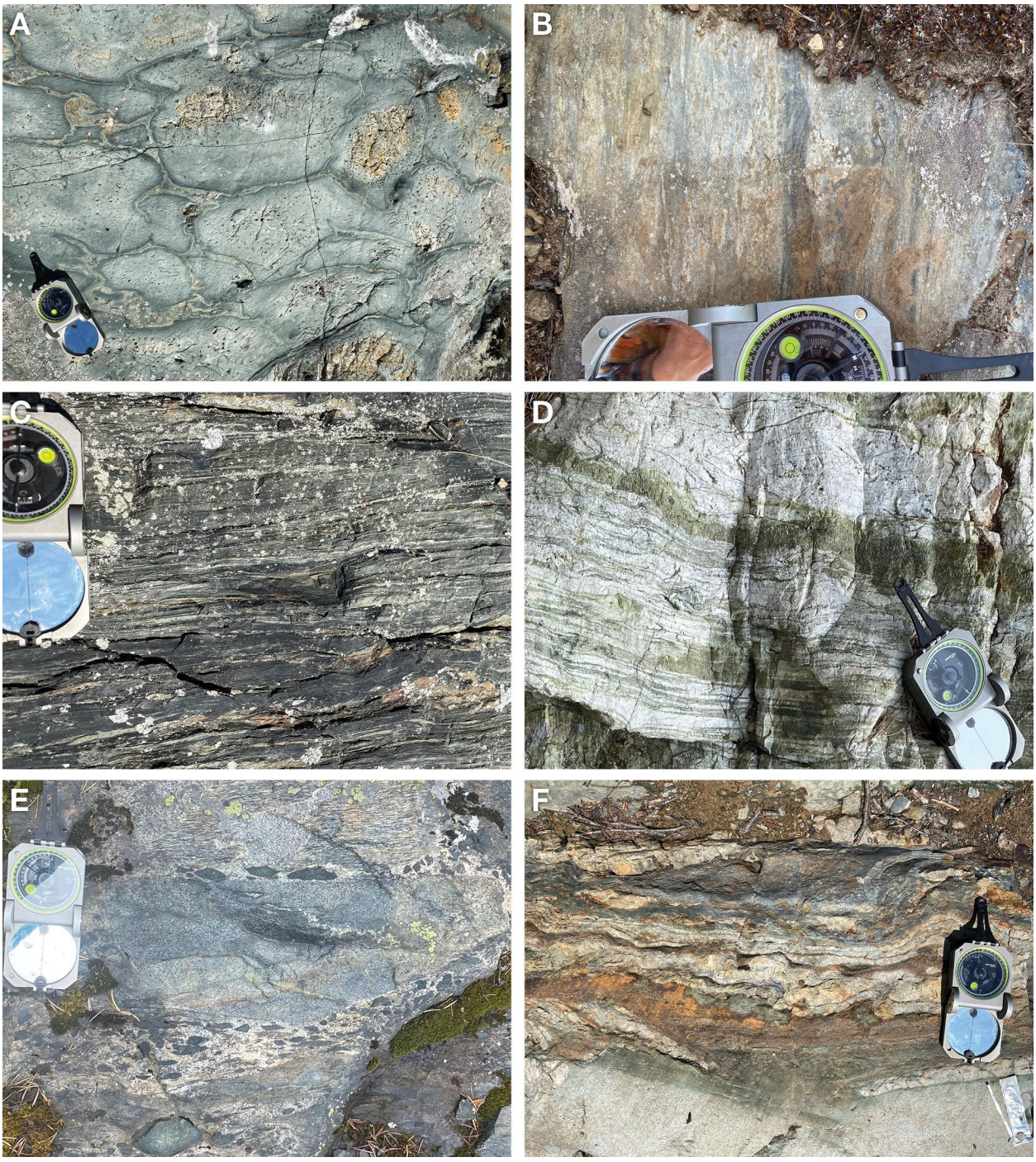


Photo 6.1. Selected photographs of geological units within Riggs and Glasgow townships. **A)** Pillowed mafic metavolcanic rocks with younging to the north-northeast (station 23LEV112: UTM 710797E 5356018N). **B)** Strained and altered intermediate to felsic metavolcanic rock in west-central Riggs Township (station 23LEV002: UTM 703040E 5356542N). **C)** Turbiditic metasedimentary rocks in northwest Riggs Township on the southern part of Wabatongushi Lake (station 23LEV032: UTM 702165E 5359687N). **D)** Paragneiss (greenish-brown) with local bands of tonalitic gneiss (whitish) in central Glasgow Township (station 23LEV145: UTM 709890E 5365659N). **E)** Polymictic clast-supported conglomerate on Wabatongushi Lake in southwest Glasgow Township (substation 23LEV0026SS: UTM 703506E 5362431N). **F)** Chert-magnetite ironstone with minor sulphides from southwest Riggs Township (station 23SGP028: UTM 702804E 5353382N). Compass for scale is 7.1 cm wide, with sighting arm pointing north. All UTM co-ordinates provided using NAD83 in Zone 16.

CHEMICAL METASEDIMENTARY ROCKS

Chemical metasedimentary rocks are observed locally within southwest Riggs Township either as 30 to 50 cm thick beds of alternating chert and magnetite bands (Photo 6.1F) or as highly strained beds with thick lenses of massive sulphide minerals and thin 1 to 2 cm bands of magnetite-rich layers. Ironstone units are distinguishable by high magnetic responses on airborne geophysical surveys (Ontario Geological Survey 1999, 2003, 2011). Additionally, ironstone is described relating to gold occurrences (and 1 copper occurrence) west of Dog Lake and south of the Lochalsh Bay stock (*see* Figure 6.2; Ontario Geological Survey 2023); this ironstone was not observed this summer.

Intrusive Rocks

Intrusive rocks within Riggs and Glasgow townships include metamorphosed Archean ultramafic to mafic intrusions, tonalitic, trondhjemitic, granodioritic intrusions, quartz-syenitic and pegmatitic granitic bodies. Proterozoic diabase dikes intrude all Archean rocks.

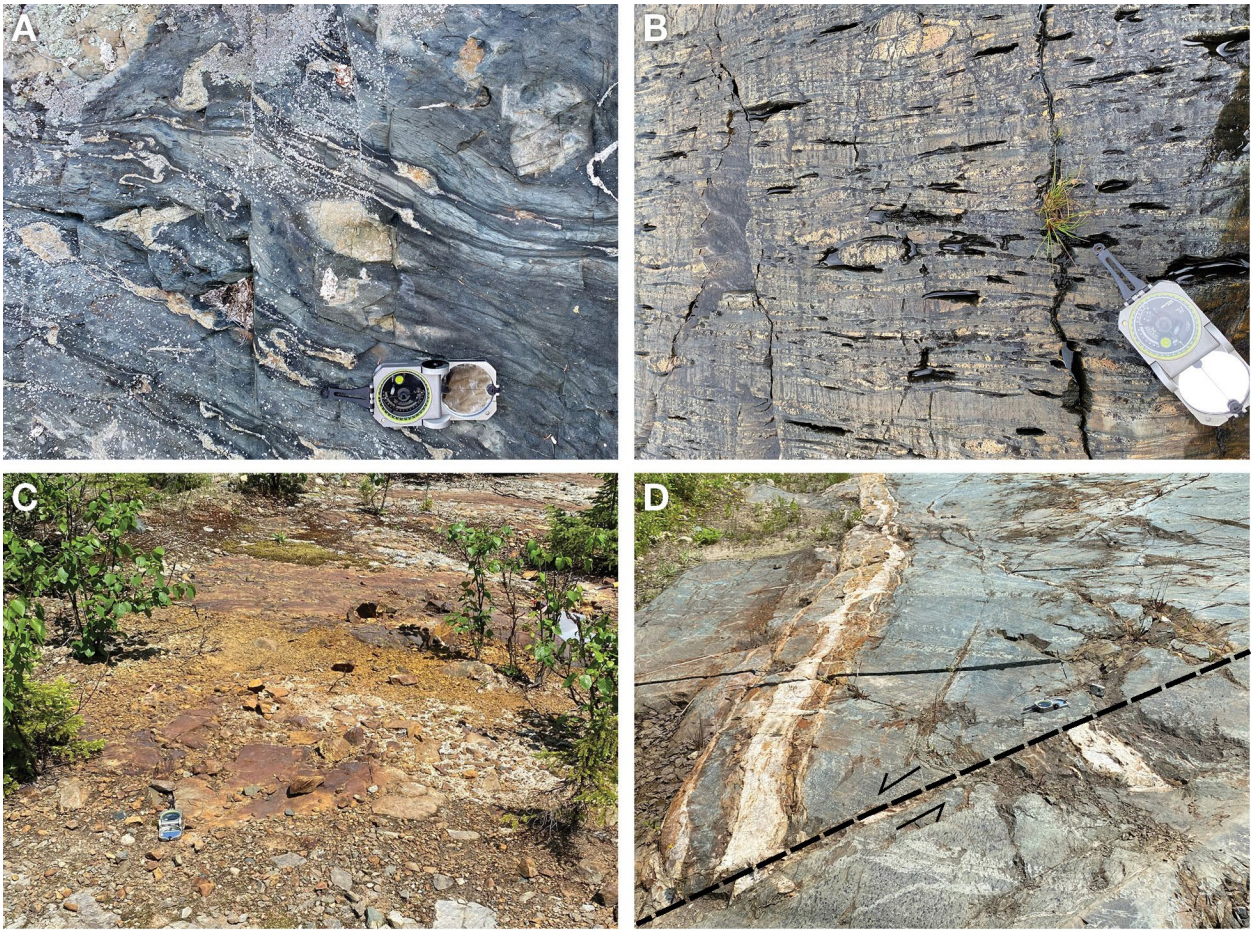


Photo 6.2. Selected photographs of structural features within Riggs Township. **A)** Primarily dextral shear sense indicators in deformed pillowed mafic metavolcanic flows along the Emily Bay deformation zone (station 23LEV095: UTM 709591E 5353004N). **B)** Deformed conglomeratic rock along Easey Lake deformation zone (substation 23LEV0291SS: UTM 711265E 5358141N). **C)** Sulphide- and ankerite-altered felsic volcanic rock with deformation along east-trending structures (station 23SGP005: UTM 702474E 5352959N). **D)** East-trending quartz-filled high-strain zone in coarse-grained metagabbroic rock offset by north-northwest-trending brittle–ductile fault indicated by black dashed line (station 23LEV050: UTM 703516E 5353377N). Compass for scale is 7.1 cm wide, with sighting arm pointing north. All UTM co-ordinates provided using NAD83 in Zone 16.

ARCHEAN INTRUSIVE ROCKS

Sills and irregular shaped bodies of fine- to coarse-grained, locally magnetic metagabbroic to metadioritic rock intrude the supracrustal rocks in southwest Riggs Township (*see* Figure 6.2). The nature of the contact between these mafic intrusive rocks and their host rock (primarily mafic metavolcanic rocks) varies: it is locally sharp, but commonly faulted or sheared with quartz veins and ankerite alteration. A subrounded olivine gabbro plug (age unknown) defines the topographic high within the Manitou Mountain nature preserve, which has not been mapped as part of this study (*see* Figure 6.2; Srivastava et al. 1974). Four nickel occurrences with 2 platinum or platinum group elements occurrences are associated with mafic intrusive units (*see* Figure 6.2). It is unclear whether the various gabbroid to dioritic bodies are related to the mafic metavolcanic rocks (e.g., feeder dikes) or represent one or multiple different mafic magmatic events in the area.

The Albert Lake stock in southern Riggs Township (*see* Figure 6.2) is a medium-grained granodiorite to tonalite, which is massive in its interior and becomes moderately to intensely foliated toward its outer contact with mafic metavolcanic and metagabbroic rocks.

The Lochalsh Bay stock, at the north end of Dog Lake (*see* Figure 6.2), comprises massive, medium- to coarse-grained quartz syenite to syenite. The central part of the stock is exposed within the Manitou Mountain nature preserve. It has been previously documented as quartz monzonite (Srivastava et al. 1974) to granodiorite and yielded an age of 2670±8 Ma (*see* Figure 6.2; Turek et al. 1996).

Quartz-feldspar porphyry intrusions occur throughout Riggs Township as relatively thin bodies that vary from granodioritic to tonalitic in composition. These dikes or sills appear to intrude preferentially near zones of moderate to intense deformation, and are intensely foliated, silicified and, locally, iron-carbonate altered. Porphyritic intrusions have yielded ages of 2694±6 Ma in West Township and 2675±6 Ma in Rennie Township (Sutcliffe and Davis 2019; Turek et al. 1996, respectively).

Central to northern Glasgow Township includes medium- to coarse-grained gneisses that vary in composition from dioritic through granitic. These rocks have undergone upper amphibolite-facies or higher metamorphism and are locally intruded by pegmatitic granite dikes. Southern Glasgow Township includes felsic intrusions located within and along the contact with clastic metasedimentary rocks near Glasgow Lake, Loch Lomond and southern Wabatongushi Lake. These intrusions comprise medium-grained, foliated granodiorite to granite that are crosscut by massive quartz-syenitic bodies. The gneisses, foliated intrusions, syenitic bodies and pegmatitic granites were previously included in the "Wabatongushi Lake granitoid complex" of Turek et al (1996). A tonalitic phase, interpreted to be part of the complex, yielded an age of 2700±1 Ma in Rennie Township (Kamo 2016; *see* Figure 6.1). Future geochronological and geochemical analyses will help determine ages, relationships and compositions, as well as constrain the deformation and clarify the geologic nature of the "Wabatongushi Lake granitoid complex" (Turek et al 1996).

PROTEROZOIC INTRUSIONS

Proterozoic mafic dikes crosscut all Archean rocks in Riggs and Glasgow townships and are distinguished by sharp, linear aeromagnetic highs (Ontario Geological Survey 1999, 2003, 2011). The dikes are composed of magnetite-bearing, fine- to medium-grained gabbro containing plagioclase phenocrysts and local glomerocrysts up to 4 cm diameter. Most dikes trend north-northwest and are interpreted to be part of the Matachewan dike swarm (2460 Ma: Bleeker et al. 2015; Osmani 1991). Dikes trending generally northeast are interpreted to be part of the Biscotasing dike swarm (*circa* 2170 Ma: Buchan, Mortensen and Card 1993).

STRUCTURAL GEOLOGY

The overall stratigraphy S_0 and bedding-parallel dominant S_1 foliation within Riggs and Glasgow townships are approximately west trending and steeply dipping to the north. Macroscale asymmetric tight to isoclinal F_1 folding of the metasedimentary stratigraphy is observed in strongly deformed exposures along Wabatongushi Lake and Dog Lake. A first-order east-trending structure is the newly identified Easey Lake deformation zone (*see* Figures 6.1 and 6.2), exposed on the southern shore of Lochalsh Bay on Dog Lake, which marks the boundary between the metavolcanic rocks and the clastic metasedimentary rocks. Along this sheared contact, conglomeratic metasedimentary rocks and minor intermediate to felsic metavolcanic rocks occur. The Easey Lake deformation zone is younger than the felsic metavolcanic rocks (2704±2 Ma: Kamo 2016) near Conboy Lake in Rennie Township (to the east of this study area), which hosts both volcanogenic massive sulphide deposit and orogenic gold occurrences (Craig 2023; Ontario Geological Survey 2023). Several second-order east-trending high-strain zones are present, are commonly ankerite altered, sulphide flooded, silicified, and are associated with orogenic gold occurrences (Photo 6.2C).

A second foliation, S_2, crosscutting the regional bedding-parallel S_0-S_1 foliation, is spatially associated with, and related to, northeast-trending deformation zones, such as the Emily Bay and Brothers Creek deformation zones. The Emily Bay deformation zone hosts the developed gold prospect Emily Bay Mine in southern Riggs Township, which is surrounded by other gold, silver and copper occurrences hosted in shear quartz-carbonate veins (Ontario Geological Survey 2023). These northeast-trending deformation zones display primarily dextral strike-slip to dextral transpressive kinematic indicators (*see* Photo 6.2A).

The Meath Lake fault is a late brittle–ductile fault that offsets all Archean rocks in the study area. Apparent offset along the fault can best be interpreted by the 5 to 7 km sinistral offset of the Easey Lake deformation zone in Meath and West townships (*see* Figure 6.1). Approaching the Meath Lake fault, orthogneisses and clastic metasedimentary rocks become brecciated with alternating metre-size blocks over approximately 10 to 15 m. This fault is consistent in orientation with others in the study area (Photo 6.2D) and throughout the belt, such as the Maskinonge Lake fault, located approximately 10 km west of the study area, which may host gold mineralization (Ma et al. 2023). Timing and duration of movement along the Meath Lake fault is unclear, but it must be older than the crosscutting Matachewan dike swarm (2460 Ma: Bleeker et al. 2015; Osmani 1991).

ACKNOWLEDGMENTS

This mapping project benefitted from the assistance of Aidan Massey-Garrison, Robin McCormick and Wulfric Harris-Stoertz. The complementary doctoral thesis study by the senior author (LEDV) is supported by the Ontario Geological Survey and by the Canada First Research Excellence Fund's Metal Earth program. Thanks to staff at the Ontario Geological Survey: Lise Robichaud and Sonia Préfontaine for guidance and support; Mathieu Levesque and Darla Bennett for community engagement; Patrick Gervais for aid with drafting figures; Monica Gaiswinkler Easton for editorial assistance; Shannon Evers, Nick Szumylo and Jeremy Creppin for aid in sample preparation. Thanks also to Alamos Gold Inc. for in-kind support of the project and valuable field discussions with Carl Nagy and Raja Yarra. The authors would like to thank Batchewana First Nation, Brunswick House First Nation, Chapleau Cree First Nation, Garden River First Nation, Michipicoten First Nation and Missanabie Cree First Nation for allowing the Ontario Geological Survey to map their traditional land use area. Special thanks to Sean at Wabatong Lodge, as well as Rod and the Missanabie community at Dog Lake Cottages and Campground for their hospitality throughout the summer.

REFERENCES

Bleeker, W., Kamo, S.L., Ames, D.E. and Davis, D.W. 2015. New field observations and U-Pb ages in the Sudbury area: Toward a detailed cross-section through the deformed Sudbury Structure; *in* Targeted Geoscience Initiative 4: Canadian Nickel-Copper-Platinum Group Elements-Chromium Ore Systems – Fertility, Pathfinders, New and Revised Models, Geological Survey of Canada, Open File 7856, p.151-156.

Buchan, K.L., Mortensen, J.K. and Card, K.D. 1993. Northeast-trending Early Proterozoic dykes of southern Superior Province: Multiple episodes of emplacement recognized from integrated paleomagnetism and U–Pb geochronology; Canadian Journal of Earth Sciences, v.30, p.1286-1296.

Corfu, F. and Sage, R.P. 1992. U–Pb age constraints for deposition of elastic metasedimentary rocks and late tectonic plutonism, Michipicoten Belt, Superior Province; Canadian Journal of Earth Sciences, v.29, p.1640-1651.

Craig, S. 2023. Mineralogical, textural, and geochemical investigation of Conboy Lake base metal and gold mineralization in the Michipicoten greenstone belt, Wawa Subprovince, Ontario; unpublished BSc thesis, Queen's University, Kingston, Ontario, 128p.

Heather, K.B. and Arias, Z. 1992. Geological and structural setting of gold mineralization in the Goudreau–Lochalsh area, Wawa gold camp; Ontario Geological Survey, Open File Report 5832, 159p.

Kamo, S.L. 2016. Part A: Report on U-Pb ID-TIMS geochronology for the Ontario Geological Survey: Bedrock mapping projects, Ontario, internal report for the Ontario Geological Survey, Jack Satterly Geochronology Laboratory, University of Toronto, Toronto, Ontario, 48p.

Ma, C., Vice, L.E.D., Nagy, C., Adam, Z.V., Shirriff, D., Lafrance, B. and Robichaud, L. 2023. Orogenic and intrusion-related gold deposits of the Michipicoten and Mishibishu greenstone belts in the Wawa region, with an emphasis on their structural timing and setting: A geological guidebook; Geological Association of Canada–Mineralogical Association of Canada–Society for Geology Applied to Mineral Deposits, Joint Annual Meeting, Sudbury, Ontario, May 25–27, 2023, Field Trip FT10, Ontario Geological Survey, Open File Report 6398, 57p.

Ontario Geological Survey 1999. Single master gravity and aeromagnetic data for Ontario, Geosoft® format; Ontario Geological Survey, Geophysical Data Set 1036.

——— 2003. Ontario airborne geophysical surveys, magnetic and electromagnetic data, grid and profile data (Geosoft® format), Wawa area; Ontario Geological Survey, Geophysical Data Set 1009b.

——— 2011. Ontario airborne geophysical surveys, magnetic and electromagnetic data, grid and profile data (ASCII and Geosoft® formats) and vector data, Magpie River–Missinaibi Lake area—Purchased data; Ontario Geological Survey, Geophysical Data Set 1237.

——— 2023. Ontario Mineral Inventory; Ontario Geological Survey, online database, September 2023 update, www.hub.geologyontario.mines.gov.on.ca. [accessed October 10, 2023]

Osmani, I.A. 1991. Proterozoic mafic dike swarms in the Superior Province of Ontario; Chapter 17 *in* Geology of Ontario, Ontario Geological Survey, Special Volume 4, Part 1, p.661-681.

Robichaud, L. 2013. Geology and mineral potential of Marsh and Lang townships, Michipicoten greenstone belt; *in* Summary of Field Work and Other Activities, 2013, Ontario Geological Survey, Open File Report 6290, p.3-1 to 3-10.

Robichaud, L. and McDivitt, J.A. 2014. Geology and mineral potential of Brackin Township, Michipicoten greenstone belt; *in* Summary of Field Work and Other Activities, 2014, Ontario Geological Survey, Open File Report 6300, p.5-1 to 5-11.

Robichaud, L., McDivitt, J.A. and Trevisan, B.E. 2015. Geology and mineral potential of Rennie and Leeson townships, Michipicoten greenstone belt; *in* Summary of Field Work and Other Activities, 2015, Ontario Geological Survey, Open File Report 6313, p.5-1 to 5-11.

Robichaud, L., Walker, J., West, S.M. and Nywening, A. 2016. Geology and mineral potential of Stover Township, Michipicoten greenstone belt; *in* Summary of Field Work and Other Activities, 2016, Ontario Geological Survey, Open File Report 6323, p.5-1 to 5-10.

Sage, R.P. and Heather, K.B. 1991. The structure, stratigraphy and mineral deposits of the Wawa area; Geological Association of Canada–Mineralogical Association of Canada–Society of Economic Geologists, Joint Annual Meeting, Toronto 1991, Field Trip A6, 118p.

Srivastava, P., Bennett, G., Elmhirst, F. and Andrews, M.D. 1974. Geological series, Missanabie area, Riggs Township, formerly Township 47, District of Algoma; Ontario Geological Survey, Preliminary Map P.944, scale 1:15 840.

Sutcliffe, C.N. and Davis, D.W. 2019. Part B: U–Pb geochronology by LA-ICPMS for samples from northern Ontario, Year 4: 2018–2019; internal report for the Ontario Geological Survey, Jack Satterly Geochronology Laboratory, University of Toronto, Toronto, Ontario, 146p.

Turek, A., Heather, K.B., Sage, R.P. and Van Schmus, W.R. 1996. U/Pb zircon ages for the Missanabie–Renabie area and their relation to the rest of the Michipicoten greenstone belt, Superior Province, Ontario, Canada; Precambrian Research, v.76, p.191-211.

Turek, A., Sage, R.P. and Van Schmus, W.R. 1992. Advances in the U–Pb zircon geochronology of the Michipicoten greenstone belt, Superior Province, Ontario; Canadian Journal of Earth Sciences, v.29, p.1154-1165.

Turek, A., Smith, P.E. and Van Schmus, W.R. 1982. Rb–Sr and U–Pb ages of volcanism and granite emplacement in the Michipicoten belt, Wawa, Ontario; Canadian Journal of Earth Sciences, v.19, p.1608-1626.

——— 1984. U–Pb zircon ages and the evolution of the Michipicoten plutonic–volcanic terrane of the Superior Province, Ontario; Canadian Journal of Earth Sciences, v.21, p.457-464.

Turek, A., Van Schmus, W.R. and Sage, R.P. 1988. Extended volcanism in the Michipicoten greenstone belt, Wawa, Ontario; abstract *in* Geological Association of Canada–Mineralogical Association of Canada, Joint Annual Meeting, St. John's 1988, Program with Abstracts, v.13, p.A127.

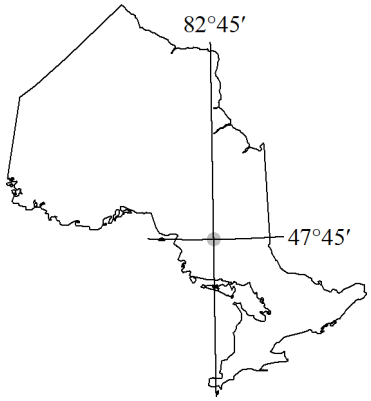
Vice, L.E.D. 2022. Preliminary geology of Meath Township, northeastern Michipicoten greenstone belt, northeastern Ontario; *in* Summary of Field Work and Other Activities, 2022, Ontario Geological Survey, Open File Report 6390, p.7-1 to 7-10.

Vice, L.E.D., Perrouty, S. and Robichaud, L. 2022. Introduction to a geochronological and structural study of supracrustal assemblages in the northeastern Michipicoten greenstone belt; *in* Summary of Field Work and Other Activities, 2022, Ontario Geological Survey, Open File Report 6390, p.8-1 to 8-8.

Walker, J. 2017. Geology and mineral potential of Bruyere Township, Michipicoten greenstone belt; *in* Summary of Field Work and Other Activities, 2017, Ontario Geological Survey, Open File Report 6333, p.6-1 to 6-10.

Walker, J. and Robichaud, L. 2016. Geology and mineral potential of Copenace Township, Michipicoten greenstone belt; *in* Summary of Field Work and Other Activities, 2016, Ontario Geological Survey, Open File Report 6323, p.6-1 to 6-9.

——— 2018. Geology and mineral potential of West Township, Michipicoten greenstone belt; *in* Summary of Field Work and Other Activities, 2018, Ontario Geological Survey, Open File Report 6350, p.5-1 to 5-10.



7. Project NE-23-002. Preliminary Geology and Mineral Potential of Cunningham Township and Part of Garnet Township, Swayze Area, Abitibi Greenstone Belt, Northeastern Ontario

T.P. Gemmell[1] and J.R.H. Creppin[1]

[1]Earth Resources and Geoscience Mapping Section, Ontario Geological Survey

INTRODUCTION

The Swayze area of the Abitibi greenstone belt has long been considered the "poor cousin" to the neighbouring Timmins, Matachewan and Kirkland Lake areas of the Abitibi greenstone belt and, therefore, has not received as much exploration attention. A regional-scale compilation mapping project in the mid-1990s (Heather 2001), which included widespread geochronological sampling, demonstrated that the Swayze area has the same episodic metavolcanic units and major faults as those found within the Abitibi greenstone belt east of the Kenogamissi Batholith (Figure 7.1; Heather 2001). The Swayze area should therefore represent a westward continuation of the fertile Abitibi greenstone belt and should have the potential to host the same types of precious and base metal mineral deposits.

This mapping project is part of a multi-year project that started in 2014 to update the geology and assess the mineral potential of the Swayze area (related project numbers: Project Unit 14-008, and Projects NE-17-001, NE-17-002, NE-18-002, NE-19-003 and NE-22-003). Field work this year focussed on Cunningham Township and part of Garnet Township (*see* Figures 7.1 and 7.2).

REGIONAL GEOLOGY

The Abitibi greenstone belt is located in the eastern part of the Wawa–Abitibi terrane of the southern Superior Province (Percival et al. 2006). It is composed predominantly of mafic to felsic metavolcanic rocks with minor ultramafic metavolcanic rocks as well as clastic and chemical metasedimentary deposits. The volcanic and sedimentary episodes in the Abitibi greenstone belt were most recently defined by Thurston et al. (2008, and references therein) and Monecke et al. (2017, and references therein). The volcanic episodes, with lithostratigraphic groups defined by Heather (2001) for the Swayze area in brackets (where applicable), are as follows: pre-2750 Ma (pre-Pacaud) episode, 2750–2735 Ma (Pacaud) episode [Chester group], 2734–2724 Ma (Deloro) episode [Marion group], 2723–2720 Ma (Stoughton–Roquemaure) episode, 2719–2711 Ma (Kidd–Munro) episode [Biscotasing group], 2710–2704 Ma (Tisdale) episode [Trailbreaker group] and 2704–2695 Ma (Blake River) episode [Swayze group]. In Ontario, rocks deposited during the volcanic episodes are overlain by rocks deposited during 2 dominantly sedimentary episodes referred to as the Porcupine-type (2690–2682 Ma) and the Timiskaming-type (2676–2670 Ma) [Ridout group] sedimentary basins.

Summary of Field Work and Other Activities, 2023,
Ontario Geological Survey, Open File Report 6405, p.7-1 to 7-10.

© King's Printer for Ontario, 2023

The Swayze area (*see* Figure 7.1) of the Abitibi greenstone belt is mainly composed of mafic, intermediate and felsic metavolcanic rocks, with local ultramafic metavolcanic rocks, clastic and chemical metasedimentary rocks and synvolcanic to syntectonic felsic to ultramafic intrusive rocks. It is bounded (*see* Figure 7.1) by the Kenogamissi Batholith (locally known as the Rice Lake batholith in the study area: *see* Becker and Benn (2003)) to the east, the Ramsey–Algoma granitoid complex to the south, the Kapuskasing Structural Zone to the west and the Nat River complex to the north (not shown on Figure 7.1).

GEOLOGY OF CUNNINGHAM AND PART OF GARNET TOWNSHIPS

The geology of Cunningham and part of Garnet townships is composed primarily of metavolcanic rocks with local units of metasedimentary rocks (Figure 7.2). The supracrustal rocks are also intruded and crosscut by the Isaiah Creek stock and mafic to ultramafic intrusive rocks with smaller bodies of felsic to intermediate intrusive rocks.

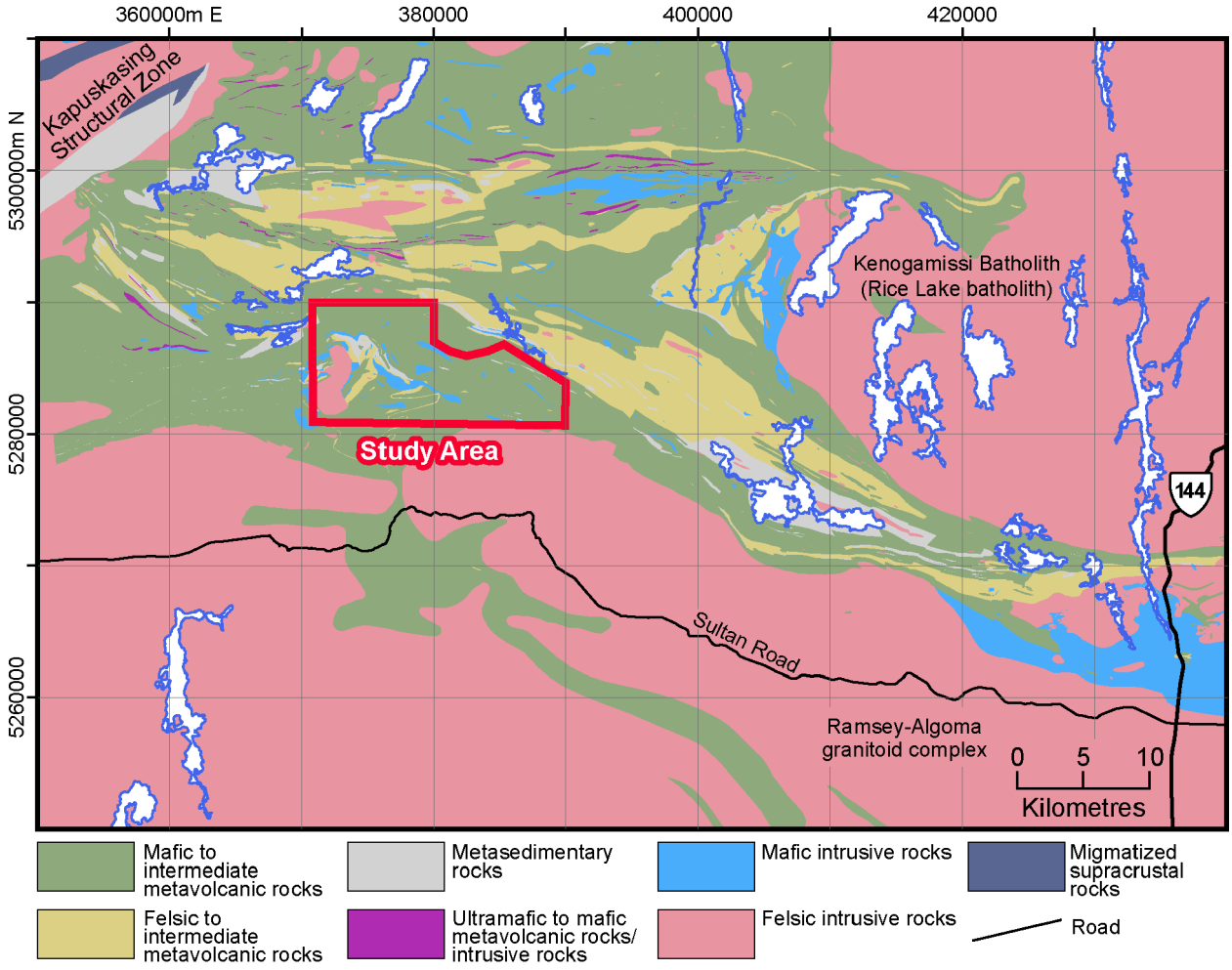


Figure 7.1. Simplified geological map of the southern Swayze area of the Abitibi greenstone belt displaying the study area (outlined by red box). Location information provided as Universal Transverse Mercator (UTM) co-ordinates using North American Datum 1983 (NAD83) in Zone 17. Geology *modified from* Ontario Geological Survey (2011).

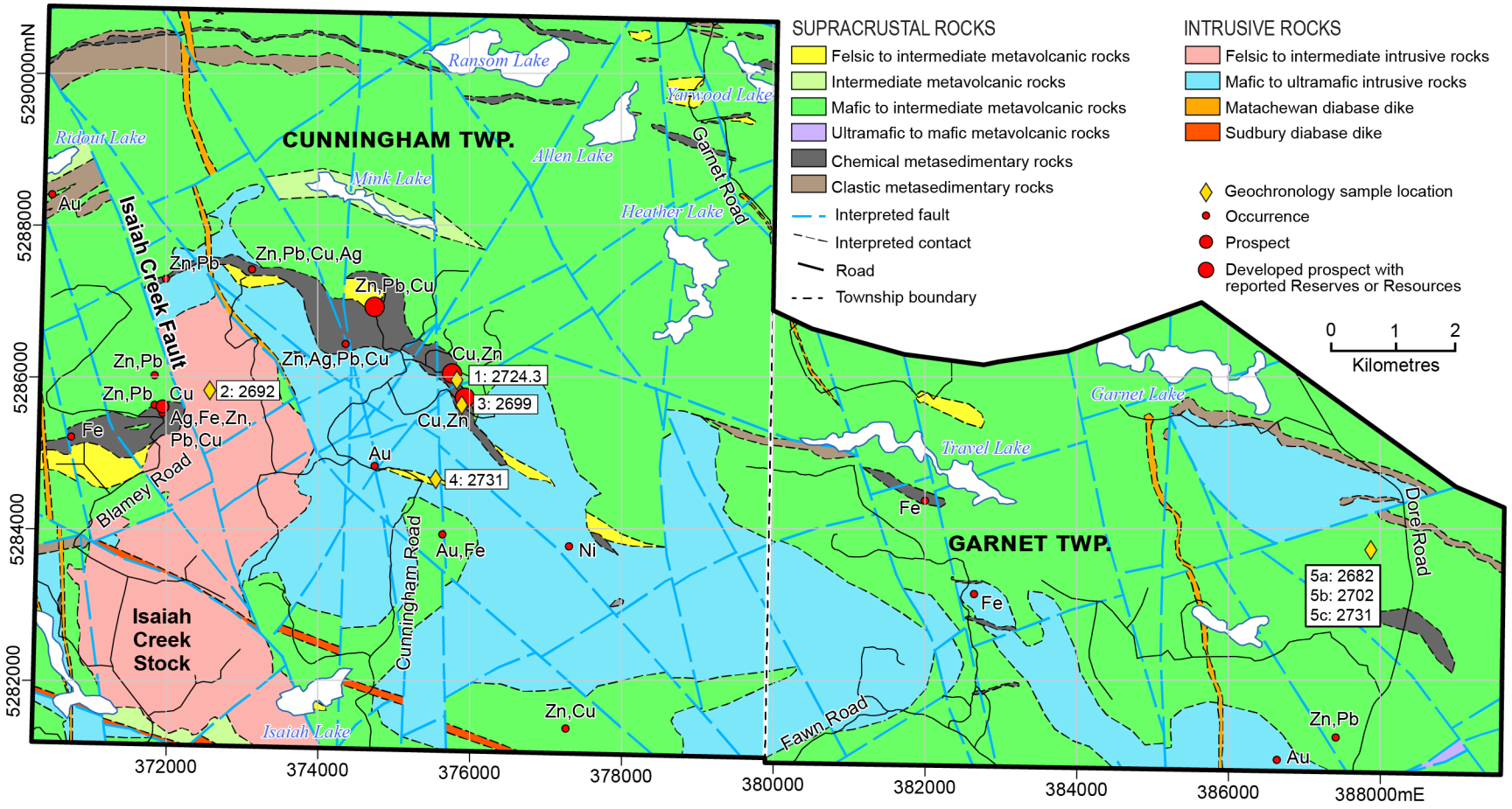


Figure 7.2. Preliminary geological map of Cunningham Township and part of Garnet Township. Geochronology data are presented in million years (Ma); *see* Table 7.1 for additional information. Ontario Mineral Inventory (OMI) (Ontario Geological Survey 2023) indicate documented primary commodities and OMI category. Abbreviations used: Ag, silver; Au, gold; Cu, copper; Fe, iron; Pb, lead; Zn, zinc. Location information provided as UTM co-ordinates using NAD83 in Zone 17.

Archean Metavolcanic Rocks

The metavolcanic rocks of the study area include abundant mafic to intermediate massive to pillowed flows with minor ultramafic to mafic flows and felsic to intermediate volcaniclastic rocks.

Mafic to intermediate and intermediate metavolcanic rocks constitute the dominant rock types within Cunningham Township and part of Garnet Township (*see* Figure 7.2). These rocks vary from dark green to light green and are typically cryptocrystalline to fine-grained, massive and pillowed lava flows (Photo 7.1A). Pillows are typically ameboid shaped, range in size from 50 to 100 cm wide and thick and are separated by thin 1 to 3 cm thick interpillow materials that locally contains pyrite or pyrrhotite. Massive, fine-grained ultramafic to mafic metavolcanic flows occur locally in southern Garnet Township (*see* Figure 7.2). These flows are typically 1 to 3 m thick and vary from moderate to dark green to an altered brown with light green serpentinized veinlets (Photo 7.1B).

Felsic to intermediate metavolcanic rocks mainly occur as narrow volcaniclastic deposits in central to southern Cunningham Township that extend locally into Garnet Township. The felsic to intermediate volcaniclastic rocks are dominantly white to light greyish green thinly bedded tuffs (Photo 7.1C) with lesser lapilli tuffs and tuff breccias. One of these units, in central Cunningham Township, yielded an age of 2724.3±0.8 Ma (van Breemen, Heather and Ayer 2006) (Table 7.1; *see* Figure 7.2, location 1). A second unit, located in an enclave in the mafic intrusive rock of central Cunningham Township, yielded an age of 2731±2 Ma (van Breemen, Heather and Ayer 2006) (*see* Table 7.1; *see* Figure 7.2, location 4).

Archean Metasedimentary Rocks

The study area has both chemical and clastic metasedimentary rocks. The chemical metasedimentary rocks can be subdivided into 2 main horizons: an ironstone horizon in northern Cunningham Township and an ironstone horizon in central Cunningham Township that extends into Garnet Township (*see* Figure 7.2). The ironstones are primarily oxide facies with lesser sulphide facies. They are predominantly composed of chert with lean alternating bands of hematized chert and locally magnetite beds (Photo 7.1D). The northern ironstone horizon is the extension of the ironstones described in Gemmell and Buyers (2022) and strikes roughly eastward with a steep dip to the south. The horizon manifests as a series of discontinuous units that have a total strike length of approximately 20 km that extends westward into Greenlaw Township. The ironstone horizon in the central portion of Cunningham Township has a roughly west-northwest strike excluding the portion of the ironstone in central Cunningham Township which wraps around the Isaiah Creek stock. This ironstone horizon likely terminates to the east in the granitoids south of Garnet Township. The central Cunningham Township ironstone horizon has a relatively consistent thickness of approximately 100 m in Garnet Township; however, local thickening (up to ~800 m in plan view) because of tight isoclinal folding in central Cunningham Township is inferred.

Clastic metasedimentary rocks are present in northern Cunningham Township and these also extend across central to southeastern Garnet Township (*see* Figure 7.2). The clastic metasedimentary rock units comprise up to approximately 400 m thick, southeast-trending, Timiskaming-style polymictic conglomerate lenses. The conglomerates are primarily matrix supported and are composed of pebble-sized clasts with lesser cobbles and boulders and are intercalated with local silty to sandy beds (Photo 7.1E). The conglomerates are polymictic with clasts, in decreasing order of abundance, of felsic to intermediate metavolcanic rocks, felsic to intermediate intrusive rocks, mafic metavolcanic rocks, massive pyrite and locally sparse chert and hematized chert. Polymictic conglomerates also occur locally at the contact between the ironstone horizon in central Cunningham Township and the metavolcanic rocks. These conglomerates have a chloritized matrix, are heavily oxidized and likely represent an erosional interface zone similar to the ones described by Thurston et al. (2008) in the Abitibi greenstone belt east of the Kenogamissi Batholith.



Photo 7.1. Selected photographs of lithological units. **A)** Fine-grained mafic pillowed flow in Cunningham Township (substation 23JC0140SS: 377825E 5285529N). **B**) Fine-grained ultramafic flow with anastomosing flow boundaries in Garnet Township (substation 23TG0151SS: 383623E 5280976N). **C**) Felsic bedded tuff in Cunningham Township (station 23TG080: 372912E 5287430N). **D**) Banded ironstone with a siliciclastic bed in Cunningham Township (station 23TG081: 372825E 5287518N). **E**) Polymictic conglomerate with volcanic, intrusive and sedimentary clasts in Garnet Township (substation 23TG0339SS: 385214E 5285208N). **F**) Massive tonalite in Cunningham Township (station 23TG015: 372579E 5283179N). Compass for scale is 22 cm long, with sighting arm pointing north. All location information provided as UTM co-ordinates using NAD83 in Zone 17.

Table 7.1. Geochronological data referred to in the text; locations and ages are shown on Figure 7.2.

No. on Figure 7.2	U/Pb Method on Zircon[a]	Age (Ma)	Interpretation	Rock Type	Easting[b] (m)	Northing[b] (m)	Source
1	TIMS	2724.3±0.8	Volcanism	Felsic metavolcanic rock	375210	5286432	van Breemen, Heather and Ayer (2006)
2	TIMS	2692±2	Emplacement	Granodiorite	372593	372593	van Breemen, Heather and Ayer (2006)
3	TIMS	2699 $^{+3}/_{-2}$	Emplacement	Quartz feldspar porphyry within felsic metavolcanic rocks	375257	5286520	van Breemen, Heather and Ayer (2006)
4	TIMS	2731±2	Volcanism	Felsic metavolcanic rock	375570	5284656	van Breemen, Heather and Ayer (2006)
5a	ICP–MS	2682±4	Emplacement	Quartz porphyry	387865	5283716	Davis, Ménard and Sutcliffe (2018)
5b	ICP–MS	2702±5	Inheritance	Quartz porphyry	387865	5283716	Davis, Ménard and Sutcliffe (2018)
5c	ICP–MS	2731±5	Inheritance	Quartz porphyry	387865	5283716	Davis, Ménard and Sutcliffe (2018)

[a] *Methods abbreviations: ICP–MS, U/Pb laser ablation inductively coupled plasma mass spectrometry; TIMS, U/Pb thermal ionization mass spectrometry.*
[b] *Locations provided as UTM co-ordinates in NAD83, Zone 17.*

Archean Intrusive Rocks

Archean intrusive rocks are present in both Cunningham and Garnet townships. These intrusive rocks can be subdivided into 3 main types: felsic to intermediate intrusions, mafic to ultramafic intrusions, and felsic to intermediate porphyritic intrusions (not represented on Figure 7.2). In addition, 2 Proterozoic gabbro dike swarms crosscut all rock types.

The most significant intrusion is the felsic to intermediate Isaiah Creek stock located in central Cunningham Township (*see* Figure 7.2). The Isaiah Creek stock is typically composed of white to light grey, but locally brownish pink weathering, tonalite (Photo 7.1F) to granodiorite with granite occurring near the centre of the intrusion. Rocks of the Isaiah Creek stock are typically porphyritic with 1 to 5 mm feldspar phenocrysts and local 1 to 5 mm quartz phenocrysts. The mafic metavolcanic rocks and gabbros surrounding the intrusion have been contact metamorphosed (Photo 7.2A). Zircons from the Isaiah Creek stock yielded an age of 2692±2 Ma (van Breemen, Heather and Ayer 2006) (*see* Table 7.1; *see* Figure 7.2, location 2). Consequently, this intrusion is older than most of the large granitoid complexes that surround the Swayze area (Becker and Benn 2003; Kamo and Hamilton 2018; van Breemen, Heather and Ayer 2006). This may indicate that the Isaiah Creek stock is synvolcanic with respect to the supracrustal rocks of the Swayze area.

Several mafic (Photo 7.2B) to ultramafic (Photo 7.2C) intrusions (up to 4 km thick) occur across the southern portion of the study area. They are fine to medium grained and equigranular with interlocking amphibole, olivine, pyroxene and plagioclase, and may include secondary chlorite and/or magnetite, talc and serpentine. These intrusions may locally represent synvolcanic intrusions.

Throughout the study area, there are also several small (metre to several hundreds of metres wide) felsic to intermediate porphyritic intrusions that are typically white to light grey and have 1 to 5 mm feldspar and/or quartz phenocrysts. Two porphyritic dikes in the study area have ages of 2699 $^{+3}/_{-2}$ Ma and 2682±4 Ma (respectively, van Breemen, Heather and Ayer 2006; Davis, Ménard and Sutcliffe 2018) (*see* Table 7.1; *see* Figure 7.2, locations 3 and 5a, respectively).

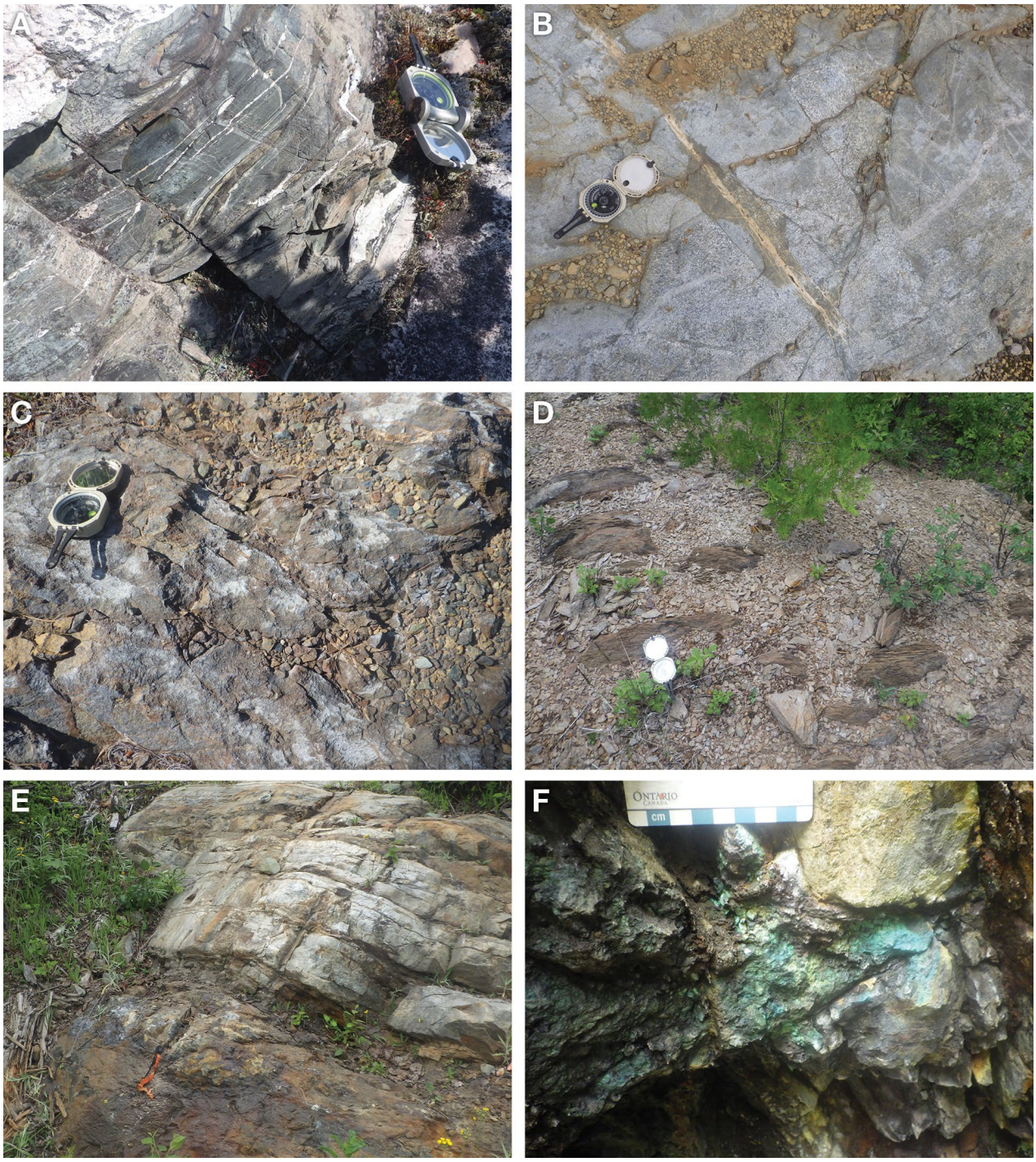


Photo 7.2. Selected photographs of lithological units. **A)** Contact between granodiorite (Isaiah Creek stock) and mafic metavolcanic country rocks in Cunningham Township exhibiting centimetre-scale Z-folding (station 23TG008: 370947E 5282203N). **B**) Medium- to coarse-grained composite gabbro in Cunningham Township with local faulting (station 23TG004: 370615E 5282775N). **C**) Medium-grained iron carbonate–bearing peridotite in Garnet Township (station 23TG053: 383752E 5281073N). **D**) Dominant high-strain zone in Cunningham Township (substation 23TG0168SS: 370481E 5288430N). **E**) Contact between barren chert beds (top of photo) and sulphidized mudstones (bottom of photo) in Cunningham Township (station 23TG041: 371313E 5285533N). **F**) Fracture-controlled pyrrhotite, pyrite, chalcopyrite, galena and sphalerite with copper-oxide staining and possible malachite in banded ironstone in Cunningham Township (station 23TG079: 373143E 5287412N). Compass for scale is 22 cm long, with sighting arm pointing north. All location information provided as UTM co-ordinates using NAD83 in Zone 17.

Proterozoic Intrusive Rocks

All Archean rocks in the field area are crosscut by 2 Proterozoic dike swarms.

Gabbro dikes of the Matachewan dike swarm (*circa* 2460 Ma: Bleeker et al. 2015), which are generally north to northwest trending, were observed in the map area (*see* Figure 7.2). These dikes can range from a few centimetres to several metres wide, and typically exhibit well-developed chilled margins. These dikes are amphibole and pyroxene rich, magnetic and locally contain euhedral to anhedral plagioclase phenocrysts.

Gabbro dikes of the Sudbury dike swarm (1238±4 Ma: Krogh et al. 1987), which are generally west-northwest trending, were also observed in the map area (*see* Figure 7.2). These dikes also display well-developed chill margins. These amphibole- and pyroxene-rich dikes generally tend to be less magnetic than the gabbros of the Matachewan dike swarm.

STRUCTURAL GEOLOGY

The dominant fabric in Cunningham and Garnet townships is a penetrative metamorphic foliation defined by sericite and chlorite that trends roughly north-northwest and is steeply dipping. It is parallel to the dominant foliation observed in Benton Township to the east (Gemmell and Szumylo 2019). The steeply dipping penetrative foliation rotates in northwestern Cunningham Township (south of the northernmost ironstone horizon (*see* Figure 7.2) to trend roughly east.

The dominant high-strain zone in the study area is located in northern Cunningham Township and extends into central Garnet Township. It is parallel to the observed regional foliation. It is characterized by the destruction of primary textures and commonly contains abundant iron-carbonate alteration (Photo7.2D). Locally, this dominant high-strain zone exhibits both sinistral and dextral kinematic indicators. Several smaller high-strain zones were also observed in the study area and these have similar trends and kinematics.

Evidence of folding was observed both at the outcrop scale (*see* Photo 7.2A) and at the map scale. Chemical metasedimentary rock units in northern Cunningham Township and in southwestern Garnet Township are interpreted to be repeated by folding. Similarly, the ironstones in northern Garnet Township (Gemmell and Buyers 2022) are also interpreted to be fold repeated. The interpreted axial traces of these folds roughly follow the regional foliation in the area. However, the exact location of the axial traces of folds is still under investigation.

Late east-northeast- and later north-northwest-trending brittle faults that exhibit both strike–slip and dip–slip components crosscut all supracrustal rocks in the study area. The Isaiah Creek fault, located in southwestern Cunningham Township, has a north-northwest strike and an apparent sinistral displacement of approximately 1.4 km.

ALTERATION AND METAMORPHISM

The earliest observed alteration is widespread vein-controlled replacement of amphiboles and feldspars by chlorite and sericite, respectively, in mafic to felsic metavolcanic rocks. Later phases of alteration overprint the supracrustal rocks within high-strain zones and include iron carbonate, sericite, chlorite and quartz alteration. The later overprinting alteration is interpreted to be related to hydrothermal fluids.

Archean rocks in the study area have undergone regional lower greenschist-facies metamorphism, with local areas of upper greenschist-facies metamorphism. Lower greenschist-facies assemblages are characterized by chlorite in the metavolcanic, metasedimentary and intrusive rocks; the upper greenschist facies is characterized by the increased amphibole content over chlorite.

MINERALIZATION

Based on the Ontario Mineral Inventory (*see* Figure 7.2; Ontario Geological Survey 2023), the ironstone horizon in central to western Cunningham Township contains 3 "developed prospects with reported reserves or resources" (from west to east: MDI41O10NE00034, MDI41O10NE00036 and MDI41O10NE00060) and 1 "prospect" (MDI41O10NE00041) (Ontario Geological Survey 2023). The 2 easternmost developed prospects (Shunsby area) were described in Gemmell (2021). All 3 prospects contain zinc (sphalerite), copper (chalcopyrite) with lesser lead (galena) and silver (*see* Figure 7.2) and occur within locally sulphidized ironstone beds and in younger fractures (Photos 7.2E and 7.2F). The mineralization style (deposit type) is still under investigation by the primary author, but was originally interpreted as volcanogenic massive sulphide by Heather (2001) and Thurston et al. (2008).

In addition to the base metal occurrences, there are 2 known occurrences of gold mineralization in both Cunningham and Garnet townships and there is 1 nickel occurrence hosted in peridotite in southern Cunningham Township.

ACKNOWLEDGMENTS

This project has benefited from the advice and guidance of Sonia Préfontaine from the Ontario Geological Survey, Rasmus Haugaard from Metal Earth (Laurentian University), and assistance of Cassandra Rousseau, Ilse Kloosterman and Lucas Perreault (junior assistants). The authors are thankful to the staff of the Ontario Geological Survey, in particular Patrick Gervais for aiding with drafting figures, Nicholas Szumylo and Shannon Evers for aiding in sample preparation, Monica Gaiswinkler Easton for aiding with final editing, and Sheree Hinz of the Resident Geologists Office for help with the Ontario Mineral Inventory information. The authors also benefited from many discussions with, and comments from, Dr. Harold Gibson from Laurentian University (Harquail School of Earth Sciences). The authors would like to thank Brunswick House First Nation, Chapleau Cree First Nation, Flying Post First Nation and Mattagami First Nation for allowing the Ontario Geological Survey to map their traditional land use area.

REFERENCES

Becker, J.K. and Benn, K. 2003. The Neoarchean Rice Lake batholith and its place in the tectonomagnetic evolution of the Swayze and Abitibi granite-greenstone belts, northeastern Ontario; Ontario Geological Survey, Open File Report 6105, 42p.

Bleeker, W., Kamo, S.L., Ames, D.E. and Davis, D. 2015. New field observations and U-Pb ages in the Sudbury area: Toward a detailed cross-section through the deformed Sudbury Structure; *in* Targeted Geoscience Initiative 4: Canadian Nickel-Copper-Platinum Group Elements-Chromium Ore Systems – Fertility, Pathfinders, New and Revised Models, Geological Survey of Canada, Open File 7856, p.151-156.

Davis, D.W., Ménard, J. and Sutcliffe, C.N. 2018. U-Pb geochronology of samples from northern Ontario. Part B: LA-ICPMS; internal report for the Ontario Geological Survey, Jack Satterly Geochronology Laboratory, University of Toronto, Toronto, Ontario, 94p.

Gemmell, T.P. 2021. Geological investigation of the Shunsby base metal prospects area, southern Swayze area of the Abitibi greenstone belt; *in* Summary of Field Work and Other Activities, 2021, Ontario Geological Survey, Open File Report 6380, p.7-1 to 7-9.

Gemmell, T.P. and Buyers, A. 2022. Preliminary geology and mineral potential of Dore and Swayze townships and part of Garnet Township, Swayze area, Abitibi greenstone belt; *in* Summary of Field Work and Other Activities, 2022, Ontario Geological Survey, Open File Report 6390, p.6-1 to 6-11.

Gemmell, T.P. and Szumylo, N. 2019. Preliminary geology and mineral potential of Heenan and Benton townships and part of Esther Township, Swayze area, Abitibi greenstone belt; *in* Summary of Field Work and Other Activities, 2019, Ontario Geological Survey, Open File Report 6360, p.9-1 to 9-10.

Heather, K.B. 2001. The geological evolution of the Archean Swayze greenstone belt, Superior Province, Canada; unpublished PhD thesis, Keele University, Keele, England, 370p.

Kamo, S.L. and Hamilton, M.A. 2018. Part A: Report on U-Pb ID-TIMS geochronology for the Ontario Geological Survey: Bedrock mapping projects, Ontario, Year 3: 2017–2018; internal report prepared for the Ontario Geological Survey, Jack Satterly Geochronology Laboratory, University of Toronto, Toronto, Ontario, 44p.

Krogh, T.E., Corfu, F., Davis, D.W., Dunning, G.R., Heaman, L.M., Kamo, S.L., Machado, N., Greenhough, J.D. and Nakamura, E. 1987. Precise U-Pb isotopic ages of diabase dykes and mafic to ultramafic rocks using trace amounts of baddeleyite and zircon; *in* Mafic Dyke Swarms, Geological Association of Canada, Special Paper 34, p.147-152.

Monecke, T., Mercier-Langevin, P., Dubé, B. and Frieman, B.M. 2017. Geology of the Abitibi greenstone belt; Chapter 1 *in* Abitibi Base and Precious Metal Deposits, Southern Abitibi Greenstone Belt, Canada, Society of Economic Geologists, Reviews in Economic Geology, v.19, p.7-50.

Ontario Geological Survey 2011. 1:250 000 scale bedrock geology of Ontario; Ontario Geological Survey, Miscellaneous Release—Data 126 – Revision 1.

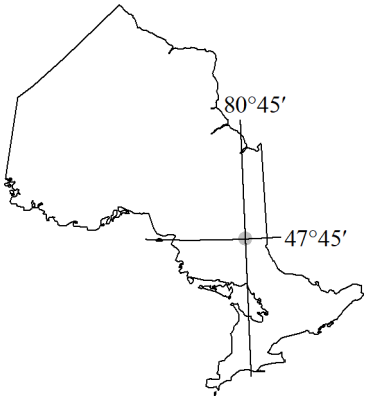
——— 2023. Ontario Mineral Inventory; Ontario Geological Survey, online database (September 2023 update), www.hub.geologyontario.mines.gov.on.ca. [accessed September 20, 2023]

Percival, J.A., Sanborn-Barrie, M., Skulski, T., Stott, G.M., Helmstaedt, H. and White, D.J. 2006. Tectonic evolution of the western Superior Province from NATMAP and Lithoprobe studies; Canadian Journal of Earth Sciences, v.43, p.1085-1117.

Thurston, P.C., Ayer, J.A., Goutier, J. and Hamilton, M.A. 2008. Depositional gaps in Abitibi greenstone belt stratigraphy: A key to exploration for syngenetic mineralization; Economic Geology, v.103, p.1097-1134.

van Breemen, O., Heather, K.B. and Ayer, J.A. 2006. U-Pb geochronology of the Neoarchean Swayze sector of the southern Abitibi greenstone belt; *in* Geological Survey of Canada, Current Research 2006-F1, 32p.

8. Project NE-23-003. Reconnaissance Bedrock Geological Mapping in Haultain, Van Hise and Nicol Townships, Abitibi Greenstone Belt, Northeastern Ontario



J. Walker[1]

[1]Earth Resources and Geoscience Mapping Section, Ontario Geological Survey

INTRODUCTION

The Gowganda silver camp came to be developed as a result of the more widespread prospecting that followed the silver discoveries in Cobalt in 1903. The region subsequently grew into a large producer of silver from 1910 to 1989 (Serigades 1968; Ontario Geological Survey 2023). The present surge in interest in critical minerals, such as cobalt, combined with the ongoing discoveries of gold in the project area has sparked renewed interest in the Gowganda camp. The geological mapping conducted in 2023 is part of a multi-year project to update the geological knowledge of the Gowganda area. Field work during the summer of 2023 focussed on detailed 1:20 000 scale mapping in Haultain Township with reconnaissance mapping into Van Hise and Nicol townships (Figure 8.1). The objectives of this project are the following: 1) to update the geological mapping in Van Hise, Haultain and Nicol townships which were last mapped in 1968 (McIlwaine 1978); 2) to characterize the major lithological units and stratigraphy; and 3) to evaluate the mineral potential of the area.

REGIONAL GEOLOGY

The project area is located in the Archean Abitibi greenstone belt (*see* Figure 8.1). The Abitibi greenstone belt is most recently subdivided by Thurston et al. (2008, and references therein) and Monecke et al. (2017, and references therein) into the following chronostratigraphic units: pre-2750 Ma episode, 2750–2735 Ma (Pacaud) episode, 2734–2724 Ma (Deloro) episode, 2723–2720 Ma (Stoughton–Roquemaure) episode, 2720–2710 Ma (Kidd–Munro) episode, 2710–2704 Ma (Tisdale) episode and the 2704–2695 Ma (Blake River) episode. Overlying the volcanic episodes in Ontario are 2 dominantly sedimentary episodes referred to the Porcupine-type (2690–2682 Ma) and the Timiskaming-type (2676–2670 Ma) sedimentary basins. Intruded into the greenstone belt area a variety of ultramafic to felsic Archean intrusions, including the Round Lake batholith (2696.9–2734.6 Ma: Ketchum, Kamo and Davis 2003; Ketchum et al. 2008; Mortensen 1993). Proterozoic mafic dikes of the Matachewan dike swarm crosscut the Archean rocks. Overlying the southern portion of the Abitibi greenstone belt, including the Proterozoic Matachewan dikes, are the sedimentary rocks of the Proterozoic Cobalt Group of the Huronian Supergroup. In the project area, the Huronian Supergroup rocks were deposited in what is known as the Cobalt Basin. Intruded into the Huronian Supergroup and older rocks are mafic intrusions of the Nipissing intrusive suite. Finally, all rocks in the study area are crosscut by the Proterozoic dikes of the Biscotasing and Sudbury swarms.

Summary of Field Work and Other Activities, 2023,
Ontario Geological Survey, Open File Report 6405, p.8-1 to 8-10.

© King's Printer for Ontario, 2023

GEOLOGY OF HAULTAIN, VAN HISE AND NICOL TOWNSHIPS

Approximately 15% of the project area consists of Archean ultramafic to felsic metavolcanic rocks and associated clastic and chemical metasedimentary rocks. Approximately 25% of the project area consists of Archean felsic to intermediate intrusive rocks, including the Round Lake batholith and Wilson Lake area granitic rocks, as well as smaller mafic to ultramafic intrusions (Figure 8.2). The remaining 60% of the project area consists of metasedimentary rocks of the Cobalt Group that overlie the Archean basement, as well as Nipissing intrusive suite mafic sills that are intruded into both the Archean basement and the Cobalt Group (*see* Figure 8.2). As noted previously, mafic dikes of the Matachewan, Biscotasing and Sudbury dike swarms also occur in the project area.

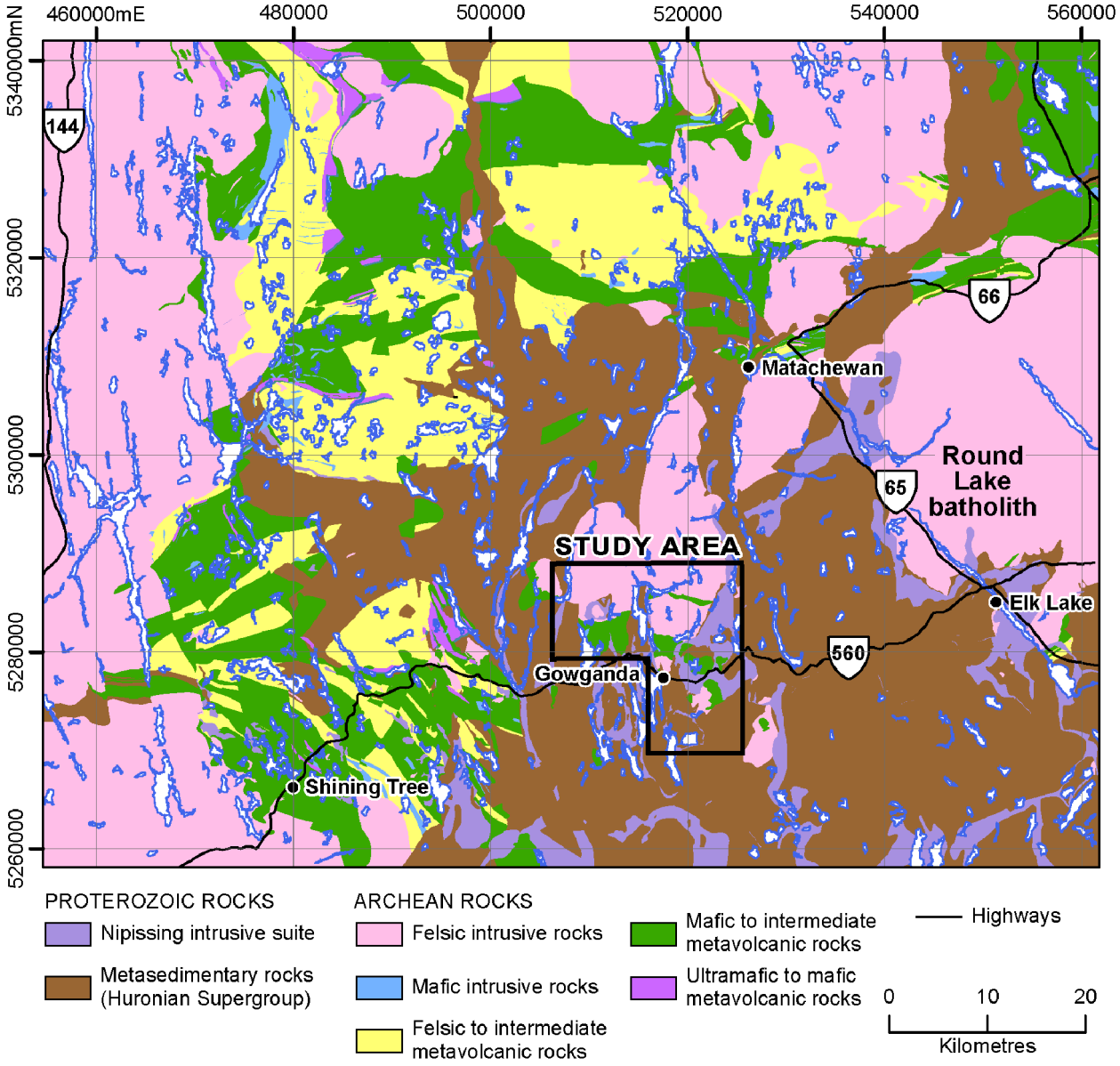


Figure 8.1. Simplified geological map of the Cobalt Embayment and Shining Tree area of the Abitibi greenstone belt showing the location of the study area (outlined with black line). Location information provided as Universal Transverse Mercator (UTM) co-ordinates using North American Datum 1983 (NAD83) in Zone 17 (*modified from* Ontario Geological Survey 2011).

Archean Metavolcanic Rocks

The metavolcanic rocks in the project area are restricted to southern Van Hise Township, central to southern Haultain Township, and central to northern Nicol Township (*see* Figure 8.2), and include ultramafic, mafic, intermediate and felsic composition rocks.

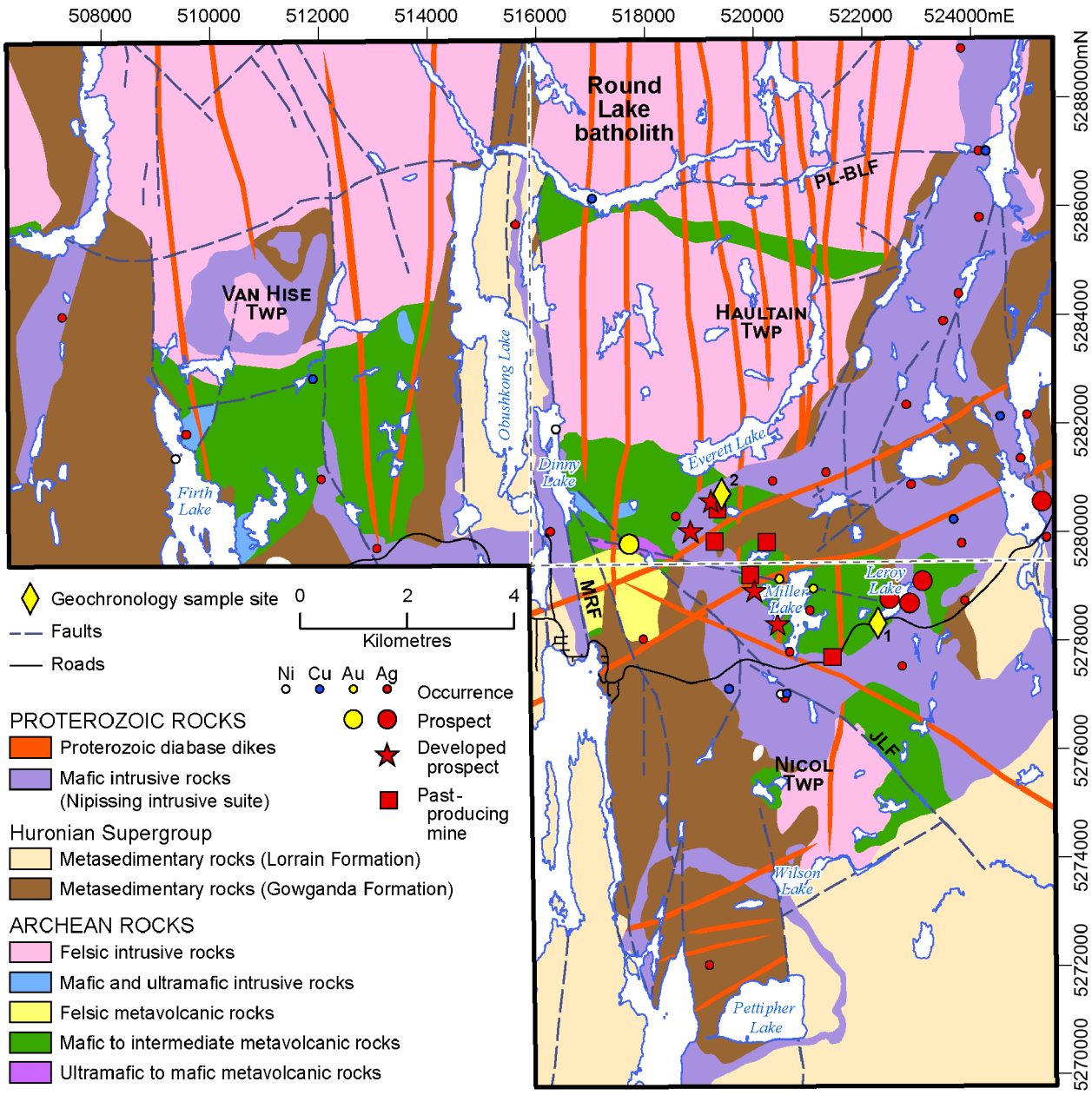


Figure 8.2. Simplified lithological map of the project area (UTM co-ordinates provided in NAD83, Zone 17). Geochronology sample locations are shown; *see* Table 8.1 for additional information. Ontario Mineral Inventory (OMI) occurrences, prospects and past-producing mines (Ontario Geological Survey 2023) show the primary commodities. Abbreviations: Ag, silver; Au, gold; Cu, copper; Ni, nickel; JLF, Jacobs Lake fault; MRF, Montreal River fault; PL-BLF, Penassi Lake–Bloom Lake fault.

Table 8.1. Summary of U/Pb ages for samples collected in Haultain and Nicol townships. Sample locations for numbers 1 and 2 are shown in Figure 8.2; "NS" is not shown because it is not an emplacement age.

No. on Figure 8.2	Mineral	Age (in Ma)	Method	Interpretation	Rock Type	Easting (m)	Northing (m)	Source
1	Zircon	2719.1±1.1	ID-TIMS	Youngest detrital grains (n=3)	Sandstone	522299	5278304	Ketchum (2002)
2	Baddeleyite	2217.5±1.6	ID-TIMS	Emplacement	Gabbro	519425	5280689	Corfu and Andrews (1986)
NS	Zircon	2703.7±2.3	ID-TIMS	Inheritance	Syenite dike	517545	5279760	Ayer et al. (2013)

Abbreviations: *ID-TIMS = isotope dilution thermal ionization mass spectrometry; NS, not shown on Figure 8.2.*
Note: *Locations are provided as UTM co-ordinates in NAD83, Zone 17.*

The extent of the ultramafic metavolcanic rocks is not well constrained. Ultramafic metavolcanic rocks have been observed in southwestern Haultain Township (*see* Figure 8.2), where they are dark grey, weakly to strongly foliated, and very fine grained. They are sporadically fragmental, with centimetre-scale fragments being angular to subangular, monolithic and many are interlocking. Rare spinifex-textured komatiites have been observed, with spinifex laths up to 3 cm long.

Mafic to intermediate metavolcanic rocks within Haultain, Nicol and Van Hise townships are typically dark to medium grey, strongly foliated and very fine-grained, although locally, they can coarsen to medium grained. Rare occurrences of pillows (Photo 8.1A), observed east of Miller Lake, are poorly developed, ameboid and decimetre in scale. The magnetic susceptibility of these rocks can vary widely, even on a single outcrop. This may be the result of a fragmental nature of the rock, which is difficult to perceive on outcrop because of strong deformation and/or perhaps because of alteration (*see* "Alteration and Metamorphism"). More investigation is needed to fully understand the magnetic susceptibility of these rocks.

Felsic to intermediate metavolcanic rocks are largely restricted to an area in northwestern Nicol Township (*see* Figure 8.2). They are largely light to medium grey, weakly foliated, very fine-grained crystal tuffs and lapilli tuffs. The quartz and feldspar crystals are millimetres in scale and comprise 20 to 30 modal % of the rock. Collins (1913) and Burrows (1926) suggested that these rocks are intrusive; however, no intrusive contacts were observed this summer and the occurrence of tuffaceous rocks suggests at least part of the area is extrusive. Nevertheless, an intrusive component cannot be ruled out at the moment.

Archean Metasedimentary Rocks

Archean metasedimentary rocks occur as clastic metasedimentary rocks and chemical metasedimentary rocks. The clastic metasedimentary rocks occur as narrow interflow units within the mafic to intermediate metavolcanic rocks in Nicol Township (Photo 8.1B). They are commonly well-sorted, very thinly parallel planar bedded sandstones. A U/Pb analysis of zircon from a sandstone in Nicol Township using isotope dilution thermal ionization mass spectrometry yielded an age of 2719.1±1.1 Ma, based on 3 concordant grains (Ketchum 2002) (*see* Figure 8.2; Table 8.1). This age was interpreted to belong to the Kidd–Munro episode (2720–2710 Ma) (Ketchum 2002); however, it could also be interpreted as part of the 2723–2720 Ma episode (Stoughton–Roquemaure) because the age lies within error of the boundary between the 2 episodes (i.e., 2720 Ma). The chemical metasedimentary rocks occur as ironstone in northwestern Nicol Township (McIlwaine 1978), but were not observed during the field season.

Archean Intrusive Rocks

Archean intrusive rocks within the project area include ultramafic intrusions, small gabbroic intrusions, large granitic bodies, such as the Round Lake batholith and the Wilson Lake area granitic rocks (*see* Figure 8.2), and smaller felsic intrusive rocks.

Ultramafic intrusive rocks are observed in south-central Van Hise Township and southwestern Haultain Township and are reported to occur in southwestern Van Hise Township (McIlwaine 1978). They are dark greenish-grey, fine-grained, massive peridotites to dunites with serpentine and talc alteration (Photo 8.1C). The outcrops are generally a distinctive rusty brown, rounded and display cooling fractures.

Mafic intrusive rocks that are spatially associated with the ultramafic intrusive rocks in central Van Hise Township are medium to dark grey, massive to locally foliated, medium-grained gabbro.

The Round Lake batholith can be subdivided spatially into 2 distinct compositional phases (McIlwaine 1978): quartz diorite and tonalite. In northern Haultain Township, the rocks observed tend to be light grey to pink, medium-grained, massive to locally foliated hornblende ± biotite quartz diorite. In central to western Haultain Township and within Van Hise Township, the rocks observed are light pink, massive, medium-grained hornblende tonalite. Previous work (McIlwaine 1978) found no potassic feldspar in stained thin sections in either rock types.

The Wilson Lake area granitic rocks occur north of Wilson Lake in central Nicol Township (*see* Figure 8.2). The rocks observed are commonly light grey to light pink, massive, medium-grained tonalite to monzonite.

Small feldspar porphyry dikes that intruded the metavolcanic rocks are common and range in thickness from centimetre to metre scale. They are foliated, pink to beige, with millimetre- to centimetre-scale euhedral to anhedral plagioclase phenocrysts.

Syenitic dikes have been observed sporadically in Haultain and Nicol townships. Where observed, they occur most commonly near the ultramafic metavolcanic rocks in southwestern Haultain Township, but are also observed in central Haultain Township and northern Nicol Township. Those observed are reddish pink, medium grained and massive, and locally contain coarse phenocrysts of biotite. Ayer et al. (2013, p.11, p.130) attempted to obtain an age from a syenite dike from the Haultain Township, but the 2703 Ma age they obtained was interpreted to be the result of inheritance, and not the age of dike emplacement. Lamprophyre dikes are uncommon in the project area, only having been observed occurring spatially associated with the syenitic dikes in southwestern Haultain Township. They are dark grey, fine to medium grained, massive and biotite rich. More investigation is needed to better understand the composition and overall relationships of these 2 types of dikes.

Proterozoic Sedimentary Rocks (Cobalt Group)

The Huronian Supergroup comprises 4 stratigraphic groups; from oldest to youngest, these are the Elliot Lake Group, Hough Lake Group, Quirke Lake Group and Cobalt Group (Robertson, Card and Frarey 1969). The Cobalt Group is the only group observed in the area and is subdivided into 4 formations: Gowganda, Lorrain, Gordon Lake and Bar River (Robertson, Card and Frarey 1969). Only the Gowganda Formation, with the Coleman Member and the Firstbrook Member (Robertson, Card and Frarey 1969), and the Lorrain Formation are observed in the map area. The Coleman Member is observed in southeastern Van Hise Township, southern, eastern and northeastern Haultain Township, and northern Nicol Township. The rocks observed are medium-grey, thinly bedded sandstones, wackes, conglomeratic

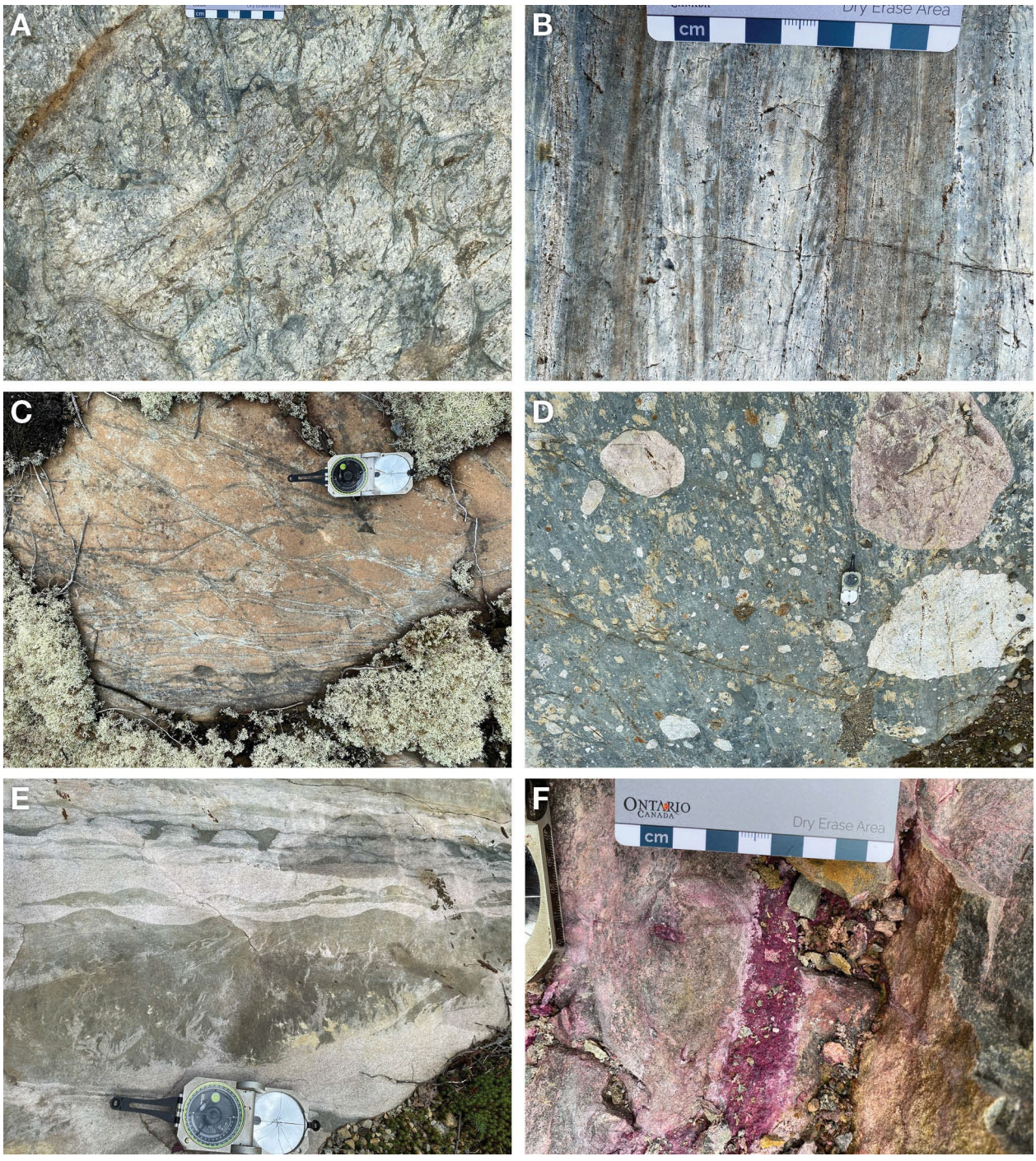


Photo 8.1. Photographs of rock units located Van Hise, Haultain and Nicol townships. **A)** Mafic pillow basalts (UTM 521885E 5278233N). **B)** Very thinly bedded Archean interflow sandstone (UTM 522291E 5278298N). **C)** Ultramafic intrusive rock displaying typical rusty brown weathering and cooling fractures (UTM 513573E 5284053N). **D)** Matrix-supported polymictic conglomerate of the Coleman Member, Gowganda Formation (UTM 520288E 5279811N). **E)** Ripple marks and soft sediment deformation features, including flame structures, in sandstones and siltstones of the Coleman Member, Gowganda Formation (UTM 520288E 5279811N). **F)** Polymetallic vein with pink colouration resulting from the presence of erythrite (UTM 520288E 5279811N). All UTM co-ordinates provided using NAD83 in Zone 17. Compass for scale in photos 8.1C, 8.1D and 8.1E is 6.9 cm wide and sighting arm points north.

sandstones or poorly sorted, matrix-supported thickly bedded to massive polymictic conglomerates (Photo 8.1D). The sandstones locally display ripple marks or soft sediment deformation structures (Photo 8.1E). The Firstbrook Member is observed in southeastern Van Hise Township and northeastern Nicol Township; the rocks are thickly laminated to thinly bedded reddish-grey, purplish and grey siltstones. The Lorrain Formation is observed in northeastern Nicol Township as light grey, massive to thickly bedded sandstones.

Proterozoic Intrusive Rocks

The Nipissing intrusive suite (2217.5±1.6 Ma: Corfu and Andrews 1986; *see* Table 8.1) in the project area occurs as gabbroic sills and dikes, locally having a saucer-shape form, that primarily intruded the rocks of the Huronian Supergroup and, to a lesser degree, Archean supracrustal and intrusive rocks. They occur as dark grey, massive, medium-grained, locally granophyric pyroxene gabbro to hornblende gabbro.

Proterozoic mafic dikes are abundant in the project area and can be delineated by their aeromagnetic signatures (Ontario Geological Survey 2017). The north-trending dikes are most common and are interpreted to be part of the Matachewan dike swarm (*circa* 2460 Ma: Bleeker et al. 2015) that intrudes all Archean rocks. The northeastern-trending dikes are interpreted to be part of the Biscotasing dike swarm (*circa* 2170 Ma: Buchan, Mortensen and Card 1993) and the northwestern-trending dikes are interpreted to be part of the Sudbury dike swarm (*circa* 1240 Ma: Krogh et al. 1988). Both the Biscotasing and Sudbury dike swarms crosscut Archean rocks, as well as the Proterozoic Huronian Supergroup sedimentary rocks and the Nipissing intrusive suite. All of these dikes range from several metres to tens of metres in thickness. Dikes of the Matachewan and Biscotasing swarms are composed of a fine- to medium-grained, massive, dark grey, locally plagioclase-phyric, gabbro. In contrast, dikes of the Sudbury dike swarm are composed of fine- to medium-grained, grey olivine gabbro.

STRUCTURAL GEOLOGY

The mafic to intermediate metavolcanic rocks in the project area are moderately to strongly foliated, with the dominant foliation changing direction from west-trending in Haultain and Van Hise townships to north-trending near Wilson Lake; this directional change suggests a major fold. Additional evidence for folding includes outcrop-scale parasitic folds and scattered perpendicular topping indicators. The felsic metavolcanic rocks locally have a northwest trend that may be related to the Jacobs Lake fault (*see* Figure 8.2). The mafic to intermediate metavolcanic rocks near Miller Lake have various foliation directions that may indicate folding or shearing. Further work is needed to fully understand the causes of the changes in foliation directions.

Faulting of varying scale occurs in the Archean supracrustal rocks and minor faulting is observed in the Proterozoic metasedimentary rocks. Faults in the project area trend in 3 main directions: north, northwest and east, with rare northeast-trending faults having been noted by previous workers (McIlwaine 1978). North-trending faults, such as the Montreal River fault (*see* Figure 8.2), appear to have influenced the deposition of the Huronian Supergroup sedimentary rocks. Northwest-trending faults, such as the Jacobs Lake fault (*see* Figure 8.2), appear to truncate the area of felsic metavolcanic rocks, as well as the Wilson Lake area granitic rocks. The east-trending Penassi Lake–Bloom Lake fault (*see* Figure 8.2) reportedly extends nearly the entire length of the project area (McIlwaine 1978), but was not observed during the reconnaissance mapping. There is some preliminary evidence for a deformation zone, extending east-southeast from south of Dinny Lake to potentially as far as Leroy Lake, which includes shearing, folding and alteration with local mineralization. Further work will be needed to validate or disprove the existence of this deformation zone.

ALTERATION AND METAMORPHISM

Alteration minerals identified in the field are albite, ankerite, calcite, chlorite, epidote, fuchsite, hematite, magnetite, pyrite, serpentine and talc. Pervasive ankerite-albite-pyrite, calcite-magnetite and fuchsite alteration appear to be spatially associated with gold mineralization. Serpentine and talc alteration were associated with the ultramafic rocks. Epidote, hematite and chlorite alteration occurred locally. No alteration was observed associated with five-element veins found in proximity to the Nipissing mafic sills.

In the project area, regional metamorphism is characterized by chlorite in the greenschist facies mafic metavolcanic rocks and as garnet in the narrow belt of amphibolite facies mafic metavolcanic rocks in northern Haultain Township. A narrow contact aureole, up to 50 m wide, occurs adjacent to the Nipissing sills.

MINERALIZATION

Mineralization in the project area is dominated by five-element vein-style mineralization associated with the Nipissing intrusive suite and gold mineralization associated with the Archean rocks. Notable mineral occurrences within the project area are shown on Figure 8.2.

Silver and cobalt mineralization occurs in polymetallic veins, interpreted to be five-element vein systems (e.g., Kissin 1992; Conrod 1989). These can be difficult to define, but typically includes nickel-cobalt-silver-arsenic mineralization, as well as various other phases, such as bismuth, commonly hosted in a carbonate vein (Kissin 1992). This style of mineralization was first discovered in Haultain Township in 1907 and led to the development of several past-producing mines (*see* Figure 8.2; McIlwaine 1978). Veins observed within the project area are millimetres to centimetres in scale, appear to pinch and swell, and can be bright pink because of the presence of erythrite (Photo 8.1F).

Gold mineralization was first discovered in the project area in 2006 by S. Swain (Swain 2009). Following the initial discovery, various parties continued to explore for gold, with some notable discoveries (*see* Figure 8.2). Gold mineralization appears spatially associated with strong alterations (*see* "Alteration and Metamorphism"); syenitic dikes are present locally. The mineralization occurs in quartz-carbonate veins and disseminated sulphides in the host rock (Transition Metals Corp., news release, November 7, 2011; Ayer et al. 2013, p.128-135).

ACKNOWLEDGMENTS

This mapping project has benefitted from the assistance of Michelle Cong-Bowers and Rizzi Balestra. Sonia Préfontaine, Manuel Duguet, George Gao and Lise Robichaud (OGS) are thanked for their valuable insight, interpretation and discussions. Sherry Swain and the exploration crews at Canada Silver Cobalt Works and Transition Metals are thanked for sharing their knowledge about local geology. Thanks go to Pat Gervais for drafting the figures of this report. Temagami First Nation/Teme-Augama Anishnabai, Matachewan First Nation and Abitibi Inland Historic Métis Community are thanked for allowing the Ontario Geological Survey to map their traditional land use area. Thanks are extended to Urs and Dianne of Auld Reekie Lodge for providing excellent accommodations for the field season.

REFERENCES

Ayer, J.A., Barrett, T.J., Creaser, R.A., Hamilton, M.A., Lafrance, B. and Stott, G.M. 2013. Section 1: Shining Tree and Gowganda Archean gold study and northern Cobalt Embayment Proterozoic vein study; report *in* Results from the Shining Tree, Chester Township and Matachewan Gold Projects and the Northern Cobalt Embayment Polymetallic Vein Project, Ontario Geological Survey, Miscellaneous Release—Data 294.

Ayer, J.A., Ketchum, J.W.F. and Trowell, N.F. 2002. New geochronological and neodymium isotopic results from the Abitibi greenstone belt, with emphasis on the timing and the tectonic implications of Neoarchean sedimentation and volcanism; *in* Summary of Field Work and Other Activities, 2002, Open File Report 6100, p.5-1 to 5-16.

Bleeker, W., Kamo, S.L., Ames, D.E. and Davis, D.[W.] 2015. New field observations and U-Pb ages in the Sudbury area: Toward a detailed cross-section through the deformed Sudbury Structure; *in* Targeted Geoscience Initiative 4: Canadian Nickel-Copper-Platinum Group Elements-Chromium Ore Systems – Fertility, Pathfinders, New and Revised Models, Geological Survey of Canada, Open File 7856, p.151-156.

Buchan, K.L., Mortensen, J.K. and Card, K.D. 1993. Northeast-trending Early Proterozoic dykes of southern Superior Province: Multiple episodes of emplacement recognized from integrated paleomagnetism and U–Pb geochronology; Canadian Journal of Earth Sciences, v.30, p.1286-1296.

Burrows, A.G. 1926. Gowganda silver area (fourth report, revised); Ontario Department of Mines, Annual Report, 1926, v.35, pt.3, p.1-61.

Collins, W.H. 1913. The geology of Gowganda Mining Division; Geological Survey of Canada, Memoir 33, p.121.

Conrod, D.M. 1989. Petrology and geochemistry of the Duncan Lake, Beaton Bay, Milner Lake, and Miller Lake Nipissing Intrusions within the Gowganda area; Ontario Geological Survey, Open File Report 5701, 210p.

Corfu, F. and Andrews, A.J. 1986. A U–Pb age for mineralized Nipissing diabase, Gowganda, Ontario; Canadian Journal of Earth Sciences, v.23, p.107-109.

Ketchum, J.W.F. 2002. U-Pb geochronological data from the Superior and Grenville Provinces of Ontario; unpublished report, Jack Satterly Geochronology Laboratory, Royal Ontario Museum, Toronto, p.14p.

Ketchum, J.W.F., Ayer, J.A., van Breemen, O., Pearson, N.J. and Becker, J.K. 2008. Pericontinental crustal growth of the southwestern Abitibi Subprovince, Canada—U-Pb, Hf, and Nd isotope evidence; Economic Geology, v.103, p.1151-1184.

Ketchum, J.W.F., Kamo, S.L. and Davis, D.W. 2003. U-Pb ages from the Superior and Grenville provinces of Ontario; unpublished report, Jack Satterly Geochronology Laboratory, Royal Ontario Museum, Toronto, 41p.

Kissin, S.A. 1992. Five-element (Ni-Co-As-Ag-Bi) veins; Geoscience Canada, v.19, p.113-124.

Krogh, T.E., Corfu, F., Davis, D.W., Dunning, G.R., Heaman, L.M., Kamo, S.L., Machado, N., Greenough, J.D. and Nakamura, E. 1988. Precise U-Pb isotopic ages of diabase dykes and mafic to ultramafic rocks using trace amounts of baddeleyite and zircon; *in* Mafic Dyke Swarms, Geological Association of Canada, Special Paper 34, p.147-152.

McIlwaine, W.H. 1978. Geology of the Gowganda Lake – Miller Lake Silver Area, District of Timiskaming; Ontario Geological Survey, Report 175, p.1-161.

Monecke, T., Mercier-Langevin, P., Dubé, B. and Frieman, B.M. 2017. Geology of the Abitibi greenstone belt; Chapter 1 *in* Abitibi Base and Precious Metal Deposits, Southern Abitibi Greenstone Belt, Canada Society of Economic Geologists, Reviews in Economic Geology, v.19, p.7-49.

Mortensen, J.K. 1993. U–Pb geochronology of the eastern Abitibi Subprovince, part 2: Noranda–Kirkland Lake area; Canadian Journal of Earth Sciences, v.30, p.29-41.

Ontario Geological Survey 2011. 1:250 000 scale bedrock geology of Ontario; Ontario Geological Survey, Miscellaneous Release—Data 126 – Revision 1.

——— 2017. Report on magnetic supergrids, 14p. [PDF document]; report *in* Ontario airborne geophysical surveys, magnetic data, grid data (ASCII and Geosoft® formats), magnetic supergrids; Ontario Geological Survey, Geophysical Data Set 1037—Revised.

——— 2023. Ontario Mineral Inventory; Ontario Geological Survey, online database, September 2023 update, www.hub.geologyontario.mines.gov.on.ca. [accessed September 27, 2023]

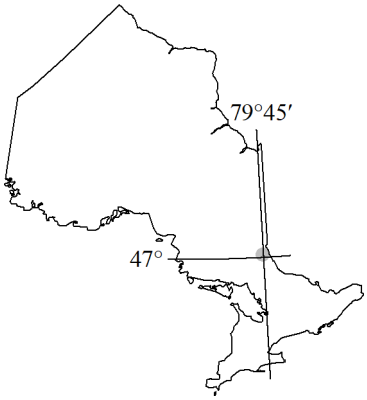
Robertson, J.A., Card, K.D. and Frarey, M.J. 1969. The federal–provincial committee on Huronian stratigraphy progress report; Ontario Department of Mines, Miscellaneous Paper 31, 26p.

Sergiades, A.O. 1968. Silver cobalt calcite vein deposits of Ontario; Ontario Department of Mines, Mineral Resources Circular 10, 498p.

Swain, S.L. 2009. Mechanical stripping and prospecting, Haultain and Nicol townships, Larder Lake Division, Claim 1248799; Kirkland Lake Resident Geologist's office, assessment file AFRO# 2.43150 AFRI# 20000005351, 13p.

Thurston, P.C., Ayer, J.A., Goutier, J. and Hamilton, M.A. 2008. Depositional gaps in Abitibi greenstone belt stratigraphy: A key to exploration for syngenetic mineralization; Economic Geology, v.103, p.1097-1134.

9. Project NE-23-001. Geology of Strathy Township, Temagami Greenstone Belt, Northeastern Ontario



P.J. MacDonald[1]

[1]Earth Resources and Geoscience Mapping Section, Ontario Geological Survey

INTRODUCTION

The Temagami greenstone belt bedrock geology mapping project is a multi-year project initiated in 2019 by the Earth Resources and Geoscience Mapping Section of the Ontario Geological Survey (*see* MacDonald 2019; MacDonald and Kamo 2021). The objectives are to 1) update township-scale bedrock geology maps, 2) investigate the geological architecture, 3) seek correlation with Abitibi greenstone belt chronostratigraphic episodes, if possible, and 4) document geological controls on mineralization.

Field work during the summer of 2023 focussed on 1:20 000 scale bedrock geology mapping in Strathy Township and the western part of Cassels Township (Figure 9.1). This article presents a brief summary of the main rock types and the geology of chosen abandoned mine sites in the study area, including select geochemical data from the Kanichee Mine site area (*see* Figure 9.1, abandoned mine site #1).

GEOLOGY OF STRATHY TOWNSHIP AND WESTERN CASSELS TOWNSHIP

The Temagami greenstone belt is a Neoarchean granite-greenstone inlier surrounded by Paleoproterozoic Huronian Supergroup metasedimentary rocks (Bennett, Dressler and Robertson 1991; Ayer et al. 2006). Based on available geochronological data, the Archean rocks of the Temagami greenstone belt correlate with multiple chronostratigraphic episodes and plutonic rock groups of the Abitibi greenstone belt (Ayer et al. 2006). The volcanic episodes in the Abitibi greenstone belt are most recently defined by Thurston et al. (2008, and references therein) and Monecke et al. (2017, and references therein). These are pre-2750 Ma (pre-Pacaud) episode, 2750–2735 Ma (Pacaud) episode, 2734–2724 Ma (Deloro) episode, 2723–2720 Ma (Stoughton–Roquemaure) episode, 2719–2711 Ma (Kidd–Munro) episode, 2710–2704 Ma (Tisdale) episode and 2704–2695 Ma (Blake River) episode. This section summarizes the supracrustal and intrusive rocks observed in Strathy Township and the western part of Cassels Township in the context of Abitibi greenstone belt chronostratigraphic episodes and plutonic groups, as well as Proterozoic metasedimentary and intrusive rocks.

Archean Supracrustal Rocks

Metavolcanic rocks throughout northwestern Strathy Township that are correlative with the pre-2750 Ma volcanic episode of the Abitibi greenstone belt (*see* Figure 9.1; Ayer et al. 2006; MacDonald and Kamo 2021). This metavolcanic package is constrained to the north by intrusive rocks of the Strathy–Chambers Batholith and Nipissing gabbro intrusive suite, and to the southeast by the Net–Vermilion

Summary of Field Work and Other Activities, 2023,
Ontario Geological Survey, Open File Report 6405, p.9-1 to 9-8.

© King's Printer for Ontario, 2023

deformation zone (*see* Figure 9.1). The package is primarily composed of south-southeast facing, calc-alkaline intermediate metavolcanic rocks, with minor basalt flows throughout, and near the top stratigraphically, thinly laminated rhyolite volcaniclastic beds (Photo 9.1A). Magnetic-jasper-chert ironstone occurs at the top of this metavolcanic package in southwestern Strathy Township (*see* Figure 9.1). Sulphide minerals are generally in low abundances throughout the package, with the exception of gossanous intermediate to felsic units proximal to Archean mafic intrusions, and minor sulphidized ironstone.

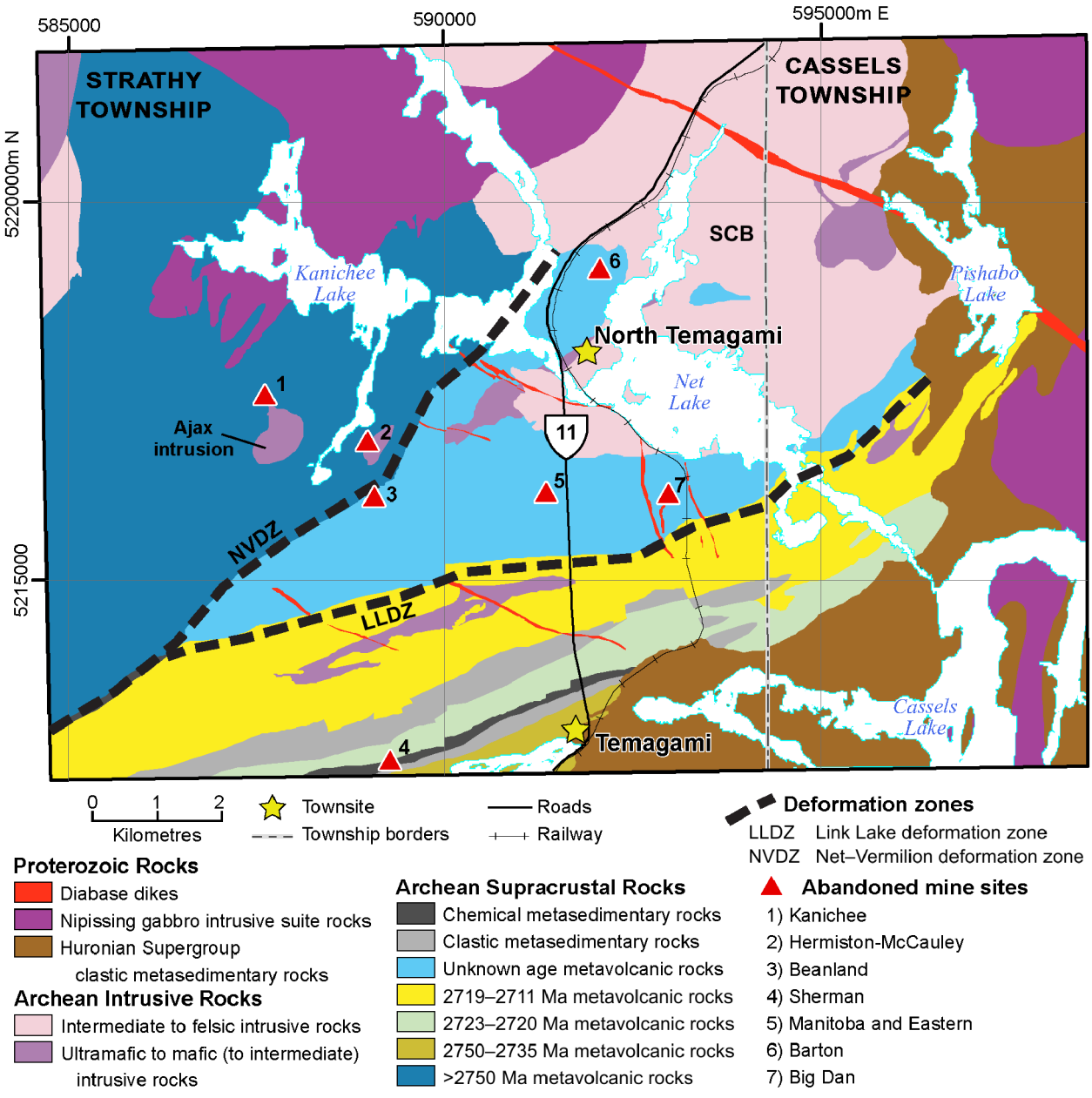


Figure 9.1. Simplified geological map of Strathy Township and western Cassels Township showing supracrustal rock units, major deformation zones and the locations of visited abandoned mine sites based on Abandoned Mines Information System (Mineral Development and Lands Branch 2022). Abbreviation: SCB, Strathy–Chambers Batholith. Location information provided as Universal Transverse Mercator (UTM) co-ordinates using North American Datum 1983 (NAD83) in Zone 17 (geology *modified from* Ayer et al. 2006).



Photo 9.1. Selected photographs of lithological features observed in Strathy Township and western Cassels Township. **A**) Thinly laminated rhyolite tuff (UTM 588646E 5217944N). **B**) Pillowed basalt flow (UTM 592626E 5215287N). **C**) Strongly deformed intermediate metavolcanic rock (UTM 589834E 5214284N). **D**) Thinly bedded siltstone grading to sandstone (UTM 591734E 5214025N). **E**) Chalcopyrite bleb within Strathy–Chambers Batholith granite (UTM 592058E 5219647N). **F**) Clast-supported polymictic conglomerate of Gowganda Formation (UTM 591919E 5213158N). Compass for scale is 22 cm long; compass point is 1 cm wide; compass points north. Location information provided as UTM co-ordinates using NAD83 in Zone 17.

Metavolcanic rocks exposed directly east of the pre-2750 Ma episode metavolcanic rocks across the Net–Vermilion deformation zone are of unknown age (*see* Figure 9.1). Termed the Arsenic Lake formation (Fyon and Crocket 1986), this package of metavolcanic rocks is bound to the northwest by the Net–Vermilion deformation zone, to the south by the Link Lake deformation zone and to the northeast by felsic to intermediate intrusive rocks of the Strathy–Chambers Batholith (*see* Figure 9.1). The Arsenic Lake formation is composed of tholeiitic massive and pillowed basalt flows (Photo 9.1B) and flow breccias. Abundant sulphide minerals and gossanous staining is a characteristic feature of the Arsenic Lake formation, with 1 to 5 cm diameter pyrite ± pyrrhotite-chalcopyrite-arsenopyrite-galena-molybdenite clots observed in most outcrop exposures.

Metavolcanic rocks, observed across southern Strathy Township and west-central Cassels Township, possibly correlative with the 2719–2711 Ma episode, have a reported age *circa* 2717 Ma for a felsic metavolcanic rock (*see* Figure 9.1; Ayer et al. 2006). This package is bound to the north by both the metavolcanic packages described above, and to the south by siliciclastic rocks (*see* Figure 9.1). It is composed of calc-alkalic intermediate to felsic metavolcanic rocks, with most primary features destroyed by strong, penetrative deformation related to the Link Lake deformation zone (Photo 9.1C). Disseminated sulphide mineralization (i.e., pyrite and sphalerite) is locally observed and is interpreted to be formed by fluids related to hydrothermal vents (Fyon and Crocket 1986) or more commonly to late, deformation-related hydrothermal iron-carbonate alteration.

Metasedimentary and metavolcanic rocks, observed from south-central Strathy Township to southwestern Cassels Township, are correlative with the 2723–2720 Ma episode, with a minimum depositional age reported at 2721.5±1.1 Ma for a sandstone (Ayer et al. 2006). The unit is located in the core of a syncline, with siliciclastic rocks at the stratigraphic base and tholeiitic basalts at the top. It is bound to the north by the strongly deformed 2719–2711 Ma episode metavolcanic rocks, to the south by 2750–2735 Ma episode metavolcanic rocks, and in the east is covered by Huronian Supergroup metasedimentary rocks (*see* Figure 9.1). The basal siliciclastic rocks are thin beds of mudstone to siltstone grading to sandstone (Photo 9.1D), overlain on the south limb by magnetite-jasper-chert ironstone. The top of the package is tholeiitic massive and pillowed basalt flows. Sulphide minerals (i.e., pyrite and pyrrhotite) are restricted to local, minor replacement of ironstone.

The last package of metavolcanic rocks, observed in south-central Strathy Township, is correlative with the 2750–2735 Ma episode (*see* Figure 9.1), with a reported age 2736 $^{+3}/_{-1}$ Ma for a felsic porphyritic flow (Bowins and Heaman 1991) collected to the south of Strathy Township. The metavolcanic package is bound to the north by the siliciclastic rocks discussed above, and is concealed to the east by Huronian Supergroup metasedimentary rocks. This rock package is composed of deformed calc-alkalic volcaniclastic rocks including lapilli-tuffs and breccias. Significant disseminated pyrite is locally observed, resulting in gossanous pods within outcrop exposures.

Archean Intrusive Rocks

Archean mafic intrusions in Strathy Township and western Cassels Township can be subdivided into 2 types based on composition. The first type comprises mafic to ultramafic intrusions located in central Strathy Township, the largest of which is the Ajax intrusion hosting the Kanichee Mine (*see* Figure 9.1). The intrusions are predominantly gabbro or pyroxenite, with lesser peridotite and anorthosite, and have geochemical affinities ranging from tholeiitic to komatiitic (Bennett 1978; James and Hawke 1984; Good 1989, and references therein). Nickel-copper-platinum group element mineralization is commonly associated with these intrusions. The mafic to ultramafic intrusions were emplaced during different episodes, suggesting they are younger than most, if not all of the metavolcanic rock packages.

The second type comprises mafic to intermediate intrusions located proximal to the 2 main deformation zones (Net–Vermilion and Link Lake deformation zones; *see* Figure 9.1). These intrusions are diorite or leucogabbroic, and have calc-alkalic geochemical affinities (Fyon and Crockett 1986). Gold mineralization is associated commonly with these more siliceous mafic intrusions. These intrusions are located within deformation zones and their elongate shape suggests they intruded during to late in the deformation event. The age of the mafic to intermediate intrusions is constrained by a porphyry dike with an age of 2687±2 Ma (Bowins and Heaman 1991) that crosscuts a diorite intrusion with the Link shear zone.

Felsic (to intermediate) Archean intrusions are observed throughout Strathy Township and western Cassels Township. The largest of these intrusions is the Strathy–Chambers Batholith, exposed in northern Strathy Township and northwestern Cassels Township. The batholith is typically medium-grained, biotite- and or hornblende-bearing quartz monzonite to granite (Bennett 1978). Disseminated, blebby and quartz veinlet–related pyrite, chalcopyrite and molybdenite mineralization is common in northeast Strathy Township (Photo 9.1E). The Strathy–Chambers Batholith is syntectonic, with a reported age of 2694.5±1.1 Ma from a sample collected in Chambers Township (MacDonald and Kamo 2021).

Proterozoic Rocks

Huronian Supergroup metasedimentary rocks of the Gowganda Formation (Cobalt Group; Bennett, Dressler and Robertson 1991) occur in southeastern Strathy Township and western Cassels Township (*see* Figure 9.1). Overall stratigraphic facing is to the east. The rocks are typically matrix-supported conglomerates, except near the Archean–Proterozoic unconformity. Proximal to the unconformity, the Gowganda Formation consists of clast-supported polymictic conglomerates with varied amounts of cobble-, pebble- and boulder-sized, rounded granitoid clasts and lesser metavolcanic clasts in a weakly chloritized mudstone matrix (Photo 9.1F). Bedding within the Gowganda Formation is generally subhorizontal with minor open folds. A well-developed vertical cleavage is present locally in exposures in and around the townsite of Temagami (*see* Figure 9.1), suggesting that at least 1 phase of penetrative deformation postdates deposition.

Proterozoic mafic intrusions include Nipissing intrusive suite gabbro sills and Sudbury swarm diabase dikes (*see* Figure 9.1). The Nipissing intrusive suite rocks have intruded Gowganda Formation metasedimentary rocks in Cassels Township, as well as pre-2750 Ma episode metavolcanic rocks in northern Strathy Township. The Nipissing intrusive suite rocks are medium-grained plagioclase- and pyroxene-bearing gabbros, and based on ages from Nipissing sills located in different parts of the Southern Province, were emplaced at 2215±2 Ma (Davey et al. 2019). Northwest-trending Sudbury diabase dikes are located throughout Strathy Township and western Cassels Township. These diabase dikes are observed most easily in roadcuts along Highway 11, crosscutting the granites in northern Strathy Township. They are composed of olivine-bearing gabbro that vary from very fine to medium grained depending on the width of the dike. The Sudbury diabase dike swarm has an age of 1238.5±4 Ma (Krogh et al. 1987).

GEOLOGY OF ABANDONED MINES SITES IN STRATHY TOWNSHIP

In Strathy Township, 7 abandoned mine sites were visited. The abandoned mine sites include a nickel-copper-platinum group element (PGE) mine, 4 gold ± silver developed prospects, an iron mine and a molybdenum developed prospect. The location of the visited abandoned mine sites are shown on Figure 9.1. Observations of each mine's mineralization style was collected from bedrock exposures and mined rock piles, and is briefly summarized.

Table 9.1. Selected geochemical data from the Kanichee Mine area.

Sample No.	Rock Type	Easting[1]	Northing[1]	Au (ppm)	Bi (ppm)	Co (ppm)	Cu (ppm)	Ni (ppm)	Pd (ppm)	Pt (ppm)	Se (ppm)	Te (ppm)
Detection Limit:				***<0.003***	***<0.02***	***<0.2***	***<0.6***	***<2***	***<0.02***	***<0.005***	***<0.2***	***<0.04***
19PM506	Gabbro	587710	5217587	<0.003	0.39	232.4	143	832	<0.02	<0.005	0.3	0.11
19PM511	Metadacite	588372	5218038	3.106	0.37	11.1	23	72	<0.02	0.009	<0.2	<0.04
22PMT001	Peridotite	587633	5217361	0.021	0.89	110.5	455.3	1445	0.05	0.023	0.6	0.08
22PMT002	Peridotite	587635	5217354	0.06	5.56	257.5	4616.1	5073	0.48	0.102	3.4	0.52
22PMT002*	Peridotite	587635	5217354	0.039	5.57	256	4612.2	4965	0.44	0.102	3.6	0.53
22PMT003	Pyroxenite	587614	5217354	0.003	0.68	89.1	355.9	1027	0.05	0.012	0.4	0.13
22PMT005	Peridotite	587571	5217427	<0.003	0.02	49.5	2.4	838	0.02	0.007	<0.2	<0.04
22PMT006	Gabbro	587572	5217427	0.097	1.89	191.9	6690.4	4847	1.02	0.19	5.6	1.79
22PMT006*	Gabbro	587635	5217354	0.192	1.9	185.6	6538.9	4744	1.01	0.183	5.7	1.71
22PMT007	Peridotite	587576	5217386	0.007	0.67	149.8	487.2	2203	0.07	0.02	0.7	0.13
22PMT009	Vein	587580	5217403	0.671	107.87	2497	1430.4	>22000	29.28	1.347	>90	53.69
22PMT011	Serpentinite	587530	5217200	0.107	7.13	196.5	10835.6	4316	2.99	0.95	7.2	4.16
22PMT012	Vein	587581	5217402	21.596	29.81	265.3	>12000	8877	7.6	0.222	25.5	16.01

Analyses completed by inductively coupled plasma mass spectrometry (ICP–MS) after a modified aqua regia extraction at the OGS Geoscience Laboratories (method code IML-101: Ontario Geological Survey 2022).

[1] Locations provided as UTM co-ordinates using NAD83 in Zone 17.

***Abbreviations:** *, lab duplicate; Au, gold; Bi, bismuth; Co, cobalt; Cu, copper; Ni, nickel; Pd, palladium; ppm, parts per million; Pt, platinum; Se, selenium; Te, tellurium.*

The Kanichee Mine (Abandoned Mine Identifier 03778), located in central Strathy Township, produced nickel, copper, platinum, palladium, gold and silver, first from underground, then from an open pit (*see* Figure 9.1, abandoned mine site #1). The mine is hosted within a pyroxenite to peridotite lobe along northwestern edge of the Ajax intrusion. Two styles of mineralization were observed along the exposed open pit's southern wall. The 2 styles include early disseminated sulphides and later structurally controlled veins. Preliminary significant assays collect by this project in and around the Kanichee Mine are reported in Table 9.1. A preliminary interpretation suggests early disseminated pyrrhotite, pentlandite and chalcopyrite represent low grade ore (~0.5% Ni and ~0.5% Cu, and <1 ppm total PGE), whereas structurally controlled veins may contain high values of palladium (up to 29.28 ppm Pd), and gold (up to 21.596 ppm Au) associated with anomalous telluride values. Gold mineralization also occurs peripheral to the intrusion within metavolcanic rocks to the north; however, if, and or how, it is related to the geological processes that formed the Kanichee Mine mineralization is unknown. Other anomalous elements from the Kanichee Mine area include bismuth, cobalt and selenium.

There are 4 gold ± silver developed prospect abandoned mine sites in central to eastern Strathy Township that were visited. The Hermiston–McCauley Mine (Abandoned Mine Identifier 03777) is located on the northside of the Net–Vermilion deformation zone, and includes a shaft (*see* Figure 9.1, abandoned mine #2). Based on ore and waste rock piles, gold mineralization is associated with quartz veining and small semi-massive zones of pyrite and arsenopyrite hosted within, or at, the margin of a diorite intrusion that intruded felsic metavolcanic rocks of the pre-2750 Ma episode. The Beanland Mine (Abandoned Mine Identifier 03780) is located south of the Net–Vermilion deformation zone and includes a shaft and small surface pit (*see* Figure 9.1, abandoned mine #3). Based on bedrock exposure along the pit wall and waste rock piles, gold and silver mineralization is associated with a narrow quartz vein (~30 cm thick) and semi-massive sulphides (pyrite, galena and arsenopyrite) hosted within mafic metavolcanic rocks of the Arsenic Lake formation. The trend of mineralization at both the Hermiston–McCauley and Beanland mines is subparallel to the northeast-trending Net–Vermillion deformation zone. The Manitoba and Eastern mines (also known as the Little Dan: Abandoned Mine Identifier 03776) is located near Highway 11 in central Strathy Township and includes 2 shafts and a portal (*see* Figure 9.1, abandoned mine #5). Based on bedrock exposures and mine rock piles, gold and silver mineralization at

Manitoba and Eastern mines is associated with north-trending, semi-massive zones of arsenopyrite, pyrite and chalcopyrite with minor quartz veins, hosted within mafic metavolcanic rocks of the Arsenic Lake formation. The Big Dan Mine (Abandoned Mine Identifier 03779) is located in eastern Strathy Township, just west of the rail line, and includes at least 1 shaft and a portal (*see* Figure 9.1, abandoned mine #7). Based on bedrock exposure and mine rock piles, gold and silver mineralization is associated with a north-trending zone of semi-massive to massive pyrite, pyrrhotite, arsenopyrite and possibly other arsenide minerals, as well as minor quartz veins, hosted within mafic metavolcanic rocks of the Arsenic Lake formation.

The Sherman Mine (Abandoned Mine Identifier 03781) produced iron from 5 pits in southern Strathy Township (*see* Figure 9.1, abandoned mine # 4). The pits were located along 2 stratigraphic horizons of ironstone. Mapping along strike, as well as observations of waste rock, suggest that mineralization was sourced predominantly from thinly laminated massive magnetic beds and jasper beds, interlayered with chert and metavolcanic rocks.

The J.W. Barton mine property (Abandoned Mine Identifier 03787), which is a developed prospect, produced minor amounts of molybdenum from 3 small shafts in northeast Strathy Township (*see* Figure 9.1, abandoned mine #6). The shafts are located within the Arsenic Lake formation metavolcanic rocks, proximal to the Strathy–Chambers Batholith. No mineralized outcrop was observed; however, ore and ore waste rock piled near the shafts suggest molybdenite occurred as disseminated millimetre- to centimetre-sized blebs hosted within narrow, white quartz veins. Molybdenite mineralization within wall rock was not observed, but may also have been mined, because other mineral inventory locations in northeastern Strathy Township have blebby molybdenite mineralization within metavolcanic rocks proximal to quartz veins and disseminated molybdenite within granitic intrusive rocks (Ontario Geological Survey 2023).

ACKNOWLEDGMENTS

The author acknowledges the project is located on the traditional land-use area of Temagami First Nation/Teme-Augama Anishnabai, Matachewan First Nation, Nipissing First Nation, Abitibi Inland Historic Métis Community (MNO Region 3) and Timiskaming First Nation, and is thankful for continued support. The author is grateful to Devon Patterson for field assistance; and to OGS staff: Sonia Préfontaine for scientific review; Darla Bennett for project support; Patrick Gervais for assisting with figures; and Monica Gaiswinkler Easton for editorial assistance. Special thanks to Candice Rogerson and David Schade for their hospitality at Andorra Accessible Cottages.

REFERENCES

Ayer, J.A., Chartrand, J.E., Grabowski, G.P.D., Josey, S., Rainsford, D. and Trowell, N.F. 2006. Geological compilation of the Cobalt–Temagami area, Abitibi greenstone belt; Ontario Geological Survey, Preliminary Map P.3581, scale 1:100 000.

Bennett, G. 1978. Geology of the northeast Temagami area, District of Nipissing; Ontario Geological Survey, Report 163, 128p.

Bennett, G.B., Dressler, B.O. and Robertson, J.A. 1991. The Huronian Supergroup and associated intrusive rocks; *in* Geology of Ontario, Ontario Geological Survey, Special Volume 4, Part 1, p.549-591.

Bowins, R.J. and Heaman, L.M. 1991. Age and timing of igneous activity in the Temagami greenstone belt, Ontario: A preliminary report; Canadian Journal of Earth Sciences, v.28, p.1873-1876.

Davey, S., Bleeker, W., Kamo, S[.L.], Davis, D.[W], Easton, [R.]M. and Sutcliffe, R.H. 2019. Ni-Cu-PGE potential of the Nipissing sills as part of the ca. 2.2 Ga Ungava large igneous province; *in* Targeted Geoscience Initiative: 2018 Report of Activities; Geological Survey of Canada, Open File 8549, p.403-419.

Fyon, J.A. and Crockett, J.H. 1986. Exploration potential for base and precious metal mineralization in part of Strathy Township, Temagami area; Ontario Geological Survey, Open File Report 5591, 46p.

Good, D.J. 1989. Platinum group element distribution in the Kanichee intrusion, District of Nipissing; Ontario Geological Survey, Open File Report 5705, 42p.

James, R.S. and Hawke, D. 1984. Geology and petrogenesis of the Kanichee layered complex, Ontario; The Canadian Mineralogist, v22, p.93-109.

Krogh, T.E., Corfu, F., Davis, D.W., Dunning, G.R., Heaman, L.M., Kamo, S.L., Machado, N., Greenough, J.D. and Nakamura, E. 1987. Precise U-Pb isotopic ages of diabase dykes and mafic to ultramafic rocks using trace amounts of baddeleyite and zircon; *in* Mafic Dyke Swarms, Geological Association of Canada, Special Paper 34, p.147-152.

MacDonald, P.J. 2019. Geological introduction to the Temagami greenstone belt mapping project; *in* Summary of Field Work and Other Activities, 2019, Ontario Geological Survey, Open File Report 6360, p.7-1 to 7-10.

MacDonald, P.J. and Kamo, S.L. 2021. New uranium–lead geochronology from the Temagami greenstone belt, northeastern Ontario; *in* Summary of Field Work and Other Activities, 2021, Ontario Geological Survey, Open File Report 6380, p.8-1 to 8-9.

Mineral Development and Lands Branch 2022. Abandoned Mines Information System; Ministry of Northern Development, Mines, Natural Resources and Forestry, online database, April 2022 update, www.hub.geologyontario.mines.gov.on.ca. [accessed October 13, 2023]

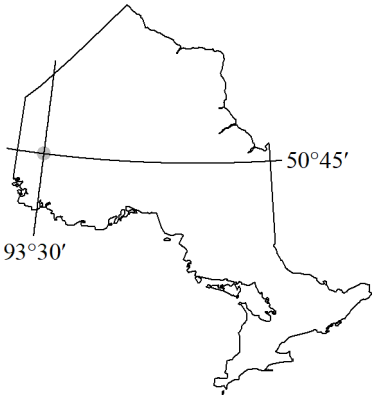
Monecke, T., Mercier-Langevin, P., Dubé, B. and Frieman, B.M. 2017. Geology of the Abitibi greenstone belt; Chapter 1 *in* Abitibi Base and Precious Metal Deposits, Southern Abitibi Greenstone Belt, Canada, Society of Economic Geologists, Reviews in Economic Geology, v.19, p.7-50.

Ontario Geological Survey 2022. Geoscience Laboratories Schedule of Fees and Services; Ontario Geological Survey, Issue 14, 33p.

——— 2023. Ontario Mineral Inventory; Ontario Geological Survey, online database, March 2023 update, www.hub.geologyontario.mines.gov.on.ca. [accessed March 28, 2023]

Thurston, P.C., Ayer, J.A., Goutier, J. and Hamilton, M.A. 2008. Depositional gaps in Abitibi greenstone belt stratigraphy: A key to exploration for syngenetic mineralization; Economic Geology, v.103, p.1097-1134.

10. Project NW-21-001. Geochronology of the LP Zone Volcanic Rocks, Red Lake Area, Uchi Subprovince, Northwestern Ontario



P.J. MacDonald[1], S.L. Kamo[2] and P.M. Malegus[3]

[1]Earth Resources and Geoscience Mapping Section, Ontario Geological Survey, Sudbury, Ontario P3E 6B5
[2]Jack Satterly Geochronology Laboratory, Department of Earth Sciences, University of Toronto, Toronto, Ontario M5S 3B1
[3]Resident Geologist Program, Ontario Geological Survey, Red Lake, Ontario P0V 2M0

INTRODUCTION

The Red Lake greenstone belt has produced over 29 million ounces of gold since its first discovery in 1925. Historical production has been predominantly sourced from structurally controlled, narrow, high-grade (visible gold-bearing) carbonate-quartz veins and quartz alteration zones within the Mesoarchean tholeiitic mafic metavolcanic rocks of the Balmer assemblage (Dubé et al. 2004). The recently discovered LP zone has an initial indicated and inferred resource of 4.89 million ounces (Pfeiffer et al. 2023). Located approximately 24 km south-southeast of Red Lake, the LP zone displays features that set it apart when compared to the gold mineralization in the Red Lake greenstone belt. The LP zone is characterized by a strongly deformed, broadly stratigraphy parallel, wide zone of disseminated gold mineralization hosted within Neoarchean calc-alkalic felsic metavolcanic rocks (Pfeiffer et al. 2023).

As part of the Red Lake bedrock mapping compilation project (*see* MacDonald and Malegus 2021), geochemical and geochronological sampling was completed in the Red Lake area during 2022 and 2023. The article presents geochronological results from a sample of the felsic metavolcanic rock that hosts LP zone mineralization (Figure 10.1).

URANIUM–LEAD GEOCHRONOLOGY ANALYTICAL METHODS

Sample preparation and isotopic analyses were carried out at the Jack Satterly Geochronology Laboratory (JSGL) at the University of Toronto. The sample was crushed and milled using standard methods (jaw crusher and Bico disk mill, respectively). Heavy mineral separation was carried out by reprocessing on a Wilfley table, followed by magnetic separation and heavy liquid (methylene iodide) methods to produce a zircon concentrate. Final sample separation was by hand picking under a microscope. Uranium–lead analysis of select zircon and rutile was carried out by chemical abrasion isotope dilution thermal ionization mass spectrometry (CA-ID-TIMS) methods, and 3 additional annealed zircon grains were analyzed by laser ablation inductively coupled plasma mass spectrometry (LA-ICP–MS) methods to quickly investigate the span of ages present. Selected rutile grains analyzed by ID-TIMS were not chemically abraded.

Summary of Field Work and Other Activities, 2023,
Ontario Geological Survey, Open File Report 6405, p.10-1 to 10-8.

© King's Printer for Ontario, 2023

Prior to CA-ID-TIMS analysis, zircon grains were thermally annealed and chemically etched (chemical abrasion; Mattinson 2005). Zircon grains were first pretreated in a muffle furnace at ~900°C for 48 hours to repair radiation damage and anneal the crystal lattice, followed by a modified single-step partial dissolution procedure in ~0.10 mL of ~50% HF and 0.020 mL 7N HNO_3 in Teflon™ dissolution vessels at 200°C for ~2 to 8 hours depending on the state of preservation of the zircon grains. Zircon and rutile were rinsed in 7N HNO_3 at room temperature prior to dissolution. A $^{205}Pb/^{235}U$ spike was added to Krogh-type Teflon™ dissolution capsules during sample loading.

The mineral grains were dissolved using ~0.10 mL of concentrated HF acid and ~0.02 mL of 7N HNO_3 at 200°C for 3 to 5 days. Samples were dried to a precipitate and redissolved in 0.15 mL of 3N HCl overnight (Krogh 1973). Uranium and lead were isolated from zircon using HCl and from rutile using HBr, then deposited onto outgassed rhenium filaments with silica gel (Gerstenberger and Haase 1997) and analyzed with a VG354 mass spectrometer using a Daly detector in pulse counting mode. Corrections to $^{206}Pb/^{238}U$ and $^{207}Pb/^{206}Pb$ ages for initial ^{230}Th disequilibrium in zircon were made assuming a Th/U ratio in the magma of 4.2. Common lead was assigned to procedural lead blank for zircon and rutile. Dead time of the measuring system for lead and uranium was 16 and 14 ns, respectively. The mass discrimination correction for the Daly detector is constant at 0.05% per atomic mass unit. Amplifier gains and Daly characteristics were monitored using the SRM 982 lead standard. Thermal mass discrimination corrections are 0.10% per atomic mass unit for lead and uranium. VG Sector software was used for lead and uranium isotopic data acquisition and in-house Visual Basic software (UtilAge) was used for data reduction.

Prior to LA-ICP–MS analysis, select zircon grains were annealed (as outlined above) and mounted on glass slides with double-sided tape and photographed under a binocular microscope. Zircon grains were then partially ablated using a 193 nm New Wave Research Inc. excimer laser and an Agilent Technologies Inc. 7900 ICP–MS. The laser was generally operated at 5 Hz and 5 J/cm^2 fluence with beam diameter between 15 to 40 µm, depending on the sample. Data were collected on ^{88}Sr (10 ms), ^{206}Pb (30 ms), ^{207}Pb (90 ms), ^{232}Th (10 ms) and ^{238}U (20 ms). Spots were pre-ablated for 1 s (5 pulses) with a large beam diameter to clean the surface, followed by a 10 s period of baseline accumulation. The laser beam was then turned on and data were collected for 25 s, followed by a washout period. Approximately 150 measurement cycles per sample were produced and ablation pits were 15 µm deep.

Data were edited and reduced using in-house VBA software (UtilLAZ program). The $^{206}Pb/^{238}U$ values showed increasing fractionation throughout zircon runs, which was caused by loss of refractory uranium, with increasing penetration depth, whereas the $^{207}Pb/^{206}Pb$ profiles were usually flat. No corrections were made for common lead, because the ^{204}Pb peak was too small to be measured precisely. Common lead (^{204}Pb) is usually present in insignificant amounts in unaltered Precambrian zircon. If present, then common lead would have the effect of pushing data to the right, displaced from the concordia curve along a shallow mixing line with slope determined by the isotopic composition of the common lead contaminant. Isotope ^{88}Sr was monitored to detect the intersection of the beam with zones of alteration or inclusions. Data showing high strontium or irregular time resolved profiles were either averaged over restricted strontium-free time windows or rejected. Two zircon standards were used: DD85-17, a quartz diorite from the Marmion batholith in northwestern Ontario (3002±2 Ma by ID-TIMS: Tomlinson et al. 2003) and DD91-1, a monzodiorite from the Pontiac Province of Quebec (2682±1 Ma: Davis 2002). Sets of 4 sample measurements were bracketed by standard measurements; differences between standards were time interpolated to correct sample measurements.

Decay constants are those of Jaffey et al. (1971). A uranium isotopic composition of 137.88 was used (Steiger and Jäger 1977). All age errors quoted, and error ellipses in the diagrams are given at 95% confidence interval. Plotting and age calculations were done using Isoplot 3.00 (Ludwig 2003).

RESULTS

Sample 22PMR029 was collected from diamond-drill core of drill-hole BR-067, at a depth of 420 m. Drill-hole BR-067 was collared at −60° toward 210° on surface at UTM 457096E 5634338N (NAD83, Zone 15). The sample is a fine-grained albite and silica-altered felsic volcanic rock (Photo 10.1A). Drill logs, provided by Kinross Gold Corp., describe this unit as an altered, aphyric felsic volcanic (also known as E32A).

Only 8 zircon grains were recovered from sample 22PMR029. A photograph of the 8 grains (Photo 10.1B) shows a diversity of crystal habits, which suggests more than 1 age population (i.e., xenocrystic, phenocrystic or eruptive). A range in the state of preservation and alteration was also observed. Most of the grains exhibited damage after chemical abrasion with only minor portions of a few grains exhibiting translucence, which is an indication of higher likelihood of concordance. Two small fragments (circled in Photo 10.1C) were deemed sufficiently well preserved to give useful CA-ID-TIMS age results. Z1 is concordant with a $^{207}Pb/^{206}Pb$ age of 2716.2±1.8 Ma (Figure 10.2; Table 10.1). Three additional grains analyzed by LA-ICP–MS appear to support this age (*see* Figure 10.2; Table 10.2). A younger date from Z2 has a $^{207}Pb/^{206}Pb$ age (i.e., minimum age) of 2645.6±3.4 Ma (1.6% discordant; *see* Figure 10.2; *see* Table 10.1). If lead loss occurred earlier in its history, the $^{207}Pb/^{206}Pb$ age could be older at 2675±15 Ma, for example, if lead loss is assumed at 500 Ma. Alternatively, this grain fragment may be as old as Z1, but affected by later hydrothermal activity; however, there is no common lead in the grain and Th/U of 0.8 is a typical magmatic value.

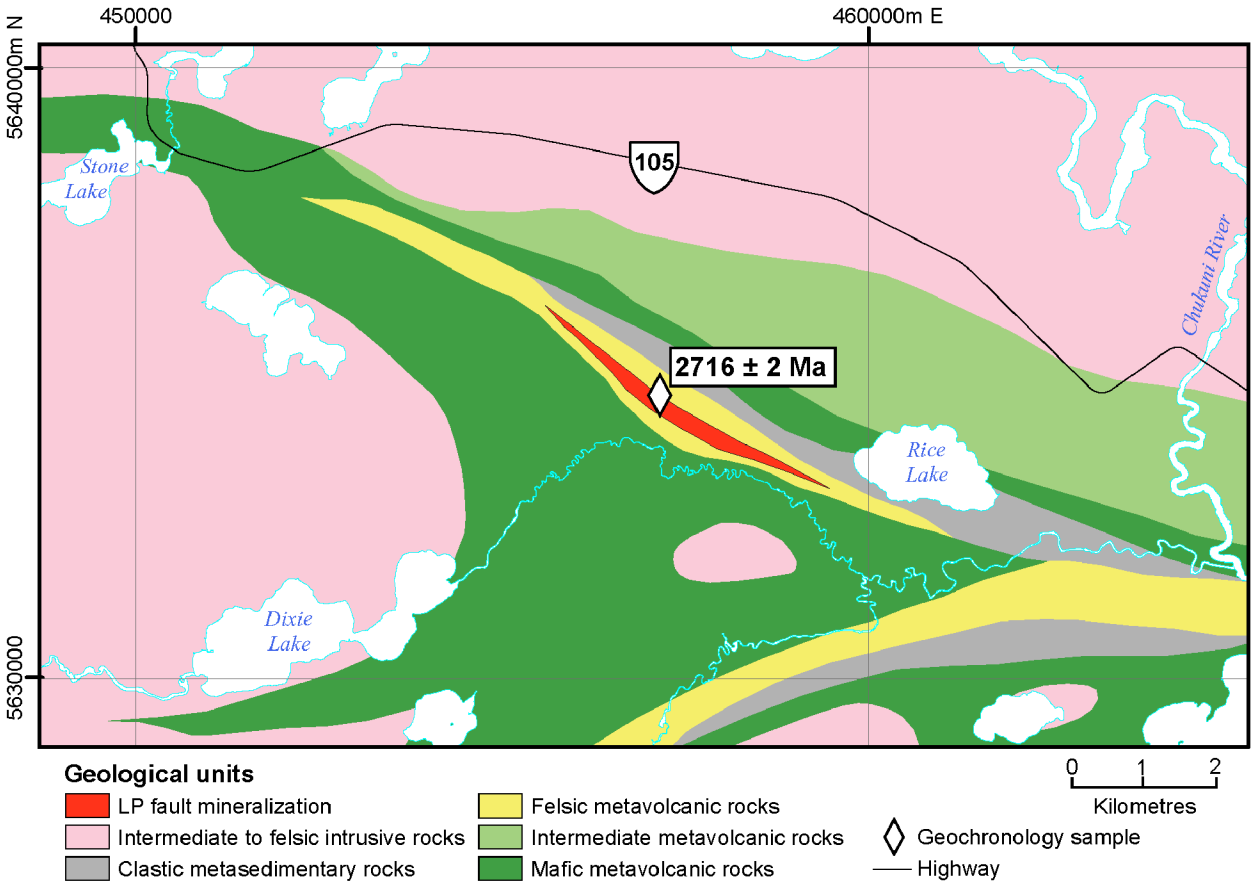


Figure 10.1. Simplified map of the geology in the region surrounding the Kinross Gold Corp. LP zone, indicating the general location of the geochronology sample (*modified from* Ontario Geological Survey 2011; BTU Metals Corp. 2020; Pfeiffer et al. 2023). Universal Transverse Mercator (UTM) co-ordinates provided in North American Datum 1983 (NAD83), Zone 15.

Abundant rutile was recovered from sample 22PMR029. Because of the typically very low uranium concentration expected in rutile (~1 ppm in this study), multi-grain fractions were selected for analysis. R1 is from 2 medium brown, translucent rutile grains (Photo 10.1D, left side) and R2 is from 3 very dark brown, facetted opaque rutile grains (*see* Photo 10.1D, right side). Multi-grain fraction R2 is subconcordant with a $^{207}Pb/^{206}Pb$ age of 2571.3±13 Ma (*see* Figure 10.2; *see* Table 10.1), which is slightly more radiogenic than R1 with data that plot to the right of R2 and is discordant (7%) from a $^{207}Pb/^{206}Pb$ age of 2758±15 Ma (*see* Figure 10.2; *see* Table 10.1). It is uncertain as to why the rutile data scatter, as they do not contain initial common loss and, therefore, may indicate crystallization over a range of time.

DISCUSSION

Intermediate to felsic lithologies of the LP zone have been previously interpreted as part of the Confederation assemblage (*circa* 2745–2735 Ma) and McNeely sequence (*circa* 2748–2742 Ma), although no age determinations existed in the area (Sanborn-Barrie et al. 2004). Recently reported ages from the LP zone include an altered aphanitic felsic unit (E32A) reported at 2729.8±3.7 Ma, a porphyritic felsic unit (E31) reported at 2722.0±1.0 Ma and metasedimentary units reported at <2720 Ma (Simmons et al. 2023). These ages suggest the rock units of the LP zone correlate with the St. Joseph assemblage (*circa* 2723 Ma) located to the northeast within the Birch–Uchi greenstone belt (Sanborn-Barrie et al. 2004; Simmons et al. 2023). The age reported by this project on zircon fragment Z1 indicates a crystallization age at 2716±2 Ma, with an additional 3 zircon grains analyzed by LA-ICP–MS supporting this age. Caution should be used because of the minor number of grains recovered; however, if accurate, this age suggests that at least some volcanic rocks within the LP zone may be younger than previously reported. This also supports the hypothesis that the LP zone felsic volcanic rocks are equivalent in age to the Bidou or Gem assemblages exposed to the west in the Rice Lake greenstone belt of Manitoba (Anderson 2008).

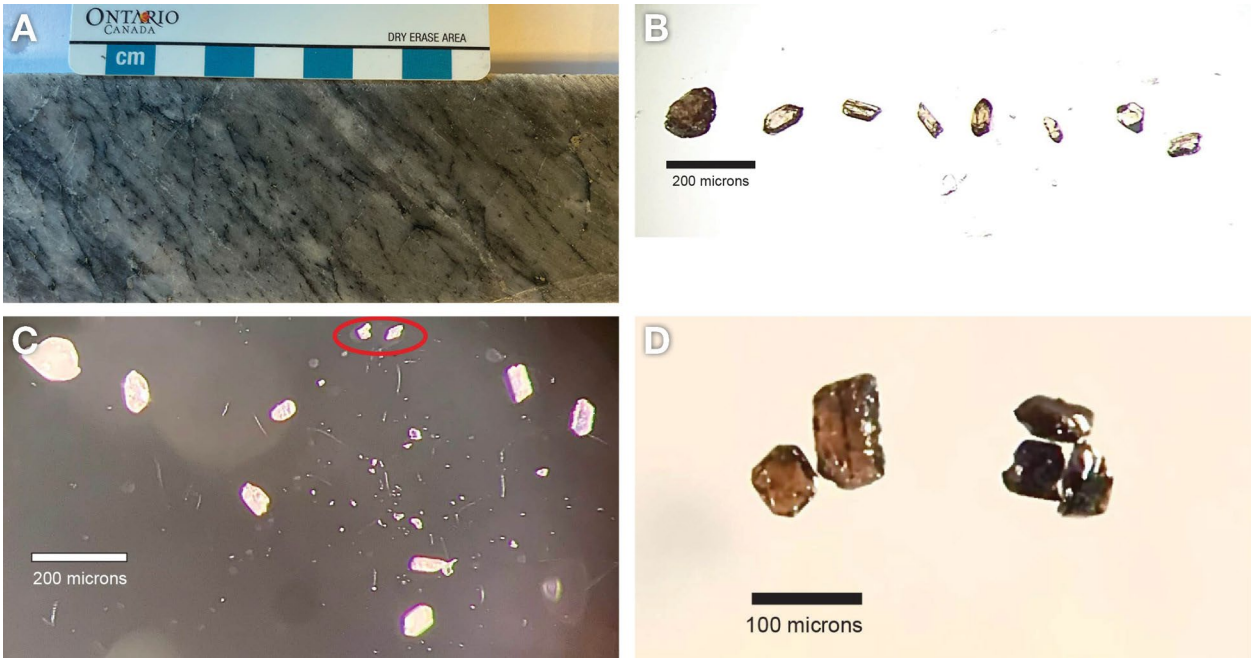


Photo 10.1. Selected photographs of sample number 22PMR029, LP zone. **A)** Diamond-drill core rock sample image of quartz-albite–altered aphanitic felsic metavolcanic rock (quartz-feldspar porphyry). **B)** Photomicrograph of 8 zircon crystals recovered from sample 22PMR029. **C)** Photomicrograph of 8 zircon crystals after chemical abrasion; only 2 small zircon fragments (circled in red) were considered sufficiently preserved to give useful age results. **D)** Photomicrograph of 2 multi-grain fractions of rutile analyzed in this study: R1 fraction to left and R2 fraction to right.

The rocks of the LP zone are strongly deformed and metamorphosed. The age presented suggests that the main stages of penetrative deformation and regional metamorphism in the area occurred at or after 2716 Ma. This broadly supports previous interpretations in the Red Lake and Birch–Uchi greenstone belts, that regional penetrative deformation and peak metamorphism occurred between 2720 and 2700 Ma (Dubé et al. 2004; Sanborn-Barrie et al. 2004, and references therein).

Gold mineralization in the Red Lake area has been interpreted to have occurred between 2723 and 2712 Ma, followed by a remobilization event at *circa* 2700 Ma (Dubé et al. 2004). The first mineralization event is coeval with the emplacement of intermediate to felsic intrusions throughout the belt during the penetrative D_2 deformation (Dubé et al. 2004). LP zone volcanism reported at 2716 Ma coincides with this reported timing of gold mineralization in the Red Lake area. Whether the gold mineralization at the LP zone is synvolcanic or is related to deformation and metamorphism remains an open question.

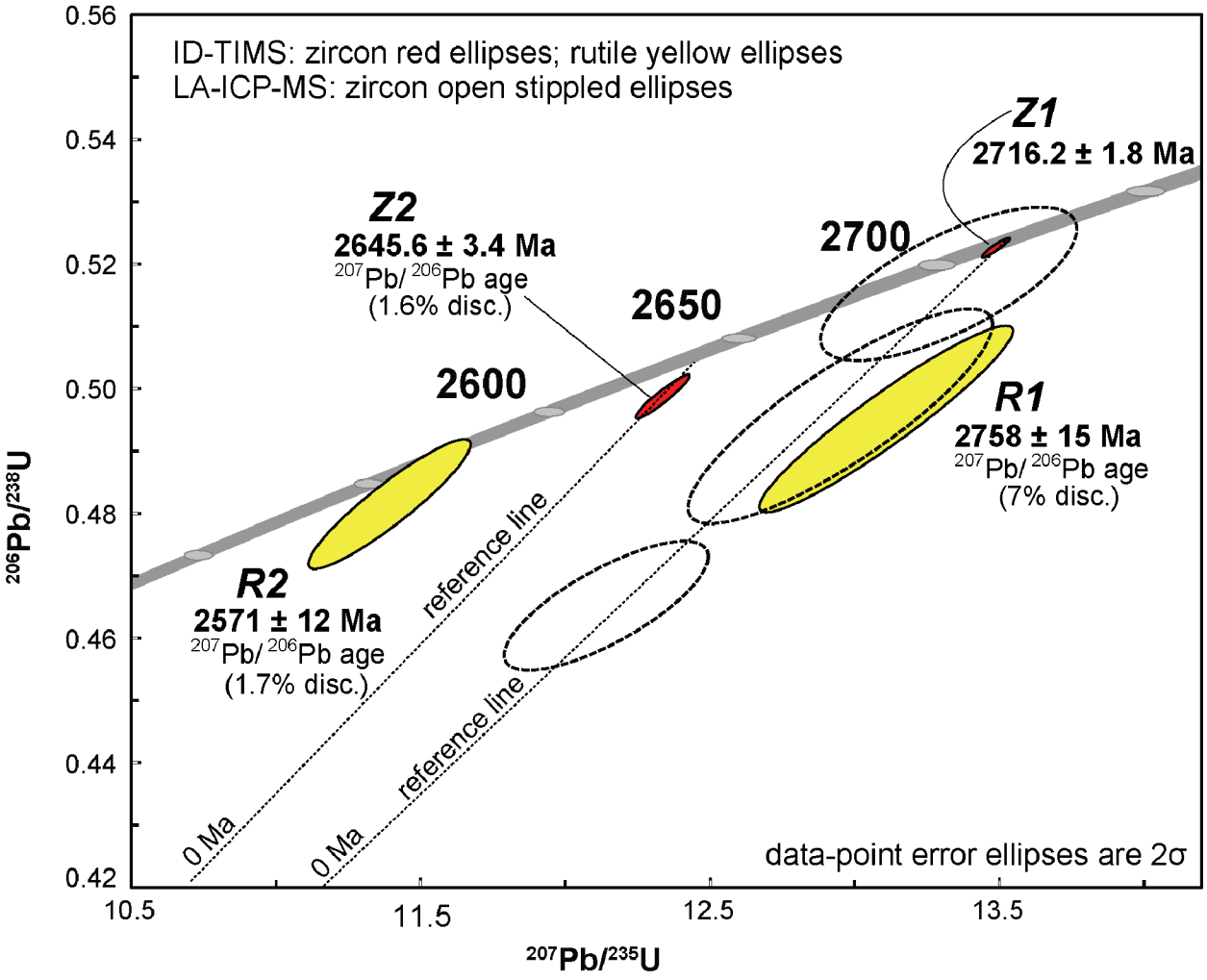


Figure 10.2. Concordia diagram of sample 22PMR029 analyzed by U/Pb CA-ID–TIMS (*modified from* Kamo 2023). The red ellipses represent 2 zircon results, yellow ellipses represent 2 multi-grain rutile results, and open ellipses represent zircon LA-ICP–MS results.

Table 10.1. Zircon and rutile U/Pb CA-ID–TIMS isotopic data from sample 22PMR029, felsic volcanic rock, LP zone, Kinross Gold Corp. Great Bear project.

Analysis No.	Weight (µg)	U (ppm)	Th/U	Pb_C (pg)	$^{206}Pb/^{204}Pb$ Measured	$^{207}Pb/^{235}U$	2σ	$^{206}Pb/^{238}U$	2σ	Error Corr.	$^{207}Pb/^{206}Pb$	2σ	$^{206}Pb/^{238}U$ Age	2σ	$^{207}Pb/^{235}U$ Age	2σ	$^{207}Pb/^{206}Pb$ Age	2σ	% Disc.
22PMR029: Felsic volcanic rock, LP zone, Kinross Gold Great Bear project (DDH BR-067: UTM 457096E 5634338N, NAD83, Zone 15, −60° towards 210°, 420 m depth)																			
Z1	1	81	0.44	0.7	3779	13.487	0.039	0.5230	0.0013	0.930	0.18703	0.00021	2711.9	5.4	2714.4	2.7	2716.2	1.8	0.2
Z2	0.5	40	0.79	0.4	1580	12.336	0.077	0.4992	0.0029	0.945	0.17921	0.00037	2610.4	12.3	2630.3	5.9	2645.6	3.4	1.6
R1	3	2	2.09	1.2	144	13.109	0.358	0.4956	0.0123	0.944	0.19182	0.00174	2595	53	2687	26	2758	15	7.2
R2	6	1	0.43	0.9	234	11.390	0.229	0.4820	0.0085	0.920	0.17140	0.00135	2536	37	2556	19	2571	13	1.7

Notes: *All zircon (z) grains have been thermally annealed and etched in HF (Mattinson 2005).*
Z is zircon, R is rutile.
Th/U calculated from radiogenic $^{208}Pb/^{206}Pb$ ratio and $^{207}Pb/^{206}Pb$ age assuming concordance.
Pb_C is total common Pb assuming the isotopic composition of laboratory blank:
assigned the isotopic composition of laboratory blank ($^{206}Pb/^{204}Pb$=18.49±0.4%; $^{207}Pb/^{204}Pb$=15.59±0.4%;$^{208}Pb/^{204}Pb$=39.36±0.4%).
$^{206}Pb/^{204}Pb$ corrected for fractionation and common Pb in the spike.
Pb/U ratios corrected for fractionation, common Pb in the spike, and blank.
Correction for ^{230}Th disequilibrium in $^{206}Pb/^{238}U$ and $^{207}Pb/^{206}Pb$ assuming Th/U of 4.2 in the magma.
Error Corr. is correlation coefficients of X–Y errors on the concordia plot.
Disc. is percent discordance for the given $^{207}Pb/^{206}Pb$ age.
Decay constants are those of Jaffey et al. (1971): ^{238}U and ^{235}U are 1.55125 ×10^{-10}/yr and 9.8485 ×10^{-10}/yr.
$^{238}U/^{235}U$ ratio of 137.88 (Steiger and Jäger 1977) used for $^{207}Pb/^{206}Pb$ model age calculations.

Table 10.2. Zircon (tape mount grains not polished) U/Pb isotopic data by LA-ICP–MS from sample 22PMR029, felsic volcanic rock, LP zone, Kinross Gold Corp. Great Bear project.

Analysis No.	U (ppm)	^{206}Pb (ppm)	Th/U	$^{207}Pb/^{235}U$	1σ	$^{206}Pb/^{238}U$	1σ	Error Corr.	$^{207}Pb/^{206}Pb$ Age	1σ	$^{207}Pb/^{235}U$ Age	1σ	$^{206}Pb/^{238}U$ Age	1σ	% Disc.
22PMR029: Felsic volcanic rock, LP zone, Kinross Gold Great Bear project (DDH BR-067: UTM 457096E 5634338N, NAD83, Zone 15, −60° towards 210°, 420 m depth)															
22PMR029-1	257	127.5	0.74	12.9	0.215	0.496	0.007	0.853	2736	14	2676	16	2597	30	6
22PMR029-2	211	98.1	0.51	12.1	0.144	0.466	0.004	0.764	2734	13	2615	11	2465	19	12
22PMR029-3	110	56.8	0.52	13.3	0.181	0.517	0.005	0.715	2714	16	2703	13	2687	21	1

Notes: *Analyses are sorted from highest to lowest $^{207}Pb/^{206}Pb$ age.*
Error Corr. is correlation coefficients for of X–Y errors on the concordia plot.
Disc. is percent discordance for the given $^{207}Pb/^{206}Pb$ age.
Relation between ages and concordia co-ordinates: $Y = {}^{206}Pb/^{238}U = EXP(L238\times(206\text{-}238Age)) - 1$; $X = {}^{207}Pb/^{235}U = EXP(L235\times(207\text{-}235Age)) - 1$.
$^{207}Pb/^{206}Pb = 137.88 \times X/Y$; U decay constants (L238 & L235) from *Jaffey et al. (1971), where L238 = 1.55125 ×10^{-10}/yr; L235 = 9.8485 ×10^{-10}/yr.*

ACKNOWLEDGMENTS

The authors would like to thank the geological staff at Kinross Gold Corp. for granting access, in-kind support and sample acquisition. We also express our appreciation to the staff of the JSGL for ongoing laboratory support. Additionally, we acknowledge Ontario Geological Survey staff Evan Hastie for project support; Manuel Duguet for scientific review; Patrick Gervais for aiding with figures; and Monica Gaiswinkler Easton for editorial assistance.

REFERENCES

Anderson, S.D. 2008. Geology of the Rice Lake area, Rice Lake greenstone belt, southeastern Manitoba (parts of NTS 52L13, 52M4); Manitoba Geological Survey, Geoscientific Report GR2008-1, 106p.

BTU Metals Corp. 2020. Artificial intelligence data evaluations identify 35 gold target areas on BTU Red Lake property; BTU Metals Corp., news release, filed July 21, 2020 with SEDAR®, *see* www.sedarplus.com, 4p. [accessed October 2, 2023]

Davis, D.W. 2002. U-Pb geochronology of Archean metasediments in the Pontiac and Abitibi subprovinces, Quebec, constraints on timing, provenance and regional tectonics; Precambrian Research, v.115, p.97-117.

Dubé, B., Williamson, K., McNicoll, V., Malo, M., Skulski, T., Twomey, T. and Sanborn-Barrie, M. 2004. Timing of gold mineralization at Red Lake, northwestern Ontario, Canada: New constraints from U-Pb geochronology at the Goldcorp high-grade zone, Red Lake Mine and the Madsen Mine; Economic Geology, v.99, p.1611-1641.

Gerstenberger, H. and Haase, G. 1997. A highly effective emitter substance for mass spectrometric Pb isotope ratio determinations; Chemical Geology, v.136, p.309-312.

Jaffey, A.H., Flynn, K.F., Glendenin, L.E., Bentley, W.C. and Essling, A.M. 1971. Precision measurement of half-lives and specific activities of ^{235}U and ^{238}U; Physical Review, v.4, p.1889-1906.

Kamo, S.L. 2023. Report on U-Pb ID-TIMS geochronology for the Ontario Geological Survey: Bedrock Mapping Projects, Ontario: 2022-2023; internal report for the Ontario Geological Survey, Jack Satterly Geochronology Laboratory, University of Toronto, Toronto, Ontario, 22p.

Krogh, T.E. 1973. A low contamination method for hydrothermal decomposition of zircon and extraction of U and Pb for isotopic age determinations; Geochimica et Cosmochimica Acta, v.37, p.485-494.

Ludwig, K.R. 2003. User's manual for Isoplot 3.00: A geochronological toolkit for Microsoft® Excel®; Berkeley Geochronology Center, Special Publication No. 4, 71p.

MacDonald, P.J. and Malegus, P.M. 2021. Introduction to the Red Lake bedrock mapping compilation project, northwestern Ontario; *in* Summary of Field Work and Other Activities, 2021, Ontario Geological Survey, Open File Report 6380, p.9-1 to 9-5.

Mattinson, J.M. 2005. Zircon U-Pb chemical abrasion ("CA-TIMS") method: Combined annealing and multi-step partial dissolution analysis for improved precision and accuracy of zircon ages; Chemical Geology, v.220, p.47-66.

Ontario Geological Survey 2011. 1:250 000 scale bedrock geology of Ontario; Ontario Geological Survey, Miscellaneous Release—Data 126 – Revision 1.

Pfeiffer, N., Sims, J., Breau, Y., Greenwood, R. and Prawasono, A. 2023. Great Bear project, Ontario, Canada: Voluntary National Instrument 43-101 technical report; NI 43-101 Technical Report, Kinross Gold Corp., filed February 13, 2023 with SEDAR®, *see* www.sedarplus.com, 243p. [accessed November 5, 2023]

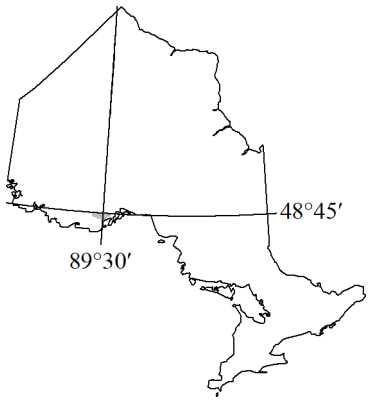
Sanborn-Barrie, M., Rogers, N., Skulski, T., Parker, J., McNicoll, V. and Devaney, J. 2004. Geology and tectonostratigraphic assemblages, east Uchi Subprovince, Red Lake and Birch–Uchi belts, Ontario; Geological Survey of Canada, Open File 4256 (also Ontario Geological Survey, Preliminary Map P.3460), scale 1:250 000.

Simmons, J., LaFrance, B., Gibson, H., Sider, P., Sherlock, R., Tinkham, D., Brueckner, S. and Hamilton, M. 2023. The Great Bear gold deposit: A gold-endowed Archean lava dome associated with a crustal-scale fault in the Red Lake greenstone belt; presentation, Metal Earth Partner Meeting, Toronto, Ontario, March 2023, Laurentian University, Harquail School of Mines, Minerals Exploration Research Centre, *The MERC Newsletter – Spring 2023*, https://mailchi.mp/laurentian/merc-newsletter-may2023, select gold "View New Videos" button to access the MERC YouTube™ channel, search on page for author surname. [accessed October 2, 2023]

Steiger, R. and Jäger, E. 1977. Subcommission of geochronology convention on the use of decay constants in geo- and cosmochronology; Earth and Planetary Science Letters, v.36, p.359-362.

Tomlinson, K.Y., Davis, D.W., Stone, D. and Hart, T.R. 2003. U-Pb age and Nd isotopic evidence for crustal recycling and Archean terrane development in the south-central Wabigoon Subprovince, Canada; Contributions to Mineralogy and Petrology, v.144, p.684-702.

11. Project NW-19-001. Precambrian Bedrock Geology Mapping in the Onion Lake and Sunshine Areas, Quetico and Wawa Subprovinces, Northwestern Ontario



G. Launay[1] and R.T. Metsaranta[1]

[1]Earth Resources and Geoscience Mapping Section, Ontario Geological Survey

INTRODUCTION

During the summer of 2023, bedrock geology mapping was conducted in the southern Quetico Subprovince and the northern margin of the Shebandowan greenstone belt north and northwest of the City of Thunder Bay. Mapping focussed mainly on parts of the Onion Lake and Sunshine 1:50 000 scale National Topographic System (NTS) areas. Additional limited mapping was also done in the adjacent Raith, East Bay, Greenwich Lake and Loon NTS areas. This mapping is part of an ongoing project to produce maps, at a scale of 1:50 000, for a large area with limited previous mapping north and northwest of the City of Thunder Bay (*see* Metsaranta 2015; Metsaranta and Walker 2019; Metsaranta and Hamilton 2020; Metsaranta and Kamo 2021; Metsaranta 2022).

In this article "map area" refers to the area in which field work was conducted in 2023 and this corresponds to the area of Figure 11.1. To aid the description of the geology, the map area has been subdivided into southern, central and northern "domains". The southern domain is primarily underlain by metavolcanic and metasedimentary rocks of the Shebandowan greenstone belt (SGB)of the Wawa Subprovince, the central domain is underlain mainly by clastic metasedimentary and granitoid rocks of the Quetico Subprovince, and the northern domain is underlain mainly by granitoid rocks, migmatite and paragneiss of the Quetico Subprovince. Most of the discussion in this article relates to the area west of Highway 527 (*see* Figure 11.1B) because the geology of the eastern portion of the map area has been described previously (*see* Metsaranta and Walker 2019; *see* Metsaranta 2022). Proterozoic intrusive rocks are present in the map area, and some have associated nickel-copper-platinum group elements mineralization. However, because of space constraints, these are not discussed in detail in this contribution.

Much of the southern domain of the map area was mapped relatively recently at a more detailed scale than 1:50 000 (e.g., Brown and Fogal 1995; Carter 1985; Scott 1990a). However, most of the central and northern domains of the map area have not been mapped previously in similar detail. Consequently, mapping efforts, and the discussion herein, are focussed primarily on the central and northern domains.

Summary of Field Work and Other Activities, 2023,
Ontario Geological Survey, Open File Report 6405, p.11-1 to 11-12.

© King's Printer for Ontario, 2023

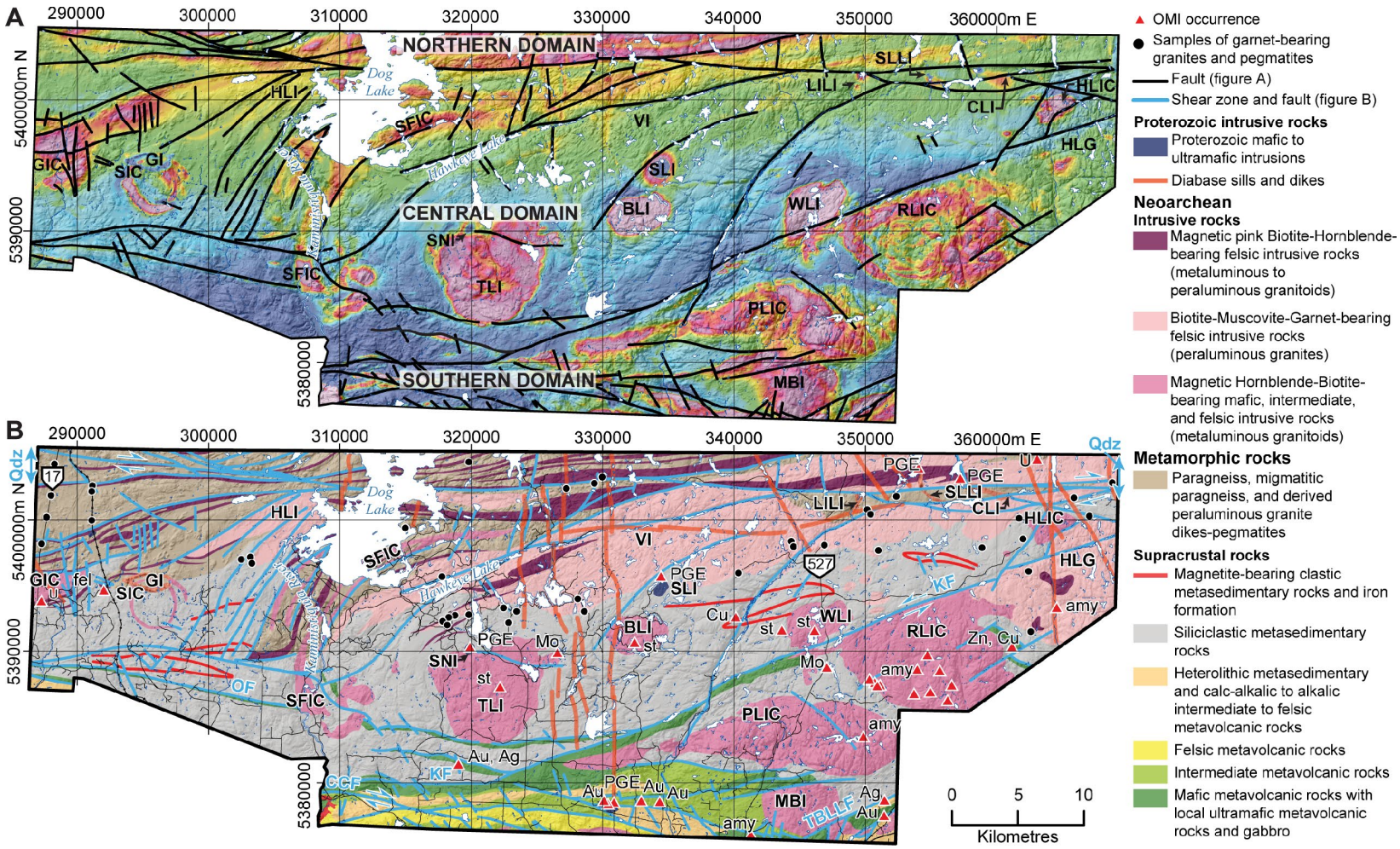


Figure 11.1. A) Total magnetic field image of the map area (Ontario Geological Survey 2017), underlain with lidar imagery (Ministry of Natural Resources and Forestry 2023). **B)** Preliminary geological map of the map area, underlain with lidar imagery, showing the location of mineral occurrences and the samples of garnet-bearing pegmatites and granites collected during the summer 2023. Geological abbreviations: BLI, Barnum Lake intrusion; CCF, Crayfish Creek fault; CLI, Current Lake intrusive complex; GI, Griff intrusion; GIC, Goldie intrusive complex; HLG, Hilma Lake granite; HLI, Hadwen Lake intrusion; HLIC, Hades Lake intrusive complex; KF, Kingfisher fault; LILI, Lone Island Lake intrusive complex; MBI, Mount Baldy intrusion; OF, Oskondaga fault; PLIC, Penassen Lakes intrusive complex; QDZ, Quetico deformation zone; RLIC, Roll Lake intrusive complex; SFIC, Silver Falls intrusive complex; SIC, Shabaqua intrusive complex; SLI, Sunday Lake intrusion; SLLI, Steepledge Lake intrusive complex; SNI, Saturday Night intrusive complex; TBLLF, Thunder Bay–Loon Lake fault; TLI, Trout Lake intrusion; VI, Voutilainen intrusion; WLI, Whitelily Lake intrusion. Commodity abbreviations: Ag, silver; amy, amethyst; Au, gold; Cu, copper; fel, feldspar; Mo, molybdenum; PGE, platinum group elements; st, granite building stone; U, uranium; Zn, zinc. Mineral occurrences are *modified from* Ontario Geological Survey (2023).Universal Transverse Mercator (UTM) co-ordinates provided using North American Datum 1983 (NAD83) in Zone 16.

SOUTHERN DOMAIN

Shebandowan Greenstone Belt and Associated Intrusions

The southern domain of the map area is underlain by rocks of the Shebandowan greenstone belt (SGB). Based on field observations and previous mapping, the SGB in the map area can be subdivided into the following units:

- bimodal mafic and felsic metavolcanic rock-dominated units, likely correlative with the Greenwater assemblage (e.g., Corfu and Stott 1998)
- intermediate metavolcanic and volcaniclastic units of uncertain tectonostratigraphic affinity
- heterolithic units of interbedded intermediate metavolcaniclastic rocks and clastic metasedimentary rocks, likely correlative to the Shebandowan and/or Auto Road assemblages (e.g., Corfu and Stott 1998)

The mafic portions of bimodal metavolcanic units in this part of the SGB comprise a mixture of massive and pillowed mafic flows (Photo 11.1A) and associated fragmental facies (pillow-breccias, flow-related breccias), gabbroic rocks (likely of synvolcanic origin) and rare ultramafic metavolcanic rocks are also present (e.g., Scott 1990a, 1990b). Thin units of magnetite-rich oxide iron formation and thin, black, sulphidic mudstone units are also locally intercalated. A felsic metavolcanic unit, mapped by Brown and Fogal (1995) and MacDonald (1939), extends in a band approximately 1 to 2 km wide from the Kaministiquia River to Dog Lake Road across the southern part of the map area. Limited field observations suggest that this unit contains both fragmental and flow-like facies. Zinc- and copper-enriched sulphide mineralization occurs locally within this interval. Based on Corfu and Stott (1998), this felsic metavolcanic unit has an age of 2718±3 Ma.

Mafic metavolcanic intervals are likely structurally intercalated by shear zones with intermediate metavolcanic and volcaniclastic rocks. These comprise a variety of monolithic and heterolithic tuff breccias, lapilli tuff and tuff. Locally, these intermediate volcaniclastic rocks are distinctly plagioclase porphyritic. Wacke and siltstone, similar in appearance to low metamorphic grade metawackes of the southern Quetico Subprovince appear to be stratigraphically intercalated with some of these intermediate metavolcanic units. These intermediate metavolcanic-dominated intervals are tentatively correlated with the Kashabowie assemblage that, based on the geochronology reported by Corfu and Stott (1998), was deposited *circa* 2695 Ma.

Heterolithic intervals, comprising a mixture of volcaniclastic rocks, including hornblende-phyric tuff breccias (Photo 11.1B), and clastic metasedimentary rocks, including trough cross-stratified, metasandstones (Photo 11.1C) and polymictic, granitoid clast–bearing conglomerates (Photo 11.1D), occur in mostly shear zone bounded units in the southern SGB area (*see* Figure 11.1B; *see also* MacDonald 1939, 1941; Kehlenbeck 1988). Geochronological constraints for what has been termed the Auto Road assemblage by Corfu and Stott (1998) suggest that granitoid cobble–bearing conglomerates within these intervals were deposited after 2682±3 Ma. Although hornblende-phyric metavolcanic rocks in this area are typically assigned to the Shebandowan assemblage (e.g., Corfu and Stott 1998), which is generally thought to have been deposited at *circa* 2690 Ma, field relationships (stratigraphic intercalation of conglomerate and tuffaceous rocks) indicate that volcanism in these heterolithic intervals likely also occurred after *circa* 2682 Ma.

Bedding and foliations throughout the SGB typically strike east to northeast and dip steeply. Metamorphic mineral assemblages indicate mainly greenschist-facies conditions. Strain within the SGB in the map area is heterogeneous and shear zones commonly mark boundaries between mappable rock units, which are not highly deformed. These shear zones are typically dextral, curvilinear and

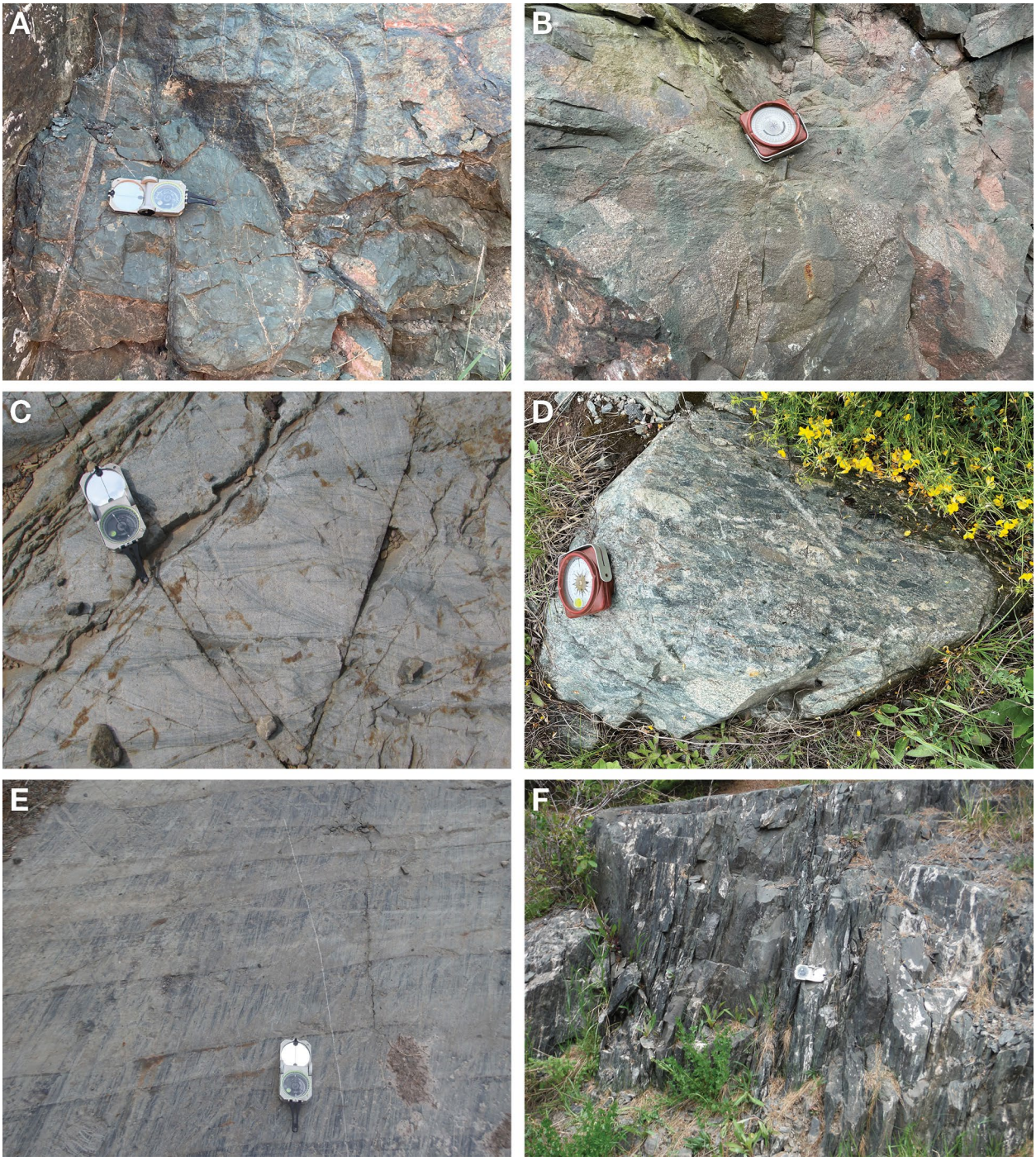


Photo 11.1. Representative photographs of the supracrustal units of the Shebandowan greenstone belt and the central domain of the map area. **A)** Pillowed mafic metavolcanic rock (23RTM197: UTM 315073E 5376695N); compass for scale is 22 cm in length. **B)** Hornblende-phyric matrix-supported calc-alkalic intermediate polymictic tuff breccia (23GAL834: UTM 312262E 5378226N); compass for scale is 10 cm in length. **C)** Cross-stratified metasandstone giving a younging direction to the south (23GAL117: UTM 329269E 5379186N); compass for scale is 22 cm in length with the sighting arm pointing north. **D)** Poorly sorted, clast-supported polymictic conglomerate (23GAL394: UTM 286451E 5387919N); compass for scale is 10 cm in length. **E)** Metawackes with graded beds giving a younging direction to the south (23GAL093: UTM 326207E 5382509N); compass for scale is 22 cm in length with the sighting arm pointing north. **F)** Sheared mafic metavolcanic panel intercalated with metawackes composing the central domain of the map area (23GAL086: UTM 326238E 5383267N); compass for scale is 22 cm in length with the sighting arm pointing north. All UTM co-ordinates are provided using NAD83 in Zone 16.

anastomosing, but, overall, are west striking and represent probably the eastward continuation of the Crayfish Creek fault system to the west. This dextral shearing is interpreted to postdate an earlier deformation event that likely structurally intercalated clastic metasedimentary rocks and deformed linear panels of mafic metavolcanic rocks immediately to the north (*see* Figure 11.1). Based on Ontario Geological Survey (2023: OMI), known gold occurrences within the SGB in the map area have a close spatial association with mapped shear zones.

The SGB was intruded by mafic mica- and amphibole-phyric lamprophyre dikes present as typically <1 m wide dikes traceable only at outcrop scales. Larger, weakly foliated, moderately to strongly magnetic metaluminous granitic intrusions, typically varying from monzogranitic to quartz monzonitic in bulk composition, form medium-sized oblate bodies in the southern part of the map area. These are broadly similar to the larger circular intrusions located farther to the north (e.g., Barnum Lake intrusion, Trout Lake intrusion; *see* Figure 11.1B).

CENTRAL DOMAIN

Clastic Metasedimentary Rocks

Most of the central domain of the map area is underlain by clastic metasedimentary rock sequences that consist mainly of texturally immature thin- to medium-bedded biotite-bearing metawackes and less abundant metasiltstones metamorphosed in the upper greenschist to the lower amphibolite facies. Porphyroblasts of garnet, cordierite and andalusite are locally present, especially near large granitoid intrusions. Despite multiple metamorphic and deformation phases affecting the map area, primary sedimentary features, such as graded beds, cross-stratification and load casts are common, and provide good younging direction indicators (Photo 11.1E). Based on the interpretation of the airborne magnetic data and new field observations, several magnetite-bearing horizons were identified in the eastern and western parts of the map area. These magnetite-bearing horizons correspond to east- to northeast-oriented tightly folded narrow magnetic anomalies on the second vertical derivative of the total magnetic field.

As highlighted by the changes of younging directions and the presence of preserved fold hinges, the metawackes were folded into steeply plunging folds with east-northeast-oriented and steeply dipping axial planes. Subvertical shear zones with a dextral strike-slip sense of shearing related to the Quetico deformation zone (QDZ) to the north and the Crayfish Creek fault to the south postdate the earlier folding event(s).

Metawackes are structurally intercalated with 105 to 120° trending panels of massive aphanitic to fine-grained mafic metavolcanic rocks corresponding to thin magnetic anomalies on the total magnetic field map (*see* Figure 11.1A). The northern contacts of these mafic metavolcanic panels are steeply north-dipping shear zones associated with a strong penetrative foliation (Photo 11.1F) that bears a steeply northwest-plunging mineral lineation underlined by chlorite. The steeply plunging lineation and kinematic indicators, such as C–S fabrics and pressure shadows around quartz porphyroblasts, locally show an apparent north-side-down sense of shearing. This apparent normal sense of shearing appears inconsistent with the regional compressive deformation observed in the map area; however, structural repetitions of these units and stratigraphy-parallel shear zones suggest that these sheared contacts are likely early thrusts, which were subsequently tilted and overturned during the folding event(s) observed in the metawackes and described previously.

Narrow, typically <1 m thick intrusions of subconcordant feldspar porphyritic intermediate to felsic dikes and amphibole- and/or mica-phyric mafic lamprophyre dikes are also common in the southern domain. Although common as outcrop-scale features, there is not a clear association of these dike suites with any of the map-scale intrusive suites depicted in Figure 11.1B.

Magnetic Metaluminous Intrusions and Intrusive Complexes

Several magnetic metaluminous intrusions and intrusive complexes occur in the central part of the map area and correspond to magnetic anomalies on the airborne total magnetic field map (*see* Figure 11.1A). These include the Barnum Lake intrusion (BLI), the Trout Lake intrusion (TLI), the Silver Falls intrusive complex (SFIC), the Shabaqua intrusive complex (SIC), and the Goldie intrusive complex (GIC).

BARNUM AND TROUT LAKE INTRUSIONS

The Trout Lake and the Barnum Lake intrusions are homogeneous and weakly deformed to undeformed porphyritic hornblende- and biotite-bearing pink quartz-monzonite. Magnetic susceptibility ranges from 10 to 15 $\times 10^{-3}$ SI units. These intrusions form regular roundish-shaped magnetic anomalies on the total magnetic field map (*see* Figure 11.1A). These intrusions of quartz-monzonite contain abundant melanocratic, angular to rounded fine- to medium-grained mafic enclaves (Photo 11.2A).

SILVER FALLS INTRUSIVE COMPLEX

The Silver Falls intrusive complex (SFIC), occurring along the Kaministiquia River and East of Dog Lake, comprises a series of elongated intrusions that are parallel to the regional fabric (*see* Figure 11.1B). The northern part of the SFIC is mainly composed of foliated medium-grained mesocratic hornblende- and biotite-bearing monzodiorite (magnetic susceptibility ~0.4–0.8 $\times 10^{-3}$ SI units), and minor leucocratic granodiorite crosscut by dikes of pink, biotite-dominated granite, and pegmatite (Photo 11.2B). The southern part of the SFIC is more differentiated and consists of a magnetic (magnetic susceptibility of ~13–18 $\times 10^{-3}$ SI units) coarse-grained to porphyritic, pink biotite-dominated monzogranite. The SFIC can be described cartographically as a 25 km long spiral-shaped body. More precisely, the long axis of the SFIC rotates counterclockwise from 80° east of Dog Lake to 200° farther south to 160° along the Kaministiquia River to the southeast (*see* Figure 11.1B). The overall shape of the SFIC suggests that this counterclockwise rotation is likely the result of the regional dextral shearing of the QDZ and was accommodated by the antithetic north- to northeast-striking sinistral shear zones occurring along the contacts between the intrusive bodies of the SFIC and the surrounding paragneiss.

SHABAQUA AND GOLDIE INTRUSIVE COMPLEXES

The Shabaqua (SIC) and the Goldie (GIC) intrusive complexes occur in the western part of the map area (*see* Figure 11.1B). Similar to the Silver Falls intrusive complex, these 2 intrusive complexes are heterogenous, and they mainly consist of foliated melanocratic medium-grained hornblende-biotite–bearing monzodiorite cut by pink quartz-monzonite and monzogranite. On the total magnetic field map, the SIC displays a narrow ring-shaped geometry crosscut to the north by an east-trending reversed magnetic polarity Proterozoic diabase intrusion (Griff intrusion; *see* Figure 11.1A).

Peraluminous Granites and Pegmatite Fields

Peraluminous granite intrusions and peraluminous granitic pegmatites are abundant in the map area. Field work in 2023 better characterized the western part of the Voutilainen intrusion (VI), mapped to the east by Metsaranta and Walker (2019) and Metsaranta (2022), the Hadwen Lake intrusion (HLI) and the granitic pegmatites occurring in their vicinity.

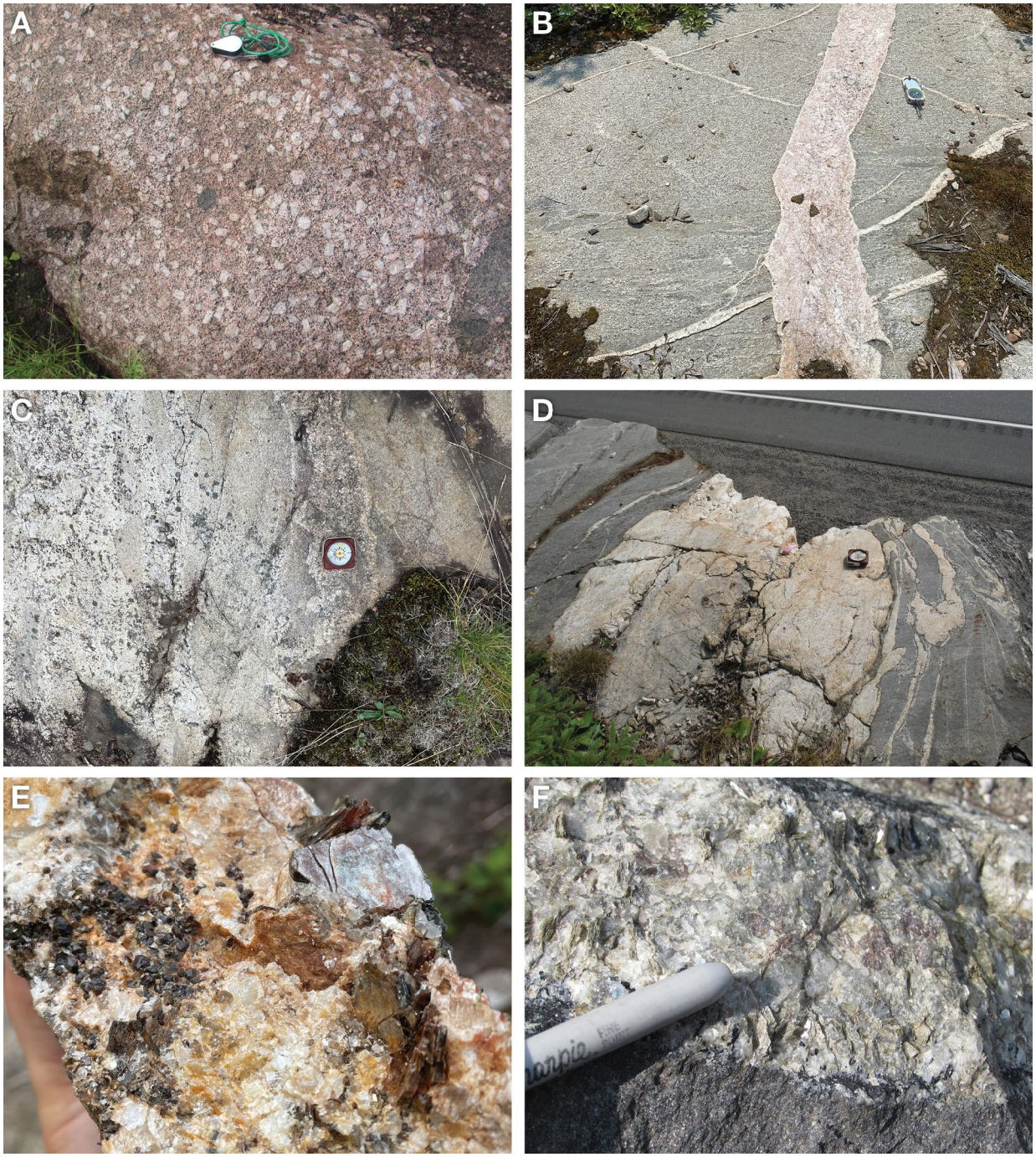


Photo 11.2. Representative photographs of the intrusive rocks occurring in the central domain of the map area. **A)** Porphyritic quartz-monzonite from the Trout Lake intrusion; note the presence of mafic enclaves (23GAL396: UTM 324419E 5385677N); hand lens for scale is 4 cm in length. **B)** Medium- to coarse-grained monzodiorite crosscut by late pink magnetite-biotite–bearing pegmatite from the Silver Falls intrusive complex (23GAL208: UTM 313914E 5397382N); compass for scale is 22 cm in length with the sighting arm pointing north. **C)** Typical exposure of the Hadwen Lake intrusion medium-grained peraluminous granite intruded by quartzofeldspathic pegmatites (23GAL669: UTM 302769E 5396584N); compass for scale is 10 cm in length. **D)** Dextrally sheared and boudinaged garnet-biotite-muscovite–bearing dike of layered pegmatite-aplite occurring along Highway 17 (23GAL384: UTM 287300E 5398121N), compass for scale is 10 cm in length. **E)** Hand specimen of garnet-muscovite–bearing pegmatite from Highway 17 (23GAL384: UTM 287300E 5398121N). **F)** Thin dike of muscovite–black and pink tourmaline–bearing pegmatite from Highway 17; note the presence of hexagonal sections of pink lithium-bearing tourmaline (elbaite?) (23GAL384: UTM 287300E 5398121N); pen for scale is 8cm in length. All UTM co-ordinates are provided using NAD83 in Zone 16.

VOUTILAINEN INTRUSION AND ONION LAKE PEGMATITES

As described by Metsaranta and Walker (2019) and Metsaranta (2022), the Voutilainen intrusion is a continuous east-northeast-striking intrusion of peraluminous granite bounded to the north by the QDZ. To the west, the Voutilainen intrusion becomes progressively narrower and consists of thin dikes of granite interdigitated within metawackes. The northern part of the Voutilainen intrusion consists of low magnetic susceptibility (~0.07–0.25 $\times 10^{-3}$ SI units) coarse-grained to white feldspar porphyritic biotite-dominated granite. Toward the south, the Voutilainen intrusion appears to evolve to a medium- to coarse-grained garnet-bearing two-mica granite. Dikes of two-mica garnet-tourmaline–bearing pegmatite, that likely belong to the Onion Lake pegmatitic field (Breaks, Selway and Tindle 2003; Metsaranta and Walker 2019; Metsaranta 2022), are present along the southern edge of the Voutilainen intrusion across the map area.

HADWEN LAKE INTRUSION AND HIGHWAY 17 PEGMATITES

The Hadwen Lake intrusion (HLI) is a northeast-striking medium- to coarse-grained peraluminous granite occurring west of Dog Lake and south of Hadwen Lake (*see* Figure 11.1B). The boundaries of the HLI are poorly exposed; thus, its contacts are mainly inferred based on limited outcrop data. However, the northwest and southeast edges of the HLI seem to correspond to northeast-striking regional deformation zones, based on mapping along strike and geophysical interpretation. The HLI consists of medium- to coarse-grained variably foliated biotite-dominated granite and two-mica granite with a low magnetic susceptibility (~0.05–0.12 $\times 10^{-3}$ SI units). The HLI is crosscut by numerous dikes of two-mica–bearing pegmatites ranging in width from centimetres to several metres (Photo 11.2C). Garnet is a common accessory mineral both in the HLI and the pegmatites crosscutting HLI granite. Pegmatitic intrusions likely derived from the HLI occur in the metawackes both north and south of the HLI. Some medium-grained niobium-tantalum oxides were observed locally in these pegmatites. Samples for whole-rock geochemical analyses were collected in 2023 to characterize the HLI and explore the rare-element potential of this intrusion and the associated pegmatites.

Numerous dikes of biotite-muscovite-garnet-tourmaline–bearing granites and granitic pegmatites occur in the westernmost part of the mapping area along Highway 17 and BFP Road. These granite dikes and pegmatites intruded strongly deformed and locally migmatitic biotite and garnet-biotite paragneiss. At least 2 generations of pegmatite can be distinguished in this area. The first generation consists of nearly concordant northeast- to east-striking, wide (up to several metres) lenses of foliated, dextrally sheared and boudinaged layered garnet-bearing aplite-pegmatites (Photos 11.2D and 11.2E). These pegmatites are mainly composed of quartz, plagioclase, potassium feldspar, biotite, muscovite and garnet with rare black tourmaline and blue apatite. The second generation of pegmatite is less common and consists of undeformed late tectonic to posttectonic north- to northeast-striking dikes that crosscut at a high angle the regional foliation. They contain potassium feldspar, plagioclase, quartz, biotite, green muscovite (lithium-rich?), garnet, blue apatite, black tourmaline and locally pink lithium-bearing tourmaline (elbaite?) (Photo 11.2F). More petrographic and mineral chemistry analyses on thin sections are required to confirm the presence of lithium-bearing minerals in these pegmatites.

NORTHERN DOMAIN

Terminology used to describe migmatites in this section is based on Sawyer (2008). The northern part of the map area was strongly affected by the QDZ. In this area, intensely sheared and metamorphosed metasedimentary rocks intruded by foliated to gneissic granitoids are exposed (Photos 11.3A and 11.3B). The former consists mainly of feldspar + quartz + biotite ± garnet ± sillimanite paragneiss to migmatitic paragneiss, and migmatite-derived garnet-bearing peraluminous granite dikes and pegmatites that were likely the product of partial melting under middle amphibolite-facies conditions of metawackes, similar to those mapped to the south. Dextrally sheared stromatic metatexites consist of interlayered unmelted,

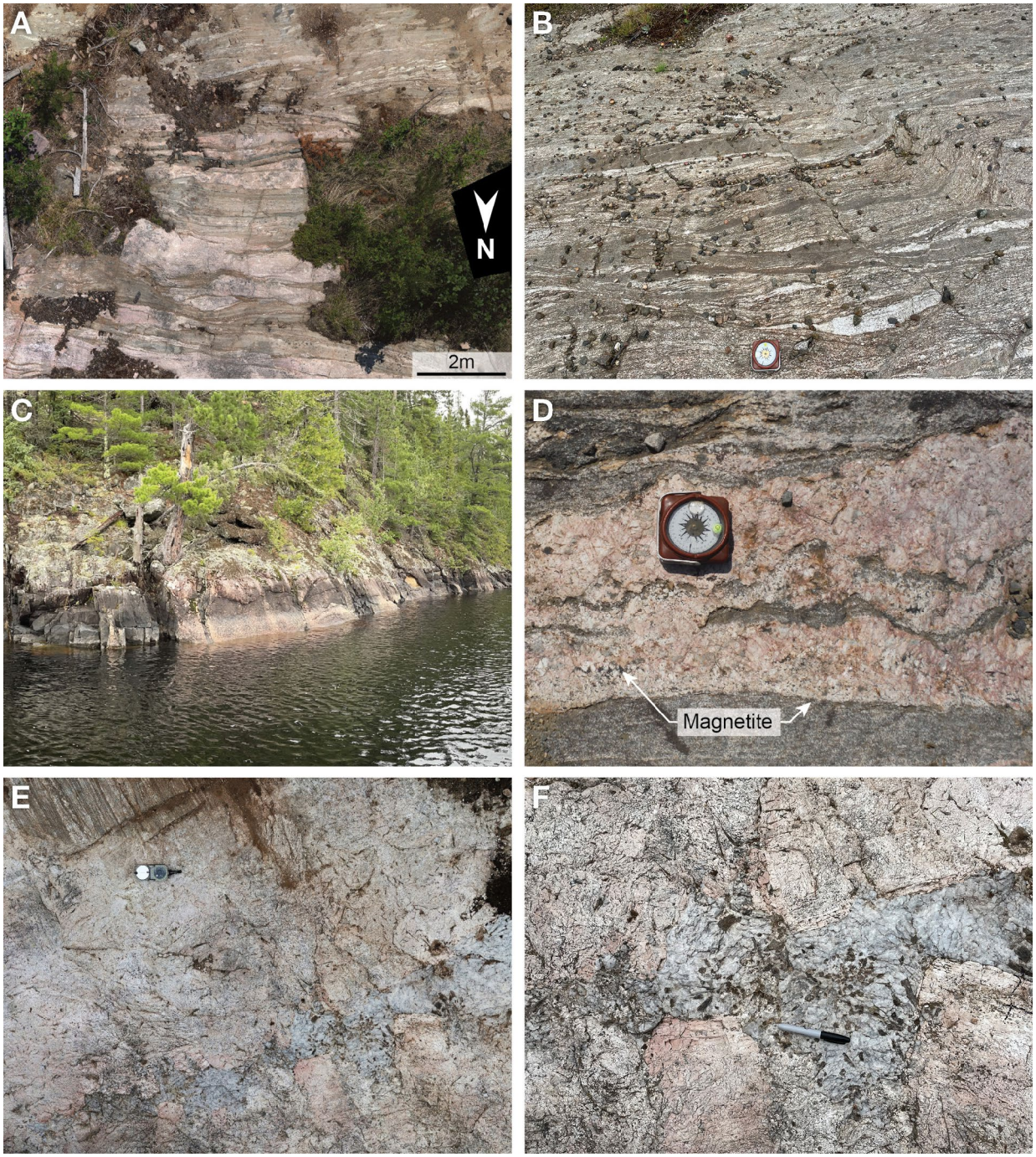


Photo 11.3. Representative photographs of the rock units occurring in the northern domain of the map area. **A)** Drone aerial photography displaying typical exposure of dextrally sheared paragneiss ± migmatitic intruded by dikes of pink magnetic granite also affected by the regional shearing (23GAL042: UTM 327149E 5402666N). **B)** Dextrally sheared stromatic metatexites intruded by a lenticular and sheared dike of peraluminous granite (23GAL771: UTM 308234E 5402906N); compass for scale is 10 cm in length. **C)** Photo showing 2 m wide dike of magnetic pink biotite-bearing granite-pegmatite intruding migmatitic paragneiss along the eastern shore of Dog Lake (23GAL831: UTM 315848E 5403865N). **D)** Close-up of magnetite-bearing pink pegmatite showing the presence of patches of magnetite (23GAL494: UTM 299091E 5405066N); compass for scale is 10 cm in length. **E)** and **F)** Undeformed north- to northeast-striking dike of garnet–pink tourmaline–bearing pegmatite discordant with the regional foliation of the paragneiss (19RM221: UTM 340510E 5405271N); in Photo 11.3E, compass for scale is 22 cm in length with the sighting arm pointing north; in Photo 11.3F, pen for scale is 14 cm in length. Note the presence of graphic feldspar megacrysts and the concentration of the pink tourmaline in the core zone of the pegmatite. All UTM co-ordinates are provided using NAD83 in Zone 16.

medium-grained dark-grey, foliated paragneiss (paleosome), and boudinaged and stretched medium- to coarse-grained quartzofeldspathic leucosomes rimmed by biotite-rich melanosome (*see* Photo 11.3B). The degree of partial melting seems to increase to the north with a volumetrically higher proportion of leucosomes. These leucosomes locally contain peritectic garnets. Although both *in-situ* versus in-source leucosomes appear to be present based on field observations, further petrographic and textural analyses are required to confirm the proportion of the 2 types of leucosomes.

Paragneiss and metatexites are intruded by east- to northeast-striking concordant lenticular dikes of magnetic (~0.13–2.94 $\times 10^{-3}$ SI units) coarse-grained pink biotite-hornblende–bearing granites and pegmatites (Photos 11.3A and 11.3C). These dikes are foliated, dextrally sheared and boudinaged, and are concentrated preferentially along intensely strained corridors. Paragneiss intruded by these magnetic pink granite-pegmatites are characterized by significantly higher values of magnetic susceptibility (ranging from 17.4 to 71.6 $\times 10^{-3}$ SI units) than typical paragneisses in this domain. This could be related to the oxidation of the paragneiss by the conversion of the iron oxides (ilmenite) and biotite to magnetite during the emplacement of these oxidized granitic melts. The presence of magnetite-rich patches and layers along the contacts between the pink granite dikes and the paragneiss supports this interpretation (Photo 11.3D). These magnetic paragneiss and pink granite dikes are coincidental with continuous east-trending high magnetic anomaly bands observed in the northern part of the area (*see* Figure 11.1A). These high-magnetic bands are crosscut by northwest-striking dextral and north- to northeast-striking sinistral faults the offsets of which are well visible on the second vertical derivative map of the total magnetic field.

As described by Metsaranta and Walker (2019) and Metsaranta (2022), the most prominent structure in this part of the map area is the QDZ, which consists of an anastomosing network of discrete shear zones that separate zones of lower strain. Kinematic indicators observed parallel to the gently plunging lineation show an obvious dextral sense of motion. However, some kinematic indicators observed on visible vertical sections of outcrops show that the QDZ points toward the existence of a thrust component in addition to the strike-slip component. These observations indicate that the QDZ is the result of a regional dextral transpressional deformation event. Field observations (e.g., dextrally sheared leucosome at the magmatic stage) show that the migmatization was coeval with the regional dextral shearing along the QDZ. Migmatites and granites account for more than 50% of the outcropping surface in this part of the map area and this suggests that the shear zone likely focussed melt ascension that, in turn, facilitated the deformation by a feedback effect. Indeed, by drastically reducing the bulk strength of the crust, the partial melting of the metawackes could cause local strain partitioning in the QDZ and explain the strong contrast of deformation intensity observed between the northern and the central domains of the map area.

Undeformed, north- to northeast-trending dikes of peraluminous granitic pegmatite crosscutting the foliation of the migmatitic paragneiss and the dextral shearing can be locally observed in this part of the map area (Photo 11.3E). They contain graphic potassium feldspar megacrysts, quartz, garnet and black to pink tourmalines that are concentrated in the core zone of the pegmatite (Photo 11.3F). These pegmatites are similar to the second generation of pegmatites observed along Highway 17 (*see* "Hadwen Lake Intrusion and Highway 17 Pegmatites").

GARNET CHEMISTRY AND CRITICAL MINERAL POTENTIAL OF THE SOUTHERN QUETICO SUBPROVINCE PEGMATITES

The map area hosts abundant peraluminous granitic pegmatites. However, no significant lithium-cesium-tantalum (LCT) mineralization has been discovered in this area. Numerous studies show that many of the LCT-type pegmatites result from the extreme fractionation of a parental peraluminous granitic intrusion (Černý 1991; London 2018). The LCT pegmatitic fields usually show a regional mineralogical and geochemical zoning pattern, with the most fractionated and enriched pegmatites

located the farthest from the inferred parental granite. Constraining this fractionation pattern is critical to identify potential fertile pegmatites and provide guidelines for exploration.

Garnet is a common accessory mineral in many peraluminous granite and granitic pegmatites observed in the map area. Numerous studies (Baldwin and von Knorring 1983; Černý 1989; Whitworth 1992; Selway, Breaks and Tindle 2005) established that the manganese contents in garnets hosted by pegmatites increase with the degree of fractionation of the pegmatitic melts and toward the core zone of the pegmatitic dikes. Consequently, the garnet composition constitutes a good exploration tool by identifying the most evolved pegmatites and constraining the fractionation pattern. The reconnaissance work, done by Breaks, Selway and Tindle (2003) along Armstrong Road, have highlighted that garnets from the Onion Lake pegmatites and the Walkinshaw Lake pegmatites are manganese rich and concluded that these pegmatites have good potential for rare-element mineralization.

To complete the garnet composition database initiated by Breaks, Selway and Tindle (2003) and constrain the fractionation pattern of the pegmatites and peraluminous granites occurring in the map area, a total of 62 samples were collected throughout the map area (*see* Figure 11.1B). Scanning electron microscopy with energy dispersive X-ray spectroscopy and electron probe microanalyses of garnets from these samples and 16 samples collected over the previous field seasons are planned during the winter of 2023–2024.

ACKNOWLEDGMENTS

We would like to thank Kate Moorhouse and Alison Griffiths for their outstanding assistance and performance during the field season. Manuel Duguet (Earth Resources and Geoscience Mapping Section, OGS) and Monica Gaiswinkler Easton (Publication Services, OGS) are thanked for their reviews and improvements to the article. Thanks to Pat Gervais (ERGMS, OGS) also for drafting assistance.

We would like to thank Fort William First Nation, Red Rock Indian Band, Métis Nation of Ontario Region 2 Thunder Bay Métis Council and Red Sky Métis Independent Nation for allowing the Ontario Geological Survey to map in their traditional land use area. Their co-operation is greatly appreciated.

REFERENCES

Baldwin, J.R. and von Knorring, O. 1983. Compositional range of Mn-garnet in zoned granitic pegmatites; The Canadian Mineralogist, v.21, p.683-688.

Breaks, F.W., Selway, J.B. and Tindle, A.G. 2003. Fertile peraluminous granites and related rare-element mineralization in pegmatites, Superior Province, northwest and northeast Ontario: Operation Treasure Hunt; Ontario Geological Survey, Open File Report 6099, 179p.

Brown, G.H. and Fogal, R.I. 1995. Precambrian geology, Ware Township; Ontario Geological Survey, Map 2616, scale 1:20 000.

Carter, M.W. 1985. Precambrian geology of Goldie Township, Thunder Bay District; Ontario Geological Survey, Preliminary Map P.2855, scale 1:15 840.

Černỳ, P. 1989. Exploration strategy and methods for pegmatite deposits of tantalum; *in* Lanthanides, Tantalum and Niobium, Springer, Berlin/Heidelberg, Germany, p.274-302.

——— 1991. Rare-element granitic pegmatites. Part I: Anatomy and internal evolution of pegmatitic deposits; Geoscience Canada, v.18, p.49-67.

Corfu, F. and Stott, G.M. 1998. Shebandowan greenstone belt, western Superior Province: U/Pb ages, tectonic implications, and correlations; Geological Society of America Bulletin, v.110, p.1467-1484.

Kehlenbeck, M.M. 1988. A fault-bounded outlier of Archean clastic rocks near Thunder Bay, Ontario; Canadian Journal of Earth Sciences, v.25, p.152-157.

London, D. 2018. Ore-forming processes within granitic pegmatites; Ore Geology Reviews, v.101, p.349-383.

MacDonald, R.D. 1939. Gorham Township and vicinity, District of Thunder Bay, Ontario; Ontario Department of Mines, Map 48C, scale 1:63 360.

——— 1941. Geology of Gorham Township and vicinity; Ontario Department of Mines, Annual Report, 1939, v.48, pt.3, 18p.

Metsaranta, R.T. 2015. Preliminary results from geological mapping of the Quetico Subprovince, the Shebandowan greenstone belt and Proterozoic rocks north of Thunder Bay; *in* Summary of Field Work and Other Activities, 2015, Ontario Geological Survey, Open File Report 6313, p.15-1 to 15-20.

——— 2022. Highlights of bedrock geology mapping in the Quetico Subprovince, north of Thunder Bay, northwestern Ontario; *in* Summary of Field Work and Other Activities, 2022, Ontario Geological Survey, Open File Report 6380, p.9-1 to 9-9.

Metsaranta, R.T. and Hamilton, M.A. 2020. A precise U/Pb age for a north-trending mafic dike from the western flank of the Marathon swarm, East Bay area, northwestern Ontario; *in* Summary of Field Work and Other Activities, 2020, Ontario Geological Survey, Open File Report 6370, p.7-1 to 7-9.

Metsaranta, R.T. and Kamo, S.L. 2021. A uranium–lead baddeleyite age for the Midcontinent Rift–related Lone Island Lake intrusion, northwestern Ontario; *in* Summary of Field Work and Other Activities, 2021, Ontario Geological Survey, Open File Report 6380, p.12-1 to 12-8.

Metsaranta, R.T. and Walker, J.A. 2019. Precambrian geology of western McGregor Township and adjacent areas, northeast of Thunder Bay; *in* Summary of Field Work and Other Activities, 2019, Ontario Geological Survey, Open File Report 6360, p.11-1 to 11-10.

Ministry of Natural Resources and Forestry 2023. Forest Resources Inventory leaf-on LiDAR; Ministry of Natural Resources and Forestry, Science and Research Branch, Forest Resource Information Unit, online data, April 10, 2022 update, https://geohub.lio.gov.on.ca/maps/lio::forest-resources-inventory-leaf-on-lidar/about. [accessed April 27, 2023]

Ontario Geological Survey 2017. Ontario airborne geophysical surveys, magnetic data, grid data (ASCII and Geosoft® formats), magnetic supergrids; Ontario Geological Survey, Geophysical Data Set 1037—Revised.

——— 2023. Ontario Mineral Inventory; Ontario Geological Survey, online database, September 2023 update, www.hub.geologyontario.mines.gov.on.ca. [accessed September 2, 2023]

Sawyer, E.W. 2008. Atlas of Migmatites; National Research Council of Canada Press, Ottawa, Ontario, The Canadian Mineralogist, Special Publication 9, 386p.

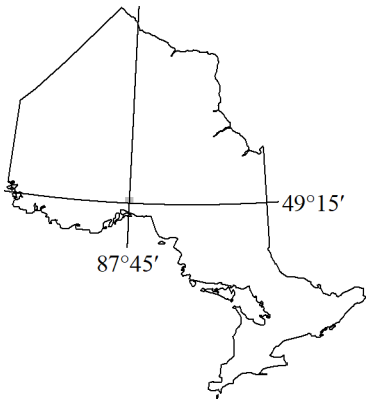
Scott, J.F. 1990a. Precambrian geology of MacGregor Township, west half, District of Thunder Bay; Ontario Geological Survey, Preliminary Map P.2985—Revised, scale 1:15 840.

——— 1990b. Geology of MacGregor Township; Ontario Geological Survey, Open File Report 5719, 82p.

Selway, J.B., Breaks, F.W. and Tindle, A.G. 2005. A review of rare-element (Li-Cs-Ta) pegmatite exploration techniques for the Superior Province, Canada, and large worldwide tantalum deposits; Exploration and Mining Geology, v.14, p.1-30.

Whitworth, M. 1992. Petrogenetic implications of garnets associated with lithium pegmatites from SE Ireland; Mineralogical Magazine, v.56, p.75-83.

12. Project NW-19-003. Archean Geology of the Georgia Lake Area, Quetico Subprovince, Northwestern Ontario



M. Duguet[1]

[1]Earth Resources and Geoscience Mapping Section, Ontario Geological Survey

INTRODUCTION

A 2 field season, 1:50 000 scale geological mapping project was started in the summer 2019 in the Georgia Lake area. The map area is represented by 1:50 000 scale National Topographic System map 42 E/5 and is located just east of Lake Nipigon. The map area includes Archean metasedimentary and intrusive rocks of the Quetico Subprovince (Superior Province), Proterozoic mafic intrusive rocks related to the Midcontinent Rift (Keweenawan sills) and several older Proterozoic dikes swarms (Figure 12.1). The Georgia Lake area was partly mapped at 1:63 360 scale in the 1960s by Pye (1964) for the western half and by Carter (1974) for the southeast corner. The rest of the map area has not been subjected to detailed mapping, but was included in the 1:250 000 compilation map of Johns, McIlraith and Stott (2003). The Georgia Lake area hosts most of the known lithium occurrences in the Quetico Subprovince, which constitutes the largest known pegmatite field in the Superior Province (Ontario Geological Survey 2019; Breaks, Selway and Tindle 2008). These pegmatites and associated S-type peraluminous granites were the subject of an extensive regional study of petrographic and chemical characteristics by Breaks, Selway and Tindle (2008).

The objectives of the project are to 1) address geoscience gaps in this area related to structure, metamorphism, plutonism and the timing of events in the Quetico Subprovince; 2) assess the level of structural control on the S-type plutonism, particularly for the rare-element pegmatites; and 3) document in more detail the different Proterozoic mafic dike swarms present in the area using geophysical interpretation, mapping, geochemistry and geochronology.

In 2023, the continuation of the field work started during the summer 2019 primarily covered the eastern part of the map area (i.e., east of Barbara Lake, *see* Figure 12.1).

SUPRACRUSTAL ROCKS OF THE QUETICO SUBPROVINCE

Mapping in the eastern part of the map area uncovered a greater quantity of metasedimentary rocks than was suggested by previous estimates (*see* for example, Breaks, Selway and Tindle 2008; or compare Figure 12.1 in this article with Figure 12.1 in Duguet 2019). Lithofacies described in Duguet (2019) for the western part of the map area apply equally to the eastern part. As noted in Duguet (2019), despite being metamorphosed in the middle to upper amphibolite facies by multiple metamorphic events, primary features in these turbidites are commonly remarkably well preserved. This is the main reason why the prefix “meta” will be omitted in this article from this point, especially when primary sedimentary features are described and discussed. Metamorphic nomenclature will be used when appropriate.

Summary of Field Work and Other Activities, 2023,
Ontario Geological Survey, Open File Report 6405, p.12-1 to 12-11.

© King’s Printer for Ontario, 2023

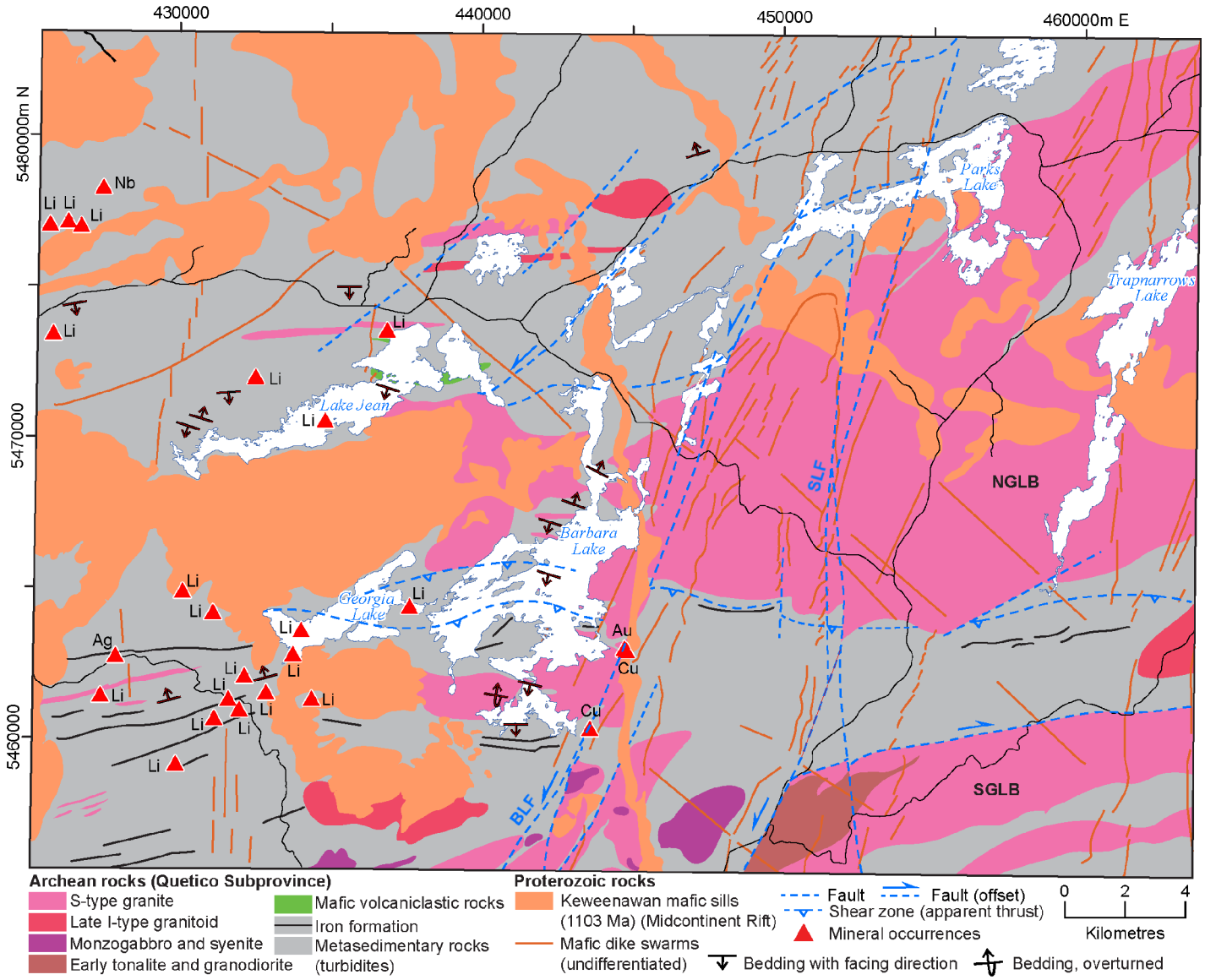


Figure 12.1. Simplified geological and structural map of the area (*modified after* Pye 1964; Carter 1974; Breaks, Selway and Tindle 2008). Mineral occurrences *from* Ontario Geological Survey (2019). Abbreviations: Ag, silver; Au, gold; Cu, copper; Li, lithium; Nb, niobium; BLF, Barbara Lake fault; SLF, Squawk Lake fault; NGLB, northern Glacier Lake batholith; SGLB, southern Glacier Lake batholith. Age of the Midcontinent Rift rocks is *from* Halls, Stott and Davis (2005). Universal Transverse Mercator (UTM) co-ordinates provided using North American Datum 1983 (NAD83) in Zone 16.

The majority of the supracrustal rocks in the study area are metasedimentary rocks derived from turbidites, and they can be organized into 2 main units that are separated from one another by a top-to-the-north thrust that is well exposed along the Barbara Lake shoreline (Duguet 2019). These units are as follows:

- The northern unit is composed mostly of massive, thick-bedded (3–5 m), very poorly sorted, greywackes. Locally, at the top of the thick beds, either laminations or thinner beds (30–40 cm thick) are present; the latter are composed of an alternation of siltstone and mudstone layers (pelites). The northern unit is well exposed along the shoreline of Parks Lake, where, despite the intense deformation, the massive aspect of sedimentary rocks in this unit is still recognizable. Boninitic volcaniclastic rocks identified during the 2019 field season interlayered with the turbidites (Duguet 2019, 2020) have not been seen in the eastern part of the map area.
- The southern unit mainly consists of thinly bedded, medium grey, metasedimentary rocks. Mudstones are interlayered with siltstones and locally some carbonate-facies iron formation. The latter are at most 1 m thick, but, despite their size, they have a strong expression on the second vertical derivative of the total magnetic field (Ontario Geological Survey 2015) and, therefore, are very good stratigraphic markers that can be followed across the entire map area.

It is possible that these 2 units represent different parts of a single turbiditic system. In this scheme, the northern unit would represent the more turbulent proximal part of the system that deposited the coarser fraction, whereas the southern unit would represent the more distal part of the system that was characterized by more intermittent laminar flows.

In the Lake Jean area, Valli, Guillot, and Hattori (2004) identified 2 main metamorphic events that affected the metasedimentary rocks. Subsequently, this was found to apply across the entire map area (*see* Duguet 2019). The first metamorphic event (M_1) is of middle pressure–middle temperature and is characterized by the assemblage garnet-staurolite-biotite-plagioclase-quartz. The second event (M_2) is into a low pressure–high temperature gradient that clearly retrogresses the earlier, M_1 Barrovian assemblages. The M_2 event is characterized by the diagnostic assemblages andalusite-cordierite-biotite or sillimanite-cordierite-biotite. The M_2 assemblages are the expression of contact metamorphism around the S-type granitic batholiths, which were emplaced at *circa* 2665 Ma (Percival and Sullivan 1988).

ARCHEAN INTRUSIVE ROCKS

The metasedimentary rocks were intruded by at least 4 types of intrusive rocks emplaced over a 50-million-year time span. These Archean intrusive rocks are described from the oldest to the youngest.

Bimodal Mafic to Felsic Intrusive Rocks

Mappable mafic intrusions were first identified by Pye (1964) (*see* Figure 12.1). These mafic intrusions are composed mostly of a well-foliated, equigranular, locally porphyritic, medium-grained, medium grey monzogabbro (Pye 1965). These intrusions coincide with magnetic highs present on the second vertical derivative of the total magnetic field (Ontario Geological Survey 2015) and are scattered along a trend parallel to the northern contact of the younger southern Glacier Lake batholith (*see* Figure 12.1). Along with their ubiquitous deformation, the location of the bodies suggests strongly that monzogabbro emplacement was controlled by a major structure. The easternmost monzogabbro intrusion, present 5 km southeast of Barbara Lake, was investigated during the 2023 field season (*see* Figure 12.1). This intrusion is very poorly exposed and the different rock types comprising it can be seen only on outcrops where younger peraluminous granites and pegmatites, more resistant to erosion, are present. Mapping by Carter (1974) identified syenite in 2 locations within that easternmost monzogabbro

intrusion. On the northern edge of the intrusion, our field investigation confirmed the presence of a pink, fine- to medium-grained, hornblende-bearing syenite. A mesocratic, medium-grained monzogabbro was also found in 3 locations. However, the relationship between the monzogabbro and the syenite could not be clearly established because they were never observed together in outcrop. Blocks of gabbro found in the area show a mylonitic fabric with clear non-coaxial shear sense indicators; unfortunately, rocks with similar textures were not observed in place.

The field relationships, the petrography and physical property measurements suggest that these syenitic and mafic intrusive rocks may be part of the sanukitoid suite (Stern, Shirey and Hanson 1989) present in most of the southern Superior Province and which range in age from 2698 to 2685 Ma in the Wabigoon Subprovince (Stevenson, Henry and Gariépy 1999). Ages of sanukitoid suite plutons in the Quetico Subprovince are bracketed between 2680 and 2670 Ma (cf. Kamo 2016; Wang et al. 2020). A sample of the syenitic part of the easternmost monzogabbro intrusion was collected for geochronology and geochemistry.

Non-magnetic gabbroic veins and sills that intruded the metasedimentary rocks were previously described in the western part of the map area (*see* Pye 1964; Duguet 2019). Additional descriptions and geochemistry of these rocks can be found in Duguet (2020). It is noteworthy that these rocks were not observed in the eastern part of the map area past the Barbara Lake fault (BLF) and the Squawk Lake fault (SLF) (*see* Figure 12.1). Interestingly, this is very similar pattern to that seen for the magnetic mafic to felsic intrusions, as the aforementioned easternmost intrusion is located just east of the BLF, but west of the SLF (*see* Figure 12.1).

Early Tonalite and Granodiorite Intrusive Rocks

In the Georgia Lake area, the presence of early tonalite and granodiorite intrusive rocks have been known for quite some time (*see* Pye 1964; Breaks, Selway and Tindle 2008), but they lacked proper mapping and geochronological characterization. In the western part of the map area, the vast majority of these intrusive rocks are quartz-feldspar porphyries emplaced parallel to the bedding of the turbidites; no sizeable body was mapped in this area (Duguet 2019). A granodiorite sampled in the western part of the study area in 2019 yielded an upper intercept U/Pb zircon age of $2676.7\ ^{+1.8}/_{-1.7}$ Ma (Kamo 2020). In the eastern part of the map area, these early tonalite and granodiorite rocks were first identified using geochemistry (Breaks, Selway and Tindle 2008); however, their geographic extent was unknown. During the summer of 2023, more of these rocks were found in the southern part of the map area. An intrusion, 4 by 2 km in size, was identified a couple of kilometres east of the monzogabbro-syenite intrusion described previously in "Bimodal Mafic to Felsic Intrusive Rocks". Outcrops are scant and most of these rocks are present as fields of chaotic blocks. Where exposed, the rock is a gneissic, light to medium grey, biotite-bearing granodiorite that is crosscut by the younger peraluminous pegmatitic granites. It can be distinguished from the S-type, biotite granite units, by its greater degree of deformation, a higher biotite content, and its magnetic susceptibility properties. For the latter, magnetic susceptibility readings for the granodiorite are between 0.10 to 0.20 $\times 10^{-3}$ SI units, which is consistently higher than the biotite granite and two-mica granites that are in the range of 0.02 to 0.05 $\times 10^{-3}$ SI units.

S-type Granites and I-type Granites

The S-type peraluminous granitoids represent by far the dominant plutonism in the area in terms of volume. Syn- to post-kinematic I-type granitoids are also present in the map area and are believed to be coeval with the S-type peraluminous granitoids (*see* Breaks, Selway and Tindle 2008). However, they will not be discussed here in detail. In the Georgia lake area, the age of the S-type plutonism has only been estimated at *circa* 2665 Ma by comparison with other parts of the Quetico Subprovince (Percival

and Sullivan 1988). Within the map area, the 2 main S-type intrusions are the southern Glacier Lake batholith (SGLB) and the northern Glacier Lake batholith (NGLB). These plutons range in composition from biotite granite to two-mica granite; the latter displaying a wide range of relative proportions between biotite and muscovite. These granites are usually massive, white, equigranular, medium to coarse grained, and may be either biotite bearing or contain 2-micas.

SOUTHERN GLACIER LAKE BATHOLITH

The southern Glacier Lake batholith (SGLB) extends along strike for over 100 km with a long axis trending approximately northeast. Ample petrographic description was provided in Pye (1965) and Breaks, Selway and Tindle (2008). Within the map area, this intrusion is exposed in the southeastern part (*see* Figure 12.1). This sector was covered by the work of Carter (1974) who mapped most of the intrusion as migmatites. This nomenclature was used by Carter (1974) to illustrate the fact that the granitic melt intruded the metasedimentary rocks as sills that range in thickness from half a metre to hundreds of metres. This configuration is especially common along the southern contact of the SGLB. In fact, true migmatitic rocks (i.e., rocks that underwent partial melting) are volumetrically rare in the map area and result from contact metamorphism of the supracrustal rocks with the granitic intrusions (melts). These structural relationships indicate that peraluminous melts were channelled along the regional composite fabric (namely $S_{0\text{-}n+1}$). Shear criteria, such as sinistral shear bands in the horizontal plan (Photo 12.1A) and top-to-the-north shear in the vertical one (Photo 12.1B), are coeval with the emplacement of the peraluminous granite; indeed, the latter rarely shows any plastic deformation, which points toward synkinematic crystallization. This strongly indicates that the emplacement of the SGLB was structurally controlled and assisted by a regional shear zone. The northern boundary of the SGLB stands in stark contrast to the southern contact. Even though in the north, the contact with the metasedimentary rocks was structurally reworked, there is a clear separation between the granite of the SGLB to the south and the host rock to the north. In addition to the differences at the boundaries of the SGLB, there are also differences along the strike of the pluton. West of the BLF (*see* Figure 12.1), the SGLB is a near continuous body with a few screens of country rock, some of them being multi-kilometres in length (Pye 1964), whereas east of this fault, the SGLB is better described as a series of sheet-like plutons with gradational contacts with the country rocks. The SGLB possesses abundant magmatic fabrics, such as biotite and muscovite schlieren and a feldspar crystal shape fabric. These magmatic foliations trend on average between 60° to 85°, which is parallel to the northern contact with the metasedimentary rocks.

The SGLB is host to both fertile granitic zones as well as pegmatite dikes. East of the BLF, no fertile granite has been identified yet. However, many pegmatite and pegmatitic granite dikes located within and outside the SGLB were observed east of the BLF. Most of these dikes are trending between north and 60° and some of them can be followed along strike over 5 to 7 km. Their thickness is also varied with the thickest ranging between 20 to 30 m. These dikes can be extremely complex texturally, varying over a few metres from potassium feldspar megacrystic fine-to medium-grained granite, to pegmatite, to aplite (Photo 12.1C). These different facies can be organized in layers that typically parallel to the trend of the dike. Accessory phases comprise garnet, cordierite and blue apatite. Tourmaline is late and usually forms in quartz myrmekitic-like pods filling interstitial spaces. A certain degree of fractionation can be seen in the field with proximal pegmatite dikes containing biotite and more distal dikes lacking biotite but containing plumose muscovite along with quartz (Photo 12.1D). For the latter, albite can also be present. It is possible that some of these dikes extended as far as into the northern Glacier Lake batholith (NGLB). However, aside from the Gathering Lake pegmatite field located outside the map area to the northeast (Breaks, Selway and Tindle 2008), no spodumene-bearing pegmatite has been observed to date east of the BLF. This contrasts strongly with the ubiquitous presence of this type of pegmatite west of the BLF. The reasons for such a difference remain to be unravel.

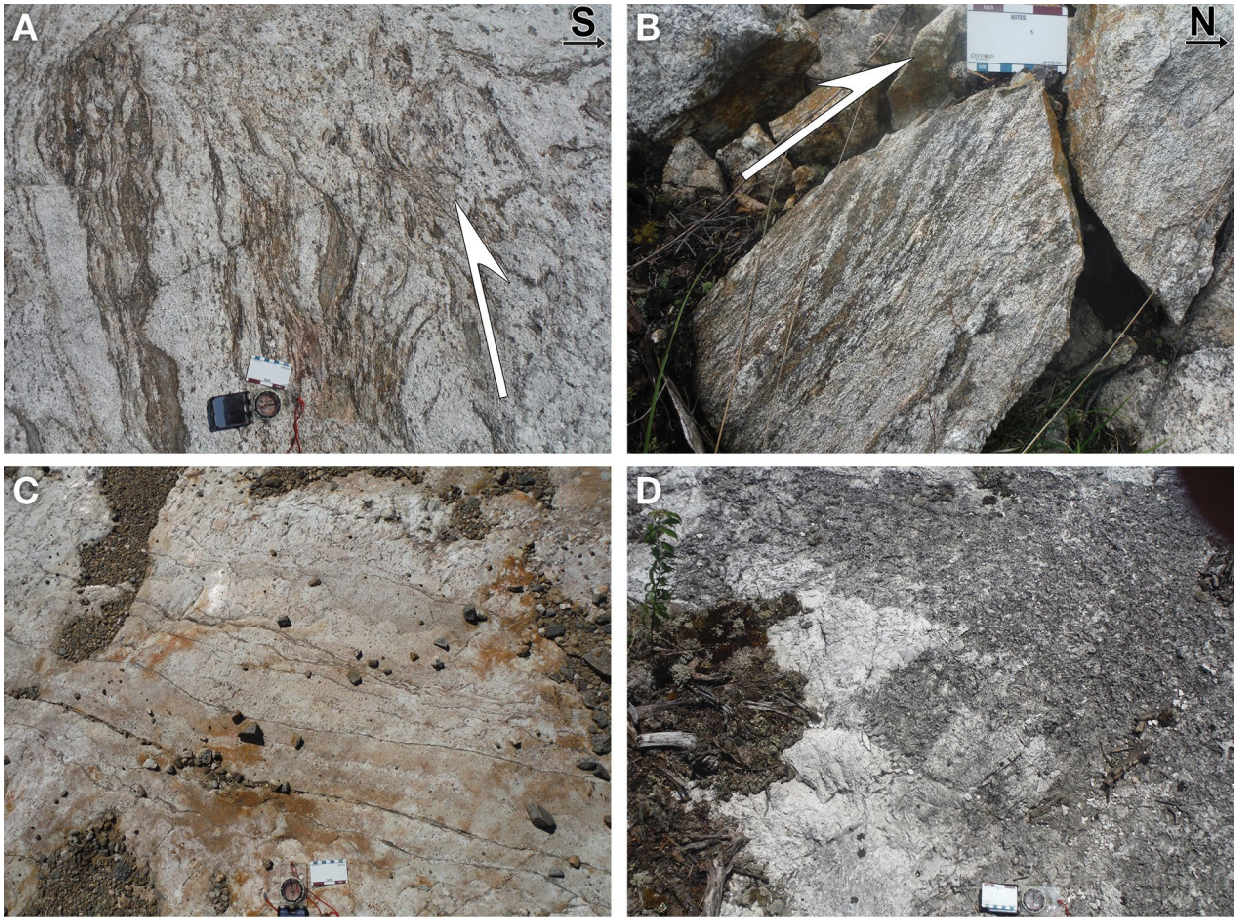


Photo 12.1. Textural features of the southern boundary of the southern Glacier Lake batholith. **A)** Metasedimentary rocks infilled with granite (UTM 462547E 5458060N). Sinistral shear bands formed during emplacement of the granitic magma. Horizontal view. **B)** Metasedimentary rocks infilled with granite (UTM 461949E 5455794N). Top-to-the north shear bands formed during emplacement of the granitic magma. Vertical view. **C)** Vari-texture in a pegmatite dike hosted in metasedimentary rocks. Dike is 4 km south of Trapnarrows Lake (UTM 458893E 5461608N). **D)** Plumose aggregate of quartz-muscovite in a pegmatite dike located south of Squawk Lake (UTM 450851E 5461983N). All UTM co-ordinates provided using NAD83 in Zone 16. Scale card in all images is 9 cm long.

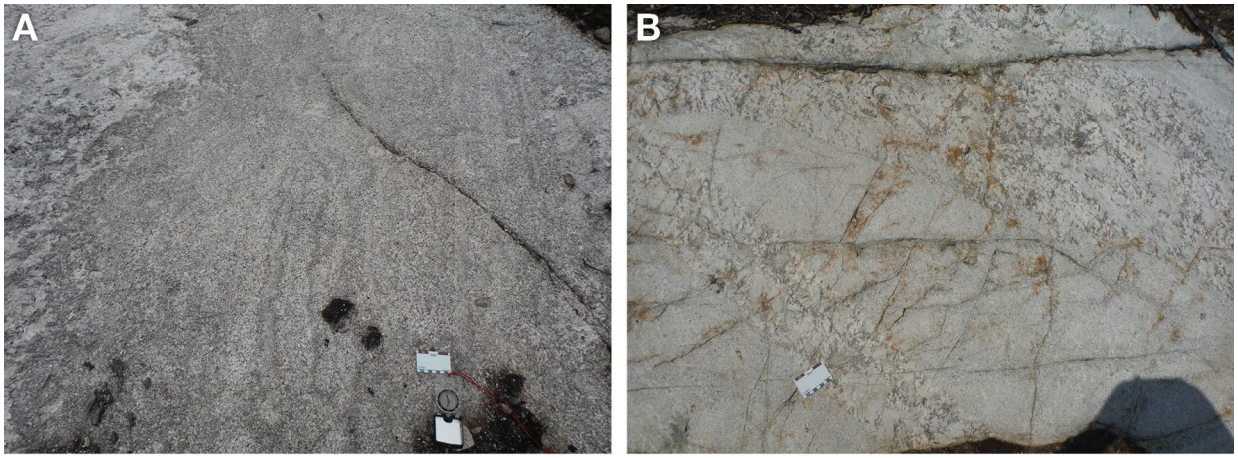


Photo 12.2. Textural features of the northern Glacier Lake batholith. **A)** Schlieren in a 2-mica granite. Note the pegmatite pod on the left side of the picture gradually transitioning into the more equigranular granite (UTM 456696E 5470143N).
B) Anastomosing network of pegmatite veins migrating into the granite (UTM 454137E 5467227N). All UTM co-ordinates provided using NAD83 in Zone 16. Scale card in all images is 9 cm long.

NORTHERN GLACIER LAKE BATHOLITH

Compared to its southern counterpart, the NGLB differs quite substantially. Notably, the NGLB displays clear boundaries with the country rock, it shows fewer visible primary structures (e.g., magmatic foliation, schlieren), nor does it show much subsolidus deformation at its boundaries. These features indicate that the structural setting during emplacement was somewhat different from that of the SGLB. Moreover, the NGLB did not seem to have generated as many pegmatite dikes as did the SGLB. Most of the visited outcrops had pegmatites, that, regardless of their nature (i.e., *in-situ* pooling of migrated melt), were present in significantly lower quantities in the NGLB, typically representing less than 5% of the outcrop areas. However, a few pooling and/or channelling areas were identified in the field and these tended to be located near the contact with the country rocks. In these pooling areas, pods of pegmatite, multiple metres in size, grade into the granite (Photo 12.2A). Other outcrops in this area contain networks of anastomosed pegmatite veins hosted in the granite (Photo 12.2B), for example, in the southeastern corner of Parks Lake. Magmatic foliation is visible clearly in these veins and is parallel to the dike contacts. These veins trend northeast on average and are parallel to the contact with the country rock.

STRUCTURAL GEOLOGY

The structural framework seen during the summer of 2023 differs little from that observed in 2019. The area is transected by megastructures that can be followed on the second vertical derivative of the total magnetic field within the map area and beyond. These megastructures are, for the most part, shear zones that, for the early ones, are responsible for the regional foliation S_1. The S_1 foliation varies greatly in intensity ranging from faint to mylonitic. The S_1 foliation affected not only the metasedimentary rocks, but also the early mafic to felsic intrusive rocks and the early generation of tonalite and granodiorite rocks. Two top-to-the-north thrusts described along the Barbara Lake shoreline (Duguet 2019) are likely coeval with, or are, late D_1, because they are crosscut by the S-type granites in the area.

A second-generation megastructure trends 60° to 70° and can be followed from Parks Lake in the northeast to Jean Lake in the southwest. This structure is prominent on the second vertical derivative of the total magnetic field (Ontario Geological Survey 2015) and is composed of at least 2 curvilinear branches that form a lens. In the Parks Lake area, the pervasive foliation dips to the northwest, but with highly varied values ranging from 45° to near vertical, whereas in the Jean Lake area, the foliation dips mainly to the north. This reversal of dip can be explained by the lensed geometry of the shear zone. In the Parks Lake area, it is likely the southern branch of the system that is exposed, whereas the northern branch is exposed in the Jean Lake area. It is possible that these 2 shear zones delineate a pop-up structure in which the part at the centre of the boudin goes up. This deformation event seems stronger in the Parks Lake area, where the metasedimentary rocks are intensely affected. Also in the Parks Lake area, primary features are rarely observed in the metasedimentary rocks, and the thickness of this shear zone is estimated at about a kilometre. In Jean Lake, a northeast-trending sinistral event was recognized by Valli, Guillot and Hattori (2004). This observation was confirmed by field work by the author in 2019, but, at that time, it could not be linked to any regional-scale event or structure. In the Jean Lake area, the S_2 foliation reworked a mostly east-trending composite $S_{0\text{-}1}$ fabric. Locally, the sinistral shearing can be seen in the pelitic layers of the metaturbidites where they defined an oblique foliation compared to the $S_{0\text{-}1}$ better preserved in the sandy layers. Sinistral shear bands were also found in the volcaniclastic rocks (Photo 12.3A). Away from this shear zone, some northeast-trending upright folds identified in the metasedimentary rocks in the Nama Creek area could be associated with this event (*see* Figure 12.1). This shear zone seems to have played a role at channelling the fractionated pegmatitic melt away from the parental peraluminous S-type granite in the area. In both the Parks Lake and Jean Lake areas, the pegmatite dikes were consistently emplaced parallel to the trend of the shear zone. This relationship is corroborated by the fact that the northern contact of the NGLB is parallel to the trend of this sinistral shear zone and, therefore, may have been geometrically constrained by this shearing event. It is

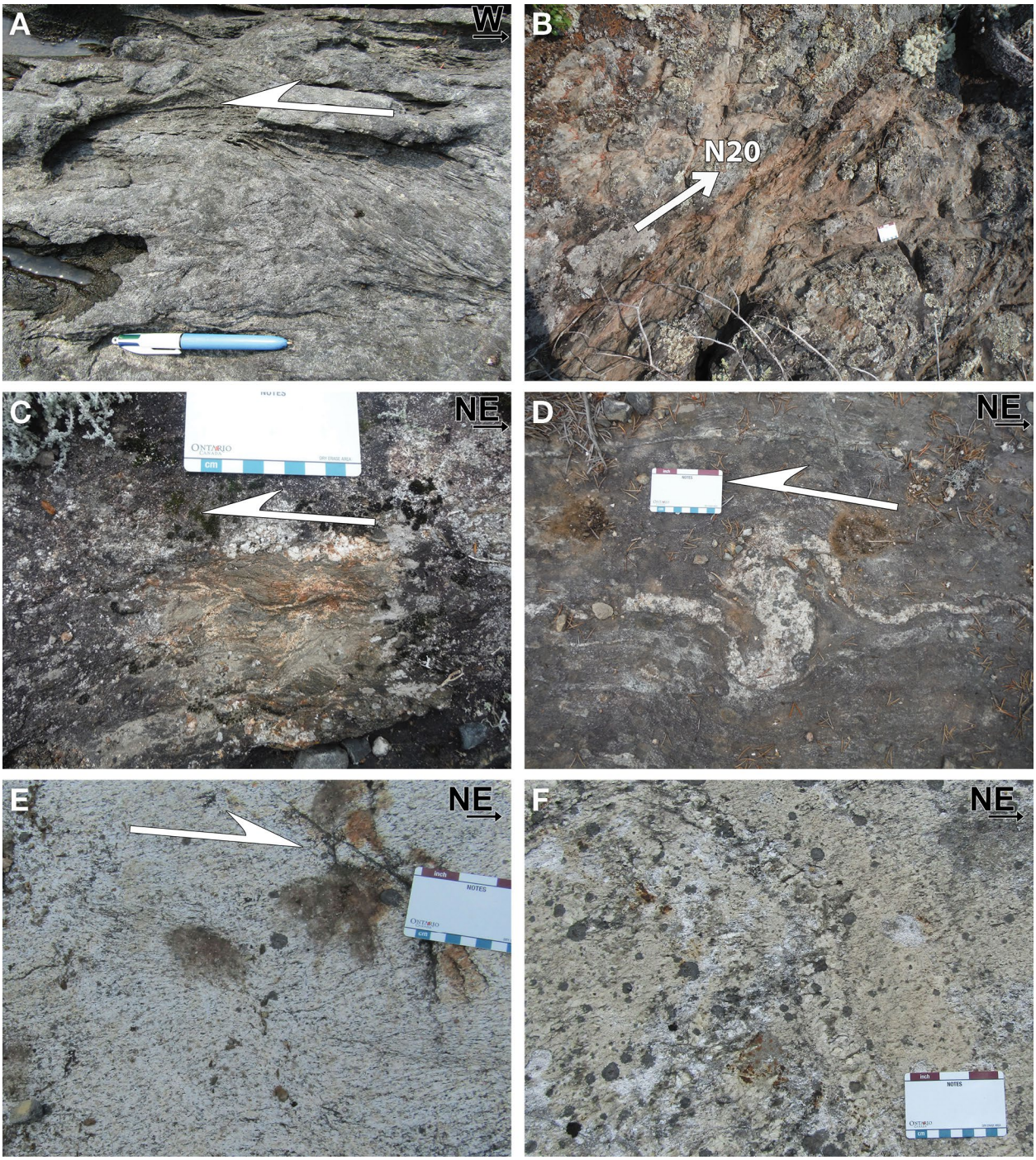


Photo 12.3. Structures and kinematic indicators in the Georgia Lake area. **A)** Sinistral shear bands affecting volcaniclastic rocks; Jean Lake shoreline (UTM 436961E 5472040N). The pen is 14 cm long. **B)** Shear zone associated with the Barbara Lake fault (BLF) and affecting the metasedimentary rocks; Parks Lake shoreline (UTM 450930E 5477946N). **C)** Greenschist displaying asymmetric boudinage giving a sinistral sense of shear. Note the undeformed granitic vein at the top of the image under the scale card that is parallel to the main foliation; Squawk Lake fault (SLF), John Ahl Road (UTM 448439E 5456310N). **D)** Peraluminous granitic vein rotated counterclockwise during shearing; Squawk Lake fault (SLF), John Ahl Road (UTM 449845E 5458058N). **E)** Dextral shear bands in the northern contact of the southern Glacier Lake batholith (UTM 453609E 5459040N). **F)** Foliation in the northern contact of the southern Glacier Lake batholith crosscutting both the pegmatite dike to the left and the granite to the right (UTM 453609E 5459040N). All UTM co-ordinates provided using NAD83 in Zone 16. Scale card in images B to F is 9 cm long.

noteworthy that this shear zone is remarkably similar in trend and kinematics to the major Gravel River shear zone, located south of the map area, which transects the Quetico Subprovince and can be followed all the way to the James Bay (*see* for example, Johns, McIlraith and Stott 2003; Rainsford and Easton 2015).

Oblique structures transecting the $S_{0\text{-}1}$ regional fabric are also prominent in the map area. A north- to northeast-trending foliation, crosscutting at a high angle the regional east-trending $S_{0\text{-}1}$ fabric, was identified in 2019 along the Barbara Lake shoreline. It has been confirmed by thin section work that this foliation was coeval with a low-pressure–high temperature metamorphism identified as M_2 (*see* "Supracrustal Rocks of the Quetico Subprovince"). As stated before, the M_2 metamorphism is the expression in the country rock of the thermal input of the S-type granitoids. Moreover, numerous granitic and pegmatitic dikes are also parallel to this fabric in the Barbara Lake area. This indicates clearly that emplacement of peraluminous granites and their associated pegmatitic fields in the area was structurally controlled. This structural control is very likely an expression of the BLF (*see* Figure 12.1). This structure, trending northeast, can be seen on the second vertical derivative of the total magnetic field (Ontario Geological Survey 2015), as well as in lidar imagery and the digital elevation model (DEM) for the map area (Ministry of Natural Resources and Forestry 2023). During the summer of 2023, similar structures were found along strike of the BLF along the Parks Lake shoreline. There, the main northeast-trending foliation is deflected along a narrow north-trending sinistral shear zone (Photo 12.3B). A similar pattern is observed farther south where the contact of the SGLB is deflected by the Barbara Lake fault (Pye 1964). Another north-trending fault, named the Squawk Lake fault (SLF), is located 7 km east of the BLF (*see* Figure 12.1). The SLF had a similar impact on the early structures. Deflection of the foliation in the metasedimentary rocks, sinistral shear sense indicators, drag folds and pegmatite dikes parallel to the fault are observed adjacent to the fault (Photos 12.3C and 12.3D). Similar to the BLF, the SLF fault is visible on the airborne magnetic survey, and the lidar and the DEM imagery. In the lidar imagery, the SLF seems to fade away just south of Parks Lake. This could mean that the SLF terminates in this area. However, when considering the trajectories of this set of faults (i.e., northeast for the BLF and north for the SLF), the possibility that they merge somewhere north of Parks Lake must be considered. Although an abundance of Quaternary till north of Parks Lake blurs the primary bedrock features, such as structural lineaments, detailed lineament analysis may be able to lift this uncertainty. Added to other evidence presented earlier in this article (e.g., absence of the mafic intrusive rocks *sensu lato* east of these faults, morphological differences in the SGLB on either side of the BLF, etc.), it is likely that the BLF and the SLF played a significant role in the geology and structural evolution of the map area. Based on the crystallization and deformation relationships with the peraluminous S-type granitoids, it also appears that the BLF and SLF may have operated at the same time as the 60° to 70°sinistral shear zone identified farther to the northwest. The full sequence of events, and the structural relationships between these 2 sets of shear zones, however, remain to be established.

The northern tectonic boundary of the south Glacier Lake batholith underwent a late dextral strike-slip shearing that affected both the two-mica granite and the metasedimentary rocks (Photo 12.3E). Within the two-mica granite itself, the deformation is clearly subsolidus with a foliation affecting the granite and crosscutting pegmatite dikes hosted within the granite (Photo 12.3F).

EXPLORATION ACTIVITY

Over the last decade, exploration for lithium has been ongoing in the Georgia Lake area where many occurrences were previously identified in the western part of the area (*see* Figure 12.1). Some of these historical occurrences, known since the mid-1950s (Pye 1965) have been reinvestigated recently. To the west, Imagine Lithium Inc. is continuing work on the Jackpot property. Historical resources at the Jackpot property were confirmed by the Imagine Lithium Inc. exploration program, which were previously estimated in 1956 at 2 million tons grading 1.09% Li_2O by Ontario Lithium Company Limited (Pye 1965). Likewise, Rock Tech Lithium Inc. has been exploring several historical properties, of which the

Nama Creek property is one of the most important. Measured resources for the Rock Tech Lithium Inc. properties was estimated at 1.89 million tonnes grading 1.04% Li_2O, with an indicated resource estimated at 4.68 million tonnes grading 1.00% Li_2O, and an inferred resource of 6.72 million tonnes grading 1.16% Li_2O (Peters and Lowicki 2018). In 2021, a preliminary economic assessment was released by Rock Tech assessing the possibility of lithium hydroxide extraction operation in the Georgia lake area (Hanrahan et al. 2021). Since 2019, exploration performed by prospectors and companies has been moving to the eastern part of the map area where nearly 100% of the available ground has been claimed.

ACKNOWLEDGMENTS

Daniel Grindall and Chris Kievit are thanked for their outstanding performance as field assistants during this summer. Wendi Lanthier of the Cedar Shores Resort is thanked for having made our stay enjoyable. This article benefitted from the visit in the field and discussions with Jason Wolf, Grant Hagedorn (OGS), Chris Beckett-Brown (OGS), Tarryn Cawood (GSC) and Jamie Cutts (GSC). Gerhard Jacob (Imagine Lithium Inc.) is warmly thanked for allowing us to look at diamond-drill cores from the Jackpot property. Also, we would like to thank Biinjitiwaabik Zaaging Anishinaabek (Rocky Bay First Nation), Bingwi Neyaashi Anishinaabek (Sand Point First Nation), Pays Plat First Nation (Pawgasheeng), Red Rock Indian Band (Opwaaganisining), Animbiigoo Zaagi'igan Anishinaabek (Lake Nipigon Ojibway), Long Lake #58 First Nation, Red Sky Métis Independent Nation and the Métis Nation of Ontario for allowing us to map on their traditional territory. Pat Gervais (OGS) drafted the figures for this article.

REFERENCES

Breaks, F.W., Selway, J.B. and Tindle, A.G. 2008. The Georgia Lake rare-element pegmatite field and related S-type, peraluminous granites, Quetico Subprovince, north-central Ontario; Ontario Geological Survey, Open File Report 6199, 176p.

Carter, M.W. 1974. Dickinson Lake area, Thunder Bay district; Ontario Geological Survey, Map 2293, scale 1:63 360.

Duguet, M. 2019. Archean and Proterozoic geology of the Georgia Lake area, Quetico Subprovince, Ontario; *in* Summary of Field Work and Other Activities, 2019, Ontario Geological Survey, Open File Report 6360, p.12-1 to 12-9.

——— 2020. Geochemistry of Archean volcaniclastic and mafic intrusive rocks, Georgia Lake area, Quetico Subprovince, northwestern Ontario; *in* Summary of Field Work and Other Activities, 2020, Ontario Geological Survey, Open File Report 6370, p.8-1 to 8-10.

Halls, H.C., Stott, G.M. and Davis, D.W. 2005. Paleomagnetism, geochronology and geochemistry of several Proterozoic mafic dike swarms in northwestern Ontario; Ontario Geological Survey, Open File Report 6171, 59p.

Hanrahan, R.J., Larder, C., Peters, K.S., Lowicki, F., Puritch, E., Feasby, D.G. and Kuchling, K. 2021. Preliminary Economic Assessment for an integrated lithium hydroxide operation from the Georgia Lake lithium project, northwest Ontario, Canada, prepared for Rock Tech Lithium Inc. by Wave International Pty Ltd., DMT GmbH & Co. KG and P&E Mining Consultants Inc.; NI 43-101 Technical Report, filed April 21, 2021, with SEDAR®, *see* www.sedarplus.com, 260p. [accessed October 18, 2023]

Johns, G.W., McIlraith, S. and Stott, G.M. 2003. Precambrian geology compilation map – Longlac sheet; Ontario Geological Survey, Map 2667, scale 1:250 000.

Kamo, S.L. 2016. Part A: Report on U-Pb ID-TIMS geochronology for the Ontario Geological Survey: Bedrock Mapping Projects, Ontario, Year 1: 2015–2016; internal report prepared for the Ontario Geological Survey, Jack Satterly Geochronology Laboratory, University of Toronto, Toronto, Ontario, 63p.

——— 2020. Part A: Report on U-Pb ID-TIMS geochronology for the Ontario Geological Survey: Bedrock Mapping Projects, Ontario Year 5: 2019-2020. internal report prepared for the Ontario Geological Survey, Jack Satterly Geochronology Laboratory, University of Toronto, Toronto, Ontario, 55p.

Ministry of Natural Resources and Forestry 2023. Forest Resources Inventory leaf-on LiDAR; Ministry of Natural Resources and Forestry, Science and Research Branch, Forest Resource Information Unit, online data, April 10, 2022 update, https://geohub.lio.gov.on.ca/maps/lio::forest-resources-inventory-leaf-on-lidar/about. [accessed April 3, 2023]

Ontario Geological Survey 2015. Ontario airborne geophysical surveys, magnetic and gamma-ray spectrometric data, grid and profile data (Geosoft® format) and vector data, Lac des Mille Lacs–Nagagami Lake area; Ontario Geological Survey, Geophysical Data Set 1078b.

——— 2019. Mineral Deposit Inventory; Ontario Geological Survey, Mineral Deposit Inventory (September 2019 update), online database.

Percival, J.A. and Sullivan, R.W. 1988. Age constraints on the evolution of the Quetico belt, Superior Province, Ontario; *in* Radiogenic and Isotope Studies: Report 2, Geological Survey of Canada, Paper 88-2, p.97-107.

Peters, K.S. and Lowicki, F. 2018. Independent technical report and updated resource estimate – Georgia Lake lithium property, Beardmore, Ontario, Canada, prepared for Rock Tech Lithium Inc. by DMT GmbH & Co. KG; NI 43-101 Technical Report, filed August 10, 2018 with SEDAR®, *see* www.sedarplus.com, 116p. [accessed October 18, 2023]

Pye, E.G. 1964. Georgia Lake area, Thunder Bay District; Ontario Department of Mines, Map 2056, scale 1:63 360.

——— 1965. Geology and lithium deposits of Georgia Lake area, District of Thunder Bay; Ontario Department of Mines, Geological Report 31, 113p.

Rainsford, D.R.B. and Easton, R.M. 2015. Ontario geophysics, mega-lineaments and gold; abstract and poster presented at KEGS symposium on Integrated Exploration for Gold in Precambrian Terranes, November 18, 2015, Toronto, Ontario.

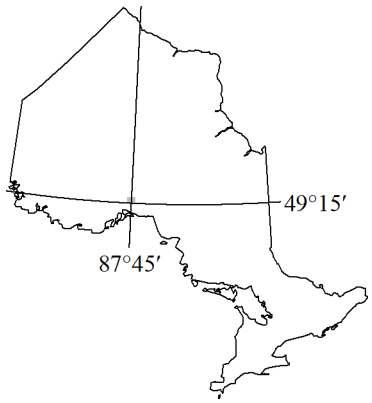
Stern, R.A., Shirey, S.B. and Hanson, G.N. 1989. Petrogenesis of mantle derived, LILE enriched Archean monzodiorite and trachyandesite (sanukitoids) in southwestern Superior Province; Canadian Journal of Earth Sciences, v.26, p.1688-1712.

Stevenson, R., Henry, P. and Gariépy, C. 1999. Assimilation-fractional crystallization origin of Archean sanukitoid suites: Western Superior Province, Canada; Precambrian Research, v.96, p.83-99.

Valli, F., Guillot, S. and Hattori, K.H. 2004. Source and tectono-metamorphic evolution of mafic and pelitic metasedimentary rocks from the central Quetico metasedimentary belt, Archean Superior Province of Canada; Precambrian Research, v.132, p.155-177.

Wang, S., Kuzmich, B., Hollings, P., Zhou, T. and Wang, F. 2020. Petrogenesis of the Dog Lake granite chain, Quetico Basin, Superior Province, Canada: Implications for Neoarchean crustal growth; Precambrian Research, v.346, article 105828, 15p.

13. Project NW-19-003. Structural Control of the Georgia Lake Lithium-Cesium-Tantalum-type Pegmatite Field, Northwestern Ontario: Preliminary Results of Lineament Analyses



M. Duguet[1] and G. Launay[1]

[1]Earth Resources and Geoscience Mapping Section, Ontario Geological Survey

INTRODUCTION

It is acknowledged that many lithium-cesium-tantalum (LCT)-type pegmatites spawn from parental peraluminous granite magmas by progressive fractionation (e.g., Wise, Müller and Simmons 2022; Bradley, McCauley and Stillings 2017, and references therein). This fractionation pattern has been documented in multiple studies that defined predictable zones of pegmatites centred on the main parent intrusion possessing very specific chemical and mineralogical compositions that reflect their degree of fractionation. Deciphering this fractionation pattern has been done commonly using geochemistry and geochronology. This type of work has indicated that melts need to travel quite long distances (up to 20 km) in order to achieve the required level of fractionation observed in LCT-type pegmatites. If the primary structural control (first order) is the geometry of the parental intrusion itself (i.e., the shape of the pluton), the distance commonly seen for melt migration in these systems must also involve some other degree of structural control (herein termed second order). One of the main difficulties when determining the level of structural control in the emplacement of LCT-type pegmatites is that most of the pegmatites are small bodies, such as dikes, sills and stocks, the emplacement of which is controlled more obviously by local structures (third order), instead of by first- and second-order structures. These local third-order structures can be difficult to link to the general regional structural framework (i.e., first- and second-order structures), even more so in areas that are distant from major shear zones. Many studies have shown, however, that deciphering even cryptic structural control of LCT-type pegmatites (or other types of ore deposits for that matter) is not beyond our reach (e.g., Silva et al. 2018; Murray, Torvela and Bills 2019). Importantly, these aforementioned studies used a variety of statistical analysis tools to quantify the level of the spatial organization of pegmatite fields compared to surrounding structures (regardless of their scale).

An example where such a study can benefit our knowledge of structural control of LCT-type pegmatite systems is located in the Georgia Lake area which hosts one of the most remarkable LCT-type pegmatite fields in Ontario (*see* Duguet, this volume). Breaks, Selway and Tindle (2008) established that there was a genetic link by melt fractionation between the parental Glacier Lake batholith *sensu lato* and the Georgia Lake pegmatite field and associated fertile granites, such as the Barbara Lake stock. This fractionation trend is identical to many others documented elsewhere in LCT-type pegmatite systems.

Field work performed by the senior author in 2019 (*see* Duguet 2019) documented the Archean history of north- to northeast-trending faults that crosscut the regional west-trending fabric. Field relationships (e.g., timing of metamorphism, deformation fabric, orientation of pegmatitic dikes parallel

Summary of Field Work and Other Activities, 2023,
Ontario Geological Survey, Open File Report 6405, p.13-1 to 13-10.

© King's Printer for Ontario, 2023

to these faults) strongly suggest that, at least in the Barbara Lake area, one of these faults, the Barbara Lake fault (BLF) (Figure 13.1A), played a significant role in channelizing granitic melt and their subsequent emplacement–crystallization. In the previously presented classification, the BLF and other faults of same orientation would qualify as second-order structures. New evidence collected during the 2023 field season in the eastern part of the area provided additional support for this interpretation (*see* Duguet, this volume).

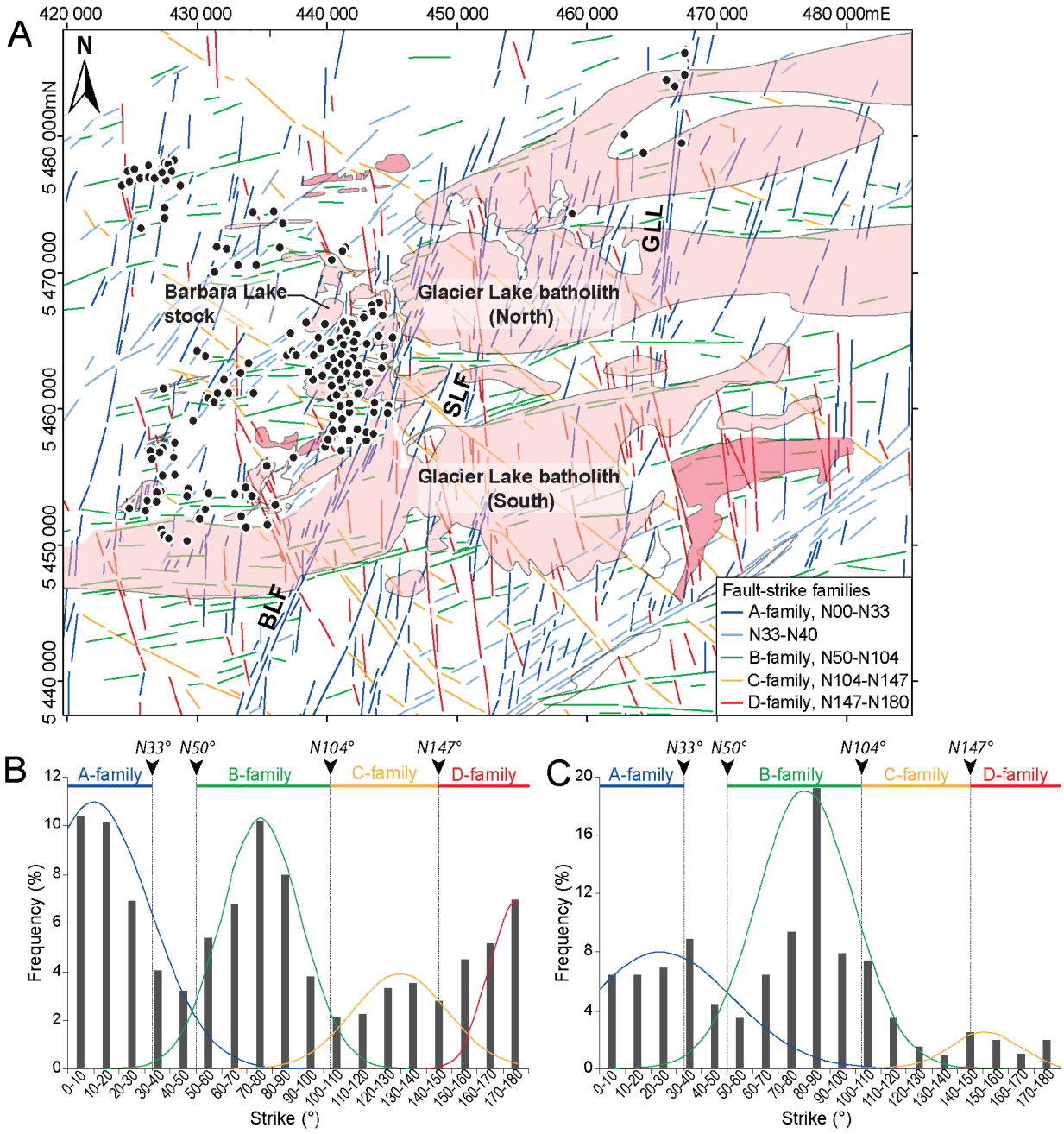


Figure 13.1. A) Lineament map based on the lineament analysis of the digital elevation model (DEM) for the Georgia Lake area. Black circles represent the pegmatite bodies documented in the area and are compiled *from* Pye (1964) and *from* Breaks, Selway and Tindle (2008). **B)** Class distribution of strike value of extracted faults within the Georgia Lake area. **C)** Class distribution of strike value of extracted pegmatite dikes within the Georgia Lake area. Abbreviations: BLF, Barbara Lake fault; SLF, Squawk Lake fault; GLL, Gathering Lake lineament. Universal Transverse Mercator (UTM) co-ordinates provided using North American Datum 1983 (NAD83) in Zone 16.

To assess the importance of the different orders of structures in the distribution of the LCT-type pegmatites in the Georgia Lake area, the spatial analysis method, outlined in Deveaud et al. (2013), was selected. That study was performed on a Phanerozoic LCT-type pegmatite field in the French Massif Central (France). In addition to the current mapping project, the Georgia Lake area was specifically chosen as a test area because of the quality of the mapping done in the 1950s by Pye (1964, 1965) who precisely documented the orientation and size of the pegmatitic bodies in the area. Preliminary results of this spatial analysis, limited to the area west of Barbara Lake, were presented by Duguet and Launay (2023); this article both summarizes that prior work and puts into perspective the field data collected during the 2023 field season.

METHODS

To constrain and discuss i) the spatial distribution of the pegmatite occurrences of Georgia Lake and ii) the spatial relationships between the pegmatites and regional-scale structural features, such as the regional foliation, shear zones, faults, and their associated lineaments, a variety of statistical tools were used, all of which are available in ESRI® ArcGIS® format. This work can be summarized into 3 stages:

- Compilation of the geology and pegmatitic bodies of the Georgia Lake area from older Ontario Geological Survey maps (e.g., Pye 1964) and data collected during the summer of 2019. In addition, the different families of lineaments occurring in the Georgia Lake area were identified and extracted from multi-directional hill-shade maps generated from Advanced Spaceborne Thermal Emission and Reflection Radiometer (ASTER) Global Digital Elevation Model (DEM) v.3 images (with 30 m of spatial resolution) using the ESRI® ArcGIS® 3D Analyst™ tool. Manual extraction of the lineaments was preferred over automatic extraction in order to discriminate the non-geological features, such as roads, railways and buildings, from true geological features. From this lineament analysis, new structural features not included in the older Ontario Geological Survey maps were identified, and the orientations of the different families of lineaments were extracted to compare with those of the pegmatites (Figures 13.1B and 13.1C).
- To characterize and quantify the level of spatial organization (i.e., clustering) of the pegmatitic bodies of the Georgia Lake area, 2 statistical methods were applied to the 203 pegmatite bodies compiled from older Ontario Geological Survey maps and data collected during this project:
  - The distance to nearest neighbour (DNN) method calculates the spacing of an individual pegmatite in a population of known density and the spatial relationship in this population (Clark and Evans 1954). A ratio (R), which represents the degree to which the distribution pattern of the observed population deviates from random expectation, is calculated. This ratio (R) ranges from 0 for an extreme clustering of the individuals to a maximum of 2.1491 for a scattered distribution. A random distribution of the population corresponds to an (R) value of 1. Herein, the calculated (R) value of 0.43 indicates a clustered distribution of the pegmatites present in the Georgia Lake area (Figure 13.2A).
  - The multi-distance spatial cluster analysis, called Ripley's K-function (Ripley 1977), and its derivatives is a complementary method to the DNN analysis that determines the degree of clustering or scattering of a set of points over a range of distances (Figure 13.2B). The second derivative (L′) of Ripley's K-function facilitates the visualization and interpretation of the distribution pattern of pegmatites for different scales (Deveaud et al. 2013). An increase of the (L′) values over a given range of distances expresses a clustering distribution of the points set, whereas a decrease of (L′) values corresponds to a scattering distribution. Constant (L′) values correspond to a random distribution of the points. The slope of the (L′) values is proportional to the rate of clustering or scattering for the considered range of

distances. The computed (L′) function for the pegmatites of the Georgia Lake area increases with distance up to 5500 m and then decreases slowly (Figure 13.2C). This highlights a clustered organization of the pegmatites up to 5500 m distance and a dispersion of these clustered groups of pegmatites beyond 5500 m. The clustering rate (slope of L′ values) of the pegmatites is high, from 0 to 2500 m, and suggests a strong control by the host rocks and/or structures on the location of the pegmatites throughout the Georgia Lake area.

- A distance-based (Euclidean distance) and density-based (kernel density) spatial analyses were performed to investigate the spatial relationships between the pegmatites and the different families of faults and/or shear zones of the Georgia Lake area. This includes the frequency analysis of
  - The shortest distance between pegmatites and the different families of structures defined by their orientations (Figure 13.3).
  - The shortest distance between pegmatites and the intersections of the structures (points).
  - The spatial densities of the structures and the intersections of the structures (Figures 13.5 and 13.4F, respectively).

For each of these spatial analyses, the frequency distributions were compared with that of a reference set of points representing "any given location" in the study area (reference distribution) to statistically distinguish true structural controls on pegmatites from apparent and insignificant spatial relationships (Deveaud et al. 2013). For this reference set, points were defined as nodes of a regular 250 m spaced grid covering the entire study area.

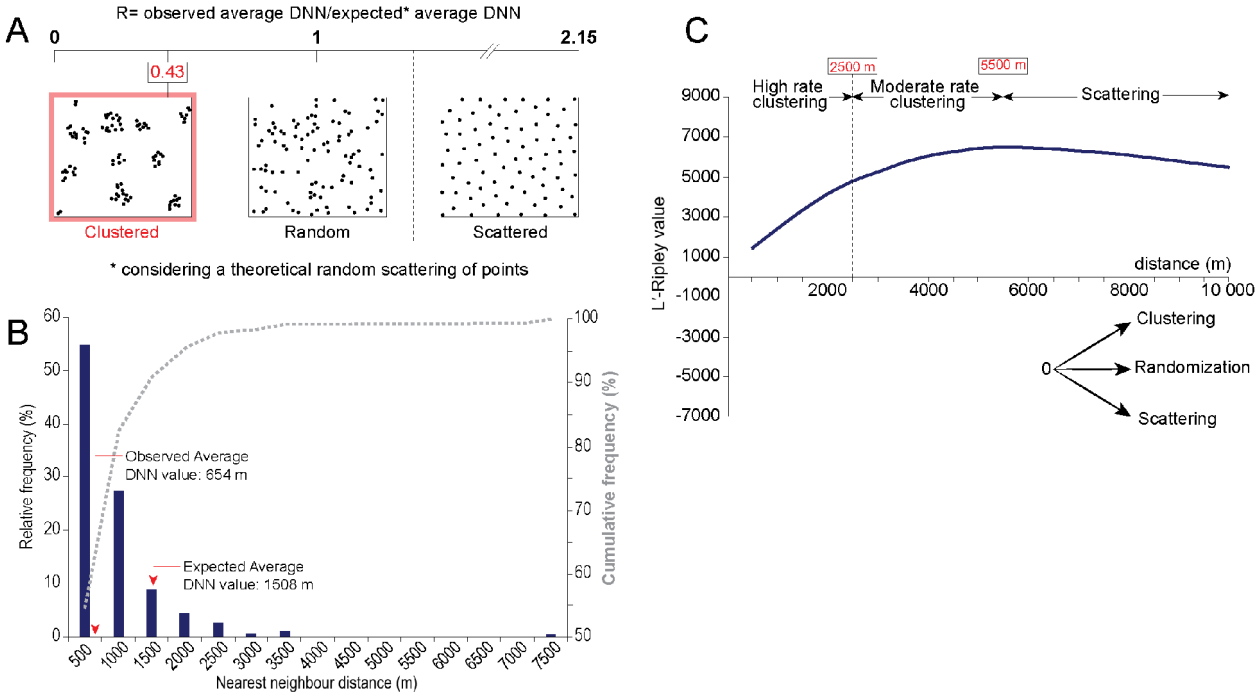


Figure 13.2. **A)** Ratio (R) computed from the observed average distance to nearest neighbour (DNN) value over the expected* average DNN value, where "*expected" = theoretical random scattering of points considered. The calculated R value of 0.43 highlights the high clustering rate of the pegmatites throughout the southern Glacier Lake batholith. **B)** Relative and cumulative frequency distributions of the distance to nearest neighbour for the 203 pegmatites considered in the entire Georgia lake area; the 500 m bin size of the histogram ranges is fixed following the Sturges's law (Sturges 1926). **C)** Ripley's L′-function computed to detect spatial deviations from a homogeneous Poisson distribution (i.e., Ripley's L′-function value = 0). The computed Ripley's L′-function value = 5000 m corresponds to a high clustering rate of the distribution of pegmatites, with a clustering distance of 2500 m and Ripley's L′-function value = 6500 m for a maximum reference distance equal to 5500 m.

RESULTS

Preliminary structural analysis of the lineaments obtained from the treatment of the ASTER Global DEM satellite images supports the presence of the north-trending Barbara Lake fault and highlights the presence of several other north- to northeast-trending fault corridors throughout the Georgia Lake area. These corridors form continuous segments over 40 to 50 km in length and are associated with high lineament densities, especially in the vicinity of the Barbara Lake stock located just east of the Barbara Lake fault (BLF) (*see* Figure 13.1). In addition, the lineament analysis assisted in identifying the main structures of the area that were categorized according to their orientation range in 4 classes (*see* Figures 13.1A and 13.1B). Of these 4 families of lineaments, 2 are clearly associated with Archean structures based on field observations. Family A corresponds to north (0°) to 30°-trending faults that crosscut at high angle the family B lineaments that were identified as the regional east-trending fabric (*see* Figure 13.1A). Particularly, the sinistral BLF and the Squawk Lake fault documented in the field (Duguet 2019; *see also* Duguet, this volume) clearly belong to family A and show prominently on the lineament analysis map (*see* Figure 13.1A).

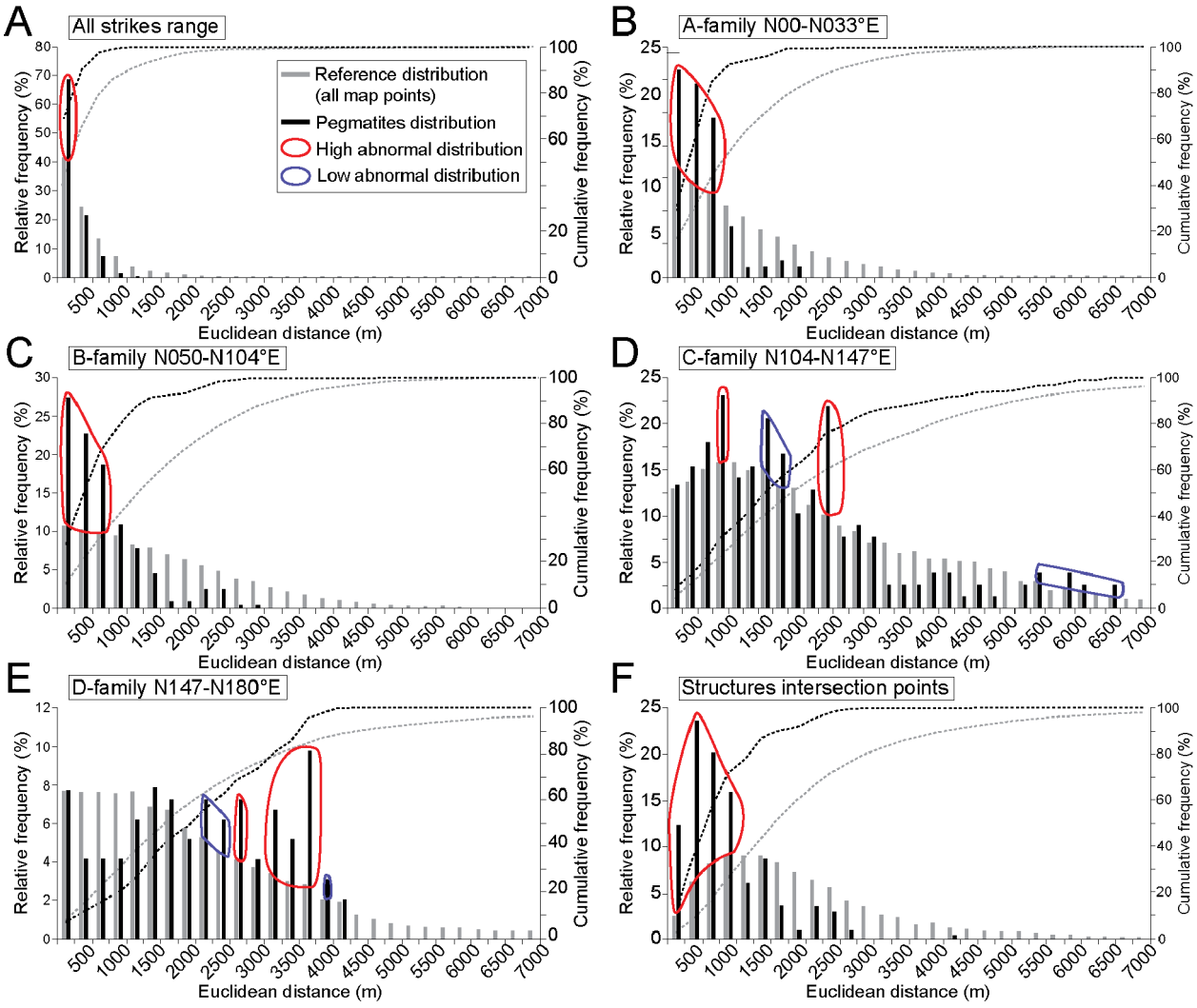


Figure 13.3. Results of statistical test for the different families of lineaments. Euclidian distances measure the frequency of the shortest distance between a pegmatite and fault and/or /shear zones, in other words, it assesses the proximity of a given pegmatite to a fault. This test was performed for **A)** all strikes range. This test was performed for each lineament family: **B)** A-family, **C)** B-family, **D)** C-family and **E)** D-family, and for **F)** all lineament intersections.

One similar lineament is present farther east and is parallel to Trapnarrows Lake, but poor outcrop exposure makes the structural relationships previously established for the BLF and the Squawk Lake fault questionable for these 2 more easterly family A structures. However, even farther east, a cluster of LCT-pegmatite, the Gathering Lake group (Breaks, Selway and Tindle 2008) is present right at the northern tip of a similar structure going along Gathering Lake (*see* Figure 13.1A). Even though the nature of families C and D remains to be assessed, family D could be a less developed branch of a conjugate set together with family A. The strong Proterozoic overprint (both dikes and faulting) in the area makes this interpretation uncertain. Orientations of pegmatite dikes correspond to families A and B (i.e., pegmatite dikes are parallel to these families) with a stronger population for the latter (*see* Figure 13.2C). One must keep in mind, however, that pegmatite dike measurements collected during the summer of 2023 in the unmapped part of the area, east of the BLF, could significantly change this distribution, switching that ratio in favour of family A. Although many pegmatite dikes seen in the eastern half of the map were emplaced parallel to the east- to northeast-trending regional fabric area (family B), pegmatitic dikes displaying trends varying from north to 40° to 50° (family A) were particularly abundant in this area (*see* Duguet, this volume). The relative proportion of these 2 families (i.e., family A and family B), therefore, remains to be quantified east of the BLF.

Euclidian distance analysis revealed a strong spatial relationship between the distribution of the known clusters of LCT-type pegmatites in the Georgia Lake area and, mainly, the faults in the area in general, regardless of their strike (Figure 13.3A), but, more importantly, with structures of families A and B. Families A and B display a peak of distance frequency at 250 m above the reference curve (i.e., high abnormal distribution) (Figure 13.3B and 13.3C). In other words, this means that 32% and 28% (relative percentage) of pegmatite bodies are 250 m away from family A and family B faults, respectively. Another 29% and 23% of pegmatites are 500 m distant from family A and family B, respectively. For reasons stated previously (e.g., detailed mapping is currently available only west of the BLF), this relationship is confirmed for only family A faults west of the BLF, with the BLF itself being included in this population. Control on pegmatite distribution by family C structures seems tenuous at best (Figure 13.3D) and non-existent for family D (Figure 13.3E). When considering the intersection of all structures (*see* Figure 13.3F), a similar relationship to that demonstrated between families A and B and the pegmatites is present. The obvious implications are that not only one or several populations of faults individually control pegmatite distribution, but that the intersection of 2 or more faults also has a strong spatial control on pegmatite distribution. This will be investigated further to assess what category(ies) of faults play the most important role in pegmatite distribution.

Kernel density diagrams show the exact same relationships previously established with the Euclidian distance analysis, but add another layer of refinement in our understanding (Figure 13.4). Kernel density diagrams allows one to assess the distribution of pegmatites compared to the density of lineament (reported to a given surface). This correlates directly with the damage zone that a shear zone does to its host rock; or, in other words, the longer the shear zone, the more damage the host rock will sustain around it. Similarly, a high density of lineament (i.e., damage) can be achieved by the intersection of several family of structures. When considering all the family groups together, pegmatites display a highly abnormal distribution for fault densities greater than 1.4 (Figure 13.4A). The same applies to families A and B (Figures 13.4B and 13.4C, respectively) in which pegmatites cluster in the highest density of lineament. Conversely, no relationship between pegmatite clustering and fault density was established for families C and D (Figures 13.4D and 13.4E, respectively). The kernel density can be represented in a map view as well, highlighting areas of maximum damage around a given family of fault. On Figures 13.5A and 13.5B, pegmatite bodies clearly cluster in areas of maximum damage around faults of families A and B (areas of high kernel density in Figures 13.5A and 13.5B, respectively).

SUMMARY

- Structures of families A and B are the main structures that control pegmatite distribution in the Georgia Lake area and are considered second-order structures (*see* Figures 13.2, 13.3 and 13.4).
- Pegmatite distribution in the Georgia Lake area is correlated also with the maximum damage zone associated with documented structures (i.e., intersection of different families of structure) (*see* Figures 13.4 and 13.5).

Altogether, these results suggest that the pegmatite melts in the Georgia Lake area were channellized along these north- to northeast-trending faults before their emplacement in adjacent subsidiary structures to form the LCT-type pegmatite bodies that are observed today.

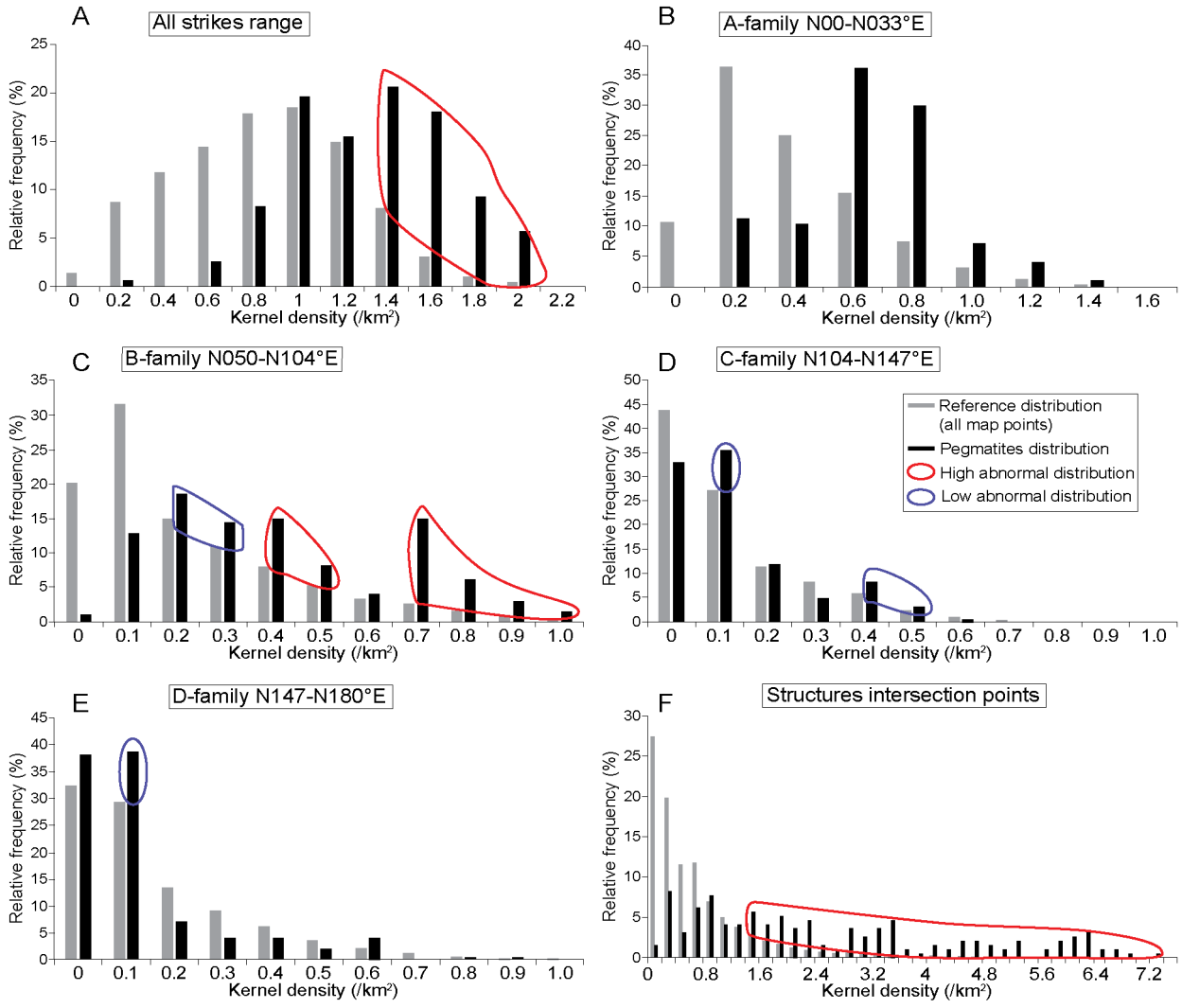


Figure 13.4. Results of statistical test for the different families of lineaments. Kernel density diagrams measure the frequency of spatial distribution of the pegmatite compared to the spatial density of faults, in other words, it assesses the spatial distribution of pegmatitic bodies compared to the damage zone of faults. This test was performed for **A)** all strikes range. This test was performed for each lineament family as **B)** A-family, **C)** B-family, **D)** C-family and **E)** D-family, and for **F)** all lineament intersections.

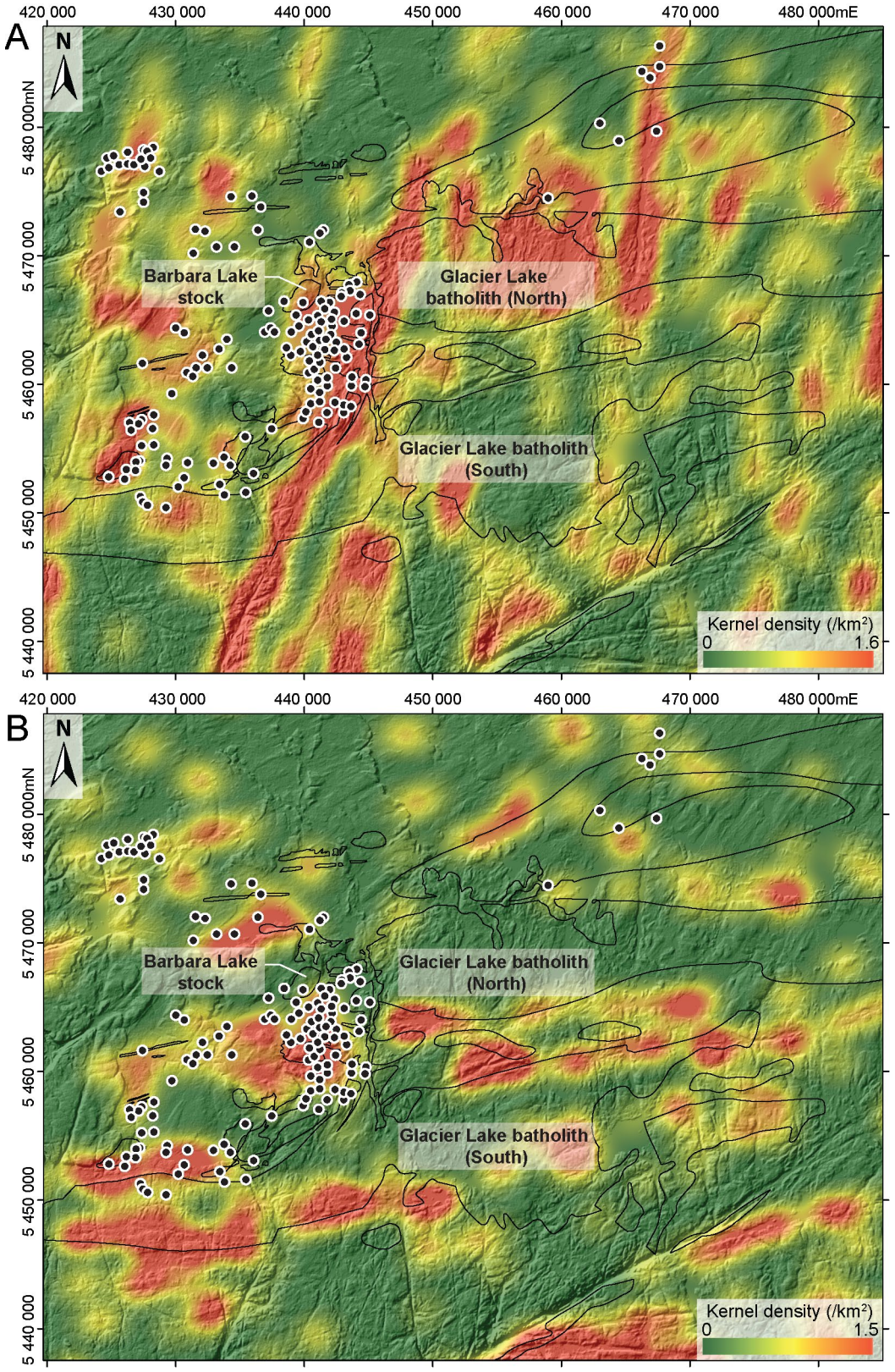


Figure 13.5. Kernel density maps for **A)** family A and **B)** family B. The black dots shown on both maps are the known pegmatite occurrences compiled *from* Pye (1964) and *from* Breaks, Selway and Tindle (2008). All UTM co-ordinates provided using NAD83 in Zone 16.

Further investigation is needed to assess the full picture of the structural control of pegmatites in the Georgia Lake area. This includes lineament analyses incorporating the newly available lidar for the area. In addition, spatial statistical analysis (i.e., Euclidian distances, kernel density diagrams) will be extended farther east (i.e., east of the BLF) and incorporating data acquired during the 2023 field season. The spatial statistical analysis performed to establish the structural control of the pegmatites will also assess the possible influence of the host rocks (i.e., granitoids versus metasedimentary rocks) in pegmatite distribution in the area. In this article, all of the different types of pegmatites present in the Georgia Lake have been treated as a single entity. An important next step will be to perform this statistical analysis for each category of pegmatites that can be identified in the Georgia Lake area.

ACKNOWLEDGMENTS

We would like to thank Biinjitiwaabik Zaaging Anishinaabek (Rocky Bay First Nation), Bingwi Neyaashi Anishinaabek (Sand Point First Nation), Pays Plat First Nation (Pawgasheeng), Red Rock Indian Band (Opwaaganisining), Animbiigoo Zaagi'igan Anishinaabek (Lake Nipigon Ojibway), Long Lake #58 First Nation, Red Sky Métis Independent Nation and the Métis Nation of Ontario for allowing us to conduct field work on their traditional territory. Pat Gervais (OGS) drafted the figures for this article.

REFERENCES

Bradley, D.C., McCauley, A.D. and Stillings, L.M. 2017. Mineral-deposit model for lithium-cesium-tantalum pegmatites; United States Geological Survey, Scientific Investigations Report 2010–5070–O, 48p. doi.org/10.3133/sir20105070O

Breaks, F.W., Selway, J.B. and Tindle, A.G. 2008. The Georgia Lake rare-element pegmatite field and related S-type, peraluminous granites, Quetico Subprovince, north-central Ontario; Ontario Geological Survey, Open File Report 6199, 176p.

Clark, P.J. and Evans, F.C. 1954. Distance to nearest neighbor as a measure of spatial relationships in population; Ecology, v.35, p.445-453.

Deveaud, S., Gumiaux, C., Gloaguen, E. and Branquet, Y. 2013. Spatial statistical analysis applied to rare-element LCT-type pegmatite fields: An original approach to constrain faults pegmatites-granites relationships; Journal of GEOsciences (formerly Journal of the Czech Geological Society), v.58, p.163-182. doi.org/10.3190/jgeosci.141

Duguet, M. 2019. Archean and Proterozoic geology of the Georgia Lake area, Quetico Subprovince, Ontario; *in* Summary of Field Work and Other Activities, 2019, Ontario Geological Survey, Open File Report 6360, p.12-1 to 12-9.

Duguet, M. and Launay, G. 2023. Structural control of the Georgia Lake lithium-cesium-tantalum-type pegmatite, A field and lineament analysis perspective, Quetico Subprovince, Ontario; abstract *in* Geological Association of Canada–Mineralogical Association of Canada–Society for Geology Applied to Mineral Deposits, Annual Meeting, Sudbury, Ontario, May 25–27, Abstracts, v.46, Geoscience Canada, v.50, p.136.

Murray, S., Torvela, T. and Bills, H. 2019. A geostatistical approach to analyzing gold distribution controlled by large-scale fault systems – An example from Côte d'Ivoire; Journal of African Earth Sciences, v.151, p.351-370.

Pye, E.G. 1964. Georgia Lake area, Thunder Bay District; Ontario Department of Mines, Map 2056, scale 1:63 360.

——— 1965. Geology and lithium deposits of Georgia Lake area, District of Thunder Bay; Ontario Department of Mines, Geological Report 31, 113p.

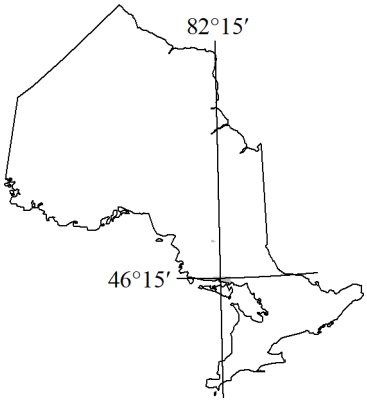
Ripley, B.D. 1977. Modelling spatial patterns; Journal of the Royal Statistical Society, Series B (Methodological), v.39, p.172-212. doi.org/10.1111/j.2517-6161.1977.tb01615.x

Silva, D., Lima, A., Gloaguen, E., Gumiaux, C., Noronha, F. and Deveaud, S. 2018. Spatial geostatistical analysis applied to the Barroso-Alvão rare-elements pegmatite field (Northern Portugal); Frontiers in Information Systems, v.1, p.67-101.

Sturges, H. 1926. The choice of class interval; Journal of the American Statistical Association, v.21, p.61-65.

Wise, M.A., Müller, A. and Simmons, W.B. 2022. A proposed new mineralogical classification system for granitic pegmatites; The Canadian Mineralogist, v.60, p.229-248. doi.org/10.3749/canmin.1800006

14. New Mafic Sill Complex Identified in the Lower Huronian Supergroup Succession: The May Township Sills



W. Bleeker[1], S.L. Kamo[2], R.M. Easton[3] and D.W. Davis[2]

[1]Geological Survey of Canada, Ottawa, Ontario K1A 0E8
[2]Jack Satterly Geochronology Laboratory, Department of Earth Sciences, University of Toronto, Toronto, Ontario M5S 3B1
[3]Earth Resources and Geoscience Mapping Section, Ontario Geological Survey, Sudbury, Ontario P3E 6B5

INTRODUCTION

The Paleoproterozoic Huronian Supergroup succession of Ontario and Quebec unconformably overlies a large part of the southern Superior craton (e.g., Roscoe 1969; Card et al. 1972; Bennett, Dressler and Robertson 1991; Roscoe and Card 1992; Young et al. 2001). Its state of deformation varies from tightly folded (and refolded) along its southernmost extent in Ontario, along the shores of Lake Huron, to essentially undeformed and flat lying farther north in Ontario and Quebec. The approximate age range of deposition for the Huronian succession is from *circa* 2500 Ma to *circa* 2250 Ma, with a firm minimum age constraint provided by abundant mafic sills of the Nipissing suite that intruded the entire succession, and which have been precisely dated at *circa* 2215 to 2217 Ma (e.g., Krogh et al. 1987; Davey et al. 2019; Kamo 2022). Although nearly all detrital zircon ages across the various formations of the Huronian Supergroup are Archean in age, and clearly derived from exhumed and eroded Archean basement of the Superior craton, there are a few younger, although minor, age modes that have been identified (*see* summary in Easton 2019; *see also* Rainbird and Davis 2006; Craddock et al. 2013; Rasmussen, Bekker and Fletcher 2013; Hill, Davis and Corcoran 2018). The most significant among these are sparse *circa* 2500 to 2510 Ma detrital grains documented in the lower rift sequence of the Huronian Supergroup, thus providing a maximum age of deposition for the base of the supergroup, and a well-defined *circa* 2310 Ma population in mudstones and cherty tuffs of the Gordon Lake Formation near the top of the supergroup (Rasmussen, Bekker and Fletcher 2013; Hill, Davis and Corcoran 2018). As there is no known source rock of that age in either the Huronian Supergroup or in the wider hinterland of the Superior craton, these zircons, with an age of 2310 Ma, must have blown in with felsic ash material from a distant source in other craton fragments (or their active margins) that at the time were contiguous with the Superior craton in what has been referred to as supercraton Superia (Bleeker 2003), that is, the larger, ancestral, cratonic landmass from which the present Superior craton originated as an internal fragment following breakup at *circa* 2100 to 2000 Ma. The same population of *circa* 2310 Ma zircons has also been identified in tuff layers of the Transvaal Basin, overlying the Kaapvaal craton fragment of southern Africa (Rasmussen, Bekker and Fletcher 2013). Together with numerous other lines of evidence, the Kaapvaal craton was, therefore, close to and contiguous with Canada's Superior craton from the late Archean to the time of Paleoproterozoic breakup and dispersal of the various cratonic fragments at *circa* 2100 to 2000 Ma (Bleeker et al. 2016).

Laterally extensive mafic sill complexes and their feeder dike swarms, commonly extending over distances of more than 1000 to 2000 km from their magmatic source areas, can provide the critical constraints for paleogeographic reconstructions of ancient terranes and cratonic fragments, that is, in their pre-breakup configuration. As a rule of thumb, if at least 2 independent, pre-breakup, large mafic magmatic events of different age can be matched and correlated across various cratonic fragments,

Summary of Field Work and Other Activities, 2023,
Ontario Geological Survey, Open File Report 6405, p.14-1 to 14-13.

© King's Printer for Ontario, 2023

it follows that these fragments were "nearest neighbours" and, therefore, likely contiguous in an ancestral landmass (Bleeker 2004; Bleeker and Ernst 2006), that is, in a "supercraton", such as Superia. Additional constraints, such as dike trends, distinct basement geological terranes and trends, and paleomagnetic information, can then be used to fine-tune their relative paleogeographic positioning (e.g., Bleeker and Ernst 2006; Ernst and Bleeker 2010; Kilian et al. 2016a, 2016b; Davey et al. 2020).

Large mafic sill complexes, such as the Nipissing sills, are of course also of interest in their own right in terms of their magmatic genesis and evolution, as hosts to various styles of mineralization (e.g., Fyon et al. 1992; Lightfoot and Naldrett 1996; Jobin-Bevans 2004, 2016; Sproule et al. 2007; Davey et al. 2019), or in terms of constraining the evolution of their host rocks, such as the Huronian succession.

It is with much of this in mind that considerable efforts have been expended to better understand the Nipissing sill complex, as well as potentially other sills and their feeder dikes, and all the various other mafic dike swarms that have intruded the southern Superior craton and/or its Huronian Supergroup cover (*see* Bleeker et al. 2015). This article briefly summarizes some key features of the Nipissing sills (*circa* 2215–2217 Ma), and then introduces evidence for a distinct and significantly older mafic sill complex intruding the lower Huronian Supergroup succession and first recognized in May Township (Jackson et al. 1994; Jackson 2001). New U/Pb geochronological data, on 3 independent samples across several townships, show that these sills, referred to as the "May Township sills", are *circa* 2258±2 Ma in age and predate the more widespread Nipissing sills by *circa* 40 million years. These sills thus add an important and sharply timed "bar" to the "magmatic barcode" (Bleeker 2004) of the southern Superior craton and may provide further critical insights into the pre-breakup paleogeography of supercraton Superia.

HURONIAN SUCCESSION AND SUPERGROUP

The Paleoproterozoic Huronian Supergroup comprises an extensive and well-preserved epicontinental sedimentary succession, locally up to approximately 10 km thick, the erosional remnants of which overlie much of the southernmost Superior craton (e.g., Card et al. 1972; Bennett, Dressler and Robertson 1991; Roscoe and Card 1992; Young et al. 2001). Close in time to the Archean–Proterozoic eon boundary, it is of global significance not only because of its exceptional preservation, but also because the sedimentary succession records 3 separate Paleoproterozoic glacial cycles (e.g., Young and Chandler 1968; Young 1973a, 1973b), as well as the Great Oxidation Event (or "GOE"; Roscoe 1969, 1973; Holland 2002; Gumsley et al. 2017) at *circa* 2400 Ma and some of the oldest unambiguous epicontinental red-bed sandstones. A summary of its stratigraphy is shown in Figure 14.1. Traditionally, it has been subdivided into 4 lithostratigraphic groups: a lowermost volcanic and siliciclastic-dominated rift succession (Elliot Lake Group) and 3 successively younger groups dominated by cyclic sequences of diamictite, siltstones and mudstones, and cross-bedded arenites (the Hough Lake, Quirke Lake and Cobalt groups, respectively; *see* Figure 14.1). The uppermost Cobalt Group, which onlaps significantly farther north across Archean basement and includes the oldest unambiguous red-bed sandstones in the upper Gowganda Formation, as well as the overlying Lorrain Formation, has been informally subdivided into a lower Cobalt Group proper, and an upper Flack Lake group (Wood 1973; Long 2009). In the finer grained siliciclastic rocks of the Gordon Lake Formation, near the base of this upper Flack Lake group, it is where the *circa* 2310 Ma tuffaceous and/or detrital zircon mode shows up for the first time (Rasmussen, Bekker and Fletcher 2013; Hill, Davis and Corcoran 2018), thus providing a maximum age of deposition for the uppermost formations of the Huronian Supergroup.

Both the timing *and* paleomagnetic constraints for the lowermost, volcanically active, rift-related Elliot Lake Group are of relatively high quality, with the earliest magmatism of mafic layered intrusions being emplaced at the base of the succession at *circa* 2480 Ma (e.g., Krogh, Davis and Corfu 1984; Clough and Hamilton 2017; *see also* Heaman cited *in* Easton 2003; Bleeker et al. 2015), and a key paleomagnetic pole (e.g., Bates and Halls 1990, and references therein) for the Matachewan dikes at

circa 2460 Ma (Heaman 1997; Halls, Stott and Davis 2005; Bleeker et al. 2015) placing the area at low latitude at that time. This is important because it favours a "snowball Earth" icehouse state for the overlying first glacial cycle, represented by the superbly preserved diamictites of the Ramsay Lake Formation. Also, the second glacial cycle (Bruce Formation) is likely to have been a "snowball Earth" icehouse event because it is overlain by thinly layered carbonates of the Espanola Formation, essentially the only carbonates in the Huronian succession and which have been argued to represent a "cap carbonate"

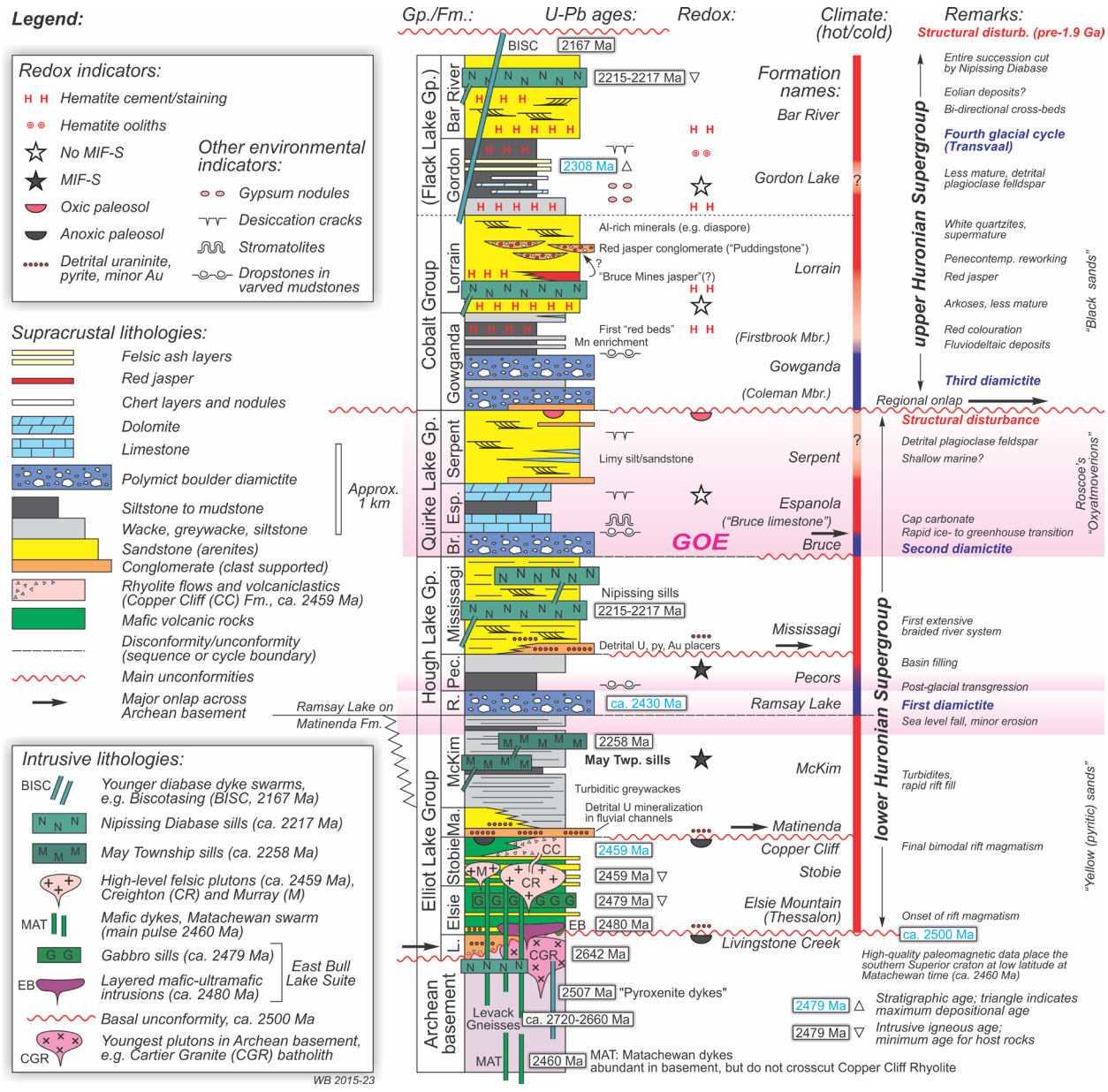


Figure 14.1. Summary stratigraphic column of the Paleoproterozoic Huronian Supergroup from 2500 to 2300 Ma, unconformably overlying Archean basement of the southern Superior craton (*from* Bleeker and Kamo 2022). *Compiled from* numerous sources: Young (1973a) and contributions therein; Bennett, Dressler and Robertson (1991); Young et al. (2001); Papineau, Mojzsis and Schmitt (2007); Gumsley et al. (2017). Age data *from* Krogh, McNutt and Davis (1982); Krogh, Davis and Corfu (1984); Corfu and Andrews (1986); Noble and Lightfoot (1992); Heaman (1997); Rasmussen, Bekker and Fletcher (2013); Bleeker et al. (2015); Davey et al. (2019). Note the May Township sills ("M") intruding the McKim Formation turbiditic greywackes at the top of Elliot Lake Group. Abbreviations: GOE, Great Oxidation Event (at *circa* 2400 Ma); MIF-S, mass-independent fractionation of sulphur (S) isotopes.

following the rapid meltdown of near-global ice sheets (Bekker et al. 2005; *see also* Kirschvink 1992; Hoffman et al. 1998; Hoffman and Shrag 2000; Kirschvink et al. 2000).

It is commonly presumed, rather uncritically (e.g., Zolnai, Price and Helmstaedt 1984; Bennett, Dressler and Robertson 1991; Young et al. 2001; Young 2019; Bradley 2008), that the Huronian Supergroup succession represents a rift to passive margin sequence, but this is mostly based on a southward-thickening wedge of volcanic and sedimentary rocks. There is, however, little direct evidence for the area having evolved into a south-facing (present co-ordinates) passive margin at *circa* 2400 to 2300 Ma. Instead, the entire succession may rather represent an extensive epicontinental rift-and-sag basin, with a south-facing passive margin only having developed much later at *circa* 2100 to 2000 Ma following breakup along the southern margin of Superia, and rifting off of the Kaapvaal, Wyoming and Karelia craton fragments. In this context, the Chocolay Group in Michigan (e.g., Larue 1981; Bekker, Karhu and Kaufman 2006), with its extensive shallow water carbonates and, importantly, devoid of any Nipissing or May Township suite mafic sills, almost certainly represents the erosional remnants of the rift to passive margin sequence at *circa* 2100 Ma.

It is, of course, possible that the epicontinental rift-and-sag basin represented by the Huronian Supergroup formed in an intra-cratonic setting, but was related and connected to a rather distal early breakup margin of the Superia supercraton—a distal margin that has yet to be identified, but was most likely situated along the eastern margin of Superia, an area now removed and obscured by the Mesoproterozoic Grenville Orogen. For the Huronian Supergroup itself, an intra-cratonic basin setting is consistent with new data from the Grenville Province south of Sudbury, indicating that only rocks of the Elliot Lake Group, and the upper Cobalt Group, are present within the immediate hanging wall of the Grenville Front (Easton, this volume, Article 18; Culshaw et al. 2023).

The successive groups of the Huronian Supergroup are separated by disconformities or minor unconformities. The most distinct of these is the lower sequence boundary of the Cobalt Group, defined by the base of the Gowganda Formation. Marked by well-preserved diamictites and polymict conglomerates, there was extensive onlap farther across the craton along this contact or unconformity (*see* Figure 14.1). At least in 1 place, northeast of Sudbury, a minor angular unconformity has been demonstrated where Gowganda Formation strata overlie previously tilted older units (Meyn 1973).

Evidence for the putative “Blezardian orogeny” at *circa* 2350 Ma (Stockwell 1982; Frarey, Loveridge and Sullivan 1982; Mungall and Hanley 2004) is lacking, however, and is largely based on confused structural relationships related to the giant Sudbury impact event and large-scale crater rebound and associated deformation at 1850 Ma (*see* discussion in Bleeker et al. 2015; Bleeker and Kamo 2022). The granite plutons in Blezard Township near the community of Copper Cliff, are now known to be A-type granites coeval with Elliot Lake Group rift magmatism, representing subvolcanic plutons related to the *circa* 2459 Ma Copper Cliff Formation (rhyolite) (Bleeker et al. 2015; *see also* Smith 2002). They do not represent orogenic granites as initially postulated or inferred (Stockwell 1982; Frarey, Loveridge and Sullivan 1982). The orientations of shatter cones associated with the Sudbury impact event at 1850 Ma closely correlate with tilted and folded bedding attitudes and, once restored into a rational pattern, indicate that the Huronian Supergroup strata were largely flat lying in the wider Sudbury area at the time of impact (Bleeker et al. 2015; Bleeker and Kamo 2022). Similarly, Nipissing gabbro sills are generally concordant with Huronian Supergroup strata and folded together with these strata only after sill emplacement. There is no documented example of a Nipissing sill clearly cutting both limbs of a pre-existing fold structure in Huronian Supergroup strata. The Huronian succession was, therefore, still largely flat lying at the time of Nipissing sill intrusion, perhaps only showing minor deformation and tilting along active faults in some areas.

THE NIPISSING SILL COMPLEX

The intrusive mafic sills of the Nipissing suite, consisting of gabbro, finer grained diabase and locally extensive granophyric "sandwich zones" below upper chilled margins, are widespread throughout the entire footprint of the preserved Huronian Supergroup succession (e.g., Card et al. 1972; Bennett, Dressler and Robertson 1991; Lightfoot and Naldrett 1996; Jobin-Bevans 2004; Fyon et al. 1992; Davey et al. 2019), and essentially have intruded all parts of the succession, as well as the proximal underlying basement (as illustrated in Figure 14.1). Nipissing suite intrusions dominantly form bedding-concordant sills, but locally become discordant and dike-like, crosscutting stratigraphy and then "silling out" again at a different level. In less tightly folded areas, such as near Cobalt, Ontario, the sills preserve distinct saucer-shaped morphologies typical of sill complexes emplaced at relatively shallow levels in flat-lying host successions where sill inflation is largely accommodated by roof uplift. The sills typically are approximately 100 m thick and have developed extensive granophyre sections in late fractionated "sandwich zones" below the upper chilled contact zones. These various differentiation processes, as first documented in the field, including mafic cumulates in the lower parts of the sills, led Bowen (1910) to define his igneous crystallization sequence or "reaction series".

Several U/Pb geochronology studies have shown that Nipissing sills were intruded between *circa* 2209 Ma and 2223 Ma (Corfu and Andrews 1986; Krogh et al. 1987; Conrod 1989, p.54; Noble and Lightfoot 1992), with subsequent studies suggesting a tighter age range of 2215 to 2217 ±2 Ma (Davey et al. 2019; Kamo 2022). Exactly coeval sills and dikes occur in "greater Karelia" (the Karjalitic sills) and Wyoming (the Clay Butte dike), and possibly in the Transvaal basin cover of the Kaapvaal craton (Hekpoort basalts?; e.g., *see* Gumsley et al. 2017; Humbert et al. 2018). Other likely correlatives are the Cheela Spring basalts and related dolerite sills in Paleoproterozoic cover of the southern Pilbara craton (Martin et al. 1998; Müller et al. 2005; Martin 2020), all of which were connected to the southern Superior craton at Nipissing time (Bleeker et al. 2016; Bleeker 2023).

The age of the Nipissing sills (2215–2217 Ma) overlaps with that of the large northeast-trending Senneterre diabase dikes documented to the northeast of the preserved footprint of Huronian cover, where these dikes crosscut the basement of the Superior craton (Buchan, Mortensen and Card 1993). The Senneterre dikes likely represent part of the feeder system to the Nipissing sills, with magma spreading out as sills once the dikes intruded upward from basement into the overlying Huronian Supergroup basin.

As stated earlier, there is strong evidence for the Huronian Supergroup succession to still be largely undeformed at Nipissing time, because the sills were emplaced concordant with bedding over large distances, locally preserving distinct saucer shapes, and only later were folded together with the host strata (Bleeker et al. 2015).

THE MAY TOWNSHIP SILLS AND THEIR URANIUM–LEAD GEOCHRONOLOGY

In the general area between Espanola and Serpent River, in the southern and more deformed part of the Huronian Supergroup south of the Murray Fault zone, many mafic sills are present, variably deformed and metamorphosed together with their host sedimentary rocks of the lower Huronian Supergroup (Figure 14.2). Although some of these (meta)gabbro and (meta)diabase sills, for instance near Espanola, are clearly part of the Nipissing intrusive suite, others are subtly different and generally lack the evolved granophyre sections that characterize many of the Nipissing sills (e.g., Lightfoot and Naldrett 1996). The sills south of the Murray Fault consist of darker metagabbro and diabase with, on average, slightly higher magnetic susceptibility values (~1.0×10^{-3} SI units) than Nipissing (meta)gabbro and diabase (~$0.4–0.8 \times 10^{-3}$ SI units). This is especially true in the corridor along Highway 17, east and west of the small town of Massey (*see*

Figure 14.2), where essentially all hill tops are deformed gabbro sills that stand up among more deeply weathered and eroded McKim Formation metagreywackes.

In an exploratory study, Jackson et al. (1994) mapped May Township and sampled some of the folded (meta)gabbro sills. One coarser metagabbro (Figure 14.3A), analyzed at the Jack Satterly Laboratory at the University of Toronto by D.W. Davis in 1995, returned a relatively precise upper intercept age of 2258±2 Ma based on several slightly discordant to concordant zircon fractions (Figure 14.3C). Following up on these initial results, the May Township sills were revisited by the senior author, confirming their distinct characteristics mentioned earlier, and a coarse plagioclase ± quartz pegmatitic segregation was sampled from a second locality along one of the deformed sills, in a small gabbro quarry just east of Massey (417625E 5118725N, Zone 17, NAD83). This sample also returned suitable accessory zircons that, despite minor complexities, are consistent with the age of *circa* 2258±2 Ma (Figure 14.3D, blue ellipses). As the exact locality of the first sample was not known in detail (S.L. Jackson, personal communication, 2017), this second sample was significant, as it established a well-located "type locality" for the May Township sills.

Since then, using the slightly different field characteristics of the May Township sills versus those of the Nipissing sills, it has become clear that the older May Township sills extend over a larger area, south of the Murray Fault, at least as far west as the community of Serpent River. An age from a third locality was obtained recently from a pegmatitic segregation in a (meta)gabbro sill from a quarry located just east of the community of Spanish (398625E 5117400N, Zone 17, NAD83), again returning a similar age (*see* Figure 14.3D, red ellipses). No baddeleyite was recovered from any of these 3 samples, which contrasts with the typical recovery of accessory minerals from Nipissing sill samples. As stated previously, the May Township sills consist of metagabbro that is typically darker (essentially black) and characterized

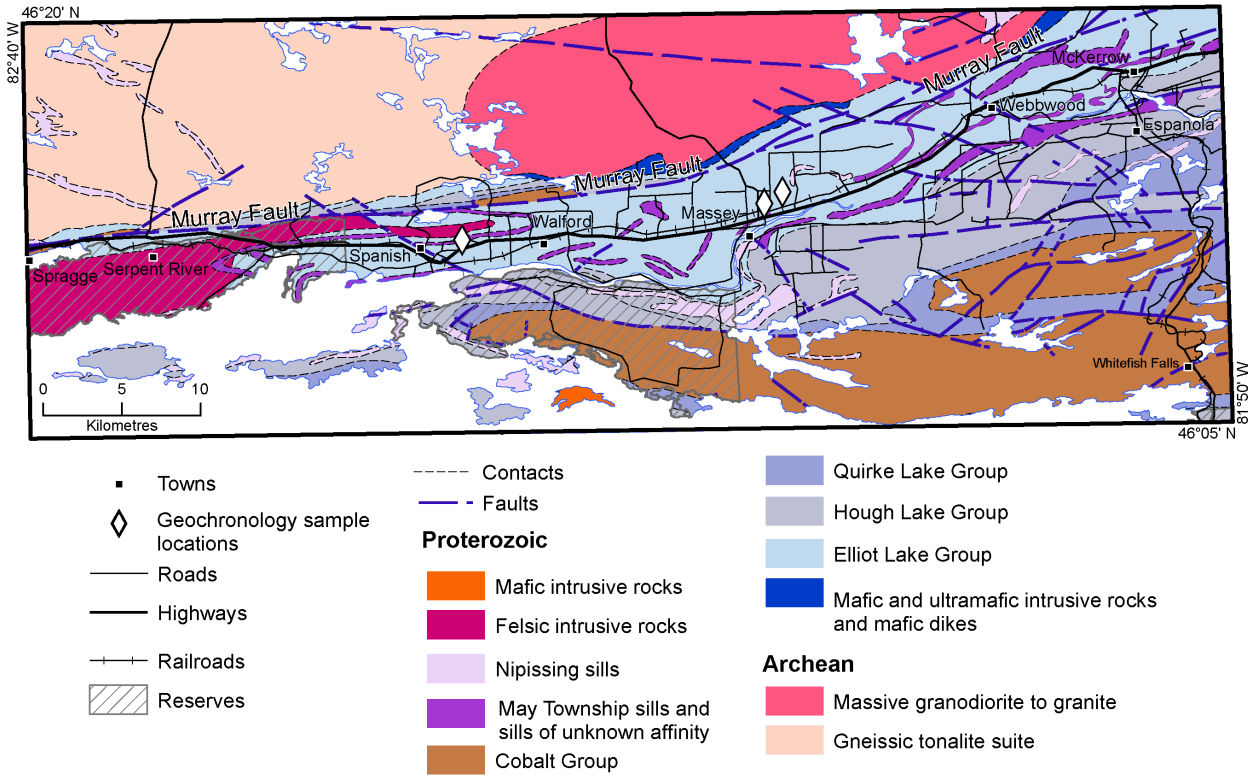


Figure 14.2. Geological sketch map for the area between Espanola and Serpent River showing the location of known and probable May Township sills, geochronology sample sites and the Murray Fault. Geology *modified from* Ontario Geological Survey (2011).

by slightly higher magnetic susceptibility values than the grey to dark green-black Nipissing sills. Many metagabbros typical of the May Township sills have sparse, somewhat larger, plagioclase phenocrysts up to 0.5 to 1.0 cm in size, in a dark amphibole-rich matrix (*see* Figure 14.3A), and their late-stage differentiated pegmatitic segregations carry zircon, not baddeleyite, and are distinct from Nipissing granophyre rich in potassium feldspar and quartz intergrowths. With the new U/Pb isotopic age confirmation, on 3 independent samples (*see* Figure 14.3D), it is clear that these more qualitative field characteristics are robust and meaningful and may help in mapping out the wider footprint of the May Township sills.

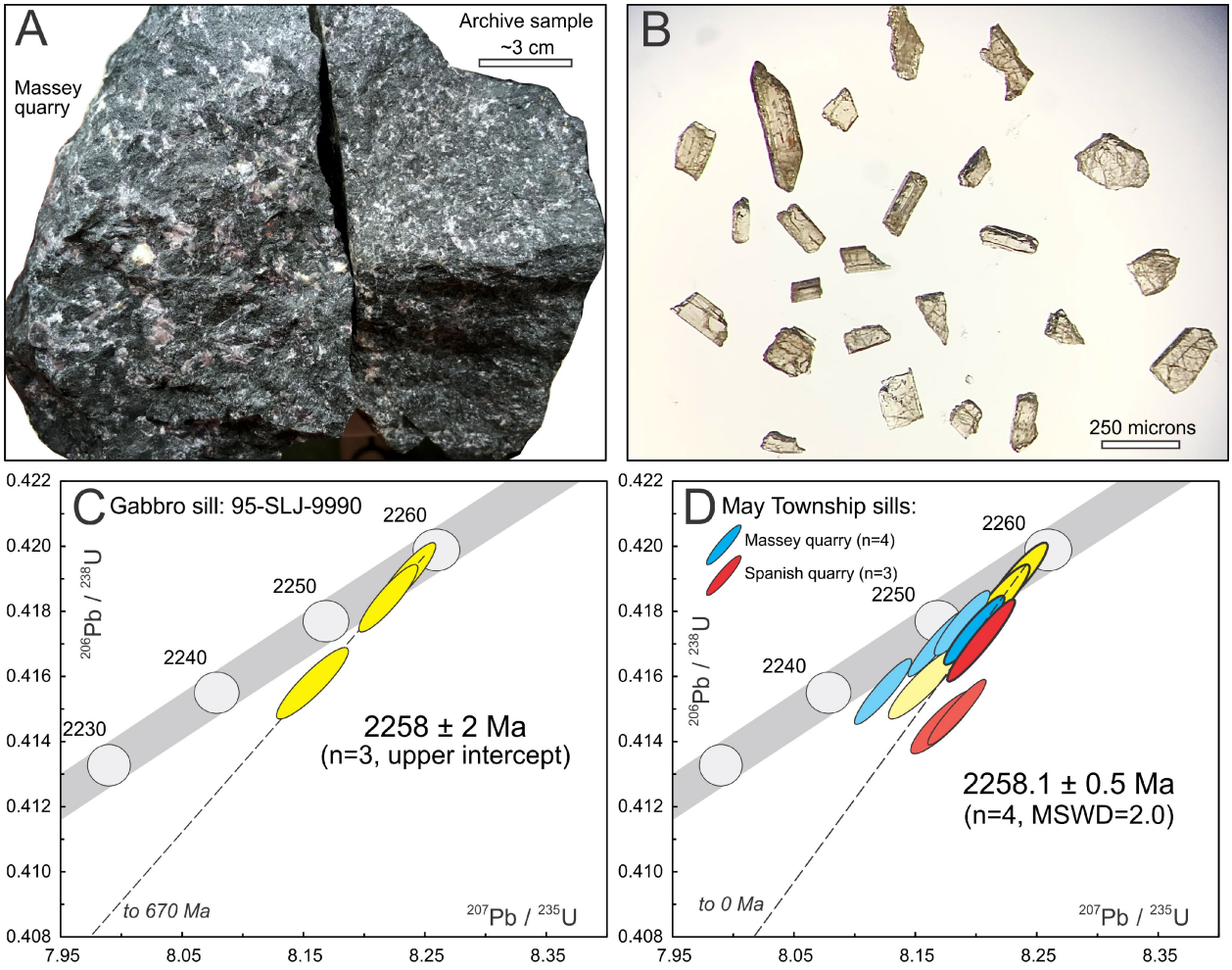


Figure 14.3. Relevant images and U/Pb concordia diagrams for the May Township sills. **A)** Images of some of the samples: an archived sample of the original sample collected by S.L. Jackson (right), and coarse pegmatitic gabbro from the Massey quarry (left). Note the large plagioclase crystals in the latter. **B)** Image of representative magmatic zircons, and fragments thereof, from the sample taken in the quarry east of Spanish. Note the varied quality of the grains, with only a limited amount of clear bits and pieces. **C)** Data on 3 zircon fractions from the original sample from May Township collected by S.L. Jackson of the Ontario Geological Survey. The middle fraction consisted of approximately 10 zircon grains and/or fragments, the other 2 fractions were single grains; all air abraded. The age shown, 2258±2 Ma, is an upper intercept of the discordia line through all 3 fractions. The lower intercept is likely meaningless. **D)** Newer data on the samples collected by the senior author, from the small quarry on Birch Lake Road in May Township (blue ellipses) and the quarry northeast of Spanish (red ellipses). All the new data are on chemically abraded single zircons and show minor scatter, but converge on the same age of 2258 Ma. A weighted mean ^{207}Pb/^{206}Pb age from the 4 most concordant data across all 3 samples (ellipses in brighter colours) is shown for reference and has an acceptable MSWD of 2.0. All data are *from* the Jack Satterly Geochronology Laboratory. The U/Pb methods used by the laboratory are described in Préfontaine and Kamo (this volume).

Given that all 3 U/Pb zircon ages overlap within uncertainty (*see* Figure 14.3D), on samples from 3 different localities up to 25 km apart, it is clear that the May Township sills form a distinct magmatic event intruding the southern Superior craton and its cover.

DISCUSSION AND CONCLUSIONS

These findings firmly establish the existence of a distinct set of mafic sills, here referred to as the May Township sills, in the lower Huronian Supergroup succession. The age of these sills, based on 3 independent samples, is 2258±2 Ma; thus, the May Township sills are *circa* 40 million years older than the Nipissing sills at 2215 to 2217 Ma. The small gabbro quarry just east of Massey, where Birch Lake Road cuts across one of the distinct gabbro ridges, and which has yielded an age of *circa* 2258±2 Ma, is easily accessible and this locality serves as an excellent "type locality". This quarry is of additional interest in that it exposes metre-scale veins and bodies of unquestionable Sudbury Breccia within the deformed May Township gabbro sill (Bleeker and Kamo 2022). The breccia and its host rocks were subsequently strongly deformed by Penokean deformation.

The May Township sills consist of variably deformed metagabbro and metadiabase that differ subtly from Nipissing (meta)gabbro and diabase, with the May Township sills being darker (not grey or dark green as is typical of Nipissing gabbro or diabase), with slightly higher magnetic susceptibility values, lacking the more evolved granophyric differentiates common to many larger Nipissing sills, and often showing sparse, somewhat larger, white plagioclase phenocrysts within dark metagabbro. Late-stage pegmatitic segregations in May Township sills do occur, but consist of coarse leucogabbro dominated by large white plagioclase crystals and minor mafic minerals ± minor quartz. These pegmatitic leucogabbro pods yielded the magmatic zircon crystals analyzed in this study. No baddeleyite was recovered in any of the samples.

The May Township sills form numerous high-standing gabbro ridges in a corridor along Highway 17 extending at least 25 km between Espanola and Serpent River and they may well extend beyond this type area (*see* Figure 14.2). The sills mostly intruded McKim Formation (meta)greywackes. The many gabbro ridges suggest there were multiple levels of sills, although several phases of folding in the area south of the Murray Fault zone almost certainly have duplicated some sills into multiple ridges. Some of the gabbro ridges clearly outline east- and west-trending, doubly plunging, upright, antiformal folds in the area, and these regional-scale folds are at least of a second generation that refold earlier folds and fabrics. The metamorphic grade of the May Township sills varies from upper greenschist to middle amphibolite facies, and in Victoria Township, and in the vicinity of the late Paleoproterozoic Cutler granite body, large garnet porphyroblasts are present.

Currently, it seems that the May Township sills are confined to the more deformed corridor south of the Murray Fault zone. This may be the result of initial access and sampling bias, but it could also indicate that the Murray Fault zone is deep rooted and provided a crustal- or lithospheric-scale (major rift fault?) structure that guided the ascent of the May Township mafic magmas and bounds their distribution. This remains to be tested by more regional exploratory surveys.

Collectively, these data add a distinct new magmatic event to southern Superior craton and a "bar" to its magmatic barcode. Thus, it is expected that magmatic ages of *circa* 2258 Ma may also show up in craton fragments that rifted off southern Superia. In this respect, the tentative identification, using sensitive high-resolution ion microprobe (SHRIMP) analyses, of zircons *circa* 2240 to 2260 Ma in Hekpoort basalt–related samples (Dorland 2004) of the Transvaal basin overlying the Kaapvaal craton may be of significance. A tentative SHRIMP zircon age of *circa* 2257±7 Ma for the Khitoostrov high-iron gabbro intrusion in Karelia may also be of interest (Zakharov et al. 2017) and adds yet another barcode match to link the ancestry of "greater Karelia" to that of southern Superia (e.g., Davey et al. 2020).

Finally, although intrusion of May Township sills in the lower Huronian Supergroup does not necessarily exclude ongoing sedimentation of the uppermost Huronian Supergroup formations, it seems likely that the May Township sill magmatism indicates a transition to a different tectono-magmatic regime and that deposition of the uppermost Cobalt Group (Flack Lake group) already had come to an end. If so, Huronian sedimentation terminated prior to *circa* 2260 Ma, perhaps accompanied by a shift in depocentres to farther south with ongoing sedimentation in the Transvaal basin of South Africa. It is interesting that neither the May Township sills, nor the younger Nipissing sills, have extrusive basalt equivalents in Canada, with possible extrusive equivalents only known from the cover of the Kaapvaal craton (Hekpoort basalts?) and Pilbara craton (Cheela Spring basalts), with both craton fragments being contiguous with the southern Superior from *circa* 2650 Ma to breakup at *circa* 2100 to 2000 Ma.

ACKNOWLEDGMENTS

We would like to thank Steve Jackson, formerly with the OGS, for digging into his memory and identifying the approximate sample locations from which some of the first samples of May Township gabbro sills were collected. Without the initial reconnaissance sampling in 1995, these mafic sills would have remained just another bunch of deformed Nipissing sills. Julie Chartrand and Pat Gervais (Earth Resources and Geoscience Mapping Section (ERGMS), OGS) kindly assisted with preparing Figure 14.2. Monica Gaiswinkler Easton (Publication Services, OGS) and Manuel Duguet (ERGMS, OGS) are thanked for proofreading and editorial handling of the manuscript. Field work and U/Pb geochronology were funded by the Geological Survey of Canada under its Targeted Geoscience Initiative (TGI). This is NRCan contribution number 20230331.

REFERENCES

Bates, M.P. and Halls, H.C. 1990. Regional variation in paleomagnetic polarity of the Matachewan dyke swarm related to the Kapuskasing Structural Zone, Ontario; Canadian Journal of Earth Sciences, v.27, p.200-211.

Bekker, A., Karhu, J.A. and Kaufman, A.J. 2006. Carbon isotope record for the onset of the Lomagundi carbon isotope excursion in the Great Lakes area, North America; Precambrian Research, v.148, no.1-2, p.145-180.

Bekker, A., Kaufman, A.J., Karhu, J.A. and Eriksson, K.A. 2005. Evidence for Paleoproterozoic cap carbonates in North America; Precambrian Research, v.137, no.3-4, p.167-206.

Bennett, G., Dressler, B.O. and Robertson, J.A. 1991. The Huronian Supergroup and associated intrusive rocks; Chapter 14 *in* Geology of Ontario, Ontario Geological Survey, Special Volume 4, Part 1, p.549-591.

Bleeker, W. 2003. The late Archean record: A puzzle in *ca*. 35 pieces; Lithos, v.71, no.2-4, p.99-134.

——— 2004. Taking the pulse of planet Earth: A proposal for a new multi-disciplinary flagship project in Canadian solid Earth sciences; Geoscience Canada, v.31, p.179-190.

——— 2023. Craton assembly and fragmentation; Geological Society of America, Abstracts with Programs, v.55, no.6, session 135-2, abstract number 391045. doi:10.1130/abs/2023AM-391045

Bleeker, W., Chamberlain, K.R., Kamo, S.L., Hamilton, M., Kilian, T.M. and Buchan, K.L. 2016. Kaapvaal, Superior and Wyoming: Nearest neighbours in supercraton Superia; 35th International Geological Congress, August 27–September, 4, 2016, Cape Town, South Africa, Paper Number 5222.

Bleeker, W. and Ernst, R.E. 2006. Short-lived mantle generated magmatic events and their dyke swarms: The key unlocking Earth's palaeogeographic record back to 2.6 Ga; *in* Dyke Swarms—Time Markers of Crustal Evolution: Selected Papers of the Fifth International Dyke Conference in Finland, Rovaniemi, Finland, July 31–August 3, 2005 and Fourth International Dyke Conference, Kwazulu-Natal, South Africa, June 26–29, 2001, A.A. Balkema, Rotterdam, p.3-26.

Bleeker, W. and Kamo, S.L. 2022. A traverse across the Sudbury Structure—Earth's largest impact crater, Day 1; *in* 68th Institute on Lake Superior Geology, Proceedings, Volume 68, Part 2, Field Trip Guidebooks, p.2-46.

Bleeker, W., Kamo, S.L., Ames, D.E. and Davis, D. 2015. New field observations and U-Pb ages in the Sudbury area: Toward a detailed cross-section through the deformed Sudbury Structure; *in* Targeted Geoscience Initiative 4: Canadian Nickel-Copper-Platinum Group Elements-Chromium Ore Systems — Fertility, Pathfinders, New and Revised Models, Geological Survey of Canada, Open File 7856, p.151-166.

Bowen, N.L. 1910. Diabase and granophyre of the Gowganda Lake district, Ontario; Journal of Geology, v.18, p.658-674.

Bradley, D.C. 2008. Passive margins through earth history; Earth-Science Reviews, v.91, p.1-26.

Buchan, K.L., Mortenson, J.K. and Card, K.D. 1993. Northeast-trending Early Proterozoic dykes of southern Superior Province: Multiple episodes of emplacement recognized from integrated paleomagnetism and U–Pb geochronology; Canadian Journal of Earth Sciences, v.30, p.1286-1296.

Card, K.D., Church, W.R., Franklin, J.M., Frarey, M.J., Robertson, J.A., West, G.F. and Young, G.M. 1972. The Southern Province; *in* Variations in Tectonic Styles in Canada, Geological Association of Canada, Special Paper 11, p.335-380.

Clough, C.E. and Hamilton, M.A. 2017. Matachewan LIP revisited: A revised, high-resolution U-Pb age for the East Bull Lake intrusion and associated units; Geological Association of Canada—Mineralogical Association of Canada, Abstracts, v.40, p.65.

Conrod, D.M. 1989. Petrology and geochemistry of the Duncan Lake, Beaton Bay, Milner Lake, and Miller Lake Nipissing intrusions within the Gowganda area; Ontario Geological Survey, Open File Report 5701, 210p.

Corfu, F. and Andrews, A.J. 1986. A U–Pb age for mineralized Nipissing diabase, Gowganda, Ontario; Canadian Journal of Earth Sciences, v.23, p.107-109.

Craddock, J.P., Rainbird, R.H., Davis, W.J., Davidson, C., Vervoort, J.D., Konstantinou, A., Boerboom, T., Vorhies, S., Kerber, L. and Lundquist, B. 2013. Detrital zircon geochronology and provenance of the Paleoproterozoic Huron (~2.4–2.2 Ga) and Animikie (~2.2–1.8 Ga) Basins, southern Superior Province; Journal of Geology, v.121, p.623-644.

Culshaw, N., Van de Kerckhove, S., Slagstad, T., Marsh, J. and Easton, R.M. 2023. Crustal evolution of the Laurentian continental margin from the Paleo- through Mesoproterozoic: A zircon U–Pb and Hf transect through the western Grenville Province, Ontario, Canada; Precambrian Research, v.386, paper 106963, 22p.

Davey, S., Bleeker, W., Kamo, S[.L.], Davis, D.[W], Easton, [R.]M. and Sutcliffe, R.H. 2019. Ni-Cu-PGE potential of the Nipissing sills as part of the ca. 2.2 Ga Ungava large igneous province; *in* Targeted Geoscience Initiative: 2018 Report of Activities; Geological Survey of Canada, Open File 8549, p.403-419.

Davey, S.C., Bleeker, W., Kamo, S.L., Vuollo, J., Ernst, R.E. and Cousens, B.L. 2020. Archean block rotation in western Karelia: Resolving dyke swarm patterns in metacraton Karelia-Kola for a refined paleogeographic reconstruction of supercraton Superia; Lithos, v.368, article 105553. doi.org/10.1016/j.lithos.2020.105553

Dorland, H.C. 2004. Provenance ages and timing of sedimentation of selected Neoarchean and Paleoproterozoic successions on the Kaapvaal Craton; unpublished PhD thesis, Rand Afrikaans University, Johannesburg, South Africa, 326p.

Easton, R.M. 2003. Geology and mineral potential of the Paleoproterozoic River Valley Intrusion and related rocks, Grenville Province; Ontario Geological Survey, Open File Report 6123, 171p.

——— 2019. What do detrital zircon studies of the Huronian Supergroup tell us? An analysis of all published data; abstract *in* 65th Institute on Lake Superior Geology, Proceedings, v.65, pt.1, p.38-39.

Ernst, R.E. and Bleeker, W. 2010. Large igneous provinces (LIPs), giant dyke swarms, and mantle plumes: Significance for breakup events within Canada and selected adjacent regions from 2.5 Ga to present; Canadian Journal of Earth Sciences, v.47, p.695-739. doi.org/10.1139/E10-025

Frarey, M.J., Loveridge, W.D. and Sullivan, R.W. 1982. A U-Pb zircon age for the Creighton Granite, Ontario; Geological Survey of Canada, Paper 82-1C, p.129-132.

Fyon, J.A., Bennett, G., Jackson, S.L., Garland, M.I. and Easton, R.M. 1992. Metallogeny of the Proterozoic Eon, northern Great Lakes region, Ontario; Chapter 25 *in* Geology of Ontario, Ontario Geological Survey, Special Volume 4, Part 2, p.1177-1215.

Gumsley, A.P., Chamberlain, K.R., Bleeker, W., Söderlund, U., de Kock, M.O., Larsson, E.R. and Bekker, A. 2017. Timing and tempo of the Great Oxidation Event; Proceedings of the National Academy of Sciences, v.114, p.1811-1816. doi.org/10.1073/pnas.1608824114

Halls, H.C., Stott, G.M. and Davis, D.W. 2005. Paleomagnetism, geochronology and geochemistry of several Proterozoic mafic dike swarms in northwestern Ontario; Ontario Geological Survey, Open File Report 6171, 59p.

Heaman, L.M. 1997. Global mafic magmatism at 2.45 Ga: Remnants of an ancient large igneous province?; Geology, v.25, p.299-302.

Hill, C.M., Davis, D.W. and Corcoran, P.L. 2018. New U-Pb geochronology evidence for 2.3 Ga detrital zircon grains in the youngest Huronian Supergroup formations, Canada; Precambrian Research, v.314, p.428-433.

Hoffman, P.F., Kaufman, A.J., Halverson, G.P. and Schrag, D.P. 1998. A Neoproterozoic snowball Earth; Science, v.281, no.5381, p.1342-1346.

Hoffman, P.F. and Schrag, D.P. 2000. The snowball Earth; Scientific American, January 2000, p.68-75.

Holland, H.D. 2002. Volcanic gases, black smokers, and the Great Oxidation Event; Geochimica et Cosmochimica Acta, v.66, p.3811-3826.

Humbert, F., de Kock, M.O., Altermann, W., Elburg, M.A., Lenhardt, N., Smith, A.J.B. and Masango, S. 2018. Petrology, physical volcanology and geochemistry of a Paleoproterozoic large igneous province: The Hekpoort Formation in the southern Transvaal sub-basin (Kaapvaal craton); Precambrian Research, v.315, p.232-256.

Jackson, S.L. 2001. On the structural geology of the Southern Province between Sault Ste. Marie and Espanola, Ontario; Ontario Geological Survey, Open File Report 5995, 55p.

Jackson, S.L., Robertson, J.A., Henderson, I. and Siemiatkowska, K.M. 1994. Precambrian geology, May Township; Ontario Geological Survey, Open File Map 233, scale 1:20 000.

Jobin-Bevans, L.S. 2004. Platinum-group element mineralization in Nipissing gabbro intrusions and the River Valley intrusion, Sudbury region, Ontario; unpublished PhD thesis, University of Western Ontario, London, Ontario, 572p.

——— 2016. Geochemical data related to a study of platinum group element mineralization in Nipissing Gabbro Intrusions and the River Valley Intrusion, Sudbury Region, Southern Province; Ontario Geological Survey, Miscellaneous Release—Data 336.

Kamo, S.L. 2022. Report on U-Pb ID-TIMS geochronology for the Ontario Geological Survey: Bedrock Mapping Projects, Ontario 2021-2022; internal report prepared for the Ontario Geological Survey, Jack Satterly Geochronology Laboratory, University of Toronto, Toronto, Ontario, 12p.

Kilian, T.M., Bleeker, W., Chamberlain, K., Evans, D.A.D. and Cousens, B. 2016a. Palaeomagnetism, geochronology and geochemistry of the Palaeoproterozoic Rabbit Creek and Powder River dyke swarms: Implications for Wyoming in supercraton Superia; *in* Supercontinent Cycles Through Earth History, Geological Society, London, Special Publication No.424, p.15-45.

Kilian, T.M., Chamberlain, K.R., Evans, D.A., Bleeker, W. and Cousens, B.L. 2016b. Wyoming on the run—Toward final Paleoproterozoic assembly of Laurentia; Geology, v.44, p.863-866.

Kirschvink, J.L. 1992. Late Proterozoic low-latitude global glaciation: The snowball Earth; *in* Geological Evolution of the Proterozoic Earth, Cambridge University Press, p.51-52.

Kirschvink, J.L., Gaidos, E.J., Bertani, L.E., Beukes, N.J., Gutzmer, J., Maepa, L.N. and Steinberger, R.E. 2000. Paleoproterozoic snowball Earth: Extreme climatic and geochemical global change and its biological consequences; Proceedings of the National Academy of Sciences, v.97, p.1400-1405.

Krogh, T.E., Corfu, F., Davis, D.W., Dunning, G.R., Heaman, L.M., Kamo, S.L., Machado, N., Greenough, J.D. and Nakamura, E. 1987. Precise U-Pb isotopic ages of diabase dykes and mafic to ultramafic rocks using trace amounts of baddeleyite and zircon; *in* Mafic Dyke Swarms, Geological Association of Canada, Special Paper 34, p.147-152.

Krogh, T.E., Davis, D.W. and Corfu, F. 1984. Precise U-Pb zircon and baddeleyite ages for the Sudbury Structure; *in* Geology and Ore Deposits of the Sudbury Structure, Ontario Geological Survey, Special Volume 1, p.431-446.

Krogh, T.E., McNutt, R.H. and Davis, G.L. 1982. Two high precision U–Pb zircon ages for the Sudbury Nickel Irruptive; Canadian Journal of Earth Sciences, v.19, p.723-728.

Larue, D.K. 1981. The Chocolay Group, Lake Superior region, USA: Sedimentologic evidence for deposition in basinal and platform settings on an early Proterozoic craton; Geological Society of America, Bulletin, v.92, p.417-435.

Lightfoot, P.C. and Naldrett, A.J. 1996. Petrology and geochemistry of the Nipissing Gabbro: Exploration strategies for nickel, copper and platinum group elements in a large igneous province; Ontario Geological Survey, Study 58, 80p.

Long, D.G.F. 2009. The Huronian Supergroup; *in* A Field Guide to the Geology of Sudbury, Ontario, Ontario Geological Survey, Open File Report 6243, p.14-30.

Martin, D.McB. 2020. Geology of the Hardey syncline—The key to understanding the northern margin of the Capricorn Orogen; Geological Survey of Western Australia, Report 203, 62p.

Martin, D.McB., Li, Z.X., Nemchin, A.A. and Powell, C.McA. 1998. A pre-2.2 Ga age for giant hematite ores of the Hamersley Province, Australia; Economic Geology, v.93, p.1084-1090.

Meyn, H.D. 1973. The Proterozoic sedimentary rocks north and northeast of Sudbury, Ontario; *in* Huronian Stratigraphy and Sedimentation, Geological Association of Canada, Special Paper 12, p.129-145.

Müller, S.G., Krapež, B., Barley, M.E. and Fletcher, I.R. 2005. Giant iron ore deposits of the Hamersley province related to the breakup of Paleoproterozoic Australia: New insights from *in situ* SHRIMP dating of baddeleyite from mafic intrusions; Geology, v.33, p.577-580.

Mungall, J.E. and Hanley, J.J. 2004. Origins of outliers of the Huronian Supergroup within the Sudbury Structure; Journal of Geology, v.112, p.59-70.

Noble, S.R. and Lightfoot, P.C. 1992. U–Pb baddeleyite ages of the Kerns and Triangle Mountain intrusions, Nipissing diabase, Ontario; Canadian Journal of Earth Sciences, v.29, p.1424-1429.

Ontario Geological Survey 2011. 1:250 000 scale bedrock geology of Ontario; Ontario Geological Survey, Miscellaneous Release—Data 126 – Revision 1.

Papineau, D., Mojzsis, S.J. and Schmitt, A.K. 2007. Multiple sulfur isotopes from Paleoproterozoic Huronian interglacial sediments and the rise of atmospheric oxygen; Earth and Planetary Science Letters, v.255, p.188-212.

Rainbird, R.H. and Davis, W.J. 2006. Detrital zircon geochronology of the western Huronian Basin; *in* 52nd Institute on Lake Superior Geology, Proceedings, Volume 52, Part 1, Program and Abstracts, p.55-56.

Rasmussen, B., Bekker, A. and Fletcher, I.R. 2013. Correlation of Paleoproterozoic glaciations based on U–Pb zircon ages for tuff beds in the Transvaal and Huronian Supergroups; Earth and Planetary Science Letters, v.382, p.173-180.

Roscoe, S.M. 1969. Huronian rocks and uraniferous conglomerates in the Canadian Shield; Geological Survey of Canada, Paper 68-40, 205p.

——— 1973. The Huronian Supergroup, a Paleoaphebian succession showing evidence of atmospheric evolution; *in* Huronian Stratigraphy and Sedimentation, Geological Association of Canada, Special Paper 12, p.31-47.

Roscoe, S.M. and Card, K.D. 1992. Early Proterozoic tectonics and metallogeny of the Lake Huron region of the Canadian Shield; Precambrian Research, v.58, p.99-119.

Smith, M.D. 2002. The timing and petrogenesis of the Creighton pluton, Ontario: An example of felsic magmatism associated with Matachewan igneous events; unpublished MSc thesis, University of Alberta, Edmonton, Alberta, 123p.

Sproule, R.A., Sutcliffe, R., Tracanelli, H. and Lesher, C.M. 2007. Palaeoproterozoic Ni–Cu–PGE mineralisation in the Shakespeare intrusion, Ontario, Canada: A new style of Nipissing gabbro-hosted mineralisation; Applied Earth Science, Institute of Mining and Metallurgy, Transactions, Section B, v.116, no.4, p.188-200.

Stockwell, C.H. 1982. Proposals for the time classification and correlation of Precambrian rocks and events in Canada and adjacent areas of the Canadian Shield; Geological Survey of Canada, Paper 80-19, 135p.

Wood, J. 1973. Stratigraphy and depositional environments of Upper Huronian rocks of the Rawhide Lake–Flack Lake area; *in* Huronian Stratigraphy and Sedimentation, Geological Association of Canada, Special Paper 12, p.73-95.

Young, G.M. ed. 1973a. Huronian Stratigraphy and Sedimentation; Geological Association of Canada, Special Paper 12, 271p.

——— 1973b. Tillites and aluminous quartzites as possible time markers for Middle Precambrian (Aphebian) rocks of North America; *in* Huronian Stratigraphy and Sedimentation, Geological Association of Canada, Special Paper 12, p.97-127.

——— 2019. Aspects of the Archean-Proterozoic transition: How the great Huronian Glacial Event was initiated by rift-related uplift and terminated at the rift-drift transition during break-up of Lauroscandia; Earth-Science Reviews, v.190, p.171-189.

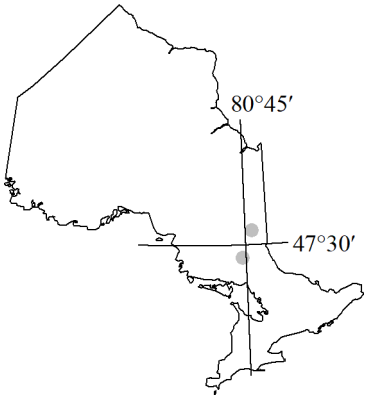
Young, G.M. and Chandler, FW. 1968. Possible glacial origin for three Precambrian (Huronian) conglomerates, north shore of Lake Huron; *in* Proceedings of the 14th Annual Institute on Lake Superior Geology, Proceedings, v.14, p.42-43.

Young, G.M., Long, D.G.F., Fedo, C.M. and Nesbitt, H.W. 2001. Paleoproterozoic Huronian basin: Product of a Wilson cycle punctuated by glaciations and a meteorite impact; Sedimentary Geology, v.141-142, p.233-254.

Zakharov, D.O., Bindeman, I.N., Slabunov, A.I., Ovtcharova, M., Coble, M.A., Serebryakov, N.S. and Schaltegger, U. 2017. Dating the Paleoproterozoic snowball Earth glaciations using contemporaneous subglacial hydrothermal systems; Geology, v.45, p.667-670.

Zolnai, A.I., Price, R.A. and Helmstaedt, H. 1984. Regional cross section of the Southern Province adjacent to Lake Huron, Ontario: Implications for the tectonic significance of the Murray Fault zone; Canadian Journal of Earth Sciences, v.21, p.447-456.

15. Project AS-19-002. A Study of Why Some Fine-Grained Sedimentary Rocks of the Gowganda Formation in Northeastern Ontario are Magnetic



R.M. Easton[1]

[1]Earth Resources and Geoscience Mapping Section, Ontario Geological Survey

INTRODUCTION

For the most part, the metasedimentary rocks of the Huronian Supergroup (*circa* 2460 to 2300 Ma; Bleeker et al. 2015; Rasmussen, Beeker and Fletcher 2013) are not magnetic and, typically, they can be regarded as relatively transparent magnetically. The exception to this generalization is the Gowganda Formation, which can contain magnetic horizons[2], especially in the lower parts of the formation (Easton, Rainsford and Préfontaine 2020, p.6-9 to 6-10; Meyn 1970a, p.80; Meyn 1971, p.17; Card, McIlwaine and Meyn 1973, p.58-59). These magnetic horizons produce magnetic patterns that differ from the response from Archean iron formation in having a sinusoidal texture of alternating highs and lows, described as a "very confused magnetic pattern that can be correlated with the structurally disturbed, magnetite-rich Gowganda" Formation mudstones (Meyn 1970a, p.32).

Although examples of magnetic horizons have been documented in many localities throughout the extent of the Gowganda Formation, the following areas were chosen for initial study because of the extent of the high magnetic response and ease of accessibility, or the availability of diamond-drill core that could be sampled. The selected areas are in Hutton and Parkin townships, and in northwest Creelman Township, in the southwestern part of the Cobalt Basin, covering an area of approximately 72 km^2 and 24 km^2, respectively (Easton, Rainsford and Préfontaine 2020) (Figure 15.1). In addition, magnetic rocks of the Gowganda Formation occur in diamond-drill core in the northern part of the Cobalt Basin, in Burt Township near Matachewan (Morrison, Dawson and Skeries 2023).

To better understand the reason why parts of the Gowganda Formation are magnetic, and any potential economic significance of these magnetic units, a reconnaissance petrographic and geochemical study of magnetic units from the Gowganda Formation was initiated in 2023. This article reports on these sampling activities and provides some preliminary results from drill-core samples from Burt Township and from surface outcrops in Hutton, Parkin, Creelman and Roberts townships (*see* Figure 15.1).

SOURCE OF MAGNETIZATION

There are 3 main potential processes that could explain the magnetic horizons found in the Gowganda Formation.

[2] *The term magnetic horizon is used because, in most cases, it is not known if the magnetic signature results from the presence of magnetite or hematite, or both. In some of the older literature (e.g., Grant 1985), it was assumed that if the rock was magnetic, it was because of the presence of magnetite.*

Summary of Field Work and Other Activities, 2023,
Ontario Geological Survey, Open File Report 6405, p.15-1 to 15-12.

© King's Printer for Ontario, 2023

- They formed from hydrothermal-rich fluids that infiltrated and altered the fine-grained parts of the formation. If this origin is correct, then one might expect an association with major structures and/or areas of more regional alteration.
- They are detrital in origin and contain magnetite and/or hematite derived from iron formation in the Archean basement or, alternatively, from adjacent magnetite-bearing Archean metavolcanic or granitic rocks (e.g., Debicki 1990). If a detrital origin is correct, then one would expect a spatial association with known Archean iron formation units and/or highly magnetic basement rocks.
- They formed from seawater through primary precipitation and subsequent diagenetic processes, but, instead of forming magnetite-chert iron formation, they formed ferruginous fine-grained clastic sedimentary rocks containing either magnetite and/or hematite. The question then becomes, is the depositional regime similar to iron deposition in the somewhat younger (*circa* 1900–1850 Ma) upper Marquette Range Supergroup (e.g., Cannon and Drenth 2023; Bekker et al. 2010); or was it similar to Neoproterozoic iron formations that were deposited in a glacial environment where there was a complex interaction between primary precipitation, diagenesis and a hydrothermal component in seawater related to mid-ocean ridge activity (e.g., Cox et al. 2013)? If the latter case, one would expect hematite, not magnetite, to be the dominant iron-oxide mineral. If either of these origins are correct, does this mean that better developed iron formation units might occur in the Huronian Supergroup, as inferred by Bleeker (2018)?

Given the size of the Cobalt Basin, and the lithological heterogeneity of the Gowganda Formation, it is possible that more than one of these processes occurred, depending on geographic location.

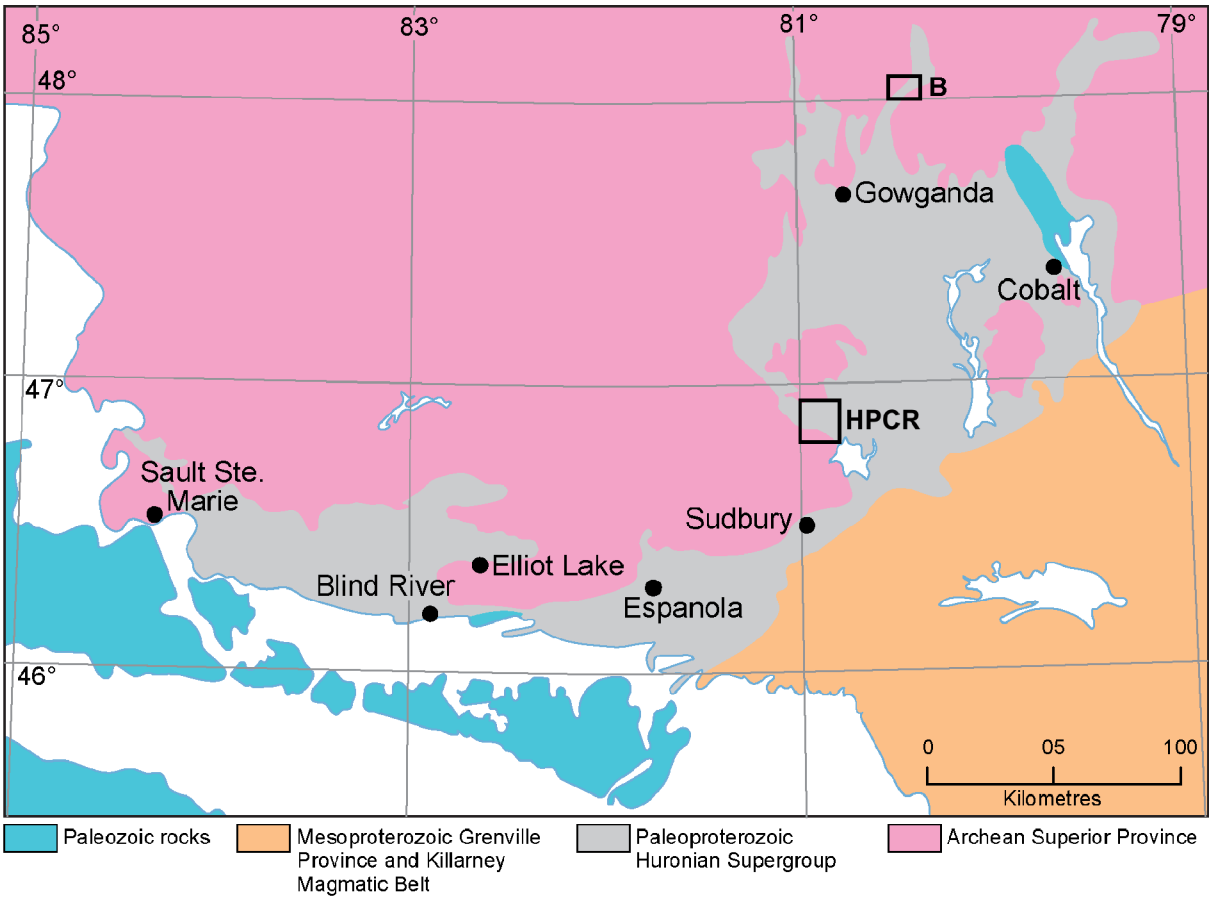


Figure 15.1. Location map showing the distribution of Huronian Supergroup rocks in northeastern Ontario and the sampling areas related to this project. Abbreviations: B, Burt Township; HPCR, area of Hutton, Parkin, Creelman and Roberts townships.

RESULTS

Definitions

Iron content: Ferruginous mudstone refers to material containing 10 to 15 weight % Fe_2O_3 (James 1954). Ironstone or iron formation refers to material containing greater than 15 weight % Fe_2O_3 (James 1954). With respect to ocean waters, ferruginous refers to $Fe^{2+}/H_2S \geq 2$ (Cox et al. 2013).

In this article, apparent stratigraphic thickness is provided based on the logged intervals in the drill core (Morrison, Dawson and Skeries 2023). Conversion to true stratigraphic thickness was not done because of known variability in the strike and dip of beds on surface near the drill collar (Moore 1963) (collar azimuth 155°, collar dip 52°), and because some historical drill-hole records document steep dips for these sedimentary rocks. Recent work by Insight Geophysics Inc. (R.A. Skeries, geologist, personal communication, November 2023), on salvaged core, suggests that dips are indeed shallow, approximately 0 to 20°; thus, the true stratigraphic thickness is approximately 2/3 the interval thickness.

Burt Township

STRATIGRAPHY

Diamond-drill hole NAN22-001 in Burt Township (551019E 5324552N, NAD83, Zone 17) contains approximately 497 m of Gowganda Formation rocks. Rainbird and Donaldson (1988) divided the Gowganda Formation into a lower, conglomerate-bearing Coleman Member and an upper mudstone- and sandstone-dominated Firstbrook Member; this terminology is in general use in the Cobalt Basin.

In drill-hole NAN22-001, the lower 188.7 m of the Gowganda Formation drill core is assigned to the Coleman Member by the author even though diamictite is present only in the lowermost 50 m of the drill core (Morrison, Dawson and Skeries 2023). The assignment of the remaining approximately 139 m of overlying laminated mudstone, siltstone and minor arenite to the Coleman Member is based on the presence of dropstones throughout the laminated mudstones and siltstones. It is the first occurrence of dropstone-free mudstone that defines the transition from the Coleman Member to the Firstbrook Member (Rainbird and Donaldson 1988, p.712). This transition appears to occur at approximately 311.8 m depth, but it is obscured by the presence of a 13.3 m thick sericitic alteration zone that affected an arenite bed. Only drill core below this altered bed was sampled as part of this study (i.e., Coleman Member).

Magnetic horizons occur in the laminated mudstone, siltstone and minor arenite unit as a 41.5 m thick zone, beginning 50.7 m above the unconformity with the Archean basement (lower magnetic zone), and as a 13.3 m thick zone beginning 163 m above the unconformity (upper magnetic zone). Photo 15.1A shows typical mudstone and siltstone layers from within the upper magnetic zone. Magnetic susceptibility readings from the lower magnetic zone range from 1.0 to 19.0 $\times 10^{-3}$ SI units, with readings from the upper magnetic zone ranging from 0.9 to 26.2 $\times 10^{-3}$ SI units (R.A. Skeries, geologist, written communication, 2023). Three samples yielding 6 thin sections were obtained from the lower magnetic zone (samples 23RME-2001A, -2001B, -2002, -2003A, -2003B), 1 sample and 1 thin section were obtained from the upper magnetic zone (sample 23RME-2004), and 1 sample and 1 thin section were obtained in non-magnetic material located 6 m above the top of the upper magnetic zone (sample 23RME-2005). The altered arenite was also sampled and a thin section prepared for comparative purposes (sample 23RME-2006). Results from petrographic study are reported below and in Table 15.1. Geochemical results were pending at the time of writing.

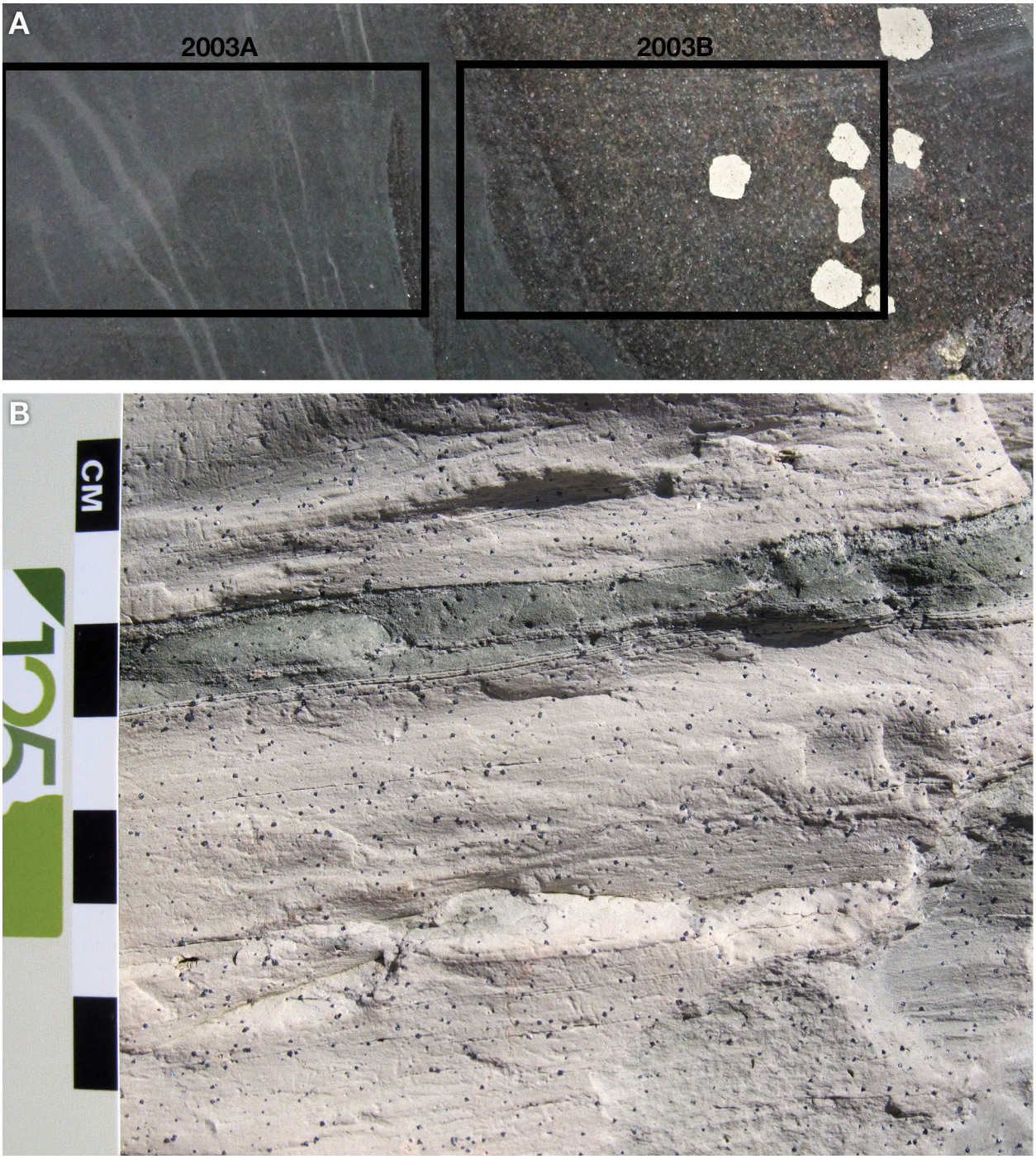


Photo 15.1. A) Section of core, 15 cm in length, showing the 2 main rock types examined in this study, with darker, fine-grained mudstone on the left and lighter, fine- to medium-grained siltstone on the right. Location of thin sections 23RME-2003A and 23RME-2003B is indicated by the black rectangles. Note large, late formed pyrite cubes in the siltstone layer. Core from interval 331.0 m to 331.15 m (upper magnetic zone), top of core is on the left. Photograph courtesy of R.A. Skeries.
B) Photograph of weakly laminated mudstone of the lower magnetic unit of the Gowganda Formation in Hutton Township. Note the small, dark, magnetic grains dispersed uniformly throughout the rock. Average magnetic susceptibility from this outcrop area was 55.5 $\times 10^{-3}$ SI units. Location: UTM 501095E 5191435N, NAD83, Zone 17. Scale card is marked in centimetres.

Table 15.1. Summary of mineralogy present in core samples from diamond-drill hole NAN22-001.

Sample Number 23RME-	Depth Interval (in m)	Average Magnetic Susceptibility ($\times 10^{-3}$ SI units)	Rock Type	Mineralogy	Detrital Grains (typically found in siltstone layers)
2006	303.0–303.3	0.1	Altered arenite	Subrounded quartz-potassium feldspar-albite clasts, muscovite-potassium feldspar-dolomite-pyrite matrix, dolomite veinlet	Quartz (subrounded), potassium feldspar, albite, zircon
2005	318.0–318.5	0.5	Laminated mudstone	Chlorite-illite-muscovite-albite-quartz-potassium feldspar-chalcopyrite-titanite-apatite-dolomite	Rock fragments, quartz (angular), albite, potassium feldspar, apatite
2004B	325.3–325.5	1–3	Laminated siltstone and mudstone	Quartz-albite-iron chlorite-illite-muscovite-potassium feldspar-hematite-titanite-apatite-large pyrite cubes (late)	Rock fragments, quartz (angular), potassium feldspar, albite, epidote, zircon
2004A	325.2–325.3	1–3	Laminated mudstone and siltstone	Iron chlorite-illite-muscovite-albite-quartz-potassium feldspar-hematite-titanite-apatite-large pyrite cubes (late), dolomite filled microcrack, quartz filled microcrack	Rock fragments, quartz (angular), potassium feldspar, albite, epidote, apatite, zircon
2003A	331.07–331.0	11	Laminated mudstone	Iron chlorite-illite-muscovite-albite-quartz-potassium feldspar-hematite-titanite-apatite	Rock fragments, quartz (angular), potassium feldspar, albite, epidote, apatite, zircon
2003B	331.08–331.5	11	Laminated mudstone and siltstone	Iron chlorite-illite-muscovite-albite-quartz-potassium feldspar-hematite-titanite-apatite-large pyrite cubes (late)	Quartz (angular), rock fragments, epidote, zircon
2002	448.3–448.2	15	Laminated mudstone	Iron chlorite-illite-muscovite-quartz-albite-potassium feldspar-hematite-apatite-synchysite	Quartz (angular)
2001B	448.4–448.3	5	Laminated siltstone and mudstone	Quartz-albite-potassium feldspar-iron chlorite-illite-muscovite-titanite-hematite-apatite	Rock fragments, quartz (angular), potassium feldspar, albite, epidote, apatite, zircon, rutile-synchysite
2001A	448.5–448.4	5	Laminated mudstone and siltstone	Quartz-iron chlorite-illite-muscovite-albite-potassium feldspar-hematite-titanite-apatite	Rock fragments, quartz (angular), potassium feldspar, albite, biotite (now chlorite)

MINERALOGY

Thin sections were examined using both optical and scanning electron microscopy, with the latter conducted at the Ontario Geological Survey Geoscience Laboratories in Sudbury using a Zeiss EVO-50 tungsten scanning electron microscope with energy dispersive spectroscopic capabilities. Results are summarized in Table 15.1.

Mineralogically, the samples from both the magnetic and the non-magnetic zones are remarkably uniform. The predominant mineralogy in the mudstone layers in both zones, which typically have a grain size of 10 μm or less, consists of quartz-albite-iron chlorite-illite transitional to muscovite-potassium

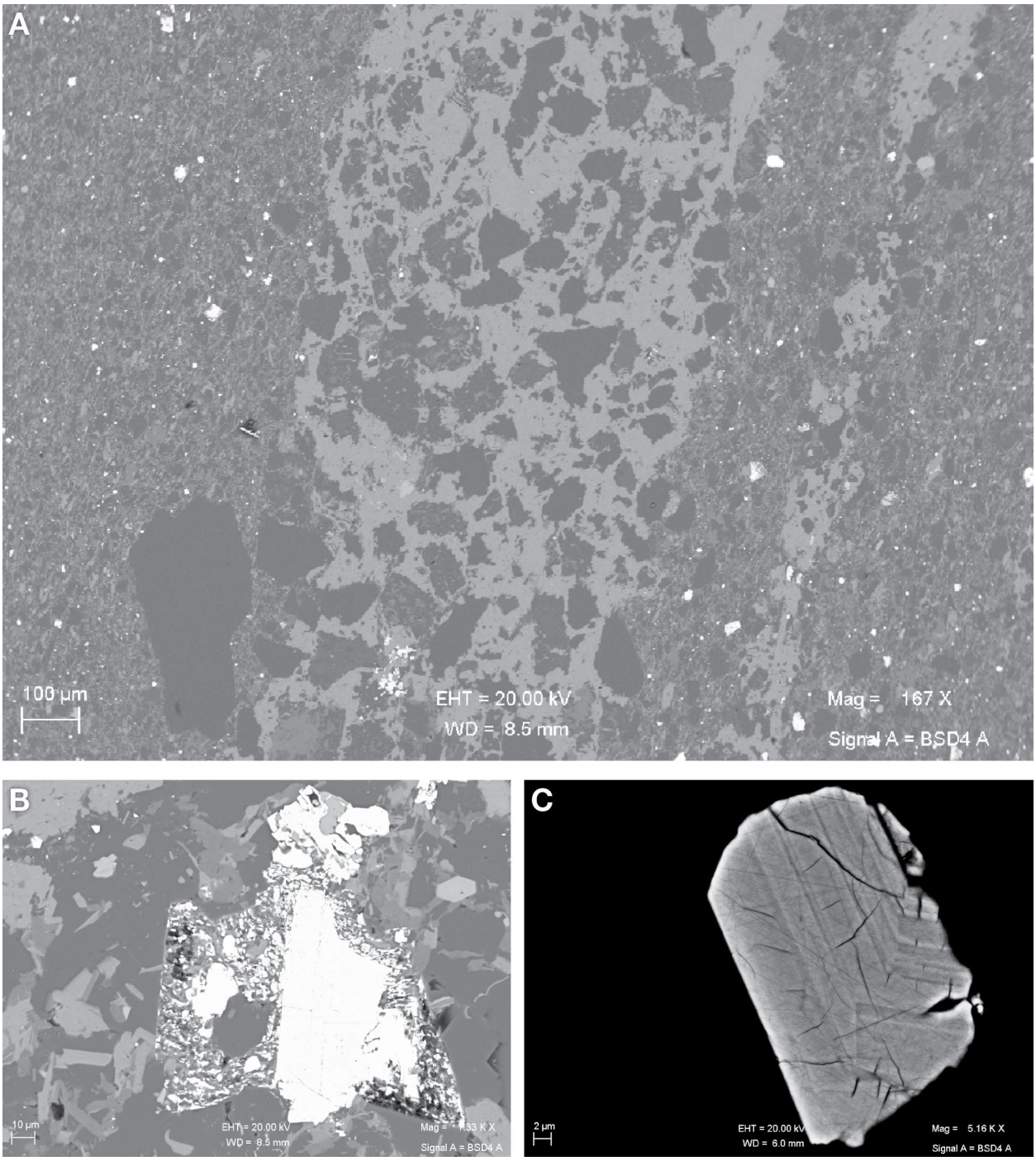


Photo 15.2. Scanning electron microscope images from sample 23RME-2001A in the lower magnetic zone showing typical textures present in the Gowganda Formation. **A)** Image showing lamination present in the sample, with typical very fine-grained mudstone layers to the left and right, with an approximately 0.7 mm thick siltstone layer in the centre of the image. Note angularity of quartz fragments (dark) that sit in a matrix of iron-chlorite (light medium grey) in the siltstone layer. Bright spots throughout the image, but most common in the mudstone layers, are hematite grains. A large quartz dropstone is present in the lower left of the image adjacent the siltstone layer. Stratigraphic top to the left. Field of view is 1.75 mm across. **B)** Image of hematite replacing a large iron chlorite grain in a siltstone layer. Field of view is 175 µm across. **C)** High contrast image of a zircon grain from a siltstone layer. Note truncation of growth laminae suggesting that the zircon is detrital in origin. Zircon grain is approximately 32 by 20 µm in size.

feldspar-hematite, with minor epidote, apatite, titanite, ulvospinel and rutile. Hematite constitutes between 5 and 15% of the mudstone in the magnetic zones. Hematite is absent in the non-magnetic zone, with the mudstones there also having slightly lower specific gravity (2.77 versus 2.81).

The dominant mineralogy in the matrix in the siltstone layers is quartz-albite-iron chlorite-illite-potassium feldspar-hematite. The siltstone consists predominantly of angular detrital quartz grains (Photo 15.2A), as well as rock fragments and detrital albite, potassium feldspar, biotite (now iron chlorite), epidote, rutile and apatite grains, as well as minor detrital zircon grains. In samples 23RME-2001A and -2001B, several sizable grains (30–80 μm) of intergrown rutile and synchysite [$Ca(Y,Ce,Nd)(CO_3)_2F$] occur in the siltstone layers and may be detrital in origin. It is not known if rutile and synchysite grew together, or if the synchysite grew epitaxially on the rutile.

The very angular nature of the quartz grains in the siltstone (*see* Photo 15.2A) is consistent with deposition in a glacial environment and with the previously inferred depositional setting of the Coleman Member (e.g., Young and Chandler 1968; Rainbird and Donaldson 1988). Overall, the mineralogy is consistent with diagenesis of the original sediment, with the absence of chloritoid indicating the rocks are unmetamorphosed, never reaching temperatures greater than 280°C (Bucher and Frey 2002, p.224).

In both magnetic zones, hematite is the only iron oxide present (Photo 15.2B). Sulphide minerals are absent in the magnetic zones, except as large (100–900 μm) pyrite grains, which appear to be of late diagenetic origin and which cut across bedding. Other oxide phases include rutile, ilmenite, ulvospinel and chromium hematite. Hematite grains are typically euhedral, 1 to 15 μm in size, and are evenly dispersed throughout the mudstone layers, but they are also common in the siltstone layers. The shape and size of the hematite grains, their uniform distribution in the layers, and their abundance in the finest grain layers, are features interpreted to be inconsistent with a detrital origin from an Archean iron formation source. Hematite compositions range from 100% iron to iron-rich grains containing minor amounts of silica, aluminum, titanium and/or manganese. Compositional variation is independent of grain size, but this compositional heterogeneity is consistent with diagenesis of a Fe-(oxy)-hydroxide precursor and/or the presence of precursor phases, such as goethite and ferrihydrite (*see* Photo 15.2B). Hematite has a reported magnetic susceptibility of 1 to 35 $\times 10^{-3}$ SI units (Grant and West 1965) and, thus, could produce the observed magnetism in the mudstones (in contrast, magnetite has a magnetic susceptibility of 1200 to 19 000 $\times 10^{-3}$ SI units; Grant and West 1965).

Although broadly similar mineralogically to the magnetic zones, a key difference is that the non-magnetic sample (23RME-2005) contains no hematite, and fine-grained (1–20 μm) sulphide minerals, typically chalcopyrite, although sparse, are present. In addition, phases, such as chlorite, mica and epidote, contain less iron and more magnesium than the same phases do in the magnetic zones, suggesting a reduction in iron supply during deposition of these stratigraphically higher mudstones. This unit also contains small shaly lenses and wisps that contain dolomite grains. Card, Innes and Debicki (1977) report the presence of minor calcareous siltstones in the Gowganda Formation near the Coleman Member–Firstbrook Member transition west of Sudbury.

The altered arenite unit consists of large subrounded grains of quartz and potassium feldspar, with a groundmass of white mica, potassium feldspar, chlorite and dolomite. Pyrite occurs throughout the rock. Several detrital zircon grains (20–60 μm, *see* Photo 15.2C) are also present.

DISCUSSION

Of the potential processes for producing the ferruginous mudstones in the Gowganda Formation in Burt Township, a post-depositional and post-diagenetic hydrothermal process or a detrital process can be ruled out. The preservation of primary sedimentary textures, the low metamorphic grade, and the absence

of any alteration features, either visual or mineralogical, rule out a hydrothermal event. Texturally, there is no evidence that the hematite in the mudstones, which consists of small (1–20 μm), euhedral grains, is detrital in origin. In addition, one would expect the presence of predominantly magnetite, not hematite, grains if the source were an Archean iron formation. Consequently, precipitation of iron from seawater and subsequent diagenesis is the most likely mechanism. The absence of chert, the predominance of hematite, and the lack of coeval banded iron formation, however, argue against the standard model for Paleoproterozoic iron formation deposition, such as the Marquette Range Supergroup (cf. Bekker et al. 2010; Cannon and Drenth 2023). As such, the model for the deposition of Neoproterozoic iron formations is proposed as the most likely origin, as further discussed in this article.

Shawma et al. (2023) have suggested that in the Gowganda to Elk Lake area, approximately 40 km south of Burt Township, the Gowganda and Lorrain formations are preserved in a paleovalley, interpreted as an ancient fjord. In the Gowganda to Elk Lake area, subglacial deposits of the Coleman Member are preserved at the base of the paleovalley, unconformably above Archean supracrustal and granitic rocks of the Abitibi Subprovince. Subsequently, the fjord was filled by glaciomarine strata sourced from a grounded tidewater ice sheet prior to climate warming (upper Coleman Member). Above the glaciomarine deposits, deltaic deposits of the Firstbrook Member represent a transition to nonglaciogenic deposition under a warm and humid climate (Shawma et al. 2023). Observations from diamond-drill hole NAN22-001 are consistent with the model of Shawma et al. (2023), with the rocks of the Coleman Member below 311.8 m depth consisting of subglacial and glaciomarine deposits.

In terms of determining why the Coleman Member contains ferruginous mudstones, the paleovalley setting proposed by Shawma et al. (2023) suggests that the environment proposed for Neoproterozoic ironstone deposition (cf. Cox et al. 2013) is applicable. In this environment, the overall chemistry of the mudstones is the result of mixing between a seawater hydrothermal (volcanic vents) and a detrital component (elements such as aluminum, potassium, sodium and titanium). Ice cover may have promoted local deep-water anoxia; however, in a paleovalley regime, the influx of oxygenated surface waters could generate iron precipitation. A decreased sulphate supply from the continent during glaciation would also have shifted Huronian deep-water chemistry from euxinic (low Fe/S values) to ferruginous (higher Fe/S values), further favouring the deposition of ferruginous mudstones and ironstones.

Hutton and Parkin Townships

FIELD OBSERVATIONS

The Gowganda Formation is well exposed in northeastern Hutton Township because of recent logging activity. In this area, conglomerate only occurs at the base of the formation, and is on the order of 15 to 25 m thick (Meyn 1970a). It is weakly magnetic (10.5×10^{-3} SI units). The majority of the formation consists of grey to grey-green weathering mudstone near the base, with very thin-bedded siltstone horizons becoming more common higher in the stratigraphy. The mudstones are typically massive or weakly parallel laminated, with laminations 1 to 3 mm thick (Photo 15.1B). Granules and pebbles, usually less than 3 cm across, are present locally, and some are obviously dropstones. Siltstone horizons become more common higher in the stratigraphy. Total stratigraphic thickness of the Gowganda Formation in Hutton Township is difficult to estimate because of the presence of numerous small-scale folds in the unit (Meyn 1970b) and the absence of distinctive marker horizons. At present, it is unclear if the Coleman Member–Firstbrook Member stratigraphic nomenclature is applicable to the Gowganda Formation in Hutton Township. Nonetheless, a distinction can be made between a lower mudstone unit that has uniformly dispersed magnetite grains (up to 0.2 mm in size) (*see* Photo 15.1B) and an upper mudstone unit that lacks obvious magnetite grains and contains more siltstone. The presence of magnetite versus hematite still needs to be confirmed through petrography. Magnetic susceptibility in the lower mudstone

unit has average values of 32.8 to 62.5 $\times 10^{-3}$ SI units, with the highest individual reading being 69.5 $\times 10^{-3}$ SI units. For comparison, olivine diabase dikes of the Sudbury dike swarm, which feature prominently in the aeromagnetic surveys, typically have values ranging from 35 to 70 $\times 10^{-3}$ SI units (Biswas 2019). In contrast, the upper mudstone unit has average values ranging from 1.5 to 6.7 $\times 10^{-3}$ SI units, but with a much greater range in individual readings than in the lower mudstone unit. The upper mudstone unit also has lower potassium, uranium and thorium contents, as determined by a handheld gamma-ray spectrometer, likely reflecting the presence of a more quartz-rich component (i.e., more siltstone). The lower mudstone unit is on the order of 450 m thick. The upper mudstone unit is at least 250 m thick; however, the top of the upper mudstone unit was not observed.

In adjacent Parkin Township to the east, the mudstone facies of the Gowganda Formation can be traced along strike for approximately 9 km. As in Hutton Township, the lower mudstone unit contains uniformly dispersed magnetic grains (up to 0.1 mm in size) and has average magnetic susceptibility values of 16.0 to 48.75 $\times 10^{-3}$ SI units, with the highest individual reading being 58.0 $\times 10^{-3}$ SI units. In the east, near the Wanapitei River, the mudstone is in fault contact with Lorrain Formation sandstone, with the sandstone having average magnetic susceptibility values of 0.08 to 0.15 $\times 10^{-3}$ SI units. In northwest Parkin Township, the Gowganda Formation mudstone is in fault contact with sandstones of the Matinenda and Mississagi formations, which also have very low average magnetic susceptibility values of 0.16 to 0.21 $\times 10^{-3}$ SI units.

In Hutton Township, the Gowganda Formation is underlain to the south by sandstone of the Serpent Formation and conglomerate of the Bruce Formation. Both units are non-magnetic, with average magnetic susceptibility of 0.16 and 0.21 $\times 10^{-3}$ SI units, respectively. A vertical roadcut in the Serpent Formation at UTM 501186E 5190624N (NAD83, Zone 17) contains well-developed shattercones, indicating that the Serpent Formation and, likely, the Gowganda Formation, were affected by deformation and/or metamorphic effects related to the Sudbury Structure, located approximately 13 km to the south.

DISCUSSION

Based on field observations, the depositional environment of the Gowganda Formation in Hutton and Parkin townships differs from that in Burt Township based on the limited presence of conglomerate and the limited development of rhythmic layering in the mudstone units, particularly the lower mudstone unit. These features suggest possible deposition in a more open basin where input of distal clastic material was limited. Nonetheless, the mechanism for the development of magnetic minerals could be similar in both areas. If the magnetic minerals in Hutton Township are indeed magnetite, only a slight increase in temperature during regional metamorphism (from ~250 to 370°C, Bucher and Frey 2002, p.224-226) would be needed to convert any early-formed hematite to magnetite.

In terms of general stratigraphic relationships, in Hutton and Parkin Township, it appears that the Huronian Supergroup units in direct contact with the Archean basement can vary between conglomerate of the Matinenda Formation, mudstone of the Pecors Formation, sandstone of the Mississagi Formation or conglomerate of the Gowganda Formation. Notably absent are turbidites of the McKim Formation and conglomerate of the Ramsay Lake Formation, and the Matinenda, Pecors and Mississagi formations are considerably thinner than they are south of the Murray Fault. These relationships are consistent, however, with observations in the River Valley area directly to the east, where the lower Huronian Supergroup is also considerably thinner than it is south of the Murray Fault (cf. Easton 2003).

Creelman Township

FIELD OBSERVATIONS

Although located only 10 km to the north of the area examined in Hutton Township, the Gowganda Formation in Creelman Township is different in both its composition and magnetic character. Conglomerate horizons are thicker and more common than to the south and occur at both the base and the top of the formation. Sandstone beds are also present in the upper part of the formation. Siltstone beds are more common throughout the township and, in some places, show evidence of soft-sediment deformation. Laminated mudstones are less common, with siliceous mudstone–siltstone sequences being more prevalent. Where mudstone is present, it is not well laminated, and contains sparse, but common, dropstones 5 to 25 cm in size. Notably absent in any of the fine-grained units were the visible disseminated magnetic grains seen in both Hutton and Parkin townships. The highest magnetic susceptibility readings came from a laminated mudstone unit, with average magnetic susceptibility values ranging from 11.2 to 15.2 $\times 10^{-3}$ SI units. Some conglomerate horizons had average magnetic susceptibility values ranging from 3.6 to 8.1 $\times 10^{-3}$ SI units. These values are much lower than those observed only 10 km to the south. Siltstones typically had magnetic susceptibility less than 1.0 $\times 10^{-3}$ SI units. As was the case to the south, total stratigraphic thickness of the Gowganda Formation in Creelman Township is difficult to estimate because of the presence of numerous small-scale folds in the unit (Meyn 1971) and the absence of distinctive marker horizons.

DISCUSSION

The depositional setting for the Gowganda Formation in Creelman Township is unclear, but is very different from that observed in Hutton and Parkin townships, despite their geographic proximity. Most notable is the greater abundance of quartz-rich rocks (siltstones and sandstones). The absence of visible magnetic grains in the mudstones in Creelman Township suggests that hematite, not magnetite, may be the primary iron phase in Creelman Township, but this awaits petrographic confirmation.

SUMMARY

The preliminary observations in this article can be summarized as follows. Magnetic units in the Gowganda Formation appear to be consist mainly of weakly to strongly laminated mudstones that occur stratigraphically above the lowermost conglomerate beds (diamictite) of the formation. Magnetic minerals are fine grained and are dispersed throughout the mudstone layers, and consist of either hematite or magnetite, with metamorphic grade being a likely determinant factor on mineralogy. Deposition of ferruginous mudstones in a glaciomarine environment, perhaps akin to the formation of Neoproterozoic ironstones, is one mechanism by which these magnetic mudstones were deposited. Petrographic and geochemical work on samples collected during the fall of 2023 will aid in either confirming or modifying these preliminary conclusions.

ACKNOWLEDGMENTS

R.A. Skeries and D. Morrison are thanked for providing access to the core from diamond-drill hole NAN22-001 for sampling purposes, as well as informative discussions on the local geological setting. S.A. Clarke of the Ontario Geological Survey Geoscience Laboratories is thanked for her assistance with using the scanning electron microscope. J.E. Chartrand of the OGS was an excellent field assistant for the Sudbury area sampling. P. Gervais prepared the figures and photographs for publication.

REFERENCES

Bekker, A., Slack, J.F., Planavsky, N., Krapez, B., Hofmann, A., Konhauser, K.O. and Rouxel, O.J. 2010. Iron Formation: The sedimentary product of a complex interplay among mantle, tectonic, oceanic, and biospheric processes; Economic Geology, v.105, p.467-508.

Biswas, S., compiler. 2019. Ontario Precambrian bedrock magnetic susceptibility geodatabase for 2001 to 2017; Ontario Geological Survey, Miscellaneous Release—Data 273 – Revision 2.

Bleeker, W. 2018. Archean BIF clasts vs. Paleoproterozoic jasper clasts? The proof is in the pudding (stone); *in* 64th Institute on Lake Superior Geology, Annual Meeting, Proceedings, v.64, pt.1, p.9-10.

Bleeker, W., Kamo, S.L., Ames, D.E. and Davis, D. 2015. New field observations and U-Pb ages in the Sudbury area: toward a detailed cross-section through the deformed Sudbury Structure; *in* Targeted Geoscience Initiative 4: Canadian Nickel-Copper-Platinum Group Elements-Chromium Ore Systems — Fertility, Pathfinders, New and Revised Models, Geological Survey of Canada, Open File 7856, p.151-166.

Bucher, K. and Frey, M. 2002. Petrogenesis of metamorphic rocks, 7th edition; Springer-Verlag, New York, 341p.

Cannon, W.F. and Drenth, B.J. 2023. Eastward transition from banded iron-formation to ferruginous clastic rocks across the central Upper Peninsula of Michigan; *in* Proceedings of the 69th Institute on Lake Superior Geology Annual Meeting, v.69, pt.1, p.21-22.

Card, K.D., Innes, D.G. and Debicki, R.L. 1977. Stratigraphy, sedimentology, and petrology of the Huronian Supergroup in the Sudbury–Espanola area; Ontario Division of Mines, Geoscience Study 16, 99p.

Card, K.D., McIlwaine, W. and Meyn, H.D. 1973. Geology of the Maple Mountain area, districts of Timiskaming, Nipissing and Sudbury; Ontario Division of Mines, Geological Report 106, 133p.

Cox, G.M., Halverson, G.P., Minarik, W.G., Le Heron, D.P., Macdonald, F.A., Bellefroid, E.J. and Strauss, J.V. 2013. Neoproterozoic iron formation: An evaluation of its temporal, environmental and tectonic significance; Chemical Geology, v.362, p.232-249.

Debicki, R.L. 1990. Stratigraphy, paleoenvironment and economic potential of the Huronian Supergroup in the southern Cobalt embayment; Ontario Geological Survey, Miscellaneous Paper 148, 154p.

Easton, R.M. 2003. Geology and mineral potential of the Paleoproterozoic River Valley Intrusion and related rocks, Grenville Province; Ontario Geological Survey, Open File Report 6123, 171p.

Easton, R.M., Rainsford, D.R.B. and Préfontaine, S. 2020. Preliminary interpretation of the Sturgeon River area aeromagnetic survey, northeastern Ontario; *in* Summary of Field Work and Other Activities, 2020, Ontario Geological Survey, Open File Report 6370, p.6-1 to 6-15.

Grant, F.S. 1985. Aeromagnetics, geology and ore environments, I. Magnetite in igneous, sedimentary and metamorphic rocks: An overview; Geoexploration, v.23, no.3, p.303-333.

Grant, F.S. and West, G.F. 1965. Interpretation theory in applied geophysics; McGraw-Hill, New York, 603p.

James, H.L. 1954. Sedimentary facies of iron-formation; Economic Geology, v.49, p.235-293.

Meyn, H.D. 1970a. Geology of Hutton and Parkin townships; Ontario Department of Mines; Geological Report 80, 78p.

——— 1970b. Hutton and Parkin townships, Sudbury District; Ontario Department of Mines, Map 2180, scale 1:31 680.

——— 1971. Geology of Roberts, Creelman and Fraleck townships; Ontario Department of Mines, Geological Report 91, 48p.

Moore, J.C.G. 1963. Burt Township and north half of Gross Township, District of Temiskaming; Ontario Department of Mines, Preliminary Map P.207, scale 1:15 840.

Morrison, D., Dawson, D.J.W. and Skeries, R.A. 2023. Insight Geophysics Inc., OJEP diamond drill hole NAN22-001, Burt gold property, Matachewan, Ontario; unpublished report, April 5, 2023, 40p.

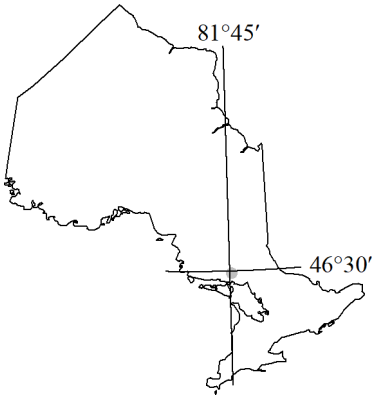
Rainbird, R.H. and Donaldson, J.A. 1988. Nonglaciogenic deltaic deposits in the early Proterozoic Gowganda Formation, Cobalt Basin, Ontario; Canadian Journal of Earth Sciences, v.25, p.710-724.

Rasmussen, B., Bekker, A. and Fletcher, I.R. 2013. Correlation of Paleoproterozoic glaciations based on U–Pb zircon ages for tuff beds in the Transvaal and Huronian Supergroups; Earth and Planetary Science Letters, v.382, p.173-180.

Shawma, N.A., McLoughlin-Coleman, T., Babechuk, M.G. and Rainbird, R.H. 2023. Paleoproterozoic (Huronian) valley-controlled deglacial-fluvial sedimentation, northern Cobalt Basin, Ontario, Canada; Sedimentary Geology, v.455, article 106421, 40p.

Young, G.M. and Chandler, FW. 1968. Possible glacial origin for three Precambrian (Huronian) conglomerates, north shore of Lake Huron; *in* Proceedings of the 14th Annual Institute on Lake Superior Geology, Proceedings, v.14, p.42-43.

16. Project NE-22-001. Occurrences of Critical Minerals in Hyman Township, Southern Province, Northeastern Ontario



C.A. Gordon[1]

[1]Earth Resources and Geoscience Mapping Section, Ontario Geological Survey

INTRODUCTION

Geological mapping of Hyman Township in the Agnew Lake area was initiated by the Ontario Geological Survey in 2022 (Gordon 2022). The area is of interest for several reasons: 1) it was last mapped over 50 years ago (Card 1965) before the establishment of the current Huronian Supergroup stratigraphy (Robertson, Card and Frarey 1969); 2) previous mapping was done with limited subdivision of the mafic intrusive rocks; 3) the area contains a past-producing uranium mine with reserves (Agnew Lake mine), a nickel-copper-platinum group elements (PGE) prospect (Kordol South showing) and numerous uranium and nickel-copper-cobalt occurrences.

This article focusses on the occurrences of critical minerals in the township (cobalt, copper, nickel, PGEs, yttrium and rare earth elements), as outlined in the Critical Minerals Strategy for the Province (Ontario 2022). Several of these occurrences were visited during the 2022 and 2023 field seasons. Although uranium is not a critical mineral (according to the 2022 strategy), it is closely associated with rare earth element concentrations in Hyman Township and, thus, can serve as a pathfinder for exploration. Similarly, thorium is not a critical mineral at present, but, in the future, demand for thorium may increase as an energy commodity (International Atomic Energy Association 2022). A summary of the critical mineral occurrences in Hyman Township from the Ontario Mineral Inventory database (Ontario Geological Survey 2023a) is presented in Table 16.1 and locations are shown on Figure 16.1.

REGIONAL GEOLOGY

Hyman Township is located approximately 50 km west-southwest of Sudbury. It straddles the boundary between the Archean Superior Province and the Paleoproterozoic Southern Province (*see* Figure 16.1). The northern quarter of the township is underlain by Archean rocks of the Birch Lake batholith (*circa* 2651 Ma: Kamo 2006, 2023) that comprise part of the Ramsey–Algoma granitoid complex. The Birch Lake batholith is intruded by numerous post-Archean dikes. The most voluminous of these is the Matachewan dike swarm (2480–2460 Ma: Heaman 1997; Bleeker et al. 2015). The southern margin of the Birch Lake batholith is overlain unconformably by supracrustal rocks of the Huronian Supergroup (2.45–2.22 Ga: Krogh, Davis and Corfu 1984; Bennett, Dressler and Robertson 1991). The Huronian Supergroup consists of metamorphosed supracrustal rocks and is subdivided into 4 groups; from lowermost to uppermost, these are the Elliot Lake, Hough Lake, Quirke Lake and Cobalt groups (Robertson, Card and Frarey 1969; Bennett, Dressler and Robertson 1991, and references therein). Within Hyman Township, the Huronian Supergroup is intruded by the Nipissing intrusive suite (2.21–2.22 Ga: Corfu and Andrews 1986; Davey et al. 2019), the Trap dike swarm (*circa* 1.75 Ga: Bleeker et al. 2015) and the Sudbury dike swarm (*circa* 1.24 Ga: Krogh et al. 1987). The Sudbury Igneous Complex,

Summary of Field Work and Other Activities, 2023,
Ontario Geological Survey, Open File Report 6405, p.16-1 to 16-13.

© King's Printer for Ontario, 2023

a remnant of an ancient meteorite crater that formed at 1850 Ma (Dietz 1964; Krogh, Davis and Corfu 1984), crops out approximately 4 km northeast and east of Hyman Township. Effects of shock metamorphism and brecciation related to the impact event extend into Hyman Township.

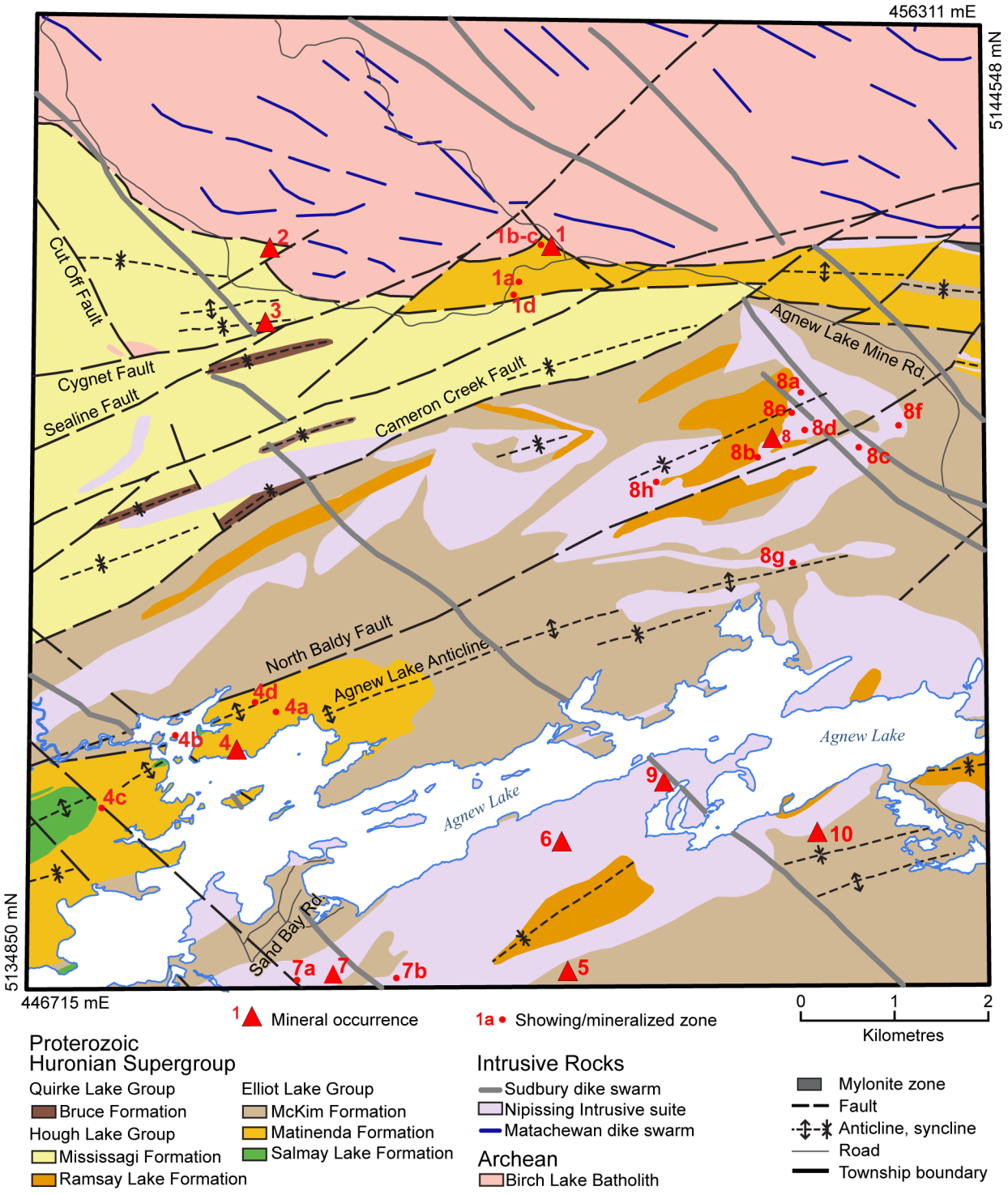


Figure 16.1. Simplified geological map of Hyman Township, based on mapping in 2022 and 2023 and *modified from* Card (1965). Mineral occurrences are labelled and are listed in Table 16.1. Universal Transverse Mercator (UTM) co-ordinates are provided using North American Datum 1983 (NAD83) in Zone 17.

Table 16.1. Ontario Mineral Inventory (OMI) occurrences in Hyman Township (Ontario Geological Survey 2023a).

Location Number in Figure 16.1	Mineral Deposit Category	Deposit Name	Commodity	OMI Number
1 (a, b, c, d)	Past-Producing Mine with Reserves	Agnew Lake Mine	U, Th, Y	MDI41I05NE00009
2	Occurrence	Richore showing	U, Th	MDI41I05NE00038
3	Occurrence	East Bay Gold Ltd., Rose showing	U, Th	MDI41I05NE00039
4 (a, b, c, d)	Occurrence	John Creek Bay, Ridge showing	U, Th	MDI41I05NE00041
5	Prospect	Kordol main zone, Kordol South prospect	Ni, Cu, Co, Pd	MDI41I05SE00069
6	Occurrence	Kordol No.2 zone, Kordol North showing	Ni, Cu, Co, Pd	MDI41I05NE00058
7 (a, b)	Occurrence	Keba and Buchy property	Ni, Cu, Co, PGE	MDI41I05SE00027
8 (a, b, c, d, e, f, g, h)	Occurrence	Woods Creek prospect (Pond showing), Main, Trevor, Raven's Cliff, Southern, Western showings	Ni, Cu	MDI41I05NE00043
9	Discretionary Occurrence	Kordol No.3 zone	Ni, Cu	MDI41I05NE00057
10	Discretionary Occurrence	Kordol No.4 zone	Ni, Cu	MDI41I05NE00056

Abbreviations: *Co, cobalt; Cu, copper; Ni, nickel; OMI, Ontario Mineral Inventory; Pd, palladium; PGE, platinum group elements; Th, thorium; U, uranium; Y, yttrium.*

Metamorphic grade in Hyman Township ranges from greenschist facies in the north to amphibolite facies in the south (Card 1978b; Gordon 2022). Early ductile deformation of Huronian Supergroup strata historically has been interpreted to have started prior to, or concurrent with, emplacement of the Nipissing intrusive suite, with regional folding continuing after the emplacement of the Nipissing sills (e.g., Card 1978a; Jackson 2001; Easton 2006a). Subsequent northwest-directed compression produced a fold-and-thrust belt along the Superior craton margin (Card et al. 1984). Much of the deformation in the study area is attributed to the Yavapai and Mazatzal orogenies (*circa* 1760 to 1650 Ma: Papapavlou et al. 2017, and references therein). The lower age limit of deformation is constrained by the age of the undeformed Sudbury dike swarm (1238±4 Ma: Krogh et al. 1987).

ECONOMIC GEOLOGY

Uranium, Thorium and Rare Earth Element Mineralization

Uranium, thorium and rare earth element (REE) mineralization associated with the Huronian Supergroup occurs in the Elliot Lake, Blind River and Agnew Lake areas, with 13 uranium-thorium mines being active in the region between 1955 and 1983 (Robertson and Gould 1983). As listed in Table 16.1 (with locations shown in Figure 16.1), there are 3 uranium occurrences and 1 past-producing mine with reserves in Hyman Township. Scintillometer measurements from field work on some of these occurrences are listed in Table 16.2. To aid the reader in the interpretation of the significance of the assay data from historical reports mentioned in subsequent sections, Table 16.3 lists the current values used by the Ontario Mineral Inventory to define an "Occurrence" or a "Prospect". The values in Table 16.3 are typically one-tenth of what would be needed for economic recovery.

GENERAL GEOLOGY

Uranium, thorium and REE mineralization is hosted predominantly in the Matinenda Formation of the lowermost Elliot Lake Group and is interpreted as a modified placer deposit (Robertson 1976). Radioactive minerals typically present include uranothorite, monazite and brannerite (Robertson 1976). Anomalous uranium and thorium contents also occur in the Birch Lake batholith (e.g., Easton 2006b).

Table 16.2. Scintillometer results for selected uranium- and thorium-mineralized units in Hyman Township.

Deposit Name	Showing Name	Location Number in Figure 16.1	Total (cpm)	K (wt. %)	U (ppm)	Th (ppm)	Host Rock
Agnew Lake Mine	Zone 3	1a	115258	6.8	172.4	**1729.2**	Quartz-pebble conglomerate
	Zone 3	1a	62700.9	3.9	52.8	**1052.2**	Quartz-pebble conglomerate
	Zone 3	1a	54630.5	5.0	102.4	**772.0**	Quartz-pebble conglomerate
	Zone 3	1a	16009.6	4.0	48.8	172.1	Polymictic conglomerate
	Zone 3	1a	14066.7	3.3	43.1	157.2	Polymictic conglomerate
	Zone 3	1a	14039.8	2.8	41.8	155.5	Polymictic conglomerate
	Zone 3	1a	14456.0	4.7	22.3	191.7	Arenite
	Zone 3	1a	18218.7	5.0	29.7	271.8	Arenite
	Zone 1	1d	64098.2	6.1	73.4	**1001.7**	Quartz-pebble conglomerate
	Zone 1	1d	43273.3	3.9	64.4	**666.4**	Quartz-pebble conglomerate
	Zone 1	1d	20132.9	3.0	16.2	**328.6**	Quartz-pebble conglomerate
	Zone 1	1d	14341.8	4.3	2.8	222.7	Quartz-pebble conglomerate
	Zone 1	1d	18382.7	3.1	33.6	260.3	Siltstone
John Creek occurrence	Ridge north	4a	52409.0	7.8	**347.8**	136.1	Oligomictic conglomerate
	Ridge north	4a	31972.7	7.8	150.9	208.2	Oligomictic conglomerate
	Ridge south	4a	15967.6	3.0	61.9	135.8	Oligomictic conglomerate
	Ridge south	4a	8292.5	2.6	25.1	80.4	Oligomictic conglomerate
	Island	4b	21519.0	6.4	128.8	74.9	Polymictic conglomerate
	Island	4b	15063.6	4.8	81.9	70.4	Polymictic conglomerate
	Island	4b	26543.2	4.6	96.5	260.7	Arenite
	Island	4b	17263.3	3.9	36.8	226.9	Arenite
	Hilltop	4c	15610.9	4.1	26.3	201.9	Quartz-granule conglomeratic sandstone
	Hilltop	4c	7504.4	2.o	13.2	105.3	Quartz-granule conglomeratic sandstone

*Values above occurrence level values are indicated in **bold** (*see *Table 16.3).*
Multiply K by 1.2046 for K_2O, Th by 1.1379 for ThO_2, U by 1.1793 for U_3O_8. All K, U and Th data were recorded using a Radiation Solutions Inc. RS-125 SuperSpec gamma-ray spectrometer, serial number 2023, calibrated on January 28, 2020, using a NaI crystal. The instrument was self-stabilizing, and data were recorded using the assay mode with a 5-minute count time. Quoted accuracy is 0.1% K, 0.4 ppm U, and 0.7 ppm Th for a sample with 7–9.3% K, 40–50 ppm U and 104–129 ppm Th.
***Abbreviations:** cpm, counts per minute; K, potassium; ppm, parts per million; Th, thorium; U, uranium; wt. %, weight percent.*

Table 16.3. Ontario Mineral Inventory (OMI) cut-off values for commodities for the mineral inventory categories "Occurrences" and "Prospects". These are the commodities present in Hyman Township (Ontario Geological Survey 2023a, 2023b).

Commodity	Grade [A] (wt. %)	Grade [A] (ppm)	Occurrence [B]	Prospect [C] True Width
Co	0.02%	200 ppm	NR	1 m
Cu	0.25%	2500 ppm	NR	1 m
Ni	0.08%	800 ppm	NR	1 m
Platinum group elements	0.5 g/t	0.5 ppm	NR	1 m
Rare earth elements	0.10% TREO	1000 ppm TREO	NR	5 m
ThO_2	0.03%	300 ppm	NR	1 m
U_3O_8	0.03%	300 ppm	NR	1 m
Y	0.05%	500 ppm	NR	1 m

[A] All values listed are arbitrarily defined as one-tenth of the minimum acceptable economic grade.
[B] Simplified, an "Occurrence" is defined as significant two-dimensional mineralization as indicated from surface rock (channel or grab) sampling.
[C] Simplified, a "Prospect" is defined as significant mineralization as indicated by three-dimensional sampling. True width minimums defined as significant, but not economic widths.
***Abbreviations:** m, metre; NR, no requirement; ppm, parts per million; TREO, total rare earth oxides; wt. %, weight percent.*

The Matinenda Formation consists of quartz and feldspathic arenites, with minor amounts of interbedded siltstone and conglomerate, and is interpreted to represent fluvial deposition (Fralick and Miall 1989). In the Agnew Lake area, uraniferous units in the Matinenda Formation crop out in 2 separate localities: 1) adjacent to the Birch Lake batholith–Huronian Supergroup contact in north-central Hyman Township, and 2) in the core of the Agnew Lake anticline in the southern half of the township (*see* Figure 16.1). This configuration is controlled by regional, kilometre-scale, northeast-trending folds and multiple generations of faults (*see* Figure 16.1; Gordon 2022, and references therein).

Mineralization is hosted in conglomeratic units and in intervening arenite and siltstone beds. Two types of conglomerate occur in the mineralized zones: 1) quartz-pebble conglomerate, and 2) polymictic conglomerate. Both conglomeratic units can contain significant uranium and thorium mineralization; however, the quartz-pebble conglomerate is typically the unit containing economic concentrations of mineralization. The quartz-pebble conglomerate contains well-rounded, well-sorted quartz pebbles and subrounded to angular feldspar granules in a coarse quartz-feldspar-sericite matrix and, locally, may be monomict (oligiomictic) and poorly sorted with pebble- and cobble-sized quartz clasts. Density packing and the amount of quartz-pebbles is varied and some of the mineralized zones contain less than 10% clasts. The quartz-pebble conglomeratic horizons do not occur as single beds over a wide thickness, but rather as a series of narrow beds separated by beds of arenite. The polymictic conglomerate unit contains poorly sorted, quartz, granitoid, shale and fine-grained mafic clasts ranging from pebble to cobble size in a grey, fine- to medium-grained sandy matrix. The polymictic conglomerate beds range from 1 to 12 m in thickness; typically much thicker than the quartz-pebble conglomerate beds. Both types of conglomerate contain varied amounts of pyrite and pyrrhotite in the matrix, locally up to 7 volume %. There is a positive correlation between the amount of sulphide, pebble density packing and uranium content (Tracanelli and MacMillan 2006). Sulphide mineralization is also concentrated along fractures and shear zones that locally contain higher uranium and thorium concentrations. Interleaved between the conglomerate beds are layers of medium- to coarse-grained, subfeldspathic to feldspathic arenite and quartz-rich siltstone, both of which contain sporadic quartz pebbles beds, and both of which contain lower grade uranium and thorium mineralization.

MINERALIZATION ADJACENT TO THE BIRCH LAKE BATHOLITH

Three previously identified uranium, thorium and/or rare earth element occurrences or past-producing mines occur along the contact between the Birch Lake batholith and the Huronian Supergroup in northern Hyman Township (*see* Figure 16.1: numbers 1, 2 and 3).

The most significant of these is the Agnew Lake Mine (*see* Figure 16.1: number 1), which operated underground from 1977 to 1980 and closed in 1983. A reported total of 1 424 924 pounds of U_3O_8 ore were recovered (MDI41I05NE00009, Ontario Geological Survey 2023a). Approximately 70 000 pounds of U_3O_8 produced was from bioleaching on surface and, in addition, the leach solution contained yttrium and light rare earth elements. At the time of closure, the estimated reserve was between 5.13 million tonnes grading 0.92 kg U_3O_8 and 5.28 million tonnes grading 0.49 kg U_3O_8 (MDI41I05NE00009, Ontario Geological Survey 2023a). No reserves for thorium, yttrium or the rare earth elements are available.

Four uranium mineralized zones occur at the Agnew Lake mine property (*see* Figure 16.1: numbers 1a to 1d) (Carrington and Wilton 1969; Thomson 1960). Only 2 zones, zones 3 and 5 (*see* Figure 16.1: numbers 1a and 1b), reportedly contained economic thicknesses of mineralization that were targeted for mining. Mineralization is hosted in quartz-pebble conglomerate (Photo 16.1A), polymictic conglomerate (Photo 16.1B) and interleaved arenite and siltstone (*see* Photo 16.1A). Bedding in the mineralized zones trends easterly and dips steeply to the south, except the north-trending part of zone 5, which occurs in an embayment adjacent to the Birch Lake batholith (Tracanelli and MacMillan 2006). Mineralized horizons are reportedly up to 900 m long and are truncated by faulting to the west and these horizons pinch-out to

the east (Carrington and Wilton 1969; Thomson 1960). The thickness of the mineralized zones ranges from 15 to 45 m, with the average economic true thickness being 1 to 2 m (Carrington and Wilton 1969; Thomson 1960). Although no thorium production was reported from the Agnew Lake mine property, the mineralized conglomerates have a ThO_2/U_3O_8 of approximately 3:1, compared to 1:2 for the Elliot Lake area ores (Carrington and Wilton 1969). This higher Th/U value was observed in the scintillometer data collected on the property and in the assay results in Tracanelli and MacMillan (2006). Thorium content ranges from 150 to 1850 ppm (*see* Table 16.2; *see also* Tracanelli and MacMillan (2006)). Tracanelli and MacMillan (2006, their Table 2) also report total rare earth element contents of between 2000 and 12 700 parts per million (ppm), which are approaching economic levels (*see* Table 16.3).

Two other showings are located on strike, and approximately 800 m to the west of the Agnew Lake Mine, also near the Birch Lake batholith–Huronian Supergroup contact. These are the Richore showing (*see* Figure 16.1: number 2) and the East Bay Gold Ltd. showing located approximately 800 m south of the Richore showing (*see* Figure 16.1: number 3). Both lie in a stratigraphic position similar to that of the Agnew Lake Mine; however, the length, width and depth of the mineralized horizons at both showings are poorly defined. Furthermore, there is some confusion at these showings as to whether or not the

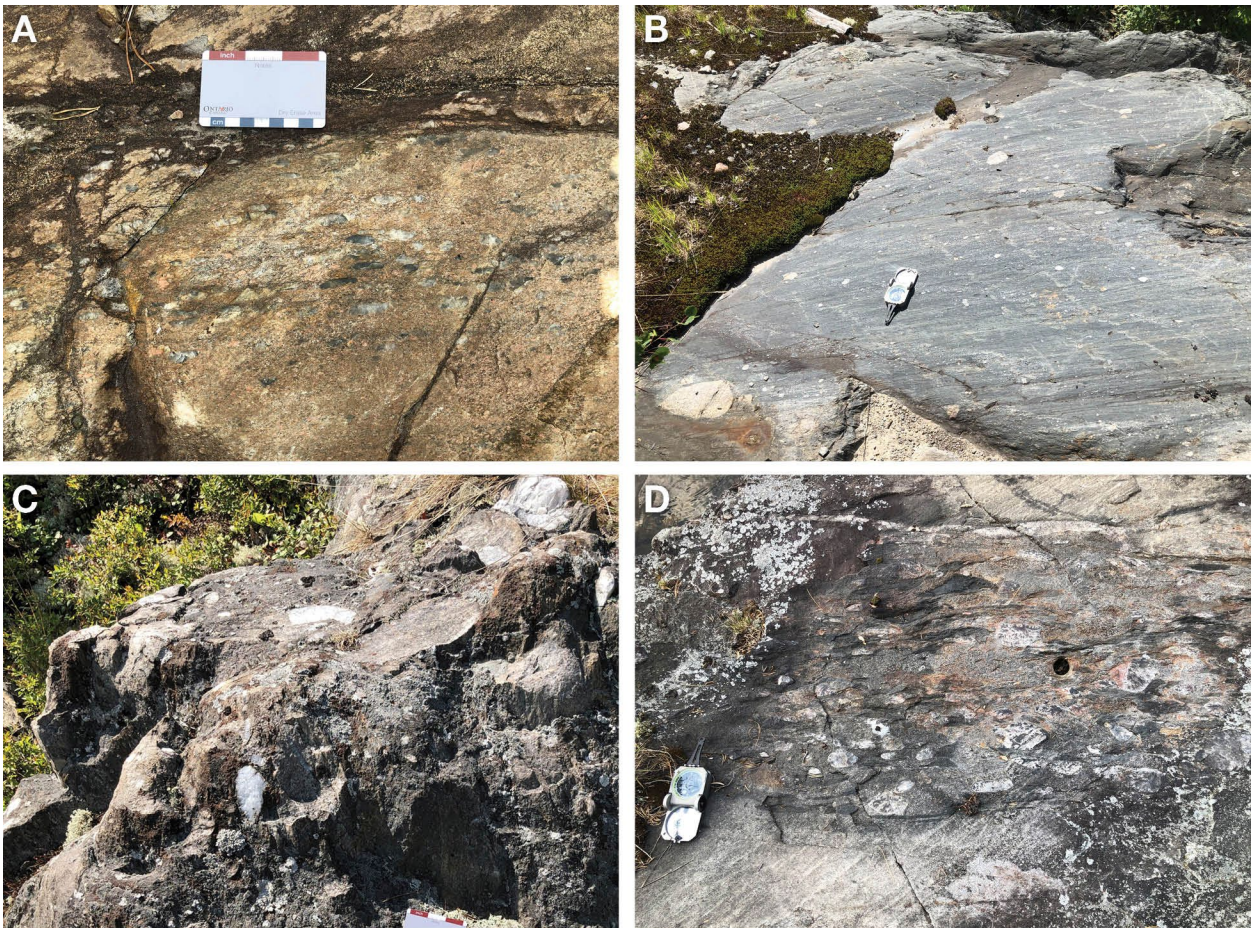


Photo 16.1. Photos of uranium- and thorium-mineralized units in the Matinenda Formation, Elliot Lake Group. **A)** Quartz-pebble conglomerate bed in feldspathic arenite, zone 3, Agnew Lake Mine property (UTM 451775E 5141955N). **B**) Polymictic conglomerate, zone 3, Agnew Lake Mine property (UTM 451746E 5141928N). **C)** Oligomictic conglomerate with pebble- and cobble-sized quartz clasts, Ridge showing, John Creek property (UTM 449091E 5137556N). **D)** Polymictic conglomerate and subfeldspathic arenite, Island showing, John Creek property (UTM 448217E 5137405N). Objects used for scale: scale card approximately 9 cm long; scintillometer approximately 25.5 cm long; open compass is 14.5 cm long. All UTM co-ordinates are provided using NAD83 in Zone 17.

mineralized conglomerates are part of the Matinenda or the Mississagi formations. These showings were not visited by the author. Despite these uncertainties, these 2 showings provide some insight into the mineral potential adjacent to the Birch Lake batholith–Huronian Supergroup contact.

The Richore showing contains mineralization hosted mainly in the Birch Lake batholith, but also in the overlying metasedimentary rocks. Three zones of radioactivity, up to 3 times that of background (40 counts per second, Lacombe 1968, p.29), are reported in the batholith. These zones range from 300 to 750 m in length and 90 to 150 m in width and occur in the batholith no more than 1500 m from the contact with the Huronian Supergroup (Lacombe 1968). Bulk samples from the batholith have values of 0.0013 to 0.0026 weight % U_3O_8 (Lacombe 1970), well below what would qualify as a mineral occurrence (*see* Table 16.3).

The East Bay Gold Ltd. showing (*see* Figure 16.1: number 3) consists of small, northeast-trending lensoidal beds of uraniferous quartz-pebble conglomerate interbedded with granule-rich conglomerate, arenite, mudstone and greywacke (Komarechka 2012). Historical drilling intersected zones with up to 1.08 pounds U_3O_8 per ton (chemical) and 1.34 pounds ThO_2 per ton (chemical) over 5.5 feet (Moody 1967, p.7). More recent assays of surface samples from a stripped area centred at UTM 448978E 5141519N (Zone 17, NAD83) within the larger property area, contained 202 ppm U, 385 ppm Th and 443 ppb Au (Komarechka 2012). Shear zones proximal to the conglomerate beds also exhibit anomalous radioactivity, up to 1000 counts per second (Komarechka 2012). The high Th/U value is similar to that observed at the Agnew Lake mine property, suggesting that this occurrence be further investigated for its rare earth element and/or thorium potential.

MINERALIZATION AT THE JOHN CREEK BAY OCCURRENCE

The John Creek Bay occurrence (*see* Figure 16.1: numbers 4a to 4d) consists of 4 uranium mineralized zones in Matinenda Formation strata that crop out in the core of the Agnew Lake anticline in southern Hyman township. These zones are exposed at the Ridge, Hill Top, Island and Cabin showings. The length and depth of the mineralized zones are poorly defined and the associated rare earth element content is unknown. In contrast to the occurrences near the Birch Lake batholith–Huronian Supergroup contact, the showings at the John Creek Bay occurrence have ThO_2/U_3O_8 of approximately 1:2, that is, closer to that of the Elliot Lake ores (*see* Table 16.2). It remains to be determined if this lower ratio means that the John Creek Bay occurrence is less prospective for thorium, yttrium and/or the rare earth elements compared to the occurrences in northern Hyman Township.

The Ridge showing (*see* Figure 16.1: number 4a) contains 2 mineralized horizons, 30 m apart, that trend east-northeast for approximately 75 m. Mineralization is hosted in oligomictic conglomeratic sandstone beds that differ from the typical uraniferous quartz-pebble conglomerate in being poorly sorted, with pebble- and cobble-sized quartz clasts. They vary from very narrow to several metres thick (Photo 16.1C). Average grades are 0.16 weight % U_3O_8 (chemical) over 0.64 m for 57 m (northern mineralized horizon) and 0.28 weight % U_3O_8 (chemical) over 0.6 m (southern mineralized horizon) (Robertson and Gould 1983).

The Island showing (*see* Figure 16.1: number 4b) contains uranium mineralized horizons of polymictic conglomerate and arenite (Photo 16.1D). The conglomerate varies from 1 to 2 m thick and trends east-northeast. Average grade is 0.152 weight % U_3O_8 (radiometric) over 2.4 m (Robertson and Gould 1983).

The Hill Top showing (*see* Figure 16.1: number 4c) occurs in thin quartz-pebble conglomerate beds intercalated with a quartz granule-rich conglomeratic sandstone. The trend of bedding parallels the nearby contact with volcanic rocks of the Salmay Lake Formation. Average grade is 0.182 weight % U_3O_8

(radiometric) (Robertson and Gould 1983). Uraniferous quartz-pebble conglomeratic beds were not observed during mapping, but elevated concentrations of uranium and thorium were noted in the granule-rich conglomeratic sandstone near the Hill Top showing and 300 m to the east (*see* Table 16.2).

The Cabin showing (*see* Figure 16.1: number 4d) was not located during mapping. It is reportedly hosted in quartz-pebble conglomerate and arenite, approximately 180 m northwest of the Ridge showing. Average grade was 0.17 weight % U_3O_8 and 0.06 weight % ThO_2 (radiometric) (Robertson and Gould 1983).

Nickel-Copper-Platinum Group Elements Mineralization

GENERAL GEOLOGY

Nickel-copper-platinum group elements (PGE) mineralization in Hyman Township is associated entirely with intrusions of the Nipissing intrusive suite, especially near the contacts of the intrusions. The Nipissing sills in the township are on trend with, and most likely part of, the same suite of gabbro bodies that host the past-producing Shakespeare nickel-copper-PGE mine in Shakespeare Township, approximately 10 km to the southwest. As listed in Table 16.1 (and shown on Figure 16.1), there is 1 nickel-copper-PGE prospect and 5 nickel-copper-PGE occurrences in Hyman Township.

Nickel-copper-PGE sulphide mineralization is associated with the larger, northeast-trending gabbroic sills that were intruded at the contact between the Ramsay Lake and McKim formations. The sills, along with their host Huronian Supergroup rocks, crop out on the northern and southern limbs of the northeast-trending Agnew Lake anticline (*see* Figure 16.1) (Gordon 2022, and references therein).

Estimates of the size of the intrusions is complicated by folding, but appears to range from 200 to 850 m in thickness and several kilometres in length. The sills are differentiated and consist of fine- to medium-grained gabbro, melagabbro and quartz gabbro. Irregular leucocratic pods occur within the main gabbroic phases. The melagabbro unit, in particular, is of economic interest as it is the main unit hosting mineralization in the Shakespeare mine area (e.g., Sproule et al. 2007). Based on mapping, the melagabbro phase of the sills in Hyman Township is 100 to 200 m thick. A breccia zone with rounded sedimentary and gabbroic clasts in a fine- to medium-grained melagabbroic matrix crops out at the base of 2 intrusions in central Hyman Township.

OCCURRENCES SOUTH OF AGNEW LAKE

The Kordol, Keba and Buchy nickel-copper-PGE occurrences (*see* Figure 16.1: numbers 5, 6 and 7) are associated with a large, folded, northeast-trending Nipissing sill south of Agnew Lake. Mineralization is exposed on surface at the Kordol South and Kordol North showings, the Kordol No.3 and No.4 zones, and at the Keba and Buchy showings.

The Kordol South showing is the main nickel-copper-PGE prospect in Hyman Township. It is a 15 m long northeast-trending zone up to 4.6 m wide that contains 10 to 40 volume % sulphide mineralization. Reported values are 1.03 weight % Cu, 0.45 weight % Ni, 0.12 weight % Co and trace palladium over 5.2 m (MDI41I05SE00069; Ontario Geological Survey 2023a). These reported values are well above the minimum values listed in Table 16.3 for a prospect. More recent work reported 160 to 388 ppb Pt+Pd+Au (combined platinum, palladium and gold) (Lapierre 2002), but these values are below the minimum values in Table 16.3. The Kordol North showing and the No.3 and No.4 zones all contain smaller, metre-size pods of sulphide mineralization. Mineralization in all of the Kordol occurrences is present as disseminated to massive pyrrhotite, pyrite and chalcopyrite hosted in melagabbro.

The Keba and Buchy property straddles the boundary with Nairn Township to the south. There are 4 showings associated with the property, 2 of which are in Hyman Township (*see* Figure 16.1: numbers 7a and 7b). The showings correspond with a northeast-trending induced polarization (IP) conductor that is at least 900 m long (Lapierre 2002). Sulphide mineralization occurs as disseminated to semi-massive and fracture-controlled pyrrhotite, chalcopyrite, pentlandite and pyrite in melagabbro (Lapierre 2002). The westernmost showing (*see* Figure 16.1: number 7a) is a 100 m long and 3 to 6 m wide zone of disseminated blebby to semi-massive pyrrhotite, minor chalcopyrite and trace pentlandite sulphide mineralization (Photos 16.2A and 16.2B). Reported values are 0.607 weight % Ni, 0.249 weight % Cu, 0.089 weight % Co and 193 ppb Pt+Pd+Au (Lapierre 2002). The cobalt, copper and nickel values are all of economic interest (*see* Table 16.3).

OCCURRENCES NEAR THE NORTH BALDY FAULT

The Nipissing sill at the Woods Creek property, also known as the Pond showing, is crosscut by the regional northeast-trending North Baldy fault and sulphide mineralization is hosted predominantly in shear and breccia zones. In this respect, it differs from most other Nipissing intrusive suite mineralized zones, which typically are contact, not shear zone hosted, deposits (e.g., Lightfoot and Naldrett 1996; Jobin-Bevans 2004, 2016).

Mineralization is exposed at the Main, Trevor, Raven's Cliff, Southern and Western contact showings and in several unnamed exposures (*see* Figure 16.1: numbers 8a to 8g) (Theyer 2005, 2007; Hart 2010a, 2010b). The Main and Trevor showings (*see* Figure 16.1: numbers 8a and 8b) as well as unnamed trenches (*see* Figure 16.1: numbers 8c, 8d and 8e) contain sulphide mineralization along shear zones, fractures and quartz veins (Photos 16.2C and 16.2D). Mineralized shear zones are strongly chloritized and trend north to east-northeast to west (Hart 2010a, 2010b). Sulphide-mineralization occurs in small patches, typically less than a metre wide, with 5 to 25% pyrrhotite and 3 to 5% chalcopyrite as blebs or disseminations and, less commonly, as semi-massive segregations (*see* Photos 16.2C and 16.2D). The host gabbro also contains metre-wide zones with up to 3% disseminated and blebby pyrrhotite and chalcopyrite. Reported values from the Main showing are 1.09 weight % Ni, 0.37 weight % Cu, 0.11 weight % Co and 301 ppb Pt+Pd (combined platinum and palladium) over 0.4 m and 0.20 weight % Cu, 0.17 weight % Ni and 132 ppb Pt+Pd over 0.9 m (Brady 2002; Theyer 2007).

The Raven's Cliff, Southern and Western contact showings (*see* Figure 16.1: numbers 8f, 8g and 8h) occur in breccia at the base of the sill. The breccia zones are 10 to 20 m thick and, in the case of the Raven's Cliff showing, at least 250 m long (Theyer 2005). Mineralization is hosted in the melagabbro breccia matrix and consists of up to 10% disseminated pyrrhotite with minor chalcopyrite and locally massive chalcopyrite and pyrrhotite pods (Photos 16.2E and 16.2F). Assay values from the Raven's Cliff showing are 0.90 weight % Cu, 0.66 weight % Ni, 0.09 weight % Co and 295 ppb Pt+Pd (Theyer 2005). The contact breccia at the Western showing is sheared, with a 3 m wide gossan in an altered breccia zone (Theyer 2005).

SUMMARY

As described herein, several critical mineral occurrences are documented in Hyman Township. Two areas in particular warrant further exploration. These include 1) the area south of the Birch Lake batholith–Huronian Supergroup contact, which is a target for yttrium, rare earth element and/or thorium mineralization; and 2) Nipissing sills in contact with major faults, such as the Pond showing, where nickel-copper-cobalt-PGE mineralization has been remobilized into shear zones.

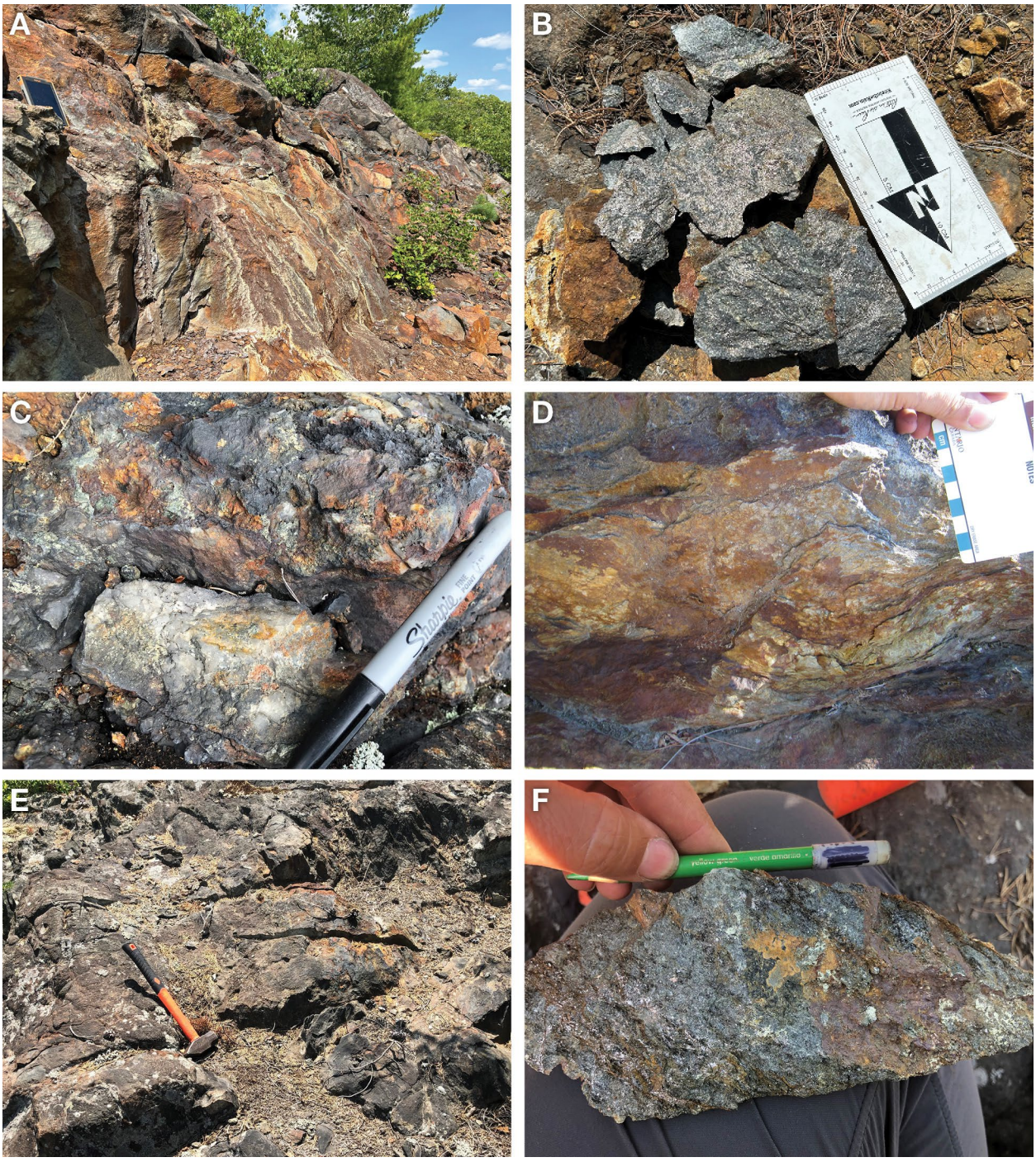


Photo 16.2. Photos of sulphide mineralized Nipissing gabbro. **A)** and **B)** Exposure of a 100 m long and 3 to 6 m wide gossan zone in melagabbro with disseminated to massive pyrrhotite and chalcopyrite, Keba and Buchy property (UTM 449300E 5134873N). **C)** Leucogabbro and intruded quartz vein containing disseminated to semi-massive chalcopyrite and pyrrhotite, unnamed showing, Wood Creek property (UTM 455078E 5140359N). **D)** Gossanous shear zone that crosscuts the Nipissing gabbro, Main showing, Woods Creek property. Shear zone is up to 1 m wide and contains disseminated pyrrhotite, pyrite and chalcopyrite (UTM 454552E 5140851N). **E)** and **F)** Polymictic breccia with disseminated pyrrhotite and chalcopyrite in melagabbro matrix, Raven's Cliff showing, Woods Creek property (UTM 455507E 5140484N). Objects used for scale: tablet is 20.5 cm long; black and white scale card is 15 cm long; marker pen is approximately 1.2 cm wide; colour scale card is 9 cm long; hammer is 40 cm long; colour pencil is 7 mm wide. All UTM co-ordinates are provided using NAD83 in Zone 17.

ACKNOWLEDGMENTS

The author would like to thank J. Courchesne, B. Gaudet, J. Gleason and E. Edwards for their assistance during the 2023 field season. R.M. Easton and M. Duguet (OGS) are thanked for their ongoing guidance on this project; and J.R.H. Creppin, J.E. Chartrand, K.H. Yeung, S.A. Evers, P. Gervais and J.F. Houle, for all the assistance with field work, equipment, databases, software logistics, sample preparation and drafting. Special thanks are extended to Atikameksheng Anishnawbek First Nation, Sagamok Anishnawbek First Nation and Whitefish River First Nation for allowing the Ontario Geological Survey to map their traditional land use area. Thanks are also extended to Vale Canada Limited, Magna Mining Inc. and Skead Holdings Ltd. for permission to access properties, and for all support that has been provided.

REFERENCES

Bennett, G.B., Dressler, B.O. and Robertson, J.A. 1991. The Huronian Supergroup and associated intrusive rocks; Chapter 14 *in* Geology of Ontario, Ontario Geological Survey, Special Volume 4, Part 1, p.549-591.

Bleeker, W., Kamo, S.L., Ames, D.E. and Davis, D. 2015. New field observations and U-Pb ages in the Sudbury area: Toward a detailed cross-section through the deformed Sudbury Structure; *in* Targeted Geoscience Initiative 4: Canadian Nickel-Copper-Platinum Group Elements-Chromium Ore Systems – Fertility, Pathfinders, New and Revised Models, Geological Survey of Canada, Open File 7856, p.151-156.

Brady, J.G. 2002. Report on diamond drill program, Woods Creek project, Hyman Township, DDH log WC-A, DDH log WC-B and DDH log WC-C, prepared for Namex Exploration Inc.; unpublished report, Sudbury Resident Geologist's office, assessment file AFRO#2.24669 AFRI# 41I05NE2008, 25p.

Card, K.D. 1965. Geology of Hyman and Drury townships, District of Sudbury; Ontario Department of Mines, Geological Report 34, 38p.

——— 1978a. Geology of the Sudbury–Manitoulin area; Ontario Department of Mines, Report 166, 238p.

——— 1978b. Metamorphism of the Middle Precambrian (Aphebian) rocks of the eastern Southern Province; *in* Metamorphism in the Canadian Shield; Geological Survey of Canada, Paper 78-10, p.269-282.

Card, K.D., Gupta, V.K., McGrath, P.H. and Grant, F.S. 1984. The Sudbury Structure: Its regional geological and geophysical setting; *in* The Geology and Ore Deposits of the Sudbury Structure, Ontario Geological Survey, Special Volume 1, p.25-43.

Carrington, J.K. and Wilton, C.K. 1969. Economic geology of Agnew Lake Mines, To be presented at the Annual Convention, Canadian Institute of Mining and Metallurgy, April 21–23, 1969, for Agnew Lake Mines Ltd. and Kerr Addison Mines Ltd.; unpublished report, Sudbury Resident Geologist's office, assessment file AFRO# Hyman 31C1 AFRI# 41I05NE0060, 21p.

Corfu, F. and Andrews, A.J. 1986. A U–Pb age for mineralized Nipissing diabase, Gowganda; Canadian Journal of Earth Sciences, v.23, p.107-109.

Davey, S., Bleeker, W., Kamo, S.L., Davis, D.W., Easton, R.M. and Sutcliffe, R.H. 2019. Ni-Cu-PGE potential of the Nipissing sills as part of the ca. 2.2 Ga Ungava large igneous province; *in* Targeted Geoscience Initiative: 2018 Report of Activities; Geological Survey of Canada, Open File 8549, p.403-419.

Dietz, R.S. 1964. Sudbury Structure as an astrobleme; Journal of Geology, v.72, p.412-434.

Easton, R.M. 2006a. Precambrian geology, Porter and Vernon townships; Ontario Geological Survey, Preliminary Map P.2845, scale 1:20 000.

——— 2006b. Geological, geochemical and geophysical data from the Porter and Vernon townships area, Southern Province; Ontario Geological Survey, Miscellaneous Release—Data 197.

Fralick, P. and Miall, A. 1989. Sedimentology of the lower Huronian Supergroup (early Proterozoic), Elliot Lake area, Ontario, Canada; Sedimentary Geology, v.63, p.127-153.

Gordon, C.A. 2022. Preliminary geology of Hyman Township, Southern and Superior provinces, Sudbury District, northeastern Ontario; *in* Summary of Field Work and Other Activities, 2022, Ontario Geological Survey, Open File Report 6390, p.13-1 to 13-10.

Hart, T.R. 2010a. Woods Creek property, 2010 exploration program, Hyman Township, Ontario, prepared for D. Beilhartz and J.G. Brady; unpublished report, Sudbury Resident Geologist's office, assessment file AFRO# 2.46332 AFRI# 20000005627, 25p.

——— 2010b. Assessment work report with assays, Woods Creek property, Hyman Township, Ontario, prepared for J. Brady and D. Beilhartz; unpublished report, Sudbury Resident Geologist's office, assessment file AFRO# 2.47175 AFRI# 20000006515, 21p.

Heaman, L.M. 1997. Global mafic magmatism at 2.45 Ga: Remnants of an ancient large igneous province?; Geology, v.25, p.299-302.

International Atomic Energy Agency 2022. Near term and promising long term options for the deployment of thorium based nuclear energy. Final report of a coordinated research project; International Atomic Energy Agency, Technical Document Series, Vienna, Austria, IAEA-TECDOC-2009, 161p.

Jackson, S.L. 2001. On the structural geology of the Southern Province between Sault Ste. Marie and Espanola, Ontario; Ontario Geological Survey, Open File Report 5995, 55p.

Jobin-Bevans, L.S. 2004. Platinum-group element mineralization in Nipissing gabbro intrusions and the River Valley intrusion, Sudbury region, Ontario; unpublished PhD thesis, University of Western Ontario, London, Ontario, 572p.

——— 2016. Geochemical data related to a study of platinum group element mineralization in Nipissing gabbro intrusions and the River Valley intrusion, Sudbury region, Southern Province; Ontario Geological Survey, Miscellaneous Release—Data 336.

Kamo, S.L. 2006. Report on U-Pb geochronological data from the southern Abitibi Subprovince, Bannockburn–Montrose and Vernon townships, and the Grenville Front region, Thistle–Sisk townships, Ontario; internal U/Pb age report prepared for the Ontario Geological Survey, Jack Satterly Geochronology Laboratory, Department of Geology, University of Toronto, Toronto, Ontario, 20p.

——— 2023. Report on U-Pb ID-TIMS geochronology for the Ontario Geological Survey: Bedrock Mapping Projects, Ontario 2022-2023; internal U/Pb age report for the Ontario Geological Survey, Jack Satterly Geochronology Laboratory, Department of Geology, University of Toronto, Toronto, Ontario, 22p.

Komarechka, R.G. 2012. HPU property, 2012 stripping property, Hyman Township, prepared for GTO Resources Inc.; unpublished report, Sudbury Resident Geologist's office, assessment file AFRO# 2.53099 AFRI# 20000007835, 38p.

Krogh, T.E., Corfu, F., Davis, D.W., Dunning, G.R., Heaman, L.M., Kamo, S.L., Machado, N., Greenough, J.D. and Nakamura, E. 1987. Precise U-Pb isotope ages of diabase dykes and mafic to ultramafic rocks using trace amounts of baddeleyite and zircon; *in* Mafic Dyke Swarms, Geological Association of Canada, Special Paper 34, p.147-152.

Krogh, T.E., Davis, D.W. and Corfu, F. 1984. Precise U-Pb zircon and baddeleyite ages for the Sudbury area; *in* The Geology and Ore Deposits of the Sudbury Structure; Ontario Geological Survey, Special Volume 1, p.431-446.

Lacombe, P.G. 1968. Report on Richore Gold Mines Limited Agnew Lake, Ontario, property, radiometric survey, prepared for Richore Gold Mines Limited; unpublished report, Sudbury Resident Geologist's office, part of assessment file AFRO# 0029 AFRI# 41I05NE0082, p.27-34.

——— 1970. Report on bulk sampling, Richore Gold Mines Limited, northern claim group, Hyman Township, Ontario; unpublished report, Sudbury Resident Geologist's office, assessment file AFRI# 41I05NE0052, 18p.

Lapierre, K. 2002. Report on the Hyman property, Hyman/Nairn townships, Sudbury, Ontario, prepared for Mustang Minerals Corp.; unpublished report, Sudbury Resident Geologist's office, assessment file AFRO# 2.24458 AFRI # 41I05NE2006, 39p.

Lightfoot, P.C. and Naldrett, A.J. 1996. Petrology and geochemistry of the Nipissing gabbro: Exploration strategies for nickel, copper and platinum group elements in a large igneous province; Ontario Geological Survey, Study 58, 80p.

Moody, G.E. 1967. Geological report, East Bay Mines Ltd., Hyman Township, Ontario; unpublished report, Sudbury Resident Geologist's office, assessment file AFRO# 63.2176 AFRI# 41I05NE0083, p.1-10.

Ontario 2022. Ontario's Critical Mineral Strategy: Unlocking the potential to drive economic recovery and prosperity; Ministry of Northern Development, Mines, Natural Resources and Forestry, 53p., www.ontario.ca/page/ontarios-critical-minerals-strategy-2022-2027-unlocking-potential-drive-economic-recovery-prosperity, also available to download: select "Download English PDF". [accessed October 16, 2023]

Ontario Geological Survey 2023a. Ontario Mineral Inventory; Ontario Geological Survey, online database, September 2023 update, www.hub.geologyontario.mines.gov.on.ca. [accessed September 20, 2023]

——— 2023b. OMI Definitions and cut-off values; document *in* Ontario Mineral Inventory, Ontario Geological Survey, online database, April 2023 update, 9p., www.geologyontario.mndm.gov.on.ca/ogsearth.html#mineral-inventory. [accessed September 20, 2023]

Papapavlou, K., Darling, J.R., Storey, C.D., Lightfoot, P.C., Moser, D.E. and Lasalle, S. 2017. Dating shear zones with plastically deformed titanite: New insights into the orogenic evolution of the Sudbury impact structure (Ontario, Canada); Precambrian Research, v.291, p.220-235.

Robertson, J.A. 1976. The Blind River uranium deposits: The ores and their setting; Ontario Division of Mines, Report 147, 73p.

Robertson, J.A., Card, K.D. and Frarey, M.J. 1969. The federal–provincial committee on Huronian stratigraphy progress report; Ontario Department of Mines, Miscellaneous Paper 31, 26p.

Robertson, J.A. and Gould, K.L. 1983. Uranium and thorium deposits of northern Ontario; Ontario Geological Survey, Mineral Deposits Circular 25, 152p.

Sproule, R.A., Sutcliffe, R., Tracanelli, H. and Lesher, C.M. 2007. Palaeoproterozoic Ni-Cu-PGE mineralisation in the Shakespeare intrusion, Ontario, Canada: A new style of Nipissing gabbro-hosted mineralisation; Applied Earth Science, Institute of Mining and Metallurgy, Transactions, Section B, v.116, no.4, p.188-200.

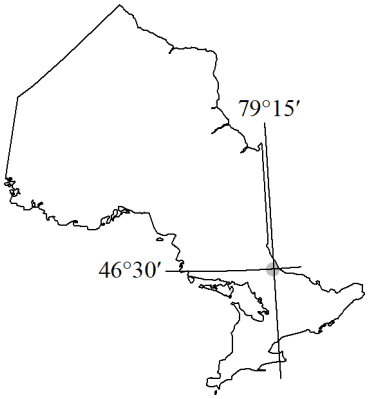
Theyer, P. 2005. Report on the results of a geological survey of the Woods Creek property, Hyman Twp., Ontario, prepared for Namex Explorations Inc.; unpublished report, Sudbury Resident Geologist's office, assessment file AFRO# 2.30689 AFRI# 20000000732, 24p.

——— 2007. Report on the results of a geological survey of the Woods Creek property, Hyman Twp., Ontario, prepared for Namex Explorations Inc.; unpublished report, Sudbury Resident Geologist's office, assessment file AFRO# 2.35217 AFRI# 20000002211, 21p.

Thomson, J.E. 1960. Uranium and thorium deposits at the base of the Huronian system in the District of Sudbury; Ontario Department of Mines, Geological Report 1, 54p.

Tracanelli, H.J. and MacMillan, D. 2006. Report of work 2005, surface diamond drilling and trenching program, Agnew Lake uranium mine property, prepared for Ursa Major Minerals Inc.; unpublished report, Sudbury Resident Geologist's office, assessment file AFRO# 2.33980 AFRI# 20000001904, 207p.

17. Project NE-22-004. Geochronological Study of a Saprolite Atop the Grenvillian Mulock Pluton near Redbridge, Northeastern Ontario



R.M. Easton[1], A.S. Marich[1] and C.J. Wall[2]

[1]Earth Resources and Geoscience Mapping Section, Ontario Geological Survey, Sudbury, Ontario P3E 6B5
[2]Pacific Centre for Isotopic and Geochemical Research, University of British Columbia, Vancouver, British Columbia V6T 1Z4

INTRODUCTION

During the course of reconnaissance mapping of the Quaternary geology of the Lake Nipissing Basin east of North Bay in 2022, an unconsolidated deposit sitting atop Precambrian basement was identified near the community of Redbridge (Marich 2022; Marich, this volume). To determine if this deposit was a regolith (loose unconsolidated rock and dust) or a saprolite (a soft, clay-rich, decomposed rock formed in place by chemical weathering), a sample of the unconsolidated material was collected for detrital zircon study. The reasoning behind this sampling approach was that a regolith would likely have a diverse detrital zircon population, whereas a saprolite would have a uniform detrital zircon reflecting the host rock. As detailed below, the detrital zircon results indicate that the deposit is indeed a saprolite.

SAMPLE DESCRIPTION

The sample site is located on the east side of North River Road, just south of the junction with Pioneer Road, approximately 2.1 km north of Highway 63 in Redbridge (UTM 635168E 5142052N, North American Datum 1983 (NAD83), Zone 17) (Figure 17.1). The sample is a reddish, coarse-grained unconsolidated deposit derived from weathered Precambrian gneissic bedrock (Photos 17.1A, 17.1B and 17.1C). The material is exposed at surface with very little (<10 cm) podzol soil cover (*see* Photo 17.1A). The bedrock units are part of the Tomiko terrane of the Grenville Province (Easton 1992). Based on existing geological maps (Lumbers 1971; Easton 2006a), the bedrock could be composed of either heterogeneous, quartzofeldspathic migmatitic gneiss or gneissic granite of the Mulock granite intrusion emplaced at *circa* 1250 Ma (*see* Figure 17.1). Evidence of horizontal banding is clear at outcrop scale (*see* Photo 17.1B). Previous U/Pb thermal ionization mass spectrometry (TIMS) upper intercept zircon ages on the Mulock granite from 2 different sample sites are $1244\ ^{+4}/_{-3}$ (Lumbers et al. 1991) and 1258±15 Ma (Davidson and van Breemen 2001), respectively. These sample sites are located approximately 19 km and 21 km, respectively, northwest of the sample site under study (*see* Figure 17.1).

Summary of Field Work and Other Activities, 2023,
Ontario Geological Survey, Open File Report 6405, p.17-1 to 17-7.

© King's Printer for Ontario, 2023

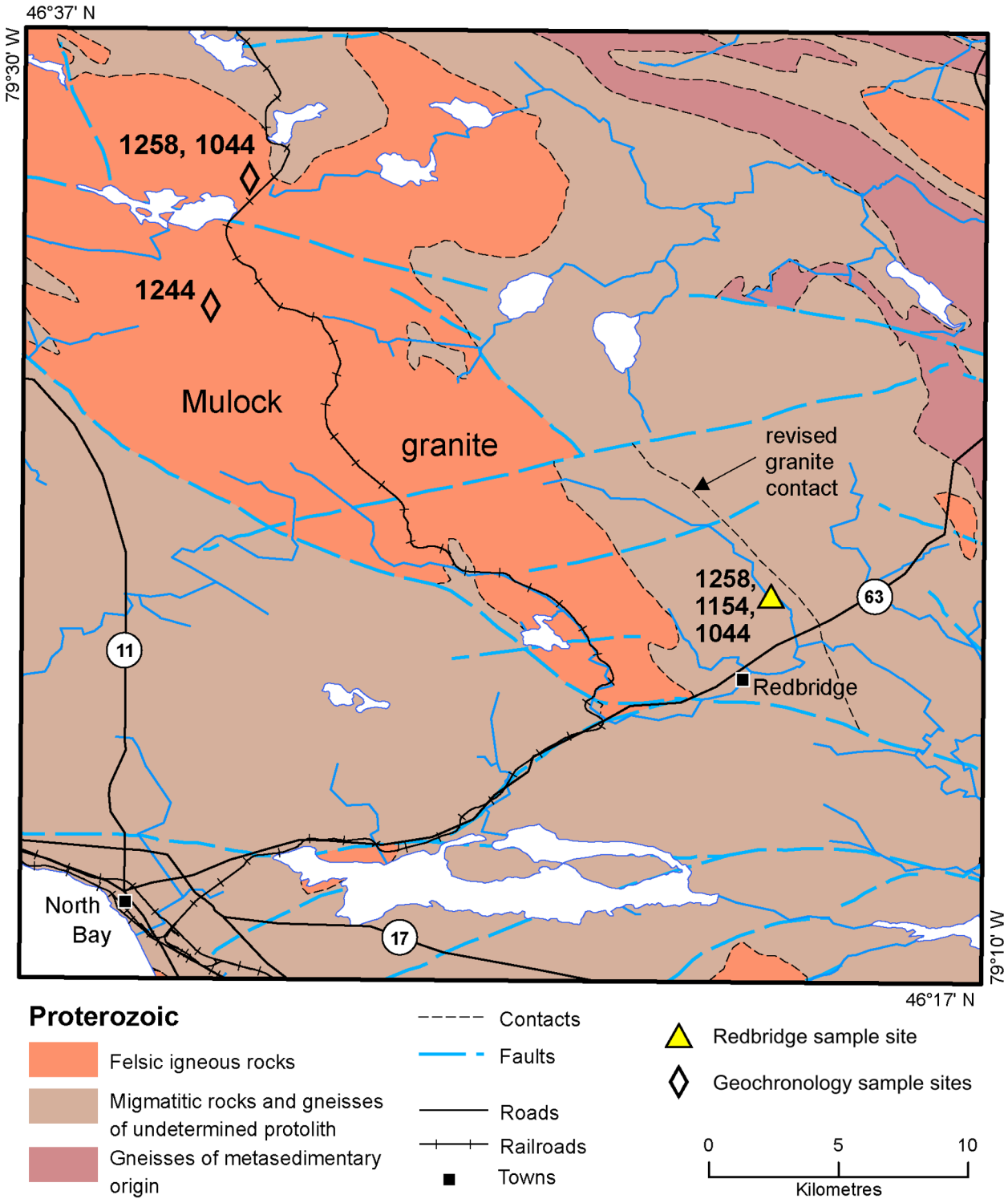


Figure 17.1. Simplified geological map of the Redbridge area showing the Mulock granite, the location of previous geochronology sample sites in the Mulock granite, and the location of the Redbridge saprolite from this study. The revised eastern contact of the Mulock granite near Redbridge is based on examination of the aeromagnetic data for the area (Ontario Geological Survey 1999), as well as the results of this study. Geology is *modified from* Ontario Geological Survey (2011).

METHODS

The sample was crushed and ground, followed by water-table, heavy-liquid and magnetic separation, at the Pacific Centre for Isotopic and Geochemical Research at the University of British Columbia. An abundant population of relatively large (~100–150 µm in long dimension), elongate, prismatic zircon crystals was separated from the sample by conventional density and magnetic methods. The entire zircon separate was placed in a muffle furnace at 900°C for 60 hours in quartz beakers to anneal minor radiation damage. Annealing enhances cathodoluminescence emission (Nasdala et al. 2002) and promotes more reproducible inter-element fractionation during laser ablation inductively coupled plasma mass spectrometry (LA-ICP–MS) (Allen and Campbell 2012). Following annealing, individual grains from all samples were hand picked under magnification based on morphology, clarity and the absence of inclusions. Then these grains were mounted in epoxy for imaging for internal structure at the University of British Columbia, using a Philips XL-30 field emission scanning electron microscope (SEM). Zircon grains were imaged using a Robinson™ cathodoluminescence detector, using a Bruker QUANTAX 200 energy-dispersive X-ray microanalysis system with XFlash® 6010 SDD detector at a voltage of 15 kV.

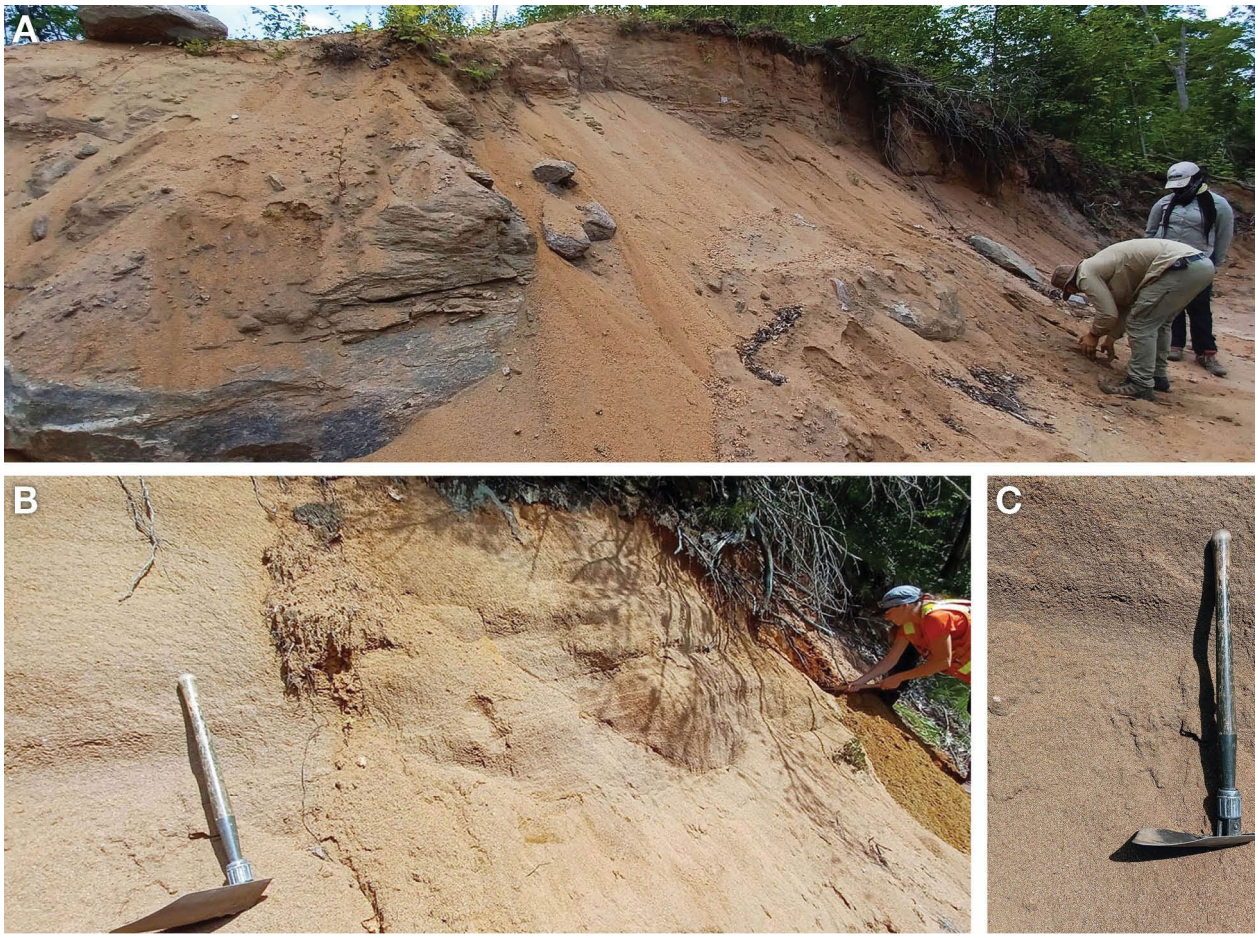


Photo 17.1. A) Wide-view of the sample site showing partly weathered rock in the lower left corner overlain by red-brown saprolite. **B)** The sample site showing the thickness and uniformity of the saprolite unit at the sample locality. **C)** Close-up view of the saprolite at the sample site. Shovel handle is 50 cm long. Site is located on the east side of North River Road north of Redbridge (UTM 635168E 5142052N, NAD83, Zone 17).

Trace element concentrations were determined in zircon and rutile by LA-ICP–MS at the Pacific Centre for Isotopic and Geochemical Research using a Resonetics (now Applied Spectra Incorporated) RESOlution M-50-LR Class I laser ablation system coupled to an Agilent Technologies 7700x quadrupole ICP–MS. Ablations were carried out with the 193 nm excimer laser, using a beam energy of 100 mJ and a pit diameter of 34 μm, with a pulse rate of 5 Hz for a duration of 30 seconds followed by 20 seconds of gas blank. Spots were chosen based on grain-scale variation observed in cathodoluminescence images and grain size, with typically 2 analyses per grain. For zircon, measurements were conducted on the masses ^{7}Li, ^{29}Si, ^{31}P, ^{45}Sc, ^{49}Ti, ^{89}Y, ^{91}Zr, ^{93}Nb, ^{139}La, ^{140}Ce, ^{141}Pr, ^{146}Nd, ^{147}Sm, ^{153}Eu, ^{157}Gd, ^{159}Tb, ^{163}Dy, ^{165}Ho, ^{166}Er, ^{169}Tm, ^{172}Yb, ^{175}Lu, ^{177}Hf, ^{188}Ta, ^{202}Hg (as a monitor for Pb), Pb (^{204}Pb, ^{206}Pb, ^{207}Pb, ^{208}Pb), ^{232}Th and U (^{235}U and ^{238}U). These masses were chosen based on high relative isotopic abundances and the absence of interferences. Sample-standard bracketing was carried out with spot analyses of synthetic glasses NIST 612 and NIST 610 between zircon analyses and the natural zircon reference materials 91500, Plesovice and Temora2.

Data were reduced using Iolite 4 software running within the WaveMetrics Igor Pro environment using the Trace Elements IS data reduction scheme (Paton et al. 2011). For zircon, NIST 612 was used as the standard and the average zirconium contents (by sample) determined by electron probe microanalysis were employed as an internal standard value for the unknowns. All concentrations were reported in parts per million with uncertainties of 2 standard deviations.

RESULTS

A total of 120 zircon grains were analyzed, with peaks present at *circa* 1045 Ma, 1174 Ma and 1253 Ma, with the peak at 1253 Ma being dominant (Figure 17.2). Of the 120 grains, 2 were greater than 20% discordant and not included in the totals presented in Table 17.1. Of the remaining 118 grains, 77 were ≤5% discordant (*see* Table 17.1). Little change in the peak positions occurs if only the grains that are ≤5% discordant are used (*see* Table 17.1).

A smaller peak at *circa* 1174 Ma likely reflects a previously undocumented metamorphic event in Tomiko terrane (*see* Table 17.1). Both the *circa* 1045 and 1170 Ma zircons have low Th/U contents of 0.06 and 0.15, respectively, with low Th/U being typical of metamorphic zircons. The age of *circa* 1174 Ma could be related to the M_1 metamorphic event of unknown age noted by Easton (2006b) and is similar to the Rb/Sr errorchron age of 1137±173 Ma obtained from the Jocko (Timberlake) pluton in western Tomiko terrane by Baer (1980). Five zircons have slightly older ^{206}Pb/^{235}U ages of 1299 to 1333 Ma and may represent grains inherited from an unknown source; only one of these 5 grains is ≤5% discordant.

Because of the uniformity of these data, and the fact that many grains were less than 1% discordant, an improved age for the Mulock granite can be obtained from this sample. Using the most concordant data only (≤1% discordant), mean ^{206}Pb/^{235}U ages with 2 sigma errors of 1047±43 Ma (n=5), 1154±50 Ma (n=2) and 1259±55 Ma (n=22) are obtained (*see* Table 17.1). Corresponding ^{207}Pb/^{206}Pb ages are 1049±90, 1152±87 and 1256±114 Ma, respectively (*see* Table 17.1).

IsoplotR (Versmeech 2018) yields a weighted mean U/Pb age of 1044±12 Ma (n=5, MSWD 1.0) for the 5 most concordant metamorphic grains using the ^{235}U decay constant of Schoene et al. (2006). Using the ^{235}U decay constant of Jaffey et al. (1971) gives an age of 1039±7 (n=5, MSWD 0.5) for the same data. The age of 1044±12 Ma is similar to the U/Pb TIMS age of M_2 metamorphism (1047±3 Ma) in Tomiko terrane reported by Easton (2006b), and the lower intercept age of 1044 $^{+126}/_{-152}$ Ma from the Mulock granite by Davidson and van Breemen (2001), both of which used the decay constants of Jaffey et al. (1971).

Table 17.1. Summary of U/Pb ages for the saprolite formed atop the Mulock granite. Data were obtained from the Pacific Centre for Isotopic and Geochemical Research at the University of British Columbia, Vancouver, British Columbia.

Th/U	$^{206}Pb/^{235}U$ Age (mean) (Ma)	Error (Ma)	$^{207}Pb/^{238}U$ Age (mean) (Ma)	Error (Ma)	$^{207}Pb/^{206}Pb$ Age (mean) (Ma)	Error (Ma)	Number of Grains
all data (n=118)*							
0.38	1306	62	1255	25	1373	132	9
0.41	1253	57	1257	25	1236	121	90
0.15	1174	57	1202	32	1108	121	8
0.05	1045	44	1049	15	1032	90	11
≤5% disc (n=77)							
0.44	1291	69	1273	30	1300	163	1
0.40	1258	56	1256	24	1252	118	62
0.12	1150	51	1150	23	1137	100	4
0.05	1046	44	1049	15	1038	90	10
≤1% disc (n=29)							
0.39	1259	55	1255	23	1256	114	22
0.15	1154	50	1150	22	1152	87	2
0.06	1047	43	1047	14	1049	90	5

**Total in table excludes 2 grains that were >20% discordant. All errors are 2 sigma.*
***Abbreviations**: disc, discordant; Ma, million years.*

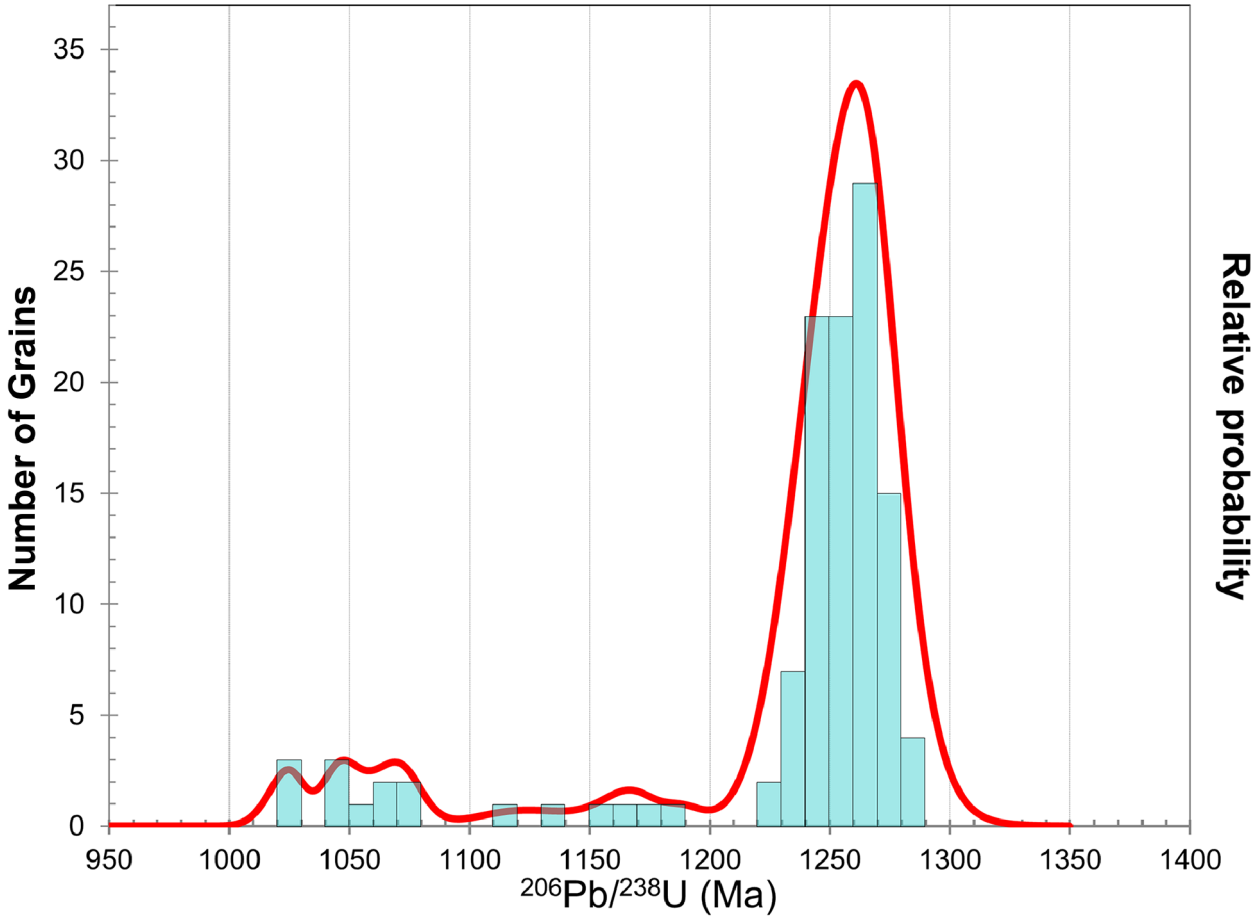


Figure 17.2. Histogram of ages for all zircons from the Redbridge saprolite sample (n=120). The prominent peak centred at *circa* 1258 Ma corresponds to the previously determined age of the Mulock granite (Davidson and van Breemen 2001).

Similarly, for the main population, a weighted mean U/Pb age of 1258±6 Ma (n=21, MSWD 0.97) is obtained for the most concordant data using the ^{235}U decay constant of Schoene et al. (2006). Using the ^{235}U decay constant of Jaffey et al. (1971) gives an age of 1240±9 Ma (n=21, MSWD 0.46). The age using the ^{235}U decay constant of Schoene et al. (2006) is almost identical to the age of 1258±15 Ma for the Mulock granite reported by Davidson and van Breemen (2001), but with somewhat improved errors. The U/Pb TIMS upper intercept zircon age reported by Davidson and van Breemen (2001) used the decay constants of Jaffey et al. (1971).

DISCUSSION

The uniform detrital zircon population of the sample and the reported ages (*see* Table 17.1) are consistent with the sampled unit being a saprolite developed atop the Mulock granite. The new data also suggest that the contact of the Mulock granite with its host migmatitic gneiss is located 3 to 4 km farther east than previously shown on existing geological maps of the area (Lumbers 1971; Easton 2006a) (*see* Figure 17.1).

ACKNOWLEDGMENTS

A.S. Marich would like to extend her thanks to J.R.H. Creppin, G.W. Hagedorn and R.P.M. Mulligan of the OGS Earth Resources and Geoscience Mapping Section (ERGMS) for field assistance and sample collection. J.E. Chartrand (ERGMS) prepared Figure 17.1; subsequently, P. Gervais (ERGMS) prepared both figures and photographs for publication.

REFERENCES

Allen, C.M. and Campbell, I.H. 2012. Identification and elimination of a matrix-induced systematic error in LA-ICP-MS $^{206}Pb/^{238}U$ dating of zircon; Chemical Geology, v.332-333, p.157-165. doi:10.1016/j.chemgeo.2012.09.038

Baer, A.J. 1980. Foliated and recrystallized granites from the Timberlake Pluton, Ontario; *in* Current Research, Part C, Geological Survey of Canada, Paper 80-1C, p.201-205.

Davidson, A. and van Breemen, O. 2001. Mid-Mesoproterozoic granitoid rocks in the North Bay area, Grenville Province, Ontario; *in* Radiogenic age and isotopic studies 14, Geological Survey of Canada, Current Research, Paper 2001-F8, 15p.

Easton, R.M. 1992. The Grenville Province; Chapter 19 *in* Geology of Ontario, Ontario Geological Survey, Special Volume 4, Part 2, p.713-904.

——— 2006a. Geology of the Songris area; Ontario Geological Survey, Preliminary Map P.2847, scale 1:50 000.

——— 2006b. Geology and mineral potential of the eastern Tomiko terrane, Grenville Province; Ontario Geological Survey, Open File Report 5554, 117p.

Jaffey, A.H., Flynn, K.F., Glendenin, L.E., Bentley, W.C. and Essling, A.M. 1971. Precision measurement of half-lives and specific activities of ^{235}U and ^{238}U; Physical Review, Part C, v.4, p.1889-1906.

Lumbers, S.B. 1971. North Bay area, Nipissing and Parry Sound districts; Ontario Department of Mines, Map 2216, scale 1:126 720.

Lumbers, S.B., Wu, T-W., Heaman, L.M., Vertolli, V.M. and MacRae, N.D. 1991. Petrology and age of the A-type Mulock granite batholith, northern Grenville Province, Ontario; Precambrian Research, v.53, p.199-231.

Marich, A.S. 2022. Quaternary geological mapping of the Lake Nipissing Basin, Highway 17 corridor, northeastern Ontario; *in* Summary of Field Work and Other Activities, 2022, Ontario Geological Survey, Open File Report 6390, p.17-1 to 17-9.

Nasdala, L., Lengauer, C.L., Hanchar, J.M., Kronz, A., Wirth, R., Blanc, P., Kennedy, A.K. and Seydoux-Guillaume, A.M. 2002. Annealing radiation damage and the recovery of cathodoluminescence; Chemical Geology, v.191, p.121-140.

Ontario Geological Survey 1999. Single master gravity and aeromagnetic data for Ontario; Ontario Geological Survey, Geophysical Data Set 1035.

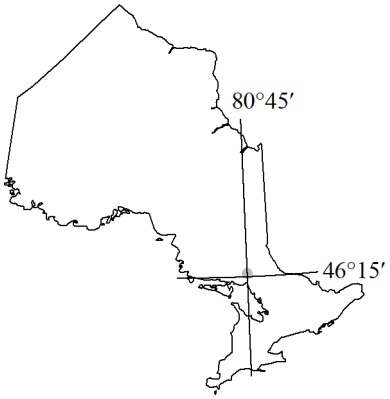
——— 2011. 1:250 000 scale bedrock geology of Ontario; Ontario Geological Survey, Miscellaneous Release—Data 126 – Revision 1.

Paton, C., Hellstrom, J., Paul, B., Woodhead, J. and Hergt, J. 2011. Iolite: Freeware for the visualisation and processing of mass spectrometric data; Journal of Analytical Atomic Spectrometry, v.26, p.2508-2518.

Schoene, B., Crowley, J.C., Condon, D.J., Schmitz, M.D. and Bowring, S.A. 2006. Reassessing the uranium decay constants for geochronology using ID-TIMS U–Pb data; Geochimica et Cosmochimica Acta, v.70, p.426-445.

Versmeech, P. 2018. IsoplotR: A free and open toolbox for geochronology; Geoscience Frontiers, v.9, p.1479-1493. doi: 10.1016/j.gsf.2018.04.001

18. Project SO-22-003. Geology of the Grenville Front Tectonic Zone Near Sudbury, Northeastern Ontario: An Update



R.M. Easton[1]

[1]Earth Resources and Geoscience Mapping Section, Ontario Geological Survey

INTRODUCTION

To fill information gaps on the 1:50 000 geological compilation map of the Sudbury area of Ames et al. (2005), a mapping project, focussing on the area around Wanup, Ontario (Figure 18.1), was initiated by the author in September 2021 (Easton 2022a, 2022b, 2023a, 2023b). Access to this study area is provided by Highways 69 and 537, Estaire Road (old Highway 69) and several local roads. The study area includes the communities of Wanup, Estaire and Wahnapitae.

Much of the study area lies within the Grenville Front tectonic zone (GFTZ), a region up to 30 km wide present between the Grenville Front and the Central Gneiss Belt of the Grenville Province (*see* Figure 18.1) (Easton 1992). A key question for this project is to determine if rocks of the Huronian Supergroup and/or Nipissing gabbros are present in the GFTZ. If they are, then the rocks in the GFTZ should be prospective for the same commodities as their counterparts in the Southern Province (especially nickel-copper-platinum group elements (PGE) in the Nipissing gabbros). If not, then what is the origin and exploration potential of the rocks in the GFTZ? This article focusses on these questions, as well as providing an update on the latest results from the project. The reader is referred to Easton (2022b, 2023b) for more detailed geological summaries of the study area and geochemical results.

RESULTS HIGHLIGHTS

Protolith of Rocks within the Grenville Front Tectonic Zone

Understanding the original source rock package(s) is important for determining its economic potential. Rock packages that are multi-deformed and multi-metamorphosed are no exception, although the identification process is more complicated. Prior work in the study area has suggested that rocks in the GFTZ include metasedimentary rocks of the Huronian Supergroup, Nipissing gabbro intrusions (*circa* 2216 Ma), and Killarney Magmatic Belt felsic intrusions (*circa* 1740 and 1450 Ma) (e.g., Dressler 1984).

As described in detail in Easton (2022b), a linear, north-northwest-trending structure almost coincident with the Wanapitei River divides the study area into 2 parts. East of the Wanapitei River, host gneisses are mostly quartzofeldspathic and contain garnet in both melasome and leucosome. Furthermore, several large ovoid plutonic bodies are present, likely related to the Killarney Magmatic Belt (*circa* 1740 Ma), including the Wanapitei Complex (6 by 2 km) and the Cleland stock (3 by 3 km) (*see* Figure 18.1). East Bull Lake intrusive suite rocks former larger, more continuous, and better-preserved bodies, including the Red Deer Lake intrusion (11 km long, up to 1 km wide). West of the Wanapitei River, the

Summary of Field Work and Other Activities, 2023,
Ontario Geological Survey, Open File Report 6405, p.18-1 to 18-7.

© King's Printer for Ontario, 2023

GFTZ is only 8 km wide, and rock units consist mainly of highly strained grey gneisses, typically migmatitic, that form thin, near-continuous belts interlayered with migmatitic amphibolite, amphibolite and garnet amphibolite. These grey gneisses could represent highly strained Archean bedrock. Possible metasedimentary units, including schists with aluminosilicate minerals locally form thin, lenticular, discontinuous bands in the package of highly strained gneissic and amphibolitic rocks. Rocks of the

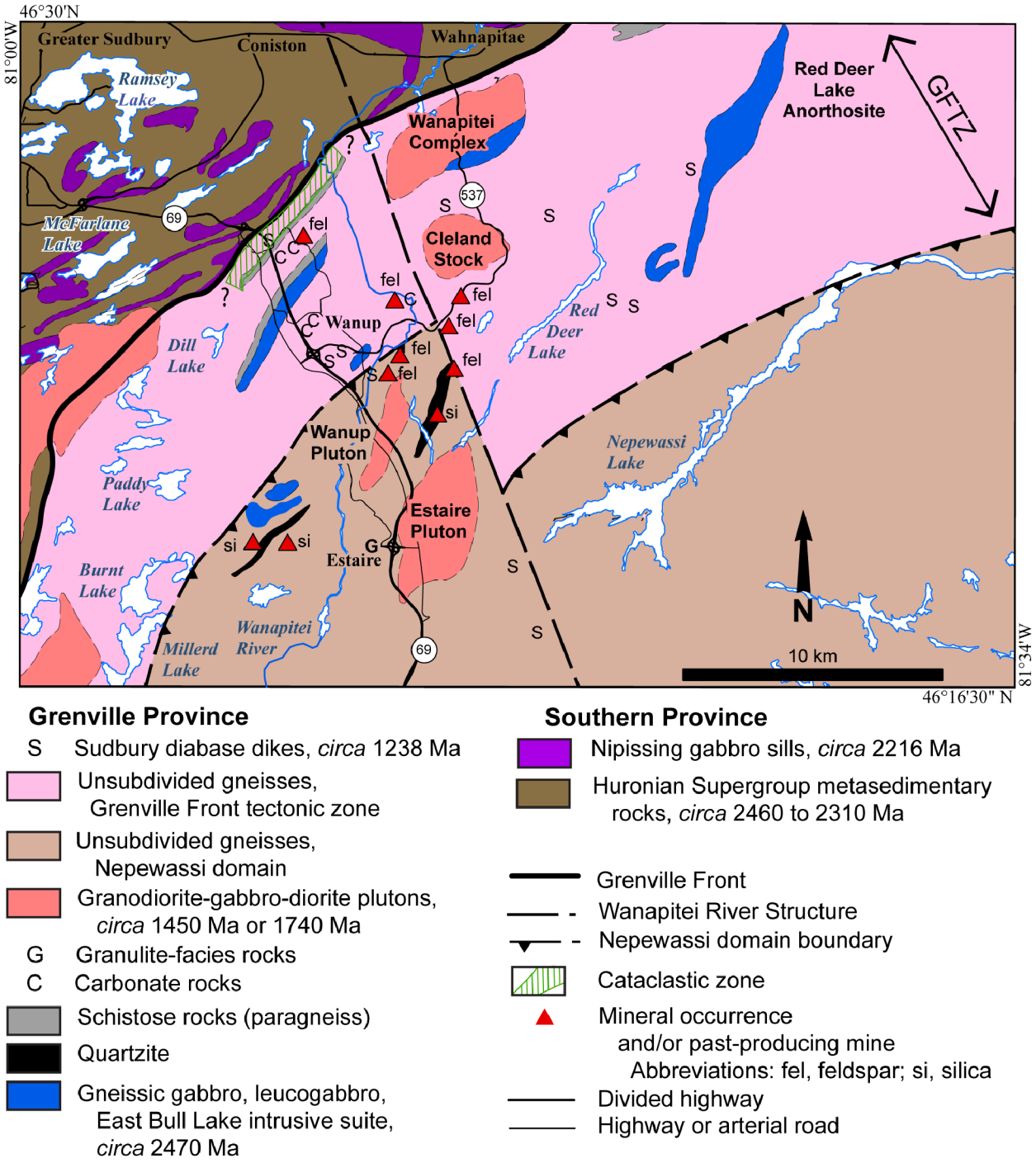


Figure 18.1. Simplified geology of the Wanup study area, showing major geological features, the newly recognized fluorine-rich cataclastic zone, industrial mineral occurrences and geological features discussed in the text (*modified from* Easton 2022b). The western and eastern extent of the cataclastic zone, represented by question marks, remains to be established. Abbreviation: GFTZ, Grenville Front tectonic zone.

East Bull Lake intrusive suite (*circa* 2475 Ma) are present and form thin, discontinuous units. Sudbury swarm (*circa* 1240 Ma) mafic dikes are large, with strike lengths of 50 to 100 m, but are discontinuous (*see* Figure 18.1). This article focusses primarily on rocks west of the Wanapitei River.

To the south, the GFTZ has been overthrust by the Nepewassi domain that contains Killarney Magmatic Belt plutons, some of which are metamorphosed at granulite facies, and lenticular belts of quartzite (*see* Figure 18.1; Easton 2014, 2022b). In the hanging wall of the Grenville Front, the lowermost 1 km has undergone late-stage cataclasis after the peak of high-grade metamorphism (hereafter referred to as the cataclastic zone). Structurally above the cataclastic zone, and south to the boundary with the Nepewassi domain, the GFTZ is characterized by numerous lenticular, anastomosing, compositionally varied, belts of highly strained gneiss that dip moderately (45–65°) to the southeast.

At present, only approximately 30% of the gneissic rocks in the GFTZ have been characterized with respect to possible protolith (Easton 2023a). Identifiable units include East Bull Lake suite mafic intrusions (platinum group element-copper potential) (*see* Easton 2022b), biotite-garnet-muscovite ± staurolite schists geochemically similar to the McKim Formation (*see* Easton 2022b), medium-grained felsites that are similar geochemically to Copper Cliff Formation rhyolites (*see* Easton 2023b), amphibolites that may be Huronian Supergroup mafic flows, and Archean tonalite gneisses. Notably absent from the GFTZ are the major Huronian Supergroup quartzite units (Matinenda, Mississagi, Serpent and/or Lorrain formations), even though rock units belonging to the Elliot Lake Group (McKim Formation, mafic and felsic volcanic rocks) appear to be present. Also absent from the GFTZ, despite their abundance and proximity to the north in the Southern Province (Bennett, Dressler and Robertson 1991; Easton 1992), are Nipissing gabbro intrusions and, to the west of the Wanapitei River, Killarney Magmatic Belt plutons.

One explanation for the absence of the main Huronian Supergroup quartzite units from the GFTZ and the Nepewassi domain is that the Southern Province does not represent a rifted passive margin sequence (e.g., Bennett, Dressler and Robertson 1991; Roscoe and Card 1992; Young et al. 2001), but rather, it was deposited in a rift-and-sag basin in an intracratonic setting (e.g., Bleeker and Kamo 2022; Bleeker et al., this volume). In the intracratonic basin setting, the Huronian Supergroup would be relatively thin on the northern and southern flanks of the basin and would consist mostly of the uppermost stratigraphic units (e.g., predominantly the Cobalt Group in both the Cobalt Basin to the northeast and possibly the quartzite slivers in the Nepewassi domain). In contrast, the lowermost stratigraphic unis would be most abundant near the centre of the basin (e.g., Elliot Lake, Quirke Lake and Hough Lake groups south of the Murray Fault) and within the GFTZ.

Garnet-rich (20–30%) horizons within the GFTZ described in Easton (2022a, 2022b) may represent metamorphosed hydrothermal alteration systems, although it is not known if they are related to volcanogenic massive sulphide alteration (zinc-copper-lead potential) or metasomatic iron and alkali-calcic alteration (gold ± copper ± iron ± cobalt potential), with the latter occurring in the Southern Province northeast of the study area (e.g., Péloquin 2023). In either case, tectonic disruption of these altered rock packages within the GFTZ will make mineral exploration difficult, because the typical alteration pathfinders for targeting these types of mineralization will not be present.

Also present in the GFTZ, west of the Wanapitei River, are several thin (30–80 cm wide) horizons of impure dolomitic marble and calc-silicate, hosted in orthogneiss (Easton 2022b). The origin of these horizons may be akin to the calcite vein-dikes present in the Central Metasedimentary Belt Boundary Zone near Bancroft (Easton 2016), rather than being sedimentary in origin. Within the cataclastic zone, calc-silicate horizons contain grossular-fluorvesuvianite-quartz assemblages (X-ray diffraction confirmed) and bastnasite, with the presence of these phases suggesting the influence of fluorine-rich fluids and rare earth element mobility in the cataclastic zone (Easton 2023b).

Fluorine-rich Alteration Zone in the Grenville Front Tectonic Zone

As documented in greater detail in Easton (2023b), an approximately 1 km wide cataclastic zone, which displays fluorine-rich alteration, is present in the immediate hanging wall of the Grenville Front west of the Wanapitei River (*see* Figure 18.1). This fluorine-rich zone warrants further exploration for critical minerals, such as niobium, the rare earth elements, tantalum, titanium and zirconium, based on the geochemical and mineralogical data indicating the mobility of these elements (Easton 2023b). All rock types within the cataclastic zone have the potential for being mineralized, although areas underlain by deformed granitic pegmatites may have greater potential for hosting niobium, tantalum and/or rare earth element mineralization. Areas underlain by calc-silicate and carbonate rocks, although volumetrically small, are good targets for rare earth element mineralization because such mineralization is likely to be hosted in minerals, such as bastnasite, from which the rare earth elements can be more easily processed. The presence of anomalous thorium and/or uranium contents in association with the critical minerals may allow the targeting of favourable rock units by using hand-held gamma-ray spectrometers (Easton 2023b).

Geochronological Constraints

Recently published laser ablation inductively coupled plasma mass spectrometry (LA-ICP–MS) U/Pb data on zircon, monazite and xenotime from pegmatites in the study area provides additional insights into its tectonic history (Pfister 2023; Pfister, Kontak and Marsh 2023). These authors, however, thought that all of the dikes were located in the GFTZ, even though more than 75% of them are actually in the Nepewassi domain. After considering the geographic location of the samples and using only the most concordant data (≤2% discordant) from the samples studied by Pfister (2023), the following constraints on the tectonic history of the study area can be identified. Note that by using only the most concordant data, some of the ages and interpretations noted herein differ slightly from those reported by Pfister (2023) and Pfister, Kontak and Marsh (2023).

NEPEWASSI DOMAIN

The Estaire pluton consists of intimately intermixed felsic and mafic magmas, with the felsic phases consisting primarily of potassium feldspar megacrystic granodiorite and monzogranite, and the mafic phases consisting primarily of gabbro, with subordinate diorite. Intrusion breccias composed of both mafic and felsic phases are common (Easton 2022a, 2014). The relationship between these different phases is well exposed on Nelson Road, and along the ramps to Highway 69, near the community of Estaire.

Although the Estaire pluton was thought to be a Killarney Magmatic Belt intrusion, until recently there was no absolute age constraint on the pluton. Two separate ages are now available from the Estaire pluton. The emplacement age, based on LA-ICP–MS data, is 1738±6 Ma (n=24; data *in* Pfister 2023, sample location not provided). This age is nearly identical to the chemical abrasion isotope dilution thermal ionization mass spectrometry (CA-ID-TIMS) age of 1739±4 Ma for the Estaire pluton obtained by Kamo (2023) on a sample collected by the author on Nelson Road (UTM 413982E 5129235N, NAD83, Zone 17). Granulite-facies metamorphism of the Estaire pluton (Easton 2022a, 2022b) occurred at 984±9 Ma based on the LA-ICP–MS data in Pfister (2023), which is similar to the CA-ID-TIMS lower intercept age of 998±12 Ma obtained by Kamo (2023).

A minimum emplacement age of the Wanup pluton is 1701±12 Ma, based on a single LA-ICP–MS zircon age from a 50 cm wide pegmatite dike cutting the pluton (data *in* Pfister 2023). Although this zircon could be inherited, a single monazite grain from the same dike has an age of 1719±8 Ma (data *in* Pfister 2023), which, combined with the zircon age, suggests that the pegmatite may be only slightly younger than emplacement of the Wanup pluton. A minimum age of *circa* 1720 Ma for the Wanup pluton

is consistent with geochemical data collected as part of this project indicating that the Estaire and Wanup plutons have geochemical characteristics suggesting that they were likely coeval (data *in* Easton 2022b). Xenotime grains from the same pegmatite dike give an age of 954±8 Ma (n=4) (data *in* Pfister 2023).

The LA-ICP–MS ages from zircon, ranging from 1425±8 to 1446±9 Ma (data *in* Pfister 2023), were obtained from 6 pegmatite dikes; these are similar in age to the Chief Lake granite located in the Southern Province. These ages indicate that Geon 14 magmatism, and/or high-grade metamorphism that formed anatectic pegmatites, is present in the Nepewassi domain. Not surprisingly, 2 of the Geon 14 pegmatite dikes intruded into the Estaire pluton contain Geon 17 zircons that likely were inherited from the pluton (data *in* Pfister 2023). Preliminary gamma-ray spectrometric and geochemical data suggest that the Geon 14 pegmatite dikes are uniformly more radiogenic (15–70 ppm U, 20–50 ppm Th) than the Grenvillian pegmatite dikes (*circa* 1030 to 960 Ma). Typically, the Geon 14 pegmatites are not zoned, and exhibit internal deformation even if the dikes are discordant to the main rock fabric. Additional work is needed to determine if radiogenic character and deformation can reliably distinguish Geon 14 dikes in the field.

Within the Nepewassi domain, there are indications of a metasomatic or metamorphic event at *circa* 1390 Ma. In the boundary between Nepewassi domain and the GFTZ, this event is recorded by growth of gem-quality monazite in a 1 m wide, garnet-bearing, peraluminous leucogranite, leucosome (Kamo 2023; Easton 2022b). Zircon from the leucosome yielded ages of 2691.7±1.5 and 1746.5±1.5 Ma (Kamo 2023). Both could be inherited grains, although the younger age could reflect initial leucosome formation. In Nepewassi domain proper, the event at *circa* 1390 Ma is recorded by zircon growth in some of the Geon 14 pegmatite dikes (data *in* Pfister 2023). This event has not been identified in the Southern Province.

Seven pegmatite dikes in Nepewassi domain were emplaced during the later stages of the Grenville orogeny, yielding LA-ICP–MS zircon ages ranging from 996±10 to 967±11 Ma and/or monazite ages of *circa* 967 Ma (data *in* Pfister 2023). Some of these late pegmatite dikes are zoned, typically with quartz-rich cores, and locally contain isolated patches that are uranium and/or thorium rich.

GRENVILLE FRONT TECTONIC ZONE

No Geon 17 pegmatite dikes were identified in the Grenville Front tectonic zone (GFTZ) in the study area west of the Wanapitei River (data *in* Pfister 2023), consistent with the absence of any orthogneisses in the GFTZ that have the geochemical characteristics of Killarney Magmatic Suite plutons. Three Geon 14 pegmatite dikes do occur within the GFTZ (data *in* Pfister 2023), although larger intrusive bodies of this age have yet to be identified in the GFTZ. The Geon 14 pegmatite dikes are commonly deformed and uniformly radiogenic, similar to the Geon 14 dikes in the Nepewassi domain.

Grenvillian pegmatite dikes predominate in the GFTZ, with LA-ICP–MS zircon ages ranging from 1036±9 to 955±11 Ma (data *in* Pfister 2023). Monazite and/or xenotime ages, where present, are typically 20 to 30 million years younger than the zircon ages, ranging from 972 to 961 Ma (data *in* Pfister 2023). This is consistent with data in Corfu and Easton (2001) indicating a relationship between age and blocking temperature in the various minerals, with zircon yielding the oldest ages at *circa* 995 Ma, followed by monazite, titanite, rutile and apatite (at *circa* 950 Ma). Similar to the Grenvillian pegmatites in the Nepewassi domain, many of these late pegmatite dikes are zoned, typically with quartz-rich cores, undeformed and, locally, may contain isolated uranium- and/or thorium-rich patches. The largest Grenvillian pegmatite dikes, which historically were exploited for feldspar and/or mica (Vos, Smith and Stevenato 1981) occur within 1.5 km of the postulated major structure along the Wanapitei River (*see* Figure 18.1; Easton 2022b). The reason for this spatial association is not fully understood.

SUMMARY

Significantly, rocks not observed in the GFTZ west of the Wanapitei River, despite their abundance and proximity to the north and/or south include quartzites, Nipissing gabbros and Killarney Magmatic Belt plutons. This means that nickel-copper-platinum group element mineralization that is associated with Nipissing gabbro intrusions (e.g., Lightfoot and Naldrett 1996) is not likely to be present south of the Grenville Front. To date, no specific mineral occurrences or mineralization styles are known to be associated with the Killarney Magmatic Belt intrusions.

In terms of the rocks of the lowermost Huronian Supergroup (mafic metavolcanic rocks, Copper Cliff Formation equivalents, McKim Formation equivalents) identified in the GFTZ, none of these units are associated with any significant mineral occurrences in the Southern Province (e.g., Roscoe and Card 1992). Given the lensoid character of these units, resulting from tectonism within the GFTZ, any mineralization, if present, would likely be of limited size. A more favourable exploration target would be the larger East Bull Lake intrusive suite bodies located within the GFTZ, especially the larger intrusions located east of the Wanapitei River (Red Deer Lake intrusion, southeastern part of the Wanapitei Complex (*see* Figure 18.1)). These intrusions are targets for contact-style nickel-copper-platinum group element mineralization (e.g., James et al. 2002).

The age data of Kamo (2023), and the data contained in Pfister (2023) and Pfister, Kontak and Marsh (2023), confirms the presence of Killarney Magmatic Belt plutonism in the Nepewassi domain, as suggested previously (Easton 2014).

ACKNOWLEDGMENTS

J.E. Chartrand provided excellent assistance in the field during both the 2021, 2022 and 2023 field seasons. J.E. Chartrand and P. Gervais assisted with the figures in this report. S.A. Clarke of the OGS Geoscience Laboratories assisted with scanning electron microscope studies of samples from the study area in April and May 2022 and in January and February 2023. This article has benefitted from discussions with M. Duguet.

REFERENCES

Ames, D.E., Davidson, A., Buckle, J.L. and Card, K.D. 2005. Geology, Sudbury bedrock compilation, Ontario; Geological Survey of Canada, Open File 4570, scale 1:50 000.

Bennett, G., Dressler, B.O. and Robertson, J.A. 1991. The Huronian Supergroup and associated intrusive rocks; Chapter 14 *in* Geology of Ontario, Ontario Geological Survey, Special Volume 4, Part 1, p.549-591.

Bleeker, W. and Kamo, S.L. 2022. A traverse across the Sudbury Structure—Earth's largest impact crater, Day 1; *in* 68th Institute on Lake Superior Geology, Proceedings, Volume 68, Part 2, p.2-46.

Corfu, F. and Easton, R.M. 2001. U-Pb evidence for polymetamorphic history of Huronian rocks in the Grenville Front tectonic zone east of Sudbury, Ontario; Chemical Geology, v.172, p.149-171.

Dressler, B.O. 1984. Sudbury geological compilation; Ontario Geological Survey, Map 2491, scale 1:50 000.

Easton, R.M. 1992. The Grenville Province; Chapter 19 *in* Geology of Ontario, Ontario Geological Survey, Special Volume 4, Part 2, p.713-904.

——— 2014. Geology and mineral potential of the Nepewassi domain, Central Gneiss Belt, Grenville Province; *in* Summary of Field Work and Other Activities, 2014, Ontario Geological Survey, Open File Report 6300, p.16-1 to 16-12.

——— 2016. Metasomatism, syenite magmatism and rare earth element and related metallic mineralization in Bancroft and Frontenac terranes, Grenville Province: A preliminary deposit model, *in* Summary of Field Work and Other Activities, 2016, Ontario Geological Survey, Open File Report 6323, p.18-1 to 18-9.

——— 2022a. Field Trip 2 – Geology of the Grenville Front and the Grenville Front tectonic zone in the Sudbury area; *in* 68th Institute on Lake Superior Geology, Sudbury, Ontario, Proceedings, v.68, pt.2, p.103-146.

——— 2022b. Geology of the Grenville Front tectonic zone near Sudbury, northeastern Ontario; *in* Summary of Field Work and Other Activities, 2022, Ontario Geological Survey, Open File Report 6390, p.12-1 to 12-15,

——— 2023a. Who were you? Insights into the lithological character of the Grenville Front tectonic zone near Wanup, Ontario; abstract *in* Geological Association of Canada–Mineralogical Association of Canada–Society for Geology Applied to Mineral Deposits, Annual Meeting, Sudbury, Ontario, May 25–27, Abstracts, v.46, Geoscience Canada, v.50, p.136-137.

——— 2023b. Critical Mineral potential in cataclastic rocks of the Grenville Front tectonic zone, southeast of Sudbury, Ontario; *in* Report of Activities 2022, Resident Geologist Program, Kirkland Lake Regional Resident Geologist Report: Sudbury District, Open File Report 6403, p.102-109.

James, R.S., Easton, R.M., Peck, D.C. and Hrominchuk, J.L. 2002. The East Bull Lake intrusive suite: Remnants of a ~2.48 Ga large igneous and metallogenic province in the Sudbury area of the Canadian Shield; Economic Geology, v.97, p.1577-1606.

Kamo, S.L. 2023. Report on U-Pb ID-TIMS geochronology for the Ontario Geological Survey: Bedrock Mapping Projects, Ontario 2022-2023; internal U/Pb age report for the Ontario Geological Survey, Jack Satterly Geochronology Laboratory, Department of Geology, University of Toronto, Toronto, Ontario, 22p.

Lightfoot, P.C. and Naldrett, A.J. 1996. Petrology and geochemistry of the Nipissing Gabbro: Exploration strategies for nickel, copper and platinum group elements in a large igneous province; Ontario Geological Survey, Study 58, 80p.

Péloquin, A.S. 2023. Metasomatic iron and alkali-calcic system in the Sudbury District; *in* Ontario Geological Survey, Resident Geologist Program, Recommendations for Exploration 2022–2023, p.59-62.

Pfister, J.D. 2023. Assessing primary versus secondary features in two pegmatite swarms with implications for the nature of pegmatitic systems; unpublished PhD thesis, Laurentian University, Sudbury, Ontario, 302p.

Pfister, J.D., Kontak, D.J. and Marsh, J.H. 2023. Unravelling 800 Ma of pegmatite formation in the western Grenville Front tectonic zone near Sudbury, Canada; Precambrian Research, v.395, article 107128, 20p.

Roscoe, S.M. and Card, K.D. 1992. Early Proterozoic tectonics and metallogeny of the Lake Huron region of the Canadian Shield; Precambrian Research, v.58, p.99-119.

Vos, M.A., Smith, B.A. and Stevenato, R.J. 1981. Industrial minerals of the Sudbury area; Ontario Geological Survey, Open File Report 5329, 156p.

Young, G.M., Long, D.G.F., Fedo, C.M. and Nesbitt, H.W. 2001. Paleoproterozoic Huronian basin: Product of a Wilson cycle punctuated by glaciations and a meteorite impact; Sedimentary Geology, v.141-142, p.233-254.

19. Project ON-22-002. An Overview of the Critical Minerals in Gold Deposits Project



E.C.G. Hastie[1], P.M. Malegus[2], D.A. Campbell[2], O.M. Burnham[3] and P.J. MacDonald[1]

[1]Earth Resources and Geoscience Mapping Section, Ontario Geological Survey
[2]Resident Geologist Program, Ontario Geological Survey
[3]Geoscience Laboratories, Ontario Geological Survey

INTRODUCTION

Gold remains one of Ontario's most significant resources; however, gold deposits are host to much more than simply gold. Many of the elements that are associated with gold and used as exploration vectors can also be highly enriched in gold deposits (e.g., antimony, arsenic, bismuth, copper, molybdenum, platinum group elements, selenium, silver, tellurium, titanium, tungsten and zinc). For example, tellurium is an element commonly found associated with gold deposits (cf. Hastie, Kontak and Lafrance 2020). The Kankberg deposit in Sweden is a global producer of tellurium and in 2022 mined 464 000 t of ore, with an average grade of 3.66 g/t Au, 10.4 g/t Ag and 164 g/t Te (Voigt and Bradley 2022). For comparison, within Ontario, gold ore samples in the Kirkland Lake area can range from 25 to 730 g/t Te (Ispolatov et al. 2008), but this is based on only 12 samples. By-product potential may also exist for many other elements in other areas of the province (e.g., molybdenum and antimony in Hemlo, antimony and nickel in Red Lake), but, again, public data that documents the concentrations of secondary metals in these gold deposits are lacking.

Many countries around the globe are investing time, effort and money in various strategies to respond to the global demand for critical minerals and materials to support the transition to a low-carbon economy. Although gold may not be on Ontario's critical mineral list (Ontario 2022), gold deposits offer the only realistic opportunity to produce several elements on the Ontario list as co-products or by-products[4]. Consequently, this current emphasis on critical minerals offers an opportunity to determine what secondary elements and recoverable phases exist in gold ores across Ontario.

The Critical Minerals in Gold Deposits project will use petrography, geochemistry and data compilation to determine answers to the following questions:

1. What are the concentrations of all elements in gold ore?
2. Are the critical mineral elements hosted in recoverable mineral phases?
3. Are critical mineral elements present in concentrations sufficient to be considered a mineral occurrence?
4. What can the elements in gold ore tell us about the geological processes responsible for the deposits?
5. What is the possibility for the production of critical mineral elements as by-products from historical tailings versus current mining operations versus future gold mining operations?

[4] *The term "critical minerals" includes both specific minerals (e.g., chromite, fluorite), as well as specific chemical elements (e.g., antimony, tellurium). In the text, the term "critical mineral elements" means elements on the Ontario Critical Minerals list (Ontario 2022).*

Summary of Field Work and Other Activities, 2023,
Ontario Geological Survey, Open File Report 6405, p.19-1 to 19-5.

© King's Printer for Ontario, 2023

More broadly, the project will involve work at the Ontario Geological Survey's Geoscience Laboratories to develop methods with increased working ranges for secondary elements and to establish new reference materials to accompany their analysis. The project will also assist in gathering data relevant to establishing updated Ontario Mineral Inventory (OMI) elemental cut-off values for mineral occurrences. Ultimately, it is hoped that the project will aid in the discovery of new mineral occurrences based on improvements in exploration models arising from this study.

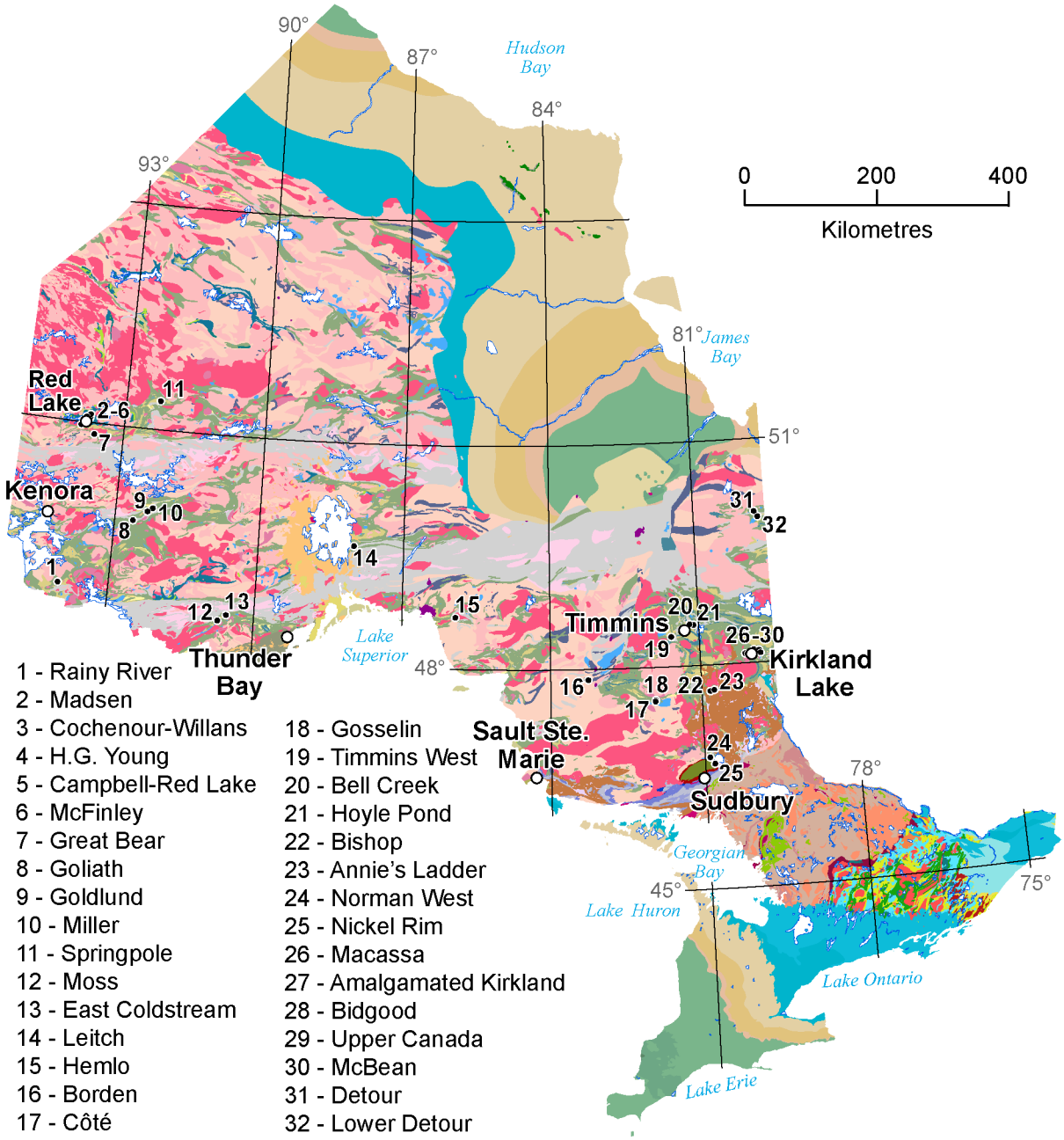


Figure 19.1. Simplified bedrock geology map of Ontario (*modified from* Ontario Geological Survey 2011) highlighting locations of deposits and occurrences that are currently part of the Critical Minerals in Gold Deposits project. Detailed legend for the geology can be found in Ontario Geological Survey (2011).

As part of this project, approximately 800 gold ore samples and select tailings from Ontario's significant gold camps, individual deposits and developing prospects will be studied. Whole-rock major and trace element geochemistry analyses will be conducted at the Ontario Geological Survey Geoscience Laboratories, Sudbury, as part of the project and to aid in method development. Ore petrography will use a combination of petrographic microscopy, scanning electron microscopy energy dispersive spectrometry (SEM–EDS) and electron probe microanalysis (EPMA). Limited external geochemical analyses (approximately 100) will be completed for over-range data and quality assurance–quality control (QA/QC) purposes.

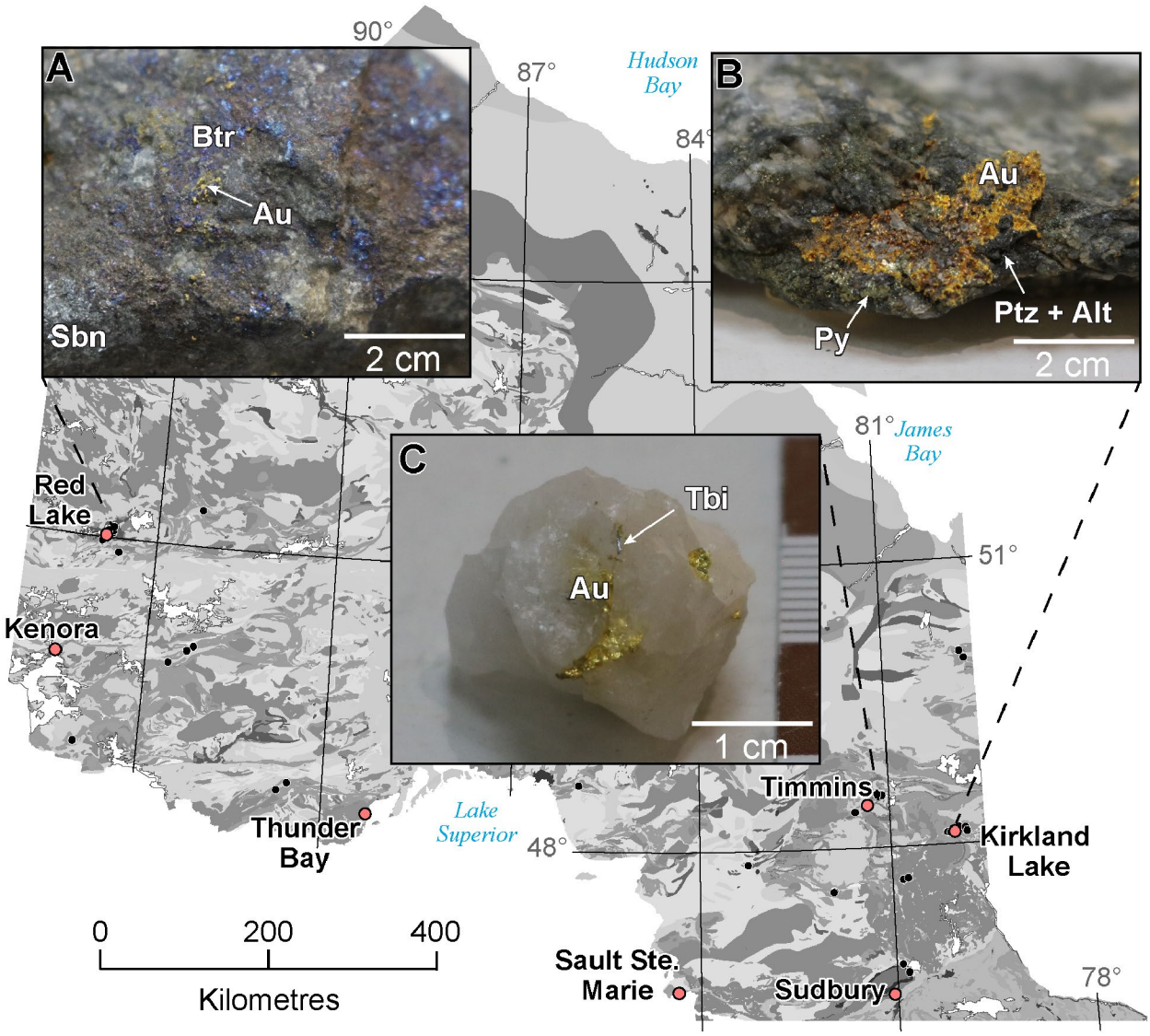


Figure 19.2. Simplified bedrock geology map of Ontario in greyscale (*modified from* Ontario Geological Survey 2011) highlighting examples of gold ore with other critical elements, such as antimony, bismuth and tellurium. **A**) Gold ore from the Cochenour-Willans Mine (sample M21202) containing gold (Au), stibnite (Sbn: Sb_2S_3) and berthierite (Btr: $FeSb_2S_4$). **B**) Gold ore from the Macassa Mine (sample M38715) containing gold (Au), pyrite (Py), petzite (Ptz: Ag_3AuTe_2) and altaite (Alt: PbTe). **C**) Gold ore from the Pamour Mine (sample M41877) containing gold (Au) and tellurobismuthite (Tbi: Bi_2Te_3). Photos were taken with the permission the Royal Ontario Museum (ROM); the sample numbers refer to the ROM sample catalogue.

SAMPLE SELECTION AND METHOD DEVELOPMENT

Work thus far has included collecting approximately 640 samples from 32 deposits (Figure 19.1) with help from industry and individual collaborators (*see* "Acknowledgments"). Data compilation of background levels of elements associated with these 32 gold deposits, among others, has assisted in establishing new OMI cut-off values for mineral occurrences that did not previously exist for certain elements (Ontario Geological Survey 2023a). Additional samples from other significant deposits and prospects will be collected over the coming year.

Method development has been ongoing since 2022 at the Geoscience Laboratories to increase working ranges on select methods pertinent to critical mineral research (e.g., method IML-101: *see* Ontario Geological Survey 2023b) and to establish a new reference material for tellurium because of the paucity of inter-laboratory reference materials with certified contents of tellurium greater than 50 ppm Te. The sample used to create this new reference material (MMTe-1) was donated from Agnico Eagle Mines Limited Macassa Mine (for further details, *see* Burnham and Hastie, this volume).

CRITICAL MINERAL POTENTIAL IN GOLD ORES

Once a fundamental baseline for secondary elements associated with gold ores can be established, then the mineral exploration industry can evaluate what element or elements may be of economic interest to them as a co-product or by-product. It is not the intention of this project to evaluate the economic viability of a given commodity, it is only to collect petrographic and geochemical data on secondary elements and comment on their occurrence in gold ores. The most likely elements on Ontario's critical mineral list (Ontario 2022) that may show elevated values in gold ores are antimony, bismuth, copper, molybdenum, nickel, platinum group elements, selenium, tellurium and zinc. Of particular interest are semi-metals, such as bismuth, antimony and tellurium (Figure 19.2), given that these are geochemically coupled throughout the natural gold refinement process in deposits. For example, they can help gold transport as polymetallic melts by depressing the melting temperature of gold, they can form gold-bearing mineral phases, such as maldonite (Au_2Bi), aurostibite ($AuSb_2$), calaverite ($AuTe_2$), sylvanite ($AgAuTe_4$) and petzite (Ag_3AuTe_2) (Tomkins, Pattison and Zaleski 2004; Tooth et al. 2011; Hastie, Kontak and Lafrance 2020), and they are important vectors in gold exploration.

ACKNOWLEDGMENTS

This project is supported through industry collaborators and special thanks are offered to companies and individuals for donating samples to the project. Company donations: Agnico Eagle Mines Ltd., Barrick Gold Corp., Evolution Mining Ltd., First Mining Gold Corp., Glencore Canada Corp., Goldshore Resources Inc., IAMGOLD Corp., Kinross Gold Corp., New Gold Inc., Newmont Corp., Pan American Silver Corp., Transition Metals Corp., Treasury Metals Inc. and West Red Lake Gold Mines Ltd. Individual donations: Dorothy Campbell and Tom Hart. In addition, special thanks to the Royal Ontario Museum (ROM) for providing access to the historic gold samples that were examined and photographed.

REFERENCES

Hastie, E.C.G., Kontak, D.J. and Lafrance, B. 2020. Gold remobilization: Insights from gold deposits in the Archean Swayze greenstone belt, Abitibi Subprovince, Canada; Economic Geology v.115, no.2, p.241-277.

Ispolatov, V., Lafrance, B., Dubé, B., Creaser, R. and Hamilton, M. 2008. Geologic and structural setting of gold mineralization in the Kirkland Lake-Larder Lake gold belt, Ontario; Economic Geology, v.103, p.309-1340.

Ontario 2022. Ontario's Critical Mineral Strategy: Unlocking the potential to drive economic recovery and prosperity; Ministry of Northern Development, Mines, Natural Resources and Forestry, 53p., www.ontario.ca/page/ontarios-critical-minerals-strategy-2022-2027-unlocking-potential-drive-economic-recovery-prosperity, also available to download: select "Download English PDF". [accessed September 20, 2023]

Ontario Geological Survey 2011. 1:250 000 scale bedrock geology of Ontario; Ontario Geological Survey, Miscellaneous Release—Data 126 – Revision 1.

——— 2023a. OMI Definitions and cut-off values; document *in* Ontario Mineral Inventory, Ontario Geological Survey, online database, April 2023 update, 9p. [accessed September 20, 2023]

——— 2023b. Geoscience Laboratories 2023 Schedule of Fees and Services, Issue 15, effective April 1, 2023; Ontario Geological Survey, Geoscience Laboratories, 36p., www.ontario.ca/page/ontario-geological-survey#section-4, under "Schedule of fees and services", *see* link to download PDF. [accessed September 20, 2023]

Tomkins, A.G., Pattison, D.R.M. and Zaleski, E. 2004. The Hemlo gold deposit, Ontario: An example of melting and mobilization of a precious metal-sulfosalt assemblage during amphibolite facies metamorphism and deformation; Economic Geology, v.99, p.1063-1084.

Tooth, B., Ciobanu, C.L., Green, L., O'Neill, B. and Brugger, J. 2011. Bi-melt formation and gold scavenging from hydrothermal fluids: An experimental study; Geochimica et Cosmochimica Acta, v.75, p.5423-5443.

Voigt, B. and Bradley, J. 2022. Boliden Summary Report, Mineral Resources and Mineral Reserves 2022, Kankberg; Boliden Mineral AB, 27p., Boliden Group, www.boliden.com/operations/exploration/mineral-reserves-and-mineral-resources, under "Mineral Resources and Mineral Reserves": beside "Boliden Area Kankberg" select "Download PDF" [accessed September 20, 2023].

20. Summary of Geophysical Projects and Activities



J. Evangelatos[1] and S. Biswas[1]

[1]Earth Resources and Geoscience Mapping Section, Ontario Geological Survey

INTRODUCTION

Geophysical services, including imaging, data compilation, interpretation and computational models, were provided in support of the Earth Resources and Geoscience Mapping section (ERGMS) bedrock mapping and groundwater programs, as well as to the Resident Geologist Program (RGP). New geophysical data were recently acquired from a ground gravity survey and are being prepared for publication.

SUPPORT FOR THE BEDROCK GEOLOGY MAPPING PROGRAM

The Ontario Geological Survey (OGS) mapping program for the 2023 field season extended across northern Ontario and included many projects. Support for this program consisted of analysis of existing geophysical data layers in preparation of mapping projects, the creation of suites of images for new projects and reviews of geological maps with respect to geophysical interpretation prior to publication.

Geophysical support was provided for the following new or ongoing mapping projects:

- Red Lake bedrock geology
- Animikie Group and Logan Igneous Suite bedrock geology and compilation
- Rowan–Kakagi bedrock geology
- North Caribou greenstone belt compilation
- Gowganda area greenstone belt bedrock geology
- Trill–Totten bedrock geology

ACQUISITION OF NEW GEOPHYSICAL DATA

A new geophysical survey, consisting of ground gravity measurements, was recently completed in the Guelph area of southern Ontario (Figure 20.1) to support the Guelph three-dimensional (3-D) sediment mapping project. The survey consisted of 3500 stations focussed along 17 profiles (Figure 20.2). The acquisition phase of the project occurred between August and September 2023, and the data are being processed at the time of writing. An increase in gravity data resolution was required to appropriately target the buried bedrock features, which were assessed to be narrower (Conway-White et al. 2022) than previously modelled (Burt and Dodge 2016). As such, despite the initial plan (Biswas and Evangelatos 2022), station spacing was halved from 100 to 50 m.

Summary of Field Work and Other Activities, 2023,
Ontario Geological Survey, Open File Report 6405, p.20-1 to 20-4.

© King's Printer for Ontario, 2023

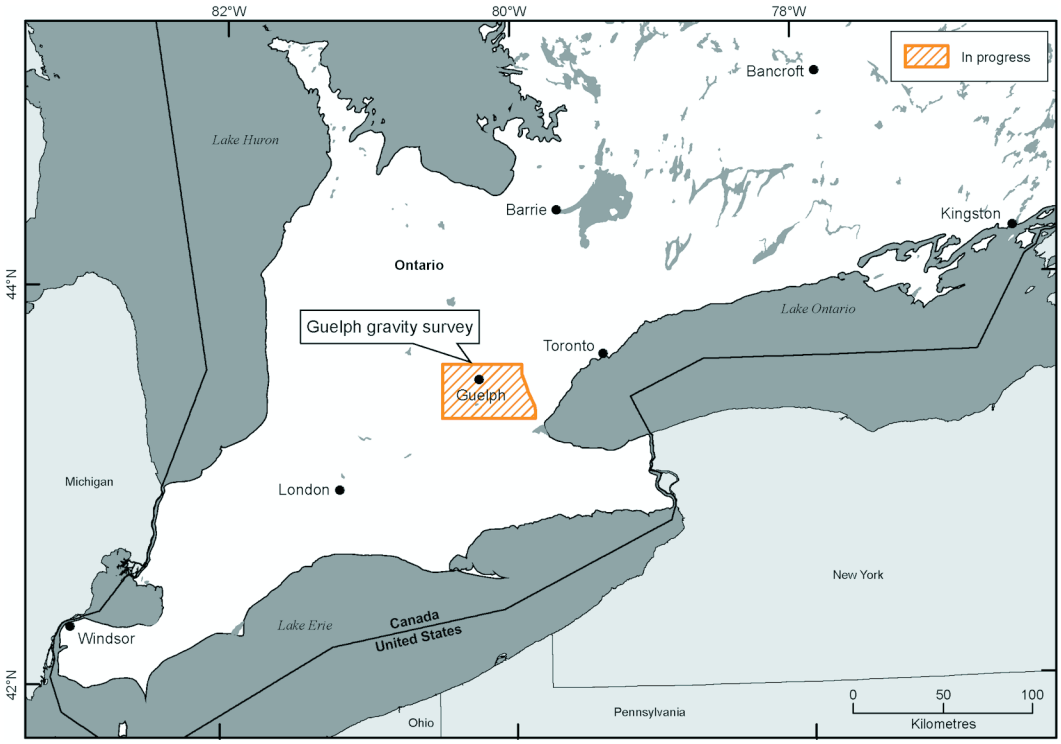


Figure 20.1. Location of ground gravity survey. The acquisition phase has been completed and the data are being processed.

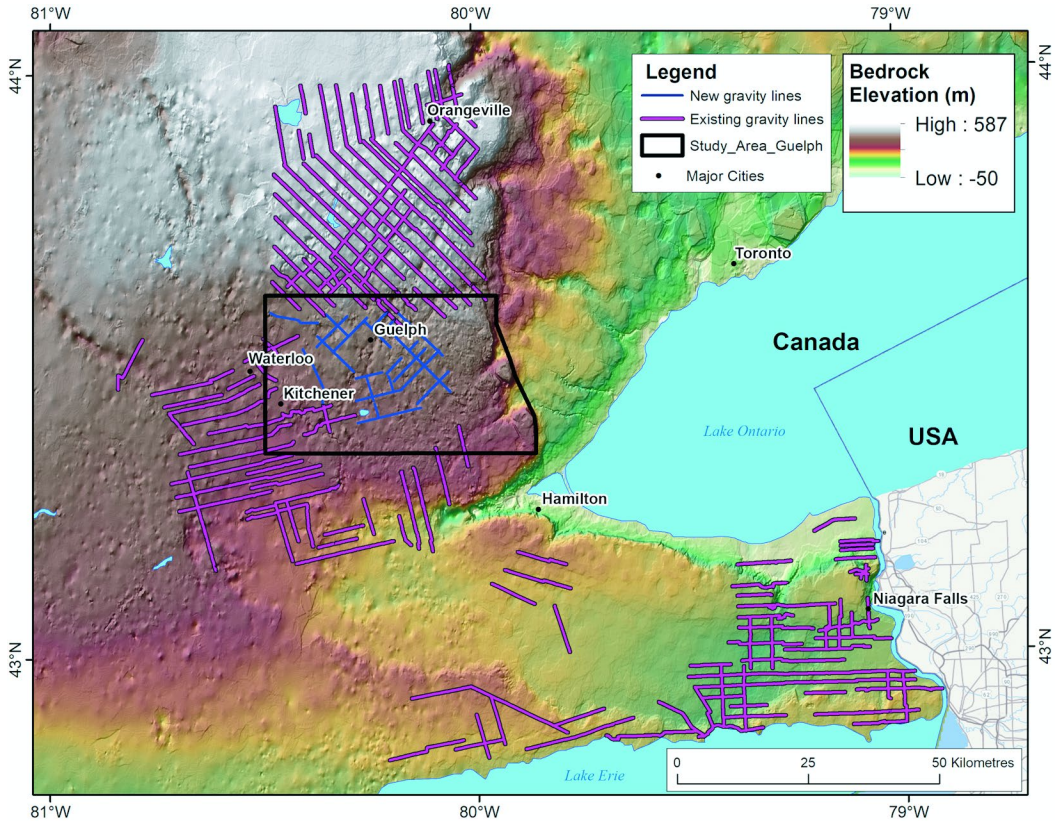


Figure 20.2. Location of the Guelph 3-D sediment mapping project area showing the new and existing gravity lines overlain on the bedrock elevation layer (Gao et al. 2006) in the region.

This survey complements the existing ground gravity surveys in the Orangeville (Ontario Geological Survey 2013), Kitchener–Waterloo (Marich et al. 2011) and Niagara Peninsula (Ontario Geological Survey 2014) areas. Figure 20.2 shows the locations of the 17 new gravity lines from the Guelph area and the pre-existing gravity lines. In late August 2023, OGS staff conducted a site visit of the gravity survey area to inspect the quality assurance and quality control (QA/QC) procedure, survey progress, and safety (Photos 20.1A to 20.1C). The results of this gravity survey will be used to identify potential thalwegs, thereby guiding the placement of boreholes. Furthermore, the gravity data, complemented by physical properties of subsurface sediments derived from borehole information, will be used to develop two-dimensional (2-D) models of the sedimentary layers and underlying bedrock along select profiles in support of the 3-D sediment mapping project in the Guelph area. The data and an accompanying report are planned to be published as a Geophysical Data Set (GDS) in 2024.

OTHER ACTIVITIES

In 2023, 17 field assistants were trained in operating the magnetic susceptibility meter. Measurements of magnetic susceptibility are used to semiquantitatively assess the concentration of magnetic minerals in outcrop. Prior to the beginning of the field season, the susceptibility meters were calibrated to OGS rock standards and their performance monitored using these same standards to ensure consistent data quality. The newly collected field measurements will be added to compilations from previous years. Data from these compilations are used by industry and academia to improve the accuracy of magnetic interpretations and, hence, subsurface models.



Photo 20.1. A) The gravity survey operator is adjusting the legs of the tripod to level the CG-6 Autograv™ gravity meter before recording gravity measurements along the roadside in the Guelph area. The orange cone is used as a safety measure to alert other road users of temporary occupation along the roadside while gravity measurements take place. **B**) A gravity survey operator walking along the roadside between gravity stations. The long staff in the operator's left hand is the global positioning system (GPS) antenna, and is used to record the horizontal and elevation co-ordinates of each station. **C**) Typical landform in the region of the survey. Note the gentle undulations that are indicative of glacial landforms.

Handheld gamma-ray spectrometers were used by geological field crews on 5 projects. As such, training on the proper use of the OGS spectrometers was provided to 8 field assistants accompanying the OGS Geoscientists during their mapping projects. Radiometric readings are very useful in the field. For example, these readings can discriminate between similar looking granitoids based on their respective concentrations of uranium, thorium and potassium. The performance of these instruments is tested for consistency throughout the year at a convenient field location off Municipal Road 35 in Sudbury.

The OGS continued to serve the public by addressing geophysical enquiries from clients in mineral exploration and by providing material support to other staff within the Ministry of Mines. An example of the latter is training provided on the use of a gamma-ray spectrometer loaned to the Mine Rehabilitation Section of the Mineral Development Branch. This instrument was used to monitor background radiation at the closed Lockerby Mine and Agnew Lake Mine. Furthermore, several in-person and virtual meetings were held with members of Indigenous communities to share knowledge of geophysics and to communicate the role of geophysics within the OGS and its overall benefits to Ontario.

As part of its commitment to maintaining and expanding its inventory of petrophysical instruments, the OGS purchased a new KT-10 magnetic susceptibility meter and a KT-10 magnetic susceptibility and conductivity meter. Repairs were made to 6 KT-10 meters and a gamma-ray spectrometer, whereas 2 KT-10 meters were found to have irreplaceably damaged parts and were thus retired.

The OGS geophysical, as well as, other geoscientific data, can be downloaded and viewed using the OGSEarth application (www.ontario.ca/ogsearth). A geophysical survey index, which can be accessed from the OGSEarth application, continues to be maintained and updated with each new release of geophysical data. This index can be downloaded as a Google Earth™ mapping service file (*.kml*) or as ESRI® files (*.shp*). Free downloads of geophysical data can be accessed from GeologyOntario (www.hub.geologyontario.mines.gov.on.ca). Hard-copy (paper) reports, maps, and physical media (CD or DVD) of digital data are also available for a nominal fee through the Publication Sales:

Tel:	705-670-5691 (local)
Toll-free:	1-888-415-9845 ext. 5691 (Canada and United States)
Fax:	705-670-5770
E-mail:	pubsales.ndm@ontario.ca

REFERENCES

Biswas, S. and Evangelatos, J. 2022. Summary of geophysical projects and activities; *in* Summary of Field Work and Other Activities, 2022, Ontario Geological Survey, Open File Report 6390, p.16-1 to 16-10.

Burt, A. and Dodge, J.E.P. 2016. Three-dimensional modelling of surficial deposits in the Orangeville–Fergus area of southern Ontario; Ontario Geological Survey, Groundwater Resources Study 15.

Conway-White, O., Steelman, C.M., Smiarowski, A., Ugalde, H., Endres, A.L., Emmanuelle A. and Parker, B.L. 2022. Improving spatial characterization of buried bedrock valleys through airborne frequency-domain electromagnetic, residual magnetic, and surface resistivity measurements; Journal of Applied Geophysics, v.199, article 104584. doi.org/10.1016/j.jappgeo.2022.104584

Gao, C., Shirota, J., Kelly, R.I., Brunton, F.R. and van Haaften, S. 2006. Bedrock topography and overburden thickness mapping, southern Ontario; Ontario Geological Survey, Miscellaneous Release—Data 207.

Marich, A.S., Priebe, E.H., Bajc, A.F., Rainsford, D.R.B. and Zwiers, W.G. 2011. A geological and hydrogeological investigation of the Dundas buried bedrock valley, southern Ontario; Ontario Geological Survey, Groundwater Resources Study 12, 248p.

Ontario Geological Survey 2013. Ontario geophysical surveys, ground gravity data, grid and point data (ASCII and Geosoft® formats) and vector data, Orangeville Area; Ontario Geological Survey, Geophysical Data Set 1072.

——— 2014. Ontario geophysical surveys, ground gravity data, grid and point data (ASCII and Geosoft® formats) and vector data, Niagara area; Ontario Geological Survey, Geophysical Data Set 1073.

21. Project ON-23-004. Determination of Indicator Minerals in Archived Fine-Fraction Non-Magnetic Heavy Mineral Concentrate Samples Using Scanning Electron Microscope Energy Dispersive Spectrometry



C. Gao[1], G.W. Hagedorn[1], D.C. Crabtree[2], S.A. Clarke[2], E.C.G. Hastie[1], G. Launay[1] and C.E. Beckett-Brown[1]

[1]Earth Resources and Geoscience Mapping Section, Ontario Geological Survey
[2]Geoscience Laboratories, Ontario Geological Survey

INTRODUCTION

Over the past 40 years, numerous Ontario Geological Survey (OGS) surficial sampling projects for indicator minerals have collected and archived voluminous amounts of samples of fine-fraction (<0.25 mm) non-magnetic heavy mineral concentrate (HMC) (Gao, Hagedorn and Crabtree 2023). In the past, only the coarse-fraction (0.25–2 mm) non-magnetic HMC samples from these previous projects have been studied through visual identification, whereas the fine-fraction non-magnetic HMC have never been analyzed, primarily because of difficulties in visual isolation of minerals in such a small grain size. Recently, selected fine-fraction non-magnetic HMC samples from the McFaulds Lake area in northern Ontario were analyzed as a pilot study using the scanning electron microscope energy dispersive X-ray spectroscopy (SEM–EDS) method (Gao et al. 2021). The McFaulds Lake ("Ring of Fire") area was selected for this pilot study because it contains world-class chromite deposits (Metsaranta et al. 2015) and previous till and stream sediment or modern alluvium sampling by the OGS indicates the potential for new chromite deposits in this area (Gao and Crabtree 2016). After the successful completion of this pilot study, this method will be used to analyze all the archived fine-fraction non-magnetic HMC samples.

OBJECTIVES AND SCOPE

The goal of this multi-year project is to analyze the archived fine-fraction non-magnetic HMC samples using automated SEM–EDS for modal mineralogy of minerals pertinent to ore deposits and critical minerals. The automated SEM–EDS method has 2 distinct advantages over visual identification. The first advantage is that it removes sampling bias and possible human error, and the second advantage is the substantial reduction of time in mineral analysis. Analyzing these legacy samples will provide complementary and value-added products to the previous surficial sampling projects that only investigated the coarse-fraction non-magnetic HMC samples. More importantly, this study has potential for documenting possible indicator minerals, such as critical mineral indicator minerals, which have not been previously identified or occur rarely in coarse-fraction non-magnetic HMC because some heavy minerals may be preferentially preserved in smaller grain size in surficial sediments through weathering and erosion (e.g., Gao et al. 2023).

Summary of Field Work and Other Activities, 2023,
Ontario Geological Survey, Open File Report 6405, p.21-1 to 21-8.

© King's Printer for Ontario, 2023

The protocols for this automation method have been developed through collaborations between the OGS Earth Resources and Geoscience Mapping Section (ERGMS) and OGS Geoscience Laboratories (Geo Labs). Analysis of the samples and release of the results will be incremental, with sample submission prioritized for areas of active OGS projects or those planned for the near future. Compiled from released OGS reports (e.g., Open File Reports and Miscellaneous Releases—Data), more than 10 000 till and stream sediment samples were collected and analyzed in the past for indicator minerals in the coarse-fraction non-magnetic HMC. However, the quality and availability of their fine-fraction non-magnetic HMC samples in the OGS archives remain largely unknown.

SAMPLE PREPARATION AND ANALYSIS

Each archived fine-fraction HMC sample is sieved to 0.125 to 0.25 mm and less than 0.125 mm fractions. Approximately 0.1 g of each sieved fraction is mounted in epoxy, such that the grains cover the surface of the sample mount without making contact at grain boundaries. The mounts are then ground to expose the grains, polished and carbon coated prior to analysis.

The analytical routine is set to cover the entire area of the polished mount. The method involves identifying individual grains using imaging techniques followed by SEM–EDS analysis from the centre of the longest axis of each grain. The analyses are processed to account for matrix effects; then, the resulting data are classified offline using a Microsoft® Excel® for Office 365 macro that identifies mineral types based on stoichiometric parameters. The results are presented as tables in 2 formats that include percent of points (% points) and areal extent (% area). In addition to the routine analysis, which is set to analyze a single second for each mineral grain, energy dispersive spectrometry filters will be added to detect and analyze some specific mineral grains, such as arsenian pyrite, sphalerite and spessartine garnet for a slightly longer time to better characterize the compositions of these minerals to help the ongoing OGS studies on gold fingerprinting (Hastie et al. 2020; Melo-Gómez et al. 2022), critical minerals in gold ores (*see* Hastie et al., this volume), and other critical mineral systems, such as lithium-cesium-tantalum type pegmatites.

RESULTS FROM THE PILOT STUDY

Results from the pilot study confirmed the anomalies of chromite grains found previously in the coarse-fraction samples, attesting to the applicability of this method in heavy mineral studies (Figures 21.1 and 21.2) (Gao et al. 2021). This study also better characterized the spatial distribution of some other heavy minerals, such as monazite, a REE-phosphate ($(Ce,La,Nd,Th)PO_4$), whereby many HMC samples, that contain none to trace amounts of this mineral in the coarse fraction, contain anomalous monazite grains in the fine fraction (Figure 21.3). Furthermore, high concentrations of lanthanum (La), cerium (Ce) and thorium (Th) in the till matrix (<0.063 mm) often coincide with fine-fraction HMC samples that contain anomalous numbers of monazite; because these elements are the major elements of this mineral, this coincidence suggests their likely derivation from monazite-bearing bedrock, thus providing insight into the nature of the source rock (Figures 21.4 and 21.5).

PROJECT STATUS

In 2023, the previous till sampling survey for gold and other indicator minerals in the Rainy River area (Bajc 1991a, 1991b) was selected for study because the results can also assist the OGS gold fingerprinting and critical mineral studies (e.g., Hastie et al. 2020). A batch of 184 fine-fraction HMC samples were retrieved from this survey and submitted to the Geo Labs for analysis. It was found that ferromagnetic minerals had not been removed from the samples. As such, they were isolated and removed using a hand-held magnetic separator. As of the time of writing, approximately 150 mounts for both the 0.125 to 0.25 mm and under 0.125 mm fractions were made and ready for polishing and carbon coating prior to analysis.

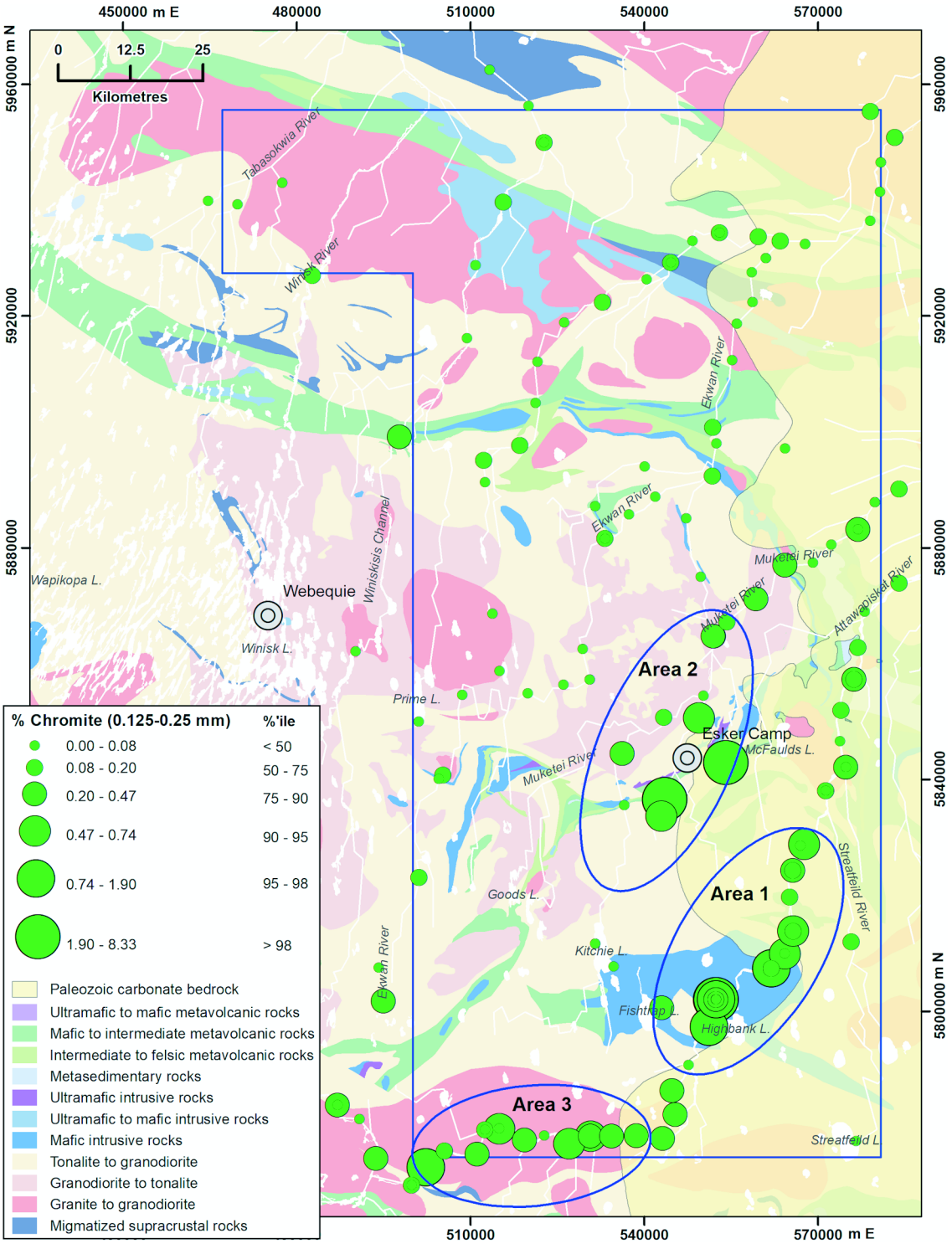


Figure 21.1. Results from a pilot study on fine-fraction (0.125–0.25 mm) non-magnetic heavy mineral concentrate (HMC) samples using the automated SEM–EDS method, which show the regional distribution of detrital chromite grains in the McFaulds Lake ("Ring of Fire") area (*from* Gao et al. 2021, Appendix 19). This pilot study analyzed 157 till and stream sediment samples, accounting for 63% of the total samples (249) collected and compiled for this area by Gao and Crabtree (2016). The plot shows the percentage of the grains of this mineral to the analyzed total grains ranging from 1100 to 5200 for each sample. To compare, this data set confirms anomalous areas 1, 2 and 3 depicted previously by the coarse-fraction detrital chromite grains (0.25–2 mm) shown below in Figure 21.2. All Universal Transverse Mercator co-ordinates provided using North American Datum 1983 (NAD83) in Zone 16.

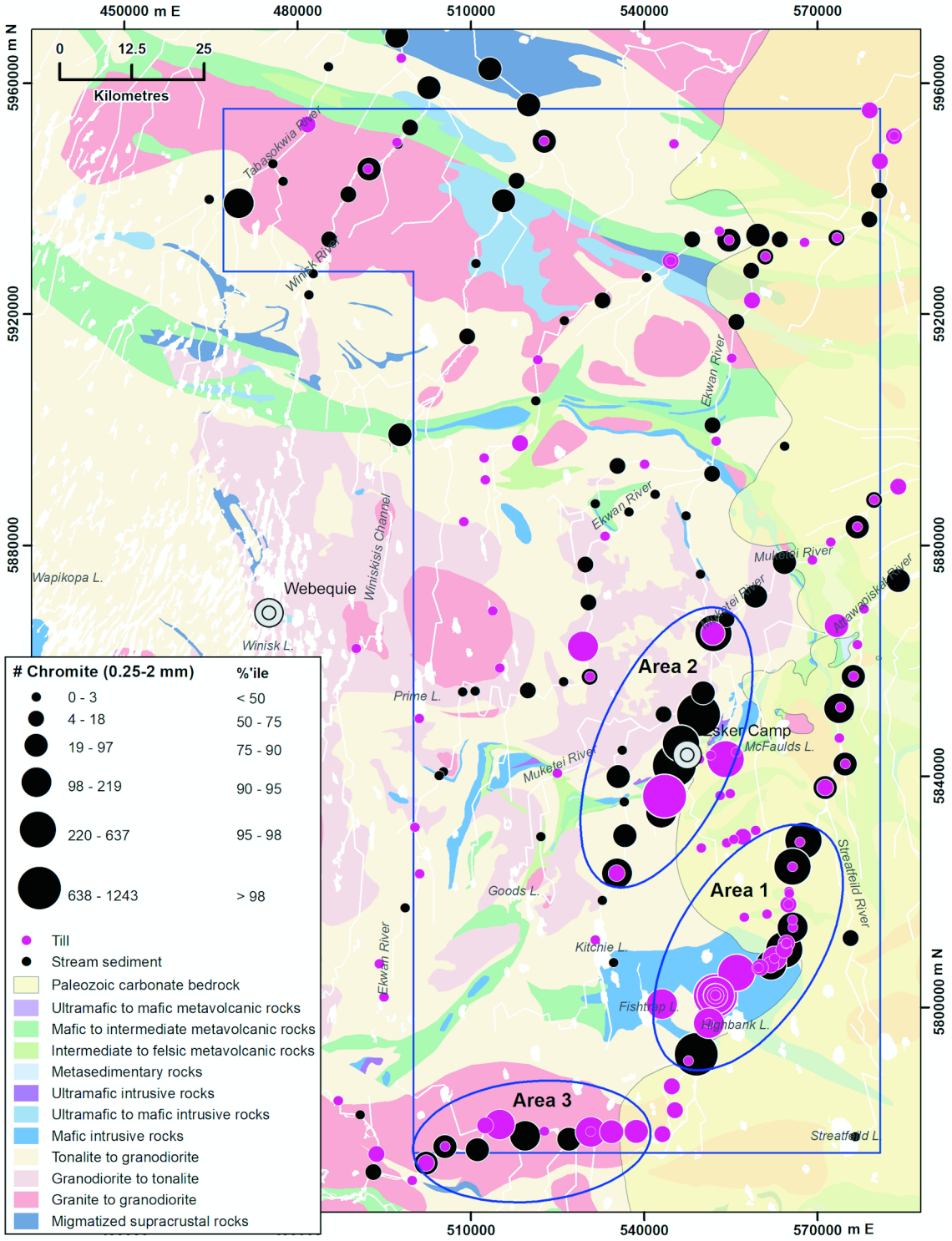


Figure 21.2. Regional distribution of detrital chromite grains isolated from visual count in coarse-fraction (0.25–2 mm) heavy mineral concentrate (HMC) samples in the McFaulds Lake ("Ring of Fire") area (*from* Gao and Crabtree 2016, Figure 24). Note that the anomalous chromite grains in areas 1, 2 and 3 are confirmed by those in the fine-fraction HMC (0.125–0.25 mm) as shown in Figure 21.1. All UTM co-ordinates provided using NAD83 in Zone 16.

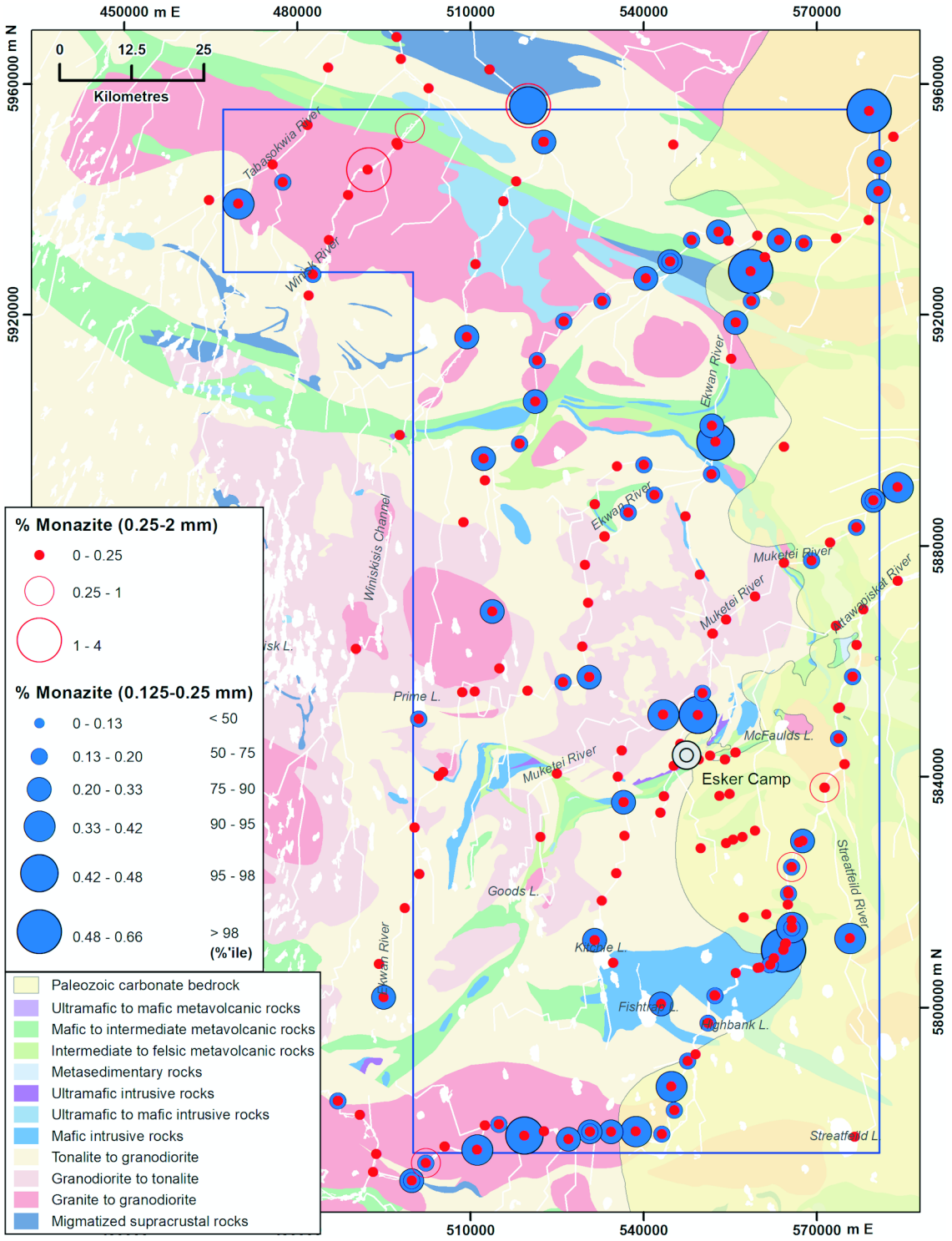


Figure 21.3. Results from the pilot study on fine-fraction (0.125–0.25 mm) non-magnetic heavy mineral concentrate (HMC) samples, showing the regional distribution of detrital monazite ($(Ce,La,Nd,Th)PO_4$) in the McFaulds Lake ("Ring of Fire") area. Monazite grains in the coarse fraction (0.25–2 mm) isolated through visual count are also shown as red-filled dots and red-outlined circles. To compare, many HMC samples that contain none to trace amounts (<0.25%) of this mineral in the coarse fraction contain anomalous (>90 percentile) monazite in the fine fraction. All UTM co-ordinates provided using NAD83 in Zone 16.

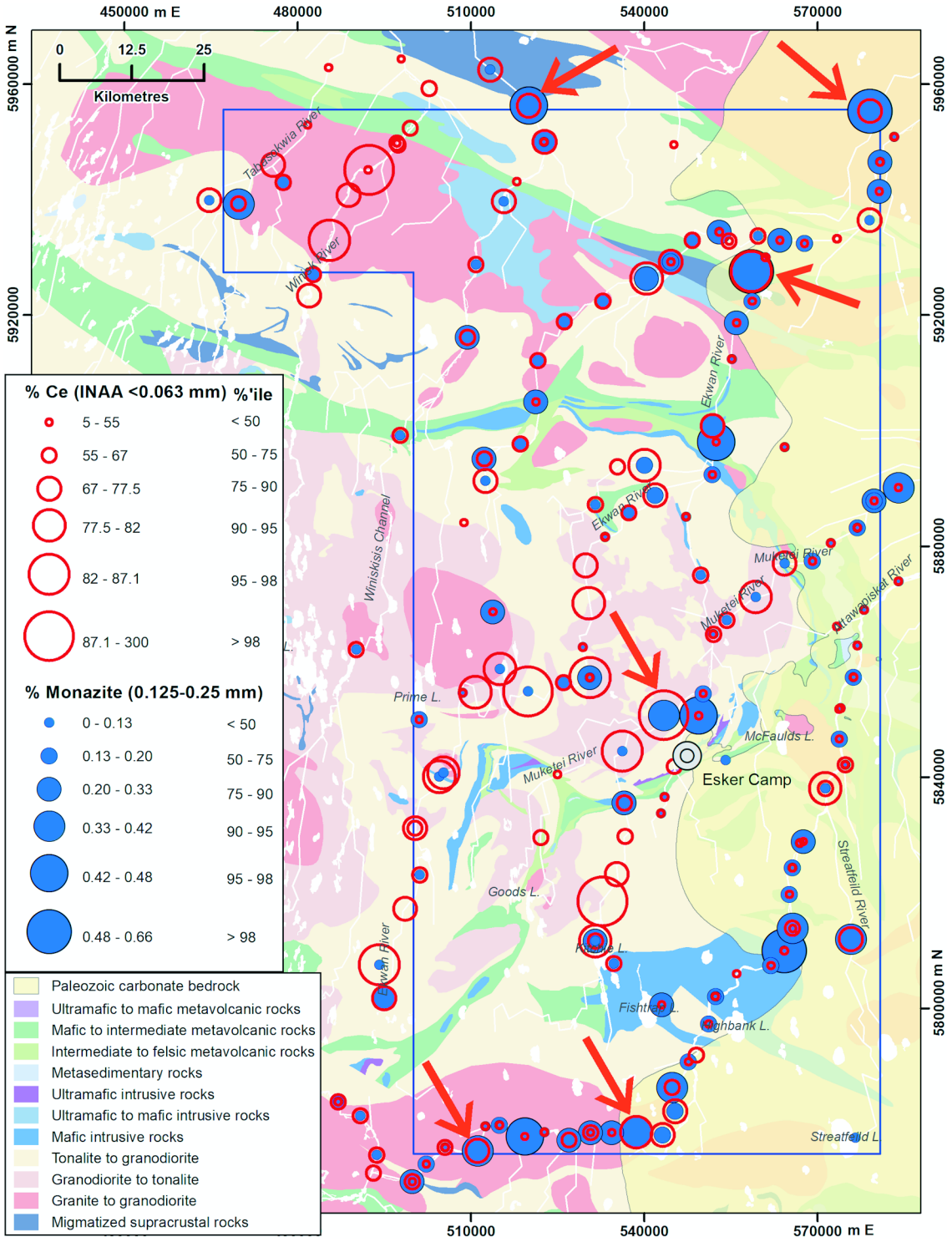


Figure 21.4. Comparison between detrital monazite grains in fine-fraction heavy mineral concentrate (HMC) and cerium (Ce) in till matrix (<0.063 mm), indicating that several samples that have anomalous numbers of monazite (>90 percentile) are, as indicated by red arrows, high to anomalously high in their concentration of cerium (>75 percentile), which is a major element of this mineral. Furthermore, most of these samples also show high to anomalously high concentration of lanthanum (La), another major element of this mineral, as shown in Figure 21.5. All UTM co-ordinates provided using NAD83 in Zone 16.

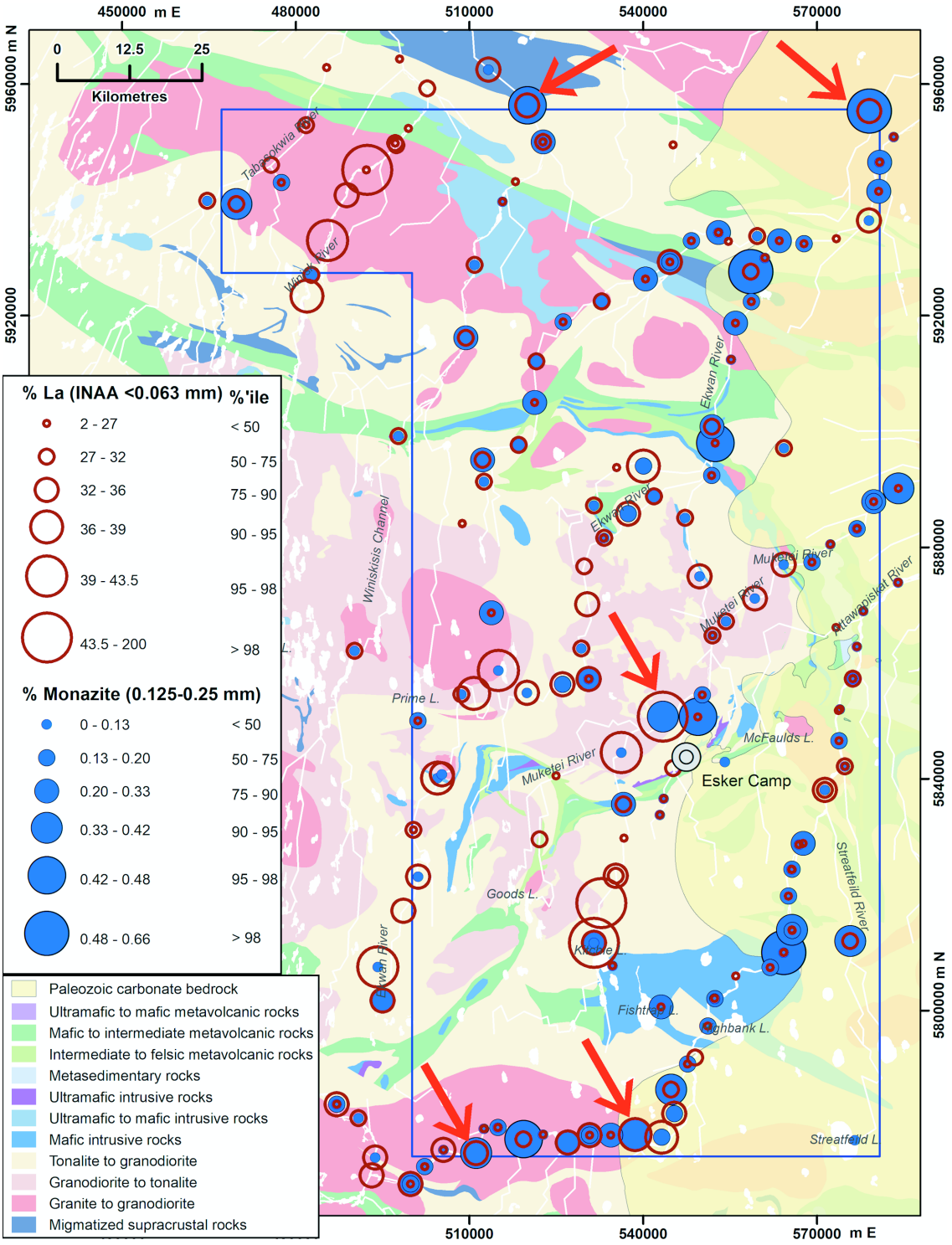


Figure 21.5. Comparison between detrital monazite grains in fine-fraction heavy mineral concentrate (HMC) and lanthanum (La) in till matrix (<0.063 mm), indicating that several samples, with anomalous amounts of this mineral (>90 percentile), are, as indicated by red arrows, high to anomalously high in their concentration of lanthanum (>75 percentile), which is a major element of this mineral. Additionally, most of these samples also show high to anomalously high concentration of cerium (Ce) (*see* Figure 21.4) and thorium (Th) (plot not provided), the other major elements of this mineral. This suggests that the elements present in anomalously high concentrations in these samples likely came from monazite-bearing bedrock. All UTM co-ordinates provided using NAD83 in Zone 16.

ACKNOWLEDGMENTS

Johanne Roux (OGS), Jose Pallot (Geo Labs) and Andy Bajc (formerly OGS) are thanked for help in retrieving the archived samples. Andrew McDonald (Laurentian University) provided insightful comments on the minerology of monazite. Manuel Duguet (ERGMS) and Riley Mulligan (ERGMS) reviewed the manuscript with many edits and helpful comments.

REFERENCES

Bajc, A.F. 1991a. Till sampling survey, Fort Frances area: Results and interpretation; Ontario Geological Survey, Study 56, 263p.

——— 1991b. Till sampling survey, Fort Frances area: Results and interpretation. Data to accompany Study 56: Ontario Geological Survey, Miscellaneous Release—Data 8.

Gao, C. and Crabtree, D.C. 2016. Results of regional till and modern alluvium sampling in the McFaulds Lake ("Ring of Fire") area, northern Ontario; Ontario Geological Survey, Open File Report 6309, 164p.

Gao, C., Crabtree, D.C., Clarke, S.A. and Yeung, K.H. 2023. Indicator mineral and bulk geochemistry data of the till and other surficial samples collected in the Pickle Lake–Cat Lake area, northern Ontario; Ontario Geological Survey, Miscellaneous Release—Data 388.

Gao, C., Crabtree, D.C., Dyer, R.D. and Clarke, S.A. 2021. Indicator mineral and geochemistry data for a till and alluvium sampling survey in the McFaulds Lake ("Ring of Fire") area, northern Ontario; Ontario Geological Survey, Miscellaneous Release—Data 322 – Revised.

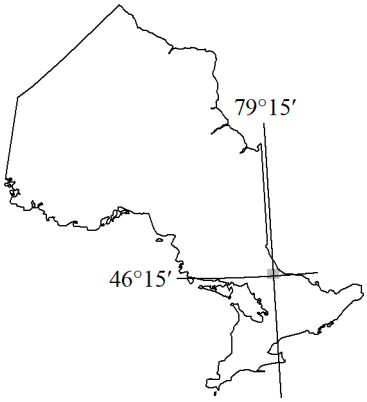
Gao, C., Hagedorn, G.W. and Crabtree, D.C. 2023. Surficial sampling in Ontario: Past, present, and future; abstract *in* Geological Association of Canada–Mineralogical Association of Canada–Society for Geology Applied to Mineral Deposits, Annual Meeting, Sudbury, Ontario, May 25–27, Abstracts, v.46, Geoscience Canada, v.50, p.143.

Hastie, E.C.G., Petrus, J.A., Gibson, H.L. and Tait, K.T. 2020. Gold Fingerprinting: Using major and trace elements associated with native gold to work toward a global gold database; *in* Summary of Field Work and Other Activities, 2020, Ontario Geological Survey, Open File Report 6370, p.10-1 to 10-10.

Melo-Gómez, J.D., Hastie, E.C.G., Gibson, H.L., Tait, K.T. and Petrus, J.A. 2022. Trace element content of gold across Ontario: An update on the Gold Fingerprinting Project; *in* Summary of Field Work and Other Activities, 2022, Ontario Geological Survey, Open File Report 6390, p.15-1 to 15-11.

Metsaranta, R.T., Houlé, M.G., McNicoll, V.J. and Kamo, S.L. 2015. Revised geological framework for the McFaulds Lake greenstone belt, Ontario; Geological Survey of Canada, Open File 7856, p. 61-73.

22. Project NE-23-007. Quaternary Geological Mapping of the Eastern Part of the Lake Nipissing Basin, Northeastern Ontario: An Update Half a Century in the Making



A.S. Marich[1]

[1]Earth Resources and Geoscience Mapping Section, Ontario Geological Survey

INTRODUCTION

Quaternary geological mapping provides insights into the surficial sediments, landforms and glacial history of a region. This report summarizes some preliminary findings from the second year of a multi-year mapping project covering the area between Hagar and Mattawa along the Highway 17 corridor in northeastern Ontario (Figure 22.1) (Marich 2022). Existing maps for this area were completed by Harrison (1972) at a scale of 1:125 000 and Boissonneau (1967) at a scale of 1:508 680. However, high-resolution mapping at a scale of at least 1:50 000 is required for many land-use planning activities, including agricultural soils suitability mapping, aggregate resource identification, as well as geotechnical and engineering applications. Thus, this project was developed to fill the gap in 1:50 000 scale mapping, as well as to improve understanding of the glacial history of the area.

This high-resolution mapping is greatly assisted by the availability of new high-resolution digital terrain models (DTMs) derived from lidar (light detection and ranging) imagery, as well as aerial photography for the region, acquired by the Ministry of Natural Resources and Forestry (Ministry of Northern Development, Mines, Natural Resources and Forestry 2022a, 2022b). The DTMs have approximately 10 cm vertical and horizontal resolution and show the land surface without vegetation or anthropogenic features, thereby permitting the delineation of landforms in much greater detail than was previously possible. The DTMs also facilitate the identification of critical locations to collect field data to better understand the composition of observed landforms and to produce detailed and accurate surficial maps.

LOCATION AND PHYSIOGRAPHY

Field work for the summer of 2023 was focussed primarily in the areas surrounding the City of North Bay, covering an area of approximately 2200 km^2 (*see* Figure 22.1).

The study area consists of primarily bedrock-controlled topography with thin (<5 m) to no sediment, except in low-lying bedrock valleys, moraines and ice-contact features where sediments can reach up to 30 m thick. The primary bedrock feature in the area is the Ottawa–Bonnechere Graben (Figure 22.2). The northern boundary of the graben is marked by a steep cliff face about 20 to 60 m high that extends from west of the study area and eastward out of the study area toward Mattawa. North of the graben, bedrock is commonly exposed at surface, except where it is locally buried by drumlins or streamlined till plains, eskers, deltas, and moraines. Modern-day Lake Nipissing occupies the broad, flat-lying topography

Summary of Field Work and Other Activities, 2023,
Ontario Geological Survey, Open File Report 6405, p.22-1 to 22-10.

© King's Printer for Ontario, 2023

present in the central Ottawa–Bonnechere Graben (*see* Figure 22.1). A series of streamlined landforms composed of bedrock or sediment cores also occupy this part of the graben. Parallel to the northern boundary of the graben is a series of lakes (including Trout Lake, Turtle Lake and Lake Talon) oriented predominantly west to east, draining eastward to the Mattawa River. To the south and southeast, topography rises to form the Almaguin (Algonquin) Highlands.

METHODS

Field work was conducted between June and August of 2023. More than 1000 observations of surface materials and landforms were made (*see* Figure 22.1). In addition, 24 C-horizon till and 2 heavy mineral sand samples were collected. Fifty ice-flow indicator measurements were also made. Sampling occurred along roads, forestry roads and trails accessed using truck or by foot. Samples were obtained from hand-dug pits (up to 1.5 m deep), roadcuts, roadside ditches, stream cutbanks and excavations. Sampling density is irregular because much of the area is covered by very thin drift; as a result, till was

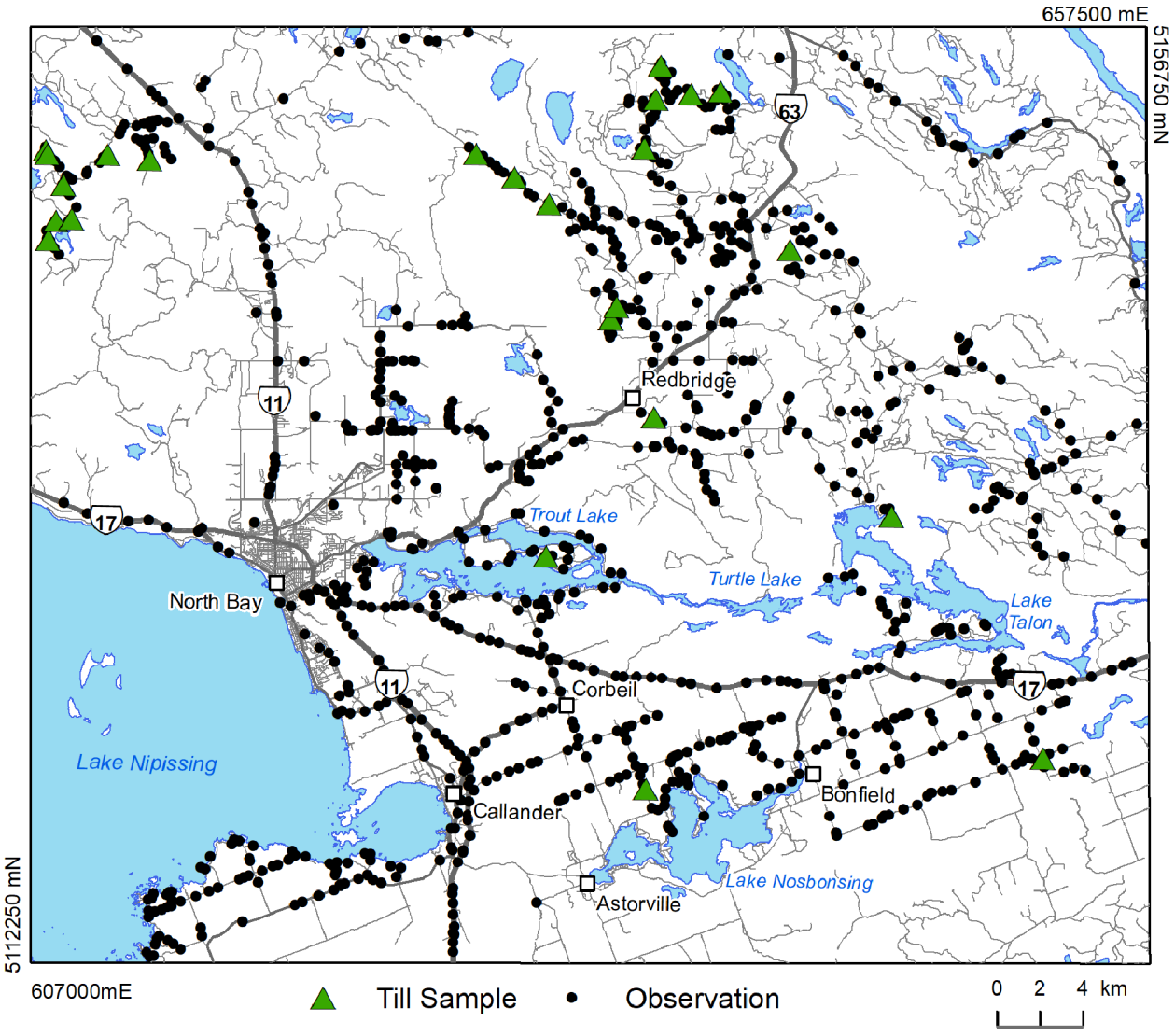


Figure 22.1. Map showing the locations of field observations and till sample sites in the study area. Observation sites are located along transportation routes and forest resource roads. Universal Transverse Mercator (UTM) co-ordinates provided using North American Datum 1983 (NAD83) in Zone 17.

sampled when it was encountered. Samples were screened in the field to remove the +5 mm fraction; this fraction will be used for pebble lithology counts. At each sample site, 2 samples of C-horizon till were collected: 1) a 10 kg sample for heavy mineral concentration and recovery of gold grains, kimberlite indicator minerals (KIM) and metamorphic/magmatic massive sulphide indicator minerals (MMSIM® [2]) and 2) a 2 to 3 kg sample for −63 µm fraction geochemical analysis and grain size determination. These sampling procedures follow standard protocols used by the Ontario Geological Survey (e.g., Bajc 1999).

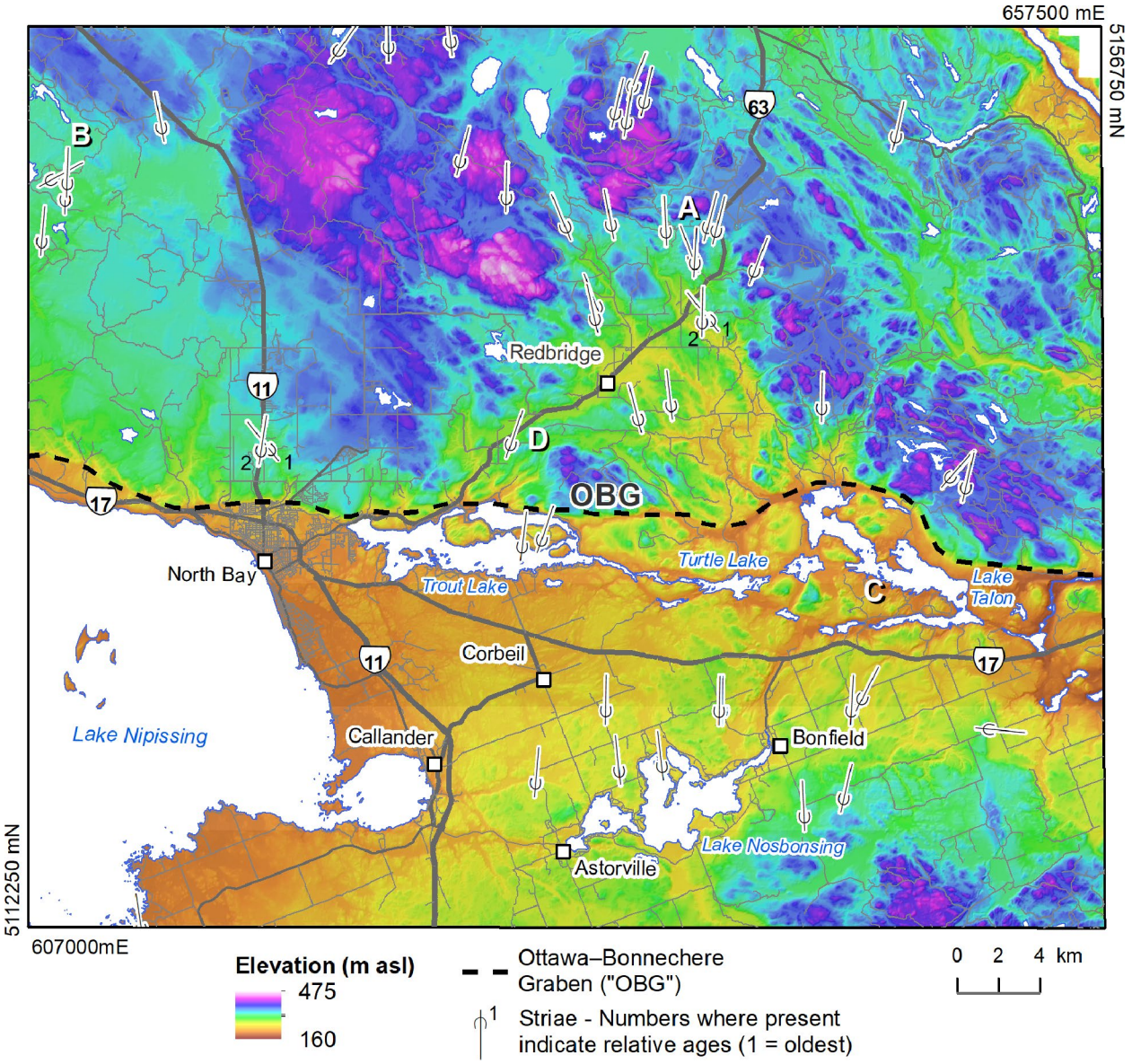


Figure 22.2. Digital terrain model (hill-shade image) of the study area (data *from* Ministry of Northern Development, Mines, Natural Resources and Forestry 2022b). In addition, ice-flow directions measured during this study are shown. The northern boundary of the Ottawa–Bonnechere Graben (OBG) is indicated by the dashed black line. Letters indicate locations of photographs in Photo 22.1. Numbers on striae symbols indicate relative ages, where 1 is the oldest. All UTM co-ordinates provided using NAD83 in Zone 17.

[2] *MMSIM is a registered trademark of Overburden Drilling Management Limited, Nepean, Ontario.*

BEDROCK GEOLOGY

The study area is located within the Central Gneiss Belt of the Grenville Province. These rocks are extremely metamorphosed and are between 1.2 to 2.7 billion years old (Figure 22.3). The most dominant rock type in the study area, occupying much of the central and western portions, are migmatitic rocks including gneisses of undetermined protolith. Felsic igneous rocks (including tonalite, granodiorite, monzonite, granite and syenite-derived gneisses) occur in the northwestern part, as well as the southern half, of the study area, and underlie Lake Nipissing. Mafic rocks, including amphibolite, gabbro, diorite and mafic gneisses, occur in small pockets in the eastern and southern portions of the study area. The northeastern part of the study area is occupied by gneisses of metasedimentary origin, which include quartzofeldspathic, pelitic to semi-pelitic, calc-silicate gneisses, as well as minor quartzite, marble and

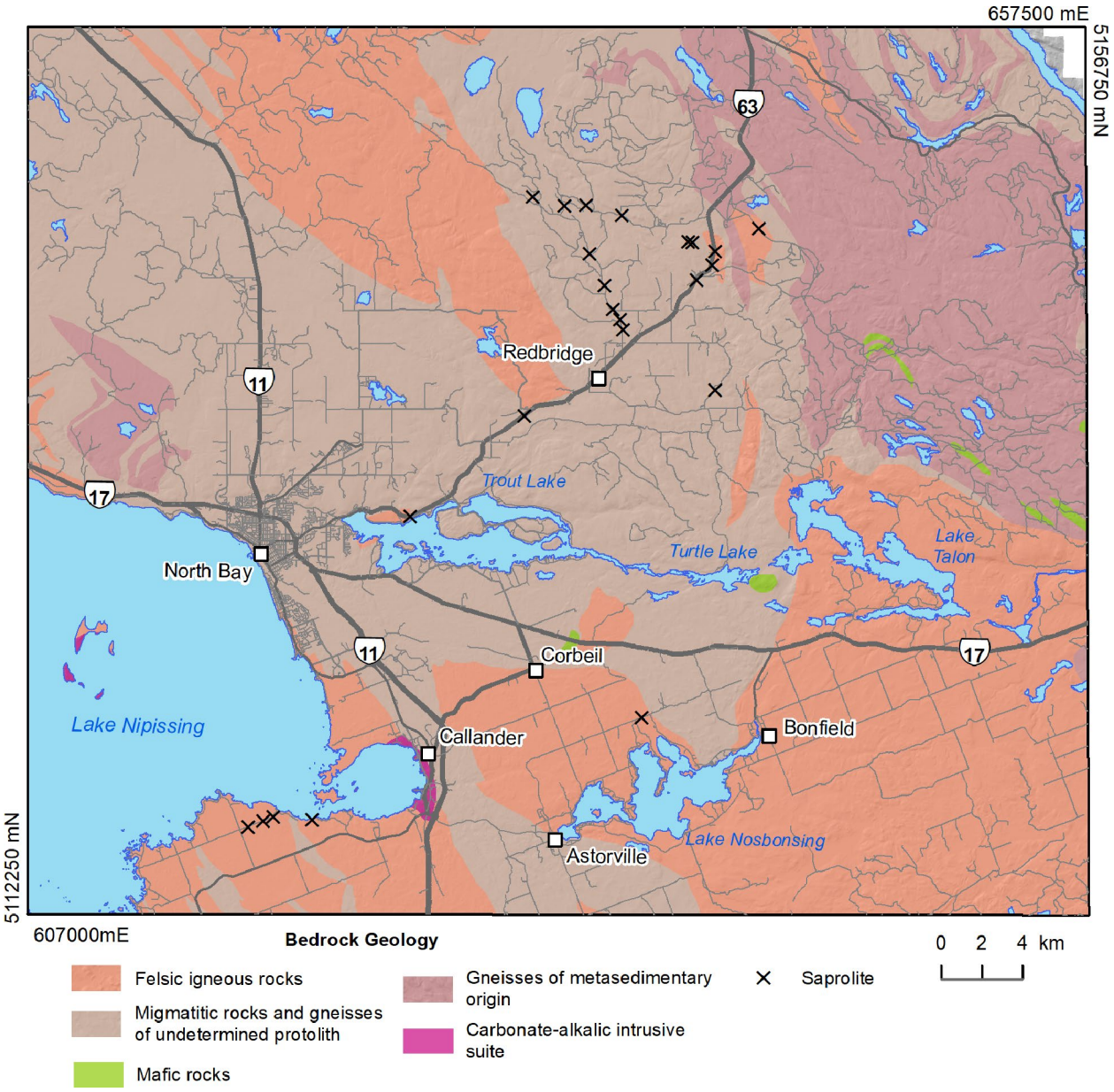


Figure 22.3. Simplified bedrock geology (*modified from* Ontario Geological Survey 2011) of the study area, including locations (indicated by ×) where saprolite was observed during the summer of 2023. All UTM co-ordinates provided using NAD83 in Zone 17.

marble breccia. Carbonatite and alkalic complexes occur as islands in Lake Nipissing, and the Callander complex occupies much of Callander Bay (located at the town of Callander at the southeastern end of Lake Nipissing) (*see* Figure 22.3). Rocks within these complexes include quartz fenite, aegirine-potassic feldspar fenite, nepheline syenite, and lamprophyre basaltic and phonolitic dikes (Lumbers 1971). The study area is crosscut by multiple diabase and pegmatite dikes, with many of the diabase dikes being associated with the extension of the Ottawa–Bonnechere Graben (Lumbers 1971). Small outliers of upper Ordovician rocks occur on the Manitou Islands and to the south of Lake Nipissing (cf. Kang and Dix 2021).

Also of note is a series of outcrops showing extreme physical and chemical weathering. The bedrock is easily sampled by hand, and its weathered components crumble to the size of very coarse-textured sand. Occurrence of this saprolite (Photo 22.1A) has been noted by both Lumbers (1971) and Harrison (1972) although little was discussed regarding its evolution and extent. Both of these studies suggest that the saprolite was found only below the lowest glacial lake levels during the last deglacial period. They observed the saprolite in hills of thin drift on both north- and south-facing slopes. The current study has expanded the aerial extent of saprolite deposits (*see* Figure 22.3). The vertical depth of weathering varies from a few metres to more than 15 m in at least 1 location near Redbridge. Lumbers (1971) and Harrison (1972) both suggested this saprolite is derived from granitic gneiss and the horizontal bedding observed



Photo 22.1. Photographs of rocks and features in the study area. **A)** Highly weathered granitic gneiss (saprolite). **B)** Glacially polished and striated bedrock; ice-flow direction is approximately from the left to right in the photograph (south-southwest). Compass is 17 cm long. **C)** Cross section through a De Geer moraine showing boulder lag at surface. Person for scale is approximately 1.8 m tall. **D)** Rhythmically bedded fine-textured glaciolacustrine sediment. Red laminae are clay, and pale greyish-brown beds are silt.

in outcrop corroborates this. A detrital zircon study of this material (*see* Easton, Marich and Wall, this volume) near Redbridge indicates that it was derived from the Mulock granite intrusion that was emplaced at *circa* 1250 Ma. The current study has also extended the contact of the Mulock granite with its host migmatitic gneiss and is now interpreted to be located 3 to 4 km farther east than previously shown on geological maps (Lumbers 1971; Easton 2006).

QUATERNARY GEOLOGY

All of northeastern Ontario was covered by the Laurentide Ice Sheet during the last glacial maximum about 20 000 years ago. The landforms and sediments observed in the modern landscape are primarily a result of events occurring the late-stage glaciation and deglaciation of the region. Deglaciation of the study area progressed between ~13 500 and 11 000 calibrated radiocarbon years before present (Dalton et al. 2020) and consisted of a retreating and thinning ice margin fronted by large proglacial lakes that included glacial lakes Algonquin and the Nipissing phase of the upper Great Lakes (e.g., Karrow 2004). Additional field work and terrain model studies are required to further refine the timing of glacial events specific to this area.

The study area is dominated by regions of exposed bedrock and thin drift. The thickest successions of sediments include till deposits that form streamlined landforms or moraine ridges, and sand sequences comprising large proglacial outwash features, eskers or ice-contact delta systems.

Ice-flow indicators (e.g., striae, grooves, chatter marks, nail head striae) were measured at 50 locations (*see* Figure 22.2; Photo 22.1B). These measurements show a general trend southward (close to 180°), with a few exceptions showing ice flow to the southwest or southeast (*see* Figure 22.2). Most of these likely reflect local ice flow around topographic obstacles (e.g., bedrock knobs). Two crosscutting striae sites show an earlier flow of 140° (i.e., southeast) with a later flow of around 180° (i.e., south). It is possible that these measurements represent 2 distinct ice-flow directions in the area: they were measured more than 20 km apart north of the City of North Bay and northeast of the community of Redbridge. Work to identify ice-flows directions in the western half of the Nipissing Basin (Marich 2022) also identified a possible older flow trending southwest to west.

The oldest sediment observed to-date in the study area is a silty sandy till with varied clast content that ranges up to about 10%. Clast lithologies are predominantly local crystalline rock of the Grenville Province with some farther-travelled Huronian Supergroup rocks, such as those of the Gowganda Formation, as well as Archean volcanic and sedimentary rocks sourced from greenstone belts farther north (e.g., the Temagami greenstone belt). The till is most commonly found in the lee-side of bedrock knobs forming crag-and-tail features, drumlins and within low-relief ridges interpreted as De Geer moraines. The streamlined features (crag-and-tail and drumlins) vary in length from a few metres to upward of a kilometre. They tend to occur in groups throughout the study area and the average orientation of the long axes of groups of these features represent local ice-flow direction at that location and are consistent with local striae measurements. The main ice-flow directions based on these landform groups vary from southeast to south to southwest across the study area from Lake Nipissing toward Mattawa.

The De Geer moraines are generally low relief (1–2 m) ridges that form parallel to the retreating ice margin and can mark yearly stillstands of the retreating ice (e.g., Lindén and Möller 2005). Although Harrison (1972) hinted at their presence, this study is the first to map De Geer moraines in the North Bay to Mattawa area. The moraines can vary in length, often with gaps between sections of the moraines, but they are generally evenly spaced (~100 m spacing). They are found as groups of moraines (fields) throughout the study area (e.g., Figure 22.4A). The De Geer moraines have been divided into 3 types based on morphology: 1) well developed, 2) topographically controlled and 3) poorly developed (Marich 2023). Well-developed De Geer moraines are continuous over approximately 5 m to tens of metres,

overprint streamlined landforms, and their spacing appears unaffected by the underlying topography. In comparison, the topographically controlled De Geer moraines rarely overprint the highest local topography, and the ridge spacing and orientation varies along their length, which is likely reflective of a thinning ice margin affected by local variations in bedrock topography. Poorly developed De Geer moraines overprint streamlined landforms and show some patterns in spacing, but are generally highly discontinuous and spacing is inconsistent over larger areas.

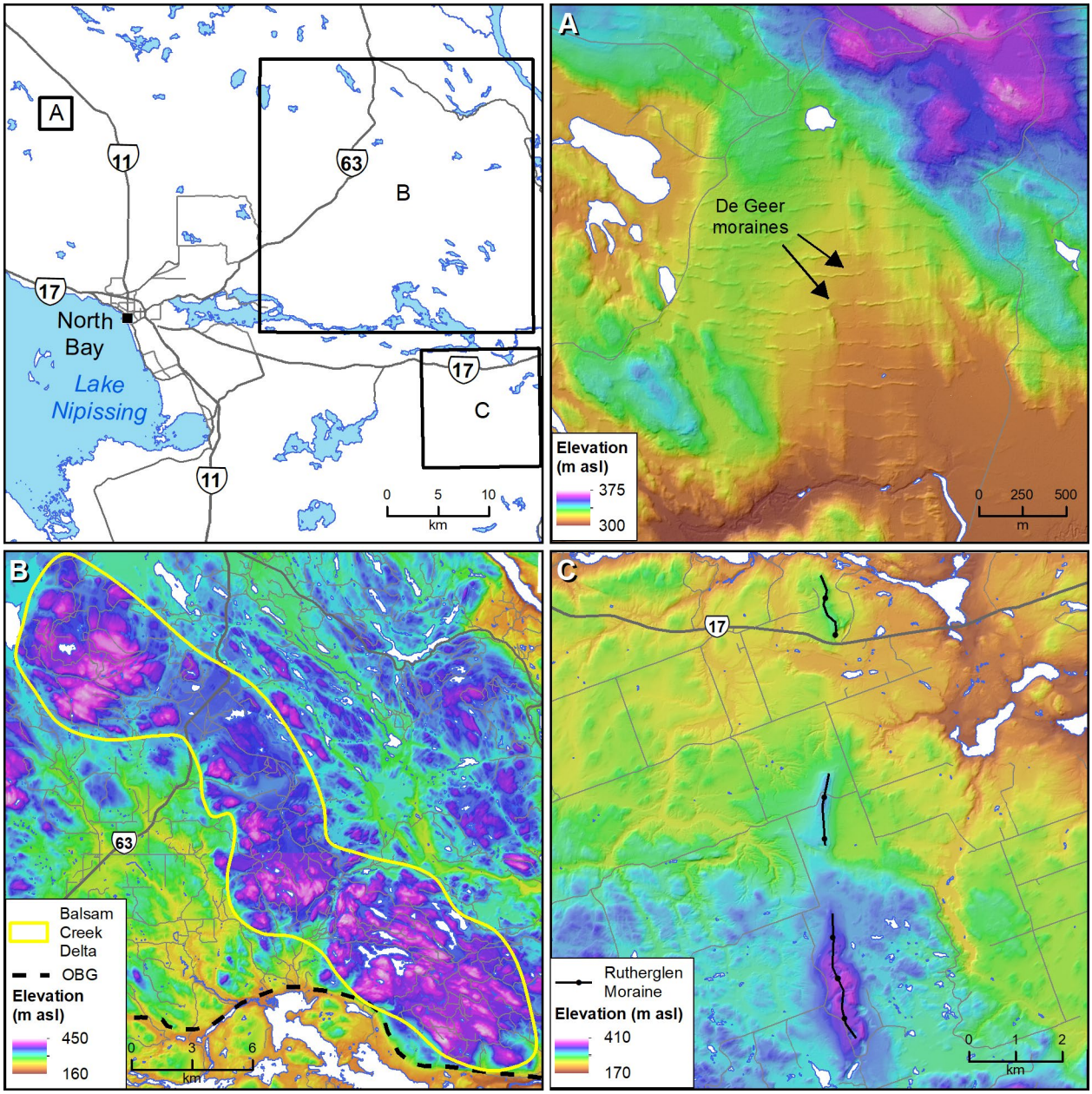


Figure 22.4. Figure in upper left shows the location of the inset figures A, B and C with respect to the boundaries of the study area. In A, B and C, the digital terrain model (hill-shade image) is based on data from the Ministry of Northern Development, Mines, Natural Resources and Forestry (2022b). **A)** Arrows point to well-developed De Geer moraines located northwest of the City of North Bay. **B)** The location of the Balsam Creek delta (yellow outline) northeast of North Bay (OBG, Ottawa–Bonnechere Graben). **C)** The location of the Rutherglen moraine east of North Bay.

The sediments observed within the De Geer moraines vary from poorly sorted, fissile, silty sandy diamicton to well-sorted to laminated and bedded sands with minor clast content. Many of the De Geer moraine ridges observed in the field were capped by a boulder lag, with clasts ranging from a few centimetres up to 1 or 2 m in diameter (Photo 22.1C). The boulder lag likely indicates a winnowing of sediment from the moraines as a result of wave action after they were formed. Till samples were collected from multiple De Geer moraines to characterize the sediment grain size and geochemistry. Samples from streamlined features underlying the De Geer moraines were also collected so a comparison could be made and to determine whether De Geer moraines are a result of reworking of existing sediments or deposits of new material brought in by the retreating glacier. In addition, 4 till fabrics (50 clasts per fabric) were measured within 4 separate well-developed De Geer moraines to provide additional information on the ice-marginal environment and ice-flow direction active during their formation.

Glaciofluvial ice-contact sands and gravels are observed within eskers and deltas within the study area. Three large esker systems oriented north-to-south, parallel to Highway 11, are located north of North Bay, with an additional large esker located just east of Bonfield. These stratified deposits are dominated by sand, but contain minor pockets of gravel. The Balsam Creek delta, located northeast of North Bay and north of the Ottawa–Bonnechere Graben, is a large flat-topped landform with a steep northeastern (up-ice) side and gradual down-ice or lakeside slope (Figure 22.4B). The landform is part of an ice-marginal complex, approximately 35 km long and approximately 6 km wide, that rises approximately 30 m above the surrounding terrain. Numerous bedrock knobs occur within the delta rising above its surface. This landform is generally sand dominated, although boulder lags were observed at several locations on the delta surface.

Another significant landform in the study area is the Rutherglen moraine (Figure 22.4C). This feature is a large north-trending ridge that is approximately 10 km long with a 2.5 km gap at its northern end. The moraine varies from approximately 500 m to 1 km in width and rises higher than 50 m above the surrounding land surface at its southern end. Along the eastern flank of the moraine is a series of terraces, developed by dropping water levels in glacial Lake Algonquin. There are fewer and less well-developed terraces on the western flank. This landform is composed primarily of ice-contact stratified drift, varying from cobble-rich gravel to medium-fine-textured sands. It is likely that this landform represents a stillstand position of the Laurentide Ice Sheet and records a major shift in ice-flow direction as it retreated from the area. Streamlined bedforms and striae measurements to the east of this linear ridge are oriented almost east-to-west and those to the west of the ridge are oriented northeast-to-southwest. A single striae measurement on the eastern flank of the Rutherglen moraine shows an ice-flow direction of 270° (i.e., west), which is unique in the area, but may reflect ice flow toward the moraine at the time of its formation (*see* Figure 22.2). This area will be targeted, during future field work, for additional ice-flow measurements to clarify this preliminary interpretation.

Much of the study area was occupied by proglacial lakes during deglaciation, resulting in deposits of silt and clay throughout the region. These sediments occupy many of the low-lying topographic areas and consist primarily of fine-textured sands or laminated silt and clay. The fine-textured sands are commonly observed adjacent to topographic highs and represent sediments deposited in nearshore glaciolacustrine environments. For example, laminated very-fine to fine-textured sands drape the flanks of the Rutherglen moraine and are underlain by laminated silt and clay. In some cases, the silt and clay are rhythmically bedded, and may be varves, although further work is required to confirm this. These rhythmically bedded sediments consist of couplets of pale grey-brown silt beds ranging in thickness from 2 to 4 cm, and pale red clay laminae commonly 2 to 4 mm thick (Photo 22.1D). The red clay laminae are striking when observed in the field and, notably, they were not observed in lake sediments of the western part of the Lake Nipissing Basin. Additional work is being conducted to further characterize the lake sediments and to identify the source of the red clay. Harrison (1972) briefly described and completed grain size analyses on these clay beds (0.4% sand, 33% silt, 67% clay), but did not elaborate on their source.

The youngest sediments observed within the study area are modern alluvium that consist of organic rich silts and sands and organic deposits (peat and muck). These deposits are observed within active river flood plains and wetlands in poorly drained low-lying areas.

FUTURE WORK

Field work is planned for the summer of 2024 in the area between North Bay and Mattawa. Future work will focus on characterizing the surficial sediments, and refinement of the understanding of glacial history in the area.

ACKNOWLEDGMENTS

The author would like to thank Cyllanie Henry and Mitchell Davies for their exceptional assistance in the field; the success of the summer's field work was largely a result of their hard work. Additional thanks go to Ontario Geological Survey (OGS) staff Riley Mulligan, Shirley Péloquin, Michael Easton and Thomas Gemmell for ongoing discussions of both Quaternary and Precambrian geology relevant to the study area.

The author would also like to thank the Algonquins of Pikwakanagan First Nation, Dokis First Nation, Nipissing First Nation, Henvey Inlet First Nation, Wolf Lake First Nation, Eagle Village First Nation, Métis Nation of Ontario – Mattawa Métis Council and Métis Nation of Ontario – Ottawa Métis Council for allowing the Ontario Geological Survey to map their traditional land use area.

A thorough and insightful review of this manuscript was completed by Riley Mulligan and is greatly appreciated.

REFERENCES

Bajc, A.F. 1999. Results of regional humus and till sampling in the eastern part of the Shebandowan greenstone belt, northwestern Ontario; Ontario Geological Survey, Open File Report 5993, 85p.

Boissonneau, A.N. 1967. Algoma, Sudbury, Timiskaming and Nipissing, surficial geology; Ontario Department of Lands and Forests, Map S465, scale 1:506 880.

Dalton, A.S., Margold, M., Stokes, C.R., Tarasov, L., Dyke, A.S., Adams, R.S., Allard, S., Arends, H.E., Atkinson, N., Attig, J.W., Barnett, P.J., Barnett, R.L., Batterson, M., Bernatchez, P., Borns, H.W., Breckenridge, A., Briner, J.P., Brouard, E., Campbell, J.E., Carlson, A.E., Clague, J.J., Curry, B.B., Daigneault, R-A., Dube-Loubert, H., Easterbrook, D.J., Franzi, D.A., Friedrich, H.G., Funder, S., Gauthier, M.S., Gowan, A.S., Harris, K.L., Hétu, B., Hooyer, T.S., Jennings, C.E., Johnson, M.D., Kehew, A.E., Kelley, S.E., Kerr, D., King, E.L., Kjeldsen, K.K., Knaeble, A.R., Lajeunesse, P., Lakeman, T.R., Lamothe, M., Larson, P., Lavoie, M., Loope, H.M., Lowell, T.V., Lusardi, B.A., Manz, L., McMartin, I., Nixon, C., Occhietti, S., Parkhill, M.A., Piper, D.J.W., Pronk, A.G., Richard, P.J.H., Ridge, J.C., Ross, M., Roy, M., Seaman, A., Shaw, J., Stea, R.R., Teller, J.T., Thompson, W.B., Thorleifson, L.H., Utting, D.J., Veillette, J.J., Ward, B.C., Weddle, T.K. and Wright, H.E. 2020. An updated radiocarbon-based ice margin chronology for the last deglaciation of the North American Ice Sheet Complex; Quaternary Science Reviews, v.234, paper 106223. doi.org/10.1016/j.quascirev.2020.106223

Easton, R.M. 2006. Geology of the Songris area; Ontario Geological Survey, Preliminary Map P.2847, scale 1:50 000.

Harrison, H.E. 1972. Quaternary geology of the North Bay–Mattawa region, Ontario–Quebec; Geological Survey of Canada, Preliminary Map 3-1971, scale 1:125 000.

Kang, H. and Dix, G.R. 2021. Upper Ordovician (Sandbian–Katian) carbonate outliers in the northern Ottawa–Bonnechere Graben (central Canada): Records of transgressions and sedimentation patterns in the Laurentian platform interior; Canadian Journal of Earth Sciences, v.58, p.1-20.

Karrow, P.F. 2004. Algonquin-Nipissing shorelines, North Bay, Ontario; Géographie physique et Quaternaire, v.58., no.2-3, p.297-304.

Lindén, M. and Möller, P. 2005. Marginal formation of De Geer moraines and their implications to the dynamics of grounding-line recession; Journal of Quaternary Science, v.20, p.113-133.

Lumbers, S.B. 1971. North Bay area, Nipissing and Parry Sound districts; Ontario Department of Mines, Map 2216, scale 1:126 720.

Marich, A.S. 2022. Quaternary geological mapping of the Lake Nipissing Basin, Highway 17 corridor, northeastern Ontario; *in* Summary of Field Work and Other Activities, 2022; Ontario Geological Survey, Open File Report 6390, p.17-1 to 17-9.

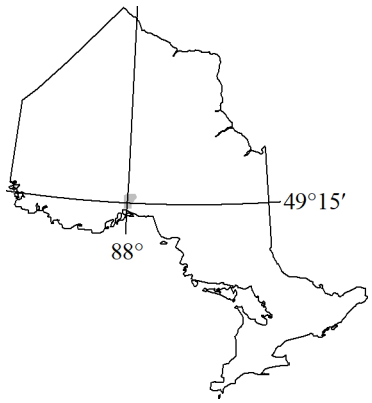
——— 2023. Drumlins, De Geers, and deltas – lidar and landform interpretations within the Lake Nipissing Basin, northeastern Ontario; abstract *in* Geological Association of Canada–Mineralogical Association of Canada–Society for Geology Applied to Mineral Deposits, Annual Meeting, Sudbury, Ontario, May 25–27, Abstracts, v.46, Geoscience Canada, v.50, p.180.

Ministry of Northern Development, Mines, Natural Resources and Forestry 2022a. Central Ontario Orthophotography Project (COOP) 2021; Ministry of Northern Development, Mines, Natural Resources and Forestry, Spatial Data Support Unit, Peterborough, Ontario.

——— 2022b. Ontario digital terrain model (lidar-derived) - Lake Nipissing 2020 DTM; Ministry of Northern Development, Mines, Natural Resources and Forestry, Provincial Mapping Unit, Peterborough, Ontario.

Ontario Geological Survey 2011. 1:250 000 scale bedrock geology of Ontario; Ontario Geological Survey, Miscellaneous Release—Data 126 – Revision 1.

23. Project NW-23-002. Till Sampling and Surficial Mapping in the Georgia Lake Area, Northwestern Ontario



G.W. Hagedorn[1] and C.E. Beckett-Brown[1]

[1]Earth Resources and Geoscience Mapping Section, Ontario Geological Survey

INTRODUCTION

Understanding the influence of the Laurentide Ice Sheet on the landscape is important for drift prospecting and local communities. Lodgment till, material deposited at the subglacial interface by a moving ice sheet, can be sampled to explore for buried mineral deposits that may be difficult to discover with more traditional exploration methods. Other types of sediments deposited by an ice sheet, such as glaciofluvial sands and gravels, are important for land-use planning considerations and material used as aggregate for infrastructure development. Furthermore, the distribution and stratigraphy of surficial sediments indicates how the ice sheet moved over the landscape constraining ice sheet reconstructions which are used in past climate modelling.

The recent focus of governments on critical minerals (Ontario 2022; Canada 2022) has made the Georgia Lake rare-element pegmatite field, an area of active exploration in Ontario, of particular interest with respect to its Quaternary geology (Figure 23.1). The region has had no detailed (1:50 000 scale) surficial mapping, with only small-scale maps available, derived from limited field work (Prest, Grant and Rampton 1968; Barnett, Cowan and Henry 1991). Furthermore, the area represents a gap in the regional till sampling distribution across Ontario, comprising an area between an Operation Treasure Hunt study area to the northwest (Dyer and Barnett 2005), Shebandowan to the southwest (Bajc 1999), Schreiber to the east (Morris 2000, 2001) and work by the Geological Survey of Canada in the Geraldton area to the north (Thorleifson and Kristjansson 1993). The southern border of the area is Lake Superior.

Deciphering the Quaternary geology of the Georgia Lake area is also important as it is close to several communities and major transport routes which require aggregates and proper understanding of the surficial sediments for further development. Additionally, glacial Lake Agassiz, the largest proglacial lake of the Laurentide Ice Sheet, drained along routes through the study area into Lake Superior during the deglaciation (Lowell et al. 2021; Fisher and Breckenridge 2022). Further study of this drainage and its routing will help understand the history of glacial Lake Agassiz and the past climate conditions.

The current project includes surficial geology mapping around the Georgia Lake rare-element pegmatite field to aid in mineral exploration and land-use planning for future deposit discovery and infrastructure development of the deposit. The mapping will take advantage of the newly released 10 cm resolution lidar (Ministry of Northern Development, Mines, Natural Resources and Forestry 2022). The project also includes regional till sampling (~10 km spacing), processed for both indicator minerals and bulk matrix geochemistry, to help identify the dispersal train from the Georgia Lake lithium-cesium-tantalum (LCT)-type pegmatites and identify if there are any other rare element pegmatites in the

Summary of Field Work and Other Activities, 2023,
Ontario Geological Survey, Open File Report 6405, p.23-1 to 23-9.

© King's Printer for Ontario, 2023

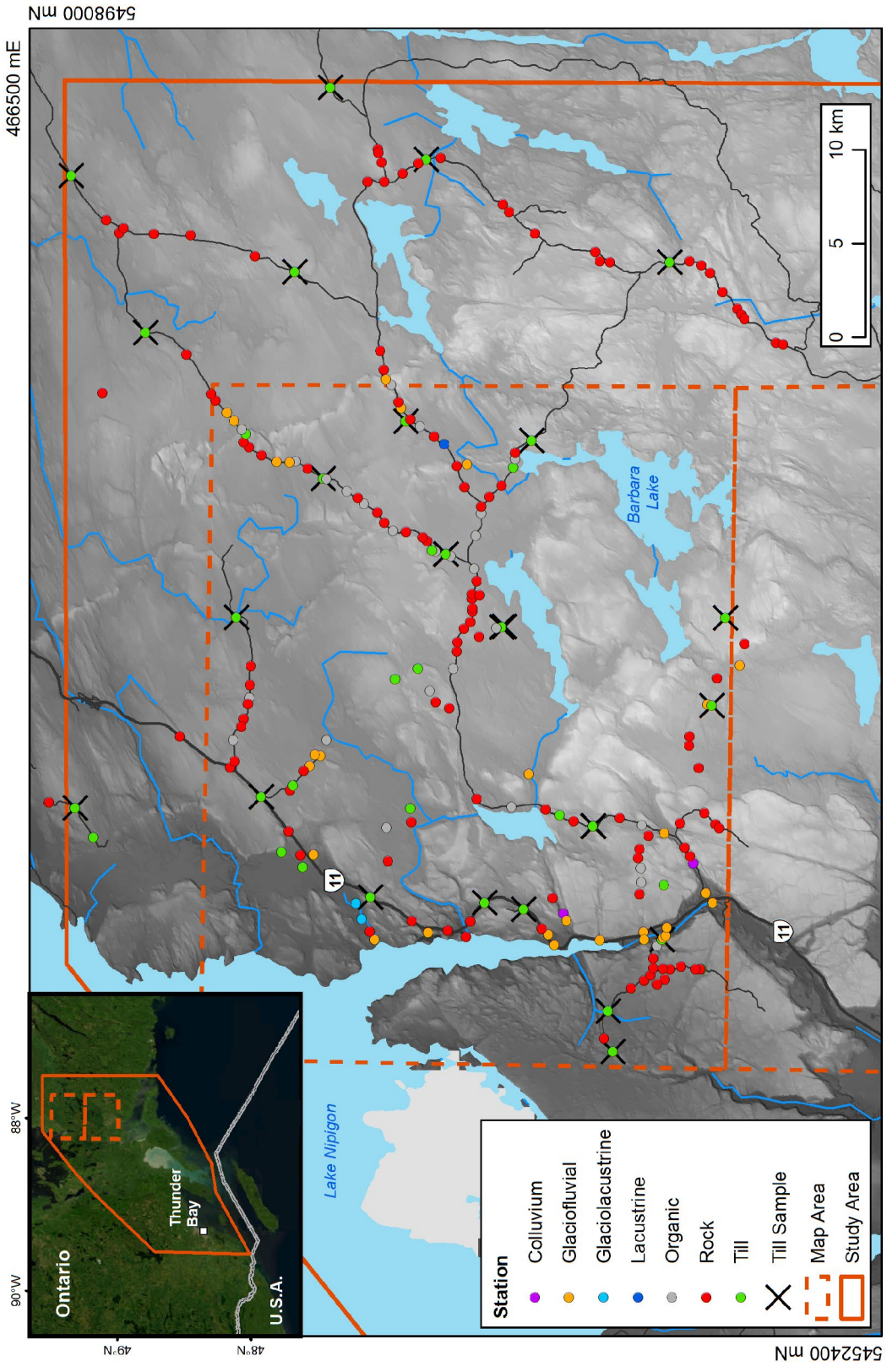


Figure 23.1. Field work during the summer of 2023 focussed on the northern part of the study area (within solid line). The 2 map areas to be completed are outlined by a dashed line, whereas the total study area for regional (10 km spacing) till sampling is outlined by the solid line. The various surficial materials encountered are represented by different colour dots (n=228). Till sample locations are indicated with an ×. Background image is the hill-shaded digital terrain model lidar (Ministry of Natural Resources and Forestry 2022). Inset map shows the study area in Ontario and the city of Thunder Bay (inset sources: Environmental Systems Research Institute, Inc. (ESRI®), Earthstar Geographics LLC and ArcGIS® User Community; image ©2023 Maxar Technologies Inc.). Universal Transverse Mercator (UTM) co-ordinates provided using North American Datum (NAD83) in Zone 16N.

region. The added benefit of till sampling is that it can also be used to assess and identify other potential mineral deposits that may be beneath the cover of surficial sediments in the study area. This article is a summary of field work completed during the summer of 2023 that focussed on the northern part of the study area (*see* Figure 23.1).

BACKGROUND

Bedrock Geology

There are 3 dominant bedrock types that underlie the northern part of the study area (Figure 23.2). The most extensive are rocks of the Archean Quetico Subprovince, which are composed of metamorphosed and ductily deformed turbidite sequences. The metasedimentary rocks of the Quetico Subprovince are relatively incompetent and are frequently eroded into lowlands. These metasedimentary rocks were intruded by several generations of plutonic rocks, of which the youngest two-mica granites are interpreted as the source for the Georgia Lake LCT-bearing pegmatites in the region (Breaks, Selway and Tindle 2008). These granites are more competent than their host rock forming a bedrock knob terrain when found at surface. The third major bedrock unit is composed of the Mesoproterozoic mafic sills of the Midcontinent Rift. The mafic sills are clearly the most resistant to erosion of the 3 dominant bedrock types, but are extensively weathered at surface where exposed. Consequently, the mafic sills create upland regions with steep relief on their flanks to form gorges. The various competency of these 3 bedrock units heavily influenced striation preservation potential, with the granite being the most suitable, although striations were observed on bedrock outcrops of all 3 units. For a detailed description of the bedrock geology, refer to Duguet (2019, 2020; *see also* Duguet, this volume).

Quaternary Geology

Previous small-scale surficial mapping shows a regionally pervasive ice flow to the southwest based on the streamlined landforms and eskers (parallel to ice flow) and the large moraine sequences (transverse to ice flow) (Prest, Grant and Rampton 1968; Barnett, Cowan and Henry 1991; Kristjansson and Thorleifson 1991). The area was covered by the Laurentide Ice Sheet until approximately 10 ka BP (Dalton et al. 2020), at which point, as a result of isostatic rebound and ice blocking of the southeastward drainage, glacial Lake Agassiz inundated the area. Glacial Lake Agassiz went through stages of filling and draining resulting from ice advance and retreat that periodically blocked drainage outlets (Lowell et al. 2021; Fisher and Breckenridge 2022).

Sediments at surface today are directly related to the glacial history of the landscape. To the north, 60 m thick sediments were documented over bedrock with 2 different till sheets in the stratigraphy (Thorleifson and Kristjansson 1993). The lower till has its material derived mostly from local bedrock sources and the upper till, which was commonly found at surface, is carbonate rich and has a distal source. Ice streams flowing to the southwest are suggested to have carried the carbonate material from the James Bay Lowland into the study area (Thorleifson and Kristjansson 1993). There is also an abundance of glaciofluvial material in the region in eskers, kames and fans, the thickest of which are observed in a meltwater channel between the Midcontinent Rift mafic sill uplands. Only limited glaciolacustrine material is found, with most occurring as a boulder lag at surface as a result of winnowing of previously deposited sediments. Modern sediments include lacustrine, alluvial and organic material of which organic and peat accumulation is most common at surface.

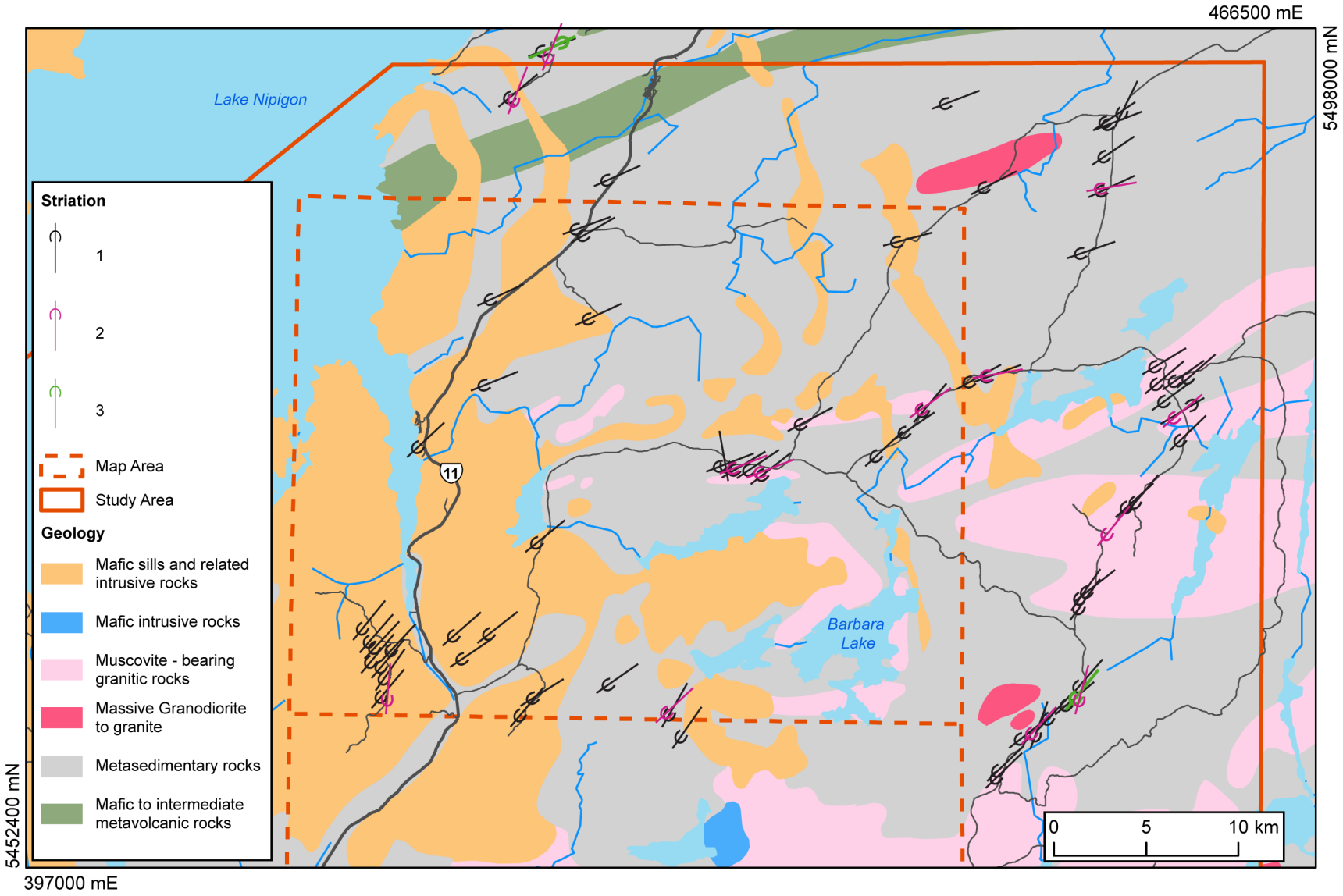


Figure 23.2. A total of 74 striation sites were visited during the summer. Of these, 14 sites had crosscutting relationships (indicated by the different colour striae symbols, where 1 is the oldest flow and 3 is the youngest flow). The more westward flows are always younger. Bedrock geology *from* Ontario Geological Survey (2011). All UTM co-ordinates provided using NAD83 in Zone 16N.

FIELD ACTIVITIES

The 2023 summer of field work focussed on the northern part of the study area, which includes the Georgia Lake rare-element pegmatite field (*see* Figure 23.1). Field observations were made primarily along roads supplemented with a few traverses into areas of particular interest. Altogether, 228 sites were visited and are subdivided into the following categories: a) 74 striation stops (14 of which showed multiple ice-flow directions), b) 25 till sampling sites and c) 129 other ground verification stops (*see* Figure 23.1).

Ice-Flow Indicators

A single ice flow is preserved at 60 striation sites and this flow was always in a southwest direction (*see* Figure 23.2). Sites with multiple flows suggest an older, more southward flow followed by a younger, southwest to west flow. One oddity is the presence of bevelled surfaces throughout the map area, which are particularly well preserved on the granite outcrops. The bevelled surfaces could be indicative of a north to northeast flow, but more field validation is needed to determine the true origins of these smoothed and striated outcrops (*see* Figure 23.2). However, the ice flow that significantly morphed the landscape is to the southwest.

Till Sampling

Till was sampled following the standardized procedures used by the Ontario Geological Survey (*see* Bajc 1999). General observations in the field suggest that 2 different till units are present. The first till unit has a grey sandy silt matrix with a larger amount of carbonate material and lower clast content (10%). In the field, this was tested and confirmed by dropping 10% HCl solution on unoxidized till matrix. This unit is comparable in composition to the upper till mentioned previously (Thorleifson and Kristjansson 1993). Chittick analyses will be conducted on collected samples to determine the concentration of total carbonate and the calcite to dolomite ratio (in 74 μm fraction). The current belief is that this carbonate material is coming from the Paleozoic carbonate bedrock in the James Bay Lowland, but further work is needed to confirm this interpretation. If true, the carbonate material in the till has been transported over 500 km, which is consistent with observations in other regions of Canada. The implication of this till sheet being present and at surface is that drift prospecting in the region would be difficult because the composition of this distal till does not reflect the local bedrock sources.

The second till unit has a brown-grey silty sand matrix with a lower amount of carbonate material and a higher clast content (15–20%). The higher proportion of the local rock types in the pebble fraction, the lack of effervescence to 10% HCl solution, sandier composition, and increased clast content of this till suggest a more local bedrock source. The brown-grey till is suited for mineral exploration purposes as it can more reliably be traced up ice to its source. This till unit is comparable to the lower till described farther north in the Beardmore–Geraldton area by Thorleifson and Kristjansson (1993). No stratigraphic relationships between the 2 tills were directly observed in the study area.

Three clast fabrics (sites 23-GWH-016, 23-GWH-049, 23-GWH-057) were completed to identify the direction of shear and, by proxy, ice-flow direction, for the deposition of the tills (Hicock et al. 1996). Fabric sites were chosen to have one in each till unit and, although 3 fabrics were completed, only 2 fabrics (sites 23-GWH-016, 23-GWH-049) had $S_1 > 0.54$ and could therefore be used for interpretation of ice-flow direction (Benediktsson et al. 2016). The clast fabric on the carbonate-rich till (site 23-GWH-049) indicates an ice-flow direction of 215°, whereas the more local till clast fabric (site 23-GWH-016) indicates an ice-flow direction of 263° (Figure 23.3). The directions of the clast fabrics match the striation record that indicates a southwestward (215°) and westward to southwestward (263°) flow for the 2 tills. The 48° difference in direction would suggest different ice-flow events as does the crosscutting relationships observed in the striation record.

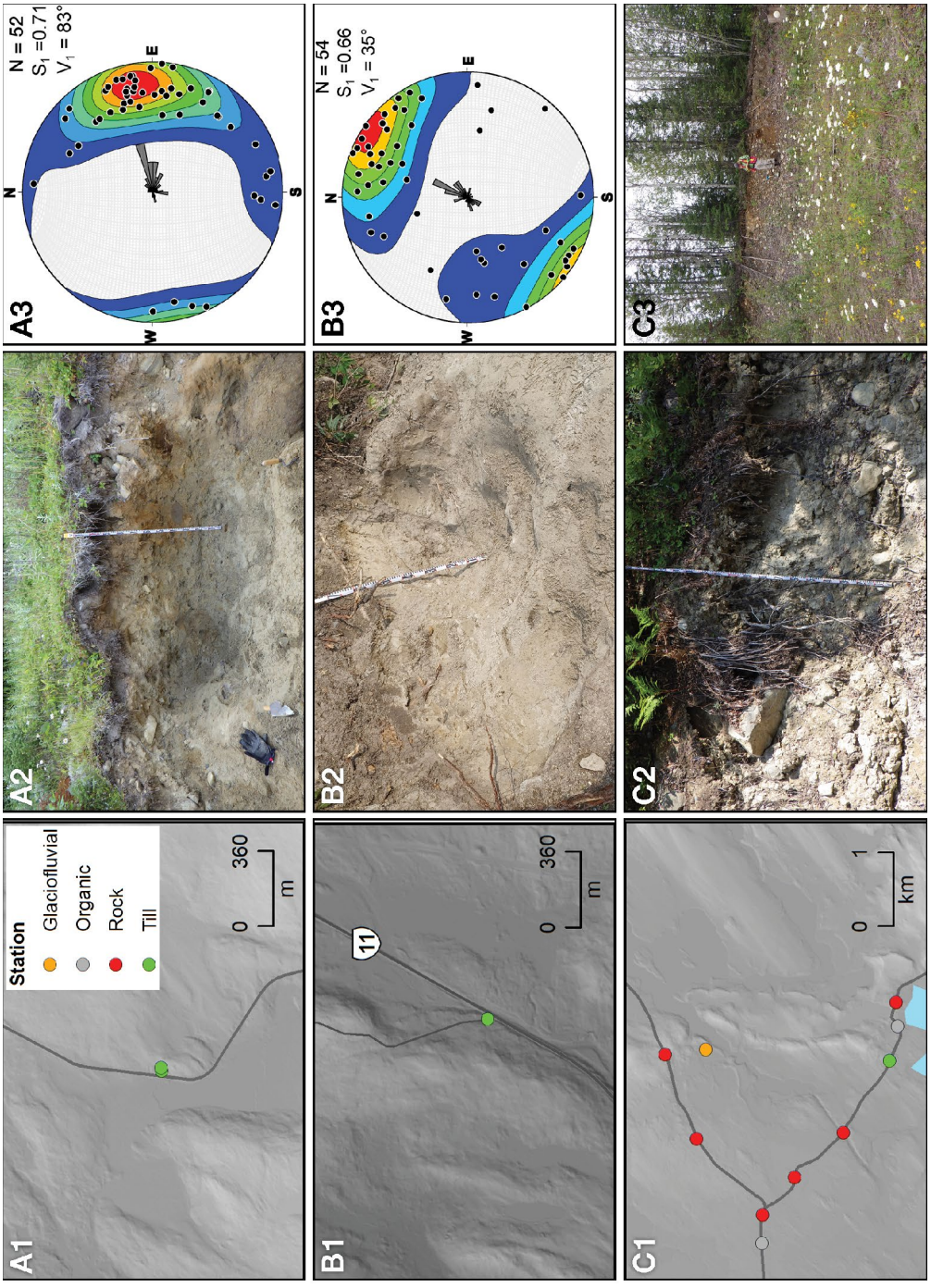


Figure 23.3. **A)** Location of site 23-GWH-016 where the local till was found at surface. The slightly streamlined landform (A1) is underlain by the brown-grey silty sand till with lag boulders and a layer of organics or peat at surface (A2) (UTM 424010E 5467858N). Measuring stick is 1.1 m. A clast fabric completed at this site indicates an ice-flow direction to the west-southwest (263°). **B)** Location of site 23-GWH-049 where the more distally sourced carbonate-rich till was found at surface. This location is in a bedrock low (B1) where the till is grey and has a sandy silt matrix, capped with a thin boulder lag (A2) (UTM 419584E 5471573N). Measuring stick is 0.7 m. A clast fabric completed at this site indicates an ice flow in the southwestward direction (216°). **C)** An esker and moraine landform assemblage that is common throughout the map area. The moraine ridge (green dot on C1) is composed of till (C2; UTM 443206E 5472118N) and has many ridges that have steeper northeastern slopes. Measuring stick (C2) is 1.8 m. An esker ends at the moraine forming a glaciofluvial fan where it meets the moraine (orange dot on C1) composed of sorted sands and gravels (C3; UTM 443355E 5474599N). All UTM co-ordinates provided using NAD83 in Zone 16N.

Surficial Mapping

All 228 sites visited will be used as ground truthing locations for surficial geology polygon delineation (*see* Figure 23.1). The abundance of glaciofluvial sands and gravels, specifically in the lower lying meltwater channels provides aggregate resources for local infrastructure development. Carbonate material is present in these sands and gravels, which could affect the suitability for certain uses.

Future Activities

The work completed this summer is the first of 3 field seasons planned. The carbonate material in the till deposits is of interest, likely being sourced from the James Bay Lowland. Additionally, work to determine the stratigraphic context of the 2 till units is important for future field work to determine which was deposited first and which is more prevalent at surface to direct drift prospecting. The bevelled surfaces are another area of interest and could indicate a northward ice flow that would also have an impact on the drift prospecting in the region. However, the southwestward ice flow is most prevalent in the study area.

Currently, the till samples collected are being prepared for submission for matrix geochemistry and indicator mineral analyses. Results from these analyses will be released as a Miscellaneous Release—Data (MRD) to aid mineral exploration in this region. Next year, the focus will be on surficial mapping and till sampling in the southern portion of the study area. During the third and final year of the project, till samples will be collected for the rest of the study area. At the end of the project, it is planned that a summary of the data will be released as an Open File Report with recommendations for exploration in the region, along with 2 surficial geology maps, at a scale of 1:50 000, for the local stakeholders to use for infrastructure development and land-use planning.

ACKNOWLEDGMENTS

George Gao and Manuel Duguet (OGS) are thanked for their reviews of this summary. Josh Brake (University of Windsor) provided great help in the field. Fort William First Nation, Red Rock Indian Band, Métis Nation of Ontario Region, Red Sky Métis Independent Nation, Animbiigoo Zaagi'igan Anishinaabek (Lake Nipigon Ojibway First Nation), Pawgasheeng (Pays Plat First Nation), Bingwi Neyaashi Anishinaabek (Sand Point First Nation), Biinjitiwaabik Zaaging Anishinaabek (Rocky Bay First Nation) Long Lake #58 First Nation, Kiashke Zaaging Anishinaabek (Gull Bay First Nation) are thanked for granting us access to their traditional lands. Kim McCollum provided fantastic accommodations at Reflection Lake Lodge.

REFERENCES

Bajc, A.F. 1999. Results of regional humus and till sampling in the eastern part of the Shebandowan greenstone belt, northwestern Ontario; Ontario Geological Survey, Open File Report 5993, 85p.

Barnett, P.J., Cowan, W.R. and Henry, A.P. 1991. Quaternary geology of Ontario, west-central sheet; Ontario Geological Survey, Map 2554, scale 1:1 000 000.

Benediktsson, Í.Ö., Jónsson, S.A., Schomacker, A., Johnson, M.D., Ingólfsson, Ó., Zoet, L., Iverson, N.R. and Stötter, J. 2016. Progressive formation of modern drumlins at Múlajökull, Iceland: Stratigraphical and morphological evidence; Boreas, v.45, p.567–583.

Breaks, F.W., Selway, J.B. and Tindle, A.G. 2008. The Georgia Lake rare-element pegmatite field and related S-type, peraluminous granites, Quetico Subprovince, north-central Ontario; Ontario Geological Survey, Open File Report 6199, 176p.

Canada 2022. The Canadian Critical Minerals Strategy. From exploration to recycling: Powering the green and digital economy for Canada and the world; Natural Resources Canada, 52p., www.canada.ca/en/campaign/critical-minerals-in-canada/canadian-critical-minerals-strategy.html. [accessed October 4, 2023]

Dalton, A.S., Margold, M., Stokes, C.R., Tarasov, L., Dyke, A.S., Adams, R.S., Allard, S., Arends, H.E., Atkinson, N., Attig, J.W., Barnett, P.J., Barnett, R.L., Batterson, M., Bernatchez, P., Borns, H.W., Breckenridge, A., Briner, J.P., Brouard, E., Campbell, J.E., Carlson, A.E., Clague, J.J., Curry, B.B., Daigneault, R-A., Dube-Loubert, H., Easterbrook, D.J., Franzi, D.A., Friedrich, H.G., Funder, S., Gauthier, M.S., Gowan, A.S., Harris, K.L., Hétu, B., Hooyer, T.S., Jennings, C.E., Johnson, M.D., Kehew, A.E., Kelley, S.E., Kerr, D., King, E.L., Kjeldsen, K.K., Knaeble, A.R., Lajeunesse, P., Lakeman, T.R., Lamothe, M., Larson, P., Lavoie, M., Loope, H.M., Lowell, T.V., Lusardi, B.A., Manz, L., McMartin, I., Nixon, C., Occhietti, S., Parkhill, M.A., Piper, D.J.W., Pronk, A.G., Richard, P.J.H., Ridge, J.C., Ross, M., Roy, M., Seaman, A., Shaw, J., Stea, R.R., Teller, J.T., Thompson, W.B., Thorleifson, L.H., Utting, D.J., Veillette, J.J., Ward, B.C., Weddle, T.K. and Wright, H.E. 2020. An updated radiocarbon-based ice margin chronology for the last deglaciation of the North American Ice Sheet Complex; Quaternary Science Reviews, v.234, paper 106223. doi.org/10.1016/j.quascirev.2020.106223

Duguet, M. 2019. Archean and Proterozoic geology of the Georgia Lake area, Quetico Subprovince, Ontario; *in* Summary of Field Work and Other Activities, 2019, Ontario Geological Survey, Open File Report 6360, p.12-1 to 12-9.

——— 2020. Geochemistry of Archean volcaniclastic and mafic intrusive rocks, Georgia Lake area, Quetico Subprovince, northwestern Ontario; *in* Summary of Field Work and Other Activities, 2020, Ontario Geological Survey, Open File Report 6370, p.8-1 to 8-10.

Dyer, R.D. and Barnett, P.J. 2005. Surficial geochemistry case studies project digital data set, Lake Nipigon region, northwestern Ontario; Ontario Geological Survey, Miscellaneous Release—Data 154.

Fisher, T.G. and Breckenridge, A. 2022. Relative lake level reconstructions for glacial lake Agassiz spanning the Herman to Campbell levels; Quaternary Science Reviews, v.294, article 107760. doi.org/10.1016/j.quascirev.2022.107760

Hicock, S.R., Goff, J.R., Lian, O.B. and Little, E.C. 1996. On the interpretation of subglacial till fabric; Journal of Sedimentary Research, v.66, p.928-934.

Kristjansson, F.J. and Thorleifson, L.H. 1991. Surficial geology, Beardmore–Geraldton, Ontario; Geological Survey of Canada, Map 1768A (also Ontario Geological Survey, Map 2535), scale 1:100 000.

Lowell, T.V., Kelly, M.A., Howley, J.A., Fisher, T.G., Barnett, P.J., Schwart, R., Zimmerman, S.R., Norris, N. and Malone, A.G. 2021. Near-constant retreat rate of a terrestrial margin of the Laurentide Ice Sheet during the last deglaciation; Geology, v.49, p.1511-1515.

Ministry of Northern Development, Mines, Natural Resources and Forestry 2022. Ontario digital terrain model (lidar-derived) - Lake Nipissing 2020 DTM; Ministry of Northern Development, Mines, Natural Resources and Forestry, Provincial Mapping Unit, Peterborough, Ontario.

Morris, T.F. 2000. Kimberlite, base metal, gold and carbonatite exploration targets, derived from overburden heavy mineral data, Killala Lake area, northwestern Ontario; Ontario Geological Survey, Miscellaneous Release—Data 52.

——— 2001. Geochemical and till pebble lithology data related to the Schreiber–Killala Lake overburden mapping and sampling program, northwestern Ontario; Ontario Geological Survey, Miscellaneous Release—Data 74.

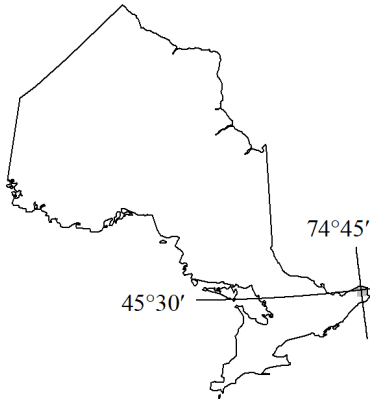
Ontario 2022. Ontario's Critical Mineral Strategy: Unlocking the potential to drive economic recovery and prosperity; Ministry of Northern Development, Mines, Natural Resources and Forestry, 53p., www.ontario.ca/page/ontarios-critical-minerals-strategy-2022-2027-unlocking-potential-drive-economic-recovery-prosperity, also available to download: select "Download English PDF". [accessed October 4, 2023]

Ontario Geological Survey 2011. 1:250 000 scale bedrock geology of Ontario; Ontario Geological Survey, Miscellaneous Release—Data 126 – Revision 1.

Prest, V.K., Grant, D.R. and Rampton, V.N. 1968. Glacial map of Canada; Geological Survey of Canada, Map 1253A, scale 1:5 000 000.

Thorleifson, L.H. and Kristjansson, F.J. 1993. Quaternary geology and drift prospecting, Beardmore–Geraldton area, Ontario; Geological Survey of Canada, Memoir 435, 146p.

24. Project SO-23-001. Paleozoic Geology of Eastern Ontario: Hawkesbury and Alexandria Areas



C. Béland Otis[1]

[1]Earth Resources and Geoscience Mapping Section, Ontario Geological Survey

INTRODUCTION

In 2017, the Earth Resources and Geoscience Mapping Section (ERGMS) of the Ontario Geological Survey (OGS) initiated a multi-year project focussing on the Paleozoic geology of eastern Ontario. The main goals of this project include producing updated 1:50 000 maps for eastern Ontario underlain by Paleozoic rocks, and to evaluate and refine the stratigraphic nomenclature and structural framework affecting the Paleozoic stratigraphy in the area (Béland Otis 2017, 2018, 2019, 2022).

Eastern Ontario is underlain by Cambrian and Ordovician platformal strata of the Ottawa Embayment of the St. Lawrence Platform. These Paleozoic rocks were last mapped by the OGS in the 1980s as a series of 20 geological bedrock maps and a summary report (Williams 1991). During the past 4 decades, this area has undergone major urban development, associated with increased land-use pressure on aggregate resources and groundwater resources. The Paleozoic rocks of eastern Ontario have significant proven and future economic potential—being the source of aggregate, dimension and building stone, calcium carbonate, silica sand, brick and tile, gypsum and other industrial minerals (Tessier et al. 2018, 2019; LeBaron et al. 2020; Mancini et al. 2021, 2022, 2023). Furthermore, the refinement of the stratigraphy can help improve the regional understanding and predictability of karst landforms (Brunton 2019).

Also, in the last 4 decades, the Cambro–Ordovician stratigraphic units of eastern Ontario have been the focus of much academic research (e.g., Dix and Molgat 1998; Dix and Al-Dulami 2011; Salad Hersi and Dix 1997, 1999; Lowe et al. 2017; Oruche and Dix 2018). These studies have introduced new stratigraphic units (or re-introduced old terms), revised formational contact definitions and relative ages of some intervals and/or proposed the application in Ontario of stratigraphic terminology used in adjacent jurisdictions instead of the current OGS nomenclature (Williams 1991; Béland Otis 2017, 2018, 2019, 2022). Furthermore, extensive discussions with ERGMS colleagues led to a new project to completely revise the Cambro–Ordovician legend of southern Ontario (Brunton et al. 2021; Béland Otis 2018, 2019, 2022).

2023 STUDY AREA AND FIELD WORK

In 2023, field work was undertaken in the Hawkesbury (NTS 31 G/10), Lachute (NTS 31 G/9), Alexandria (NTS 31 G/7) and Vaudreuil (NTS 31 G/8) map areas (Figure 24.1). In addition, some outcrops and quarries were mapped in the adjacent Winchester (NTS 31 G/3), Cornwall (NTS 31 G/2) and Huntingdon (NTS 31 G/1) areas to the south, although additional field work is needed to complete mapping these areas. In Ontario, the Lachute and Vaudreuil areas each represent less than 125 km^2 (*see* Figure 24.1) and data from these areas will be combined with the maps produced for the

Summary of Field Work and Other Activities, 2023,
Ontario Geological Survey, Open File Report 6405, p.24-1 to 24-9.

© King's Printer for Ontario, 2023

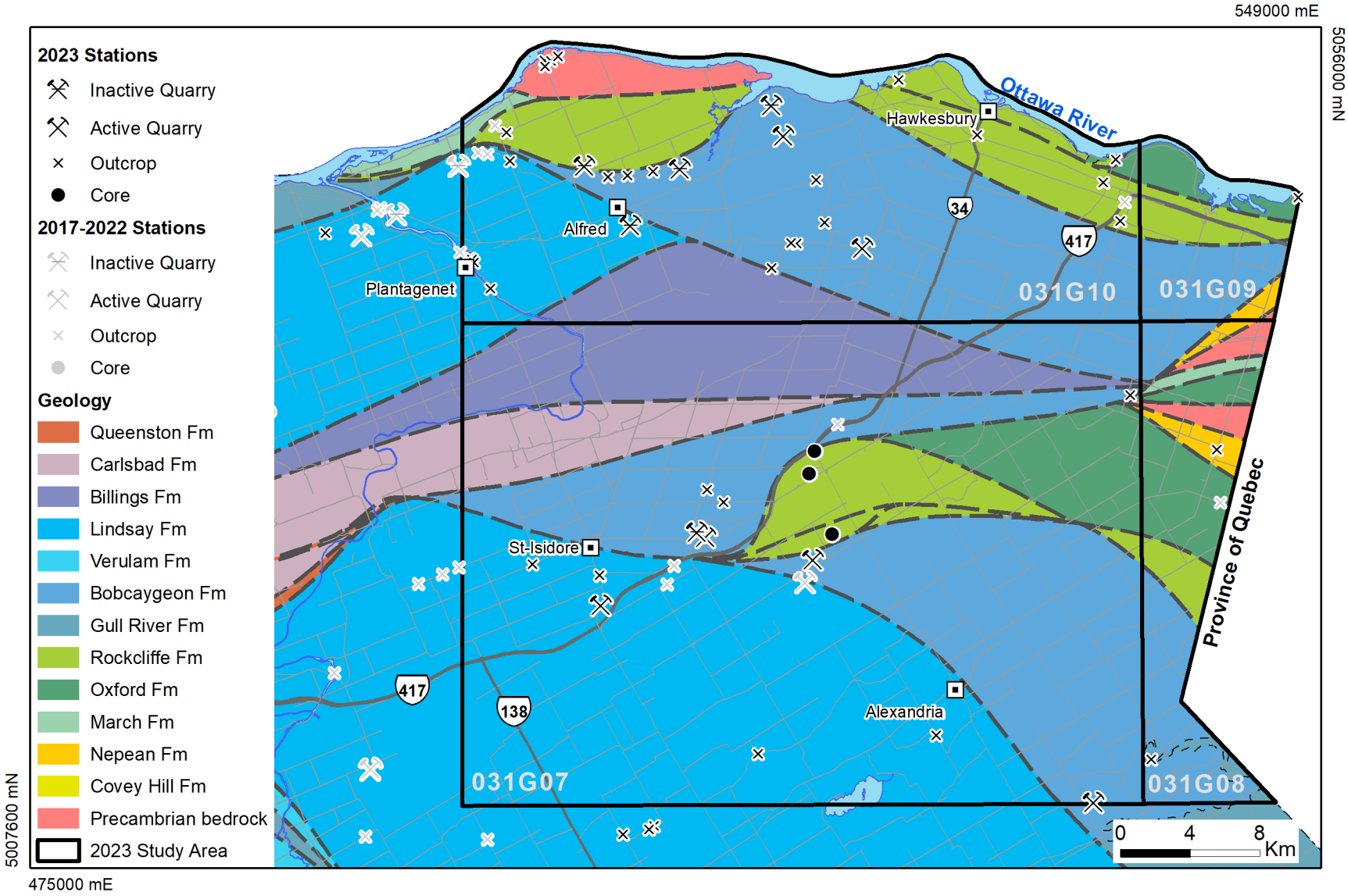


Figure 24.1. Geological bedrock geology of eastern Ontario based on previous mapping (*from* Armstrong and Dodge 2007; *modified from* Williams 1991) showing the locations of the 2023 study area and mapping stations (outcrop and quarries). Abbreviation: Fm = Formation. Numbers (e.g., 031G07) indicate the National Topographic System (NTS) map number. All Universal Transverse Mercator (UTM) co-ordinates provided using North American Datum 1983 (NAD83) in Zone 18.

Hawkesbury and Alexandria areas. The 2023 field season involved the examination of 43 outcrops, 6 active and 6 inactive quarries (*see* Figure 24.1). Most of these 55 stations were sampled for geochemical and thin section analyses. This mapping also included the examination of 3 cores stored at the Oil, Gas and Salt Resources Library (OGSRL) in London, Ontario.

The previous OGS mapping of the area took place in 1982 by Williams, Rae and Wolf (1985, 1986). Fewer than 50% of their stations could be revisited because they are no longer accessible. The uneven distribution and quality of the existing outcrops (e.g., predominantly bedding planes and/or riverbeds) made it challenging to determine the stratigraphic position of many outcrops.

PALEOZOIC STRATIGRAPHY OF THE HAWKESBURY–LACHUTE AND ALEXANDRIA–VAUDREUIL AREAS

Paleozoic sedimentary rocks subcrop across the entire study area, except for the area south of the Ottawa River, near the community of Lefaivre, where Precambrian rocks are at surface. Previously published maps also show Precambrian basement subcrops in a fault block near Sainte-Anne-de-Prescott in Ontario, in part based on the presence of nearby outcrops in the province of Quebec (Wilson 1941a, 1941b; Williams, Rae and Wolf 1985).

The oldest Paleozoic rock unit present in the eastern Ontario area is the Covey Hill Formation of the Potsdam Group, equivalent to the Ausable Formation (Williams 1991; Lowe et al. 2017). This unit is mainly composed of feldspathic and quartzitic conglomerate to sandstone. Although a Covey Hill Formation outcrop has not been identified in the study area, its presence has been confirmed in diamond-drill holes (Williams, Rae and Wolf 1985; Williams 1991; Lowe et al. 2017). Prior OGS mapping also suggested that the unit subcrops near the Quebec border in the Vaudreuil map area (Williams, Rae and Wolf 1985).

The uppermost unit of the Potsdam Group, the Nepean Formation is mainly composed of quartz arenite and was observed at only 1 locality in the easternmost portion of the study area. The unit has also been intercepted by a few diamond-drill cores (Williams 1991; Lowe at al 2017). Because the Nepean Formation is correlative with the Keeseville Formation of New York State, Lowe at al. (2017) suggested that the American name should take priority and be used in Canada.

The Potsdam Group is overlain by the Beekmantown Group. The Beekmantown Group, according to the OGS nomenclature, is subdivided into the March and Oxford formations. However, more recent studies suggest it should be subdivided into the Theresa, Beauharnois and Carillon formations or the Theresa, Fort Cassin and Providence Island formations, in ascending order (Williams 1991; Bernstein 1992; Landing and Westrop 2006; Oruche and Dix 2021). The March Formation (Theresa Formation) does not crop out in the study area, but has been intersected in diamond-drill cores. It is composed of interbedded calcareous sandstone that transitions upward into dolostone. The Oxford Formation (Beauharnois and Carillon formations) was observed near the Ottawa River and in some creeks in the easternmost portion of the study area. The lowest strata of the unit comprise dark grey, medium- to thin-bedded, dolostone beds that can be somewhat quartzitic near the base (Beauharnois Formation). Above these, a general upward increase in dolomudstone and shale is observed (Carillon Formation). An excellent exposure of these upper Beekmantown Group beds was observed in 2023 at Pointe-Fortune, near the Carillon dam and is shown in Photo 24.1B.

The Rockcliffe Formation disconformably overlies the Beekmantown Group (Wilson 1946; Dix and Molgat 1998). In all of the areas previously mapped for this project (Béland Otis 2017, 2018, 2019, 2022), it is composed of greenish gray to maroon, calcareous to non-calcareous, generally fine- to medium-grained, sublitharenite to lithic wacke with a general upward increase in shale content. Near Hawkesbury,

an additional cross-bedded calcarenitic facies is present, which previously has been referred to by a variety of names, including the St. Martin Formation; St. Martin Member of the Rockcliffe Formation; the Laval Formation; and the Hog's Back Formation (Wilson 1946; Williams 1991; Bolton, Steele-Petrovich and Munro 1991; Salad Hersi and Dix 1997).

The Ottawa Group, comprising a series of limestones, dolostones and shales, disconformably overlies the Rockcliffe Formation (Wilson 1946; Williams 1991). Many stratigraphic nomenclatures have been proposed for this succession and it is currently the focus of a stratigraphic revision by the OGS (Brunton et al. 2021). The lowest rock unit consists of medium-bedded tabular greenish grey silty dolostones interbedded with fine crystalline limestones, shales and calcareous sandstones. In eastern Ontario, these rocks are mapped by Williams (1991) as the lower member of the Gull River Formation, whereas in the bordering jurisdictions (e.g., New York State and Quebec), they are recognized as the Pamelia Formation of the Black River Group (Okulitch 1939; Wilson 1946; Clark 1972; Fisher 1977; Williams 1991). The top dolomitic bed represents the upper contact of the unit. The upper member of the Gull River Formation, equivalent to the Lowville Formation of the Black River Group of Quebec and



Photo 24.1. Photographs of selected sites visited during 2023 field work. **A**) Lindsay Formation at the St-Isidore quarry, Colacem Canada Inc. The lower bench seen here to the left is approximately 12 m high. **B**) Thin- to medium-bedded, stromatolitic, brownish grey mudstone beds, with some yellow to orange weathering, of the Oxford Formation (Carillon Formation) at the Carillon dam near Pointe–Fortune. **C**) Heavily bioturbated ripple marks with crests parallel to hammer of the thinly bedded storm beds of the Verulam Formation along the South Nation River just east of Plantagenet. **D**) Bentonite bed (at base of hammer and pen) found in the wackestone of the Lower Bobcaygeon Formation (Chaumont Formation) at the McMillan quarry near Laggan. Hammer handle in B, C and D is 33 cm long.

New York State, consists of tabular bedded, fine crystalline dark grey limestone and generally weathers bluish grey (Williams 1991; Salad Hersi and Dix 1999). Birds-eye textures and *Tetradium* colonies are characteristic of that unit. Within the 2023 study area, the Gull River Formation (lower and/or upper member) is best exposed at the McMillan, McLeod and Green Valley quarries.

The lower member of the Bobcaygeon Formation of eastern Ontario is characterized by thick to massive beds of finely crystalline dark brownish grey heavily burrowed limestone with stylolites (Williams 1991). Within Ontario and adjacent jurisdictions, these strata have been given many stratigraphic names (Coboconk, Chaumont, Watertown, and Leray formations) but have generally been attributed to the uppermost units of the Black River Group (Clark 1972; Fisher 1977; Salad Hersi and Dix 1999; Armstrong and Carter 2010; Oruche, Dix and Kamo 2018). In the study area, the best locations to examine these strata are the L'Orignal, MacLeod, McMillan and Green Valley quarries, as well as an outcrop north of Alfred.

The lower member of the Bobcaygeon Formation is generally overlain by a few metres to a few centimetres of thinly bedded muddy limestone, mapped previously as the middle member of the Bobcaygeon Formation and recently defined by Oruche, Dix and Kamo (2018) as the L'Orignal Formation. Within the study area, this unit is best observed at the L'Orignal quarry and at the Alfred outcrop. This unit is directly overlain by the upper member of the Bobcaygeon Formation and comprises highly variable facies both horizontally and vertically. Because it correlates to the Rockland and Hull formations of eastern Ontario, many authors, both prior to and following the 1980s OGS mapping, associate this unit with these formations (*see* Raymond 1914, 1921; Wilson 1946; Uyeno 1974; Oruche, Dix and Kamo 2018). The Rockland Formation is described as thick-bedded packstone, whereas the Hull Formation consists of thinly bedded dark grey carbonate mudstones to brown cross-bedded crinoidal grainstones and can contain chert (Uyeno 1974; Oruche, Dix and Kamo 2018).

The upper contact of the Bobcaygeon Formation with the Verulam Formation is rarely observed in outcrop because of the shaly nature of the latter. Indeed, the Verulam Formation is characterized by thin-bedded shale, interbedded with thin to medium undulating and fossiliferous wackestone to grainstone (Williams 1991; Dix and Al-Dulami 2011). Major components of the limestone beds include intraclasts, echinoderms, bryozoans, brachiopods and trilobites. During the 2023 field season, the Verulam Formation was identified only near the quarry floor of the St-Isidore quarry and along South Nation River near Plantagenet (Photos 24.1A and 24.1C).

The upper contact of the Verulam Formation with the Lindsay Formation was placed at the uppermost shale bed greater than 5 cm thick, as discussed by Williams (1991). The Lindsay Formation is composed of thin- to thick-bedded, light to dark grey, nodular wackestone to packstone with some 2 to 3 cm thick calcareous shale interbeds. The St-Isidore quarry is one of the best exposures of the Lindsay Formation (Photo 24.1A). The upper Eastview Member, composed of dark brownish micrite, and the upper geological contact of the Lindsay Formation were not observed during the 2023 field season, but have been identified in local diamond-drill cores (Williams 1991).

The youngest Paleozoic strata, found in the eastern Ontario area, are a succession of Ordovician shales composed of the Billings, Carlsbad and Queenston formations. Only the first 2 formations are present within the study area and no outcrop was found. The Billings Formation largely comprises dark grey to black noncalcareous shale, but, near the top, there is a general increase of siltstone and limestone beds. The upper contact with the Carlsbad Formation is defined as the base of the lowest limestone bed greater than 2 cm thick (Williams 1991). The Carlsbad Formation is composed of interbedded shale, fossiliferous siltstone and limestone. The unit becomes quite calcareous near the top and its upper contact is the lower limit of the Queenston Formation red shales.

STRUCTURAL GEOLOGY OF THE HAWKESBURY–LACHUTE AND ALEXANDRIA–VAUDREUIL AREAS

The Ottawa Embayment of the St. Lawrence Platform is a structurally complex rift basin (Williams 1991). Numerous normal faults cross the basin, generally parallel to the Ottawa River. Within the 2023 study area, however, the exact location and orientation of these structures was difficult to map because of limited exposure and the presence of a thick Quaternary succession over the Paleozoic bedrock. Since the last OGS geological mapping, a new high-resolution aeromagnetic survey has been acquired (Ontario Geological Survey 2014). Although the Paleozoic succession in Ontario is nonmagnetic, structures in the underlying magnetic Proterozoic bedrock may be reflected in the sedimentary cover. Structural trends identified in the Precambrian basement (Magnus and Easton 2015) will be studied and possibly integrated in future maps.

DISCUSSION AND FUTURE WORK

Additional work is required to improve the quality and accuracy of the geological maps for eastern Ontario because of a lack of outcrops. First, the recently digitized geological descriptions of the outcrops mapped by the OGS in the 1980s will be integrated with the newly acquired field data. Second, data from well records (water, geotechnical and hydrocarbon exploration) will be used in the production of the map(s). Third, lidar imagery, which is now available for the entire study area, will be used to help delineate the Paleozoic rock units according to their specific topographic features and assist in the measurement of bedrock elevations and possibly the thickness of the stratigraphic units.

Regional correlation of the Ottawa graben strata to the more structurally stable platformal strata of south-central Ontario is challenging. This is the main reason why the Cambro-Ordovician legend revision project was proposed (Brunton et al. 2021). Initial field work and discussions for that project seems to confirm that, although units can be correlated throughout southern Ontario by texture, fossil assemblage and bedding style, there is significant variation in mineralogy, thickness and even colour. Additional literature review, field work, core logging and discussions will be needed before any standardized legend is established.

Facies variations in stratigraphic units was also observed within the Ottawa graben. This can be explained by various factors, such as syntectonic sedimentation, sea-level fluctuations and deposition over an irregular, faulted crystalline basement. Within the study area, these variations occur mostly in the Gull River and Bobcaygeon formations (Brunton et al. 2021). Now that these strata are mapped from Arnprior to the Quebec border, the following variations are recognized: 1) the lower and upper Gull River Formation units are generally much darker in the southeast of the Ottawa basin; 2) the lower member of the Bobcaygeon Formation varies in thickness from a few metres to more than 10 m and the unit, usually composed of wackestone, can also contain rudstones, but this was observed at only a limited number of stations; and finally 3) the shaly middle member of the Bobcaygeon Member does not seem to be present in the study area and the upper member of the Bobcaygeon Formation exhibits so many different facies that it is still unclear how many stratigraphic names and/or units should be used to characterize this upper member (e.g., Rockland, Hull, Kirkfield, Napanee formations).

To resolve these subregional correlation challenges, additional field work and core logging will be needed, but also U/Pb zircon geochronology on newly discovered bentonite horizons (e.g., Photo 24.1D). Characterizing the mineralogy, chemistry and age of these bentonites will enable improved stratigraphic correlations within the Ottawa graben and across south-central and southwestern Ontario. The OGS is also working to establish a regional chemostratigraphic profile using stable carbon and oxygen isotopes to assist

in regional correlations (Brunton et al. 2021; Hahn 2022; Atasiei et al. 2022). This data set will build on previously published profiles (Barta and al. 2007; Paton and Brett 2020; Oruche, Dix and Kamo 2018), and, when paired with absolute ages derived from bentonite, will provide a powerful and high-resolution data set.

ACKNOWLEDGMENTS

The author wishes to acknowledge the assistance of Elizabeth Edwards during the field season and to thank Frank Brunton and Katie Hahn (ERGMS) for their insight in the field. Also, the author would like to thank quarry owners and operators (including Colacem Canada Inc., Green Infrastructure Partners Inc., Lafarge Canada Inc., A.L. Blair Construction Ltd.), as well as private land owners, for granting access and allowing sample collection on their properties. The author would like to thank the Algonquins of Pikwakanagan First Nation for allowing the Ontario Geological Survey to map their traditional land use area. The author is also thankful to all the ERGMS staff, particularly Kei Yeung (GIS technical help) and Julien Bonin (drafting figures). Finally, the Geoscience Laboratories and the Publication Services Unit staff are acknowledged for their help throughout this project.

REFERENCES

Armstrong, D.K. and Carter, T.R. 2010. The subsurface Paleozoic stratigraphy of southern Ontario; Ontario Geological Survey, Special Volume 7, 301p.

Armstrong, D.K. and Dodge, J.E.P. 2007. Paleozoic geology of southern Ontario; Ontario Geological Survey, Miscellaneous Release—Data 219.

Atasiei, D., Tsujita, C.J., Brunton, F.R., Jin, J. and Yeung, K.H. 2022. Stratigraphy and sedimentology of Upper Ordovician strata, with emphasis on the Collingwood and Rouge River members, southern Ontario and Manitoulin Island; *in* Summary of Field Work and Other Activities, 2022, Ontario Geological Survey, Open File Report 6390, p.20-1 to 20-6.

Barta, N.C., Bergström, S.M., Saltzman, M.R. and Schmitz, B. 2007. First record of the Ordovician Guttenberg ^{13}C excursion (GICE) in New York State and Ontario: Local and regional chronostratigraphic implications; Northeastern Geology and Environmental Sciences, v.29, p.276-298.

Béland Otis, C. 2017. Paleozoic geology of eastern Ontario; *in* Summary of Field Work and Other Activities, 2017, Ontario Geological Survey, Open File Report 6333, p.22-1 to 22-11.

——— 2018. Paleozoic geology of eastern Ontario: Ottawa area; *in* Summary of Field Work and Other Activities, 2018, Ontario Geological Survey, Open File Report 6350, p.22-1 to 22-10.

——— 2019. Paleozoic geology of eastern Ontario: Arnprior–Quyon area; *in* Summary of Field Work and Other Activities, 2019, Ontario Geological Survey, Open File Report 6360, p.20-1 to 20-10.

——— 2022. Paleozoic geology of eastern Ontario: Russell–Thurso area; *in* Summary of Field Work and Other Activities, 2022, Ontario Geological Survey, Open File Report 6390, p.23-1 to 23-8.

Bernstein, L. 1992. A revised lithostratigraphy of the Lower–Middle Ordovician Beekmantown Group, St. Lawrence Lowlands, Quebec and Ontario; Canadian Journal of Earth Sciences, v.29, p.2677-2694.

Bolton, T.E., Steele-Petrovich, H.M. and Munro, I. 1991. Middle Ordovician (Chazyan) stratigraphy, and bryozoan and conodont faunas in the Hawkesbury region, eastern Ontario; Geological Survey of Canada, Bulletin 412, p.1-33.

Brunton, F.R. 2019. Karst map of southern Ontario: An update; *in* Summary of Field Work and Other Activities, 2019, Ontario Geological Survey, Open File Report 6360, p.21-1 to 21-9.

Brunton, F.R., Béland Otis, C., Hahn, K.E. and Yeung K.H. 2021. Progress on the development of a new stratigraphic framework for the Paleozoic geology of southern Ontario; *in* Summary of Field Work and Other Activities, 2021, Ontario Geological Survey, Open File Report 6380, p.16-1 to 16-9.

Clark, T.H. 1972. Montréal area; Ministère des Richesses Naturelles du Québec, Geological Report 152, 244p.

Dix, G.R. and Al-Dulami, M.J. 2011. Late Ordovician (Chatfieldian) catastrophic volcanism and abrupt carbonate platform-interior subsidence: A tectonic link across a Taconian foreland basin (Québec Embayment) due to inherited crustal weakness; Geological Society of America Bulletin, v.123, p.1988-2004.

Dix, G.R. and Molgat, M.P. 1998. Character of the Middle Ordovician Sauk-Tippecanoe sequence boundary in the Ottawa Embayment (eastern Ontario): Possible evidence for platform-interior, Taconic tectonism; Canadian Journal of Earth Sciences, v.35, p.603-619.

Fisher, D.W. 1977. Correlation of the Hadrynian, Cambrian and Ordovician rocks in New York State; New York State Museum and Science Service, Map and Chart Series 25, 75p.

Hahn, K.E. 2022. Paleozoic geology of the Kingston area, eastern Ontario; *in* Summary of Field Work and Other Activities, 2022, Ontario Geological Survey, Open File Report 6390, p.22-1 to 22-10.

Landing, E. and Westrop, S.R. 2006. Early Ordovician faunas, stratigraphy, and sea level history of the middle Beekmantown Group, northeastern New York; Journal of Paleontology, v.80, p.958-980.

LeBaron, P.S., Sabiri, N., Laidlaw, D.A., Hinz, S.L.K. and Fortner, L. 2020. Report of Activities 2019, Resident Geologist Program, Southern Ontario Regional Resident Geologist Report: Southeastern and Southwestern Ontario Districts and Petroleum Operations; Ontario Geological Survey, Open File Report 6368, 72p.

Lowe, D.G., Arnott, R.W.C., Nowlan, G.S. and McCracken, A.D. 2017. Lithostratigraphic and allostratigraphic framework of the Cambrian–Ordovician Potsdam Group and correlations across Early Paleozoic southern Laurentia; Canadian Journal of Earth Sciences, v.54, p.550-585.

Magnus, S.J. and Easton, R.M. 2015. Precambrian geology of eastern Ontario interpreted from aeromagnetic and compiled geological data—northeast sheet; Ontario Geological Survey, Preliminary Map P.3792, scale 1:100 000.

Mancini, L.A., Dorado-Troughton, M., Sabiri, N., LeBaron, P.S., Hinz, S.L.K., Dorland, G. and Fortner, L. 2022. Report of Activities 2021, Resident Geologist Program, Southern Ontario Regional Resident Geologist Report: Southeastern Ontario and Southwestern Ontario Districts and Petroleum Operations; Ontario Geological Survey, Open File Report 6386, 65p.

Mancini, L.A., Dorado-Troughton, M., Swiercz, J., LeBaron, P.S., Hinz, S.L.K., Sabiri, N., Dorland, G. and Fortner, L. 2023. Report of Activities 2022, Resident Geologist Program, Southern Ontario Regional Resident Geologist Report: Southeastern Ontario and Southwestern Ontario Districts and Petroleum Operations; Ontario Geological Survey, Open File Report 6404, 78p.

Mancini, L.A., Meek, R.D., Sabiri, N., LeBaron, P.S., Rodriguez Miguel, L.M., Hinz, S.L.K., Dorland, G., Patterson, C. and Fortner, L. 2021. Report of Activities 2020, Resident Geologist Program, Southern Ontario Regional Resident Geologist Report: Southeastern Ontario and Southwestern Ontario Districts and Petroleum Operations; Ontario Geological Survey, Open File Report 6376, 67p.

Okulitch, V.J. 1939. The Ordovician section at Coboconk, Ontario; Royal Canadian Institute, Transactions, v.33, p.319-339.

Ontario Geological Survey 2014. Ontario airborne geophysical surveys, magnetic data, grid and profile data (ASCII® and Geosoft® formats) and vector data, eastern Ontario area; Ontario Geological Survey, Geophysical Data Set 1075.

Oruche, N.E. and Dix, G.R. 2021. Sequence stratigraphy of a Middle to Upper Ordovician foreland succession (Ottawa Embayment, central Canada): Evidence for tectonic control on sequence architecture along southern Laurentia; Basin Research, v.33, p.779-808.

Oruche, N.E., Dix, G.R. and Kamo, S.L. 2018. Lithostratigraphy of the upper Turinian–lower Chatfieldian (Upper Ordovician) foreland succession, and a U–Pb ID–TIMS date for the Millbrig volcanic ash bed in the Ottawa Embayment; Canadian Journal of Earth Sciences, v.55, p.1079-1102.

Paton, T.R. and Brett, C.E. 2020. Revised stratigraphy of the middle Simcoe Group (Ordovician, upper Sandbian–Katian) in its type area: An integrated approach; Canadian Journal of Earth Sciences, v.57, p.184-198.

Raymond, P.E. 1914. The Trenton Group in Ontario and Quebec; *in* Summary Report for the Year 1912, Geological Survey of Canada, p.342-350.

——— 1921. A Contribution to the description of the fauna of the Trenton Group; Geological Survey of Canada, Museum Bulletin 31, 67p.

Salad Hersi, O. and Dix, G.R. 1997. Hog's Back Formation: A new (Middle Ordovician) stratigraphic unit, Ottawa Embayment, eastern Ontario, Canada; Canadian Journal of Earth Sciences, v.34, p.588-597.

——— 1999. Blackriveran (lower Mohawkian, Upper Ordovician) lithostratigraphy, rhythmicity, and paleogeography: Ottawa Embayment, eastern Ontario, Canada; Canadian Journal of Earth Sciences, v.36, p.2033-2050.

Tessier, A.C., LeBaron, P.S., Charbonneau, S.J., Laidlaw, D.A., Wilson, A.C. and Fortner, L. 2018. Report of Activities 2017, Resident Geologist Program, Southern Ontario Regional Resident Geologist Report: Southeastern Ontario and Southwestern Ontario Districts and Petroleum Operations; Ontario Geological Survey, Open File Report 6341, 93p.

Tessier, A.C., LeBaron, P.S., Smith, A.C., Laidlaw, D.A., Bousquet, P. and Fortner, L. 2019. Report of Activities 2018, Resident Geologist Program, Southern Ontario Regional Resident Geologist Report: Southeastern Ontario and Southwestern Ontario Districts and Petroleum Operations; Ontario Geological Survey, Open File Report 6356, 94p.

Uyeno, T.T. 1974. Conodonts of the Hull Formation, Ottawa Group (Middle Ordovician), of the Ottawa–Hull area, Ontario and Quebec; Geological Survey of Canada, Bulletin 248, 31p.

Williams, D.A. 1991. Paleozoic geology of the Ottawa–St. Lawrence Lowland, southern Ontario; Ontario Geological Survey, Open File Report 5770, 292p.

Williams, D.A., Rae, A.M. and Wolf, R.R. 1985. Paleozoic geology of the Alexandria–Vaudreuil area, southern Ontario; Ontario Geological Survey, Preliminary Map P.2719, scale 1:50 000.

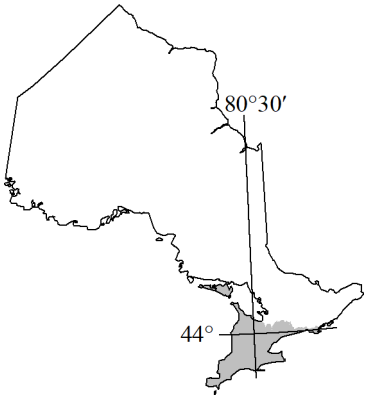
——— 1986. Paleozoic geology of the Hawkesbury–Lachute area, southern Ontario; Ontario Geological Survey, Preliminary Map P.2718, scale 1:50 000.

Wilson, A.E. 1941a. Valleyfield; Geological Survey of Canada, Map 660A, scale 1: 126 720.

——— 1941b. L'Orignal; Geological Survey of Canada, Map 662A, scale 1: 126 720.

——— 1946. Geology of the Ottawa–St. Lawrence Lowland, Ontario and Quebec; Geological Survey of Canada, Memoir 241, 66p.

25. Project SO-21-002. Stratigraphy and Sedimentology of Upper Ordovician Strata, Southern Ontario and Manitoulin Island



D. Atasiei[1], C.J. Tsujita[1], F.R. Brunton[2,1], J. Jin[1] and K.H. Yeung[2]

[1]Department of Earth Sciences, University of Western Ontario, London, Ontario N6G 2V4
[2]Earth Resources and Geoscience Mapping Section, Ontario Geological Survey, Sudbury, Ontario P3E 6B5

INTRODUCTION

Although the Ordovician stratigraphy of southern Ontario has been studied for more than a century, several inconsistencies remain between surface and subsurface stratigraphic nomenclature. Rock units with the same stratigraphic name have different lithologic and/or paleontological definitions and subdivisions depending on their geographic location. The Upper Ordovician carbonate-dominated succession of Ontario occurs in a large area along the St. Lawrence Platform, extending from the Ottawa region to the Niagara Escarpment and to Windsor. This carbonate depositional system was punctuated by a suite of organic-rich shales and mixed shale-carbonate units between the lower Katian (Trentonian) normal marine carbonates of the underlying Verulam–Cobourg formations and overlying upper Katian Blue Mountain and Georgian Bay formations.

As noted in Atasiei et al. (2021, 2022), one of the main goals of this study is to compare the stratigraphic-rank criteria for parts of the Upper Ordovician succession in southern Ontario, including, in ascending order: the Collingwood member of the Cobourg Formation of the Trenton Group (should it be a formational-rank unit and how does it correlate with the Utica Formation regionally); and the Rouge River member of the overlying Blue Mountain Formation. At present, no systematic formation-rank geologic picks or stratigraphic nomenclature have been agreed upon for these Upper Ordovician strata in southern Ontario.

This work will build upon the collaborative studies (2015 to 2023) between the Ontario Geological Survey (OGS), Geological Survey of Canada (GSC), the staff of the Oil, Gas and Salt Resources Library (OGSRL), and faculty and students of the Department of Earth Sciences of the University of Western Ontario (UWO). The broader objective of this study is to provide an interpretation of the paleoenvironmental factors that led to the disappearance of the broad carbonate factory and the accumulation of organic-rich Collingwood member carbonates (marlstones) and Rouge River member mixed shale and minor carbonate rock units, respectively. In recent years, there have been numerous studies concerning the Late Ordovician environmental crisis and ocean anoxia based on widespread black shales and, therefore, part of this study will attempt to address this phenomena in the southern Ontario portion of Laurentia.

PREVIOUS WORK

The historical development of stratigraphic nomenclature for the Upper Ordovician in southern Ontario is complex (Figure 25.1; Winder 1961; Hamblin 1999, 2018; Brunton et al. 2023).

Summary of Field Work and Other Activities, 2023,
Ontario Geological Survey, Open File Report 6405, p.25-1 to 25-11.

© King's Printer for Ontario, 2023

Raymond (1914; *see also* Raymond 1916) introduced the term Collingwood and over the past century it has undergone many changes in stratigraphic position and formational rank and has also been assigned to different stratigraphic groups (e.g., Simcoe versus Trenton groups). Likewise, the term "Rouge River" has been referred to under different names (e.g., originally "Gloucester" by Raymond (1914) and "Whitby" by Liberty (1964)) and different stratigraphic ranks (e.g., formation versus member).

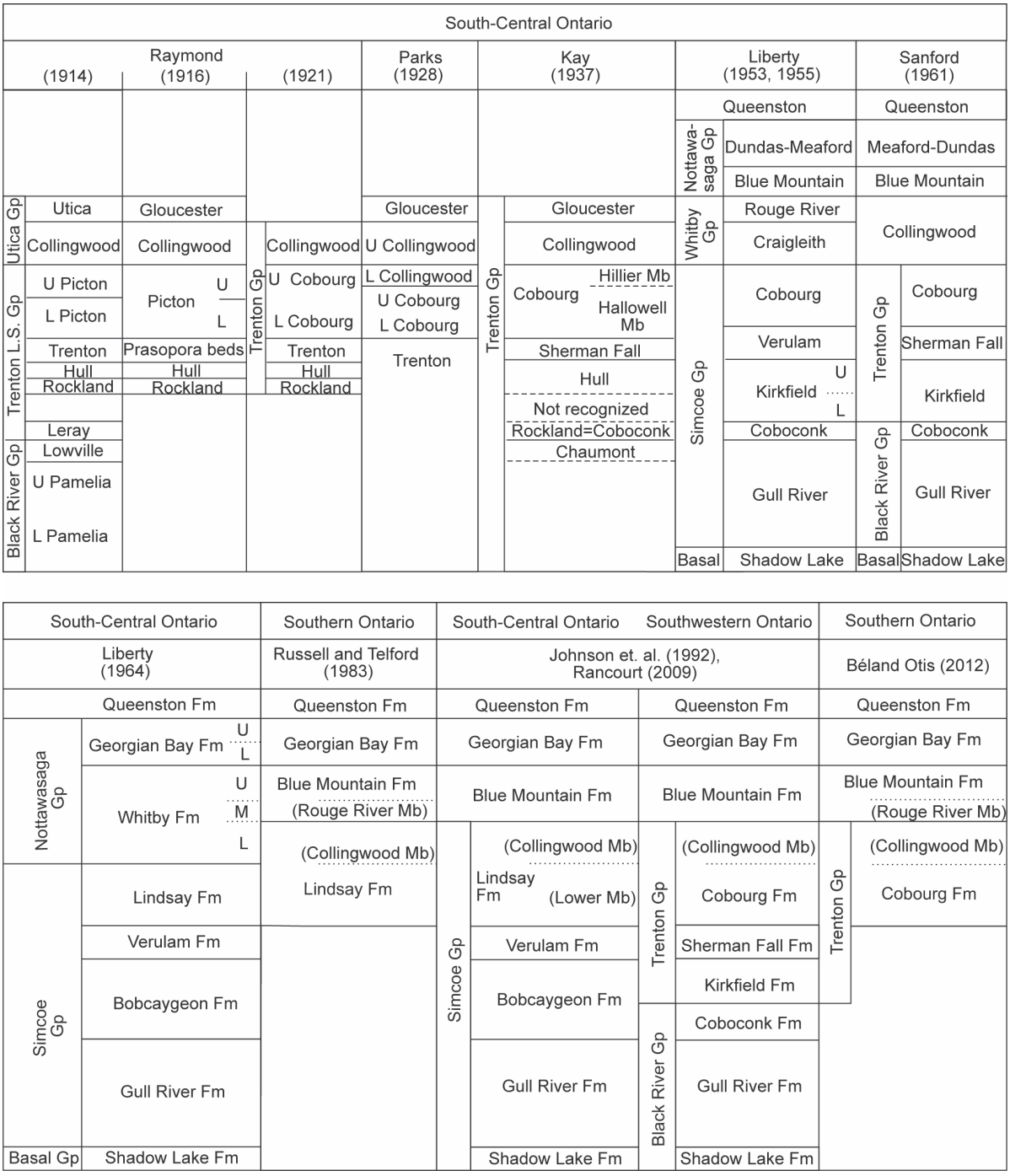


Figure 25.1. Chart of selected stratigraphic nomenclature for part of Upper Ordovician Paleozoic geology, southern Ontario. Abbreviations: Fm, Formation; Gp, Group; L, lower; Mb, member, U, upper. Nomenclature, as noted in the chart, is *from* Raymond (1914, 1916, 1921); Parks (1928); Kay (1937); Liberty (1953, 1955); Sanford (1961); Liberty (1964); Russell and Telford (1983); Johnson et al. (1992); Rancourt (2009); and Béland Otis (2012).

Although the authors agree with the latest stratigraphic assignments of lithofacies by the OGS (*see* Béland Otis 2012), some discrepancies remain regarding formational-rank geologic picks for some of the wells examined by this study; further work is ongoing.

OBJECTIVES

The main objectives of this study are to characterize and redefine formational rank geologic contacts of the Cobourg through the Blue Mountain succession. A total of 13 cores were examined in the summers of 2022 and 2023 (Table 25.1; Figure 25.2). The cores were drilled at sites located mostly within southwestern and south-central Ontario. Key cores were chosen based upon completeness of available core coverage and geophysical data through the interval of interest, as well as achieving areal coverage from Manitoulin Island to Toronto, including wells in Lake Erie. Outcrops in the vicinity of Sheguiandah on Manitoulin Island, Delphi Point in Collingwood area, and Rouge River type section in Toronto (Whitby) area were measured during the summer of 2023 to both study the formational-rank geologic contacts at these sites and to look along strike within units for diagnostic features, such as phosphatic lag deposits, invertebrate faunas and sedimentary bedforms. The results are currently being compiled for journal articles and will be included in an MSc thesis (in preparation by D. Atasiei).

RESEARCH METHODS

Formational-rank geologic contacts were identified based upon lithofacies descriptions of rock cores and drill cuttings relative to geophysical well logs (gamma-ray—neutron—density), combined with outcrop descriptions (Figure 25.3). Field work focussed on core descriptions and photography of key lithologic units to define rock unit contacts and to reconcile observed lithofacies variations–contacts with geophysical well log data, as well as to define geological contacts in outcrops located throughout Manitoulin Island and southwestern Ontario. As clay and organic matter content vary widely through the interval and area of interest, gamma-ray logs have proven to be the most useful tool in recognizing lithologic contacts (*see* Figure 25.3). Only one of the cores studied does not have gamma-ray logs associated with them (*see* Table 25.1).

Fossil type and abundance vary significantly through the studied succession and have proven valuable in the recognition of formational-rank boundaries and smaller cycles within the studied interval. Detailed descriptions of the taphonomic and paleoecologic attributes of these strata will aid in the interpretation of oxygen fluctuation, depositional dynamics and faunal patterns that may reveal the underlying processes responsible for the extreme variations in organic matter preservation within this succession. Data collected during this project will enable improved delineation of the paleoenvironmental changes recorded in the stratigraphic interval.

In addition to lithostratigraphic work, the cores have been sampled for trace element analysis and stable carbon and oxygen isotopic analysis to detect chemostratigraphic trends and/or anomalies that may aid in the recognition of unit boundaries. Select samples were chosen for petrographic analysis to determine microstructures and mineral content characteristic of specific units. Scanning electron microscopy electron dispersive spectrometry (SEM–EDS) was undertaken on select samples to examine sedimentary microfabrics and compositional attributes not visible by other methods.

Table 25.1. Wells selected for subsurface stratigraphic study of the uppermost Cobourg Formation, the Collingwood Formation, and the Rouge River member of the Blue Mountain Formation. Cores with photos have been logged and the formation picks have been compared to those in the records (specifically Ministry of Natural Resources and Forestry "Form 7: Drilling and Well Completion Report") located at the Oil, Gas and Salt Resources Library (www.ogsrlibrary.com), London, Ontario. The well core without associated geophysical logs is indicated in **bold**.

Licence Number	Name	Core Number	Photographed (Yes or No)	Latitude (degrees North)	Longitude (degrees West)
T012159	Dundee East, Lake Erie 45 – E4C	1130	No	42.73641667	−80.07358333
T006120	OGS 83-1 Halton, Nassagaweya 9-VII	1104	Yes	43.53479139	−79.95857611
T006056	OGS 82-4 Wiarton, Albemarle 4-24-1W	862	Yes	44.79185583	−81.23234972
T002252	Geological Survey of Canada No 2, Russell 24-II	151	Yes	45.32047222	−75.39594444
T006078	OGS 82-3, Yarmouth Township, 3-9-1	861	Yes	42.67076833	−81.16139472
T006045	OGS 82-2 Chatham, Harwich 1-25-IECR	860	Yes	42.38782250	−82.07989500
H000015	OGS Deep Hole No. 1 Corbetton, Melancthon 251-II	1098	Yes	44.14021583	−80.35862222
N000262	OGS CLGD No. 1, Collingwood 27-VII	CLGD 1	No	44.53397972	−80.41429167
N000257	OGS CLGD No. 2, Collingwood 24-VIII	CLGD 2	No	44.51392000	−80.42696250
N000261	**OGS CLGD No. 3, Collingwood 26-VII**	**CLGD 3**	**No**	**44.53286306**	**−80.39755917**
N000258	OGS CLGD No. 4B, Collingwood 25-IV	CLGD 4B	No	44.53420194	−80.35379000
N000255	OGS CLGD No. 7A, Collingwood 10-I	CLGD 7A	No	44.46744194	−80.27927000
N000264	OGS CLGD No. 16, Collingwood 40-XII	CLGD 16	No	44.58801639	−80.51334639

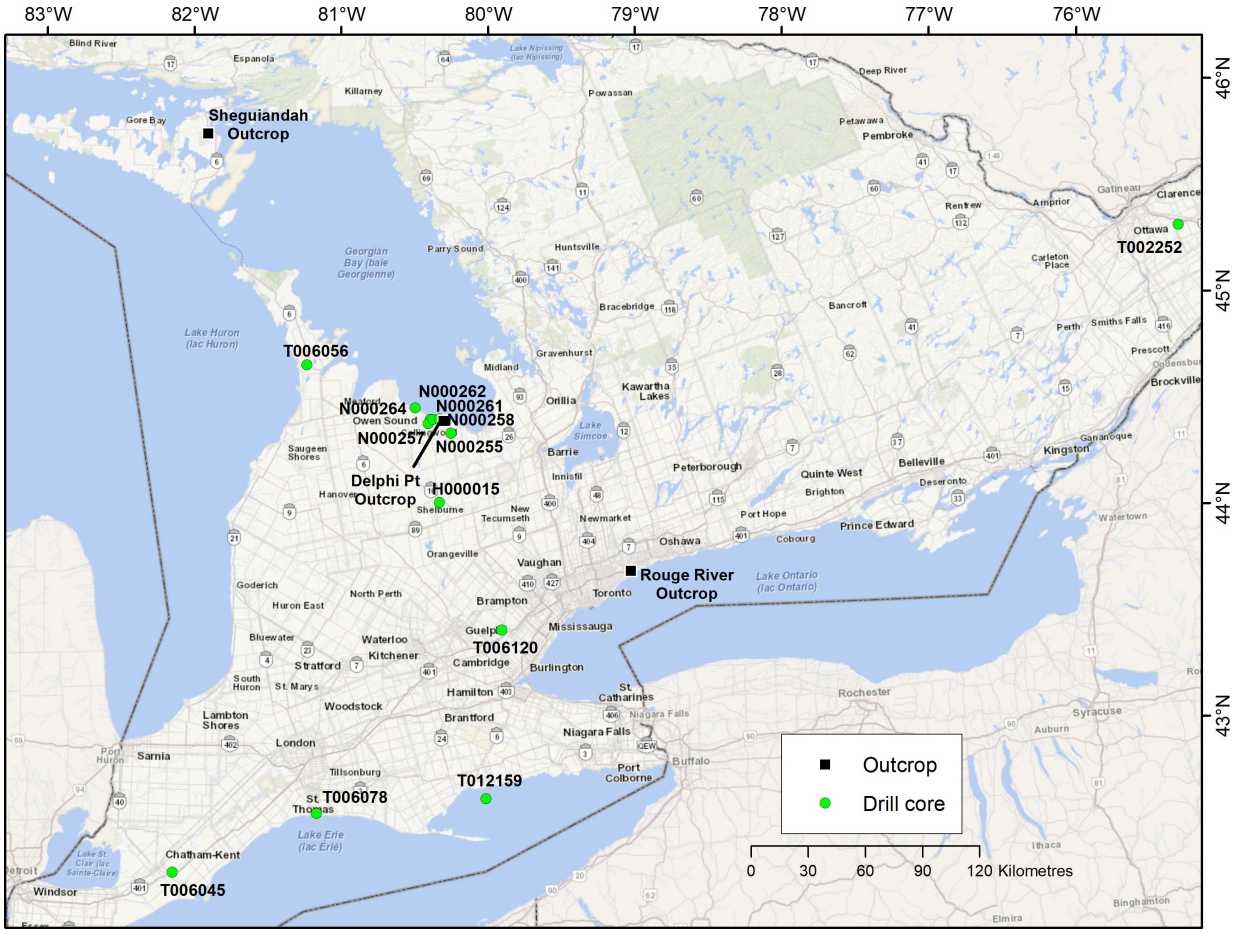


Figure 25.2. Map of southern Ontario showing drill sites corresponding to cores examined in 2022 and 2023 (green dots) and 3 key outcrops (black squares) on Manitoulin Island (Sheguiandah site), Collingwood (Delphi Point) and Toronto (Rouge River type section). Observations on the cored wells will be used to define formational-rank contacts in order to define stratigraphic relationships of the Upper Trenton Group (Cobourg Formation) through to the basal Blue Mountain Formation.

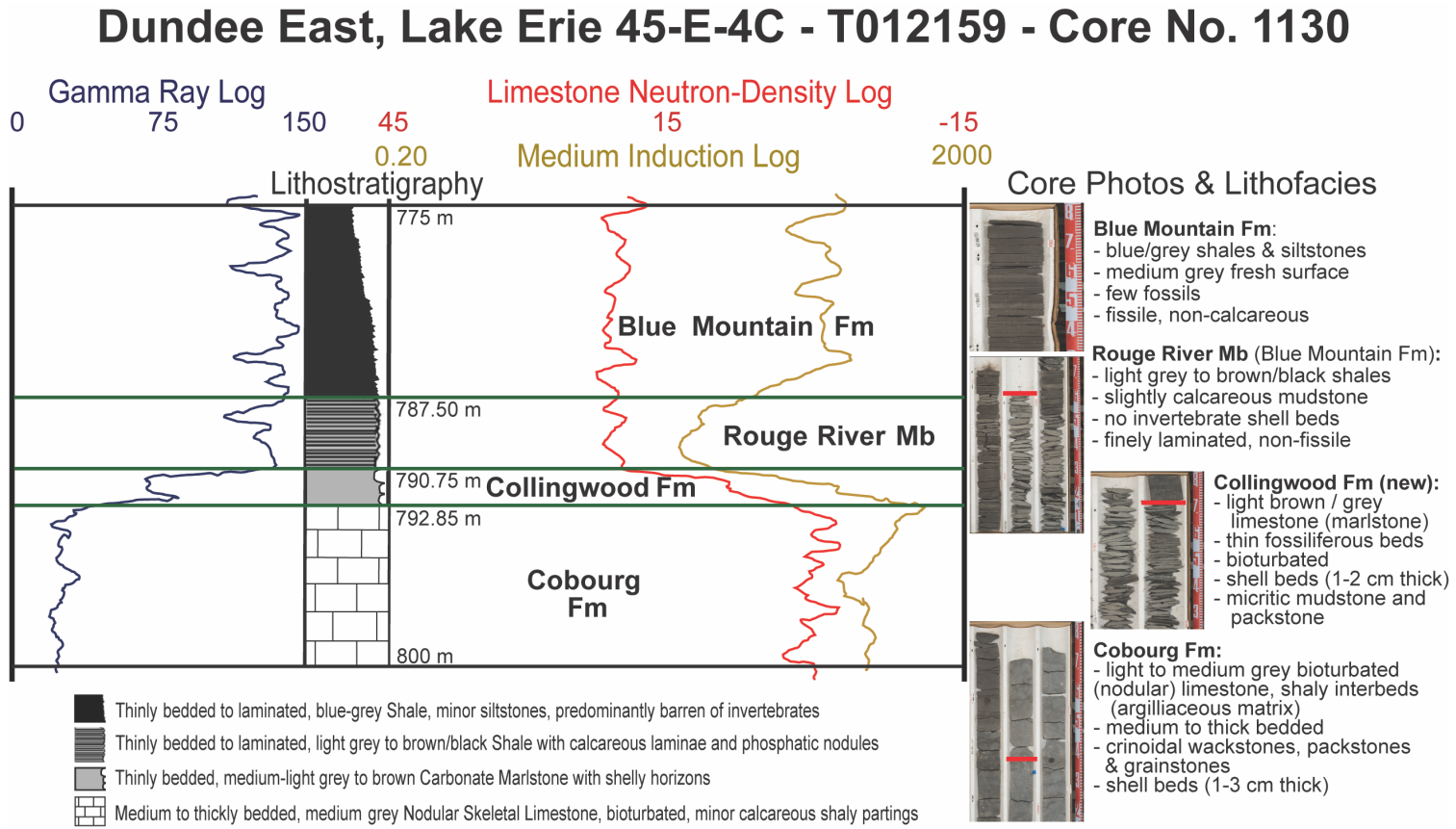


Figure 25.3. Stratigraphic log for Dundee East, Lake Erie 45–E4C, Licence Number T012159, Core number 1130. Revised formation and member picks are shown in green lines. These lines are adjusted approximately 1.7 m between the gamma-ray log obtained on the core versus the borehole gamma-ray log shown in figure. The basal Cobourg Formation, which is a highly bioturbated nodular limestone with calcareous shaly interbeds, has a relatively low gamma-ray signature (blue line) because of low terrigenous clay and/or feldspar content. The stepped increase in gamma-ray signature reflects the disconformable contact between the Cobourg Formation and overlying carbonate marlstones of the Collingwood Formation. The limestone neutron-density profile (red line) reflects an inferred decrease in hydrogen concentration associated with a reduction in permeability vertically. The resistivity medium-induction log (gold line) records variably conductive lithofacies vertically. The 3 geophysical profiles appear to reflect cyclic deposition vertically from the Collingwood Formation through Rouge River Member and basal Blue Mountain Formation succession. The red marker lines in the core photos reflect contacts between various formational and member rank units in the core. Abbreviations: Fm, Formation; Mb, member; the gamma-ray log reflects GAPI, gamma-ray American Petroleum Industry (API) units[3].

[3] *16.5 American Petroleum Institute (API) units correspond to a concentration of radioactive elements equal to 1 microgram of radium per ton. The gamma-ray probes used in oil logging give comparable responses from one probe to another because of their common calibration. Clays have an activity of 100 to 200 API, sands 30 to 80 API, and limestone 10 to 50 API.*

PRELIMINARY STRATIGRAPHIC REVISIONS

Currently, this study suggests 2 preliminary changes to the stratigraphic nomenclature in use in southern Ontario. The first is to remove the Collingwood member from the Cobourg Formation and elevate it to formational rank, that is, the Collingwood Formation. The second change is to confirm that the Rouge River member, although lithologically distinctive, is indeed the basal member of the Blue Mountain Formation and, thus, stays at member rank. The collection of additional lithological, geochemical and geophysical data to support the change to formational rank for the Collingwood member strata is currently part of an MSc thesis study by Atasiei at the University of Western Ontario. The data acquired by the MSc thesis study will be used to officially redefine the Collingwood Formation as outlined in the North American Stratigraphic Code (North American Commission on Stratigraphic Nomenclature 2021, p.172-173). The rationale for these suggested changes is outlined briefly in the next 4 sections.

Cobourg Formation

Raymond (1921) named the Cobourg Formation for a succession of Ordovician strata in the Prince Edward County to Cobourg region of south-central Ontario. Raymond (1921) recognized 2 members, which Kay (1937, p.278) named the Hallowell and Hillier members. There have been numerous attempts to further subdivide the Cobourg Formation into subunits (other than the Collingwood member and lower member) or lithofacies; however, these subdivisions have proven difficult to apply regionally (*see* Figure 25.1). This upper part of the Trenton Group was referred to historically as Middle Ordovician, but is now assigned to the Upper Ordovician Epoch. Sinclair (1958) was among the first to designate an Upper Ordovician age for at least the upper Hillier Member. Presently, the Cobourg Formation is used mainly in the subsurface stratigraphic nomenclature of southwestern Ontario by the petroleum industry, Ministry of Natural Resources and Forestry (MNRF) staff and OGSRL staff. In contrast, the correlative term Lindsay Formation, defined by Liberty (1969), is used in the outcrop belt of south-central and southeastern Ontario by GSC and OGS staff (*see* Figure 25.1; *see* discussion in Caley 1936; Sproule 1936; Sanford 1961; Liberty 1969; Winder and Sanford 1972; Armstrong and Carter 2010; Brunton et al. 2017). Recent revisions to the lithostratigraphy of southern Ontario by the OGS have adopted Cobourg Formation as the preferred name for this interval (Brunton et al. 2017; Brunton and Brintnell 2020).

The Cobourg Formation (not including the “Collingwood member” lithofacies) comprises light to dark grey, argillaceous limestones and calcareous clay seams with minor interbeds of crystalline crinoidal packstones to grainstones (2 to >60 cm thick). The succession is medium to thickly bedded and contains shaly partings and thin shaly beds and weathers as grey loose to irregular rubbly limestones (Sproule 1936). In general, coarsely crystalline skeletal packstone and grainstone interbeds tend to be more abundant toward the base of the formation and fine upward to wackestones and lime mudstones (Melchin et al. 1994). The planar tabular bedded limestones are typically fine- to coarse-crystalline, horizontally to low-angle cross-laminated, skeletal packstones and grainstones, probably deposited by storms (Armstrong and Carter 2010). The uppermost units of the Cobourg Formation also can be selectively dolomitized and darker grey and are variably intensely bioturbated. Some regional variations are observed at the top of the Cobourg Formation because the top of the Trenton Group is variably eroded (*see* Caley 1936; Sproule 1936). The contact between the overlying Collingwood Formation (new rank) thinly bedded to laminated carbonate marlstones and the underlying Cobourg Formation *senso stricto* is distinctive and disconformable (*see* Figure 25.3; Caley 1936; Sproule 1936; Liberty 1955).

Collingwood Formation (New Rank)

This stratigraphic interval is a key focus of this study. Raymond (1912) named this stratigraphic unit the lower Utica Formation, based on observations mainly from the Ottawa graben region, but did not designate a type section for the Collingwood unit. Raymond (1914, 1916) subsequently designated this stratigraphic unit as the Collingwood portion of the Utica Group (*see* Figure 25.1). Raymond (1912, 1914) described the Collingwood unit as layers of finely crystalline (fine-grained) relatively pure blue limestone with alternating thicker units of soft brown shale. Kay (1937) assigned the lower Collingwood carbonate beds as belonging to the bioturbated nodular limestone beds of the Cobourg Formation (Hillier member) and the overlying shales as upper Collingwood rock units. Liberty (1955) recognized the disconformable nature of contact with the underlying Cobourg Formation and renamed this stratigraphic unit as the Craigleith Formation of the Whitby Group and, subsequently, as the "Lower Whitby Formation" within the Nottawasaga Group (*see* Figure 25.1; Liberty 1964). Russell and Telford (1983) formally defined the Collingwood Member as the uppermost member of the Lindsay Formation (outcrop belt equivalent of the Cobourg Formation), based mainly on lithologic characteristics identified in the shallow subsurface near its outcrop belt.

As outlined above, the rocks comprising the Collingwood Formation have had a long and complicated nomenclatural history (*see also* reviews by Russell and Telford 1983; Churcher et al. 1991; Rancourt 2009; Hamblin 1999, 2018). Collingwood Formation lithofacies range up to approximately 10 m thick (Johnson et al. 1992). The authors generally follow the most recent geochemical and stratigraphic studies of the upper Cobourg Formation through the Blue Mountain Formation interval undertaken by Béland Otis (2012, 2015a, 2015b), except that a significant time break or disconformity is suggested as occurring between the underlying bioturbated limestones of Cobourg Formation and the lithologically and faunally distinctive thinly bedded carbonate marlstones of the overlying Collingwood Formation.

Consequently, because of the distinctive lithological character of the Collingwood lithofacies, the fact that both its upper and lower contacts represent time breaks, the fact that the lithofacies occurs throughout southern Ontario, and the fact that many previous authors considered it to be a formational-rank unit, the authors recommend that the Collingwood strata be designated as a formation, not a member.

Rouge River Member (Basal Blue Mountain Formation)

Liberty (1955) named the shales immediately above the Collingwood Formation carbonate marlstones as the Rouge River Formation (*see* Figure 25.1). He subsequently referred to this succession as the "middle member" of the Whitby Formation (Liberty 1969; Liberty and Bolton 1971). Russell and Telford (1983) referred to this interval as the Rouge River Member of the Blue Mountain Formation, which corresponds approximately to the Utica Formation of Raymond (1912, 1914) and the "Gloucester" Formation (Raymond 1916). Parks (1928) treated the Rouge River strata as equivalent to the "upper Gloucester" unit. In his study of Paleozoic rocks of the Toronto area, Caley (1940, p.14) equated the Rouge River Formation strata to the Gloucester unit of "upper Billings Shale" of the Ottawa area (*see* Figure 25.1). In the Rouge River type area, northeast of Toronto, Miller (1942; and noted in Liberty 1969, p.68) reported the common occurrence of mud cracks that are spatially associated with phosphatic lag layers (referred to as nodules by Miller 1942) in the Rouge River area, supporting a shallow-water origin with hiatuses in deposition of unknown duration within these organic-rich shale units. Although the presence of mud cracks has proven difficult to observe in the cores selected for this study, the phosphatic layers are readily evident.

The authors concur that this stratigraphic interval is a basal member of the overlying Blue Mountain Formation because the 2 successions are similar lithologically. Consequently, the authors recommend that the Rouge River rocks remain at member status. The fact the member is not present everywhere in southern Ontario supports this recommendation. It appears that the Rouge River Member represents initial shallow-water shale deposition with minor calcareous intervals, including the development of phosphatic nodules and the preferential preservation of organic material in select areas of southern Ontario. These lithofacies reflect distinctive paleo-oceanographic conditions following deposition of the underlying Collingwood Formation carbonate marlstones. The organic-rich Rouge River Member strata were subsequently covered by transgressive deepening-upward shale deposits. These overlying shales are similar lithologically to the shales of the Rouge River Member, but lack the phosphatic lag deposits, skeletal-bearing intervals and organic-rich layers.

Blue Mountain Formation

Parks (1928) named the Blue Mountain Formation and described it as a sparsely fossiliferous succession comprising soft bluish grey to grey shales (*see* discussion in Russell and Telford 1983; Armstrong and Carter 2010). Liberty (1969) reassigned this succession to the upper Thornbury Member of the Whitby Formation. Russell and Telford (1983) redefined this succession as the Blue Mountain Formation (*see* Figure 25.1). Although a combination of gamma-ray, neutron and resistivity geophysical logs appear to be helpful in delineating the contact between the Rouge River Member and overlying Blue Mountain Formation (*see* Figure 25.3), not all cores used in this study have such logs and the Rouge River Member appears to be missing in some of the cores.

FUTURE WORK

Next steps include a more detailed examination of the Collingwood Formation and Rouge River member lithofacies, both in subsurface and outcrop. It is hoped that this will result in identifying descriptive characteristics of the units that will enable correlation of the relatively thin stratigraphic wedge present in Ontario (Collingwood Formation and Rouge River member) relative to the much thicker Utica Formation (shale) and its coeval formations in other jurisdictions (e.g., Brett and Baird 2002; Baird and Brett 2002; note that the Utica Formation is defined differently in Quebec than in New York State, but, in both jurisdictions, it overlies the Trenton Group) and build upon the regional characterization of these units by the OGS (Béland Otis 2012, 2015a, 2015b). The study will include a sedimentological and sequence stratigraphic approach to assess the interplay between regional tectonic influences relative to sedimentation processes, in addition to carrying out more detailed studies of the organic-rich units similar to those of Rancourt (2009), Sweeney (2014) and Hamblin (2018).

ACKNOWLEDGMENTS

This research forms part of a MSc thesis study at the University of Western Ontario by Dan Atasiei. The authors thank staff at the Oil, Gas and Salt Resources Library in London, Ontario (manager Jordan Clark, and staff Ramen Tolo, Elizabeth Lenkic, R. Connor MacLeod, and summer students) for their help in compiling key cores examined in this study, and for core handling, photography and sampling for thin sections. Rhys Paterson and Shuo Sun are thanked for assisting D. Atasiei with understanding of the subsurface data available at the core library.

REFERENCES

Armstrong, D.K. and Carter, T.R. 2010. The subsurface Paleozoic stratigraphy of southern Ontario; Ontario Geological Survey, Special Volume 7, 301p.

Atasiei, D., Brunton, F.R., Jin, J. and Yeung, K.H. 2021. Stratigraphy and sedimentology of Upper Ordovician strata, southern Ontario and Manitoulin Island; *in* Summary of Field Work and Other Activities, 2021, Ontario Geological Survey, Open File Report 6380, p.17-1 to 17-3.

Atasiei, D., Brunton, F.R., Jin, J., Phillips, A.R. and Yeung, K.H. 2022. Stratigraphy and sedimentology of Upper Ordovician strata, with emphasis on the Collingwood and Rouge River members, southern Ontario and Manitoulin Island; *in* Summary of Field Work and Other Activities, 2022, Ontario Geological Survey, Open File Report 6390, p.20-1 to 20-6.

Baird, G.C. and Brett, C.E. 2002. Indian Castle Shale: Late synorogenic siliciclastic succession in an evolving Middle to Late Ordovician foreland basin, eastern New York State; Physics and Chemistry of the Earth, v.27, p.203-230.

Béland Otis, C. 2012. Preliminary results: Potential Ordovician shale gas units in southern Ontario; *in* Summary of Field Work and Other Activities, 2012, Ontario Geological Survey, Open File Report 6280, p.29-1 to 29-12.

——— 2015a. Upper Ordovician organic-rich mudstones of southern Ontario: Drilling project results; Ontario Geological Survey, Open File Report 6312, 59p.

——— 2015b. Geological, geochemical and geophysical data from the Ordovician shales drilling program and the regional sampling program, southern Ontario; Ontario Geological Survey, Miscellaneous Release—Data 326.

Brett, C.E. and Baird, G.C. 2002. Revised stratigraphy of the Trenton Group in its type area, central New York: Sedimentology and tectonics of a Middle Ordovician shelf-to-basin succession; Physics and Chemistry of the Earth, v.27, p.231-263.

Brunton, F.R. and Brintnell, C. 2020. Early Silurian sequence stratigraphy and geological controls on karstic bedrock groundwater flow zones, Niagara Escarpment region and the subsurface of southwestern Ontario; Ontario Geological Survey, Groundwater Resources Study 13.

Brunton, F.R., Carter, T., Logan, C., Clark, J., Yeung, K., Fortner, L., Freckelton, C., Sutherland, L. and Russell, H.A.J. 2017. Lithostratigraphic compilation of Phanerozoic bedrock units and 3D geological model of southern Ontario; abstract *in* Regional-scale groundwater geoscience in southern Ontario: An Ontario Geological Survey, Geological Survey of Canada, and Conservation Ontario Geoscientists open house, Guelph, Ontario, March 1–2, 2017, Geological Survey of Canada, Open File 8212, p.3. doi.org/10.4095/299759

Brunton, F.R., Hahn, K.E., Béland Otis, C.B. and Julig, P.J. 2023. Paleozoic geology of Manitoulin Island and adjacent North Channel Islands, northeastern Ontario: A geological guidebook; Geological Association of Canada–Mineralogical Association of Canada–Society for Geology Applied to Mineral Deposits, Joint Annual Meeting, Sudbury, Ontario, May 25–27, 2023, Field Trip FT04 Guidebook, Ontario Geological Survey, Open File Report 6388, 64p.

Caley, J.F. 1936. The Ordovician of Manitoulin Island, Ontario, Canada; Geological Survey of Canada, Memoir 202, p.21-92.

——— 1940. Palaeozoic geology of the Toronto–Hamilton area, Ontario; Geological Survey of Canada, Memoir 224, 284p.

Churcher, P.L., Johnson, M.D., Telford, P.G. and Barker, J.F. 1991. Stratigraphy and oil shale resource potential of the Upper Ordovician Collingwood Member, Lindsay Formation, Southwestern Ontario; Ontario Geological Survey, Open File Report 5817, 98p.

Hamblin, A.P. 1999. Upper Ordovician strata of southwestern Ontario: Synthesis of literature and concepts; Geological Survey of Canada, Open File 3729, 34p.

——— 2018. Stratigraphic architecture, sedimentology, and resource potential of the Upper Ordovician Nottawasaga Group of southwestern Ontario, surface and subsurface: tectonics and sequence stratigraphy in the distal Appalachian Foreland; Geological Survey of Canada, Open File 8153, 86p.

Johnson, M.D., Armstrong, D.K., Sanford, B.V., Telford, P.G. and Rutka, M.A. 1992. Paleozoic and Mesozoic geology of Ontario; Chapter 20 *in* Geology of Ontario, Ontario Geological Survey, Special Volume 4, Part 2, p.907-1008.

Kay, M. 1937. Stratigraphy of the Trenton Group; Geological Society of America, Bulletin, v.48, p.233-302.

Liberty, B.A. 1953. Preliminary map, Alliston, Simcoe, York and Dufferin counties, Ontario; Geological Survey of Canada, Paper 53-9, 3p., 1 sheet, scale 1:63 360.

——— 1955. Stratigraphic studies of the Ordovician System in central Ontario; Proceedings of the Geological Association of Canada, v.7, p.139-147.

——— 1964. Upper Ordovician stratigraphy of the Toronto area; *in* Geology of Central Ontario, American Association of Petroleum Geologists–Society of Economic Paleontologists and Mineralogists, Guidebook, p.43-54.

——— 1969. Paleozoic geology of the Lake Simcoe area, Ontario; Geological Survey of Canada, Memoir 335, 201p.

Liberty, B.A. and Bolton, T.E. 1971. Paleozoic geology of the Bruce Peninsula area, Ontario; Geological Survey of Canada, Memoir 360, 163p.

Melchin, M.J., Brookfield, M.E., Armstrong, D.K. and Coniglio, M. 1994. Stratigraphy, sedimentology and biostratigraphy of the Ordovician rocks of the Lake Simcoe area, south-central Ontario; Geological Association of Canada–Mineralogical Association of Canada, Joint Annual Meeting, Waterloo 1994, Field Trip A4 Guidebook, 101p.

Miller, M.L. 1942. Stratigraphy of the Rouge River–Oshawa area; unpublished Master of Arts thesis, University of Toronto, Toronto, Ontario, 59p.

North American Commission on Stratigraphic Nomenclature 2021. North American Stratigraphic Code, 2021 edition; Stratigraphy, v.18, no.3, p.153-204. doi.org/10.29041/strat.18.3.01

Parks, W.A. 1928. Faunas and stratigraphy of the Ordovician black shales and related rocks in Southern Ontario; Transactions of the Royal Society of Canada, 3rd Series, v.22, section 4, p.39-90.

Rancourt, C. 2009. “Collingwood” strata in south-central Ontario – A petrophysical chemostratigraphic approach to comparison and correlation using geophysical borehole logs; unpublished MSc thesis, University of Toronto, Toronto, Ontario, 65p.

Raymond, P.E. 1912. Invertebrates. Notes on field work in the Ottawa Valley; Geological Survey of Canada, Summary Report 1911, p.351-357.

——— 1914. The Trenton Group in Ontario and Quebec; Geological Survey of Canada, Summary Report 1912, p.342-350.

——— 1916. Expedition to the Baltic provinces of Russia and Scandinavia. Part 1, The correlation of the Ordovician strata of the Baltic Basin with those of eastern North America; Bulletin, Museum of Comparative Zoology, v.56, p.179-187.

——— 1921. A contribution to the description of the fauna of the Trenton Group; Geological Survey of Canada, Museum Bulletin 31, 67p.

Russell, D.J. and Telford, P.G. 1983. Revisions to the stratigraphy of the Upper Ordovician Collingwood beds of Ontario—A potential oil shale; Canadian Journal of Earth Sciences, v.20, p.1780-1790.

Sanford, B.V. 1961. Subsurface stratigraphy of Ordovician rocks in southwestern Ontario; Geological Survey of Canada, Paper 60-26, 54p.

Sinclair, G.W. 1958. Age of the Ordovician Cobourg "Formation"; abstract, Geological Society of America, Bulletin, v.69, no.12, p.1643.

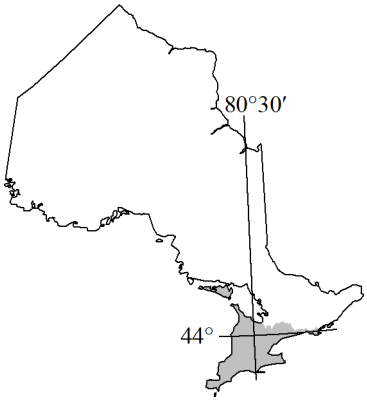
Sproule, J.C. 1936. A study of the Cobourg Formation; Geological Survey of Canada, Memoir 202, p.93-117.

Sweeney, S.N. 2014. Allostratigraphy of the Upper Ordovician Blue Mountain Formation, southwestern Ontario, Canada; unpublished MSc thesis, The University of Western Ontario, London, Ontario, 301p.

Winder, C.G. 1961. Lexicon of Paleozoic names in southwestern Ontario; University of Toronto Press, Toronto, Ontario, 121p.

Winder, C.G. and Sanford, B.V. 1972. Stratigraphy and paleontology of the Paleozoic rocks of southern Ontario; 24th International Geological Congress, Montreal, Quebec, Excursion A45-C45, 73p.

26. Project SO-22-004. Revisiting the Cambrian Stratigraphy of Southwestern Ontario: Next Steps



A.R. Phillips[1], F.R. Brunton[2,1] and K.H. Yeung[2]

[1]Department of Earth Sciences, The University of Western Ontario, London, Ontario N6G 2V4
[2]Earth Resources and Geoscience Mapping Section, Ontario Geological Survey, Sudbury, Ontario P3E 6B5

INTRODUCTION

This project involves an examination of basal Paleozoic sedimentary rocks and underlying variably weathered crystalline basement rocks in key wells across southwestern and southcentral Ontario. These predominantly subsurface Cambrian and Ordovician strata are the least understood and documented part of the Paleozoic succession in southern Ontario (Figure 26.1).

Sanford and Quillian (1959) used 130 sets of drill cuttings and drillers logs from approximately 200 wells to map the thickness and distribution of the Cambrian strata in the subsurface of southern Ontario. In the 6 decades since then, more than 900 wells have been drilled into this interval, including several wells under the waters of Lake Erie where the Cambrian section attains a thickness of greater than 175 m. Included in this recent data set are sets of drill cuttings from 900 wells, and drill cores from 129 wells, all of which allow for a better understanding of the stratigraphy and sedimentology of this complex section. These data, in combination with geophysical logs from more than 725 of the wells, also allow for a much better understanding of porosity and permeability trends within this geologic section. This modern data set allows for improved correlations and subdivisions of strata that historically has been lumped together as the "basal beds".

There are more than 20 mostly small, but prolific hydrocarbon reservoirs in the basal siliciclastic-dominated succession of southwestern Ontario (Bailey Geological Services Ltd. and Cochrane 1984; Bailey 2005; Trevail 1990; Dorland 2004; Dorland et al. 2019). Despite this, little is known about the precise age, depositional systems and stratigraphic correlations of the host strata or the formational fluid temperatures, pressures, and porosity and/or permeability values of various rock units. The rock units are generally thought to represent deposition from progressive onlap of Early Paleozoic seas over a broad undulatory Proterozoic basement surface (referred to simplistically as the Algonquin Arch). Subsequently, localized and episodic erosion of these largely unlithified sediments occurred prior to the Ordovician marine transgression(s) and associated onset of carbonate-dominated sedimentation that cover these strata (*see* Hamblin 1998a, 1998b, 2011). Paleotopographic irregularities, and syndepositional and later faulting of the Cambrian and Precambrian basement rocks, appear to have had some local control on the preserved sedimentary rock characteristics and distribution.

A better understanding of the stratigraphy and distribution of Cambrian strata in the subsurface of southern Ontario is important to our general understanding of the Paleozoic history of Ontario and thus has broad and direct relevance to many clients. The relationship of the Cambrian strata to the underlying Proterozoic basement and structures and deep formational fluid characteristics may help us to develop

Summary of Field Work and Other Activities, 2023,
Ontario Geological Survey, Open File Report 6405, p.26-1 to 26-7.

© King's Printer for Ontario, 2023

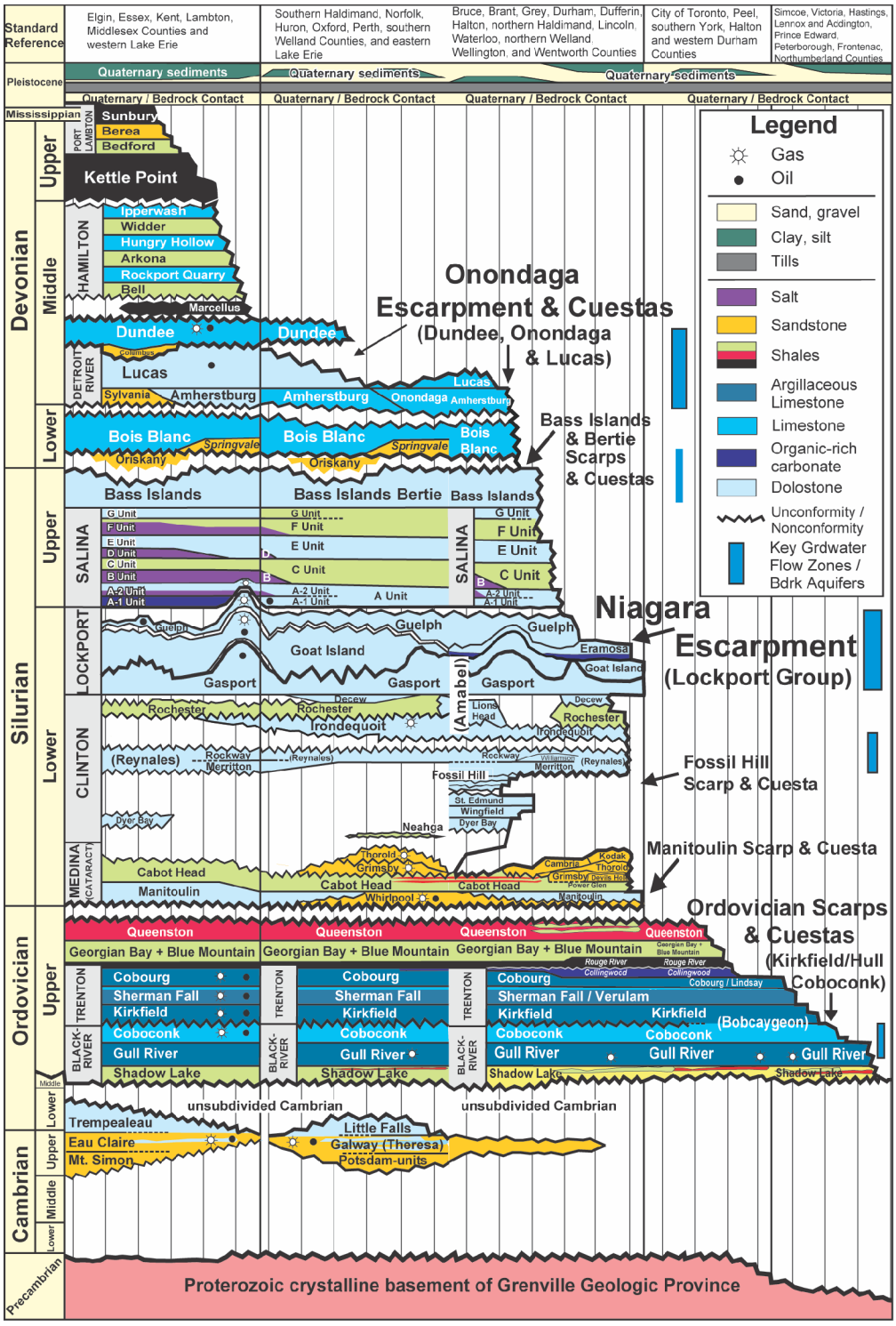


Figure 26.1. Revised terminology of Paleozoic strata for south-central and southwestern Ontario (*modified after* Winder 1961; Beards 1967; Winder and Sanford 1972; Armstrong and Carter 2010; Brunton et al. 2017). Group names are in capitals, members in italics, and abandoned or geographically restricted formation names in brackets. The remaining horizontal black zig-zag lines reflect unconformities, or sequence boundaries. Stepped karstic cuestas and key escarpments are labelled on the right side. The Phanerozoic bedrock topography is depicted by the erosional line (uppermost, thickened, black zig-zag line). The line thicknesses signify inferred missing time intervals (note: Cambrian, Lower to Middle Ordovician and Lower Silurian gaps in sedimentation). The relative thicknesses of rock units are not to scale.

a more robust structural framework for southwestern Ontario that will assist in our understanding of deep regional formational fluid flow, deep disposal of brines and other waste, and other potential deep storage. This project also links directly with other Ontario Geological Survey (OGS) Paleozoic initiatives, including 1) the ongoing three-dimensional (3-D) Paleozoic modelling work using Leapfrog® Works; 2) updates to Paleozoic lithostratigraphic chart and map legend for southern Ontario; and 3) the development of a modern lexicon of Paleozoic names for southern Ontario (*see* Brunton et al. 2021).

PREVIOUS WORK

The last subsurface project of these basal sedimentary rock units, sponsored by the OGS, was in the 1980s (Bailey Geological Services Ltd. and Cochrane 1984). That study, based on oil and gas well records, consisted of a resource evaluation for the Cambrian units of southwestern Ontario, structure contour maps for the top of the underlying Proterozoic bedrock and for the top of the overlying Upper Ordovician Shadow Lake Formation, and isopach maps for all units found between these 2 surfaces. As such, that project did not separate out the Cambrian rock units (*see also* Trevail 1990; Carter, Trevail and Easton 1996; Easton and Carter 1991; Al et al. 2011; Raven et al. 2011).

The Cambrian–Lower Ordovician strata in the subsurface of southwestern Ontario was last examined in some detail over 60 years ago (Sanford and Quillian 1959). They subdivided the Cambrian succession into 3 formations and applied stratigraphic nomenclature from the Michigan Basin to the west side of southwestern Ontario and Appalachian Foreland Basin nomenclature to the east side (*see also* Hamblin 1998a, 1998b, 2011). Although these terms are now out-of-date and, in some instances, are used elsewhere for much younger strata, they remain in current usage (Armstrong and Carter 2010; Carter et al. 2019; *see* Figure 26.1). Bailey (2005) revisited the Cambrian succession in the subsurface using geophysical gamma-ray logs and drill cuttings. Bailey used Michigan Basin stratigraphic terms and proposed a complex model of repeated cycles of onlap, tilting, uplift and erosion.

The Cambrian section, where it is thickest in southwestern Ontario, typically has a basal dolomitic sandstone interval that is overlain by a transitional mixed feldspathic quartz sandstone and carbonate succession, which is often capped by a thick dolostone section that is variably oölitic. Early workers attempted to correlate the drill cuttings from the Cambrian wells in southwestern Ontario to the outcrop belts in Wisconsin or New York (e.g., Cohee 1945, 1947, 1948a, 1948b; Roliff 1954; Sanford and Quillian 1959). The Cambrian section is absent over a large portion of southwestern Ontario that is known as the Algonquin Arch. In this area, the Proterozoic basement rocks are variably weathered (paleosols) and covered by a varied siliciclastic and mixed carbonate Upper Ordovician (Black River–Trenton) succession that makes for direct correlation to outcrops of eastern Ontario and upstate New York difficult.

STUDY AREA AND FIELD WORK

The proposed subsurface mapping initiative covers southwestern and southcentral Ontario (Figure 26.2). These basal Paleozoic rocks are largely restricted to the subsurface and are known only through hydrocarbon exploration and/or development drilling and deep stratigraphic cores. Twenty key wells were selected from the more than 1225 Cambrian–Precambrian wells in the Oil, Gas and Salt Resources Library (OGSRL) database (*see* Figure 26.2; Table 26.1) to provide a representative distribution across southern Ontario. Preference was given to wells with the most complete data, including drill core, drill cuttings and modern geophysical logs. The well databases of adjacent jurisdictions were also reviewed to identify wells with geophysical logs, drill cuttings and core descriptions and/or core analyses.

Phase 1 of the study was conducted in 2022 and involved the selection of key cores and well cuttings for high-resolution photography by staff at the OGSRL in London, Ontario. All 20 key wells have a suite of geophysical logs that have been integrated with the lithofacies descriptions to better characterize formational rank geologic picks and aid in correlation to other key wells. These wells will serve as fenceposts to expand the correlations to the entire database of 1225 wells intersecting the Cambrian in southwestern Ontario. The 20 key wells selected for this study were drilled between 1962 and 2012. Fifteen of the 20 wells have drill core, including 9 that have the entire Cambrian interval cored. Those that do not have core over the entire section have drill cuttings available for examination. The staff at the OGSRL in London, Ontario, have largely completed photography of key drill cuttings samples and the cores of the 20 key wells.

The main focus of Phase 2 of the study (2023 field season) has been to 1) complete descriptions of drill cuttings; 2) core photography of odd-sized core boxes; 3) provide more detailed core descriptions of key wells; 4) examine 4 cores from eastern Michigan and northern Ohio to correlate with the 20 key wells in southwestern Ontario; and 5) sample key facies within cores for petrographic analyses. Petrographic examination of 200 thin sections from select wells is currently underway. The final product of Phase 2 will be an Open File Report (draft to be completed by the end of 2023) that will include stratigraphic and sedimentologic descriptions, formational-rank revisions, and petrographic analyses that will be compared to selected well test, production and injection data to further understand porosity and permeability trends within the various Cambrian rock units.

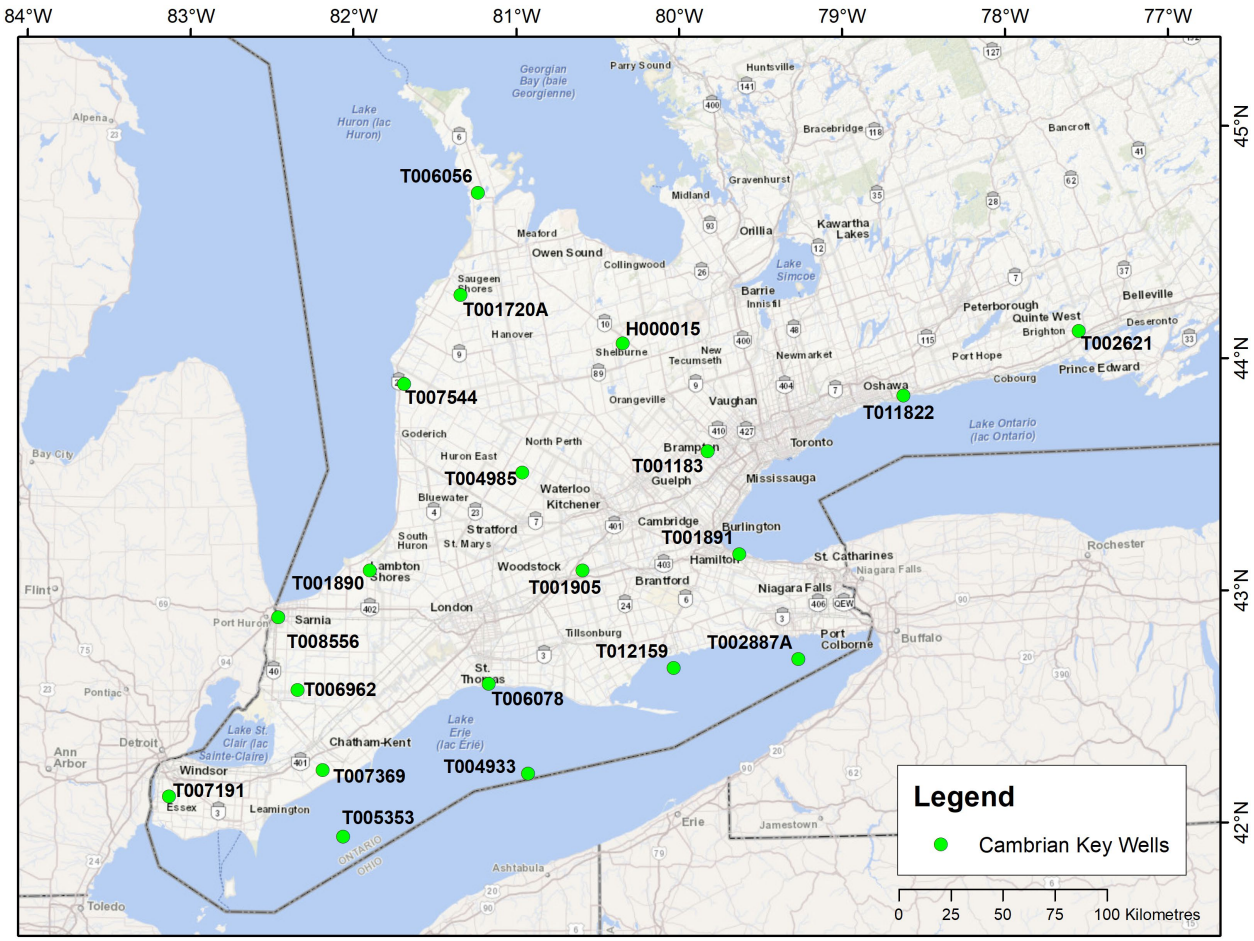


Figure 26.2. Map showing the 20 key Cambrian wells to be examined as part of this study; details about the wells are provided in Table 26.1.

Table 26.1. Key wells selected for subsurface stratigraphic study of the Cambrian succession in southwestern Ontario. Well locations are shown on Figure 26.2 (labelled with Well Licence number). Numbers for core and cuttings in this table correspond to file numbers assigned to drill core boxes and drill cuttings trays at the Oil, Gas, and Salt Research Library in London, Ontario.

Number	Well Licence	County	Township, Location [a]	Well Name	Completion Date	Well Logs [b]	Core Number	Cuttings Number
1	T007191	Essex	Anderdon 2-11-V	Pembina - Maxus	Nov 11, 1987	CNL–LDT, DLL, BHCS, FMS	none	9354-55
2	T007369	Kent	Raleigh 1-17-XIII	Ram/BP No. 5	Aug 20, 1988	CNL–LDT, DLL, BHCS, EPT	986	9508-09
3	T005353	Kent	Lake Erie 284-U-4	Consumers' 13730	July 8, 1980	CNL–FDC, DLL	1030	6921-23
4	T006962	Lambton	Sombra 2-26-V	Ram No. 89	May 14, 1986	CNL–LDT, DLL, BHCS	none	9145-46
5	T008556	Lambton	Sarnia 2-11-RIVIR	Imperial Brine Disposal No. 1	Nov 17, 1997	CN–ZDL, DLL–MLL, BHC-AC	1074	10762-64
6	T001890	Lambton	Bosanquet 3-18-IV	Home-CDR-Union Thedford	Jan 28, 1965	AV, GRD	543	5550-51
7	T006078	Elgin	Yarmouth 3-9-I	OGS 82-3	Mar 11, 1983	TDT, IRT	861	9341-51
8	T004933	Elgin	Lake Erie 184-K-3	Consumers' 13603	July 14, 1979	CNL–FDC, DLL	700	4065-67
9	T012159	Haldimand	Lake Erie 45-E-4C	Dundee East Lake Erie	Sept 11, 2012	CNT–SPeD, AIL, CSL	1130	11774-76
10	T001905	Oxford	Blenheim 3-23-I	Kewanee Gobles No. 40	Dec 14, 1964	GR–N, DENL	150	5530-31
11	T004985	Perth	Elma 2-36-XIV	Petromark et al.	July 20, 1979	GR–N, DENL	none	4068-69
12	T007544	Huron	Ashfield 2-6-XWD	BP No. 1	Jan 6, 1990	CN–ZDL, DLL–MLL, BHC-AC	none	9434-35
13	T001720A	Bruce	Saugeen 2-29-II	BP-Triad (A)	Aug 2, 1964	GR–N, DENL	985	5421-22
14	T006056	Bruce	Albemarle 4-25-IW	OGS 82-4 Wiarton	Nov 22, 1982	GR-SDD, SDN, FEL	862/1103	9352-53
15	H000015	Dufferin	Melancthon 7-251-II	OGS Deep Hole No. 1 - Corbetton	Mar 10, 1982	GR-LSD, SDN, CSS, FEL	1098	9301-06
16	T001183	Peel	Chinguacousy 1-14-VIW	M & M Oil & Gas No. 1	Feb 23, 1962	GR–N	none	3797-98
17	T001891	Wentworth	Saltfleet 2-11-I	Imperial No. 891	Jan 16, 1965	GR–N, DENL	259	5557-58
18	T002887A	Welland	Lake Erie 24-T-3	CPOG Welland No. 2A	Nov 7, 1969	SNP, FDC, BHCS, DILL	648	7559-61
19	T011822	Durham	Darlington 3-12-BFC	St. Mary's Cement DH08-01	Aug 30, 2008	GR–Cond	1121	Core
20	T002621	Hastings	Murray 2-6-III	Consumers' 31758	Nov 26, 1968	GR–N	137	7389-89

[a] *Onshore locations are provided as township, tract, lot and concession. Offshore locations as Lake Erie, block, tract and quadrant.*

[b] *Types of well logs: AIL, Array Induction Log (Weatherford); AV, Acoustic Velocity Log (Welex); BHC-AC, Borehole Compensated Acoustilog (Western Atlas); BHCS, Borehole Compensated Sonic Log (Schlumberger); CN–ZDL, Compensated Neutron–Z-Densilog (Western Atlas); CNL–FDC, Compensated Neutron Log–Formation Density Compensated (Schlumberger); CNL–LDT, Compensated Neutron Log–Litho Density Tool (Schlumberger); CNT–SPeD, Dual Spaced Neutron–Photo Density (Weatherford); CSL, Compensated Sonic (Weatherford); CSS, Compensated Sonic Sonde (BPB Wireline); DENL, Density Log (Welex, Great Guns); DILL, Dual Induction-Laterolog (Schlumberger); DLL, Dual Laterolog (Schlumberger); DLL–MLL, Dual Laterolog–Micro Laterolog (Western Atlas); EPT, Electromagnetic Propagation Tool (Schlumberger); FDC, Compensated Formation Density Log (Schlumberger); FEL, Focused Electric Log (BPB Wireline); FMS, Formation Microscanner (Schlumberger); GR–Cond, Gamma Ray-Apparent Conductivity (Golder Associates); GR–DENL, Density Log (Welex); GR–N, Radioactivity Log, Nuclear Log or Gamma Ray–Neutron (Welex, Birdwell, Great Guns); GR-LSD, Gamma Ray-Long Spaced Density (BPB Wireline); GR-SDD, Gamma Ray-Slim Dual Density (BPB Wireline); GRD, Guard Log (Welex); IRT, Induction Resistivity Tool (Schlumberger); SDN, Slim Dual Neutron (BPB Wireline); SNP, Sidewall Neutron Porosity Log (Schlumberger); TDT, Thermal Decay Time Tool (Schlumberger).*

ACKNOWLEDGMENTS

The initial 2 phases of this study have been supported financially by the Ministry of Natural Resources and Forestry (MNRF) and the Ministry of Mines, in collaboration with staff at the Oil, Gas and Salt Resources Library in London, Ontario.

REFERENCES

Al, T., Beauheim, R., Crowe, R., Diedrichs, M., Frizzell, R., Kennell, L., Lam, T., Parmenter, A. and Semec, B. 2011. Geosynthesis; Nuclear Waste Management Organization (NWMO), Toronto, Ontario, NWMO DGR-TR-2011-11, 448p.

Armstrong, D.K. and Carter, T.R. 2010. The subsurface Paleozoic stratigraphy of southern Ontario; Ontario Geological Survey, Special Volume 7, 301p.

Bailey, S.M. 2005. A comparison of the Cambrian reservoir rocks onlapping the SE and NW sides of the Algonquin Arch in SW Ontario – A regional correlation project; *in* Proceedings, Ontario Petroleum Institute, 44th Annual Meeting, London, Ontario, v.44, Technical Paper 5, 20p.

Bailey Geological Services Ltd. and Cochrane, R.O. 1984. Evaluation of the conventional and potential oil and gas reserves of the Cambrian of Ontario; Ontario Geological Survey, Open File Report 5499, 72p.

Beards, R.J. 1967. Guide to the subsurface Palaeozoic stratigraphy of southern Ontario; Ontario Department of Energy Resources Management, Paper 67-2, 19p.

Brunton, F.R., Béland Otis, C., Hahn, K.E. and Yeung, K.H. 2021. Progress on the development of a new stratigraphic framework for the Paleozoic geology of southern Ontario; *in* Summary of Field Work and Other Activities, 2021, Ontario Geological Survey, Open File Report 6380, p.16-1 to 16.9.

Brunton, F.R., Carter, T., Logan, C., Clark, J., Yeung, K., Fortner, L., Freckelton, C., Sutherland, L. and Russell, H.A.J. 2017. Lithostratigraphic compilation of Phanerozoic bedrock units and 3D geological model of southern Ontario; *in* Regional-Scale Groundwater Geoscience in Southern Ontario: An Ontario Geological Survey, Geological Survey of Canada, and Conservation Ontario Open House; Geological Survey of Canada, Open File 8212, p.3. doi.org/10.4095/299750

Carter, T.R., Brunton, F.R., Clark, J.K., Fortner, L., Freckelton, C., Logan, C.E., Russell, H.A.J., Somers, M., Sutherland, L. and Yeung, K.H. 2019. A three-dimensional geological model of the Paleozoic bedrock of southern Ontario; report [PDF] *in* Ontario Geological Survey, Groundwater Resources Study 19 / Geological Survey of Canada, Open File 8618, 56p.

Carter, T.R., Trevail, R.A. and Easton, R.M. 1996. Basement controls on some hydrocarbon traps in southern Ontario, Canada; *in* Basement and Basins of Eastern North America, Geological Society of America, Special Paper 308, p.95-107.

Cohee, G.V. 1945. Stratigraphy of Lower Ordovician and Cambrian rocks in the Michigan Basin; United States Geological Survey, Oil and Gas Investigations, Preliminary Chart no.9.

——— 1947. Cambrian and Ordovician rocks in recent wells in southeastern Michigan; American Association of Petroleum Geologists, Bulletin, v.31, p.293-307.

——— 1948a. Thickness and lithology of Upper Ordovician and Lower and Middle Silurian rocks in the Michigan Basin; United States Geological Survey, Oil and Gas Investigations, Preliminary Chart no.33.

——— 1948b. Cambrian and Ordovician rocks in Michigan Basin and adjoining areas; American Association of Petroleum Geologists Bulletin, v.32, p.1417-1448.

Dorland, M. 2004. Cambrian reservoirs of southwestern Ontario; Ontario Oil & Gas Magazine, 2004 Edition, Ontario Petroleum Institute, London, Ontario, p.20-22.

Dorland, M., Colquhoun, I., Carter, T.R., Phillips, A., Fortner, L., Clark, J. and Hamilton, D. 2019. Ontario Oil and Gas Plays 2. Cambrian and Ordovician conventional plays; Ontario Oil & Gas Magazine, 2019 Edition, Ontario Petroleum Institute, London, Ontario, p.34-41.

Easton, R.M. and Carter, T.R. 1991. Extension of Grenville basement beneath southwestern Ontario; Ontario Geological Survey, Open File Map 162, scale 1:1 013 760.

Hamblin, A.P. 1998a. Upper Cambrian strata of southwestern Ontario: Summary of literature; Geological Survey of Canada, Open File Report 3663, 10p.

——— 1998b. Upper Cambrian and Lower (Middle?) Ordovician sandstones of the Ottawa Embayment: Summary of literature; Geological Survey of Canada, Open File 3670, 10p.

——— 2011. Detailed outcrop and core measured sections of Upper Cambrian and Middle Ordovician sandstones (and associated facies), southwestern Ontario; Geological Survey of Canada, Open File 6856, 41p.

Raven, K., McCreath, D., Jackson, R., Clark, I., Heagle, D., Sterling, S. and Melaney, M. 2011. Descriptive Geosphere Site Model: OPG's Deep Geologic Repository for low and intermediate level waste; Nuclear Waste Management Organization (NWMO), Toronto, Ontario, NWMO DGR-TR-2011-24, 426p.

Roliff, W.A. 1954. The pre-Middle Ordovician rocks of southwestern Ontario; Proceedings of the Geological Association of Canada, v.6, part II, p.103-109.

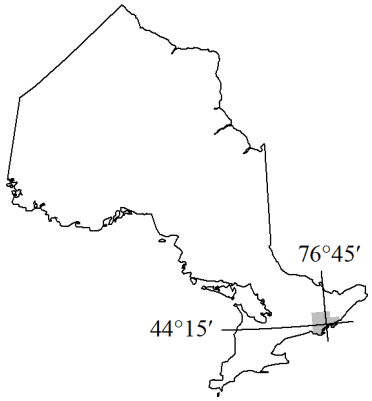
Sanford, B.V. and Quillian, R.G. 1959. Subsurface stratigraphy of Upper Cambrian rocks in southwestern Ontario; Geological Survey of Canada, Paper 58-12, 33p.

Trevail, R.A. 1990. Cambro–Ordovician shallow water sediments, London area, southwestern Ontario; *in* Subsurface geology of southwestern Ontario: A core workshop; American Association of Petroleum Geologists, 1990 Eastern Section Meeting, London, Ontario, p.29-50.

Winder, C.G. 1961. Lexicon of Paleozoic names in southwestern Ontario; University of Toronto Press, Toronto, Ontario, 121p.

Winder, C.G. and Sanford, B.V. 1972. Stratigraphy and paleontology of the Paleozoic rocks of southern Ontario; 24th International Geological Congress, Montreal, Quebec, Excursion A45-C45, 73p.

27. Project SO-22-001. Paleozoic Geology of Eastern South-Central Ontario: Tweed–Kaladar and Belleville–Wellington Areas



K.E. Hahn[1]

[1]Earth Resources and Geoscience Mapping Section, Ontario Geological Survey

INTRODUCTION

In 2022, the Ontario Geological Survey (OGS) initiated a multiyear mapping project focussed on the Paleozoic geology of eastern south-central Ontario (Figure 27.1). This work builds on current OGS mapping projects in eastern Ontario, which, over the past few years, have helped inform several revisions to the Ordovician stratigraphic nomenclature in eastern Ontario (Béland Otis 2017, 2018, 2019, 2022; Hahn 2022). These mapping projects are contributing to a formalized revision to Paleozoic stratigraphic nomenclature for use in Ontario led by the OGS (Brunton et al. 2021).

The study area encompasses the region from Belleville to Gananoque and is bounded by Lake Ontario to the south and the Precambrian–Paleozoic unconformity in the north (*see* Figure 27.1). The study area is represented by 10 National Topographic System (NTS) maps and was last mapped by the OGS in the 1980s (Carson 1981a, 1981b, 1981c, 1982a, 1982b). A detailed summary report does not exist to accompany these maps and, since their publication, only minor revisions to the maps were made for publication of the seamless Paleozoic geology map of southern Ontario (Armstrong and Dodge 2007). Prior to mapping by the OGS, the study area was mapped in the 1960s by Liberty (1963, 1971) and the stratigraphic nomenclature in use by the OGS for this part of Ontario is based on the work of Liberty (1969) (Figure 27.2).

The Paleozoic bedrock near Kingston has been the subject of many academic studies and thesis projects (e.g., McFarlane 1992; Salad Hersi and Dix 1999; Lowe et al. 2017; James, Narbonne and Armstrong 2020; Oruche and Dix 2018). The bulk of these studies employ stratigraphic nomenclature that is not in use by the OGS, but rather includes nomenclature that predates the work of Liberty (1969) or is more commonly used in New York State (*see* Figure 27.2).

This project has 3 goals:

1. reconcile the nomenclature and stratigraphic framework of the Paleozoic bedrock in the study area with proposed revisions to OGS Paleozoic stratigraphic nomenclature (*see* Brunton et al. 2021; Béland Otis 2017, 2018, 2019, 2022; Hahn 2022)
2. establish a regional chemostratigraphic profile using stable carbon and oxygen isotopes to assist in regional correlation
3. update the mapped formational-rank contacts between the various Paleozoic units as well as along the Precambrian–Paleozoic unconformity

Summary of Field Work and Other Activities, 2023,
Ontario Geological Survey, Open File Report 6405, p.27-1 to 27-11.

© King's Printer for Ontario, 2023

In addition, the Ordovician sedimentary rocks of eastern south-central Ontario are important sources for aggregate and groundwater resources and the updated mapping will contribute to better land-use planning in the region. Anticipated products of this project include 10 geological maps, at a scale of 1:50 000, and an Open File Report.

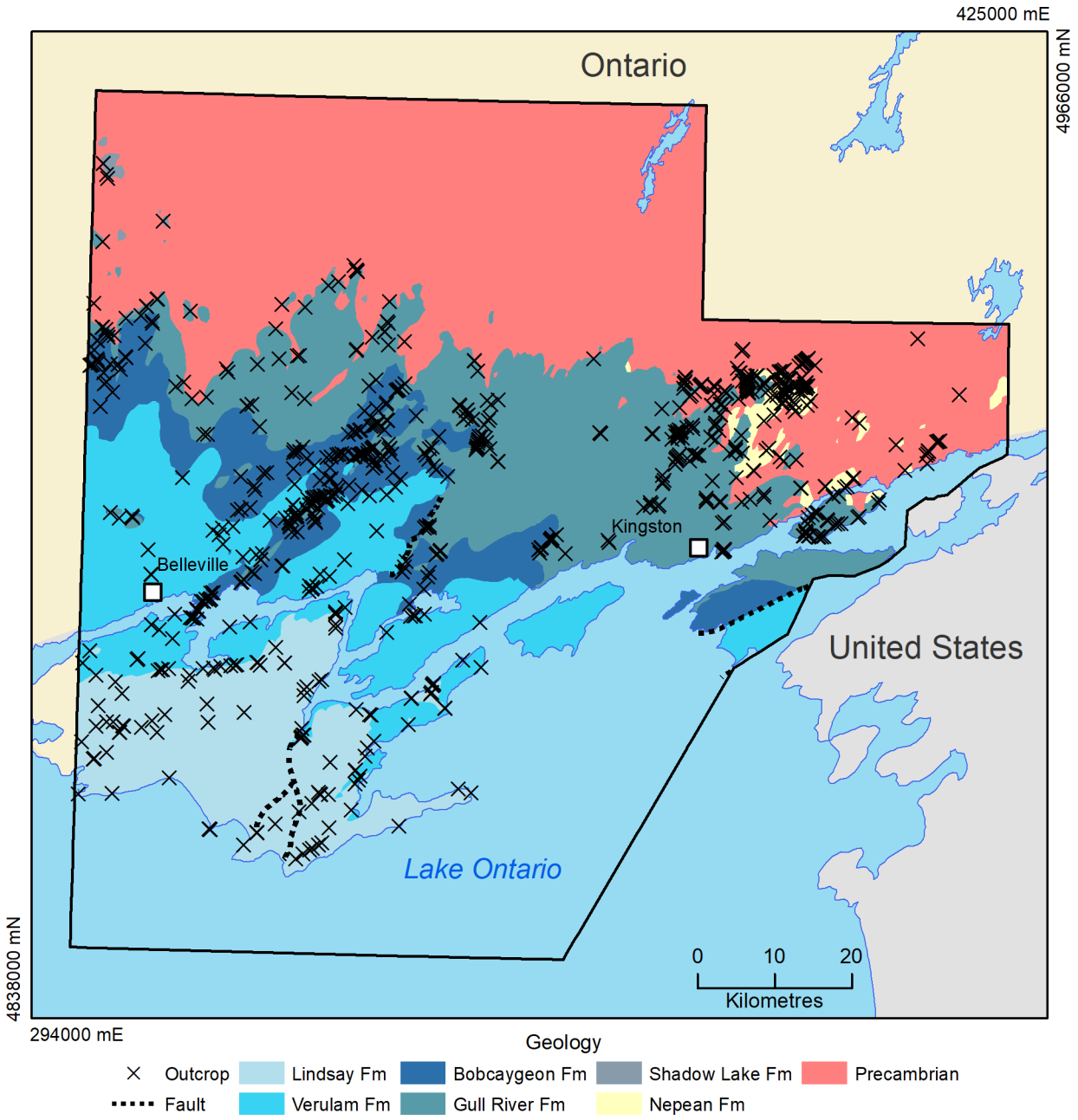


Figure 27.1. General bedrock geology (*from* Armstrong and Dodge 2007; *modified from* Carson 1981a, 1981b, 1981c, 1982a, 1982b) of the study area showing the locations of 2023 outcrop stations mapped and drill cores logged. Universal Transverse Mercator (UTM) co-ordinates provided using North American Datum 1983 (NAD83) in Zone 18. Major cities in the areas shown with small white box outlined in black. Abbreviation: Fm, Formation.

2023 STUDY AREA AND FIELD WORK

The 2023 field season focussed on 5 of the 10 maps representing the entire study area and included mapping in the Tweed–Kaladar (NTS 31C/7) and Belleville–Wellington (NTS 31 C/3 and 30 N/14) areas. Additionally, some outcrops and quarries were visited in the Gananoque–Wolfe Island (NTS 31 C/8 and 31 C/1) area as follow up to work conducted in 2022 (Hahn 2022). The 2023 season included the documentation of 740 outcrops, 14 active quarries and 19 inactive quarries (*see* Figure 27.1). A total of 144 samples were taken for whole-rock geochemical analyses and thin sections. Additionally, 2 outcrops were sampled at a 50 cm vertical spacing interval for stable carbon and oxygen isotope analysis.

Extensive upgrades to roads have occurred since the region was last mapped in 1980 and 1981 (Carson 1981a, 1981b, 1981c, 1982a, 1982b). This road work has resulted in many of the outcrops previously mapped being covered. Additionally, many outcrops indicated on the original maps are located on private property and others are now covered by landscaping. In some places, roadwork has exposed new outcrops in ditches and the construction of new subdivisions near Belleville has temporarily exposed bedrock at surface.

PALEOZOIC STRATIGRAPHY OF THE TWEED–KALADAR AND BELLEVILLE–WELLINGTON AREAS

The oldest Paleozoic sedimentary rocks in the study area are the siliciclastic sedimentary rocks of the Potsdam Group (*see* Figure 27.2). They crop out mainly in the easternmost part of the Gananoque–Wolfe Island and Tichborne–Sydenham map areas as outliers sitting unconformably on Precambrian basement rock. The Potsdam Group was not observed in the Tweed–Kaladar or Belleville–Wellington map areas and currently it is not known if it is present in the subsurface. According to the OGS stratigraphy, the Potsdam Group is subdivided into 2 formations: the Covey Hill Formation and the overlying Nepean Formation. Only the Nepean Formation has been previously described by the OGS in the project area (Carson 1982a; Armstrong and Dodge 2007), although recent work in the study area by Lowe et al. (2017) identified outcrops possibly belonging to the Covey Hill Formation. Lowe et al. (2017) proposed that the formational names from New York State have historical precedence and that the Potsdam Group should follow a tripartite subdivision. Using this nomenclature, the Covey Hill Formation would be equivalent to the Ausable Formation and the Nepean Formation would be equivalent to the Hannawa Falls and Keeseville formations (Lowe et al. 2017) (*see* Figure 27.2). A more detailed overview of the proposed changes can be found in Béland Otis (2017, 2018, 2019, 2022).

In the study area, the Potsdam Group is overlain by the Simcoe Group, which includes the Shadow Lake, Gull River, Bobcaygeon, Verulam and Lindsay formations (*see* Figure 27.2).

From the Kingston area to the Lake Simcoe region of Ontario, the Shadow Lake Formation crops out most commonly near the Precambrian–Paleozoic unconformity. It is present in only a few small outcrops in the Tweed–Kaladar map area. The Shadow Lake Formation is composed of red and green sandstone, siltstone and shale and may include clasts of the underlying basement and/or large quartz clasts. In eastern Ontario, the Shadow Lake Formation has been included as part of the Pamelia Formation (e.g., McFarlane 1992; Salad Hersi and Dix 1999). The upper contact with the Gull River Formation is gradational and is generally marked at the first occurrence of a thick carbonate bed; however, there has been considerable debate as to how to define this contact (e.g., Liberty 1969, 1971; Carson 1981a, 1981b, 1982a, 1982b, 1982c; Melchin et al. 1994).

Elsewhere in Ontario, the Gull River Formation is subdivided into a lower and upper member (central Ontario and Ottawa graben; Liberty 1963, 1969, 1971) or a lower, middle and upper member (Kingston area; Carson 1981b, 1982a, 1982b; Armstrong and Dodge 2007) (*see* Figure 27.2).

In the Tweed–Kaladar and Belleville–Wellington map areas, it is unsubdivided (Carson 1981a, 1981c). In the Tweed–Kaladar map area, outcrops of the Gull River Formation occur as outliers in the Precambrian rocks in the northern part of the map area and in 2 inliers north of the city of Belleville. In the Belleville–Wellington map area, the Gull River Formation crops out in topographic lows along the Salmon River. The lower member of the Gull River Formation is generally a dark grey-brown, finely crystalline limestone, whereas the middle member is typified by thin- to medium-bedded, interbedded limestone, dolostone and dolomitic limestone, ranging from pale grey to whitish grey (limestone), to pale green or pale yellow. Varying amounts of rounded, frosted, quartz sand and/or silt can be present in beds throughout the lower and middle members. In general, beds are tabular. A variety of sedimentary features are present throughout both members including intraclastic horizons, ooid beds, mud cracks, microbial lamination, vertical and horizontal burrows, salt hoppers, dissolved-out gypsum laths, pink calcite-filled vugs and bird's-eye texture. Both members contain a restricted marine fauna of predominantly molluscs, ostracods and arthropods, with some occurrences of stromatolites and rare crinoids.

The upper member of the Gull River Formation consists of medium- to massive-bedded, dark grey to dark brown tabular limestone (Photo 27.1A). Several distinct lithofacies are present including thick to massive beds of bivalve floatstone (Photo 27.1B) with ooid packstone to grainstone matrix, beds of wackestone to packstone with abundant fragments of *Tetradium* corals, and angular and chaotic intraclast-bearing beds. In the Tweed–Kaladar and Belleville–Wellington map areas, the upper Gull River Formation appears to lack the distinctive stromatolite bioherm-bearing horizons that are present to the east near Kingston (Hahn 2022). The uppermost part of the Gull River Formation, best represented by an outcrop at Kingsford, consists of massive, finely crystalline, bioturbated limestone beds and is dark brown on fresh surfaces and weathers grey. These characteristic beds of the upper member of the Gull River Formation correspond to the Chaumont Formation (Liberty 1963, 1971) (*see* Figure 27.2).

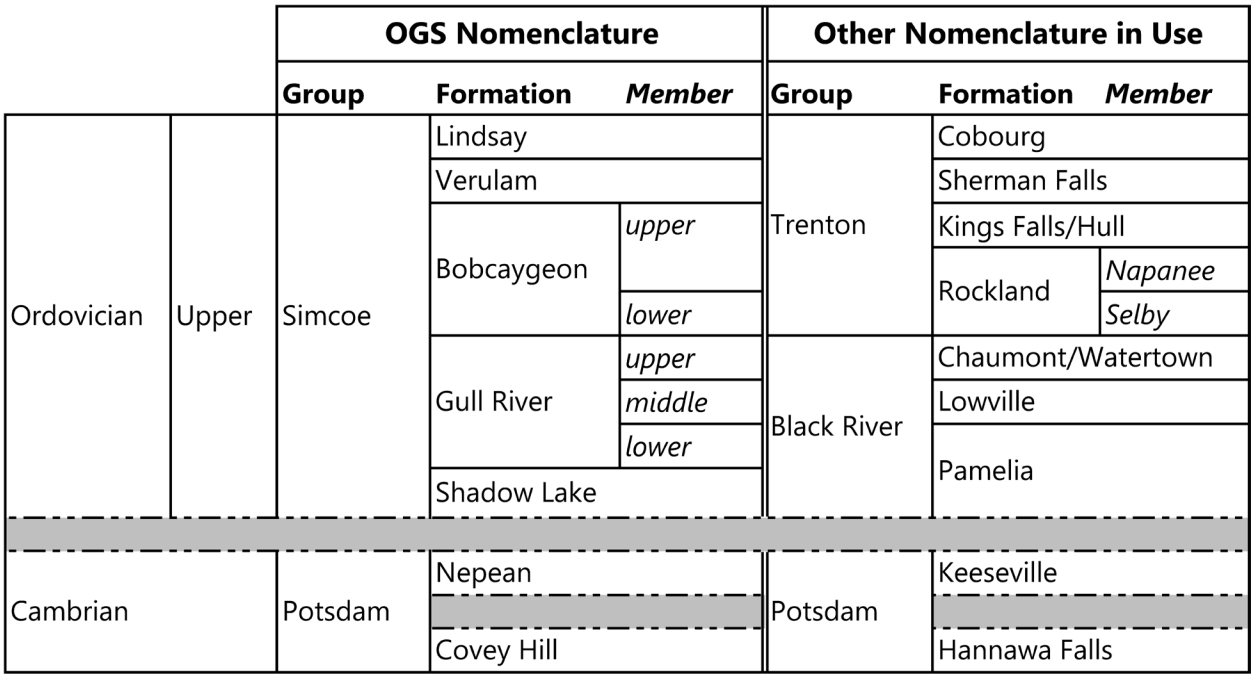


Figure 27.2. Terminology of Paleozoic strata in eastern Ontario and the study area; a more extensive review of other nomenclature in use in the Ottawa graben can be found in Béland Otis (2017). The Napanee and Selby members (mb) are members of the Rockland Formation (e.g., Kay 1937; Cameron and Mangion 1977). It is currently unknown how much of the proposed nomenclature in the Ottawa graben can be extended to the study area. Grey areas outlined by dashed lines represent disconformities. *See* Hahn (2022) for additional information.



Photo 27.1. Selected photographs from the large Kingsford outcrop along Desoronto Road, Kingsford, Ontario. This outcrop covers the Gull River–Bobcaygeon formational transition (Black River Group–Trenton Group). **A**) Continuous section of the Gull River Formation showing the thinner bedding style of Lowville Formation (lowest ledge) and massive bedding of Chaumont Formation (upper 2 ledges). **B**) Bivalve floatstone in the Gull River Formation (Lowville Formation; lower part of outcrop). Scale card is marked in centimetres. **C**) Scoured contact (yellow line) between bioturbated mudstone (bottom) and grainstone (top) from near the top of the outcrop. The unit is stratigraphically above the massive beds in Photo 27.1A (Bobcaygeon Formation). **D**) Thin-bedded, brachiopod-rich, dark coloured limestone with a petroliferous odour in the Bobcaygeon Formation from the top of the Kingsford outcrop (Selby member?).

The Bobcaygeon Formation forms a wide band trending approximately northwest across the Tweed–Kaladar map area and is present along both sides of the Salmon River in the Belleville–Wellington map area. In the western part of the study area, the Bobcaygeon Formation is largely covered by thick drift and only limited roadcut exposures are present, whereas in the central part of the study area the Bobcaygeon Formation crops out mainly as a flat, planar, limestone plain. In the vicinity of the Salmon River, roadcuts and small escarpments are present, which allow for better observation of the unit. Previous descriptions of the Bobcaygeon Formation in the study area are vague (Liberty 1963; Carson 1981a, 1981c), and somewhat inconsistent with descriptions of it to the west (Lake Simcoe area; Liberty 1971; Armstrong 2000) and the east (Ottawa region; Williams 1991). Distinguishing features of the Bobcaygeon Formation include a change from the restricted marine fauna of the underlying strata to an increase in crinoids, brachiopods and bryozoans, an overall increase in shale content, and an increase in common hardground surfaces and storm beds (Photo 27.1C). This suggests a general upward-deepening trend and a transition to more open marine conditions, but with hiatuses, for this succession.

The lower and upper members of the Bobcaygeon Formation were previously described in the Tweed–Kaladar and Belleville–Wellington map areas (Carson 1981a, 1981c). In both map areas, the 2 members are described as fine- to medium-crystalline, pale to dark brown and grey limestone, interbedded with calcarenites (Carson 1981a, 1981c). In general, the lower member is more resistant to weathering, whereas the upper member is typically thinner bedded and contains shale seams. Other authors (e.g., Kay 1937; Cameron and Mangion 1977) have termed these units the Selby and Napanee members of the Rockland Formation (equivalent to the lower Bobcaygeon Formation?) and the overlying Hull Formation may be absent (equivalent to the upper Bobcaygeon Formation of eastern Ontario) (*see* Figure 27.2). The Selby member, defined by Kay (1937) along Selby Creek (Lennox and Addington County), is described as dark-grey to black, medium- to fine-textured petroliferous limestone that weathers buff. Although the type section was not found during this field season, several outcrops matching this description and having a strong petroliferous odour were observed. The most notable occurrence was near the top of the large outcrop at Kingsford (Photo 27.1D). The Napanee member is defined as a grey-blue, medium-textured, heavy-ledged limestone with shaly partings (Kay 1937). It is a terrace and scarp-forming unit and crops out over the higher topography on both sides of the Salmon River (Kay 1937). It is currently unclear how the “Bobcaygeon Formation” of the study area correlates to the “Bobcaygeon Formation” of eastern (L’Orignal Formation?: e.g., Oruche, Dix and Kamo 2018; Béland Otis 2019) and central Ontario (Kirkfield Formation?: e.g., Sanford 1993; Paton and Brett 2020).

The Verulam Formation is present in the southern part of the Tweed–Kaladar map area, where it is mainly covered by thick drift. In the northern part of the Belleville–Wellington map area, it is mainly exposed along the Lake Ontario shoreline and as the lower part of escarpments present along the Verulam–Lindsay formational contact throughout Prince Edward County. Many of the shoreline outcrops of the Verulam Formation that were shown on previous maps are now covered by different forms of erosion control. In general, the Verulam Formation is described as interbedded wackestone, packstone and grainstone beds between 5 and 25 cm thick, with shale seams (Photo 27.2A). In outcrop, shale-rich beds display recessive weathering, and outcrops tend to be quite rubbly. The most common fauna in the Verulam Formation includes brachiopods, bryozoans and crinoids (Photo 27.2B).

The Lindsay Formation is present throughout the southern part of the Belleville–Wellington map area. It is a fossiliferous, bioturbated limestone with shaly partings (Photo 27.2C). In outcrop, depending on weathering style, it can form either thick, resistant-weathering ledges of thinner, irregularly bedded nodular limestone, or it can be recessively weathering and, displays a crumbly weathering with breaks along shale partings. The overall texture is nodular and wackestone, packstone and grainstone beds can all be found.

STRUCTURAL GEOLOGY OF THE TWEED–KALADAR AND BELLEVILLE–WELLINGTON MAP AREAS

The Paleozoic strata in the study area are generally flat lying or display shallow dips (<5° to the south). Locally, beds can be tilted up to 20° in the vicinity of Precambrian inliers. Strike is varied near these inliers, where the tilted bedding likely represents Paleozoic sedimentary rocks draping Precambrian bedrock highs, not tectonic deformation. Several large normal faults are documented in the study area. The Salmon and Napanee rivers both follow the trend of normal faults with vertical displacement of up to 30 m (Carson 1981c). Tilted bedding at Massasauga Point, as well as a small Precambrian inlier in Prince Edward County, follow the same trend as the Salmon River. Several small Precambrian inliers near the Salmon River also follow the same linear trend. The control between deep basement structures and normal faulting is currently unknown. Normal faulting also occurs in Prince Edward County from Picton and extending to the south. In this case, the west block of the fault is downthrust approximately 30 m and the fault possibly splits into 2 smaller faults to the south (Carson 1981c). Further work using modern digital elevation data will assist in more accurately estimating the amount of displacement along faults, as well as better determining their location and extent.

DISCUSSION AND FUTURE WORK

Part of the current mapping study includes detailed geochemical sampling at key outcrops and drill cores. Sampling for stable carbon and oxygen isotopes was undertaken at the Kingsford outcrop at a 50 cm vertical spacing. This outcrop represents a continuous section from the upper Gull River Formation (Lowville and Chaumont formations) through to at least part of the lower Bobcaygeon Formation (Selby member?). A bentonite bed near the base of the outcrop may serve as a marker bed, or provide an isotopic age, to help constrain the relative ages for the stratigraphic units. This can then be combined with stable isotope chemostratigraphy as a tool to correlate the stratigraphic succession locally, and perhaps in a regional and/or global context.

Despite the extensive scientific literature regarding the stratigraphic interval spanning the Gull River through Bobcaygeon formations, also termed the Black River–Trenton groups boundary, considerable confusion still exists related to delineating formational and group rank boundaries. The nomenclature of Upper Ordovician sedimentary rocks in eastern and south-central Ontario varies both geographically and between the outcrop belts and the subsurface. In south-central Ontario, these strata are named the Simcoe Group (Liberty 1969), whereas in eastern Ontario, they are referred to as the Ottawa Group (Wilson 1946). In the subsurface of southwestern Ontario, they are referred to as the Black River and Trenton groups (Sanford 1961). Ongoing work by the OGS aims to address the confusion by producing a revised list of Cambro-Ordovician stratigraphic units for use in Ontario (Brunton et al. 2021).

The main challenge in the Tweed–Kaladar and Belleville–Wellington map areas is whether the Bobcaygeon Formation can be further subdivided and how these subdivisions of the Bobcaygeon Formation fit into a regional stratigraphic framework. For instance, in the Ottawa graben, the lower member of the Bobcaygeon Formation was previously defined as being characterized by thick beds of finely crystalline dark brownish grey heavily burrowed limestone (Williams 1991). Equivalent strata elsewhere in Ontario have been given different names (Coboconk, Chaumont, Watertown, and/or Leray formations), but are generally considered Black River in age (Clark 1972; Fisher 1977; Salad Hersi and Dix 1999; Armstrong and Carter 2010; Oruche, Dix and Kamo 2018; Brunton et al. 2021; Béland Otis 2017, 2018, 2019, 2022) (*see* Figure 27.2). In the study area, these same rocks have been mapped as part of the upper Gull River Formation (or unit D of Liberty 1971).

There is confusion in the literature as to what the correlative units are for the Selby and Napanee members of the Rockland Formation. Some of the literature states that the Selby member is the lateral equivalent of both the Coboconk and Chaumont formations (e.g., Kay 1937; Cameron and Mangion 1977; McFarlane 1992; James, Narbonne and Armstrong 2020) (*see* Figure 27.2). In 2 locations visited this summer, rocks fitting the description of the Selby member were observed to overlie rocks corresponding to the Chaumont Formation. Thus, the potential relationship to the Coboconk Formation is unresolved.

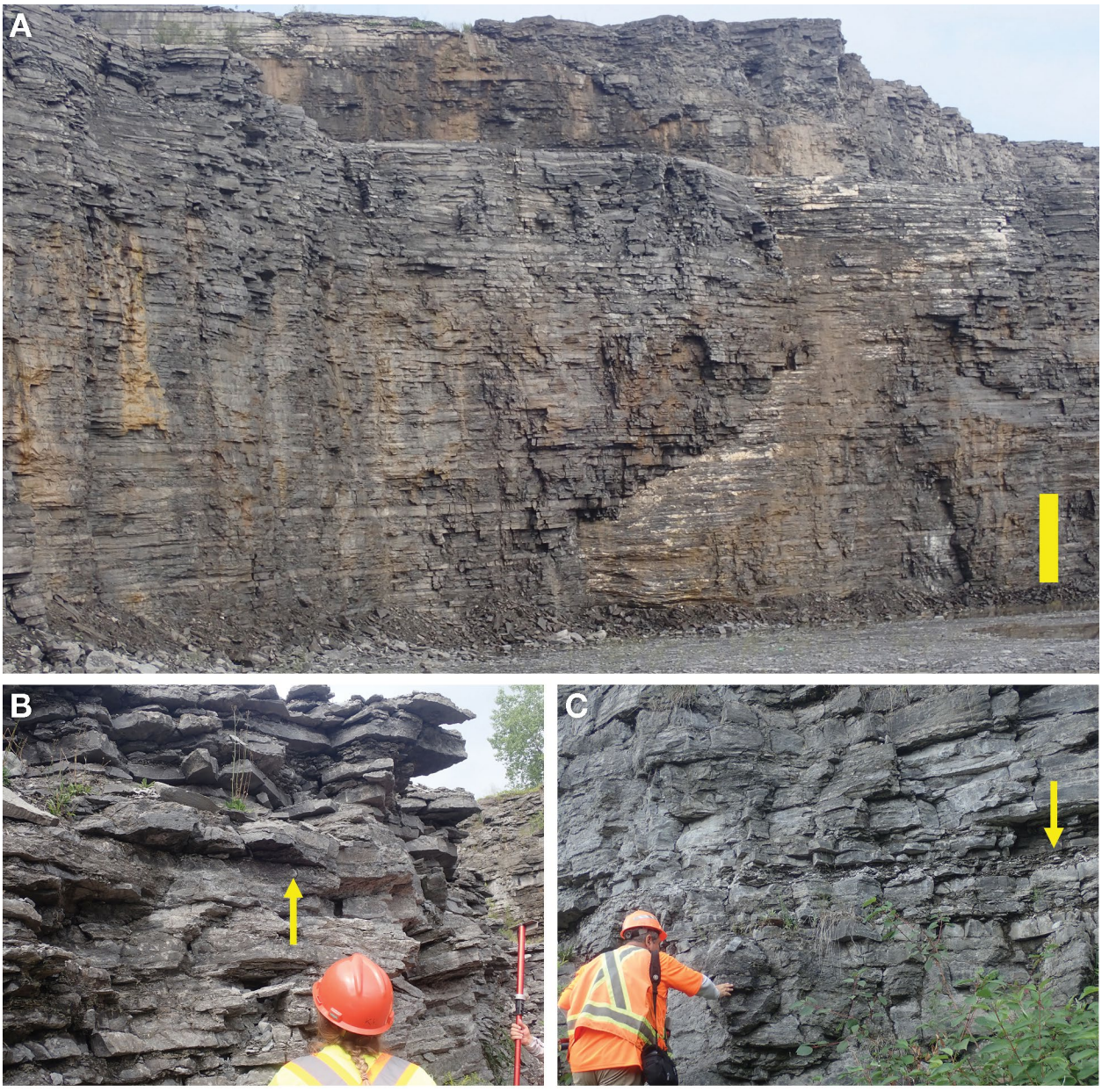


Photo 27.2. Selected photographs from the Picton Quarry. **A)** Verulam Formation from the lowest level of the Picton Quarry (yellow bar is 1.5 m). **B)** Lumpy bedding style of *Prasopora* bryozoan-rich beds (yellow arrow) in the Verulam Formation. **C)** Transition between the thinner bedded, shale-rich limestone of the Verulam Formation (yellow arrow) to heavily bioturbated beds of the Lindsay Formation.

Key questions to be addressed based on the 2023 field season results include the following:

- How regionally extensive are the Selby and Napanee members of Kay (1937) and do they warrant map-scale subdivision (at 1:50 000 scale)?
- What is the relationship between the Selby and Napanee members to rock units of similar age in central Ontario and eastern Ontario?
- Can the Selby and Napanee members be identified in the subsurface of southwestern Ontario?

ACKNOWLEDGMENTS

The author wishes to acknowledge the assistance of Sydney Gardner (Queen's University) during the field season, as well as Kei Yeung (GIS technical help, OGS) and Julien Bonin (drafting figures, OGS) who are gratefully acknowledged for providing help with preparing maps and figures. The author would like to thank the Algonquins of Pikwakanagan First Nation, Alderville First Nation, Curve Lake First Nation, Hiawatha First Nation, Mississaugas of Scugog Island First Nation, Mohawks of the Akwesasne and the Mohawks of the Bay of Quinte for allowing the Ontario Geological Survey to map their traditional land use area. The Mohawks of the Bay of Quinte are also acknowledged for allowing us to map on their territory and for their time in accompanying us. Finally, Catherine Béland Otis and Frank Brunton (OGS) are thanked for many lively discussions, technical expertise, and for reviewing this report.

REFERENCES

Armstrong, D.K. 2000. Paleozoic geology of the northern Lake Simcoe area, south-central Ontario; Ontario Geological Survey, Open File Report 6011, 43p.

Armstrong, D.K. and Carter, T.R. 2010. The subsurface Paleozoic stratigraphy of southern Ontario; Ontario Geological Survey, Special Volume 7, 301p.

Armstrong, D.K. and Dodge, J.E.P. 2007. Paleozoic geology of southern Ontario; Ontario Geological Survey, Miscellaneous Release—Data 219.

Béland Otis, C. 2017. Paleozoic geology of eastern Ontario; *in* Summary of Field Work and Other Activities, 2017, Ontario Geological Survey, Open File Report 6333, p.22-1 to 22-11.

——— 2018. Paleozoic geology of eastern Ontario: Ottawa area; *in* Summary of Field Work and Other Activities, 2018, Ontario Geological Survey, Open File Report 6350, p.22-1 to 22-10.

——— 2019. Paleozoic geology of eastern Ontario: Arnprior–Quyon area; *in* Summary of Field Work and Other Activities, 2019, Ontario Geological Survey, Open File Report 6360, p.20-1 to 24-10.

——— 2022. Paleozoic geology of eastern Ontario: Russell–Thurso area; *in* Summary of Field Work and Other Activities, 2022, Ontario Geological Survey, Open File Report 6390, p.23-1 to 23-8.

Brunton, F.R., Béland Otis, C., Hahn, K.E. and Yeung K. 2021. Progress on the development of a new stratigraphic framework for the Paleozoic geology of southern Ontario; *in* Summary of Field Work and Other Activities, 2021, Ontario Geological Survey, Open File Report 6380, p.16-1 to 16-9.

Cameron, B. and Mangion, S. 1977. Depositional environments and revised stratigraphy along the Black River–Trenton boundary in New York and Ontario; American Journal of Science, v.277, p.486-502.

Carson, D.M. 1981a. Paleozoic geology of the Kaladar–Tweed area, southern Ontario; Ontario Geological Survey, Preliminary Map P.2411, scale 1:50 000.

——— 1981b. Paleozoic geology of the Tichborne–Sydenham area, southern Ontario; Ontario Geological Survey, Preliminary Map P.2413, scale 1:50 000.

——— 1981c. Paleozoic geology of the Belleville–Wellington area, southern Ontario; Ontario Geological Survey, Preliminary Map P.2412, scale 1:50 000.

——— 1982a. Paleozoic geology of the Gananoque–Wolfe Island area, southern Ontario; Ontario Geological Survey, Preliminary Map P.2496, scale 1:50 000.

——— 1982b. Paleozoic geology of the Bath–Yorkshire Island area, southern Ontario; Ontario Geological Survey, Preliminary Map P.2497, scale 1:50 000.

Clark, T.H. 1972. Montréal area; Ministère des Richesses Naturelles du Québec, Geological Report 152, 244p.

Fisher, D.W. 1977. Correlation of the Hadrynian, Cambrian and Ordovician rocks in New York State; New York State Museum and Science Service, Map and Chart Series 25, 75p.

Hahn, K.E. 2022. Paleozoic geology of the Kingston area, eastern Ontario; *in* Summary of Field Work and Other Activities, 2022, Ontario Geological Survey, Open File Report 6390, p.22-1 to 22-10.

James, N.P., Narbonne, G.M. and Armstrong, A.K.R. 2020. Aragonite depositional facies in a Late Ordovician calcite sea, eastern Laurentia; Sedimentology, v.67, p.3513-3532.

Kay, G.M. 1937. Stratigraphy of the Trenton Group; Geological Society of America, Bulletin, v.48, p.233-302.

Liberty, B.A. 1963. Geology of Tweed, Kaladar, and Bannockburn map areas, Ontario, with special emphasis on Middle Ordovician stratigraphy; Geological Survey of Canada, Paper 63-14, 15p.

——— 1969. Paleozoic geology of the Lake Simcoe area, Ontario; Geological Survey of Canada, Memoir 355, 201p.

——— 1971. Paleozoic geology of the Wolfe Island, Bath, Sydenham, and Gananoque map-areas, Ontario; Geological Survey of Canada, Paper 70-35, 12p., 4 maps.

Lowe, D.G., Arnott, R.W.C., Nowlan, G.S. and McCracken, A.D. 2017. Lithostratigraphic and allostratigraphic framework of the Cambrian–Ordovician Potsdam Group and correlations across Early Paleozoic southern Laurentia; Canadian Journal of Earth Sciences, v.54, p.550-585.

McFarlane, R.B. 1992. Stratigraphy, paleoenvironmental interpretation, and sequences of the Middle Ordovician Black River Group, Kingston, Ontario, Canada; unpublished PhD thesis, Queen's University, Kingston, Ontario, 167p.

Melchin, M.J., Brookfield, M.E., Armstrong, D.K. and Coniglio, M. 1994. Stratigraphy, sedimentology and biostratigraphy of the Ordovician rocks of the Lake Simcoe area, south-central Ontario; Geological Association of Canada–Mineralogical Association of Canada, Joint Annual Meeting, Waterloo, Ontario, Guidebook for Field Trip A4, 101p.

Oruche, N.E. and Dix, G.R. 2021. Sequence stratigraphy of a Middle to Upper Ordovician foreland succession (Ottawa Embayment, central Canada): Evidence for tectonic control on sequence architecture along southern Laurentia; Basin Research, v.33, p.779-808.

Oruche, N.E., Dix, G.R. and Kamo, S.L. 2018. Lithostratigraphy of the upper Turinian–lower Chatfieldian (Upper Ordovician) foreland succession, and a U–Pb ID–TIMS date for the Millbrig volcanic ash bed in the Ottawa Embayment; Canadian Journal of Earth Sciences, v.55, p.1079-1102.

Paton, T.R. and Brett, C.E. 2020. Revised stratigraphy of the middle Simcoe Group (Ordovician, upper Sandbian–Katian) in its type area: An integrated approach; Canadian Journal of Earth Sciences. v.57, p.184-198.

Salad Hersi, O. and Dix, G.R. 1999. Blackriveran (lower Mohawkian, Upper Ordovician) litho-stratigraphy, rhythmicity, and paleogeography: Ottawa Embayment, eastern Ontario, Canada; Canadian Journal of Earth Sciences, v.36, p.2033-2050.

Sanford, B.V. 1961. Subsurface stratigraphy of Ordovician rocks in southwestern Ontario; Geological Survey of Canada, Paper 60-26, 54p.

——— 1993. Stratigraphic and structural framework of Upper Middle Ordovician rocks in the Head Lake–Burleigh Falls area of south-central Ontario; Géographie Physique et Quaternaire, v.47, no.3, p.253-268.

Williams, D.A. 1991. Paleozoic geology of the Ottawa–St. Lawrence Lowland, southern Ontario; Ontario Geological Survey, Open File Report 5770, 292p.

Wilson, A.E. 1946. Geology of the Ottawa–St. Lawrence Lowland, Ontario and Quebec; Geological Survey of Canada, Memoir 241, 66p.

28. Project ON-21-005. Keeping it Simple: Geological Information on Water Well Records



A.K. Burt[1], K.H. Yeung[1], D. Grant[2] and R.P.M. Mulligan[1]

[1]Earth Resources and Geoscience Mapping Section, Ontario Geological Survey, Sudbury, Ontario P3E 6B5
[2]Aardvark Drilling Inc., 25 Lewis Road Unit C, Guelph, Ontario N1H 1E9

INTRODUCTION

Geological information on water well records is an important source of subsurface data for many geological, geotechnical and hydrogeological projects; however, the reliability of the data is an ongoing problem. Core or grab samples may be retrieved and logged by a trained technologist during the construction of monitoring wells for geotechnical and environmental projects. In contrast, domestic and agricultural water wells are typically drilled using methods that produce only cuttings, and geological materials are identified and recorded by well technicians who have little or no geological expertise.

Traditionally, paper well records are submitted to the Ministry of Environment, Conservation and Parks (MECP) whereupon staff populate and maintain a database that is publicly accessible through the Water Well Information System (WWIS). More recently, a direct data entry form has been implemented that may be completed by the well technician or office staff. In each case, field descriptions are restricted to 1 colour field, with 1 of 9 possible terms, and 3 material fields, with 1 of 82 possible terms (Table 28.1). Local terms and lengthy descriptions must be interpreted and there is a potential to decrease the accuracy of the resulting data (Figure 28.1). Many of the terms in the current WWIS are redundant or have limited geological or hydrogeological meaning, whereas others describe minerals rather than rock types or simply do not reflect the geology typically present in Ontario. A previous investigation of how individual terms are used and combined revealed a cumbersome database with 36 495 unique combinations of terms (Burt et al. 2021, 2022). Of those, 20 000 combinations occur only once or twice in the database, whereas just 100 combinations comprise approximately 60% of the records, suggesting that there is considerable potential for simplification.

The Ontario Geological Survey (OGS) is collaborating with a team of water supply well technicians, geotechnical drillers, MECP staff and other stakeholders on a project to improve the quality and consistency of geological information available from the WWIS. Phase 1 of the project focusses on improving new well records submitted to MECP, by developing a new electronic and step-wise system with a simpler and more meaningful set of terms for describing geological materials on water well records (Burt et al. 2023). The system will need to accommodate records generated by well technicians working on water supply, geotechnical and environmental projects. It will also need to reflect language used in *Ontario Water Resources Act* R.R.O. 1990, Regulation 903 WELLS (Ontario 1990) (Warren Lusk, Lusk Geo Inc., personal communication, 2023). Phase 2 will convert the geological information within existing well records in the WWIS to the new system. Only phase 1 activities are described in this article.

Summary of Field Work and Other Activities, 2023,
Ontario Geological Survey, Open File Report 6405, p.28-1 to 28-7.

© King's Printer for Ontario, 2023

Table 28.1. Terms currently used to describe geological materials in the Ministry of Environment, Conservation and Parks (MECP) water well database (WWIS). Terms listed in column 1 are used in all 3 material ("Mat") fields. Terms listed in column 2 are only used in material fields 2 and 3 ("Mat2" and "Mat3", respectively).

Terms* used in Mat1, Mat2 and Mat3 fields (primary materials)
Basalt
Boulders
Chert
Clay
Coarse gravel
Coarse sand
Conglomerate
Dolomite
Feldspar
Fill
Fine gravel
Fine sand
Flint
Gneiss
Granite
Gravel
Greenstone
Greywacke
Gypsum
Hardpan
Iron formation
Limestone
Marble
Marl
Medium gravel
Medium sand
Muck
Other
Overburden
Pea gravel
Peat
Prev. drilled **
Previously dug
Quartz
Quartzite
Quicksand
Rock
Sand
Sandstone
Schist
Shale
Silt
Slate
Soapstone
Stones
Till
Topsoil
Unknown type
Wood fragments

Terms* used in Mat2 and Mat3 fields (modifiers)
Cemented
Clayey
Clean
Coarse-grained
Crystalline
Dark-coloured
Dense
Dirty
Dry
Fine-grained
Fosiliferous **
Fractured
Gravelly
Hard
Layered
Light-coloured
Limy
Loose
Medium-grained
Packed
Porous
Sandy
Shaley
Sharp
Silty
Soft
Sticky
Stoney
Thick
Thin
Very
Water-bearing
Weathered

Colours
Black
Blue
Blue-grey
Brown
Green
Grey
Red
White
Yellow

** **Note**: All terms, including those marked specifically with **, are exactly as used in the MECP WWIS database.*

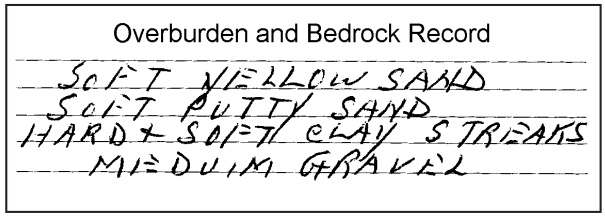
PHASE ONE

Initially, a review was undertaken to evaluate whether systems used in other jurisdictions could be applied to Ontario. Approaches varied from not including geological descriptions in the well record database to free-form descriptions to forms (paper or digital) with separate columns for recording observations about colour, materials, hardness and moisture. Pick-lists are typically used on digital forms and have the potential to reduce confusion and complexity, but only where the lists include geological materials most likely to be encountered, reflect the geological expertise of typical users, are not overly lengthy or cumbersome, and prevent geological improbabilities. Annotated photographs of different geological materials, laminated reference cards and training videos released by some jurisdictions may increase the potential for improving the reliability of the descriptions.

Proposed System and Terminology

The jurisdictional review guided development of a two-step system for entering geological materials on Ontario water well records. The unit depth and 1 of 5 material categories (fill, previously constructed, overburden (sediment), overburden (unconsolidated rock) or consolidated bedrock) are selected in step 1 (Table 28.2) and, if done systematically and consistently, would be an improvement over many historical records. At the time of writing, a separate category is being considered for rubbly, weathered and unconsolidated rock: the so-called interface aquifer zone found between the Quaternary sediment cover and competent bedrock. It is likely that many of the ambiguous formation descriptions currently available through WWIS, for example instances of rock over sediment, result from difficulties in naming materials within this zone. Using Google Search™ (the most likely source to be consulted for information) reveals that definitions of overburden typically refer to both soil and rock above the feature or zone of interest. Furthermore, this separation reflects the language of *Ontario Water Resources Act* R.R.O. 1990, Regulation 903 s. 13 (12) "The casing of a drilled well that obtains water from bedrock, other than from the weathered bedrock zone, shall be sealed into the bedrock with suitable sealant to prevent impairment of the quality of the ground water and the water in the well. O.Reg. 372/07 s. 13 (7)" (Ontario 1990).

A



B

General Colour	Most Common Material	Other Materials	General Description
RED	MSND		
	MSND		
	CLAY		
	GRVL		

C

Step 1	Colour	Sediment						Bedrock				Notes
		Primary	Secondary	Tertiary	Qualifer	Hardness	Moisture	Lithology	Qualifer	Hardness	Moisture	
sediment	yellow	sand				soft						
sediment		silt				soft						putty sand
sediment		clay			layered	hard						
sediment		medium gravel										

Figure 28.1. Comparison of geological descriptions on **A)** an original well record, **B)** the digital version obtained from the Ministry of Environment, Conservation and Parks (MECP) Water Well Information System and **C)** the same record entered into the proposed system. This example was selected from the list of Ambient Groundwater Geochemistry Project (AGGP) sampled wells (Hamilton 2021). It highlights the loss of information arising from the need to interpret local terms ("putty sand"), as well as data entry errors.

Table 28.2. Proposed terms for recording unit depths and material categories in Step 1.

From	To	Select from	Next action
Unit start depth	Unit end depth	Fill	Go to next unit
		Previously constructed	Activates construction method list
		Overburden (sediment) Overburden (unconsolidated rock) Consolidated bedrock	Activates detailed geological description lists (*see* Tables 28.3 and 28.4)

Table 28.3. Proposed terms for describing overburden–sediment in step 2. Terms in **bold** are new.

Colour	Primary Material	Secondary Material	Tertiary Material	Qualifier	Hardness	Moisture	
Black	Topsoil	Clay	Clay	Layered	Hard	Dry	
Blue	Peat	Silt	Silt	**Lost circulation**	Soft	Wet	
Blue-grey	Clay	Sand	Sand	Till	Loose		
Brown	Silt	Gravel	Gravel	Weathered	Cemented		
Green	Sand	Cobbles	Cobbles	Wood			
Grey	Fine sand	Boulders	Boulders	Other			**Free-form text**
Orange	Medium sand						
Pink	Coarse sand						
Red	Gravel						
Tan	Fine gravel						
White	Medium gravel						
Yellow	Coarse gravel						
Other	Cobbles						
	Boulders						

Table 28.4. Proposed terms for describing unconsolidated rock and consolidated bedrock in step 2. Terms in **bold** are new.

Colour	Primary Material	Qualifier	Hardness	Moisture	
Black	Dolostone	Fractured	Hard	Dry	
Blue	Limestone	Layered	Soft	Wet	
Blue-grey	Mudstone	**Lost circulation**			
Brown	Sandstone	Weathered			
Green	Shale	Other			**Free-form text**
Grey	**Shale and limestone**				
Orange	Basalt				
Pink	Granite				
Red	Greenstone				
Tan	Marble				
White	Quartzite				
Yellow	Slate				
Other	Other				

If the term fill or previously constructed are selected, no further geologic description is necessary for that unit. Step 2 is activated if overburden or bedrock are selected as the material category, where a series of optional pick-lists for colour, lithology, qualifiers, hardness and moisture will be made available to the submitter (Tables 28.3 and 28.4). Many of the 82 terms used in the current system will be retained or slightly modified, whereas others (39) will be abandoned (Table 28.5). For example, the choices for bedrock lithology will be restricted to common or locally important rock types, such as granite, limestone, sandstone and mudstone, whereas minerology terms, such as feldspar and chert will be abandoned. There are also a few new terms, such as mudstone and lost circulation. Although the terms on the pick-lists have

Table 28.5. Terms to be abandoned. Terms in *italic* will be modified in the new system. For example, clayey will become clay.

Rock	Sediment	Qualifiers and Other Terms
Chert	*Clayey*	Clean
Conglomerate	*Silty*	Dirty
Crystalline	*Sandy*	Light-coloured
Feldspar	Quicksand	Dark-coloured
Flint	*Gravelly*	Thick
Fosiliferous **	Pea gravel	Thin
Gneiss	*Stoney*	Fine-grained
Greywacke	Hardpan	Medium-grained
Gypsum	Marl	Coarse-grained
Iron formation	Muck	Dense
Limy	Overburden	Packed
Quartz		Porous
Rock		Sticky
Schist		Sharp
Shaly		Unknown type
Soapstone		Very
		*Prev. drilled **
		Previously dug

***Note**: All terms, including those marked specifically with **, are exactly as used in the MECP WWIS database.*

been developed following an in-depth assessment of the frequency, distribution and typical combinations of current terms, referencing digital copies of original water well records as required (www.ontario.ca/page/map-well-records [accessed September 5 2023]), further refinements may be necessary following ongoing testing and review.

Internal Testing

A province-wide database of geological descriptions has been assembled from original water well records to evaluate the proposed system and lists of terms. Wells sampled as part of the Ambient Groundwater Geochemistry Program (AGGP) have been used because they include both overburden and bedrock wells on a 10 by 10 km grid with increased density in areas of focussed study (Hamilton 2021). The database was then expanded to include a subset of wells from across the province (Figure 28.2).

Pick-lists created using the proposed system and terms are being used to populate the remainder of the database. Any descriptions not easily translated into the new system are noted in a separate column (*see* Figure 28.1). A team of well technicians will then be consulted to determine the most probable material. For example, descriptions of “putty sand” likely refer to coarse, water saturated, silt. Further testing will include comparing the populated database to published surficial and bedrock geology maps. It is anticipated that these tests will highlight both omissions in the proposed terms and where to focus future training efforts.

Stakeholder Review

In conjunction with internal testing, the proposed system and lists of terms are currently undergoing preliminary stakeholder review. Well technicians, managers and company owners representing water supply, geotechnical and environmental industries have been invited to comment, as have survey geoscientists and geological and engineering technicians from consulting companies. Presentations at the southern Ontario regional-scale groundwater geoscience open house in 2021 and 2023 were recorded and are available on the Geological Survey of Canada Groundwater Geoscience YouTube™ channel

(Burt et al. 2022, 2023). Similar presentations and follow-up discussions are planned for an upcoming Ontario Groundwater Association meeting and the 2023 OGS Virtual Showcase to increasing exposure and solicit feedback on the proposed system.

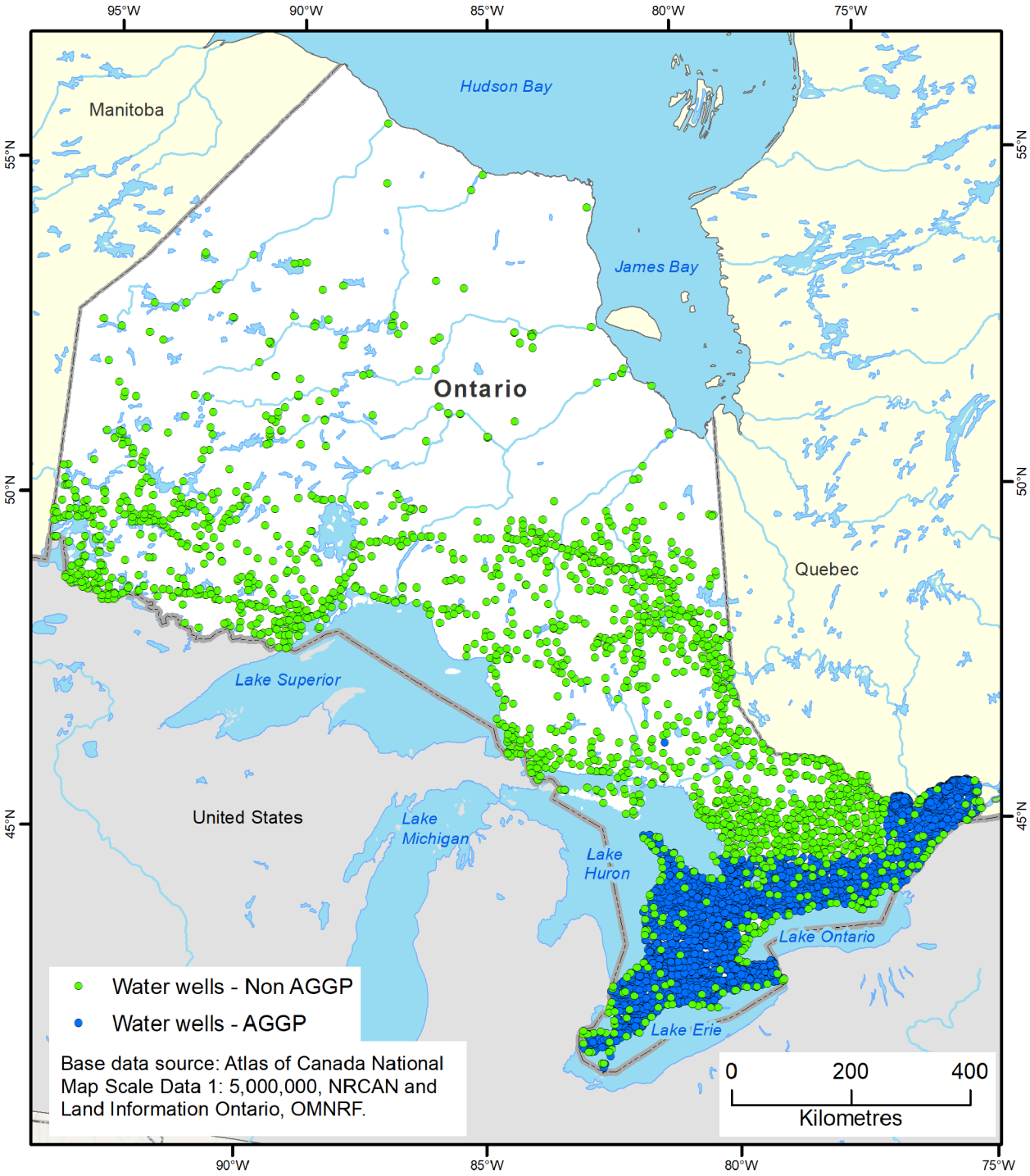


Figure 28.2. Location of water wells used to evaluate the proposed system. Shown in blue are 3616 wells sampled as part of the Ambient Groundwater Geochemistry Project (AGGP) (Hamilton 2021). An additional 1834 randomly selected wells from WWIS are shown in green. Well record data from the Ministry of Environment, Conservation and Parks (MECP), Water Well Information System (WWIS) contains information licenced under the Open Government Licence – Ontario (https://data.ontario.ca/dataset/well-records) [accessed September 6, 2023].

This review process is a critical step in finalizing the list of terms that will be recommended to MECP. The process has revealed considerable interest in creating training materials suitable for printed reference cards and mobile devices. Photographs of cuttings, core and hand samples, simple descriptions, tips for identifying materials, and typical drill responses have been suggested. Publicly accessible documentation such as this would be a valuable project outcome and contributions will be sought from the wider drilling community.

ACKNOWLEDGMENTS

The success of this project is dependent on the contributions by well technicians, managers and consultants representing the water supply, geotechnical and environmental industries. Frank Brunton, Manuel Duguet, Michael Easton and Riku Metsaranta (OGS) guided development of the bedrock lithology list.

Stakeholder review is ongoing, and the time and expertise offered is gratefully acknowledged. At the time of writing, feedback has been received from the following: Mike Grant (Marathon Drilling Co. Ltd.), Rachel Borne (Elements Geo Corp.), Peter Gray (MTE Consultants Inc.), Warren Lusk (Lusk Geo Inc.), Peter LeBaron (OGS), Vanessa Felix (Pioneer Construction Inc.), Matt Krukowski (OGS), Brett MacAskell (NWO Well Services Ltd.), David Walker (Walker Drilling Ltd.), Julie Selway (Tearlach Resources Limited), Channing Robbins (Pontil Drilling), Tim Collins (Geo-Environmental Drilling Inc.), Kyle Fitter (Hole Products, LLC), Randall Goodwin (Kodiak Drilling), Brennon McMahan (Choice Sonic Drilling Ltd.), Kevin Langille (Langille Well Drilling), Ann Wilson (Highland Water Well Drilling Inc.), Bryan Watson (G. Hart & Sons Well Drilling Ltd.), and Kelsey Proks (exp Global Inc.).

REFERENCES

Burt, A.K., Grant, D., Kelly, A., Mulligan, R.P.M., Yeung, K.H. and Brunton, F.R. 2023. Lithological lock-down – Standardizing geological descriptions in well records; *in* Regional-scale groundwater geoscience in southern Ontario: The 2023 Ontario Geological Survey, Geological Survey of Canada, and Conservation Ontario Geoscientists Open House, Ontario Geological Survey, Open File Report 6387, p.7, oral presentation available at www.youtube.com/watch?v=sEXnYhE6gpk&t=9s. [accessed October 6, 2023]

Burt, A.K., Mulligan, R.P.M., Brunton, F.R., Yeung, K.H., Spina, N.E., and Cheng, T. 2021. Improving geological nomenclature in Ontario Well Records; *in* Summary of Field Work and Other Activities 2021, Ontario Geological Survey, Open File Report 6380, p.20-1 to 20-5.

——— 2022. Towards a simplified, standardized nomenclature for geological materials in well records; *in* Regional-scale groundwater geoscience in southern Ontario: The 2021 Ontario Geological Survey, Geological Survey of Canada, and Conservation Ontario Geoscientists Open House, Ontario Geological Survey, Open File Report 6378, p.3, oral presentation available at www.youtube.com/watch?v=BjrmCXLRCGY. [accessed October 6, 2023]

Hamilton, S.M. 2021. Ambient groundwater geochemical and isotopic data for southern Ontario, 2007–2019; Ontario Geological Survey, Miscellaneous Release—Data 283 – Revision 2.

Ontario 1990. *Ontario Water Resources Act*, Revised Regulations of Ontario 1990, Regulation 903 Wells, as amended 2020 O.Reg 461/19, under *Ontario Water Resources Act*, R.S.O. 1990, c. O.40, as amended 2021, c. 4, Sched. 10, s. 4; available at www.ontario.ca/laws/regulation/900903. [accessed October 6, 2023]

29. Project ON-23-005. A Unified Stratigraphic Framework for the Provincial Groundwater Monitoring Network



R.P.M. Mulligan[1], A.K. Burt[1], K.H. Yeung[1] and F.R. Brunton[1]

[1]Earth Resources and Geoscience Mapping Section, Ontario Geological Survey

INTRODUCTION

Groundwater is 1 of Ontario's most significant natural resources, supplying drinking water to millions of residents, irrigation for agriculture, and playing a vital role in sustaining natural ecosystems. The Provincial Groundwater Monitoring Network (PGMN) is a network of observation wells across the province designed to monitor long-term and real-time variations in groundwater levels and chemistry. This is done to improve understanding of the influence of changing climate patterns and to provide baseline information for resource allocation decisions, interference complaints, and drought response used by municipalities, conservation authorities, Ontario ministries and academia. The PGMN was initiated in 2000 and currently (as of the time of writing) consists of 522 wells across the province, with a concentration in southern Ontario (Ministry of Environment, Conservation and Parks 2023; Figure 29.1). The present database contains information on wells screened in both bedrock (n=215) and sediment-hosted (n=307) groundwater flow systems as well as the intervening interface zone.

Since its inception, the PGMN has undergone enhancements, such as the addition of new wells into the network, and the inclusion of rain gauges, stream gauges, geochemical analyses, climate stations and real-time telemetry. At present, stratigraphic information, beyond the lithological descriptions contained in linked water well records, is assigned on an *ad hoc* basis, which hinders regional evaluations of groundwater flow systems and surface water–groundwater interactions across different parts of the province. This project aims to provide a stratigraphic assessment of screened and open-hole intervals for wells in the PGMN, through a multifaceted analysis of geological, hydrological and geochemical data. A product of this effort will be the development of a new, standardized hydrostratigraphic framework for sediment-hosted aquifers in the province.

METHODS

The PGMN database contains the following information for each well: geographic location (co-ordinates and ground elevation), well construction (drill method, year, well diameter, drill depth, well screen or open hole depth, and piezometer depth), screen interval lithology (materials report in the water well information system (WWIS) record) and classification (bedrock, sediment and/or interface). At many locations (95 sites), wells were drilled on private lands where confidentiality agreements preclude the release of location information.

Summary of Field Work and Other Activities, 2023,
Ontario Geological Survey, Open File Report 6405, p.29-1 to 29-6.

© King's Printer for Ontario, 2023

Integration of Available Geological Data

As a first step, the PGMN database was split into multiple spreadsheets to facilitate the integration of available geological data. Individual spreadsheets helped organize the available data into thematic tables containing geographic information, well construction information, well lithological information, Quaternary stratigraphic data, bedrock stratigraphic data, hydrogeological data and geochemical data. The location of the PGMN wells were imported into ESRI® ArcMap® and ESRI® ArcPro® to code the well locations with the best available geological information based on published maps, reports and three-dimensional (3-D) models (Table 29.1). Additionally, terrain and surficial geological data, including elevation data, elevation source, physiographic region, surficial material and permeability, surface landform, surface hydrostratigraphic unit (*see* "Assessing Well Screen Stratigraphy") and 3-D sediment model area name(s), were added to the database for each well.

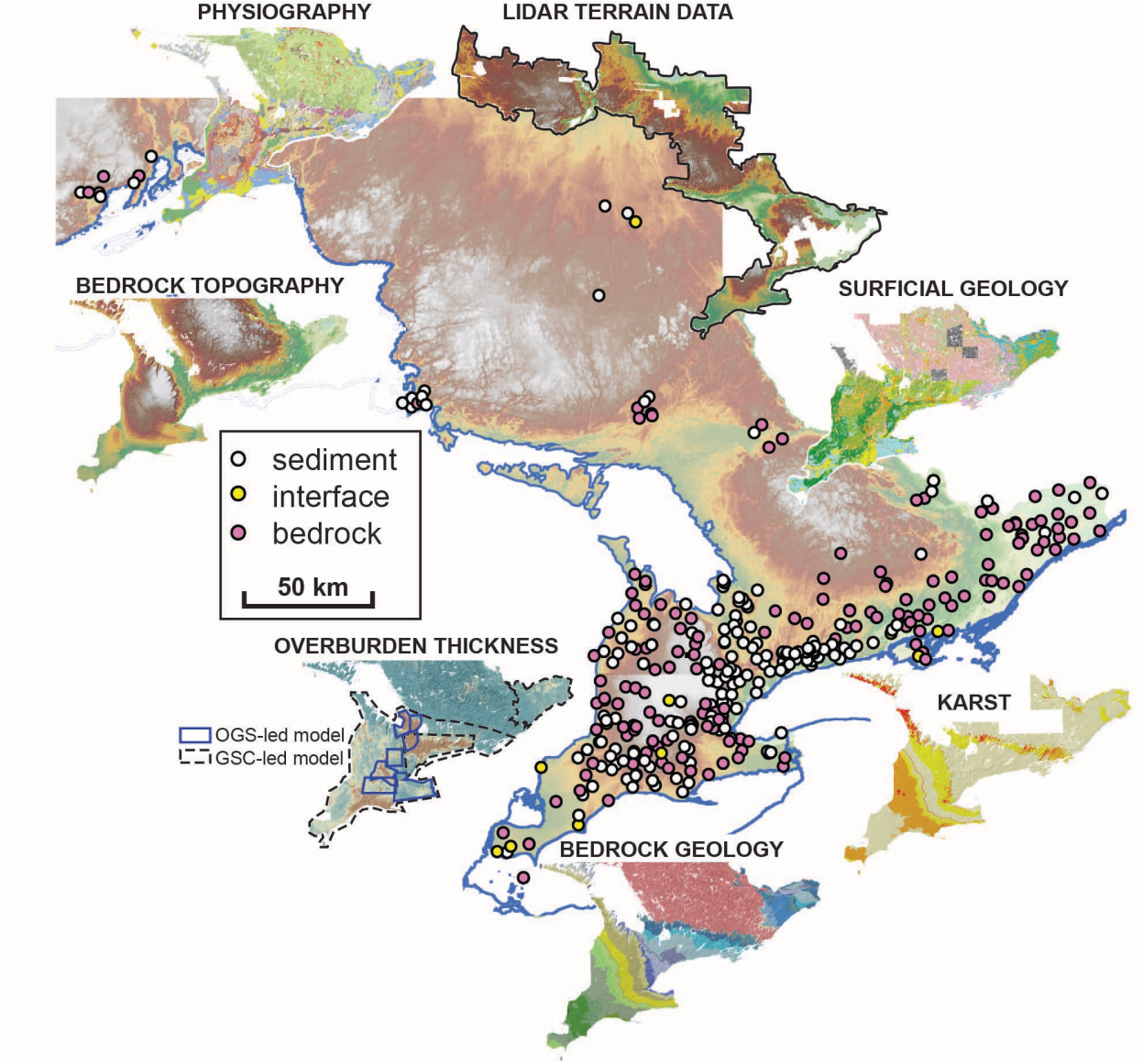


Figure 29.1. Distribution of Provincial Groundwater Monitoring Network (PGMN) wells screened in sediment (shown as white-filled circles), interface zone (shown as yellow-filled circles) and bedrock units (shown as pink-filled circles). Inset maps show available geological, terrain and 3-D model data to be incorporated into the PGMN database to aid in stratigraphic assessment of screen intervals (*see* Table 29.1 for references). Data are overlain on a digital elevation model and hillshade.

Table 29.1. Geological, terrain and 3-D model data available to incorporate into Provincial Groundwater Monitoring Network (PGMN) database for wells on public land. Numbers in each column indicate the number of wells for which coverage is available or unavailable.

Coverage	Lidar[1]	Physiography[2]	Surficial Geology[3]	Overburden Thickness and/or Bedrock Topography[4]	Bedrock Lithology[5]	Karst[6]	3-D Bedrock Model[7]	3-D Surficial Model[8]
Available	400	394	400	391	427	166	330	330
Unavailable	27	33	27	36	0	261	97	97

[1]*FRI T2 lidar and Ontario lidar projects (Ministry of Natural Resources and Forestry 2022, 2023).*

[2]*Ontario Geological Survey (2007).*

[3]*Includes areas mapped at 1:50 000 scale or better. Compilation for southern Ontario (Ontario Geological Survey 2010).*

[4]*Gao et al. (2006).*

[5]*Ontario Geological Survey (2011) and Armstrong and Dodge (2007).*

[6]*Includes wells within "*known*", "*potential*" and "*inferred*" karst areas in Brunton and Dodge (2008).*

[7]*Carter et al. (2019, 2021).*

[8]*Includes Ontario Geological Survey 3-D models in progress and ongoing provincial-scale modelling (Logan et al. 2020).*

Wells in the PGMN database were then divided into sediment- (and interface) screened wells and bedrock-screened wells. Additional information about distance to nearest cored borehole, nearest borehole identifier, modelled screen stratigraphic unit, a unified stratigraphic name for screened interval, and information on the hydraulic confinement of the screened zone was also assigned to each well. For bedrock-hosted wells, additional data to be added to the spreadsheet include bedrock topography, subcropping lithology and formation name and 3-D model coverage.

Assessing Well Screen Stratigraphy

A multifaceted workflow is being implemented to assess well screen stratigraphy within the PGMN. First, bedrock wells within the recently published 3-D model of Paleozoic stratigraphy for southern Ontario (Carter et al. 2019, 2021) will be directly assigned stratigraphic data from the model layers. Bedrock wells outside the 3-D model domain will be evaluated on an individual basis. A simplified stratigraphic scheme to incorporate the wide range of bedrock terrains and rock types is in development.

A similar approach is being applied to PGMN wells screened in Quaternary sediments overlying bedrock. Existing 3-D model layers will be directly assigned to screened intervals wherever possible. Unlike the bedrock wells, where a single model now provides stratigraphic information down to the formation name, Quaternary sediments have yet to undergo a standardized evaluation of stratigraphic information. A wide range of names and terminology exists for aquifers and aquitards across the province. Discrepancies in the terminology arise from the large number of investigations that have been completed, but focus on different aspects of the same sediment packages. For example, municipal well field investigations are typically focussed on the characterization of water-producing zones with less focus on overlying confining units, whereas watershed-scale hydrogeological studies require integration of greater number and variety of lithologic units. Additionally, geological investigations span multiple decades and the names for both the timing of events and the sediments that were deposited are constantly undergoing refinement as new data are collected and knowledge improves (e.g., Russell, Sharpe and Cummings 2011). The Ontario Geological Survey (OGS) has developed a standardized naming convention for model layers, but spatial and temporal variations in glacial processes and depositional environments create a situation where the same model layer name may be applied to sediment packages of vastly different ages and geneses (Mulligan et al. 2023). Where 2 OGS models overlap and there is disagreement between the named unit at the well screen interval, the coding of the more recent model will be assigned. Where models from 2 different sources overlap, the well will be attributed with the layer

names from each model, along with the new, unified, stratigraphic information in development. Any PGMN wells located outside completed 3-D model boundaries will be evaluated individually based on the lithological data contained in the linked WWIS record and surrounding records, and local terrain data.

FUTURE WORK AND DELIVERABLES

The initial stratigraphic assessment of PGMN well screens has demonstrated a need for a critical analysis of existing naming conventions in use in the province and for a single, unified framework that can describe pan-provincial hydrostratigraphy. Significant time lags exist between glacial events affecting different parts of the province and different lobes of the ice sheet advanced and retreated asynchronously. At a given time, some areas were still covered by glaciers, coarse-grained sediments were being deposited in stratified moraine systems and thick laminated muds were deposited in low-lying basins. A useful provincial-scale hydrostratigraphic framework must therefore be devoid of temporal terms, such as the widely used stadial–interstadial and the more recent phase–interphase (Karrow, Dreimanis and Barnett 2000) systems that have long formed the benchmark for Quaternary stratigraphic studies.

Instead, a combined morpho-hydrostratigraphic approach is being adopted to emphasize the important hydraulic functions of stratigraphic relationships of prominent sediment packages and surficial landforms. For example, stratified interlobate moraines in southern Ontario have long been known to host prolific aquifers (Martin and Frind 1998; Howard et al. 1995; Sharpe and Russell 2023). The difference between the Oak Ridges and Orangeville–Waterloo moraines is the time in which they were deposited, with the former postdating the latter by approximately 3000 years. Recent improvements in subsurface data collection have revealed the striking similarities in bulk stratigraphy of these regionally significant moraine systems. Each moraine system broadly consists of tripartite succession comprising a basal sand and gravel, a widespread fine-grained unit, and an upper sand rich unit (Bajc and Shirota 2007; Bajc and Dodge 2011; Burt and Dodge 2016; Sharpe and Russell 2023). These successions overlie a regional till deposited during the last glacial maximum and are partially overridden by younger fine-grained tills and associated glaciolacustrine deposits that create hydraulic confinement along the moraine flanks. Improved understanding of the relative timing of deposition of these large, stratified moraine systems is of critical importance for better understanding regional ice sheet dynamics and the possible links to paleoclimate variability. From an applied perspective, however, the timing of deposition is inconsequential to their function, allowing the sediment packages within these moraines to be grouped within a single morpho-hydrostratigraphic unit that includes all partially confined, ice-contact stratified deposits.

In this regard, the development of a unified stratigraphic framework is geared toward the hydrogeological applications of Quaternary sediments and landforms in the province, but will ultimately provide valuable guidance in the effort to standardize a lexicon for the Quaternary glacial sediment systems in the province. The aim is to develop a hierarchical approach that allows for flexibility to accommodate observations from studies of vastly different scales ranging from a one-unit Quaternary package to a unified framework designed to standardize high-resolution 3-D model layer names and surficial sediment units into provincially significant depositional systems, while preserving some of the local differences that arise from the diverse geological settings.

The enhancements to the PGMN database through assignment of best available stratigraphic information to screened intervals will be accompanied by a Groundwater Resources Study report that outlines the data, methods, interpretations and intended uses of the new geological information. Additionally, information hosted within the database will be made available as geospatial data stored on the Ministry of Environment, Conservation and Parks (MECP) PGMN portal (www.ontario.ca/page/map-provincial-groundwater-monitoring-network) and the OGS GeologyOntario hub (www.hub.geologyontario.mines.gov.on.ca).

Following the successful incorporation of the geological and stratigraphic data into the PGMN database, future efforts may include the addition of available hydrogeological (i.e., specific capacity) and geochemical data, particularly for wells that have been sampled as part of the ongoing OGS Ambient Groundwater Geochemistry Project (AGGP) and associated studies (Hamilton 2021).

ACKNOWLEDGEMENTS

This project was initiated by Hazen Russell (Geological Survey of Canada) and Don Cummings (DC Geo Consulting and Carleton University). Ongoing discussions with MECP staff Heather Brodie-Brown, Vasily Rogojin, George Zhang and Dajana Grgic will assist in guiding next steps. We thank the many external clients for comments and suggestions following the 2023 Southern Ontario Groundwater Geoscience Open House.

REFERENCES

Armstrong, D.K. and Dodge, J.E.P. 2007. Paleozoic geology of southern Ontario; Ontario Geological Survey, Miscellaneous Release—Data 219.

Bajc, A.F. and Dodge, J.E.P. 2011. Three-dimensional mapping of surficial deposits in the Brantford–Woodstock area, southwestern Ontario; Ontario Geological Survey, Groundwater Resources Study 10, 86p.

Bajc, A.F. and Shirota, J. 2007. Three-dimensional mapping of surficial deposits in the Regional Municipality of Waterloo, southwestern Ontario; Ontario Geological Survey, Groundwater Resources Study 3, 41p.

Brunton, F.R. and Dodge, J.E.P. 2008. Karst map of southern Ontario, including Manitoulin Island; Ontario Geological Survey, Groundwater Resource Study 5.

Burt, A.K. and Dodge, J.E.P. 2016. Three-dimensional modelling of surficial deposits in the Orangeville–Fergus area of southern Ontario; Ontario Geological Survey, Groundwater Resources Study 15, 175p.

Carter, T.R., Brunton, F.R., Clark, J.K., Fortner, L., Freckelton, C., Logan, C.E., Russell, H.A.J., Somers, M., Sutherland, L. and Yeung, K.H. 2019. A three-dimensional geological model of the Paleozoic bedrock of southern Ontario; Ontario Geological Survey, Groundwater Resources Study 19, Geological Survey of Canada, Open File 8618. doi.org/10.4095/315045

Carter, T.R., Logan, C.E., Clark, J.K., Russell, H.A.J., Brunton, F.R., Cachunjua, A., D'Arienzo, M., Freckelton, C., Rzyszczak, H., Sun, S. and Yeung, K H. 2021. A three-dimensional geological model of the Paleozoic bedrock of southern Ontario, version 2; Geological Survey of Canada, Open File 8795, 103p. doi.org/10.4095/328297

Gao, C., Shirota, J., Kelly, R.I., Brunton, F.R. and Van Haaften, S. 2006. Bedrock topography and overburden thickness mapping, southern Ontario; Ontario Geological Survey, Miscellaneous Release—Data 207.

Hamilton, S.M. 2021. Ambient groundwater geochemical and isotopic data for southern Ontario, 2007–2019; Ontario Geological Survey, Miscellaneous Release—Data 283 – Revision 2.

Howard, K.W.F., Eyles, N., Smart, P.J., Boyce, J.I., Gerber, R.E., Salvatori, S.L. and Doughty, M. 1995. The Oak Ridges moraine of southern Ontario: A groundwater resource at risk; Geoscience Canada, v.22, p.101-120.

Karrow, P.F., Dreimanis, A. and Barnett, P.J. 2000. A proposed diachronic revision of Late Quaternary time-stratigraphic classification in the eastern and northern Great Lakes area; Quaternary Research, v.54, p.1-12.

Logan, C.E., Russell, H.A.J., Bajc, A.F., Burt, A.K., Mulligan, R.P.M. and Sharpe, D.R. 2020. A three-dimensional surficial geology model of southern Ontario: Progress report; *in* Southern Ontario groundwater project 2014–2019: Summary report, Geological Survey of Canada, Open File 8536, 245p. doi.org/10.4095/321078

Martin, P.J. and Frind, E.O. 1998. Modeling a complex multi-aquifer system: The Waterloo moraine; Ground Water, v.36, p.679-690.

Ministry of Environment, Conservation and Parks 2023. Map: Provincial Groundwater Monitoring Network, online database, www.ontario.ca/page/map-provincial-groundwater-monitoring-network. [accessed July 4, 2023]

Ministry of Natural Resource and Forestry. 2022. Forest Resources Inventory leaf-on LiDAR; Ministry of Natural Resources and Forestry, Science and Research Branch, Forest Resources Information Unit, online data, April 10, 2022 update, https://geohub.lio.gov.on.ca/maps/lio::forest-resources-inventory-leaf-on-lidar/about. [accessed September 22,2023]

——— 2023. Ontario digital terrain model (lidar-derived); Ministry of Natural Resources and Forestry, Science and Research Branch, Provincial Mapping Unit, online data, September 21, 2023 update, https://geohub.lio.gov.on.ca/maps/mnrf::ontario-digital-terrain-model-lidar-derived/about. [accessed September 23, 2023]

Mulligan, R.P.M., Burt, A.K., Brunton, F.R. and Yeung, K.H. 2023. Towards a Hydrogeological Understanding of the Provincial Groundwater Monitoring Network; abstract *in* Regional-scale groundwater geoscience in southern Ontario: The 2023 Ontario Geological Survey, Geological Survey of Canada, and Conservation Ontario Geoscientists Open House, Ontario Geological Survey, Open File Report 6387, p.36.

Ontario Geological Survey 2007. Physiography of southern Ontario; Ontario Geological Survey, Miscellaneous Release—Data 228.

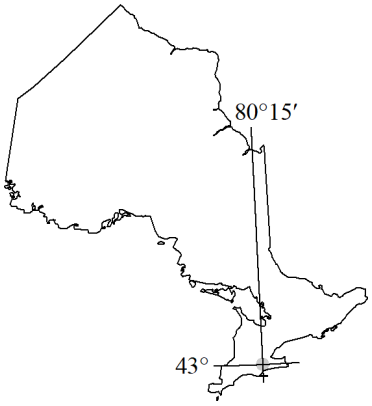
——— 2010. Surficial geology of southern Ontario; Ontario Geological Survey, Miscellaneous Release—Data 128 – Revised.

——— 2011. 1:250 000 scale bedrock geology of Ontario; Ontario Geological Survey, Miscellaneous Release—Data 126 – Revision 1.

Russell, H.A.J., Sharpe, D.R. and Cummings, D.I. 2011. Sediment-aquifer play types in a list of 30 key Canadian aquifers; *in* Geohydro–2011, Joint Meeting of the Canadian Quaternary Association and the Canadian Chapter of the International Association of Hydrogeologists, Proceedings, 8p.

Sharpe, D.R. and Russell, H.A.J. 2023. Sedimentary architecture and glacial hydraulic significance of the stratified Oak Ridges moraine, southern Ontario, Canada; Boreas, v.52, p.341-380.

30. Project SO-23-002. Ambient Groundwater Geochemistry Project: Six Nations of the Grand River



L.M. Colgrove[1] and K.M. Dell[1]

[1]Earth Resources and Geoscience Mapping Section, Ontario Geological Survey

INTRODUCTION

Work undertaken as part of the Ambient Groundwater Geochemistry Project (AGGP) has mapped out ambient, baseline groundwater chemistry across the province since 2007. Data collected as part of the project has allowed mapping of regional patterns of chemistry in groundwater that is controlled by the bedrock and overburden geology. The latest published database includes extensive chemical analyses for 6231 samples across southern Ontario (Hamilton 2021). A gap in sampling density was identified on the federal reserve land of Six Nations of the Grand River (hereafter shortened to Six Nations) (Figure 30.1). Six Nations is the most highly populated First Nation reserve in Canada, with nearly 12 000 community members living on the reserve as of March 2023. Although the town of Ohsweken had a water treatment plant constructed in 2013, which draws water from the Grand River, much of the community depends on private wells, "trucked in" water stored in cisterns and/or purchased bottled water.

Whereas the original target of sampling 1 bedrock and 1 overburden well every 100 km^2 has been accomplished or attempted through the AGGP, several offshoot projects and collaborations have resulted in a higher sample density in certain regions. Included in these offshoot projects are 2 projects that collected samples at 4 times the original target density (i.e., 1 sample per 25 km^2). These 2 projects are located adjacent to the gap identified at Six Nations, further emphasizing the absence of data in that area. The following studies were conducted in the region around Six Nations as part of the AGGP:

1. The Niagara Peninsula and Brant County were first sampled under the AGGP at a 100 km^2 sample density in 2010 in an effort to characterize groundwater geochemistry of southwestern Ontario (Hamilton, Freckelton and Mariotti 2010).
2. An undergraduate BSc thesis was completed using 97 AGGP samples across the Niagara Peninsula collected during the 2010 field work (Matheson 2012).
3. The Niagara Peninsula was sampled at a higher sampling density (1 bedrock and 1 overburden sample per 25 km^2) and with more comprehensive analyses in 2015 to support a MSc thesis (Smal 2016).
4. The north shore of Lake Erie west of the Niagara Peninsula was resampled to increase the density (1 bedrock and 1 overburden sample per 25 km^2) to conduct a more comprehensive analysis of the groundwater chemistry. This was a collaborative effort between the Ontario Geological Survey (OGS) and the Ministry of Natural Resources and Forestry and was intended to characterize and understand groundwater-related gases and anomalous groundwater chemistry in the region.

Summary of Field Work and Other Activities, 2023,
Ontario Geological Survey, Open File Report 6405, p.30-1 to 30-7.

© King's Printer for Ontario, 2023

The mapping and academic studies highlighted above have identified the groundwater in the Niagara Peninsula as an anomaly in southern Ontario because of high total dissolved solids (TDS), major ions (especially sulphate), hydrogen sulphide, methane and other parameters. The federal reserve land of Six Nations is directly adjacent to the Niagara anomaly; therefore, it is likely that groundwater on the reserve has similar chemistry. This would be consistent with reports of poor water quality in the community.

A sampling campaign to address this gap in the AGGP data set at Six Nations was carried out at the beginning of September 2023. This activity was conducted in close collaboration with the Environmental Task Force of the Band Council of Six Nations of the Grand River (ETF). The purpose of this work was to 1) fill in the sample gap that exists at Six Nations, 2) map the ambient groundwater conditions at Six Nations, 3) establish the western extent of anomalous chemistry observed in the Niagara Peninsula and 4) build relationships with the Six Nations community and to better understand the needs of the community.

STUDY AREA

The study area encompasses the federal reserve boundary of Six Nations of the Grand River in southern Ontario, which covers approximately 180 km^2. The study area is bordered by the counties of Haldimand, Norfolk and Brant, and is east of the city of Brantford and southwest of the city of Hamilton. Land use on the reserve is largely rural-residential and agricultural.

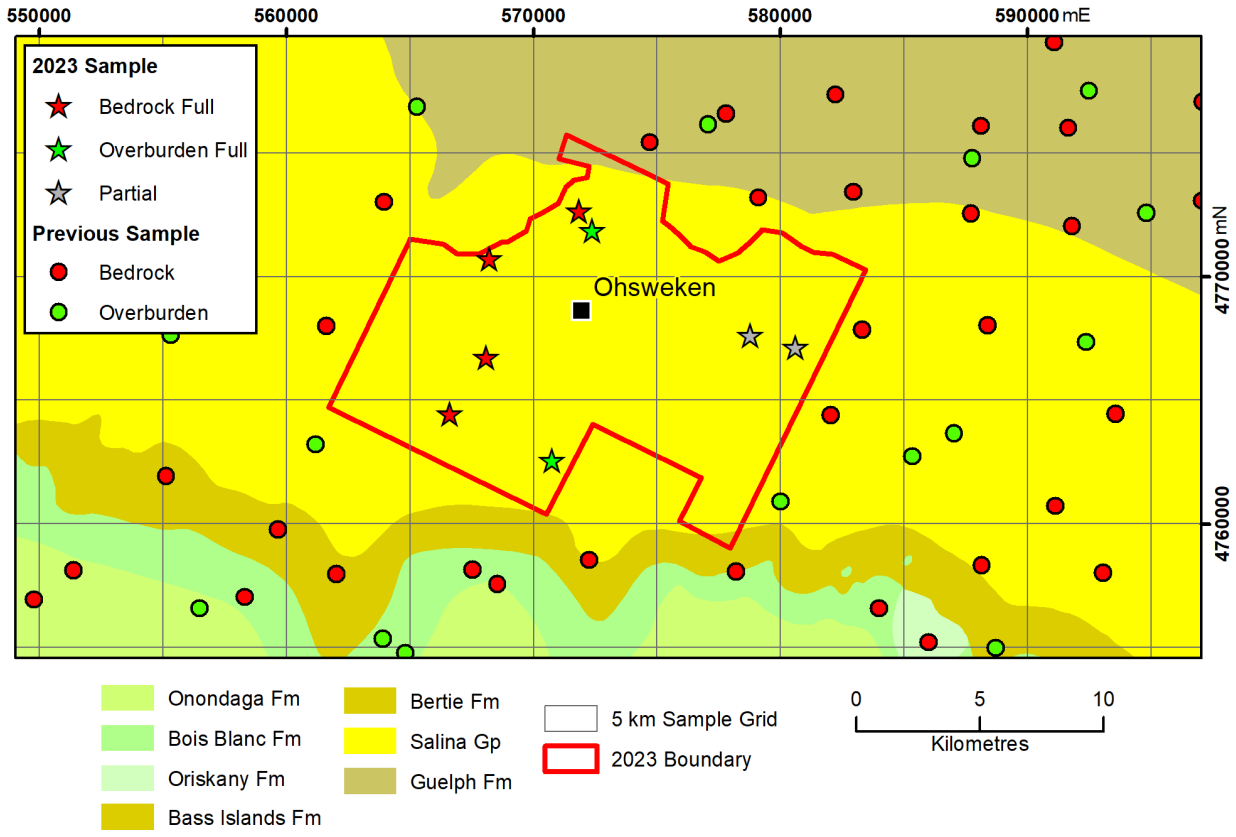


Figure 30.1. The extent of the 2023 study area (shown by red outline) and the location of samples. Location information provided as Universal Transverse Mercator (UTM) co-ordinates using North American Datum 1983 (NAD83) in Zone 17.

The study area lies within the Appalachian Basin, east of the Algonquin Arch. The Salina Group and Guelph and Bertie formations comprise the bedrock geology of Six Nations (*see* Figure 30.1):

- The upper Silurian Salina Group subcrops over the majority of the study area. It is composed of dolostone with intermittent shale layers and gypsum nodules (Armstrong and Dodge 2007; Armstrong and Carter 2010).
- The lower Silurian Guelph Formation is a dolostone unit that covers a small portion of the study area at its northern extent.
- The upper Silurian Bertie Formation is an argillaceous dolostone (Armstrong and Carter 2010) that subcrops in a very small area in the southeast.

The study area is located between 2 bedrock topographic highs: the Niagara Escarpment to the north and the Onondaga escarpment to the south. The bedrock depression between them is known as the Salina Trough and is filled with glacial sediments to a drift thickness greater than on the adjacent cuestas. Overburden geology of the Niagara Peninsula generally includes 4 units: sand, silt and gravel of the lower drift unit at the bottom; clay, silty clay and clayey silt of the lower glaciolacustrine unit; silt and clay of the Halton Drift unit; and silt and clay of the upper glaciolacustrine unit (Burt 2015).

METHODS

Site Selection

Sampling conducted as part of the AGGP typically involves door-to-door cold-calling to find participants with viable wells. Sampling at Six Nations was conducted differently, with well-owners being approached ahead of time and sampling proceeding by way of scheduled appointments. This approach was adopted in accordance with the ETF to not only work on First Nation land in a respectful way, but also to increase community awareness and participation in the project, and to facilitate sampling efficiency. The following steps were involved in site selection:

- A 5 km by 5 km sample grid was utilized across the study area to identify necessary samples to achieve 1 bedrock and 1 overburden sample in each grid square ("node") (*see* Figure 30.1). It should be noted that in many parts of the province, distinct overburden and bedrock aquifers are not being simultaneously exploited by residential wells because of the hydrogeological characteristics of the area. In such areas, both samples are attempted, but often only 1 or the other is obtained.
- The Ministry of Environment, Conservation and Parks (MECP) Well Water Information System (WWIS) was used by OGS personnel to identify potential wells to sample. Potential sampling wells were favoured based on 1) location within the node, 2) drilled well construction, 3) a younger age for the well, 4) the presence of a well tag, and 5) the agreement of the well record with mapped drift thickness.
- Following the analysis above, the location and identification of desirable wells were provided to the ETF who approached the homeowners to set up sampling appointments.
- In areas with limited sampling opportunities, flyers were left at households where a drilled well was observed on the property in an effort to increase participation.

Table 30.1. Details of the analytical suite requested for AGGP samples collected in 2023.

Laboratory	Bottle Name	Analytes	Volume	Preservative
OGS Geoscience Laboratories	Metals	ICP–MS suite of 58 elements	60 mL, filtered	Nitric acid
	Anions	Br, Cl, F, I, NO_3, NO_2, PO_4, SO_4	60 mL, filtered	none
	Hg	Hg	60 mL, filtered	Hydrochloric acid
	DIC/DOC	Dissolved inorganic carbon, dissolved organic carbon	60 mL, filtered	none
SGS Canada	Bacteria	Total coliform, fecal coliform	250 mL, unfiltered	Sodium thiosulphate
	Nutrients	Total Kjeldahl nitrogen, NH_3	60 mL, unfiltered	Sulphuric acid
	PO_4, F	PO_4, F	60 mL, filtered	none
	Sulphide	Dissolved S^{2-}	60 mL, filtered	Zinc acetate and sodium hydroxide
	Anions	Br, Cl, SO_4, NO_3, NO_2, NO_2+NO_3	60 mL, filtered	none
	Colour	Colour	500 mL, unfiltered	none
	DIC/DOC	Dissolved inorganic carbon, dissolved organic carbon	60 mL, filtered	none
Isotope Tracer Technologies	Tritium	^3H	250 mL, unfiltered	none
	Isotopes	$\delta^{18}O$-H_2O, δ^2H-H_2O	120 mL, unfiltered	none
Jan Veizer	Dissolved Gases	C1, C2, C3, CO_2, N_2, Ar+O_2	125 mL, unfiltered	Copper sulphate
	^{13}C-CH_4	$\delta^{13}C$-CH_4, δ^2H-CH_4	125 mL, unfiltered	Copper sulphate
	S-isotopes	$\delta^{34}S$-S^{2-}, $\delta^{34}S$-SO_4, $\delta^{18}O$-SO_4	250 mL, unfiltered	Zinc acetate
Saskatchewan Research Council	Gross Alpha-Beta	Gross alpha-beta	1 L, unfiltered	none
	Radon	Radon	2 × 40 mL, unfiltered	none
Field lab and extra	Iodide	Iodide	60 mL, unfiltered	Nickel acetate
	Spare	to be determined	250 mL, unfiltered	none
	Field gases	CH_4, CO_2	600 mL, unfiltered	none

Abbreviation: *ICP–MS, inductively coupled plasma mass spectrometry.*

Field Methods

Field protocols were consistent with AGGP methodology described by Hamilton, Brauneder and Mellor (2007) and Hamilton and Brauneder (2008).

At the beginning of each sampling day, the field probes were verified and/or calibrated in the morning. The YSI™ multiparameter probe (YSI-EXO1™) was calibrated daily for pH, conductivity and dissolved oxygen, whereas oxidation reduction potential (ORP) was calibrated once at the start of the field season. An additional YSI-ODO™ (optical dissolved oxygen) probe was also used and calibrated daily.

At each site, a well-owner interview and well inspection were completed to gather information about the well and groundwater, and to determine the viability of taking a sample. To collect the sample, sampling hoses were connected to a tap providing untreated water, as pictured in McEwan et al. (2015). Water was run through a flow cell containing the YSI™ multiparameter probe, which was used to assess purging of house plumbing and the well. Purging was determined to be complete once stable readings of temperature, pH, conductivity, optical dissolved oxygen and dissolved oxygen were achieved, which was typically after approximately 250 L of purged water.

A total of 22 bottles were filled at each site for subsequent analysis (*see* Table 30.1 for details) and several on-site measurements were made. Parameters measured using the YSI™ and YSI-ODO™ probes were logged and recorded. Alkalinity was determined on-site by titrating to 3 end-points using 1.6 N sulfuric acid (H_2SO_4) and a bromocresol green-methyl red indicator. If detected by smell, or

reported by the homeowner, hydrogen sulphide was measured using the methylene blue method. The bottle for determination of total and fecal coliform was filled directly from the faucet after thorough disinfection of the tap. Daily shipments to laboratories were conducted to observe the short holding times (the shortest being 48 hours) for several parameters (e.g., bacteria, radon).

Dissolved gas composition and iodide concentration were analyzed in the field at a temporary laboratory set up at the base camp. For dissolved gas analysis, 600 mL of water were collected in an O-ring sealed 1200 mL glass bottle and allowed to temperature-equilibrate overnight with the bottle overturned. Methane, carbon dioxide and oxygen levels were measured in the headspace using an RKI Eagle 2™ portable multigas monitor the following morning. Iodide concentrations were determined using an ion selective electrode (ISE).

Quality control samples, including standards, blanks and duplicates (accounting for more than 10% of the total number of samples), were inserted into the analytical sequence prior to submission and analysis by the laboratories.

PRELIMINARY RESULTS

Sample Coverage

A total of 8 sample stations were accessed and used to obtain 7 full samples (including 1 duplicate) and 2 partial samples (*see* Figure 30.1):

- 5 full samples were collected from drilled wells completed in bedrock
- 1 full sample was collected from a dug well and 1 full sample was collected from a drilled well completed in overburden
- 2 partial samples were taken at wells that went dry during the purging process

The sample coverage is largely on the western side of the reserve. The inconsistent sample coverage is attributed to several factors. First, access to wells in the town of Ohsweken (*see* Figure 30.1) and surrounding areas was limited because they are serviced by the municipal water distribution system. Second, because of the dominantly clay overburden in the study area, most overburden wells are large-diameter, concrete wells and are often serviced with trucked-in water. Therefore, opportunities to access competent samples from overburden units in the study area were limited. Third, areas of poor water quality are difficult to sample using the AGGP protocols because residents are likely to abandon wells yielding undesirable water that is expensive to treat. This was a common occurrence in the 2023 study area, with many residents having resorted to using cisterns.

Data

Samples were submitted to laboratories (*see* Table 30.1) during field work; however, because the work was conducted in September, most analytical results were pending at the time of writing. Preliminary results for specific conductivity and iodide obtained in the field are provided (Figure 30.2), although full quality control analysis has not yet been conducted. Readings of specific conductivity ranged from approximately 1900 to 3500 µS/cm, with the exception of 1 of the partial samples from a shallow well that was approximately 700 µS/cm. These levels are consistent with previous AGGP samples from the surrounding area and suggest that groundwater in Six Nations has levels of dissolved solids consistent with the elevated concentrations present in the Niagara anomaly. Iodide concentrations ranged from 4 to 108 ppb, with the highest concentrations found in bedrock wells at the north end of the study area (*see* Figure 30.2). Iodide in the samples from Six Nations is within the range of those of AGGP samples from the surrounding area.

Upon receipt of all data, quality control analyses will be conducted, and reports will be prepared for each of the participating well owners and for the ETF. Ultimately, the data will be integrated into the next revision of the AGGP database for southern Ontario.

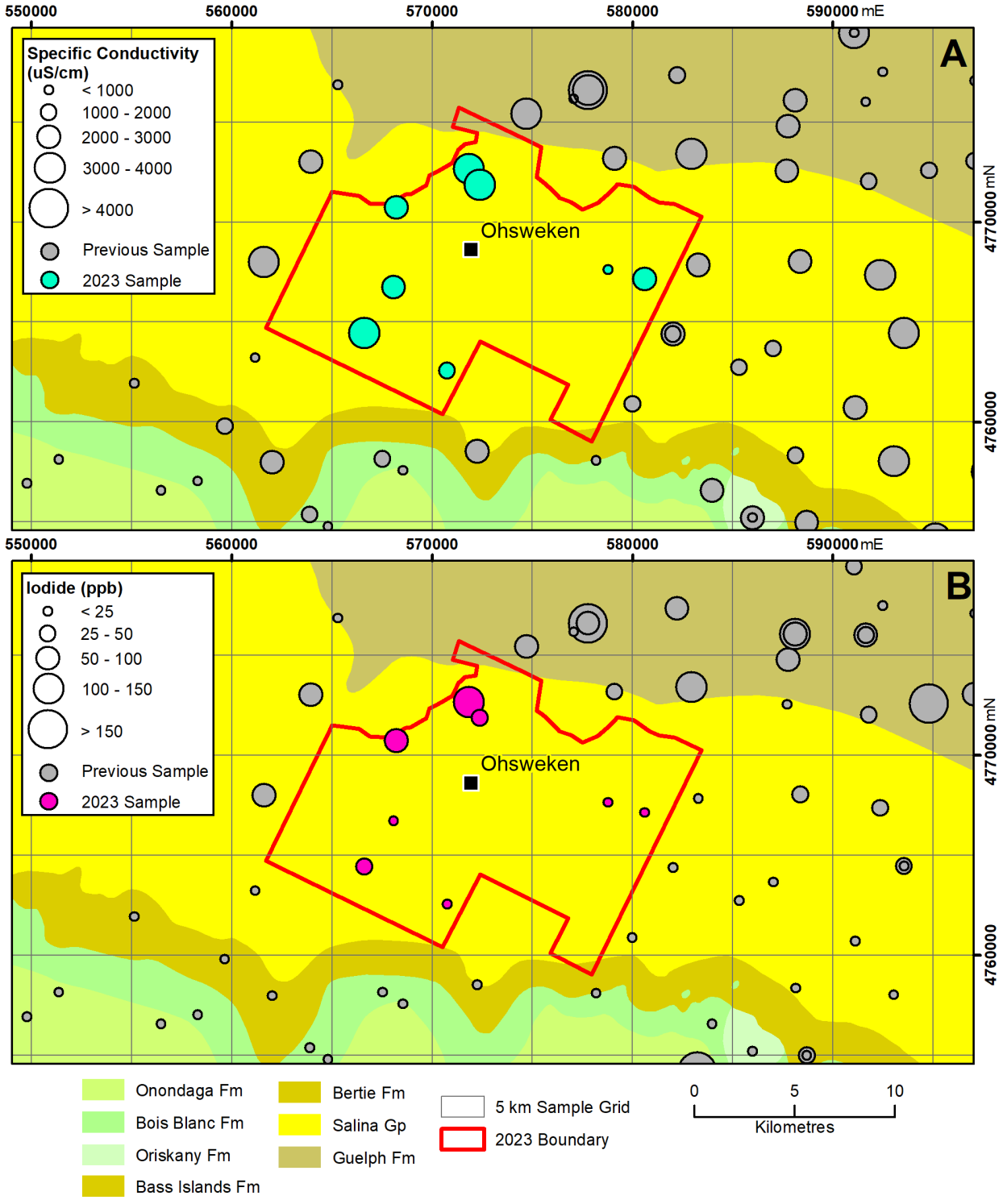


Figure 30.2. A) Specific conductivity and **B)** iodide concentrations for the samples collected in 2023 (within the red outline). Data from existing AGGP samples from the surrounding area are also shown for comparison. Location information provided as UTM co-ordinates using NAD83 in Zone 17.

ACKNOWLEDGMENTS

This project would not have been possible without the exceptional help and support of the Environmental Task Force of Six Nations, especially Rod Whitlow and Julia Zazzarini who generously gave their time to promote this project and accompany us in the field. Thank you as well to Dr. Stewart Hamilton who made the introduction between the Ontario Geological Survey and the Environmental Task Force. We would like to thank the community for its support of this work and the well owners for participating. Our colleagues Kei Yeung, Abigail Burt, Chris Beckett-Brown, Lizane Pamer, Darla Bennett and Mathieu Levesque helped get the project mobilized and provided ongoing support.

REFERENCES

Armstrong, D.K. and Dodge, J.E.P. 2007. Paleozoic geology of southern Ontario; Ontario Geological Survey, Miscellaneous Release—Data 219.

Armstrong, D.K. and Carter, T.R. 2010. The subsurface Paleozoic stratigraphy of southern Ontario; Ontario Geological Survey, Special Volume 7, 301p.

Burt, A.K. 2015. Quaternary stratigraphy of the Niagara Peninsula revealed with three-dimensional mapping; *in* Summary of Field Work and Other Activities, 2015, Open File Report 6313, p.35-1 to 35-17.

Hamilton, S.M. 2021. Ambient groundwater geochemical and isotopic data for southern Ontario, 2007–2019; Ontario Geological Survey, Miscellaneous Release—Data 283 – Revision 2.

Hamilton, S.M. and Brauneder, K. 2008. The ambient groundwater geochemistry project: Year 2; *in* Summary of Field Work and Other Activities, 2008, Ontario Geological Survey, Open File Report 6226, p.34-1 to 34-7.

Hamilton, S.M., Brauneder, K. and Mellor, K.J. 2007. The ambient groundwater geochemistry project – southwestern Ontario; *in* Summary of Field Work and Other Activities, 2007, Ontario Geological Survey, Open File Report 6213, p.23-1 to 23-5.

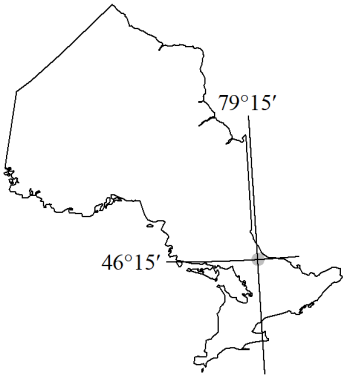
Hamilton, S.M., Freckelton, C.N. and Mariotti, R. 2010. The ambient groundwater geochemistry program: Completion of sampling of southwestern Ontario; *in* Summary of Field Work and Other Activities, 2010, Ontario Geological Survey, Open File Report 6260, p.34-1 to 34-4.

Matheson, E. 2012. Analysis of anomalous groundwater geochemistry of the Niagara Peninsula, Ontario, Canada; unpublished BSc thesis, Queen's University, Kingston, Ontario, 164p.

McEwan, C.A., Hamilton, S.M., Slater, G.F. and Campbell, J.D. 2015. Geochemical and isotopic sampling to delineate sources of highly mineralized groundwater on the Niagara Peninsula; *in* Summary of Field Work and Other Activities, 2015, Open File Report 6313, p.37-1 to 37-8.

Smal, C.A. 2016. Natural and anthropogenic sources controlling regional groundwater geochemistry on the Niagara Peninsula; unpublished MSc thesis, McMaster University, Hamilton, Ontario, 288p.

31. Project NE-23-006. Aggregate Resources Inventory of the North Bay Area, Central Nipissing District, Northeastern Ontario



L.A. Handley[1]

[1]Earth Resources and Geoscience Mapping Section, Ontario Geological Survey

INTRODUCTION

During the summer of 2023, field work for an aggregate resources study was conducted in the North Bay area of northeastern Ontario. The study area covers approximately 940 km^2 of the Statistics Canada Nipissing Census Division and is centred on the City of North Bay on the eastern shores of Lake Nipissing in northeastern Ontario (Figure 31.1). The study area is represented by all or parts of the following 1:50 000 scale map sheets of the National Topographic System (NTS): Kiosk (31 L/2), Powassan (31 L/3) and North Bay (31 L/6).

The purpose of this study is to characterize and inventory the sand and gravel deposits and bedrock within the study area to assess their potential as aggregate resources. Field observations were made at 812 localities, including 404 auger or roadcut sections of surficial materials, 408 bedrock outcrops and 56 existing pits or quarries. These field observations will be integrated with historical aggregate quality and gradation tests performed by the Ministry of Transportation (MTO), as well as water-well records from the Ministry of Environment, Conservation and Parks (MECP), to evaluate both the quantity and quality of aggregate resources within the North Bay area.

PREVIOUS WORK

Previous work on the inventory of aggregate resources for the North Bay area was completed in 1984 by the Ontario Geological Survey (Ontario Geological Survey 1984). This older study does not follow the current "Aggregate Resource Inventory Paper" (ARIP) standard format of the Ontario Geological Survey (OGS), but does include relevant data that have been incorporated into the current study. A new high-resolution digital terrain model (DTM), derived from light detection and ranging (lidar) data acquired from the Ministry of Natural Resources and Forestry (MNRF) (Ministry of Northern Development, Mines, Natural Resources and Forestry 2022), has been used to help delineate and refine aggregate deposit boundaries. Data and observations from regional Quaternary geology mapping completed by the Geological Survey of Canada (Harrison 1972; Figure 31.2) and the most recent compilation of OGS bedrock geology mapping (Ontario Geological Survey 2011; Figure 31.3) have also been used in this study. An OGS Quaternary mapping project covering the entire study area is currently underway and will complement this aggregate assessment (*see* Marich, this volume).

Summary of Field Work and Other Activities, 2023,
Ontario Geological Survey, Open File Report 6405, p.31-1 to 31-9.

© King's Printer for Ontario, 2023

PHYSIOGRAPHY AND SURFICIAL GEOLOGY

The western part of the study area is characterized by flat terrain with numerous lakes and rivers. The southeastern and northern parts of the study area are characterized by the more rugged Precambrian Shield landscape. The study area encompasses portions of 3 physiographic regions: the Nipissing–Mattawa lowland, the Northern upland and the Algonquin highland (Chapman and Putnam 1984).

The Nipissing–Mattawa lowland physiographic region, located between North Bay and Rutherglen in the centre of the study area, is associated with extensive glacial lake sediments draped in areas of low topographic relief between bedrock outcrops (*see* Figure 31.2). The lake sediments consist mainly of varved clays with some rhythmically bedded sands (Harrison 1972). Minor ridges and several large end-moraine segments, drumlins and eskers are also important elements of the surface topography in this part of the study area (Harrison 1972).

The Northern upland physiographic region is located north of the City of North Bay and is bounded to the south by the Ottawa–Bonnechere Graben fault scarp. The Northern upland physiographic region has moderate relief (~90 m; Harrison 1972) and is dominated by Precambrian bedrock outcrops with a thin till cover at high elevations.

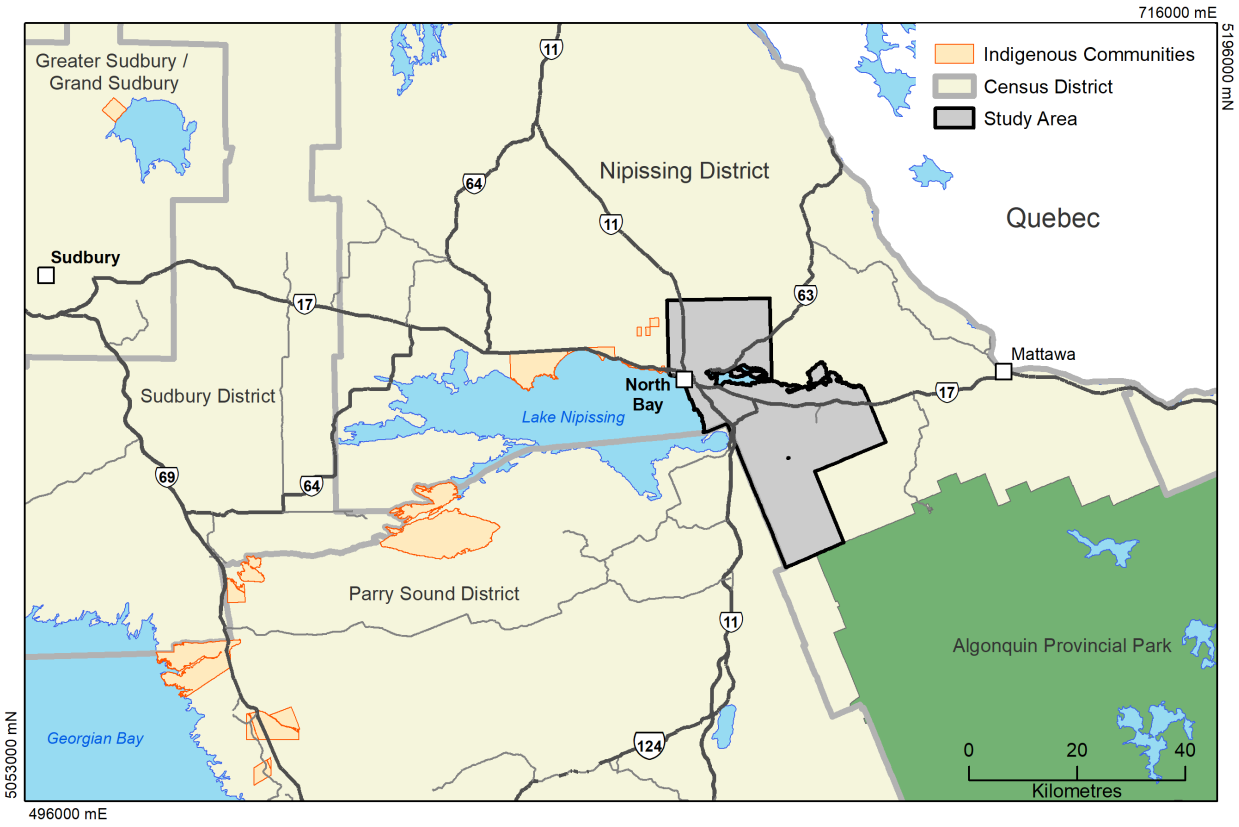


Figure 31.1. Location map showing the study area (grey) within the Nipissing District and the surrounding area, northeastern Ontario. Universal Transverse Mercator (UTM) co-ordinates provided using North American Datum 1983 (NAD83) in Zone 17.

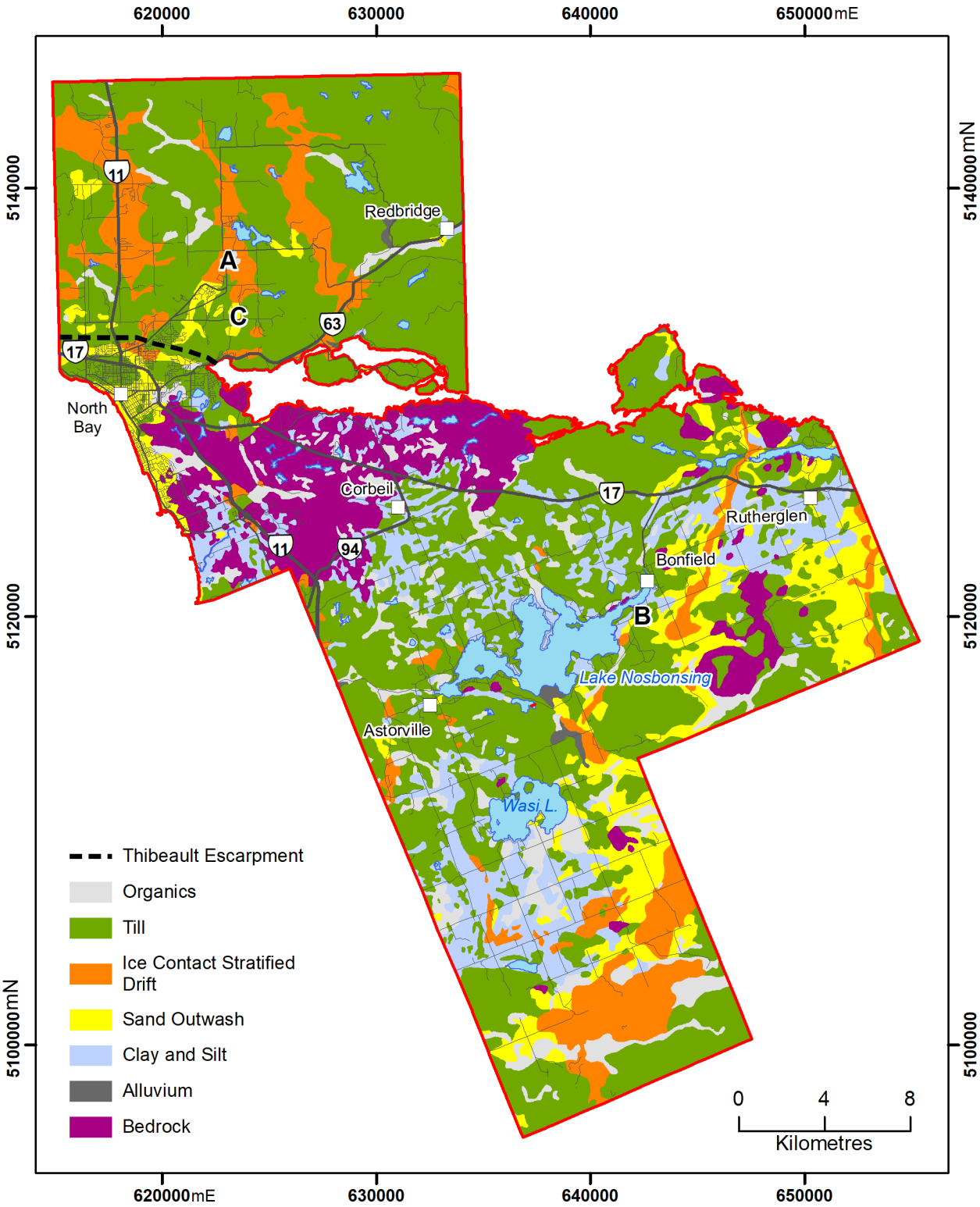


Figure 31.2. Surficial geology map of the study area (geology *modified from* Harrison 1972). The Thibeault escarpment is indicated by the black dashed line. Note: the original map colours have been updated, but no changes have been made to the original polygon boundaries. Letters on the map indicate locations of photographs in Photo 31.1. All UTM co-ordinates provided using NAD83 in Zone 17.

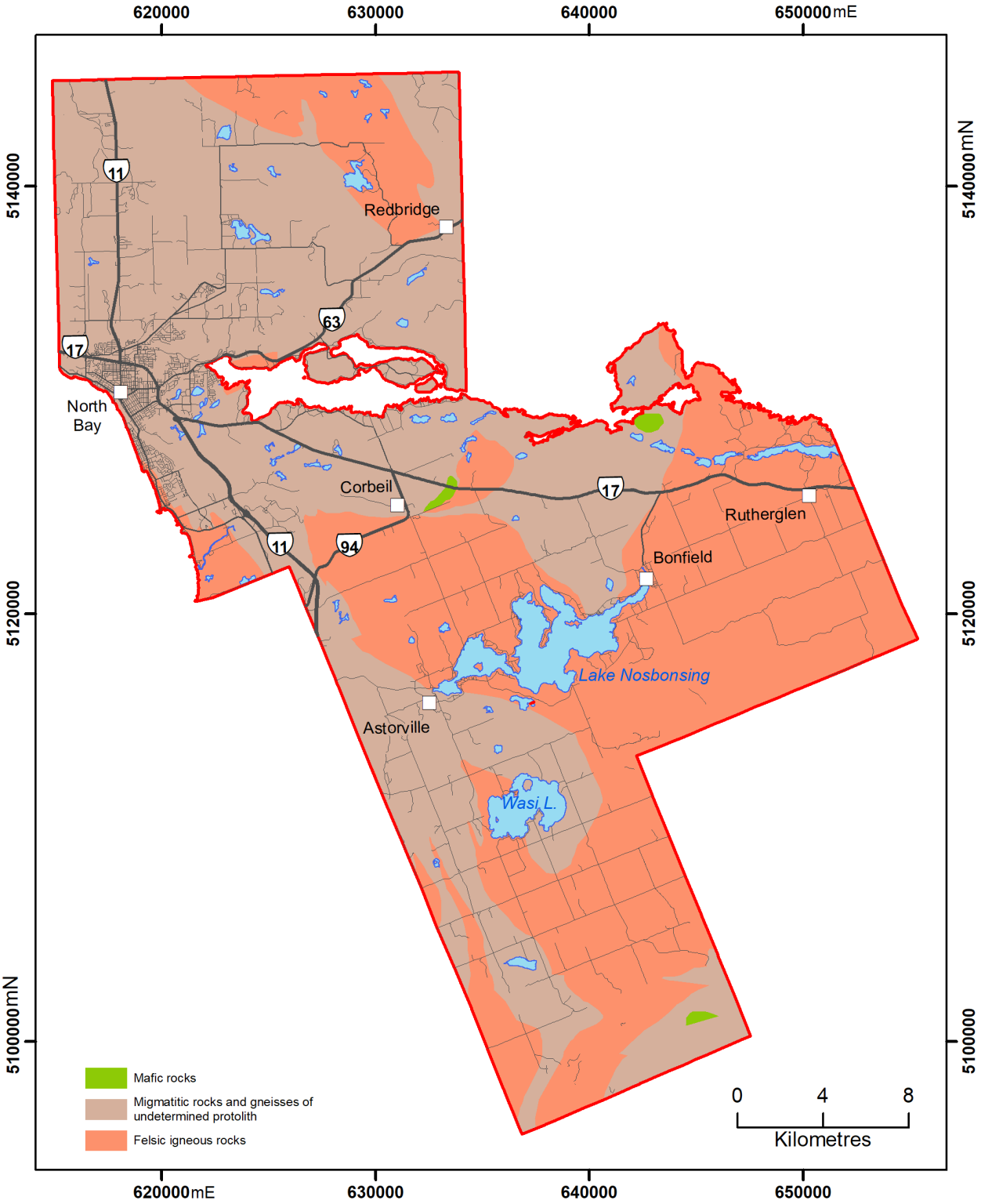


Figure 31.3. Simplified Precambrian bedrock geology map of the study area (*modified from* Ontario Geological Survey 2011). All UTM co-ordinates provided using NAD83 in Zone17.

Similarly, the Algonquin highland physiographic region is characterized by knolls of Precambrian (Grenville Province) bedrock locally overlain by a thin veneer of glacial sediments (*see* Figure 31.2). Relief is typically highly varied, with exposed rounded bedrock knobs and ridges ranging from 15 to 60 m high (Chapman and Putnam 1984). Many of the valleys, depressions and low-lying areas within this physiographic region are filled with outwash sand and gravel, which could potentially become an increasingly more important aggregate resource as other major deposits become depleted.

The thickness and distribution of surficial materials, including sand and gravel deposits, are largely the result of glacial activity during the Late Wisconsin when the Laurentide Ice Sheet advanced through, and subsequently retreated from, the area. Previous work suggests drift thickness in the study area is generally less than 5 m, although it may locally exceed 30 m in thickness in some low-lying bedrock valleys, as well as where ice-contact deposits occur (Harrison 1972). Figure 31.2 shows the distribution of these Quaternary deposits within the study area.

As the ice advanced to the southwest, it deposited an extensive veneer of compact, stony sandy till (Ontario Geological Survey 1984). This is the oldest sediment observed within the study area. Field observations show the thickness and distribution of this material to be very irregular and change quickly over a short distance, even as little as over a few metres. As is typical for glaciated terrains, the till is commonly found in the lee of exposed bedrock knobs, in drumlins, moraines and smaller low-relief ridges that are interpreted as De Geer moraines (Lindén and Möller 2005). Clasts in the till are predominantly subangular local crystalline rocks of the Grenville Province. The low fines content in the till suggests that the material could be suitable for low-grade specification aggregate products for road-building and construction applications.

The largest aggregate deposit by volume in the study area is the broad northeast-trending Genesee moraine, located in the southern portion of the Chisolm Township south of the City of North Bay. The Genesee moraine was formed by meltwaters flowing off the ice margin as it retreated from the Algonquin highland into the Nipissing–Mattawa lowland (Ontario Geological Survey 1984). This meltwater was confined by the ice margin and the higher topographic elevation of highland, resulting in the deposition of sediment in Chisolm Township and in small morainic deposits south of the town of Powassan (Ontario Geological Survey 1984). The composition of the Genesee moraine is predominantly sandy with several gravelly, esker-like ridges near the eastern side of the deposit. These ridges contain good pockets of crushable gravel that have been extracted from small pits for local use. The aggregate from these pits is acceptable for a wide range of load-bearing specification products for road-building and construction industries.

As the ice retreated northward from the Genesee moraine, it uncovered the Fossmill outlet (Harrison 1972). During this outlet phase, meltwater ponded and covered most of the Nipissing–Mattawa lowland depositing considerable amounts of subglacial sand and gravel in a southeast-trending esker through the present-day Bonfield Township (Harrison 1972). The Bonfield esker is a single segmented ridge, approximately 9 to 18 m high, composed predominantly of good crushable gravel (Harrison 1972). The ridge is flanked by thin outwash deposits and grades into finer grained deltaic sediments.

Glaciofluvial ice-contact sand and gravel material was also observed in 3 large parallel south-trending esker systems just north of the City of North Bay (Photo 31.1A). The northern portions of the esker deposits are well defined and predominantly contain pebble and cobble gravel (Ontario Geological Survey 1984). The middle portions of the eskers also contain coarser aggregate (i.e., cobbles and boulders), but the coarser material is overlain by slightly finer textured outwash sediments that were deposited at a later time (Photo 31.1B). Many large commercial pits, operating in the central and western esker deposits, currently supply much of the road-building and construction aggregate used by the City of North Bay. The southern portions of these esker deposits comprise extensive sandy deltaic sequences,

which were deposited in the deep water that ponded against the Thibeault escarpment (Ontario Geological Survey 1984). Several small pits are currently operating in the southern portions of the esker deposits; however, they are only able to supply a limited amount of fine aggregate products (i.e., septic and blending sands).

The younger south-trending Rutherglen moraine is a large glacial landform in the study area that is approximately 10 km in length and varies from 0.5 to 1 km in width. The moraine is a broad, irregular and segmented hummocky ridge with observed local relief of 46 m (Harrison 1972). It is largely composed of ice-contact stratified drift with larger clasts and a highly varied medium sand to a much coarser cobble gravel matrix. There are several small overgrown pits in the southern portion of the moraine that exposed some of the predominantly fine-textured sands. However, in the northern portion, there are considerable amounts of crushable gravel in irregular pockets and lenses within the exposed sand.

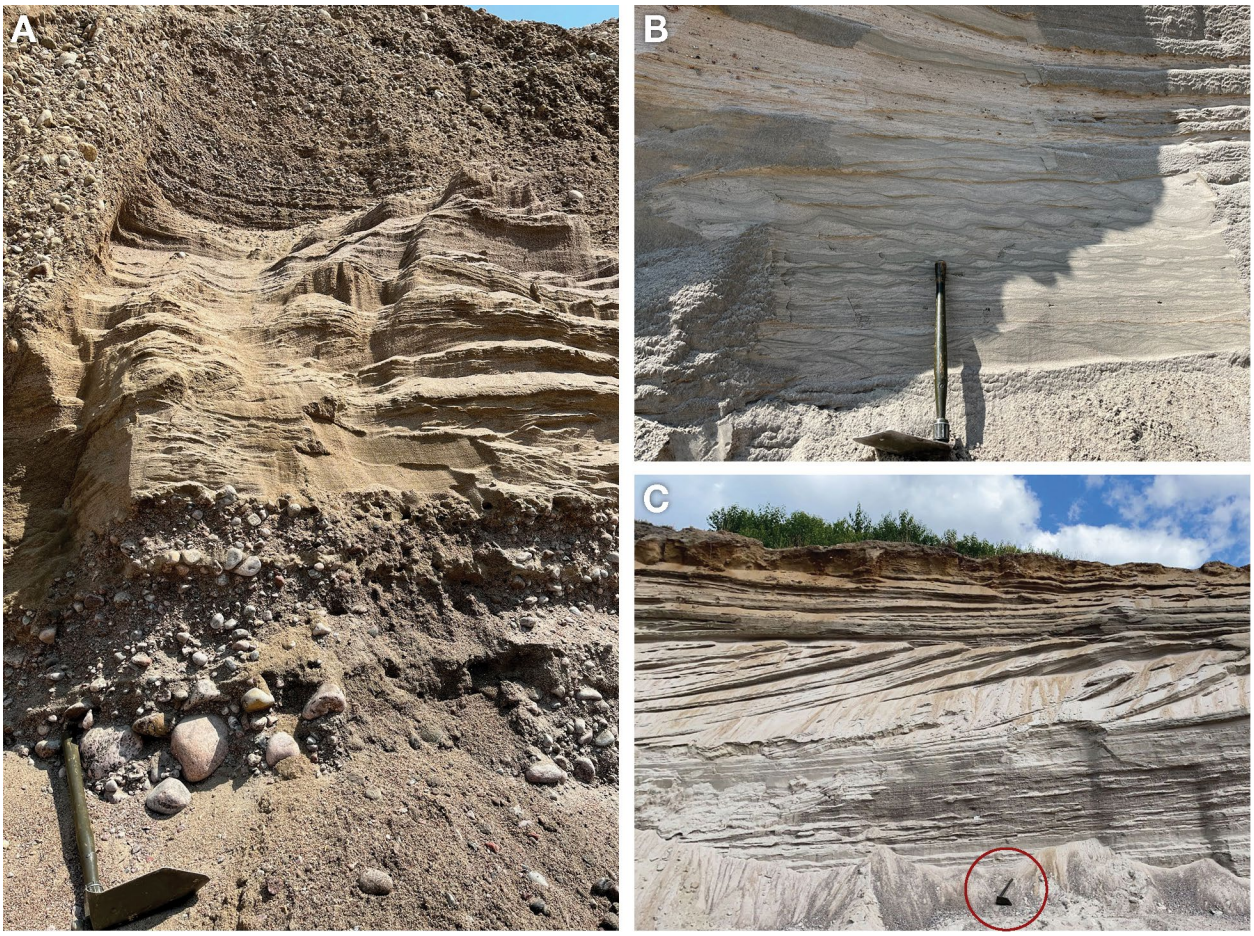


Photo 31.1. Representative photographs of sand and gravel deposits in the study area. **A)** Typical glaciofluvial deposits found north of the City of North Bay. **B)** Typical rippled fine- to medium-textured sand observed in deltaic deposits south of the City of North Bay. **C)** Typical rippled sand and sandy foreset beds interpreted as deltaic deposits within the City of North Bay. The handle of the shovel used for scale in all photos is 40 cm long; in Photo 31.1C, the location of the shovel is indicated by a red circle. Approximate photo locations are indicated on Figure 31.2.

The De Geer moraines are low-relief ridges of 1 to 2 m in height that formed parallel to the retreating ice (Lindén and Möller 2005; *see also* Marich, this volume, article 22, Figure 22.4B). Although mapping of these moraines is not completed, their presence was suggested by Harrison (1972) and are now being further investigated by an OGS mapping project (*see* Marich 2022; *see also* Marich, this volume). Field observations indicate that the sediments in the De Geer moraines are mainly poorly sorted to well-laminated silty sand beds with minor clasts (<5%). There is currently no aggregate extraction from the De Geer moraines, but further investigation may reveal larger pockets of laminated sand beds that could be used for low-grade specification aggregate for construction applications and local uses.

During deglaciation, much of the study area was occupied by proglacial lakes resulting in the deposition of fine-textured silt and clay. These glaciolacustrine sediments were observed in the low-lying areas surrounding or between bedrock knobs or other topographic highs. In deeper basins, the sediment was observed to be silt and clay and gradually became sandier in shallower water environments. Sandy deltas were deposited where rivers entered the lakes and these can form valuable sand resources (Photo 31.1C). Muddy glaciolacustrine deposits have implications for aggregate exploration and extraction because these deposits can drape older viable deposits.

Postglacial erosional and depositional processes have played a minor role in modifying the physiography of the North Bay area. The youngest sediments observed within the study area are peat and muck accumulating in poorly drained low-lying topographic areas and organic-rich alluvial silts and sands on active river floodplains.

SAND AND GRAVEL RESOURCES

In brief, gravel resources in the study area are locally thick but, typically, are not extensive. Overall, the low proportion and occurrence of gravel in the study area poses challenges for the production of crushed aggregate for present and future use. The main crushable aggregate resources are concentrated in the 3 north-trending esker complexes that occur in the northern portion of the City of North Bay, a larger esker in Bonfield Township and several eskers in the southern portion of Chisolm Township. Other sources of crushable aggregate in the project area are found in isolated pockets of gravel, deposited in eskers and moraines, where many small pits have opened for local use. These pockets tend to form small deposits and are scattered throughout the study area. The textural and lithological quality of the gravel deposits are generally good. The initial aggregate quality assessment in the area suggests that the coarse aggregate found in most of the deposits are derived from locally sourced crystalline rocks of the Grenville Province (good quality) with only some farther travelled Huronian Supergroup clasts (lower quality). Most of the aggregates are well suited for higher grade load-bearing aggregate products. Aggregate quality limitations include the locally high proportions of oversized clasts and/or coarse-grained gneissic rock clasts because these larger gneissic clasts are susceptible to rapid weathering (Ontario Geological Survey 1984). Furthermore, deposits rich in Huronian Supergroup clasts may be susceptible to alkali–silica reactivity (Rogers et al. 2000).

Sand resources, however, are plentiful in the study area and several pit operations have recently opened. These new operations exploit sandy outwash complexes and glacial lake deltaic deposits in areas associated with glacial meltwaters. Several larger pits have also been developed in the sandy flanks of the southern portion of the esker complexes north of the Thibeault escarpment and the City of North Bay. Some of these pits have permanent onsite processing facilities and produce blending sand for hot mix asphalt and concrete aggregate applications. Large resources of material are still available and unexploited; however, excess amounts of fines (silt and clay) severely limit the uses of the sand in some areas.

BEDROCK GEOLOGY AND RESOURCE POTENTIAL

The study area lies in the northwestern portion of the Central Gneiss Belt of the Grenville Province (Figure 31.3). These rocks are highly metamorphosed gneisses that are between 1.2 to 2.7 billion years old and have been intruded by 1.4 to 1.5 billion year old granitic and monzonitic plutons (Easton 1992, 2006). The most dominant rock type in the study area consists of migmatitic rocks, including gneisses derived from unknown protoliths, covering most of the central and northern portions of the study area. Although these units have not been known to be quarried in the past, they may be suitable for some crushed products (Ontario Geological Survey 1984). However, it is important to mention that coarse gneisses, containing large amounts of biotite with well-developed foliation, are susceptible to chemical and mechanical weathering and, therefore, may **not** be well suited for load-bearing aggregate products.

The second most dominant rock type, occupying the south and western portions of the study area, include younger intrusive plutonic rocks (*see* Figure 31.3). These plutonic rocks comprise tonalite, granodiorite, monzonite and granite that have undergone metamorphism and display gneissic and recrystallization textures (Ontario Geological Survey 1984; Easton 2006). These rock types are the most common in the North Bay area and are suitable for a variety of road-base, asphalt and concrete products. Careful selection of bedrock is important for concrete products because some of the felsic rocks with higher feldspar and quartz content are known to cause deleterious chemical reactions, such as alkali–silica reactivity. Alkali–silica reactivity is known to cause a reaction between the highly alkaline cement paste and reactive non-crystalline silica resulting in premature concrete deterioration (Rogers et al. 2000).

Mafic plutonic rocks are also present in a few small localized areas in the central portion of the study area. These rocks include amphibolite, gabbro, diorite and mafic gneisses. These rocks are volumetrically limited, and their potential has not yet been determined.

Using bedrock-derived crushed stone resources may become increasingly more important in the future, especially in the aggregate-poor, thinly drift-covered, central portion of the North Bay area.

NEXT STEPS

The information gathered from this field investigation will be used to update the existing older ARIP (Ontario Geological Survey 1984) providing much-needed aggregate resources data for the North Bay area. This study will confirm many of the subdivisions that were observed previously and will be used in conjunction with the most recent Quaternary mapping to provide new aggregate resources maps delineating primary, secondary and tertiary aggregate resources available for future use. An accompanying report will include detailed descriptions and assessments of sand and gravel and bedrock-derived aggregate resources in the study area.

ACKNOWLEDGMENTS

The author would like to thank all of the landowners and pit and quarry operators for granting access to their lands and operations that were covered during this field study. The author would also like to thank Nipissing First Nation, Henvey Inlet First Nation, Dokis First Nation and the Algonquins of Ontario for allowing the Ontario Geological Survey to map their traditional land use areas. Thanks are also extended to Hayden Orr (Canadore College) for assistance in the field.

REFERENCES

Chapman, L.J. and Putnam, D.F. 1984. The physiography of southern Ontario; Ontario Geological Survey, Special Volume 2, 270p.

Easton, R.M. 1992. The Grenville Province; Chapter 19 *in* Geology of Ontario, Chapter 19, Ontario Geological Survey, Special Volume 4, Part 2, p.713-904.

——— 2006. Geology and mineral potential of the eastern Tomiko terrane, Grenville Province; Ontario Geological Survey, Open File Report 5554, 117p.

Harrison, H.E. 1972. Quaternary geology of the North Bay-Mattawa region, Ontario – Quebec; Geological Survey of Canada, Preliminary Map 3-1971, scale 1:125 000.

Lindén, M. and Möller, P. 2005. Marginal formation of De Geer moraines and their implications to the dynamics of grounding-line recession; Journal of Quaternary Science, v.20, p.113-133.

Marich, A.S. 2022. Quaternary geological mapping of the Lake Nipissing Basin, Highway 17 corridor, northeastern Ontario; *in* Summary of Field Work and Other Activities, 2022; Ontario Geological Survey, Open File Report 6390, p.17-1 to 17-9.

Ministry of Northern Development, Mines, Natural Resources and Forestry 2022. Ontario digital terrain model (lidar-derived) - Lake Nipissing 2020 DTM; Ministry of Northern Development, Mines, Natural Resources and Forestry, Provincial Mapping Unit, Peterborough, Ontario.

Ontario Geological Survey 1984. Aggregate resources inventory of the North Bay area, districts of Nipissing and Parry Sound; Ontario Geological Survey, Aggregate Resources Inventory Paper 70, 82p.

——— 2011. 1:250 000 scale bedrock geology of Ontario; Ontario Geological Survey, Miscellaneous Release—Data 126 – Revision 1.

Rogers, C., Grattan-Bellew, P.E., Hooton, R.D., Ryell, J. and Thomas, M.D.A. 2000. Alkali-aggregate reactions in Ontario; Canadian Journal of Civil Engineering, v.27, p.246-260.

This page left blank intentionally

Geoscience Laboratories

32. Revised Methods for the Multi-Element Analysis of Vegetation by Acid-Digestion and Inductively Coupled Plasma Mass Spectrometry at the Geoscience Laboratories



O.M. Burnham[1] and E.G. Amyotte[2]

[1]Geoscience Laboratories, Ontario Geological Survey
[2]Resident Geologist Program, Ontario Geological Survey

INTRODUCTION

In the summer of 2022, in support of a pilot study led by Resident Geologist Program (RGP) staff to refine the application of biogeochemical techniques to the exploration tools for lithium-cesium-tantalum (LCT) pegmatites, the Geoscience Laboratories (Geo Labs) embarked on a review of the methods used for the multi-element analysis of vegetation after acid digestion, with an emphasis on the large-ion lithophile (LILE) and high field strength elements (HFSE) that are typically enriched in such deposits. Methods of drying, comminution, ashing, acid digestion and analysis were examined using in-house and interlaboratory reference materials before analyzing a suite of 119 samples of black spruce, grey alder and humus collected from the Georgia Lake area (Amyotte et al. 2022).

PREVIOUS WORK

Although the Geo Labs have traditionally employed a combination of concentrated nitric acid (HNO_3) and hydrogen peroxide (H_2O_2) to oxidize the organic matter and solubilize analytes in vegetation samples prior to their analysis by inductively coupled plasma atomic emission spectrometry (ICP–AES) (under method codes SOL-VEG and IAT-100), over the last 20 years, this method has been rarely used. Clients have more commonly opted for customized methods that involve various wet or dry ashing methods followed by multi-acid digestions (commonly modified after the Geo Labs open-all-in-one or closed-all-in-one methods, method codes SOL-OAIO and SOL-CAIO, respectively) to promote more complete recoveries and requested analyses by inductively coupled plasma mass spectrometry (ICP–MS) because of its greater sensitivity and wider elemental range. Given the renewed interest in biogeochemical exploration methods, in particular those that might be applied to the exploration for critical minerals, and the wider range of elements that might be of interest, in 2022–2023, the default methods for vegetation digestion and analysis at the Geo Labs moved from the purely oxidative HNO_3 and H_2O_2 digestion to a method that incorporates hydrofluoric (HF), perchloric ($HClO_4$) and hydrochloric (HCl) acids to maximize the recovery and retention of the full range of lithophile trace elements, with full elemental analysis by ICP–MS.

Summary of Field Work and Other Activities, 2023,
Ontario Geological Survey, Open File Report 6405, p.32-1 to 32-18.

© King's Printer for Ontario, 2023

REVISED METHOD

Sample Preparation

Prior to digestion and/or analysis, all samples need to be dried and milled to produce representative and homogeneous fine-grained materials that are stable and can be easily subsampled.

DRYING

Tests of drying temperature and duration indicated that, although fir twigs and needles and/or fresh spruce tips could be adequately dried for milling by either 72 hours at 45°C, 24 hours at 80°C, or 12 to 24 hours at 150°C, there was a systematic loss or low recoveries of several analytes with increasing temperature (Figure 32.1). Despite the apparent slight (~ 30%) loss of mercury when drying is carried out at 80°C, to optimize production and to match the drying temperatures used for the interlaboratory reference materials used for quality control (e.g., NIST 1575 or 1575a, pine needles, dried at 85°C), this temperature was chosen for the routine drying temperature. For samples to be ashed before digestion, loss of volatile elements during drying at 80°C is a minor concern. However, in cases where such analytes might be determined in unashed material, longer drying at a lower temperature (e.g., 45°C) would be required.

MILLING

During method development, dried samples were initially milled through a small Wylie cutting mill, in which the material was pulverized by rotating blades until it passed through an internal 20-mesh sieve. This mill was easily able to process the dried leaves, needles and moss submitted from the pilot study, but was unable to pulverize more woody materials, such as twigs and bark, and was found to impart significant concentrations of silver, bismuth, indium, nickel, lead, antimony and tin (Table 32.1). Accordingly, production was moved to a more robust Fritsch Pulverisette mill. Although harder to clean between samples, the Fritsch mill is more robust, so able to process a wider range of sample media, and imparts considerably less contamination (*see* Table 32.1).

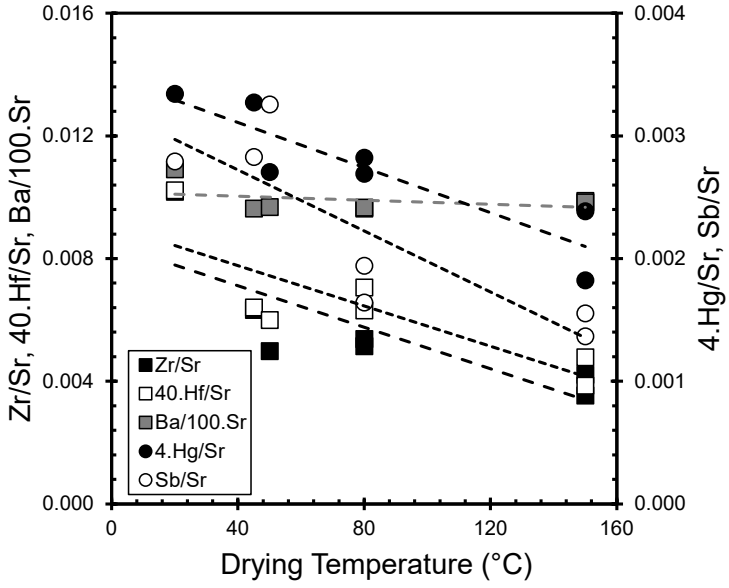


Figure 32.1. Recovery of zirconium, hafnium, barium, mercury and antimony from fir needles and twigs by aqua regia extraction (without ashing) as a function of drying temperature. Concentrations are ratioed to Sr to correct for loss on drying, Sr and Ba are assumed to be immobile during drying. Whereas the decrease in measured Hg and Sb contents may reflect volatilization during drying, the lower recovery of Zr and Hf at higher drying temperatures may reflect the creation of non-aqua regia leachable components.

Table 32.1. Estimated contamination during milling of vegetation samples through different mills. Data obtained by ICP–MS analysis after closed-vessel digestion of ashed material (method code IMC-100), except where indicated.

	Ag[a] (ppb)	As[a] (ppb)	Au[a] (ppb)	Ba (ppb)	Be (ppb)	Bi (ppb)
Agate[b]	0.79	45	0.039	3400	1.45	0.49
Wiley Mill	**49**	17.7	0.174	3500	0.17	**138**
Fritsch Mill	0.93	7.8	0.0141	4200	0.11	0.24

	Cd (ppb)	Ce (ppb)	Co (ppb)	Cr (ppb)	Cs (ppb)	Cu (ppb)
Agate[b]	25.1	34	8.8	60	5.2	3800
Wiley Mill	39	4	29.6	52	8.6	7300
Fritsch Mill	31.4	2.78	10.8	137	9.8	4500

	Dy (ppb)	Er (ppb)	Eu (ppb)	Ga (ppb)	Gd (ppb)	Hf (ppb)
Agate[b]	1.27	0.81	0.34	16.6	1.98	2.63
Wiley Mill	0.24	0.15	0.1	8.6	0.17	1.02
Fritsch Mill	0.17	0.13	0.02	9.7	0.17	0.77

	Ho (ppb)	In (ppb)	La (ppb)	Li (ppb)	Lu (ppb)	Mo (ppb)
Agate[b]	0.26	0.01	16.6	72	0.08	520
Wiley Mill	0.05	**12.7**	2.07	66	0.03	560
Fritsch Mill	0.03	ND	1.32	74	0.05	620

	Nb (ppb)	Nd (ppb)	Ni (ppb)	Pb (ppb)	Pd[a] (ppb)	Pr (ppb)
Agate[b]	1.6	13.9	226	12.7	0.0225	4.1
Wiley Mill	ND	0.78	**58 000**	**55 000**	ND	0.4
Fritsch Mill	ND	0.91	460	15.8	ND	0.29

	Rb (ppb)	Sb (ppb)	Sc (ppb)	Se[a] (ppb)	Sm (ppb)	Sn (ppb)
Agate[b]	6900	1.04	1.92	16.4	2.55	0.88
Wiley Mill	7200	**220**	0.48	27.2	0.55	**33 000**
Fritsch Mill	7400	**9.3**	0.51	19.5	0.35	**10.1**

	Sr (ppb)	Ta (ppb)	Tb (ppb)	Te[a] (ppb)	Th (ppb)	Ti (ppb)
Agate[b]	1430	0.03	0.32	1.56	7.2	610
Wiley Mill	1580	ND	0.03	2.42	0.4	115
Fritsch Mill	1720	ND	0.03	0.86	0.36	167

	Tl (ppb)	Tm (ppb)	U (ppb)	V (ppb)	W (ppb)	Y (ppb)
Agate[b]	0.48	0.08	1.28	12.4	0.54	6.8
Wiley Mill	1.05	0.04	0.38	5.8	**8**	2.18
Fritsch Mill	0.41	0.02	0.33	10.6	**8**	1.13

	Yb (ppb)	Zn (ppb)	Zr (ppb)
Agate[b]	0.67	30 200	100
Wiley Mill	0.18	31 400	41
Fritsch Mill	0.13	36 000	39

[a] *ICP–MS analysis after aqua regia extraction (method code IML-100).*

[b] *Results for agate used as a control, representing an estimate of the composition of the material before milling. For each test, approximately 200 g of hard wheat kernels was processed through each mill, from 5 g were ashed and analyzed.*

Note: *Text in* **bold** *indicates marked contamination added during milling.*

Abbreviation: *ND, not detected.*

ASHING

To preconcentrate the sample and remove organic components, which is critical when perchloric acid is present in the acid mixtures used for the final digestion, samples are ashed by stepped heating using a LECO TGA-701 Thermogravimetric Analyzer. From room temperature to 105°C, samples are heated in a nitrogen atmosphere and the temperature ramped in 20°C increments. They are then heated in air to 485°C (again, ramping the temperature in 20°C increments), held at 485°C for 5 hours in an oxygen atmosphere and finally cooled in air to room temperature before being transfer to sealed vials in a desiccator. At each change in temperature or atmosphere, the conditions are held until a constant mass is attained, allowing all reactions to proceed to completion. During ashing, at least 3 separate episodes of mass loss are seen (Figure 32.2): initial loss of moisture from room temperature to 105°C, loss of volatiles at 180 to 240°C and combustion of light volatile matter at 300 to 380°C (Gonzaga Fraga et al. 2020). Some samples show an additional charring stage at 380 to 440°C. During the pilot study, average ash contents ranged from 2.1 to 6.2 weight %, signifying a sixteen- to fifty-fold increase in concentration relative to the originally collected materials. For samples with low ash contents (< 4% weight%), it was generally necessary to ash duplicate 2 to 2.5 g sample aliquots to obtain sufficient material for analysis (0.1–0.2 g).

Acid Digestion

CLOSED-VESSEL DIGESTIONS

To maximize the recovery of trace elements during acid digestion and minimize blanks, ashed vegetation samples are processed using the closed vessel multi-acid digestion routinely used for whole-rock lithogeochemical analysis (Geo Labs method code SOL-CAIO, *see* Burnham et al. 2002), modified to include an additional pre-oxidation stage with concentrated nitric acid and to employ a reduced volume of the main hydrofluoric acid-bearing acid mixture (a 10:1:1 mixture of concentrated HF, HCl and $HClO_4$).

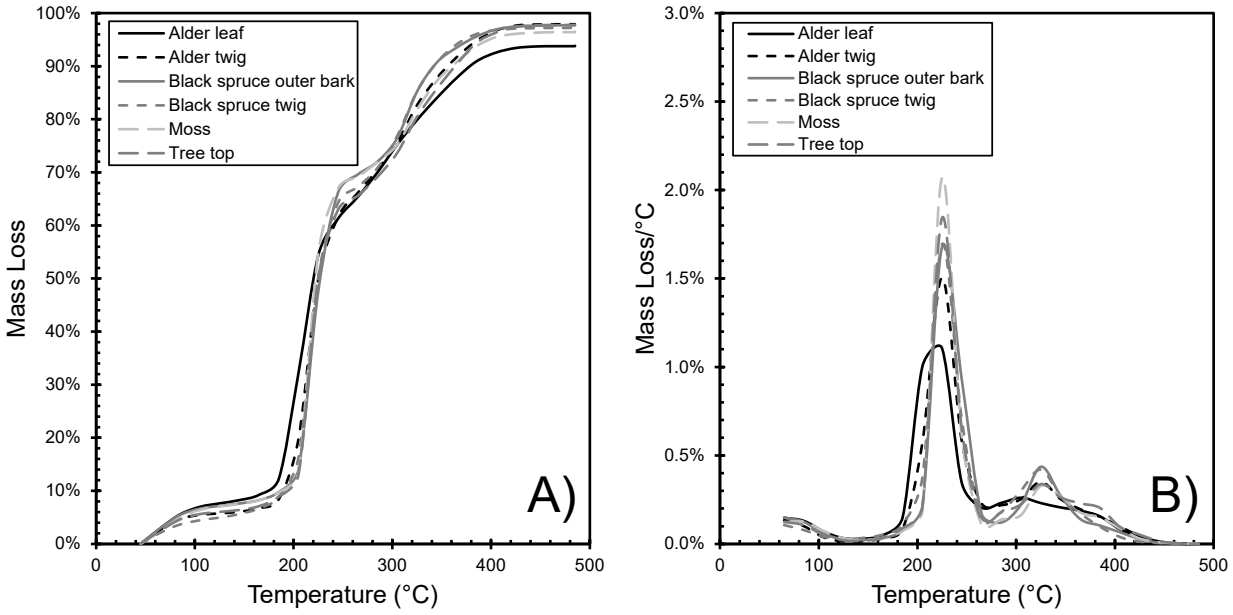


Figure 32.2. Average **A)** thermogravimetric (TG) and **B)** differential thermogravimetric (DTG) profiles obtained during the ashing of the vegetation materials collected during the LCT pegmatites biogeochemical exploration pilot study. Ashing was carried out by stepped heating at 20°C temperature intervals in an atmosphere of nitrogen (ambient to 105°C), air (105°C to 485°C) and oxygen (5 hours at 485°C).

In a 60 mL PFA digestion vessel, 6 mL of concentrated nitric acid is added to 0.1 to 0.2 g ashed sample and the mixture evaporated to near dryness on a 110°C hotplate. Once dry, 7.5 mL (half the normal volume) of the HF–HCl–$HClO_4$ acid mixture is added, after which the closed-vessel sample digestion is carried out as normal for lithogeochemical samples, with 1 week spent sealed in the digestion vessel in a 110°C oven followed by conditioning of the sample solution through repeated dry downs and acid re-dissolutions to produce a solution in 10% v/v nitric acid containing trace HCl and HF to ensure analyte stability.

AQUA REGIA EXTRACTIONS

Although, by preparing samples using the closed-vessel digestion method routinely applied to lithogeochemical samples, better recoveries were expected for elements that require hydrofluoric or perchloric acid to bring them into or stabilize them in solution, the specific elements affected and the possible magnitude of the improvements in recovery were unclear. Freshly ashed aliquots of selected samples of black spruce, grey alder and humus vegetation samples from the pegmatite pilot study and selected QC materials therefore were also prepared using the routine Geo Labs modified aqua regia extraction method and analyzed by ICP–MS (method codes SOL-ARD and IML-100) to compare the results obtainable. Whereas closed-vessel digestions require 2 weeks to complete and involve multiple dry-down stages, aqua regia extractions are simpler to carry out and can be completed in less than 3 days, so offer considerable time savings.

Whether closed-vessel digestions or aqua regia extractions were used, because digestions are carried out on ashed samples, the analyses benefitted from the preconcentration afforded by sample ashing.

Analysis

All sample solutions were analyzed using the routine ICP–MS methods applied to either closed-vessel digestions (analysis method code IMC-100) or aqua regia extractions from soil, sediment and humus samples (analysis method code IML-100), with concentrations corrected for loss-on-ignition during data processing. Analyses were carried out on a Thermo iCAP-Q ICP–MS and calibrated against digested certified rock reference materials (AC-E, BE-N, GSD-12, GSR-1, GSS-6 by method code IMC-100) and/or acid-matrix-matched solutions made up from NIST traceable single or multi-elemental stock solutions (method code IML-100 and a supplementary solution for method code IMC-100, *see* Burnham and Schweyer 2004). Signal intensities were corrected for drift and/or evaporation using a Ru-Re internal standard added during solution preparation and were processed offline using in-house created data reduction routines. Where necessary, interferences were corrected using interelement correction factors determined from synthetic solutions analyzed within the runs.

RESULTS

Results for the multi-acid digestions and aqua regia extractions of the interlaboratory and in-house quality control materials (NIST 1571, orchard leaves; NIST 1573 and 1573a, tomato leaves; NIST 1575 and NIST 1575a, pine needles; MRB-43, an in-house unashed peat reference material[3]) are presented in Tables 32.2 to 32.8. These data, and those obtained for selected samples of black spruce, grey alder and humus collected as part of the vegetation pilot study, are compared graphically in Figures 32.3 to 32.7.

[3] *In-house unashed peat reference material MRB-43 and its ashed equivalent (MRB-42) are fen peats collected from the Holland Marsh, Ontario in 1982 as sample codes 1878P and 1878A, respectively. They were dried, milled, homogenized, split and bottled by the Ontario Geological Survey.*

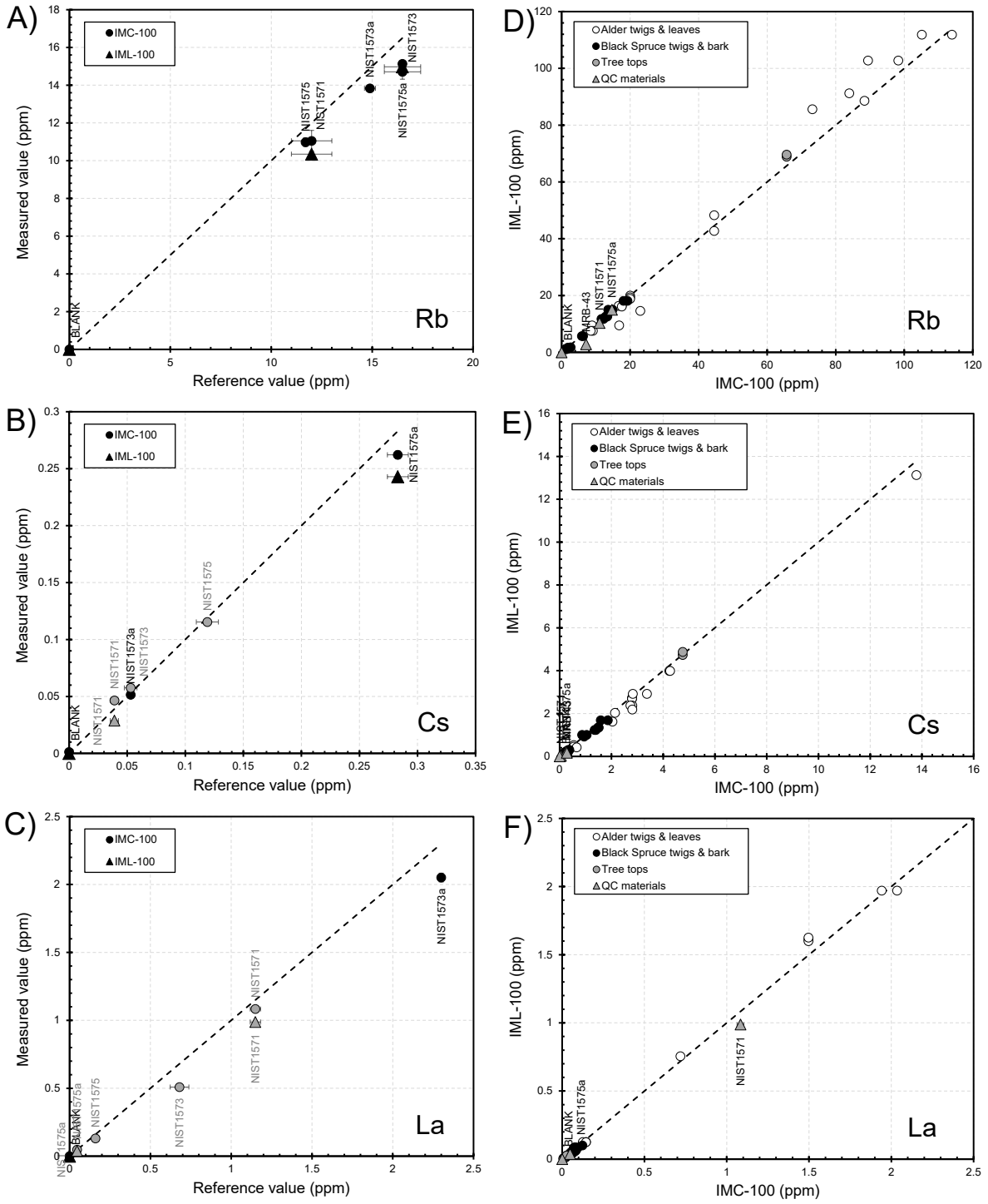


Figure 32.3. Comparison of rubidium, cesium and lanthanum concentrations obtained for interlaboratory vegetation reference materials (NIST 1571, NIST 1573, NIST 1573a, NIST 1575 and NIST 1575a), selected vegetation samples collected as part of the Georgia Lake pilot study (Amyotte et al. 2022) and/or the in-house peat reference material (MRB-43) after ashing and either closed-vessel digestion (method code SOL-CAIO) or aqua regia extraction (method code SOL-ARD) followed by ICP–MS analysis (method codes IMC-100 and IML-100). **Plots A), B) and C)**: Recovery relative to reference values from either NIST-issued certificates of analysis (solid black symbols), where available, or published values (grey symbols: NIST 1571, NIST 1573, NIST 1573a and NIST 1575, Roelandts and Gladney 1998; NIST 1575a, Sucharová and Suchara 2006). **Plots D), E) and F)**: Comparison of data obtained for samples prepared by closed-vessel and aqua regia extraction methods. Dashed lines indicate 1:1 agreement between data. Error bars represent 95% confidence intervals on reference values.

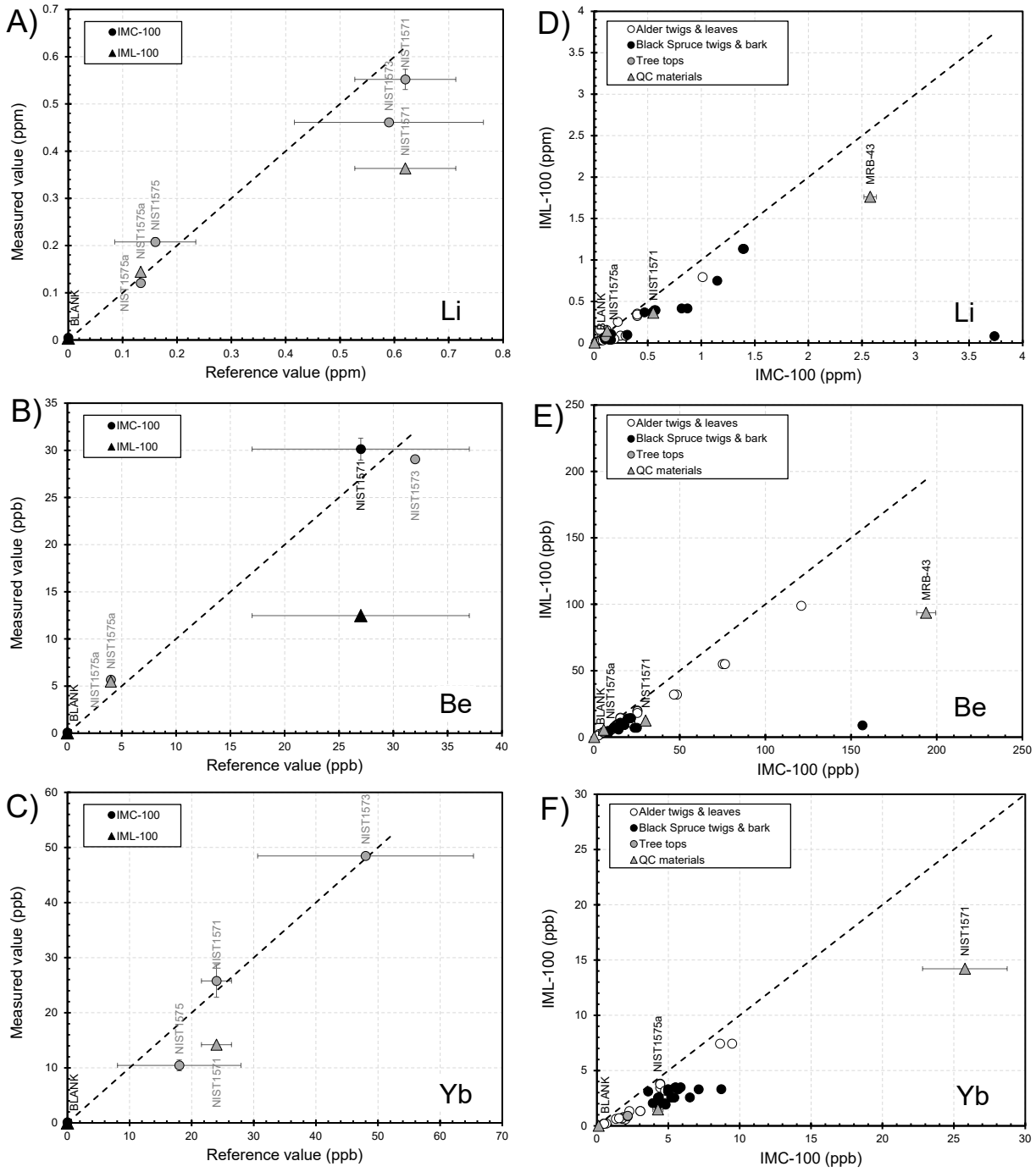


Figure 32.4. Comparison of lithium, beryllium and ytterbium concentrations obtained for interlaboratory vegetation reference materials (NIST 1571, NIST 1573, NIST 1575 and NIST 1575a), selected vegetation samples collected as part of the Georgia Lake pilot study (Amyotte et al. 2022) and/or the in-house peat reference material (MRB-43) after ashing and either closed-vessel digestion (method code SOL-CAIO) or aqua regia extraction (method code SOL-ARD) followed by ICP–MS analysis (method codes IMC-100 and IML-100). **Plots A), B) and C)**: Recovery relative to reference values from either NIST-issued certificates of analysis (solid black symbols), where available, or published values (grey symbols: NIST 1571, NIST 1573 and NIST 1575, Roelandts and Gladney 1998; NIST 1575a, Sucharová and Suchara 2006). **Plots D), E) and F)**: Comparison of data obtained for samples prepared by closed-vessel and aqua regia extraction methods. Dashed lines indicate 1:1 agreement between data. Error bars represent 95% confidence intervals on reference values.

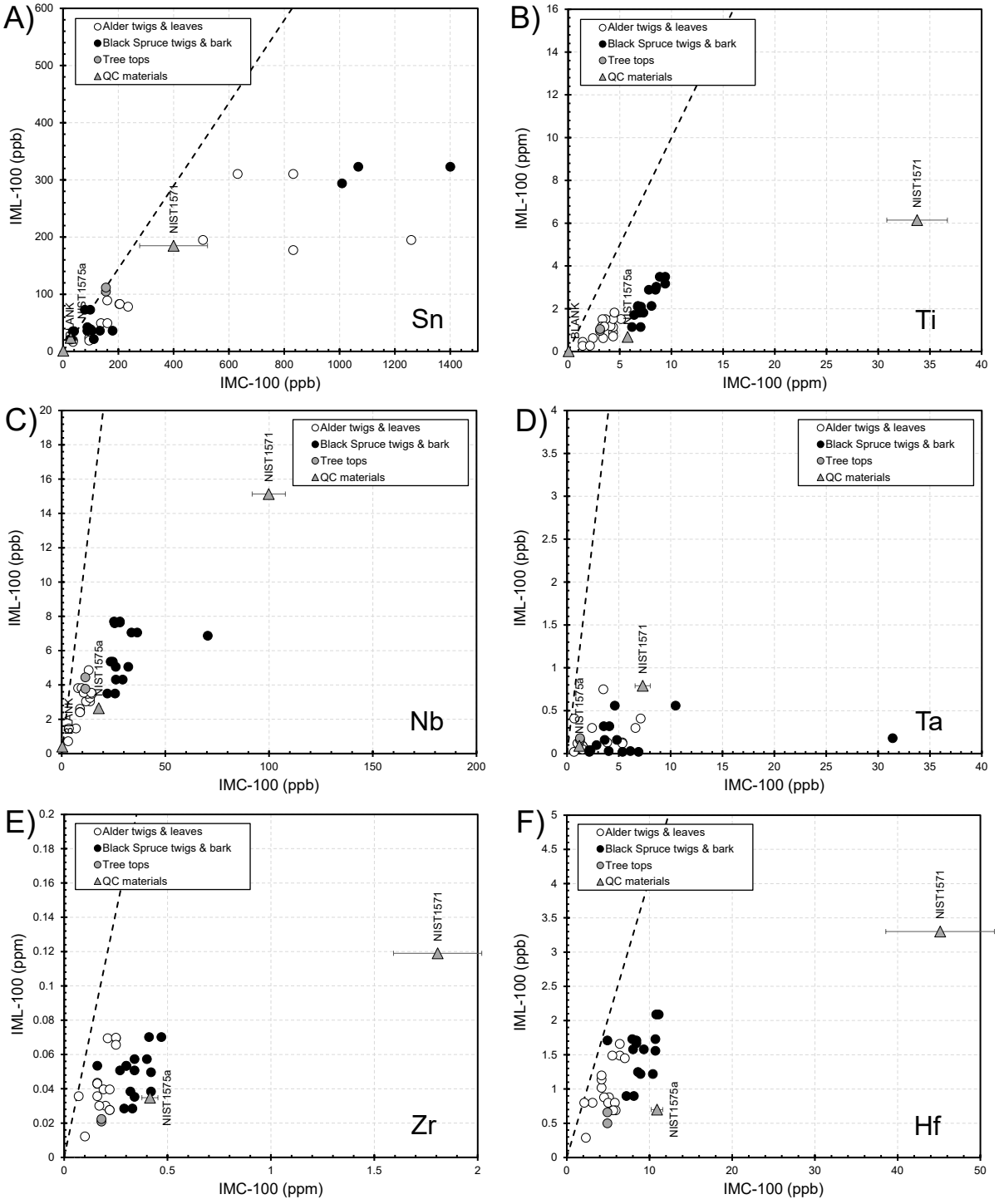


Figure 32.5. Comparison of the concentrations of **A)** tin, **B)** titanium and the high field-strength elements (HFSE) **C)** niobium, **D)** tantalum, **E)** zirconium and **F)** hafnium obtained for interlaboratory vegetation reference materials (NIST 1571 and NIST 1575a) and selected vegetation samples collected as part of the Georgia Lake pilot study (Amyotte et al. 2022) after ashing and either closed-vessel digestion (method code SOL-CAIO) or aqua regia extraction (method code SOL-ARD) followed by ICP–MS analysis (method codes IMC-100 and IML-100). Dashed lines indicate 1:1 agreement between data. Few reference values are available for the high field-strength elements in NIST reference materials so the accuracy of the analyses could not be demonstrated. Error bars represent 1 standard deviation on measured values.

In general, the multi-acid digestions and aqua regia extractions yield similar and, where certified or published concentrations are available, accurate results for most of the alkali elements (Ba, Cs, Rb and Sr), base metals (Co, Cu, Mo, Ni, Pb and Zn), light rare-earth elements (LREE: La, Ce, Pr and Nd) and select semimetal and transition metals (e.g., Cd, Bi, In, Sb, V and W) in the vegetation samples and the reference materials used in the study (Figure 32.3). However, as expected, for many elements, the recovery by aqua regia extractions appears to be incomplete. Whereas the concentrations obtained by multi-acid digestions for beryllium, chromium, gallium, the high field-strength elements (HFSE: Hf, Nb, Ta, Th, U, Zr), lithium, the heavy rare-earth elements (HREE: Er, Tm, Yb and Lu), scandium, tin, tellurium, thallium and yttrium agree well with their certified and/or published concentrations (Figure 32.4), those obtained by aqua regia extractions show either erratic or low recoveries, in particular for hafnium, niobium, tin, tantalum, titanium and zirconium (Figure 32.5). Because the closed vessel digestions and aqua regia extractions were applied to different ashed aliquots of the original pulverized material, some of the variable recovery might be accounted for sample heterogeneity. However, in general, aqua regia extractions appear to be less efficient for many elements that could be of interest during critical mineral exploration, justifying the use of more lengthy but more quantitative mixed acid digestions.

Because only the IML-100 method provides data for arsenic, selenium and the precious metals (Ag, Au and Pd) and the reference materials used in the study are not well characterized for many of these elements, it was not possible to assess the accuracy of the analysis of many of these elements in the ashed samples. Based on single analyses of NIST 1571 (orchard leaves) and NIST 1575a (pine needles), silver, arsenic and selenium appear to be effectively recovered and analyzed from ashed samples by an aqua regia extraction and ICP–MS analysis (Figure 32.7), but, because of its volatilization during ashing, mercury was absent in the ashed material: all measured mercury contents were below the estimated limited of detection and are not presented in Tables 32.3 to 32.6.

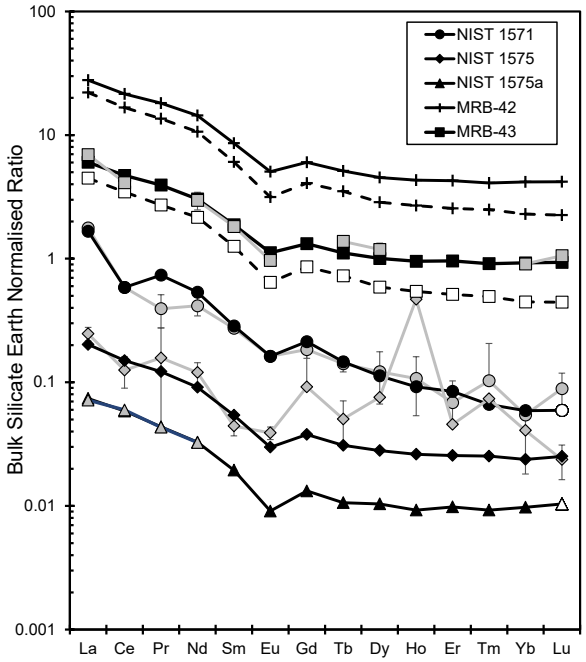


Figure 32.6. Bulk silicate Earth normalized rare-earth element plots for 4 of the principal reference materials used in the study (NIST 1571, orchard leaves; NIST 1575, pine needles; NIST 1575a, pine needles; MRB-43, unashed peat). Black symbols and black solid lines: concentrations obtained by method code IMC-100. Open symbols and dashed lines: concentrations obtained by aqua regia extractions. Grey symbols and grey solid lines: reference values from either NIST-issued certificates of analysis, where available, or published values (NIST 1571 and NIST 1575, Roelandts and Gladney 1998; NIST 1575a, Sucharová and Suchara 2006; MRB-43, OGS unpublished INAA data, 2002). Error bars represent 95% confidence intervals on reference values.

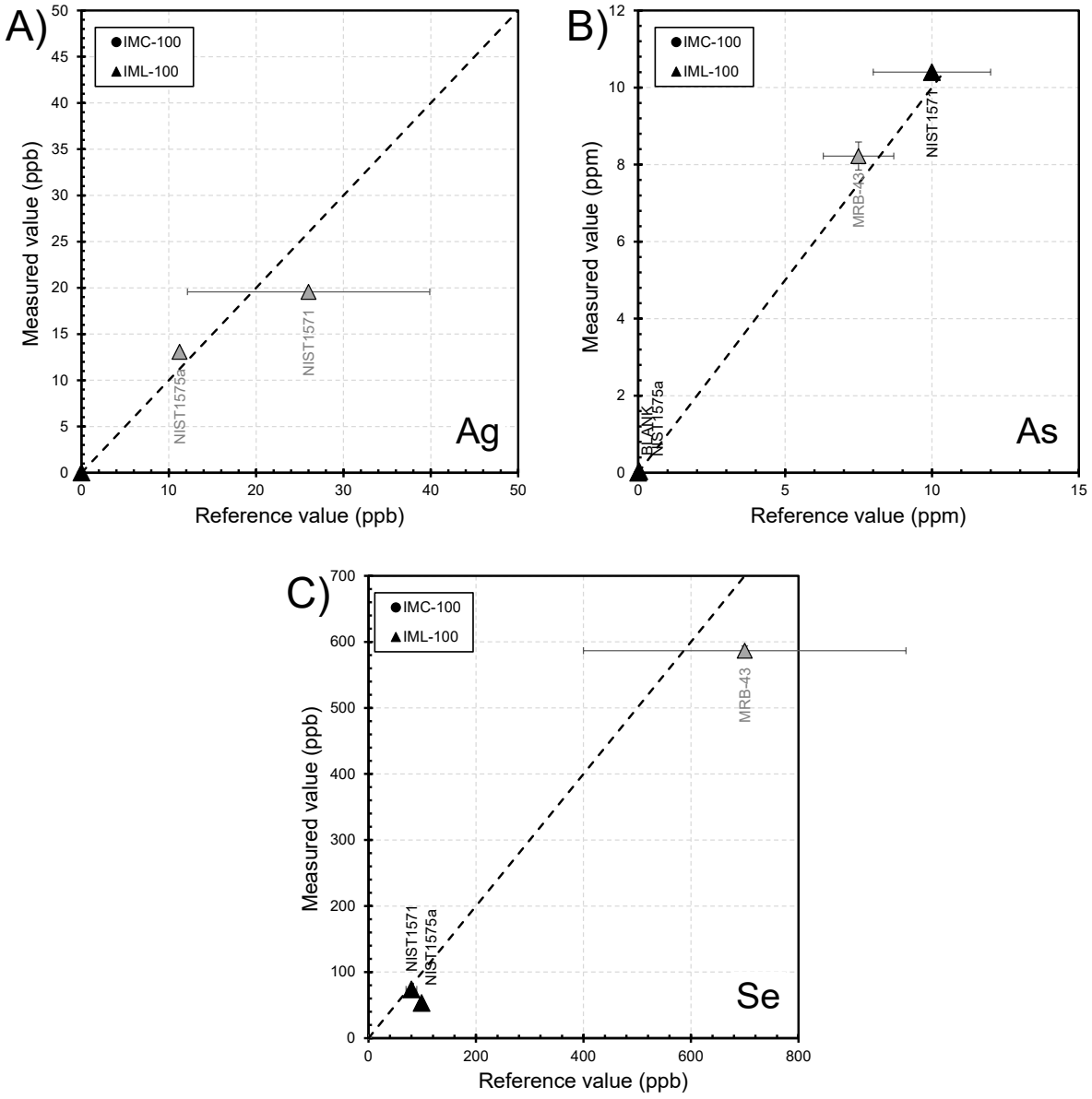


Figure 32.7. Recovery of **A)** silver, **B)** arsenic and **C)** selenium from interlaboratory vegetation reference materials (NIST 1571 and NIST 1575a) and/or the in-house peat reference material (MRB-43) after ashing and either closed-vessel digestion (method code SOL-CAIO) or aqua regia extraction (method code SOL-ARD) followed by ICP–MS analysis (method codes IMC-100 and IML-100). Reference values from either NIST-issued certificates of analysis (solid black symbols), where available, or published values (grey symbols: NIST 1571, Roelandts and Gladney, 1998; NIST 1575a, Sucharová and Suchara 2006). Dashed line indicates 1:1 agreement. Error bars represent 95% confidence intervals on reference values and 1 standard deviation of measured values.

Table 32.2. Summary of trace element concentrations determined in NIST 1571 (orchard leaves) interlaboratory reference material.

	Li (ppm)	Be (ppb)	Sc (ppb)	Ti (ppm)	V (ppm)	Cr (ppm)
Reference value	0.62 ± 0.09	27 ± 10	61 ± 4	20 ± 2	0.51 ± 0.03	2.6 ± 0.3
IMC-100 (n=7)	0.55 ± 0.02	30 ± 1	80 ± 6	34 ± 3	0.68 ± 0.05	3.0 ± 0.3
IML-100 (n=1)	0.4	12	38	6	0.4	2.2

	Co (ppb)	Ni (ppm)	Cu (ppm)	Zn (ppm)	Ga (ppb)	As (ppm)
Reference value	160 ± 10	1.3 ± 0.2	12 ± 1	25 ± 3	99 ± 16	10 ± 2
IMC-100 (n=7)	163 ± 10	1.41 ± 0.09	13.2 ± 0.2	27 ± 3	157 ± 11	NM
IML-100 (n=1)	118	1.1	12	24	83	10

	Se (ppb)	Rb (ppm)	Sr (ppm)	Y (ppm)	Zr (ppm)	Nb (ppb)
Reference value	80 ± 10	12 ± 1	37 ± 1	0.48	2.0 ± 0.8	NA
IMC-100 (n=7)	NM	11.1 ± 0.6	33.8 ± 0.6	0.52 ± 0.02	1.8 ± 0.2	100 ± 8
IML-100 (n=1)	74	10	33	0.4	0.12	15

	Mo (ppb)	Pd (ppb)	Ag (ppb)	Cd (ppb)	In (ppb)	Sn (ppb)
Reference value	300 ± 100	NA	26 ± 14	110 ± 10	1.6 ± 0.5	290 ± 46
IMC-100 (n=7)	232 ± 7	NM	NM	110 ± 8	1.8 ± 0.4	400 ± 120
IML-100 (n=1)	227	0.4	20	116	1.2	185

	Sb (ppb)	Te (ppb)	Cs (ppm)	Ba (ppm)	La (ppm)	Ce (ppm)
Reference value	2900 ± 300	10 ± 2	0.039 ± 0.003	43.0 ± 1.0	1.15 ± 0.03	0.98 ± 0.05
IMC-100 (n=7)	3300 ± 510	7 ± 3	0.046 ± 0.003	44.2 ± 0.6	1.08 ± 0.02	0.98 ± 0.03
IML-100 (n=1)	2900	4	0.029	42	1	0.8

	Pr (ppm)	Nd (ppm)	Sm (ppb)	Eu (ppb)	Gd (ppb)	Tb (ppb)
Reference value	0.10 ± 0.03	0.52 ± 0.09	111 ± 5	25 ± 1	100 ± 15	14 ± 2
IMC-100 (n=7)	0.187 ± 0.005	0.67 ± 0.02	116 ± 10	25 ± 1	116 ± 4	14.5 ± 0.9
IML-100 (n=1)	0.16	0.6	92	20	96	12

	Dy (ppb)	Ho (ppb)	Er (ppb)	Tm (ppb)	Yb (ppb)	Lu (ppb)
Reference value	82 ± 37	16 ± 8	30 ± 2	7 ± 7	24 ± 2	6 ± 2
IMC-100 (n=7)	76 ± 4	13.7 ± 0.5	37 ± 3	4.5 ± 0.4	26 ± 3	4.0 ± 0.4
IML-100 (n=1)	58	10	23	2.7	14	1.8

	Hf (ppb)	Ta (ppb)	W (ppb)	Au (ppb)	Tl (ppb)	Pb (ppm)
Reference value	29 ± 3	8 ± 3	40 ± 18	13 ± 2	41 ± 10	45 ± 3
IMC-100 (n=7)	45 ± 7	7.3 ± 0.7	56 ± 4	NM	37 ± 1	49 ± 4
IML-100 (n=1)	3	0.8	41	1.4	32	43

	Bi (ppb)	Th (ppb)	U (ppb)
Reference value	87 ± 26	64 ± 6	29 ± 5
IMC-100 (n=7)	28 ± 3	62 ± 12	35 ± 3
IML-100 (n=1)	26	35	20

Notes: *Reference values from NIST-issued certificate of analysis or Roelandts and Gladney (1998).*
Abbreviations: *NA, not available. NM, not measured.*

Table 32.3. Summary of trace element concentrations determined in NIST 1573 (tomato leaves) interlaboratory reference material.

	Li (ppm)	**Be (ppb)**	**Sc (ppb)**	**Ti (ppm)**	**V (ppm)**	**Cr (ppm)**
Reference value	0.6 ± 0.2	32	172 ± 13	78 ± 12	1.2 ± 0.2	4.5 ± 0.5
IMC-100 (n=1)	0.46	29	142	87	1.4	3.9

	Co (ppb)	**Ni (ppm)**	**Cu (ppm)**	**Zn (ppm)**	**Ga (ppb)**	**As (ppm)**
Reference value	530 ± 25	1.2 ± 0.1	11 ± 1	62 ± 6	66 ± 45	0.27 ± 0.05
IMC-100 (n=1)	438	1.2	10	60	281	NM

	Se (ppb)	**Rb (ppm)**	**Sr (ppm)**	**Y (ppm)**	**Zr (ppm)**	**Nb (ppb)**
Reference value	67	16.5 ± 0.1	44.9 ± 0.3	NA	NA	NA
IMC-100 (n=1)	NM	15	41	0.46	6.2	233

	Mo (ppb)	**Pd (ppb)**	**Ag (ppb)**	**Cd (ppb)**	**In (ppb)**	**Sn (ppb)**
Reference value	570	NA	100 ± 250	2900	1	184 ± 62
IMC-100 (n=1)	467	NM	NM	2430	0.91	87

	Sb (ppb)	**Te (ppb)**	**Cs (ppm)**	**Ba (ppm)**	**La (ppm)**	**Ce (ppm)**
Reference value	39	0.6 ± 0.2	0.053 ± 0.005	58 ± 3	0.68 ± 0.06	1.36 ± 0.09
IMC-100 (n=1)	46	1.4	0.058	61	0.51	1

	Pr (ppm)	**Nd (ppm)**	**Sm (ppb)**	**Eu (ppb)**	**Gd (ppb)**	**Tb (ppb)**
Reference value	0.17 ± 0.04	0.56 ± 0.02	83 ± 6	24 ± 6	69 ± 19	11 ± 3
IMC-100 (n=1)	0.11	0.41	84	18	74	12

	Dy (ppb)	**Ho (ppb)**	**Er (ppb)**	**Tm (ppb)**	**Yb (ppb)**	**Lu (ppb)**
Reference value	62 ± 12	11 ± 5	36 ± 32	NA	48 ± 17	9 ± 2
IMC-100 (n=1)	74	3.9	45	7.5	48	6.9

	Hf (ppb)	**Ta (ppb)**	**W (ppb)**	**Au (ppb)**	**Tl (ppb)**	**Pb (ppm)**
Reference value	251 ± 72	220	NA	0.6 ± 0.4	38 ± 15	6.3 ± 0.3
IMC-100 (n=1)	153	15	62	NM	28	5.5

	Bi (ppb)	**Th (ppb)**	**U (ppb)**
Reference value	NA	170 ± 30	61 ± 3
IMC-100 (n=1)	8.5	147	53

Notes: *Reference values from NIST-issued certificate of analysis or Roelandts and Gladney (1998). NIST 1573 not analyzed by IML-100.*
Abbreviations: *NA, not available. NM, not measured.*

Table 32.4. Summary of trace element concentrations determined in NIST 1573a (tomato leaves) interlaboratory reference material.

	Li (ppm)	**Be (ppb)**	**Sc (ppb)**	**Ti (ppm)**	**V (ppm)**	**Cr (ppm)**
Reference value	NA	NA	100 ± 0	NA	0.835 ± 0.01	1.99 ± 0.06
IMC-100 (n=2)	0.515 ± 0.004	25 ± 2	103.8 ± 0.2	58 ± 2	0.81 ± 0.01	1.92 ± 0.07

	Co (ppb)	**Ni (ppm)**	**Cu (ppm)**	**Zn (ppm)**	**Ga (ppb)**	**As (ppm)**
Reference value	570 ± 20	1.59 ± 0.07	4.7 ± 0.14	30.9 ± 0.7	NA	0.112 ± 0.004
IMC-100 (n=2)	523 ± 11	1.59 ± 0.02	4.532 ± 0.004	28.2 ± 0.3	154 ± 3	NM

	Se (ppb)	**Rb (ppm)**	**Sr (ppm)**	**Y (ppm)**	**Zr (ppm)**	**Nb (ppb)**
Reference value	54 ± 3	14.89 ± 0.27	85	NA	6.1	NA
IMC-100 (n=2)	NM	13.84 ± 0.04	79 ± 1	0.96 ± 0.03	4.89 ± 0.04	180.3 ± 0.9

	Mo (ppb)	**Pd (ppb)**	**Ag (ppb)**	**Cd (ppb)**	**In (ppb)**	**Sn (ppb)**
Reference value	460 ± 0	NA	17 ± 0	1520 ± 40	NA	NA
IMC-100 (n=2)	394 ± 7	NM	NM	1,280 ± 130	1.77 ± 0.04	76 ± 10

	Sb (ppb)	**Te (ppb)**	**Cs (ppm)**	**Ba (ppm)**	**La (ppm)**	**Ce (ppm)**
Reference value	63 ± 6	NA	0.053	63	2.3	2
IMC-100 (n=2)	57 ± 1	35 ± 17	0.0515 ± 0.0006	58 ± 2	2.05 ± 0.03	1.61 ± 0.03

	Pr (ppm)	**Nd (ppm)**	**Sm (ppb)**	**Eu (ppb)**	**Gd (ppb)**	**Tb (ppb)**
Reference value	NA	1.6	190	66	170 ± 0	24
IMC-100 (n=2)	0.354 ± 0.006	1.26 ± 0.06	198 ± 18	38 ± 2	196 ± 5	23 ± 2

	Dy (ppb)	**Ho (ppb)**	**Er (ppb)**	**Tm (ppb)**	**Yb (ppb)**	**Lu (ppb)**
Reference value	NA	NA	NA	NA	NA	NA
IMC-100 (n=2)	123 ± 11	3.9 ± 0.1	71 ± 5	9.1 ± 0.3	53 ± 3	7.7 ± 0.7

	Hf (ppb)	**Ta (ppb)**	**W (ppb)**	**Au (ppb)**	**Tl (ppb)**	**Pb (ppm)**
Reference value	140 ± 0	14	NA	NA	NA	4.2
IMC-100 (n=2)	124 ± 1	12.5 ± 0.5	22.8 ± 0.2	NM	23 ± 2	0.63 ± 0.03

	Bi (ppb)	**Th (ppb)**	**U (ppb)**
Reference value	NA	120 ± 0	35 ± 0
IMC-100 (n=2)	3.8 ± 0.3	106 ± 3	42.8 ± 0.3

Notes: *Reference values from NIST-issued certificate of analysis or Roelandts and Gladney (1998). NIST 1573a not analyzed by IML-100.*
Abbreviations: *NA, not available. NM, not measured.*

Table 32.5. Summary of trace element concentrations determined in NIST 1575 (pine needles) interlaboratory reference material.

	Li (ppm)	**Be (ppb)**	**Sc (ppb)**	**Ti (ppm)**	**V (ppm)**	**Cr (ppm)**
Reference value	0.16 ± 0.07	NA	41 ± 5	14 ± 6	0.38 ± 0.05	2.6 ± 0.2
IMC-100 (n=4)	0.208 ± 0.009	14.3 ± 0.4	41 ± 2	17.2 ± 0.8	0.399 ± 0.009	2.01 ± 0.09

	Co (ppb)	**Ni (ppm)**	**Cu (ppm)**	**Zn (ppm)**	**Ga (ppb)**	**As (ppm)**
Reference value	123 ± 11	2.7 ± 0.2	2.9 ± 0.3	65 ± 2	90	0.21 ± 0.04
IMC-100 (n=4)	110 ± 3	2.26 ± 0.06	2.81 ± 0.05	67 ± 8	125 ± 12	NM

	Se (ppb)	**Rb (ppm)**	**Sr (ppm)**	**Y (ppm)**	**Zr (ppm)**	**Nb (ppb)**
Reference value	47 ± 6	11.7 ± 0.1	4.8 ± 0.2	0.084	0.18	NA
IMC-100 (n=4)	NM	11.0 ± 0.2	4.42 ± 0.06	0.117 ± 0.004	0.92 ± 0.07	53 ± 2

	Mo (ppb)	**Pd (ppb)**	**Ag (ppb)**	**Cd (ppb)**	**In (ppb)**	**Sn (ppb)**
Reference value	140 ± 38	NA	100 ± 170	210 ± 19	NA	NA
IMC-100 (n=4)	108 ± 2	NM	NM	184 ± 20	1.5 ± 0.2	257 ± 28

	Sb (ppb)	**Te (ppb)**	**Cs (ppm)**	**Ba (ppm)**	**La (ppm)**	**Ce (ppm)**
Reference value	190 ± 9	NA	0.119 ± 0.010	7.1 ± 0.5	0.16 ± 0.02	0.21 ± 0.06
IMC-100 (n=4)	168 ± 17	3.3 ± 0.3	0.115 ± 0.002	7.04 ± 0.10	0.131 ± 0.004	0.251 ± 0.006

	Pr (ppm)	**Nd (ppm)**	**Sm (ppb)**	**Eu (ppb)**	**Gd (ppb)**	**Tb (ppb)**
Reference value	0.04 ± 0.03	0.15 ± 0.03	18 ± 3	6.0 ± 0.7	50 ± 50	5 ± 2
IMC-100 (n=4)	0.031 ± 0.001	0.114 ± 0.002	22 ± 2	4.6 ± 0.3	20.6 ± 0.4	3.06 ± 0.08

	Dy (ppb)	**Ho (ppb)**	**Er (ppb)**	**Tm (ppb)**	**Yb (ppb)**	**Lu (ppb)**
Reference value	51	70	20 ± 25	5	18 ± 10	1.6 ± 0.5
IMC-100 (n=4)	18.9 ± 0.9	3.9 ± 0.1	11.2 ± 0.4	1.72 ± 0.10	10.5 ± 1.0	1.7 ± 0.1

	Hf (ppb)	**Ta (ppb)**	**W (ppb)**	**Au (ppb)**	**Tl (ppb)**	**Pb (ppm)**
Reference value	20 ± 25	8	57	0.7 ± 0.7	40 ± 7	10.8 ± 0.5
IMC-100 (n=4)	24 ± 2	3.9 ± 0.5	50 ± 3	NM	28 ± 4	9.9 ± 0.2

	Bi (ppb)	**Th (ppb)**	**U (ppb)**
Reference value	NA	37 ± 3	20 ± 4
IMC-100 (n=4)	21.5 ± 0.5	33.1 ± 0.8	17.3 ± 0.7

Notes: *Reference values from NIST-issued certificate of analysis or Roelandts and Gladney (1998). NIST 1575 not analyzed by IML-100.*
Abbreviations: *NA, not available. NM, not measured.*

Table 32.6. Summary of trace element concentrations determined in NIST 1575a (pine needles) interlaboratory reference material.

	Li (ppm)	**Be (ppb)**	**Sc (ppb)**	**Ti (ppm)**	**V (ppm)**	**Cr (ppm)**
Reference value	0.13325	4	10.1 ± 0.3	NA	0.12575	0.37525
IMC-100 (n=3)	0.121 ± 0.008	5.7 ± 0.3	10.6 ± 0.4	5.8 ± 0.1	0.110 ± 0.004	0.32 ± 0.01
IML-100 (n=1)	0.1	5	9	0.7	0.1	0.3

	Co (ppb)	**Ni (ppm)**	**Cu (ppm)**	**Zn (ppm)**	**Ga (ppb)**	**As (ppm)**
Reference value	61 ± 2	1.47 ± 0.1	2.8 ± 0.2	38 ± 2	76.25	0.039 ± 0.002
IMC-100 (n=3)	57.8 ± 0.4	1.34 ± 0.04	2.73 ± 0.04	34.3 ± 0.2	34 ± 7	NM
IML-100 (n=1)	58	1	2	35	22	0.04

	Se (ppb)	**Rb (ppm)**	**Sr (ppm)**	**Y (ppm)**	**Zr (ppm)**	**Nb (ppb)**
Reference value	99 ± 4	16.5 ± 0.9	6.4975	0.035	NA	NA
IMC-100 (n=3)	NM	14.7 ± 0.4	6.10 ± 0.06	0.046 ± 0.002	0.42 ± 0.04	18 ± 1
IML-100 (n=1)	53	15	6	0.02	0.03	3

	Mo (ppb)	**Pd (ppb)**	**Ag (ppb)**	**Cd (ppb)**	**In (ppb)**	**Sn (ppb)**
Reference value	14	NA	11.25	233 ± 4	NA	40
IMC-100 (n=3)	13.6 ± 0.6	NM	NM	196.6 ± 0.9	ND	27.6 ± 1.0
IML-100 (n=1)	12	0.3	13	170	0.1	24

	Sb (ppb)	**Te (ppb)**	**Cs (ppm)**	**Ba (ppm)**	**La (ppm)**	**Ce (ppm)**
Reference value	8.75	NA	0.283 ± 0.009	6 ± 0.2	0.0465	0.1
IMC-100 (n=3)	6.6 ± 0.8	1.3 ± 0.7	0.262 ± 0.003	5.3 ± 0.2	0.048 ± 0.003	0.098 ± 0.002
IML-100 (n=1)	6	0.4	0.2	5	0.04	0.07

	Pr (ppm)	**Nd (ppm)**	**Sm (ppb)**	**Eu (ppb)**	**Gd (ppb)**	**Tb (ppb)**
Reference value	0.011	0.04075	NA	NA	NA	NA
IMC-100 (n=3)	0.0111 ± 0.0003	0.041 ± 0.005	7.9 ± 0.9	1.4 ± 0.2	7.2 ± 0.4	1.052 ± 0.002
IML-100 (n=1)	0.009	0.03	5	1	5	0.8

	Dy (ppb)	**Ho (ppb)**	**Er (ppb)**	**Tm (ppb)**	**Yb (ppb)**	**Lu (ppb)**
Reference value	NA	NA	NA	NA	NA	NA
IMC-100 (n=3)	7.0 ± 0.4	1.38 ± 0.05	4.3 ± 0.2	0.63 ± 0.06	4.3 ± 0.4	0.7 ± 0.1
IML-100 (n=1)	3	0.8	2	0.3	1	0.3

	Hf (ppb)	**Ta (ppb)**	**W (ppb)**	**Au (ppb)**	**Tl (ppb)**	**Pb (ppm)**
Reference value	NA	NA	NA	NA	16	0.167 ± 0.015
IMC-100 (n=3)	10.9 ± 0.7	1.2 ± 0.2	5.1 ± 0.4	NM	15.1 ± 0.6	0.151 ± 0.001
IML-100 (n=1)	0.7	0.09	4	0.3	3	0.1

	Bi (ppb)	**Th (ppb)**	**U (ppb)**
Reference value	NA	13.25	5
IMC-100 (n=3)	1.81 ± 0.08	14.8 ± 0.4	6.1 ± 0.4
IML-100 (n=1)	2	9	4

Notes: *Reference values from NIST-issued certificate of analysis or Sucharová and Suchara (2006).*
Abbreviations: *NA, not available. NM, not measured.*

Table 32.7. Summary of trace element concentrations determined in MRB-42 (ashed peat, sample code 1878A) in-house quality control material.

	Li (ppm)	Be (ppb)	Sc (ppb)	Ti (ppm)	V (ppm)	Cr (ppm)
IMC-100 (n=7)	12.6 ± 0.3	913 ± 33	5310 ± 100	2005 ± 84	45 ± 1	35 ± 1
IML-100 (n=3)	8.0 ± 0.2 [a]	515 ± 7	3409 ± 100	571 ± 12	38.2 ± 0.8	26.3 ± 0.3

	Co (ppb)	Ni (ppm)	Cu (ppm)	Zn (ppm)	Ga (ppb)	As (ppm)
IMC-100 (n=7)	8120 ± 240	26.2 ± 0.3 [a]	832 ± 26	183 ± 6	8090 ± 130	NM
IML-100 (n=3)	7021 ± 140	23.2 ± 0.1	736 ± 5	143.8 ± 0.4	4252 ± 95	36.4 ± 0.8

	Se (ppb)	Rb (ppm)	Sr (ppm)	Y (ppm)	Zr (ppm)	Nb (ppb)
IMC-100 (n=7)	NM	31 ± 2	829 ± 13	20.1 ± 0.4 [a]	109 ± 4 [a]	5520 ± 140 [a]
IML-100 (n=3)	2382 ± 53	16.0 ± 0.3	733 ± 17	13.3 ± 0.3	12.53 ± 0.09	397 ± 5

	Mo (ppb)	Pd (ppb)	Ag (ppb)	Cd (ppb)	In (ppb)	Sn (ppb)
IMC-100 (n=7)	5480 ± 100	NM	NM	525 ± 23 [a]	40 ± 3 [a]	4859 ± 96
IML-100 (n=3)	5442 ± 11	12.0 ± 2	3462 ± 170	390 ± 12	26.9 ± 0.5	4268 ± 70

	Sb (ppb)	Te (ppb)	Cs (ppm)	Ba (ppm)	La (ppm)	Ce (ppm)
IMC-100 (n=7)	1404 ± 33	84 ± 18	1.00 ± 0.05	582 ± 11	18 ± 1	36 ± 2
IML-100 (n=3)	1244 ± 46	65.6 ± 1.0	0.770 ± 0.004	336 ± 5	14.3 ± 0.3	27.9 ± 0.3

	Pr (ppm)	Nd (ppm)	Sm (ppb)	Eu (ppb)	Gd (ppb)	Tb (ppb)
IMC-100 (n=7)	4.6 ± 0.3	18 ± 1	3490 ± 220	779 ± 19	3270 ± 240	507 ± 34
IML-100 (n=3)	3.44 ± 0.08	13.3 ± 0.2	2462 ± 56	485.4 ± 2	2219 ± 27	347 ± 6

	Dy (ppb)	Ho (ppb)	Er (ppb)	Tm (ppb)	Yb (ppb)	Lu (ppb)
IMC-100 (n=7)	2979 ± 86 [a]	626 ± 15 [a]	1833 ± 61 [a]	271 ± 9 [a]	1793 ± 40 [a]	276 ± 9 [a]
IML-100 (n=3)	1927 ± 21	401 ± 4	1,115 ± 7	169.6 ± 0.6	1011 ± 6	151.7 ± 2

	Hf (ppb)	Ta (ppb)	W (ppb)	Au (ppb)	Tl (ppb)	Pb (ppm)
IMC-100 (n=7)	2800 ± 270	350 ± 9 [a]	965 ± 48	NM	100 ± 4	210 ± 5 [a]
IML-100 (n=3)	263 ± 5	6.4 ± 1	750.0 ± 3	18.6 ± 0.4	21.9 ± 0.6	105 ± 2

	Bi (ppb)	Th (ppb)	U (ppb)
IMC-100 (n=7)	132 ± 7	3690 ± 340	6020 ± 280 [a]
IML-100 (n=3)	113 ± 4	2935 ± 19	5833 ± 50

Notes: *Reference values not available for MRB-42.*
[a]Mean concentrations after outlier removal (n=6).
Abbreviations: *NA, not available. NM, not measured.*

Table 32.8. Summary of trace element concentrations determined in MRB-43 (unashed peat, sample code 1878P) in-house quality control material.

	Li (ppm)	Be (ppb)	Sc (ppb)	Ti (ppm)	V (ppm)	Cr (ppm)
Reference value	NA	NA	1050 ± 110	420 ± 78.7	9.4 ± 0.4	8 ± 1.2
IMC-100 (n=9)	2.58 ± 0.06	194 ± 6	1159 ± 24	433 ± 7	9.9 ± 0.1 [a]	9.1 ± 0.2 [a]
IML-100 (n=5)	1.8 ± 0.1	94 ± 6	644 ± 25	89 ± 4	7.4 ± 0.2	5.8 ± 0.2

	Co (ppb)	Ni (ppm)	Cu (ppm)	Zn (ppm)	Ga (ppb)	As (ppm)
Reference value	2000 ± 400	5.7 ± 0.9	NA	37.7 ± 3.1	NA	7.5 ± 1.2
IMC-100 (n=9)	1769 ± 39	6.0 ± 0.2	186 ± 4	40.6 ± 0.8	1727 ± 36	NM
IML-100 (n=5)	1523 ± 69	5.08 ± 0.10	181 ± 4	40 ± 1	760 ± 7	8.2 ± 0.4

	Se (ppb)	Rb (ppm)	Sr (ppm)	Y (ppm)	Zr (ppm)	Nb (ppb)
Reference value	700 ± 300	6.3 ± 1.6	192.8 ± 19.9	NA	NA	NA
IMC-100 (n=9)	NM	7.1 ± 0.1 [a]	178 ± 3	4.44 ± 0.10	28 ± 1	1189 ± 20 [a]
IML-100 (n=5)	587 ± 7	2.8 ± 0.1	162 ± 3	2.70 ± 0.06	1.74 ± 0.02	105 ± 2

	Mo (ppb)	Pd (ppb)	Ag (ppb)	Cd (ppb)	In (ppb)	Sn (ppb)
Reference value	1000 ± 700	NA	500 ± 0	NA	8.9 ± 12.5	NA
IMC-100 (n=9)	1205 ± 26	NM	NM	475 ± 10	9.5 ± 0.9	5260 ± 310
IML-100 (n=5)	1200 ± 10	3.2 ± 0.5	362 ± 21	485 ± 17	7.7 ± 0.2	3097 ± 79

	Sb (ppb)	Te (ppb)	Cs (ppm)	Ba (ppm)	La (ppm)	Ce (ppm)
Reference value	296.4 ± 22.9	NA	0.25 ± 0.04	122.6 ± 16.7	4.5 ± 0.3	6.9 ± 0.9
IMC-100 (n=9)	333 ± 11	19 ± 2	0.281 ± 0.007	124 ± 2 [a]	3.97 ± 0.08 [a]	7.8 ± 0.2 [a]
IML-100 (n=5)	282 ± 14	19 ± 3	0.171 ± 0.008	74 ± 1	2.9 ± 0.1	5.8 ± 0.2

	Pr (ppm)	Nd (ppm)	Sm (ppb)	Eu (ppb)	Gd (ppb)	Tb (ppb)
Reference value	NA	3.7 ± 0.6	740 ± 70	148.8 ± 15.3	NA	136.5 ± 14.9
IMC-100 (n=9)	1.01 ± 0.02 [a]	3.89 ± 0.09 [a]	763 ± 32	172 ± 7	719 ± 28	110 ± 4
IML-100 (n=5)	0.69 ± 0.01	2.70 ± 0.05	511 ± 7	99 ± 1	467 ± 8	72 ± 1

	Dy (ppb)	Ho (ppb)	Er (ppb)	Tm (ppb)	Yb (ppb)	Lu (ppb)
Reference value	800 ± 100	NA	NA	NA	400 ± 20	71.3 ± 5.4
IMC-100 (n=9)	677 ± 22	142 ± 6	420 ± 15	62 ± 3	408 ± 21	63 ± 4
IML-100 (n=5)	397 ± 5	81 ± 1	225 ± 4	33.6 ± 0.6	197 ± 2	30.0 ± 0.6

	Hf (ppb)	Ta (ppb)	W (ppb)	Au (ppb)	Tl (ppb)	Pb (ppm)
Reference value	1000 ± 90	84.5 ± 13.4	NA	15.4 ± 6.6	NA	NA
IMC-100 (n=9)	722 ± 29	78 ± 2	210 ± 4 [a]	NM	56 ± 2	73 ± 2
IML-100 (n=5)	47 ± 2	1.5 ± 0.1	136 ± 4	13 ± 9	25 ± 1	66 ± 2

	Bi (ppb)	Th (ppb)	U (ppb)
Reference value	NA	800 ± 100	1190 ± 160
IMC-100 (n=9)	64 ± 2 [a]	826 ± 19	1383 ± 66
IML-100 (n=5)	61 ± 1	586 ± 7	1248 ± 24

Notes: *Reference values from unpublished OGS INAA data (2002).*
[a]Mean concentrations calculated after outlier removal (n=8).
Abbreviations: *NA, not available. NM, not measured.*

CONCLUSIONS

By ashing and digesting samples using the closed-vessel digestion method routinely applied to lithogeochemical samples, elements requiring hydrofluoric or perchloric acid to bring them into or stabilize them in the solution appear to be quantitatively recovered, with accurate results achieved for a wide range of trace elements with concentrations that range from a few parts per billion (ng/g, e.g., Be, Th, U and the HREE) to tens or hundreds of parts per million (µg/g, e.g., Ba, Pb and Sr) in the dried samples.

For analytes that are easily extracted from the ashed samples, including the alkali elements (Ba, Cs, Rb and Sr), base metals (Co, Cu, Mo, Ni, Pb and Zn), LREE (La, Ce, Pr and Nd) and select semimetals and transition metals (e.g., Cd, Bi, In, Sb, V and W), a simpler aqua regia extraction can achieve similar recoveries to the closed-vessel technique. However, for beryllium, chromium, gallium, the HFSE, lithium, the HREE, scandium, tin, tellurium, thallium and yttrium, aqua regia extractions show incomplete recoveries.

Analysis of vegetation samples by ICP–MS collected over known lithium-cesium-tantalum (LCT) pegmatite mineralization shows strong enrichment in LILE, including lithium, rubidium, cesium and beryllium. The presence of HFSE enrichment has yet to be evaluated.

Further work on other mineralization styles may be merited, to determine possible applications and analytical requirements. A typical analytical package might pair analyses of closed-vessel digested ashed material and aqua regia extracted ashed and unashed material to cover the full spectrum of trace elements including lithophile elements, semimetals, precious metals and mercury.

ACKNOWLEDGMENTS

At all stages of the project, the work was assisted by Geo Labs staff. Thanks go to Matt Eles for his work on drying and milling of the vegetation samples, Glenna Keating and Natalie Chretien for their work to develop methods for sample ashing, and to Jose Pallot and Michelle Moore for their work in solution preparation and analysis.

Thunder Bay RGP staff, Sophie Churchley, Greg Paju, Justin Jonsson, Colleen Kurcinka and Sergio Bautista are recognized for their support in field sampling and providing geological expertise on the project.

REFERENCES

Amyotte, E.G., Kurucz, S.V., Paju, G.F., Jonsson, J.R.B. and Kurcinka, C.E. 2022. Investigation of biogeochemical exploration techniques to aid in the exploration for lithium-cesium-tantalum pegmatite dikes: Project description and preliminary observations; *in* Summary of Field Work and Other Activities, 2022, Ontario Geological Survey, Open File Report 6390, p.31-1 to 31-7.

Burnham, O.M., Hechler, J.H., Semenyna, L. and Schweyer, J. 2002. Mineralogical controls on the determination of trace elements following mixed acid dissolution; *in* Summary of Field Work and Other Activities, 2002, Ontario Geological Survey, Open File Report 6100, p.36-1 to 36-12.

Burnham, O.M. and Schweyer, J. 2004. Trace element analysis of geological samples by ICP–MS at the Geoscience Laboratories: Revised capabilities due to improvements to instrumentation; *in* Summary of Field Work and Other Activities, 2004, Ontario Geological Survey, Open File Report 6145, p.54-1 to 54-20.

Gonzaga Fraga, L., João Silva, J., Teixeira, S., Soares, D., Ferreir, M. and Teixeira, J. 2000. Influence of operating conditions on the thermal behavior and kinetics of pine wood particles using thermogravimetric analysis; Energies, v.13, p.2756-2777.

Roelandts, I. and Gladney, E.S. 1998. Consensus values for NIST biological and environmental standard reference materials; Fresenius Journal of Analytical Chemistry, v.360, p.327-338.

Sucharová, J. and Suchara, I. 2006. Determination of 36 elements in plant reference materials with different Si contents by inductively coupled plasma mass spectrometry: Comparison of microwave digestion assisted by three types of digestion mixtures; Analytica Chimica Acta, v.576, p.163-176.

33. Characterization of New In-House Quality Control Materials for Tellurium Analysis: Results of a Round Robin Study



O.M. Burnham[1] and E.C.G. Hastie[2]

[1]Geoscience Laboratories, Ontario Geological Survey
[2]Earth Resources and Geoscience Mapping Section, Ontario Geological Survey

INTRODUCTION

The analysis of matrix-matched reference materials (RMs), either in-house quality control materials or certified interlaboratory reference materials, is a critical component of any geochemical quality assurance program to demonstrate accuracy and precision during analysis, to provide assurance that analyses meets the necessary standards for use, to allow validation and calibration of measurements, and to ensure the metrological traceability and validity of results under ISO Standard 17025 (International Organization for Standardization 2017). Whereas there are many well-characterized reference materials targeted towards the analysis of nonmineralized rock types or the principle economic components of ores[3], for many of the elements on Ontario's Critical Minerals list (Ontario 2022), there are few reference materials that are characterized with suitable concentrations and/or matrices to allow them to be used for quality control on mineralized samples where the critical minerals are present at levels that could make them co-products or by-products during mineral processing. A survey of the characterized concentrations of critical minerals in currently or historically available reference materials from 6 of the main interlaboratory reference material suppliers (African Mineral Industry Standards, AMIS; Canadian Certified Reference Material Program, CCRMP; Chinese National Analysis Centre for Iron and Steel, NACIS; Ore Research and Exploration, OREAS; South African Reference Materials, SARM; and United States Geological Survey, USGS) and/or included within the GeoRem database (Jochum et al. 2005) indicates that, while there is an adequate supply of materials with lithium, niobium, tin, antimony, uranium, vanadium, base metal (e.g., cobalt, copper, nickel, and zinc), chromium and platinum group metal contents above the cut-offs required for the indication of a mineral occurrence in the Ontario Mineral Inventory (OMI) database (Ontario Geological Survey 2023), there are few readily available materials with the cesium, gallium, germanium, scandium and/or zirconium contents needed to meet the OMI cut-offs and only one (the CCRMP copper concentrate CCu-1e with 61.8 ± 4.7 ppm Te) that would meet the 50 ppm cut-off for tellurium (Figure 33.1).

With the increasing interest in tellurium as a co-product or by-product of gold production and the need to validate the analyses of tellurium at elevated concentrations in a wider range of matrices to support the Critical Minerals in Gold Deposits project (Project ON-22-002: *see* Hastie et al., this volume), the OGS Geoscience Laboratories (Geo Labs) and Earth Resources and Geological Mapping Section (ERGMS) collaborated to characterize a suite of in-house quality control materials for tellurium and other major and trace elements of interest to critical mineral exploration through a round-robin study of a new

[3] *In August 2023, GeoRem (http://georem.mpch-mainz.gwdg.de), an online database reference materials of geological and environmental interest, listed almost 60 000 analyses of 3800 reference materials.*

Summary of Field Work and Other Activities, 2023,
Ontario Geological Survey, Open File Report 6405, p.33-1 to 33-18.

© King's Printer for Ontario, 2023

in-house material and 3 existing ones. Samples were circulated to 6 laboratories that offered tellurium and other trace element analyses by a range of methods in mineralized samples and reporting ranges that covered the concentration ranges present in the candidate materials. This report summarizes the initial results of this study, with preliminary assigned concentrations for tellurium and selected trace elements in the 4 materials. Because of analytical difficulties at a participating laboratory, a set of analyses needed to be repeated and the revised data have yet to be reported. Once received, the assigned values may need to be revised.

MATERIAL SELECTION

Existing MRB-Series In-House Reference Materials

The Geo Labs has a long-established program for the preparation, analysis, characterization and use of in-house quality control materials. Many of the earliest of these materials were prepared when the Geo Labs was affiliated with the Minerals Research Branch (part of the Ontario Ministry of Natural Resources) and were created in relatively small quantities (rarely exceeding 100 kg), using representative rock types identified by OGS geologists (MRB-7 to MRB-18 and MRB-29 to MRB-32) augmented with

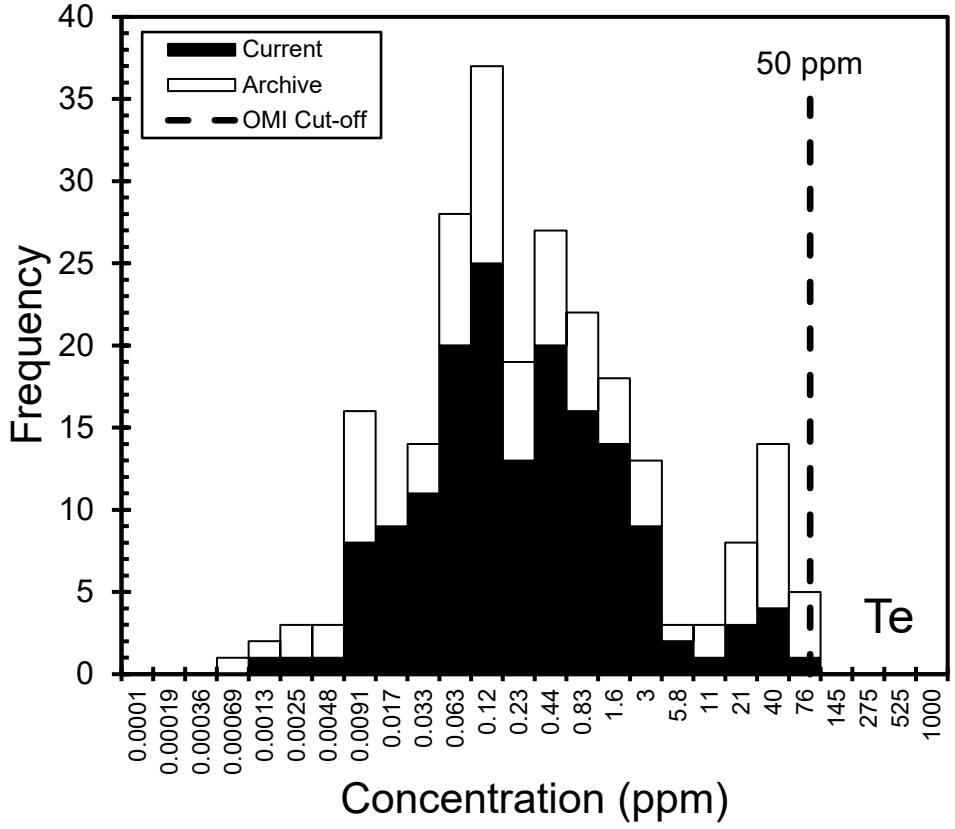


Figure 33.1. Distribution of the tellurium concentrations of 1069 current and archived reference materials available from 6 of the main interlaboratory reference material suppliers (African Mineral Industry Standards, AMIS; Canadian Certified Reference Material Program, CCRMP; Chinese National Analysis Centre for Iron and Steel, NACIS; Ore Research and Exploration, OREAS; South African Reference Materials, SARM; United States Geological Survey, USGS) relative to the cut-off required for the indication of a mineral occurrence in the Ontario Mineral Inventory (OMI) database (Ontario Geological Survey 2023). A single material (a CCRMP copper concentrate) exceeds the 50 ppm Te OMI cut-off.

Table 33.1. Approximate elemental and mineral compositions of candidate reference materials based on X-ray diffraction (XRD), scanning electron microscopy (SEM), and reconnaissance whole-rock analyses.

Material Name	Mass Available (kg)	Description	Mineralogy	Major Element Composition
MRB-25	1.85	Base-metal poor, Ag–Au reference material	**Major Minerals** 70% Quartz 16% Pyrite 9.8% Ankerite + Siderite 2.3% Mica **Minor Minerals** apy, fam, cst, Au, saf, hes, skt, Ag-rich ttr, sph, vol, alt, Bi, tsm, ptz, clr	**Major Elements** ~8 wt % S 700 ppm Σ(Co, Ni, Cu, Zn) 80 ppm Pb **Trace Elements** ~60 ppm Au ~50 ppm Te
MRB-28	3	Base-metal, sulphide-rich, Ag–Au reference material	**Major Minerals** 59% Quartz 16% Pyrite 8.2% Sphalerite 4.3% Mica 2.6% Galena 3.0% Ankerite + Siderite **Minor Minerals** plb-pea, aca, ap, eng-fam, hes, cer, cv, aik, cvl	**Major Elements** ~15 wt % S 0.55 wt % Cu 4.1 wt % Pb 6.8 wt % Zn **Trace Elements** 40 ppm Au 3400 ppm Ag ~320 ppm Te
MRB-34	0.5	Base-metal poor, Au reference material	**Major Minerals** 95% Quartz 2.9% Pyrite 0.23% Chlorite **Minor Minerals** pyh, sd, Au, ccp, rt, sp	**Major Elements** 2.75 wt % S ~725 ppm Σ(Co, Ni, Cu, Zn) 5–10 ppm Pb **Trace Elements** 400 ppm Au ~40 ppm Te
MMTe-1	4.5	Base-metal poor, Au reference material	**Major Minerals** 51% Potassium Feldspar 35% Quartz 6.5% Ankerite + Siderite 4.6% Pyrite ± Molybdenite **Minor Minerals** alt, Au, clv, ptz	**Major Elements** ~2.7 wt % S ~350 ppm Σ(Co, Ni, Cu, Zn) 130 ppm Pb **Trace Elements** 250 ppm Au 360–380 ppm Te

Minor Mineral abbreviations: *aca, acanthite; Ag-rich ttr, silver-rich tetrahedrite; aik, aikinite;* ***alt, altaite****; ap, apatite; apy, arsenopyrite; ccp, chalcopyrite; cer, cerussite;* ***clr, coloradoite****;* ***clv, calaverite****; cst, cassiterite; cv, covellite;* ***cvl, cervelleite****; eng-fam, enargite–famatinite solid solution;* ***hes, hessite****; plb-pea, polybasite–pearceite solid solution; pyh, pyrrhotite;* ***ptz, petzite****; rt, rutile; saf, safflorite; sd, siderite; skt, skutterudite; sp, sphalerite; sph, stephanite;* ***tsm, tsumoite****;* ***vol, volynskite*** *(*modified from *Warr 2021). Text in* **bold** *indicates tellurium-bearing phases.*

Elements: *Ag, silver; Au, gold; Bi, bismuth; Co, cobalt; Cu, copper; Ni, nickel; Pb, lead; S, sulphur; Te, tellurium; Zn, zinc. Σ(Co, Ni, Cu, Zn) = total Co, Cu, Ni and Zn.*

mineralized samples for use during precious metal analysis (MRB-19 to MRB-28 and MRB-34 to MRB-38: Lightfoot et al. 1991; Richardson 1995). Although the mineralized materials were initially only characterized for their platinum group element and/or gold and silver contents, recent reconnaissance analyses toward the improved characterization of the MRB-series reference materials indicated that several were enriched in tellurium, including MRB-25, MRB-28 and MRB-34, and that these materials span a range of chemical and major mineral compositions, with tellurium predominantly contained as a range of silver, lead, bismuth, mercury and/or gold tellurides (Table 33.1), making them suitable candidate materials for further characterization.

New Material (MMTe-1)

To supplement the MRB-series and increase the range of matrices and tellurium concentrations considered in the study, a sample of tellurium-rich gold ore (MMTe-1) was donated from Agnico Eagle Mines Limited Macassa Mine. In contrast to the other candidate reference materials and commercially available tellurium-rich reference materials, such as the CCRMP CCu-1 series copper concentrates, MMTe-1 contains quartz and feldspar, with high gold and tellurium contents but low sulphur, so it better matches the compositions of samples expected to be submitted as part of the Critical Minerals in Gold Deposits project.

MATERIAL PREPARATION

The in-house reference material MMTe-1 was jaw crushed to -10-mesh using a Boyd crusher fitted with chromium steel plates, and ball-milled in alumina in 150 to 200 g batches to -230 mesh (<63 µm). Because the MRB series contained a large fraction of oversized material, with 15 to 40% greater than 63 µm, each material was screened to -230 mesh and the oversize fraction repulverized. After (re)pulverization, all materials were rehomogenized by repeated splitting and blending in 800 to 900 g batches using a T2C Turbula® Schatz geometry mixer before bottling in 35 to 50 g aliquots for final use. A total of 37 jars of MRB-25 (50 g), 61 jars of MRB-28 (50 g), 12 jars of MRB-34 (40 g) and 128 jars of MMTe-1 (35 g) were created.

Homogeneity Testing

Because of the small number of units produced and time constraints on the project, an independent test of homogeneity was not carried out before circulation of the reference materials for characterization. As a result, the uncertainty resulting from sample heterogeneity is combined with the "within-laboratory" uncertainty in the final assessment of the materials.

ROUND-ROBIN CHARACTERIZATION

Analytical Methods

A 50 g aliquot of each of the in-house reference materials (separated during bottling) and 10 g aliquots of 2 traceability materials (the most recent CCRMP copper concentrate CCu-1e and OREAS 603c, a high-sulphidation epithermal gold-silver-copper ore from Ore Research and Exploration) were circulated in a blind round-robin study to 5 commercial laboratories that offered tellurium and other trace element analyses by a range of methods in mineralized samples and reporting ranges that covered the concentration ranges present in the reference materials. Prior to circulation, individual laboratories were consulted to ensure that the optimal methods were chosen.

Sample analysis was based on a one-stage nested design, with each laboratory being asked to perform 5 analyses of each reference material and 3 analyses of each traceability material. To aid analysis, the laboratories were supplied with the expected concentration ranges for tellurium, the enriched base and precious metals (e.g., copper, lead, zinc, silver, and gold), cadmium, antimony, barium and sulphur in all materials. Analyses were primarily carried out by inductively coupled plasma mass spectrometry (ICP–MS) and/or inductively coupled plasma optical emission spectrometry (ICP–OES) after either a hydrofluoric-bearing mixed acid digestion, aqua regia extraction, or sodium peroxide fusion. Additional data were obtained for total carbon and sulphur, base metals, silver, the major element oxides, and selected trace elements at the Geo Labs using method codes IRC-100 (total carbon and sulphur by LECO combustion and infra-red analysis), AAF-104 (cobalt, copper, nickel, lead and zinc by flame atomic absorption spectrometry

(AAS) after HF-$HClO_4$-HNO_3 digestion), AAF-200 (Ag analysis by flame AAS, after HF-HNO_3 digestion), XRF-M01 and XRF-M02 (wavelength dispersive X-ray fluorescence (WD–XRF) on fused glass beads) and XRF-T05 (WD–XRF on pressed powder pellets).

Although the laboratories were requested to report data unscreened for reporting limits and with more precision than usual so that the maximum amount of data could be gathered for each material, this request could not be easily accommodated within the commercial laboratories QC protocols, reducing the number of laboratory means and/or the ability to estimate the within-laboratory precision for several analytes.

Data Reduction

Prior to detailed data reduction, the contributed data were examined to confirm that they met the requirements of the experimental design of the certification program with respect to the number of data contributed and to identify outliers that could be explained for technical reasons, the most obvious of which was identifiable interlaboratory bias. Statistical outliers in the form of single results within an individual laboratory data set were also identified, but not rejected at this stage. For the purposes of the characterization, each data set was considered to have originated from a separate laboratory, even if they were contributed by the same organization or company.

For each analyte, individual laboratory means ($\bar{y}_i$) were initially calculated from the reported data for each of the in-house reference materials and the accompanying traceability materials using Equation 1:

$$\bar{y}_i = \frac{1}{n_i} \sum_{j=1}^{n_i} y_{ij} \qquad (1)$$

where $\bar{y}_i$ is the mean of the j repeat analyses performed by laboratory i, and
n_i is the number of repeat analyses that were performed by laboratory i.

The laboratory means for the traceability materials were then converted to "z-scores" using Equation 2:

$$z = \frac{(\bar{y}_i - y_a)}{\sigma_a} \qquad (2)$$

where y_a is the assigned value for the traceability material, representing the best estimate of the true value of the concentration of the analyte, and
σ_a is the between-laboratory standard deviation assigned to analyte on the certificate of analysis for the traceability material.

Because systematic interlaboratory biases have long been recognized as one of the primary sources of uncertainty in the determination of consensus values for reference materials (e.g., Youden 1960), the calculated z-scores were used to screen the laboratory means for accuracy and consistency before they were combined to produce the compilation means and uncertainties for each analyte. Where a laboratory mean for an analyte in the traceability material of a similar matrix was outside 2 between-laboratory standard deviations of the assigned value (i.e., $|z| > 2$), the mean was rejected on the grounds of method bias and removed from further calculations. For sulphur-poor samples (<10 weight % S: MRB-25, MRB-34, and MMTe-1), acceptance was based on the results obtained for OREAS 603c (3.67 weight % S). For sulphur-rich samples (>10 weight % S: MRB-28), CCu-1e (24 weight % S) was used. The results of this screening are illustrated for tellurium and tin in Figure 33.2.

Because of the high copper and silver contents of both traceability materials (22.9 weight % Cu and 205 ppm Ag in CCu-1e; and 1.21 weight % Cu and 294 ppm Ag in OREAS 603e) and the high zinc content of CCu-1e (3.02 weight % Zn) relative to both the reporting ranges for some or all the commercial laboratories (1 weight % Cu, 100–200 ppm Ag and 0.5–1 weight % Zn) and the concentrations in the in-house reference materials, it was not possible or meaningful to use the data obtained for the traceability materials to verify the accuracy of the contributed data. In such cases, where the concentrations for the in-house reference materials were within the reporting range for the method, the data were provisionally accepted pending the rejection of statistical outliers.

Having screened out laboratory method means showing potential bias based on the results for the traceability materials, the remaining laboratory means were statistically screened for poor precision and/or residual outliers or bias by the application of the Cochran and Grubbs statistical tests, using the appropriate number of degrees of freedom and 5% chance of false rejection. Whereas the Cochran test can flag multiple data sets as possessing statistically poor precision, the Grubbs test only flags the most discrepant mean; if more than a single outlier is present, the test either rejects only the most anomalous value or results in a false negative and the acceptance of all data.

The final assigned concentrations for the reference materials were calculated from the grand mean of accepted laboratory means ($\bar{\bar{y}}$) for each analyte, according to Equation 3:

$$\bar{\bar{y}} = \frac{\sum_{i=1}^{p} n_i \bar{y}_i}{\sum_{i=1}^{p} n_i} \quad (3)$$

where $\bar{y}_i$ is the mean of the data from laboratory *i*,
n_i is the number of repeat analyses performed by laboratory *i*, and
p is the number of laboratory means after the removal of inaccurate and/or potentially inaccurate data.

Because the final data assessment was based on a one-stage nested design, within-laboratory and between-laboratory uncertainties were estimated from one-way analyses of variance (ANOVA) of the accepted laboratory data. Because any particular result (y_{ij}) can be expressed by Equation 4:

$$y_{ij} = \mu + \alpha_i + \varepsilon_{ij} \quad (4)$$

where μ is the grand mean of the laboratory means ($\bar{\bar{y}}$),
α_i is the error because of laboratory *i*, and
ε_{ik} is the measurement error.

The uncertainty in the measurement error, ε_{ik}, (the within-laboratory standard deviation) can be estimated from Equation 5:

$$\sigma_{within} = \sqrt{MS_W} \quad (5)$$

where MS_W is the mean square within parameter of the ANOVA.

And the uncertainty in the error because of laboratory *i*, α_i, (the between-laboratory standard deviation) can be estimated from Equation 6:

$$\sigma_{between} = \sqrt{\frac{MS_B - MS_W}{n_i}} \quad (6)$$

where MS_B is the mean square between parameter of the ANOVA.

The combined standard uncertainty (standard deviation of the mean of the contributing laboratory data, *u*) was calculated from the within- and between-laboratory standard deviations (σ_{withn} and $\sigma_{between}$) according to Equation 7:

$$u = \sqrt{\frac{\sigma^2_{between} + \sigma^2_{within}/n_i}{p}} \quad (7)$$

which was expanded to provide the reference material uncertainty (*U*) at a 95% confidence level, using an expansion factor given by Student's *t* factor at *p-1* degrees of freedom[4]:

$$U = t_{p-1,\,0.95} \cdot u \quad (8)$$

[4] *For an infinite number of analyses, n, the number of degrees of freedom, df = n-1, also approaches infinity, and t_{n-1} approaches 1.96 for 95% confidence, but as the number of analyses decreases, t_n increases to 2.36 for 8 analyses (df = 7) and 4.3 for 3 analyses (df = 2). Because t increases rapidly with decreasing number of analyses, the spread in data for analytes characterized by only a few laboratories must be considerably smaller than that for a widely analyzed analyte if the final uncertainty is to be within an acceptable range.*

During the characterization of the reference materials, the target expanded uncertainties for the final values were set at 0.33 H_a ($U/H_a < 0.33$), where H_a is a fitness-for-purpose criterion derived from the Horwitz function (Horwitz, Kamps and Boyer 1980; Horwitz and Albert 1995):

$$H_a = 0.02 \cdot c^{0.8495} \quad (9)$$

where H_a is the target between-laboratory reproducibility observed at analyte concentration c, with both c and H_a expressed as mass ratios.

This is consistent with the target uncertainties suggested in the IAG "Protocol for the Certification of Geological Reference Materials" (Kane et al. 2003; Kane and Potts 2007).

RESULTS

Table 33.2 to Table 33.5 present the compilation means, expanded uncertainties (U) and within- and between-laboratory standard deviations (σ_{within} and $\sigma_{between}$) obtained by this study for the 4 in-house reference materials. For many of the analytes, the number of accepted laboratory means for each material was low (often between 3 and 5), primarily because of the incomplete recovery of many major and trace elements by aqua regia extraction methods, leading to low recoveries from both the traceability materials and in-house reference materials (e.g., tin in Figure 33.2) and the immediate rejection of the laboratory means. Because a large proportion of the data sets were obtained using aqua regia based methods (6 of the 13 multi-elemental methods used aqua regia extractions for solution preparation), this considerably reduced the number of data sets available. Only arsenic, cobalt, copper, nickel, zinc, selenium, molybdenum, silver, cadmium, indium, tellurium, mercury and bismuth appeared not to show a systematic low bias for aqua regia based analyses compared to either the reference concentrations for the traceability materials and/or the concentrations obtained by other methods.

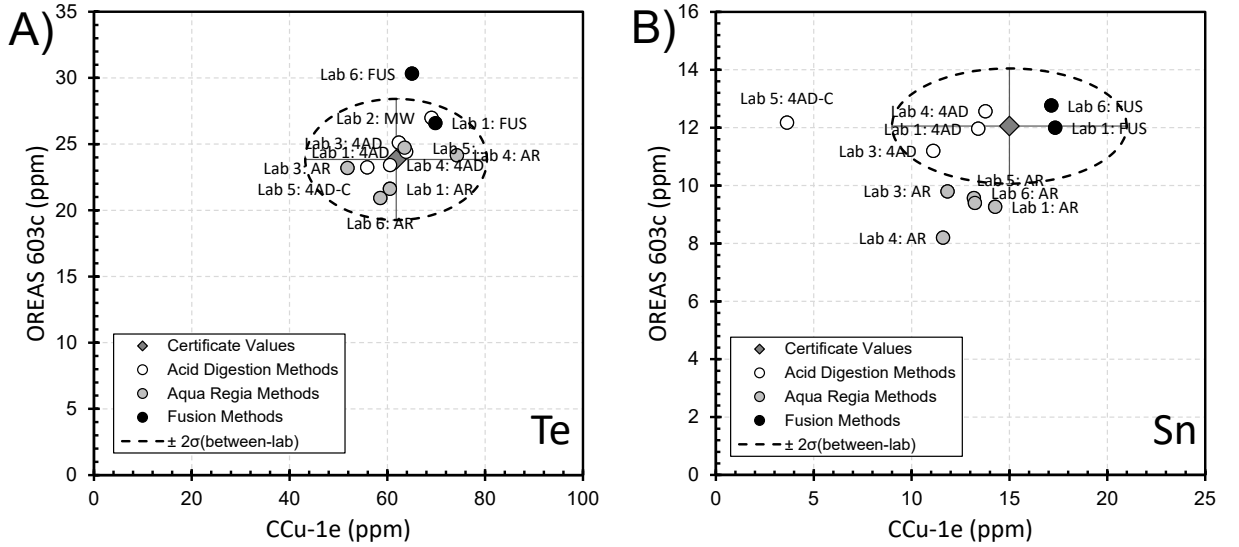


Figure 33.2. Mean concentrations of **A)** tellurium and **B)** tin reported for the traceability materials by laboratories participating in the round-robin characterization of Geo Labs in-house reference materials. Values plotting outside the ellipse (i.e., not within 2 between-laboratory standard deviations of the assigned value) were inferred to exhibit method bias. Unless otherwise stated, where the laboratory mean for an analyte in the matrix-matched traceability material was outside of the acceptable range, the mean was rejected and removed from further calculations. For low sulphur samples (<10 weight % S: MRB-25, MRB-34, and MMTe-1), acceptance was based on the results obtained for OREAS 603c. For high sulphur samples (>10 weight % S: MRB-28), acceptance was based on the results for CCu-1e.

Table 33.2. Assigned values and uncertainties for in-house reference material MMTe-1.

Analyte	Units	Total Data Sets	Accepted Data Sets	Assigned Value	Within-Lab Std. Dev.	Between-Lab Std. Dev.	Expanded Uncertainty at 95% Confidence
Preferred							
Ag	ppm	12	8	16.60	0.51	0.41	0.39
Bi	ppm	10	9	1.974	0.044	0.070	0.056
Co	ppm	14	8	9.04	0.23	0.20	0.18
Cu	ppm	15	10	290.9	4.8	3.8	3.1
Mo	ppm	13	11	1,228	22	30	21
Provisional							
Ni	ppm	14	9	20.17	0.72	0.74	0.62
Indicative							
Ce	ppm	10	4	131.2	3.1	3.6	6.2
Hg	ppm	5	5	1.56	0.05	0.11	0.14
Pb	ppm	15	5	127.1	2.8	5.7	7.2
Sc	ppm	9	4	3.18	0.06	0.21	0.34
Th	ppm	11	4	11.2	0.2	0.7	1.2
U	ppm	11	5	4.11	0.10	0.25	0.32
Y	ppm	12	5	14.1	0.4	0.9	1.1
Yb	ppm	5	4	1.00	0.05	0.07	0.11
Information							
SiO_2	wt %	2	1	70.01	0.06	NA	NA
TiO_2†	wt %	10	3	0.402	0.009	NA	0.010
$Fe_2O_3^{Total}$	wt %	10	4	4.061	0.060	0.045	0.083
Al_2O_3	wt %	10	5	9.0	0.2	0.9	1.2
MnO	wt %	11	6	0.0582	0.0014	0.0035	0.0037
MgO	wt %	10	5	0.803	0.019	0.046	0.058
CaO	wt %	10	5	2.03	0.02	0.12	0.15
Na_2O	wt %	9	4	0.203	0.005	0.012	0.020
K_2O	wt %	10	4	5.94	0.10	0.09	0.15
P_2O_5	wt %	9	4	0.175	0.002	0.008	0.013
S	wt %	8	4	2.73	0.03	0.15	0.24
As	ppm	11	8	4.69	0.42	1.17	0.99
Ba††	ppm	13	3	3355	16	39	99
Be	ppm	8	3	2.14	0.05	0.24	0.60
Cd	ppm	9	7	0.20	0.05	0.13	0.12
Cr†	ppm	13	3	98	6	9	23
Cs	ppm	11	6	2.73	0.15	0.29	0.31
Dy	ppm	5	3	3.09	0.08	0.09	0.24
Er	ppm	5	3	1.27	0.03	0.06	0.15
Eu	ppm	5	3	2.10	0.05	0.11	0.29
Ga	ppm	11	5	17.6	0.5	3.5	4.3
Gd	ppm	5	3	5.72	0.17	0.16	0.44
Ge††	ppm	5	2	2.98	0.24	NA	0.96
Hf†	ppm	9	2	5.07	0.04	0.09	0.87
Ho	ppm	5	4	0.493	0.037	0.049	0.083

Notes:$Fe_2O_3^{Total}$, total Fe expressed as Fe_2O_3.
†Fusion and closed-vessel digestions only.
††Non-acid based preparation methods only.
***Abbreviation:** NA, not available; Std. Dev., standard deviation.*

Table 33.2, *continued*.

Analyte	Units	Total Data Sets	Accepted Data Sets	Assigned Value	Within-Lab Std. Dev.	Between-Lab Std. Dev.	Expanded Uncertainty at 95% Confidence
Information							
In	ppm	8	8	0.0317	0.0031	0.0086	0.0073
La	ppm	11	3	67.5	1.4	2.7	7.0
Li	ppm	7	3	7.36	0.17	0.38	0.96
Lu	ppm	3	2	0.145	0.009	NA	0.035
Nb	ppm	7	5	6.0	0.3	1.7	2.1
Nd	ppm	5	4	54.6	1.7	2.5	4.2
Pr	ppm	5	2	15.1	0.3	0.2	2.1
Rb	ppm	11	4	175.3	5.3	4.0	7.3
Sb	ppm	11	5	5.5	0.2	0.8	1.0
Se	ppm	8	4	1.32	0.43	0.17	0.41
Sm	ppm	5	3	8.58	0.22	0.31	0.82
Sn	ppm	9	5	1.11	0.04	0.21	0.27
Sr	ppm	13	6	1485	19	72	76
Ta	ppm	7	3	0.24	0.01	0.04	0.11
Tb	ppm	5	3	0.55	0.03	0.15	0.37
Te	ppm	11	10	364	6	31	22
Tl	ppm	11	8	1.09	0.04	0.36	0.30
Tm	ppm	4	2	0.16	0.01	0.01	0.10
V	ppm	13	4	139	3	26	42
W	ppm	10	5	33.2	1.1	7.3	9.1
Zn	ppm	14	10	27.7	1.1	3.6	2.6
Zr†	ppm	11	3	227	3	8	20

Notes: $Fe_2O_3^{Total}$*, total Fe expressed as* Fe_2O_3*.*
†Fusion and closed-vessel digestions only.
††Non-acid based preparation methods only.
Abbreviation: *NA, not available; Std. Dev., standard deviation.*

The loss of data sets was compounded for a number of analytes, where there were clear method biases seen within and between different multi-acid digestion and/or fusion methods that were explicable on technical grounds:

- For titanium, chromium and the high field strength elements, such as zirconium and hafnium, acid digestions in closed-vessels yielded concentrations that were notably higher than those from open-beaker digestions and showed better agreement with data obtained using fusion-based methods or single analyses on pressed powder pellets (Figure 33.3). In such cases, it was inferred that the routine multi-acid digestions failed to digest one or more acid-resistant phases and that the more rigorous preparation methods yielded the best estimates of the materials' compositions. The laboratory means obtained using the routine methods were therefore removed from the calculations, generally leaving 3 or fewer laboratory means from which to calculate consensus values.

Table 33.3. Assigned values and uncertainties for in-house reference material MRB-25.

Analyte	Units	Total Data Sets	Accepted Data Sets	Assigned Value	Within-Lab Std. Dev.	Between-Lab Std. Dev.	Expanded Uncertainty at 95% Confidence
Preferred							
Cd	ppm	11	9	1.206	0.051	0.076	0.061
In	ppm	8	7	0.1011	0.0067	0.0059	0.0061
Provisional							
As	ppm	11	10	784	14	24	18
Co	ppm	14	12	76.9	2.5	2.6	1.8
Cu	ppm	14	13	136.8	3.8	5.1	3.2
Ga	ppm	10	5	4.19	0.15	0.18	0.24
Ni	ppm	14	10	108.0	2.6	5.4	4.0
Indicative							
CaO	wt %	10	5	2.548	0.044	0.018	0.033
Pb	ppm	14	7	988	20	30	29
Rb	ppm	10	4	10.67	0.29	0.44	0.74
Sc	ppm	9	4	8.63	0.20	0.54	0.87
Sr	ppm	12	5	42.4	1.1	1.8	2.3
Zn	ppm	14	11	382	11	22	15
Information							
SiO_2	wt %	2	2	70.2	0.4	1.23	11.15
TiO_2†	wt %	7	3	0.238	0.002	0.007	0.017
$Fe_2O_3^T$	wt %	10	4	12.65	0.14	0.37	0.60
Al_2O_3	wt %	10	5	2.459	0.043	0.050	0.067
MnO	wt %	11	5	0.0817	0.0017	0.0035	0.0044
MgO	wt %	10	5	1.508	0.027	0.034	0.045
Na_2O	wt %	9	4	0.1348	0.0038	0.0028	0.0052
K_2O	wt %	10	5	0.513	0.012	0.015	0.020
P_2O_5	wt %	9	3	0.0560	0.0009	0.0025	0.0062
S	wt %	8	5	7.91	0.13	0.48	0.60
Ag	ppm	11	9	81.4	6.7	NA	2.3
Ba	ppm	13	6	70.4	3.0	3.2	3.7
Be	ppm	4	2	0.170	0.008	0.004	0.047
Bi	ppm	12	12	14.35	1.18	0.78	0.60
Ce	ppm	9	4	3.07	0.42	0.22	0.46
Cr†	ppm	13	4	159	6	19	31
Cs	ppm	8	5	0.132	0.025	0.025	0.034
Dy	ppm	5	4	1.02	0.06	0.27	0.44
Er	ppm	5	2	0.78	0.05	NA	0.21
Eu	ppm	5	3	0.36	0.03	0.05	0.14
Gd	ppm	5	3	0.94	0.04	0.21	0.51
Ge††	ppm	4	1	0.9	0.1	NA	NA
Hf†	ppm	7	1	0.52	0.01	NA	NA
Hg	ppm	4	3	29.5	0.8	0.6	1.8
Ho	ppm	4	3	0.20	0.01	0.09	0.22
La	ppm	8	4	1.22	0.17	0.12	0.23

Notes:$Fe_2O_3^{Total}$, total Fe expressed as Fe_2O_3.
†Fusion and closed-vessel digestions only.
††Non-acid based preparation methods only.
***Abbreviation:** NA, not available; Std. Dev., standard deviation.*

Table 33.3, *continued*.

Analyte	Units	Total Data Sets	Accepted Data Sets	Assigned Value	Within-Lab Std. Dev.	Between-Lab Std. Dev.	Expanded Uncertainty at 95% Confidence
Information							
Li	ppm	7	3	2.93	0.07	0.40	1.00
Lu	ppm	2	2	0.118	0.010	0.002	0.045
Mo	ppm	10	8	0.96	0.72	0.05	0.27
Nb	ppm	6	4	0.35	0.03	0.29	0.46
Nd	ppm	5	3	2.48	0.18	0.14	0.39
Pr	ppm	5	2	0.49	0.09	0.02	0.39
Sb	ppm	12	5	5.01	0.46	0.68	0.88
Se	ppm	9	4	7.6	0.4	0.8	1.3
Sm	ppm	5	3	0.79	0.04	0.08	0.20
Sn	ppm	11	6	12.5	1.2	3.1	3.3
Ta	ppm	5	1	0.043	0.001	NA	NA
Tb	ppm	3	2	0.177	0.008	0.002	0.038
Te	ppm	12	10	51.3	5.1	7.1	5.3
Th	ppm	8	3	0.117	0.028	NA	0.031
Tl	ppm	10	8	0.066	0.006	0.031	0.026
Tm	ppm	3	2	0.10	0.01	0.01	0.11
U	ppm	3	2	0.04	0.00	0.01	0.11
V	ppm	12	5	49.2	1.2	3.4	4.3
W	ppm	7	4	990	31	155	248
Y	ppm	11	5	4.3	0.3	2.1	2.6
Yb	ppm	5	4	0.65	0.07	0.18	0.30
Zr†	ppm	11	3	17.1	0.7	0.8	2.1

Notes: $Fe_2O_3^{Total}$*, total Fe expressed as* Fe_2O_3*.*
†Fusion and closed-vessel digestions only.
††Non-acid based preparation methods only.
Abbreviation: *NA, not available; Std. Dev., standard deviation.*

- In the materials that contain high concentrations of barium in the presence of sulphides (e.g., MMTe-1, MRB-28 and OREAS 603c), all acid-based methods yielded lower values than those using fusion or pressed pellet preparation methods most likely as a result of oxidation of the sulphides and precipitation of insoluble barium sulphate during solution preparation (*see* Figure 33.3). In such cases, it was inferred that acid-based methods failed to quantitatively recover barium and that the non-acid-based methods yielded the best estimates of the materials' compositions. The 3 laboratory means obtained using non-acid-based methods were therefore used for the calculation of consensus values for these materials.
- Although the means from several laboratories and/or methods (including both aqua regia extractions and multi-acid digestions) matched the certified concentrations for germanium by acid digestion in OREAS 603e (0.16 ± 0.09 ppm Ge), leading to their initial acceptance, it is likely that the certified concentrations considerably underestimate the germanium content of the material as a result of volatilization of germanium as a volatile fluoride during the digestions used during the certification round of that material. The 2 laboratory means obtained using a sodium peroxide fusion followed with analysis by ICP–OES or ICP–MS indicate that the concentration of germanium in OREAS 603e might be considerably higher (around 4 ppm Ge: *see* Figure 33.3). Once again, the 3 laboratory means obtained using non-acid-based methods were therefore used for the calculation of consensus values for these materials.

Table 33.4. Assigned values and uncertainties for in-house reference material MRB-28.

Analyte	Units	Total Data Sets	Accepted Data Sets	Assigned Value	Within-Lab Std. Dev.	Between-Lab Std. Dev.	Expanded Uncertainty at 95% Confidence
Preferred							
Co	ppm	13	7	11.24	0.39	0.41	0.41
In	ppm	10	10	3.15	0.11	0.19	0.14
Provisional							
Cd	ppm	12	11	337	7	21	14
Mo	ppm	12	7	7.86	0.39	0.32	0.34
Rb	ppm	10	4	101.1	1.6	2.5	4.1
U	ppm	10	9	57.0	1.1	4.3	3.4
Indicative							
CaO	wt %	10	8	1.189	0.020	0.020	0.018
As	ppm	11	9	560	14	22	18
Cu	ppm	14	10	5417	95	220	160
Information							
SiO_2	wt %	2	2	47.6	0.3	1.0	9.3
TiO_2†	wt %	8	3	0.1024	0.0020	0.0027	0.0070
$Fe_2O_3^T$	wt %	10	7	13.75	0.25	0.38	0.37
Al_2O_3	wt %	10	4	5.15	0.08	0.15	0.25
MnO	wt %	11	5	0.3090	0.0051	0.0063	0.0083
MgO	wt %	10	5	0.620	0.014	0.014	0.019
Na_2O	wt %	6	1	0.061	0.005	NA	NA
K_2O	wt %	10	2	1.57	0.03	0.02	0.23
Ag	ppm	5	2	2100	100	1400	12 900
Ba††	ppm	13	3	6360	73	69	190
Bi	ppm	12	10	430	9	35	25
Cr†	ppm	13	3	77	4	18	44
Ge††	ppm	7	2	3.9	0.3	0.1	1.5
Hf†	ppm	9	1	1.30	0.07	NA	NA
Hg	ppm	4	3	20.2	0.6	0.6	1.6
Ni	ppm	12	7	11.7	0.4	1.3	1.2
Pb	ppm	7	5	41 500	1200	10 200	12 700
Sb	ppm	12	5	404	11	21	27
Sc	ppm	8	2	2.4	0.1	0.4	3.7
Se	ppm	9	4	9.7	0.4	2.5	4.0
Sm	ppm	5	4	2.7	0.2	0.8	1.2
Sn	ppm	11	8	12.7	0.4	1.5	1.3
Sr	ppm	12	8	36	2	29	24
Te	ppm	12	11	339	14	50	34
Tl	ppm	11	8	1.26	0.04	0.56	0.47
V	ppm	11	3	14	0	8	20
W	ppm	10	4	26.9	2.9	1.2	2.8
Y	ppm	11	7	7.3	0.2	1.4	1.3
Zn	ppm	6	3	69 430	1540	1420	3910
Zr†	ppm	11	3	55	4	15	37

Notes:$Fe_2O_3^{Total}$, total Fe expressed as Fe_2O_3.
†Fusion and closed-vessel digestions only.
††Non-acid based preparation methods only.
***Abbreviation:** NA, not available; Std. Dev., standard deviation.*

Table 33.5. Assigned values and uncertainties for in-house reference material MRB-34.

Analyte	Units	Total Data Sets	Accepted Data Sets	Assigned Value	Within-Lab Std. Dev.	Between-Lab Std. Dev.	Expanded Uncertainty at 95% Confidence
Preferred							
Cd	ppm	13	11	5.59	0.15	0.35	0.24
Co	ppm	14	10	43.71	0.95	1.17	0.89
In	ppm	8	7	0.0888	0.0063	0.0032	0.0040
Ni	ppm	13	10	30.10	0.87	1.09	0.83
Provisional							
MnO	wt %	11	4	0.01969	0.00044	NA	0.00031
Rb	ppm	10	4	1.87	0.07	0.07	0.12
Indicative							
MgO	wt %	10	4	0.258	0.004	0.007	0.012
Mo	ppm	11	10	3.04	0.20	0.40	0.29
Sc	ppm	8	4	1.62	0.05	0.10	0.17
Y	ppm	11	5	1.18	0.05	0.09	0.11
Zn	ppm	14	11	350	14	17	12
Information							
SiO2	wt %	2	1	88.27	0.08	NA	NA
TiO_2†	wt %	10	2	0.0494	0.0017	0.0006	0.0088
$Fe_2O_3^T$	wt %	10	4	5.48	0.06	0.12	0.19
Al_2O_3	wt %	10	5	1.005	0.011	0.031	0.039
CaO	wt %	10	5	0.916	0.014	0.032	0.040
Na_2O	wt %	9	4	0.230	0.006	0.007	0.012
K_2O	wt %	10	4	0.0833	0.0039	NA	0.0028
P_2O_5	wt %	7	4	0.00600	0.00103	NA	0.00073
S	wt %	8	4	2.79	0.04	0.14	0.22
Ag	ppm	12	9	20.7	1.9	2.4	2.0
Ba	ppm	10	5	16.7	0.6	2.0	2.5
Be	ppm	2	2	0.07	0.01	0.05	0.42
Ce	ppm	9	3	1.20	0.05	0.08	0.22
Cr†	ppm	12	4	298	9	27	43
Cs	ppm	9	5	0.110	0.003	0.043	0.054
Dy	ppm	4	2	0.206	0.002	0.008	0.071
Er	ppm	5	3	0.128	0.010	0.022	0.057
Eu	ppm	2	2	0.051	0.005	0.005	0.048
Ga	ppm	10	5	1.52	0.09	0.13	0.17
Gd	ppm	5	2	0.200	0.011	NA	0.045
Ge††	ppm	1	1	1.1	0.2	NA	NA
Hf†	ppm	6	1	0.18	0.02	NA	NA
Hg	ppm	5	5	0.39	0.07	0.09	0.12
Ho	ppm	1	1	0.048	0.003	NA	NA
La	ppm	8	4	0.58	0.05	0.06	0.11
Li	ppm	7	3	2.19	0.15	0.29	0.73
Lu	ppm	1	1	0.022	0.002	NA	NA
Nb	ppm	7	4	0.58	0.04	0.13	0.20

Notes:$Fe_2O_3^{Total}$, total Fe expressed as Fe_2O_3.
†Fusion and closed-vessel digestions only.
††Non-acid based preparation methods only.
***Abbreviation:** NA, not available; Std. Dev., standard deviation.*

Table 33.5, *continued*.

Analyte	Units	Total Data Sets	Accepted Data Sets	Assigned Value	Within-Lab Std. Dev.	Between-Lab Std. Dev.	Expanded Uncertainty at 95% Confidence
Information							
Nd	ppm	5	3	0.687	0.056	0.017	0.076
Pb	ppm	11	3	6.0	1.5	NA	1.6
Pr	ppm	4	1	0.159	0.010	NA	NA
Sb	ppm	10	4	0.18	0.09	0.08	0.14
Se	ppm	6	2	1.00	0.05	NA	0.20
Sm	ppm	5	4	0.161	0.035	0.030	0.054
Sr	ppm	11	3	7.56	0.18	0.19	0.51
Ta	ppm	5	2	0.4	0.0	0.4	3.8
Tb	ppm	1	1	0.033	0.002	NA	NA
Te	ppm	12	11	36.2	1.2	4.8	3.3
Th	ppm	7	3	0.0974	0.0038	NA	0.0043
Tl	ppm	3	2	0.012	0.001	0.005	0.049
Tm	ppm	1	1	0.020	0.001	NA	NA
U	ppm	5	4	0.065	0.006	0.022	0.035
V	ppm	11	5	17.8	0.5	1.5	1.9
W	ppm	10	4	6.33	0.14	0.52	0.83
Yb	ppm	4	4	0.134	0.043	NA	0.030
Zr[†]	ppm	9	2	6.0	0.9	0.5	5.6

Notes:$Fe_2O_3^{Total}$, total Fe expressed as Fe_2O_3.
[†]Fusion and closed-vessel digestions only.
[††]Non-acid based preparation methods only.
***Abbreviation:** NA, not available; Std. Dev., standard deviation.*

According to the guidelines set out by ISO Guide 35 (International Organization for Standardization 2006) or the IAG Certification Protocol (Kane et al. 2003; Kane and Potts 2007), certification for an analyte requires at least 15 individual laboratory measurements or 10 results that originate from at least 2 different methods of analysis that are in agreement. Because of the low number of accepted laboratory means for many of the analytes and/or the limited number of methods found to give acceptable values for specific ones, none of the final values presented in Tables 33.2 to 33.5 can be considered to be certified, despite the occasional close agreement between laboratories, and so must be designated a lower status.

When it comes to non-certified values, there is less rigour in the definition of terms. For the purposes of this study, the following designations were used:

- "Preferred" values:
  $p \geq 7$, $u < H_a/3$ (good agreement between many of the laboratories), and $\sigma_{within} < 2H_a/3$ (acceptable repeatability)
- "Provisional" values:
  Similar to Preferred but with fewer accepted data sets ($p = 4 – 6$), poorer between laboratory agreement ($u = H_a/3 - 2H_a/3$), or poorer repeatability ($\sigma_{within} = 2H_a/3 – 3H_a/2$)
- "Indicative" values:
  Similar to Provisional, but with 2 of the 3 criteria poorer than required for Preferred status (i.e., $p = 4 – 6$, $u = H_a/3 - 2H_a/3$, or $\sigma_{within} = 2H_a/3 – 3H_a/2$).
- "Information" values:
  $p < 4$, $u > 2H_a/3$ or $\sigma_{within} > 3H_a/2$.

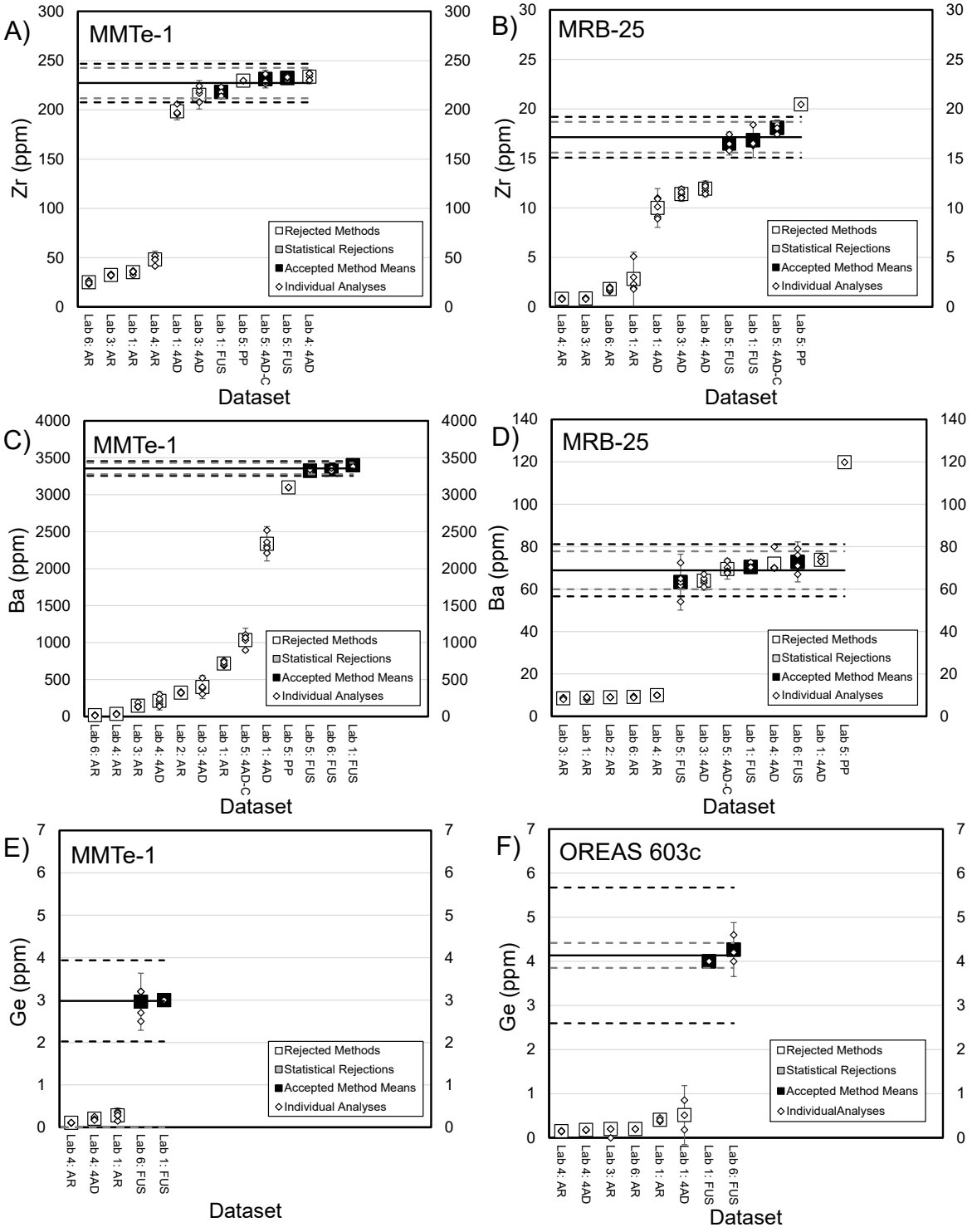


Figure 33.3. Mean concentrations reported for **A)** zirconium in MMTe-1, **B)** zirconium in MRB-25, **C)** barium in MMTe-1, **D)** barium in MRB-25, and **E)** germanium in MMTe-1 and **F)** germanium in OREAS 603c by laboratories participating in the round-robin characterization of Geo Labs in-house reference materials, illustrating selected analytical problems not adequately screened for by the analysis of the traceability materials. Solid dashed lines indicate the assigned values; black dashed lines, the 95% confidence intervals on the assigned values and grey dashed lines, between-laboratory standard deviations on the assigned values. Method codes: 4AD, multi-acid digestions (open-vessel); 4AD-C multi-acid digestions (closed-vessel); AR, aqua regia extractions; FUS, sodium peroxide or lithium metaborate fusions; PP, pressed pellet. Because only a single analysis was performed on a pressed pellet, pressed pellet data were used for information, but not included in the statistical analysis.

Based on these designations, it was possible to assign preferred values to only 2 to 5 analytes, provisional values to only 1 to 5 analytes, and indicative values to only 2 to 8 analytes in each material. All other analytes, including tellurium, were assigned information values. In the case of tellurium, this results from the broad spread in the laboratory means (e.g., $u/H_a = 0.81 – 1.36$: Figure 33.4), despite screening of data for laboratory biases, rather than the lack of data sets (p = 10–11) or poor analytical precision ($\sigma_{within} = 0.53$ for MMTe-1 and 0.69–2.24 for the MRB-series reference materials). Once the final set of laboratory data for tellurium have been received, it is hoped that the data set for tellurium can be refined to reduce the spread in the laboratory means to yield a more definitive value for the element. With additional analyses of the 4 materials by alternate techniques (e.g., metaborate fusion with ICP–MS analysis or more rigorous analysis by WD–XRF), it might also be possible to refine the values for several of the other elements. In the meantime, the values given in Tables 33.1 to 33.4 can be used as interim quality control values during analyses of tellurium and other critical mineral elements at elevated concentrations to support the Critical Minerals in Gold Deposits and other projects conducted by or in collaboration with the OGS.

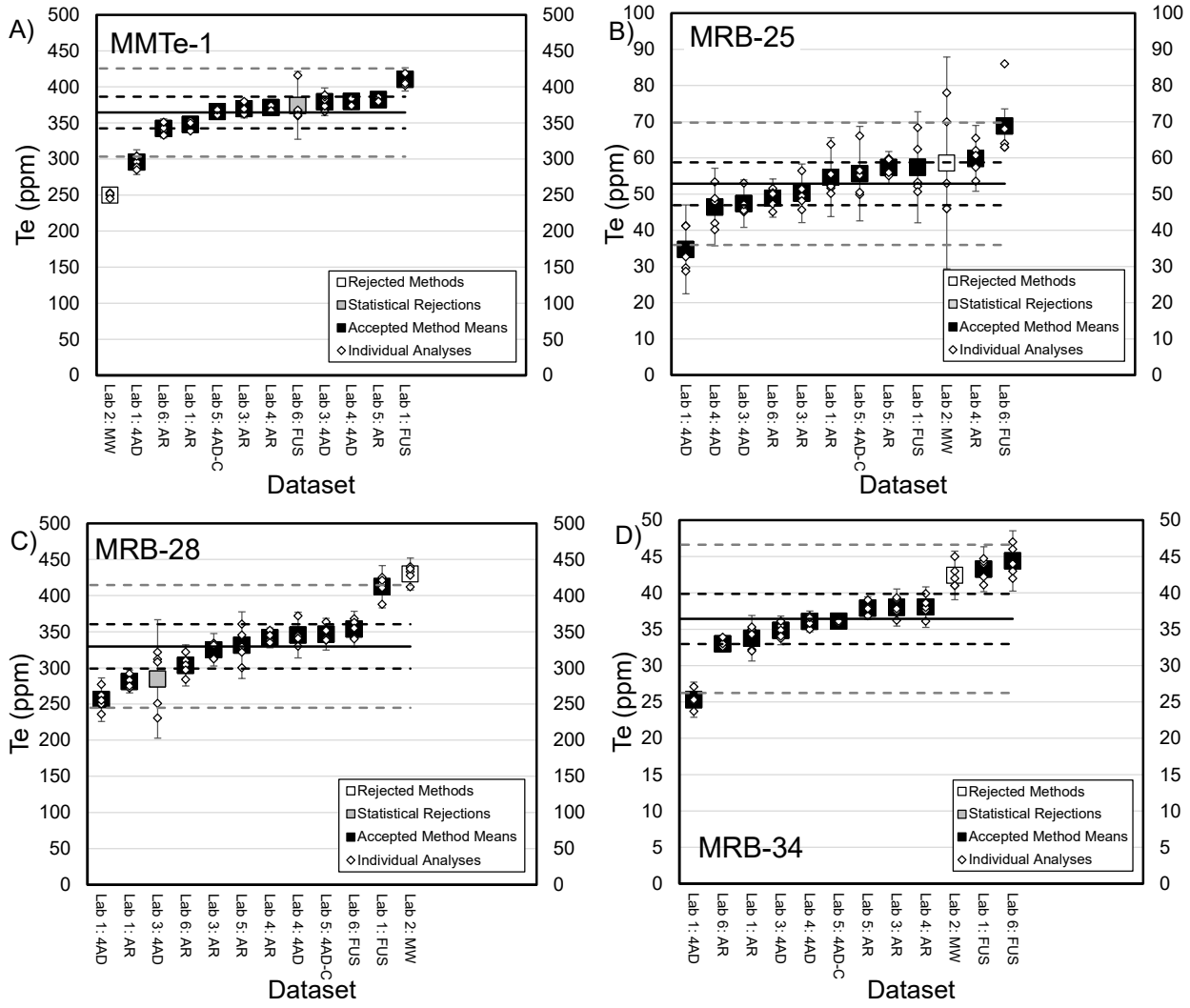


Figure 33.4. Mean concentrations reported for **A)** tellurium in MMTe-1, **B)** tellurium in MRB-25, **C)** tellurium in MRB-28, and **D)** tellurium in MRB-34 by laboratories participating in the round-robin characterization of Geo Labs in-house reference materials. Symbols as in Figure 33.3. Data by microwave digestion (MW) from Lab 2 rejected on analytical grounds (the contribution of sample gold to the gold added as an internal standard during solution preparation). These analyses are being repeated.

SUMMARY

Through a round-robin study, using commercial and government laboratories, preliminary concentrations have been assigned for major and trace elements in 4 in-house reference materials to be used for quality control during analyses of tellurium and other critical mineral elements at elevated concentrations to support the Critical Minerals in Gold Deposits and other projects conducted by or in collaboration with the OGS. The data obtained by this study allow the in-house quality control materials to be used as monitors of for both precision *and* accuracy during internal and external analyses of samples collected as part of the OGS's response to Ontario's Critical Mineral Strategy (Ontario 2022).

Because of analytical difficulties, the data set for tellurium was incomplete at the time of data compilation and only information values could be assigned to the analyte because of poor inter-laboratory agreement. Once the final data are received, it is hoped that the data set for tellurium can be refined to reduce the spread in the laboratory means to yield a more definitive value for the element.

Because the methods applied to the in-house reference materials were chosen to produce the optimal data for tellurium and were dominated by mixed acid digestions, predominantly in open-vessels and aqua regia extractions, they often failed to fully access or report many of the lithophile major and trace elements, leading to poor recoveries and/or method bias. This resulted in a limited number of acceptable laboratory means for many analytes in each material and the assignment of only information values. To better constrain the compositions of the 4 materials, additional analyses will be carried out using alternative techniques and the assigned compositions updated.

ACKNOWLEDGMENTS

This project was assisted by numerous ERGMS and Geo Labs staff including Nathan Guitard for pulverizing and bottling the materials, Natalie Chretien, Glenna Keating, Jose Pallot, Michelle Moore, Fareeda Amirault and Sandra Clarke for assistance in characterizing the materials prior to their selection. Special thanks go to the staff of Agnico Eagle Mines Limited Macassa Mine for donating the starting material for MMTe-1 to the project. Thanks go to the commercial laboratories (ALS Canada Ltd., North Vancouver; Agat Laboratories Ltd., Mississauga; Activation Laboratories Ltd., Ancaster; SGS Canada Inc., Lakefield; Bureau Veritas Mineral Laboratories, Vancouver) for their assistance in method selection and analysis.

REFERENCES

Horwitz, W. and Albert, R. 1995. Precision in analytical measurements: expected values and consequences in geochemical analyses; Fresenius' Journal of Analytical Chemistry, v.351, p.507-511.

Horwitz, W., Kamps, L.R. and Boyer, K.W. 1980. Quality assurance in the analysis of foods for trace constituents; Journal of the Association of Official Analytical Chemists, v.63, p.1344-1354.

International Organization for Standardization 2017. General requirements for the competence of testing and calibration laboratories; International Organization for Standardization, Geneva, Switzerland, ISO Standard 17025, 30p.

——— 2006. Reference materials – General and statistical principles for certification, 3rd ed.; International Organization for Standardization, Geneva, Switzerland, ISO Guide:2006, 64p.

Jochum, K.P., Nohl, U., Herwig, K., Lammel, E., Stoll, B. and Hofmann A.W. 2005. GeoReM: A new geochemical database for reference materials and isotopic standards; Geostandards and Geoanalytical Research, v.29, p.333-338. http://georem.mpch-mainz.gwdg.de [v.35, accessed May 14, 2023].

Kane, J.S. and Potts, P.J. 2007. ISO best practices in reference material certification and use in geoanalysis; Geostandards and Geoanalytical Research, v.31, p.361-378.

Kane, J.S., Potts, P.J., Wiedenbeck, M., Carignan, J. and Wilson, S. 2003. International Association of Geoanalysts' protocol for the certification of geological and environmental reference materials; Geostandards Newsletter: The Journal of Geostandards and Geoanalysis, v.27, p.227-244.

Lightfoot, P.C., Chai, G., Hodge, A.E. and Rowell, D. 1991. An update report on the certification of the OGS in-house standard reference materials; *in* Summary of Field Work and Other Activities, 1991, Ontario Geological Survey, Miscellaneous Paper 157, p.231-233.

Ontario 2022. Ontario's Critical Mineral Strategy: Unlocking the potential to drive economic recovery and prosperity; Ministry of Northern Development, Mines, Natural Resources and Forestry, 53p., www.ontario.ca/page/ontarios-critical-minerals-strategy-2022-2027-unlocking-potential-drive-economic-recovery-prosperity, also available to download: select "Download English PDF". [accessed October 24, 2023]

Ontario Geological Survey 2023. OMI Definitions and cut-off values; document *in* Ontario Mineral Inventory, Ontario Geological Survey, online database, April 2023 update, 9p., www.geologyontario.mndm.gov.on.ca/ogsearth.html#mineral-inventory. [accessed October 24, 2023]

Richardson, J.M. 1995. 1995 Update report on the composition of the Geoscience Laboratories in-house reference materials (MRB Series); *in* Summary of Field Work and Other Activities, 1995, Ontario Geological Survey, Miscellaneous Paper 164, p.198-203.

Warr, L.N. 2021. IMA–CNMNC approved mineral symbols; Mineralogical Magazine, v.85, p.291-320.

Youden, W.J. 1960. The sample, the procedure, and the laboratory; Analytical Chemistry, v.32, p.23A-37A.

34. Summary of Quality Control Data for the Geoscience Laboratories Methods IML-100, IML-101, LOI-2ST, LOI-3ST and LOI-4ST



V.L. Hingst[1]

[1]Geoscience Laboratories, Ontario Geological Survey

INTRODUCTION

This article summarizes the results of analyses for quality control samples for the Geoscience Laboratories' test methods IML-100, IML-101, LOI-2ST, LOI-3ST and LOI-4ST. The IML-100 test method is the inductively coupled plasma mass spectrometric (ICP–MS) analysis of minor and trace elements in soils, humus, and unconsolidated sediments after a modified aqua regia extraction. The IML-101 test method is designed for the ICP–MS analysis of mineralized rocks after a modified aqua regia extraction. The loss on ignition (LOI) test methods are measures of the changes in weight during heating to drive off volatiles and/or remove components by thermal decomposition and/or burning in an oxygen-rich atmosphere. The different LOI test methods represent different temperature programs, where:

- The LOI-2ST test method includes heating under nitrogen gas to 105°C, oxygen to 500°C and total LOI at 500°C;
- The LOI-3ST test method includes heating under nitrogen gas to 105°C, oxygen to 500°C, oxygen to 1000°C and total LOI at 1000°C;
- The LOI-4ST test method includes heating under nitrogen gas to 105°C, oxygen to 371°C, oxygen to 500°C, oxygen to 1000°C and total LOI at 1000°C.

The quality control data for the IML-100, IML-101 and the LOI methods were summarized from September 14, 2018, to August 17, 2023, and capture results obtained since the last Summary of Field Work QC summary in 2018 (Hargreaves 2018).

ACKNOWLEDGMENTS

The author would like to thank Natalie Chretien, Marcus Burnham, Brent Handford, Glenna Keating and Michelle Moore for their help in preparing this article.

REFERENCES

Hargreaves, J.C. 2018. Summary of quality control data for the Geoscience Laboratories methods IML-100, IML-101, IMW-100, LOI-2ST, LOI-3ST and LOI-4ST; *in* Summary of Field Work and Other Activities, 2018, Ontario Geological Survey, Open File Report 6350, p.29-1 to 29-14.

Lynch, J. 1990. Provisional elemental values for eight new geochemical lake sediment and stream sediment reference materials LKSD-1, LKSD-2, LKSD-3, LKSD-4, STSD-1, STSD-2, STSD-3 and STSD-4; Geostandards Newsletter, v.14, p.153-167.

——— 1999. Additional provisional elemental values for LKSD-1, LKSD-2, LKSD-3, LKSD-4, STSD-1, STSD-2, STSD-3 and STSD-4; Geostandards Newsletter, v. 23, p. 251-260.

Summary of Field Work and Other Activities, 2023,
Ontario Geological Survey, Open File Report 6405, p.34-1 to 34-10.

© King's Printer for Ontario, 2023

Table 34.1. Summary of results obtained by the IML-100 test method for routine in-house and certified reference materials from September 14, 2018 to August 17, 2023.

Material	Provider	Description	Ag (ppm)	As (ppm)	Au (ppm)	Ba (ppm)	Be (ppm)
In-house Reference Material							
RAFT-2	In-house	Sediment	1.12 ± 0.04 (147)	85.4 ± 2.6 (147)	0.020 ± 0.009 (147)	102.0 ± 2.6 (147)	0.75 ± 0.04 (147)
Certified Reference Materials							
LKSD-2	CANMET	Lake sediment	0.785 ± 0.027 (39)	9.6 ± 0.4 (39)	0.006 ± 0.022 (39)	215 ± 5 (39)	0.70 ± 0.04 (39)
Certificate			*0.8 ± 0.2*	*9 ± 3*	*NA*	*211 ± 12*	*NA*
LKSD-3	CANMET	Lake sediment	2.64 ± 0.10 (21)	25.8 ± 1.3 (21)	0.0032 ± 0.0006 (21)	172 ± 16 (21)	0.65 ± 0.03 (21)
Certificate			*2.4 ± 0.4*	*23 ± 6*	*NA*	*169 ± 10*	*NA*
LKSD-4	CANMET	Lake sediment	0.229 ± 0.012 (21)	14.2 ± 0.4 (21)	0.0019 ± 0.00030 (21)	136.8 ± 3.0 (21)	0.437 ± 0.020 (21)
Certificate			*0.2 ± 0.1*	*12 ± 3*	*NA*	*135 ± 4*	*NA*
STSD-1	CANMET	Stream sediment	0.316 ± 0.012 (9)	20.0 ± 0.5 (9)	0.006 ± 0.005 (9)	278 ± 4 (9)	0.427 ± 0.028 (9)
Certificate			*0.3 ± 0.1*	*17 ± 5*	*NA*	*261 ± 9*	*NA*
STSD-3	CANMET	Stream sediment	0.427 ± 0.007 (4)	25.4 ± 0.5 (4)	0.0030 ± 0.0008 (4)	680 ± 8 (4)	1.15 ± 0.04 (4)
Certificate			*0.4 ± 0.1*	*22 ± 6*	*NA*	*692 ± 62*	*NA*

Material	Provider	Description	Bi (ppm)	Cd (ppm)	Ce (ppm)	Co (ppm)	Cr (ppm)
In-house Reference Material							
RAFT-2	In-house	Sediment	4.88 ± 0.16 (147)	2.43 ± 0.06 (147)	45.2 ± 1.1 (147)	40.4 ± 1.3 (147)	36.1 ± 1.2 (147)
Certified Reference Materials							
LKSD-2	CANMET	Lake sediment	1.12 ± 0.05 (39)	0.821 ± 0.023 (39)	97.7 ± 2.4 (39)	15.1 ± 0.4 (39)	28.7 ± 1.0 (39)
Certificate			*NA*	*0.8 ± 0.2*	*NA*	*17 ± 1*	*29 ± 3*
LKSD-3	CANMET	Lake sediment	3.0 ± 0.3 (21)	0.529 ± 0.015 (21)	80.2 ± 2.3 (21)	28.4 ± 0.9 (21)	52.3 ± 1.7 (21)
Certificate			*NA*	*0.6 ± 0.3*	*NA*	*30 ± 2*	*51 ± 5*
LKSD-4	CANMET	Lake sediment	0.494 ± 0.022 (21)	1.99 ± 0.04 (21)	39.8 ± 1.1 (21)	9.13 ± 0.22 (21)	20.1 ± 0.8 (21)
Certificate			*NA*	*1.9 ± 0.5*	*NA*	*11 ± 1*	*21 ± 2*
STSD-1	CANMET	Stream sediment	0.439 ± 0.028 (9)	0.900 ± 0.016 (9)	36.6 ± 1.2 (9)	14.1 ± 0.4 (9)	28.2 ± 0.8 (9)
Certificate			*NA*	*0.8 ± 0.2*	*NA*	*14 ± 2*	*28 ± 3*
STSD-3	CANMET	Stream sediment	1.330 ± 0.011 (4)	1.120 ± 0.006 (4)	41.8 ± 1.0 (4)	13.6 ± 0.4 (4)	33.3 ± 0.9 (4)
Certificate			*NA*	*1.0 ± 0.2*	*NA*	*14 ± 1*	*34 ± 6*

Notes: *Compiled data given as mean ± 1 standard deviation of results (number of measurements). Certificate value is average ± 1 standard deviation of the mean; Certificate values are provisional and for partial extraction (concentrated HNO_3-concentrated HCl; Lynch 1999).*
Abbreviations: *CANMET = Canada Centre for Mineral and Energy Technology; NA = not available.*

Table 34.1, ***continued.***

Material	Provider	Description	Cs(ppm)	Cu (ppm)	Dy (ppm)	Er (ppm)	Eu (ppm)
In-house Reference Material							
RAFT-2	In-house	Sediment	0.79 ± 0.05 (147)	602 ± 17 (147)	2.73 ± 0.08 (147)	1.42 ± 0.05 (147)	0.924 ± 0.024 (147)
Certified Reference Materials							
LKSD-2	CANMET	Lake sediment	1.43 ± 0.08 (39)	33.8 ± 1.2 (39)	5.28 ± 0.16 (39)	2.91 ± 0.10 (39)	1.36 ± 0.04 (39)
Certificate			*NA*	*36 ± 3*	*NA*	*NA*	*NA*
LKSD-3	CANMET	Lake sediment	1.49 ± 0.08 (21)	32.4 ± 1.3 (21)	3.59 ± 0.12 (21)	1.91 ± 0.07 (21)	0.995 ± 0.027 (21)
Certificate			*NA*	*34 ± 3*	*NA*	*NA*	*NA*
LKSD-4	CANMET	Lake sediment	1.08 ± 0.05 (21)	29.3 ± 0.8 (21)	2.96 ± 0.07 (21)	1.69 ± 0.04 (21)	0.899 ± 0.028 (21)
Certificate			*NA*	*30 ± 3*	*NA*	*NA*	*NA*
STSD-1	CANMET	Stream sediment	1.17 ± 0.07 (9)	34.7 ± 0.8 (9)	3.94 ± 0.13 (9)	2.21 ± 0.06 (9)	1.05 ± 0.03 (9)
Certificate			*NA*	*36 ± 2*	*NA*	*NA*	*NA*
STSD-3	CANMET	Stream sediment	2.93 ± 0.06 (4)	35.6 ± 0.9 (4)	3.45 ± 0.04 (4)	1.91 ± 0.04 (4)	1.016 ± 0.015 (4)
Certificate			*NA*	*38 ± 2*	*NA*	*NA*	*NA*

Material	Provider	Description	Ga (ppm)	Gd (ppm)	Hf (ppm)	Hg (ppm)	Ho (ppm)
In-house Reference Material							
RAFT-2	In-house	Sediment	4.91 ± 0.17 (39)	7.11 ± 0.22 (39)	0.061 ± 0.008 (39)	0.157 ± 0.007 (39)	1.023 ± 0.030 (39)
Certified Reference Materials							
LKSD-2	CANMET	Lake sediment	5.00 ± 0.20 (14)	7.08 ± 0.19 (14)	0.064 ± 0.007 (14)	0.161 ± 0.008 (14)	1.03 ± 0.04 (14)
Certificate			*NA*	*NA*	*NA*	*0.16 ± 0.019*	*NA*
LKSD-3	CANMET	Lake sediment	5.88 ± 0.19 (21)	5.01 ± 0.16 (21)	0.088 ± 0.008 (21)	0.283 ± 0.007 (21)	0.680 ± 0.024 (21)
Certificate			*NA*	*NA*	*NA*	*0.29 ± 0.036*	*NA*
LKSD-4	CANMET	Lake sediment	4.08 ± 0.11 (21)	3.65 ± 0.08 (21)	0.018 ± 0.004 (21)	0.180 ± 0.006 (21)	0.585 ± 0.015 (21)
Certificate			*NA*	*NA*	*NA*	*NA*	*NA*
STSD-1	CANMET	Stream sediment	3.82 ± 0.14 (9)	4.85 ± 0.10 (9)	0.015 ± 0.003 (9)	0.1111 ± 0.0026 (9)	0.772 ± 0.023 (9)
Certificate			*NA*	*NA*	*NA*	*0.110*	*NA*
STSD-3	CANMET	Stream sediment	5.15 ± 0.12 (4)	4.28 ± 0.05 (4)	0.0127 ± 0.0017 (4)	0.298 ± 0.008 (4)	0.667 ± 0.006 (4)
Certificate			*NA*	*NA*	*NA*	*0.09*	*NA*

Notes: *Compiled data given as mean ± 1 standard deviation of results (number of measurements). Certificate value is average ± 1 standard deviation of the mean; Certificate values are provisional and for partial extraction (concentrated HNO_3-concentrated HCl; Lynch 1999).*
Abbreviations: *CANMET = Canada Centre for Mineral and Energy Technology; NA = not available.*

Table 34.1, ***continued.***

Material	Provider	Description	In (ppm)	Ir (ppm)	La (ppm)	Li (ppm)	Lu (ppm)
In-house Reference Material							
RAFT-2	In-house	Sediment	0.0982 ± 0.0025 (147)	0.0030 ± 0.0003 (146)	29.7 ± 0.8 (147)	7.9 ± 0.5 (147)	0.170 ± 0.006 (147)
Certified Reference Materials							
LKSD-2	CANMET	Lake sediment	0.0598 ± 0.0015 (39)	< 0.0006 (39)	56.4 ± 1.4 (39)	15.4 ± 0.9 (39)	0.386 ± 0.013 (39)
Certificate			*NA*	*NA*	*NA*	*NA*	*NA*
LKSD-3	CANMET	Lake sediment	0.0440 ± 0.0013 (21)	< 0.0006 (22)	42.5 ± 1.2 (21)	20.9 ± 1.0 (21)	0.249 ± 0.009 (21)
Certificate			*NA*	*NA*	*NA*	*NA*	*NA*
LKSD-4	CANMET	Lake sediment	0.0524 ± 0.0014 (21)	< 0.0006 (21)	21.1 ± 0.5 (21)	9.2 ± 0.4 (21)	0.235 ± 0.007 (21)
Certificate			*NA*	*NA*	*NA*	*NA*	*NA*
STSD-1	CANMET	Stream sediment	0.0411 ± 0.0009 (9)	< 0.0006 (9)	21.6 ± 0.6 (9)	8.7 ± 0.5 (9)	0.310 ± 0.010 (9)
Certificate			*NA*	*NA*	*NA*	*NA*	*NA*
STSD-3	CANMET	Stream sediment	0.0482 ± 0.0004 (4)	< 0.0006 (4)	24.4 ± 0.7 (4)	18.8 ± 1.0 (4)	0.2566 ± 0.0007 (4)
Certificate			*NA*	*NA*	*NA*	*NA*	*NA*

Material	Provider	Description	Mo (ppm)	Nb (ppm)	Nd (ppm)	Ni (ppm)	Pb (ppm)
In-house Reference Material							
RAFT-2	In-house	Sediment	3.15 ± 0.07 (147)	0.55 ± 0.03 (147)	26.8 ± 0.6 (147)	863 ± 33 (147)	96.8 ± 2.9 (147)
Certified Reference Materials							
LKSD-2	CANMET	Lake sediment	1.17 ± 0.06 (39)	1.50 ± 0.09 (39)	52.5 ± 1.2 (39)	23.7 ± 0.7 (39)	38.3 ± 1.9 (39)
Certificate			*2 ± 0.7*	*NA*	*NA*	*23 ± 3*	*40 ± 7*
LKSD-3	CANMET	Lake sediment	1.03 ± 0.05 (21)	2.22 ± 0.11 (21)	39.1 ± 1.1 (21)	46.2 ± 1.3 (21)	24.4 ± 1.5 (21)
Certificate			*2 ± 0.9*	*NA*	*NA*	*44 ± 4*	*26 ± 5*
LKSD-4	CANMET	Lake sediment	1.74 ± 0.03 (21)	1.15 ± 0.09 (21)	22.4 ± 0.6 (21)	32.1 ± 1.0 (21)	90.7 ± 1.8 (21)
Certificate			*2 ± 0.6*	*NA*	*NA*	*32 ± 5*	*93 ± 8*
STSD-1	CANMET	Stream sediment	1.05 ± 0.05 (9)	0.65 ± 0.04 (9)	25.1 ± 0.7 (9)	20.9 ± 0.5 (9)	33.3 ± 1.3 (9)
Certificate			*2 ± 0.5*	*NA*	*NA*	*18 ± 3*	*34 ± 4*
STSD-3	CANMET	Stream sediment	6.13 ± 0.14 (4)	1.122 ± 0.020 (4)	24.43 ± 0.10 (4)	28.1 ± 0.4 (4)	40.1 ± 0.8 (4)
Certificate			*7 ± 2*	*NA*	*NA*	*25 ± 3*	*39 ± 5*

Notes: *Compiled data given as mean ± 1 standard deviation of results (number of measurements). Certificate value is average ± 1 standard deviation of the mean; Certificate values are provisional and for partial extraction (concentrated HNO_3-concentrated HCl; Lynch 1999).*
Abbreviations: *CANMET = Canada Centre for Mineral and Energy Technology; NA = not available.*

Table 34.1, ***continued.***

Material	Provider	Description	Pd (ppm)	Pr (ppm)	Pt (ppm)	Rb (ppm)	Rh (ppm)
In-house Reference Material							
RAFT-2	In-house	Sediment	0.050 ± 0.022 (146)	7.08 ± 0.16 (147)	0.038 ± 0.016 (147)	8.3 ± 0.5 (147)	0.0079 ± 0.0020 (146)
Certified Reference Materials							
LKSD-2	CANMET	Lake sediment	< 0.004 (39)	14.0 ± 0.3 (39)	< 0.0013 (39)	18.1 ± 0.9 (39)	< 0.006 (39)
Certificate			*NA*	*NA*	*NA*	*NA*	*NA*
LKSD-3	CANMET	Lake sediment	< 0.004 (21)	10.45 ± 0.28 (21)	< 0.0013 (21)	25.9 ± 0.9 (21)	< 0.006 (21)
Certificate			*NA*	*NA*	*NA*	*NA*	*NA*
LKSD-4	CANMET	Lake sediment	< 0.004 (21)	5.63 ± 0.13 (21)	< 0.0013 (21)	10.3 ± 0.4 (21)	< 0.006 (21)
Certificate			*NA*	*NA*	*NA*	*NA*	*NA*
STSD-1	CANMET	Stream sediment	< 0.004 (5)	6.15 ± 0.17 (9)	< 0.0013 (5)	8.3 ± 0.3 (9)	< 0.006 (5)
Certificate			*NA*	*NA*	*NA*	*NA*	*NA*
STSD-3	CANMET	Stream sediment	< 0.004 (4)	6.24 ± 0.06 (4)	< 0.0013 (4)	16.4 ± 0.5 (4)	< 0.006 (4)
Certificate			*NA*	*NA*	*NA*	*NA*	*NA*

Material	Provider	Description	Sb (ppm)	Sc (ppm)	Se (ppm)	Sm (ppm)	Sn (ppm)
In-house Reference Material							
RAFT-2	In-house	Sediment	1.30 ± 0.05 (147)	3.24 ± 0.21 (147)	7.7 ± 0.4 (147)	4.80 ± 0.14 (147)	2.98 ± 0.06 (147)
Certified Reference Materials							
LKSD-2	CANMET	Lake sediment	0.68 ± 0.04 (39)	6.0 ± 0.3 (39)	0.98 ± 0.15 (39)	9.33 ± 0.24 (39)	1.37 ± 0.04 (39)
Certificate			*1.2 ± 0.5*	*NA*	*NA*	*NA*	*NA*
LKSD-3	CANMET	Lake sediment	0.94 ± 0.04 (21)	6.40 ± 0.21 (21)	0.85 ± 0.13 (21)	6.75 ± 0.19 (21)	1.15 ± 0.04 (21)
Certificate			*1.4 ± 0.5*	*NA*	*NA*	*NA*	*NA*
LKSD-4	CANMET	Lake sediment	1.22 ± 0.06 (21)	3.96 ± 0.19 (21)	2.16 ± 0.09 (21)	4.24 ± 0.11 (21)	3.24 ± 0.07 (21)
Certificate			*1.5 ± 0.6*	*NA*	*NA*	*NA*	*NA*
STSD-1	CANMET	Stream sediment	2.38 ± 0.09 (9)	4.8 ± 0.4 (9)	1.59 ± 0.04 (9)	5.19 ± 0.15 (9)	1.72 ± 0.19 (9)
Certificate			*2.0 ± 1.0*	*NA*	*NA*	*NA*	*NA*
STSD-3	CANMET	Stream sediment	3.11 ± 0.09 (4)	4.30 ± 0.18 (4)	1.59 ± 0.09 (4)	4.77 ± 0.06 (4)	1.446 ± 0.011 (4)
Certificate			*2.4 ± 1.2*	*NA*	*NA*	*NA*	*NA*

Notes: *Compiled data given as mean ± 1 standard deviation of results (number of measurements). Certificate value is average ± 1 standard deviation of the mean; Certificate values are provisional and for partial extraction (concentrated HNO_3-concentrated HCl; Lynch 1999).*
Abbreviations: *CANMET = Canada Centre for Mineral and Energy Technology; NA = not available.*

Table 34.1, ***continued.***

Material	Provider	Description	Sr (ppm)	Ta (ppm)	Tb (ppm)	Te (ppm)	Th (ppm)
In-house Reference Material							
RAFT-2	In-house	Sediment	21.6 ± 1.0 (147)	0.0018 ± 0.0013 (147)	0.495 ± 0.016 (147)	2.36 ± 0.05 (147)	1.19 ± 0.12 (147)
Certified Reference Materials							
LKSD-2	CANMET	Lake sediment	26.8 ± 1.2 (39)	0.0025 ± 0.0006 (39)	0.938 ± 0.028 (39)	0.059 ± 0.005 (39)	8.7 ± 0.4 (39)
Certificate			*32 ± 6*	*NA*	*NA*	*NA*	*NA*
LKSD-3	CANMET	Lake sediment	27.7 ± 1.4 (21)	0.0026 ± 0.0010 (21)	0.649 ± 0.024 (21)	0.052 ± 0.010 (21)	8.0 ± 0.4 (21)
Certificate			*36 ± 8*	*NA*	*NA*	*NA*	*NA*
LKSD-4	CANMET	Lake sediment	39.6 ± 0.9 (21)	0.0038 ± 0.0018 (21)	0.508 ± 0.012 (21)	0.137 ± 0.005 (21)	1.98 ± 0.09 (21)
Certificate			*41 ± 5*	*NA*	*NA*	*NA*	*NA*
STSD-1	CANMET	Stream sediment	30.0 ± 0.8 (9)	0.0036 ± 0.0007 (9)	0.674 ± 0.025 (9)	0.070 ± 0.004 (9)	0.917 ± 0.031 (9)
Certificate			*28 ± 6*	*NA*	*NA*	*NA*	*NA*
STSD-3	CANMET	Stream sediment	65.2 ± 1.6 (4)	0.0032 ± 0.0005 (4)	0.591 ± 0.009 (4)	0.0692 ± 0.0017 (4)	1.81 ± 0.09 (4)
Certificate			*67 ± 5*	*NA*	*NA*	*NA*	*NA*

Material	Provider	Description	Ti (ppm)	Tl (ppm)	Tm (ppm)	U (ppm)	V (ppm)
In-house Reference Material							
RAFT-2	In-house	Sediment	242 ± 31 (147)	0.270 ± 0.008 (147)	0.192 ± 0.006 (147)	8.37 ± 0.22 (147)	25.7 ± 1.3 (147)
Certified Reference Materials							
LKSD-2	CANMET	Lake sediment	728 ± 57 (39)	0.279 ± 0.007 (39)	0.401 ± 0.014 (39)	6.37 ± 0.17 (39)	45.2 ± 2.0 (39)
Certificate			*1010 ± 166*	*NA*	*NA*	*NA*	*48 ± 10*
LKSD-3	CANMET	Lake sediment	1137 ± 59 (21)	0.280 ± 0.009 (21)	0.262 ± 0.010 (21)	3.67 ± 0.09 (21)	52.8 ± 2.1 (21)
Certificate			*1410 ± 236*	*NA*	*NA*	*NA*	*55 ± 13*
LKSD-4	CANMET	Lake sediment	535 ± 39 (21)	0.412 ± 0.011 (21)	0.240 ± 0.008 (21)	29.8 ± 0.7 (21)	32.4 ± 1.2 (21)
Certificate			*660 ± 86*	*NA*	*NA*	*NA*	*32 ± 10*
STSD-1	CANMET	Stream sediment	360 ± 40 (9)	0.249 ± 0.008 (9)	0.305 ± 0.011 (9)	6.71 ± 0.09 (9)	49.1 ± 1.5 (9)
Certificate			*539 ± 130*	*NA*	*NA*	*NA*	*47 ± 11*
STSD-3	CANMET	Stream sediment	398 ± 17 (4)	0.295 ± 0.011 (4)	0.259 ± 0.003 (4)	8.29 ± 0.15 (4)	56.8 ± 2.3 (4)
Certificate			*614 ± 130*	*NA*	*NA*	*NA*	*61 ± 22*

Notes: *Compiled data given as mean ± 1 standard deviation of results (number of measurements). Certificate value is average ± 1 standard deviation of the mean; Certificate values are provisional and for partial extraction (concentrated HNO_3-concentrated HCl; Lynch 1999).*

Abbreviations: *CANMET = Canada Centre for Mineral and Energy Technology; NA = not available.*

Table 34.1, ***continued.***

Material	Provider	Description	W (ppm)	Y (ppm)	Yb (ppm)	Zn (ppm)	Zr (ppm)
In-house Reference Material							
RAFT-2	In-house	Sediment	0.40 ± 0.04 (147)	14.4 ± 0.3 (147)	1.20 ± 0.04 (147)	117 ± 3 (147)	0.28 ± 0.14 (147)
Certified Reference Materials							
LKSD-2	CANMET	Lake sediment	0.42 ± 0.05 (39)	28.7 ± 0.6 (39)	2.56 ± 0.09 (39)	193 ± 6 (39)	3.44 ± 0.26 (39)
Certificate			*NA*	*NA*	*NA*	*200 ± 6*	*NA*
LKSD-3	CANMET	Lake sediment	0.43 ± 0.20 (21)	19.0 ± 0.5 (21)	1.67 ± 0.05 (21)	137 ± 7 (21)	5.2 ± 0.4 (21)
Certificate			*NA*	*NA*	*NA*	*139 ± 10*	*NA*
LKSD-4	CANMET	Lake sediment	0.25 ± 0.06 (21)	16.9 ± 0.4 (21)	1.56 ± 0.04 (21)	185 ± 4 (21)	0.80 ± 0.10 (21)
Certificate			*NA*	*NA*	*NA*	*189 ± 10*	*NA*
STSD-1	CANMET	Stream sediment	0.32 ± 0.14 (9)	24.1 ± 0.7 (9)	1.98 ± 0.07 (9)	165.2 ± 2.9 (9)	0.54 ± 0.17 (9)
Certificate			*NA*	*NA*	*NA*	*165 ± 8*	*NA*
STSD-3	CANMET	Stream sediment	1.34 ± 0.29 (4)	20.0 ± 0.5 (4)	1.678 ± 0.020 (4)	188 ± 6 (4)	0.61 ± 0.03 (4)
Certificate			*NA*	*NA*	*NA*	*192 ± 11*	*NA*

Notes: *Compiled data given as mean ± 1 standard deviation of results (number of measurements). Certificate value is average ± 1 standard deviation of the mean; Certificate values are provisional and for partial extraction (concentrated HNO_3-concentrated HCl; Lynch 1999).*

Abbreviations: *CANMET = Canada Centre for Mineral and Energy Technology; NA = not available.*

Table 34.2. Summary of results obtained by the IML-101 test method for routine in-house and certified reference materials from September 14, 2018 to August 17, 2023.

Material	Provider	Description	Ag (ppm)	As (ppm)	Au (ppm)	Bi (ppm)	Cd (ppm)
In-house Reference Material							
RAFT-2	In-house	Sediment	1.16 ± 0.09 (545)	83 ± 4 (544)	0.019 ± 0.005 (544)	4.96 ± 0.18 (544)	2.45 ± 0.14 (544)
Certified Reference Materials							
SdAR-H1	IAG	Sediment	84 ± 6 (182)	406 ± 13 (182)	4 ± 4 (182)	5.09 ± 0.15 (182)	25.5 ± 0.6 (182)
Certificate			*76 ± 6**	*396 ± 24**	*NA*	*5.1 ± 0.4**	*25 ± 1**
WPR-1a	CANMET	Peridotite	1.05 ± 0.08 (314)	10.2 ± 1.2 (314)	0.045 ± 0.025 (314)	0.123 ± 0.011 (314)	0.59 ± 0.06 (314)
Certificate			*1.02 ± 0.10*	*9.3 ± 1.1*	*0.05**	*0.122 ± 0.011*	*0.598 ± 0.086*

Material	Provider	Description	Co (ppm)	Cu (ppm)	Hg (ppm)	In (ppm)	Ir (ppm)
In-house Reference Material							
RAFT-2	In-house	Sediment	40.8 ± 1.4 (545)	607 ± 30 (545)	0.176 ± 0.021 (544)	0.100 ± 0.005 (543)	0.0034 ± 0.0010 (544)
Certified Reference Materials							
SdAR-H1	IAG	Sediment	56.2 ± 1.6 (182)	1181 ± 30 (182)	7.32 ± 0.21 (182)	10.01 ± 0.20 (182)	< 0.003 (182)
Certificate			*55.6 ± 1.4*	*1160 ± 20*	*7.3 ± 0.6**	*9.5 ± 0.5**	*NA*
WPR-1a	CANMET	Peridotite	212 ± 13 (314)	2939 ± 187 (314)	0.055 ± 0.012 (314)	0.074 ± 0.005 (313)	0.0041 ± 0.0011 (314)
Certificate			*213 ± 17*	*2990 ± 160*	*0.05**	*0.0899 ± 0.0047***	*0.02**

Material	Provider	Description	Mo (ppm)	Ni (ppm)	Pb (ppm)	Pd (ppm)	Pt (ppm)
In-house Reference Material							
RAFT-2	In-house	Sediment	3.15 ± 0.14 (544)	869 ± 48 (545)	98 ± 4 (545)	0.050 ± 0.010 (544)	0.040 ± 0.022 (544)
Certified Reference Materials							
SdAR-H1	IAG	Sediment	64.1 ± 1.5 (182)	226 ± 6 (182)	3978 ± 98 (182)	0.44 ± 0.04 (182)	0.13 ± 0.07 (182)
Certificate			*64* ± 3	*230* ± 5	*3890* ± 80	*NA*	*NA*
WPR-1a	CANMET	Peridotite	0.79 ± 0.07 (314)	4343 ± 274 (314)	7.3 ± 0.5 (314)	0.63 ± 0.06 (314)	0.26 ± 0.06 (314)
Certificate			*0.9**	*4390 ± 220*	*7.92 ± 0.89*	*0.614 ± 0.025*	*0.452 ± 0.030*

Notes: *Compiled data given as mean ± 1 standard deviation of results (number of measurements). Certificate values are average ± $\sigma_{between\text{-}lab}$.*
Abbreviations: *CANMET = Canada Centre for Mineral and Energy Technology; IAG = International Association of Geoanalysts; NA = not available.*
**Information values.*
***Provisional values.*
****Provisional values based on non-2-acid digestion methods.*

Table 34.2, ***continued.***

Material	Provider	Description	Sb (ppm)	Se (ppm)	Sn (ppm)	Te (ppm)	Tl (ppm)
In-house Reference Material							
RAFT-2	In-house	Sediment	1.31 ± 0.06 (544)	7.5 ± 0.5 (544)	3.06 ± 0.12 (544)	2.35 ± 0.13 (544)	0.274 ± 0.011 (544)
Certified Reference Materials							
SdAR-H1	IAG	Sediment	529 ± 20 (182)	16.1 ± 1.6 (182)	1.7 ± 0.7 (182)	10.09 ± 0.26 (182)	9.73 ± 0.27 (182)
Certificate			*505 ± 27**	*15 ± 3**	*2.9 ± 0.4**	*NA*	*9.5 ± 1**
WPR-1a	CANMET	Peridotite	1.58 ± 0.21 (314)	6.6 ± 0.6 (314)	0.74 ± 0.18 (314)	1.13 ± 0.09 (314)	0.068 ± 0.006 (314)
Certificate			*3.13 ± 0.39*	*7.7 ± 1.0****	*1.16 ± 0.17****	*0.958 ± 0.075****	*0.0752 ± 0.0063***

Material	Provider	Description	Zn (ppm)
In-house Reference Material			
RAFT-2	In-house	Sediment	118 ± 4 (545)
Certified Reference Materials			
SdAR-H1	IAG	Sediment	3889 ± 105 (182)
Certificate			*3680 ± 60*
WPR-1a	CANMET	Peridotite	128 ± 8 (314)
Certificate			*160 ±18*

Notes: *Compiled data given as mean ± 1 standard deviation of results (number of measurements). Certificate values are average ± $\sigma_{between\text{-}lab}$.*
Abbreviations: *CANMET = Canada Centre for Mineral and Energy Technology; IAG = International Association of Geoanalysts; NA = not available.*
**Information values.*
***Provisional values.*
****Provisional values based on non-2-acid digestion methods.*

Table 34.3. Summary of results obtained by the LOI-2ST test method for routine in-house and certified reference materials from September 14, 2018 to August 17, 2023.

Material	Provider	Description	Nitrogen 105°C (wt %)	Oxygen 500°C (wt %)	Total LOI 500°C (wt %)
In-house Reference Material					
RAFT-2	In-house	Sediment	4.8 ± 0.5 (11)	23.93 ± 0.16 (11)	28.5 ± 0.5 (11)
Certified Reference Material					
STSD-1	CANMET	Stream Sediment	4.39 ± 0.24 (7)	24.86 ± 0.21 (7)	29.25 ± 0.23 (7)
Certificate			*NA*	*NA*	*29.7 ± 0.8*

Notes: *Compiled data given as mean ± 1 standard deviation of results (number of measurements).*
Abbreviations: *CANMET = Canada Centre for Mineral and Energy Technology; NA = not available.*

Table 34.4. Summary of results obtained by the LOI-3ST test method for routine in-house and certified reference materials from September 14, 2018 to August 17, 2023.

Material	Provider	Description	Nitrogen 105°C (wt %)	Oxygen 500°C (wt %)	Oxygen 1000°C (wt %)	Total LOI 1000°C (wt %)
In-house Reference Material						
LK-NIP-1	In-house	Diabase	0.177 ± 0.029 (13)	0.25 ± 0.08 (13)	-0.31 ± 0.06 (13)	0.11 ± 0.04 (13)
ODL-1	In-house	Dolomitic Limestone	0.26 ± 0.07 (60)	1.06 ± 0.13 (60)	38.88 ± 0.13 (60)	40.20 ± 0.05 (60)
ORCA-1	In-house	Rhyolite	0.08 ± 0.03 (41)	0.383 ± 0.027 (41)	0.30 ± 0.03 (41)	0.77 ± 0.04 (41)
QS-1	In-house	Calcareous Shale	0.88 ± 0.20 (36)	1.95 ± 0.22 (36)	8.49 ± 0.22 (36)	11.32 ± 0.19 (36)
RAFT-2	In-house	Sediment	4.9 ± 0.5 (64)	24.27 ± 0.17 (64)	1.05 ± 0.08 (64)	30.3 ± 0.4 (64)
RV-1	In-house	Melagabbro	0.14 ± 0.04 (42)	0.04 ± 0.05 (42)	1.96 ± 0.05 (42)	2.14 ± 0.06 (42)
Certified Reference Material						
STSD-1	CANMET	Stream Sediment	4.41 + 0.18 (85)	25.12 + 0.16 (85)	1.16 + 0.08 (85)	30.69 + 0.17 (85)
Certificate				*29.7 ± 0.8†*	*NA*	*31.6**

Notes: *Compiled data given as mean ± 1 standard deviation of results (number of measurements).*
Abbreviations: *CANMET = Canada Centre for Mineral and Energy Technology; NA = not available.*
†Total loss on ignition to 500°C (LOI_{105} + LOI_{500}).
**Provisional value.*

Table 34.5. Summary of results obtained by the LOI-4ST test method for routine in-house and certified reference materials from September 14, 2018 to August 17, 2023.

Material	Provider	Description	Nitrogen 105°C (wt %)	Oxygen 371°C (wt %)	Oxygen 500°C (wt %)	Oxygen 1000°C (wt %)	Total LOI 1000°C (wt %)
In-house Reference Materials							
RAFT-2	In-house	Sediment	5.2 ± 0.4 (20)	22.40 ± 0.28 (20)	1.33 ± 0.18 (20)	1.51 ± 0.06 (20)	30.44 ± 0.29 (20)
RV-1	In-house	Melagabbro	0.15 ± 0.06 (4)	0.157 ± 0.016 (4)	-0.106 ± 0.029 (4)	1.98 ± 0.06 (4)	2.19 ± 0.10 (4)
Certified Reference Materials							
STSD-1	CANMET	Stream Sediment	4.45 + 0.20 (11)	23.0 + 0.4 (11)	1.63 + 0.32 (11)	1.60 + 0.07 (11)	30.69 + 0.19 (11)
Certificate				*29.7 ± 0.8†*		*NA*	*31.6**

Notes: *Compiled data given as mean ± 1 standard deviation of results (number of measurements).*
Abbreviations: *CANMET = Canada Centre for Mineral and Energy Technology; NA = not available.*
†Total loss on ignition to 500 °C = (LOI_{105} + LOI_{371} + LOI_{500}).
**Provisional value.*

35. Revision of the Calibration for Major Element Analysis of Geological Samples by Wavelength Dispersive X-ray Fluorescence at the Geoscience Laboratories



G.L. Keating[1]

[1]Geoscience Laboratories, Ontario Geological Survey

INTRODUCTION

In 2019, the Geoscience Laboratories (Geo Labs) initiated the replacement of the 2 ageing Axios® wavelength dispersive x-ray fluorescence (WD–XRF) spectrometers. As a result, the first instrument was replaced in September 2020 and the second, in March 2021. Both Axios® spectrometers were replaced with Malvern-Panalytical® Zetium® spectrometers equipped with dual detection "cores" that combine wavelength dispersive and energy dispersive systems and allow analysis in either or both modes. The existing WD–XRF analytical application could not be electronically copied to the new spectrometer software, therefore the analytical application had to be manually transferred for the Geo Labs method codes XRF-M01 and XRF-M02 (major and minor element analysis by WD–XRF on fused glass beads) on the spectrometer installed in March 2021.

The transfer of the major element application presented an opportunity to address sample preparation issues and improve corrections for the methods. The new calibrations use the same fundamental parameters algorithms (Willis and Duncan 2008) as were used in previous versions of the application to generate XRF-M01 and XRF-M02 test method results.

BACKGROUND

The primary goal with the purchase and commissioning of the new instruments was to at least match previous performance of the XRF-M01 and XRF-M02 test methods (Keating and Burnham 2012). The secondary goals were to make improvements to sample preparation and overlap corrections.

To improve sample preparation, during fusion, the dilution was changed from 1 part calcined sample with 6 parts flux, a 7× dilution, to 1 part calcined sample with eight 8 parts flux, a 9× dilution. This results in improved dissolution, improved overlap corrections, does not compromise lower reporting limits, and reduces cross contamination issues. No changes were made to associated loss-on-ignition methods; therefore, no re-evaluation was required for these methods.

With any change to a calibration or instrumentation, it is necessary to verify the performance of the methods and update the statistics and reporting limits. This article presents a summary of the work done to transfer the application and generate the new calibrations for the XRF-M01 and XRF-M02 analytical application and to determine the revised figures of merit for these test methods based on those calibrations.

Summary of Field Work and Other Activities, 2023,
Ontario Geological Survey, Open File Report 6405, p.35-1 to 35-7.

© King's Printer for Ontario, 2023

ANALYTICAL WORK

The new analytical application includes both the XRF-M01 and XRF-M02 test methods and it was transferred using the parameters in use by Geo Labs in the previous versions of this analytical application. The same analytes are reported with the new application as were reported with the previous versions of the XRF-M01 and XRF-M02 test methods, for a total of 20 analytes plus losses on ignition at 105 and 1000°C. All the measuring parameters were carefully optimized based on the types of samples received in the past and in anticipated projects.

A total of 103 certified reference materials (CRMs) and 5 synthetic materials were used to calibrate the spectrometer for the XRF-M01 and XRF-M02 application. All reference materials were freshly prepared using the same preparation method and same dilution as those used to prepare samples. The calibration and sample analysis results are initially expressed as "volatile free" (or ignited) values using the spectrometer control software (SuperQ, Malvern-PANalytical 2020). The loss-on-ignition values are then used to recalculate the XRF-M01 and XRF-M02 test methods results so that the sample analytical results are expressed on an "as submitted" basis, accompanied by the loss-on-ignition values (moisture and total loss-on-ignition).

To estimate the lower limit of detection (LLoD) for each analyte, duplicate pairs of samples and reference materials prepared in the Geo Labs were used, analyzed with the new application and the results expressed on an "as submitted" basis, in the same way as routine samples for the XRF-M01 and XRF-M02 test methods. Between March and June, 2022, 282 fused beads (141 duplicate pairs) were analyzed twice, at least 4 weeks apart.

An independent set of CRMs (AGV-2, AL-I, AN-G, BCR-32, BCS-353, BCS-368, BCS-381, BHVO-2, BIR-1A, BXMG-3, DTS-2B, FeR-2, FeR-3, FeR-4, FK-N, GS-N, GSD-11, GSP-2, GSR-2, GSR-3, GTS-2A, GYP-A, IPT-62, JDo-1, JLs-1, MO-7, NIM-P, NIST 69B, NIST-694, OKUM-1, ORCA-1, QS-1, SARM-40, STSD-1, SX67-05, SY-4, TIG-1, UB-N and WMG-1A), that are not included in the calibration regressions and with a wide variety of compositions, were freshly prepared using the same preparation method as that used for samples. These materials were measured multiple times (8 to 20 times each) between March and June 2022, to verify the accuracy and precision of the new application.

METHOD VERIFICATION

The measurement of sample and reference material duplicate pairs were used to estimate the LLoDs. By using duplicate analyses carried out on separate sample aliquots and analyzed on different days at least 4 weeks apart, it was possible to obtain an estimate of the overall "method" uncertainty as a function of concentration for each analyte that includes most of the major sources of variation (including those from sample preparation and within-run or between-run instrumental variations) and from which the method LLoD can be calculated. The sample pairs were chosen to represent a broad range of rock types and, as much as possible, to ensure all sample types were represented over the entire desired range of analysis. The uncertainty and LLoD calculations were based on the seminal article published by Thompson and Howarth (1976).

The data were grouped into 21 groups of 13 sample pairs, each sample pair averaged, and relative difference calculated. For each group, the mean concentration, group median difference, relative difference (%) and expected difference (95% relative uncertainty) were calculated. The LLoDs and optimal precisions that are achievable by the method were estimated from the regression of median differences against the group means. To minimize the effect of the highest concentration groups on the regression and the uncertainty in the calculated LLoDs, only the lowest concentration groups (points

closest to the LLoD) were used to calculate the LLoDs for most elements. In most cases, at least 18 groups (234 sample pairs) were used in the calculation, but as few as 6 groups (78 sample pairs) were used for some elements. A summary of the figures of merit obtained for the revised XRF-M01 and XRF-M02 test methods, based on duplicate analyses, is given in Table 35.1, along with the number of groups used in their estimation.

The CRMs used to verify the accuracy and precision of the XRF-M01 and XRF-M02 test methods were measured multiple times (8 to 20 times each) between March and June 2022, to calculate the new figures of merit. A summary of the figures of merit obtained from the CRM analyses is given in Table 35.2 (XRF-M01) and Table 35.3 (XRF-M02).

A typical set of plots used to evaluate the LLoD statistics, along with accuracy and precision plots for the data, are shown for total Fe expressed as Fe_2O_3 in Figure 35.1.

When the LLoDs for analytes were compared to the previously published LLoDs for the XRF-M01 and XRF-M02 test methods (Keating and Burnham 2012), it was determined that no changes were required to the existing lower reporting limits for the XRF-M01 and XRF-M02 test methods.

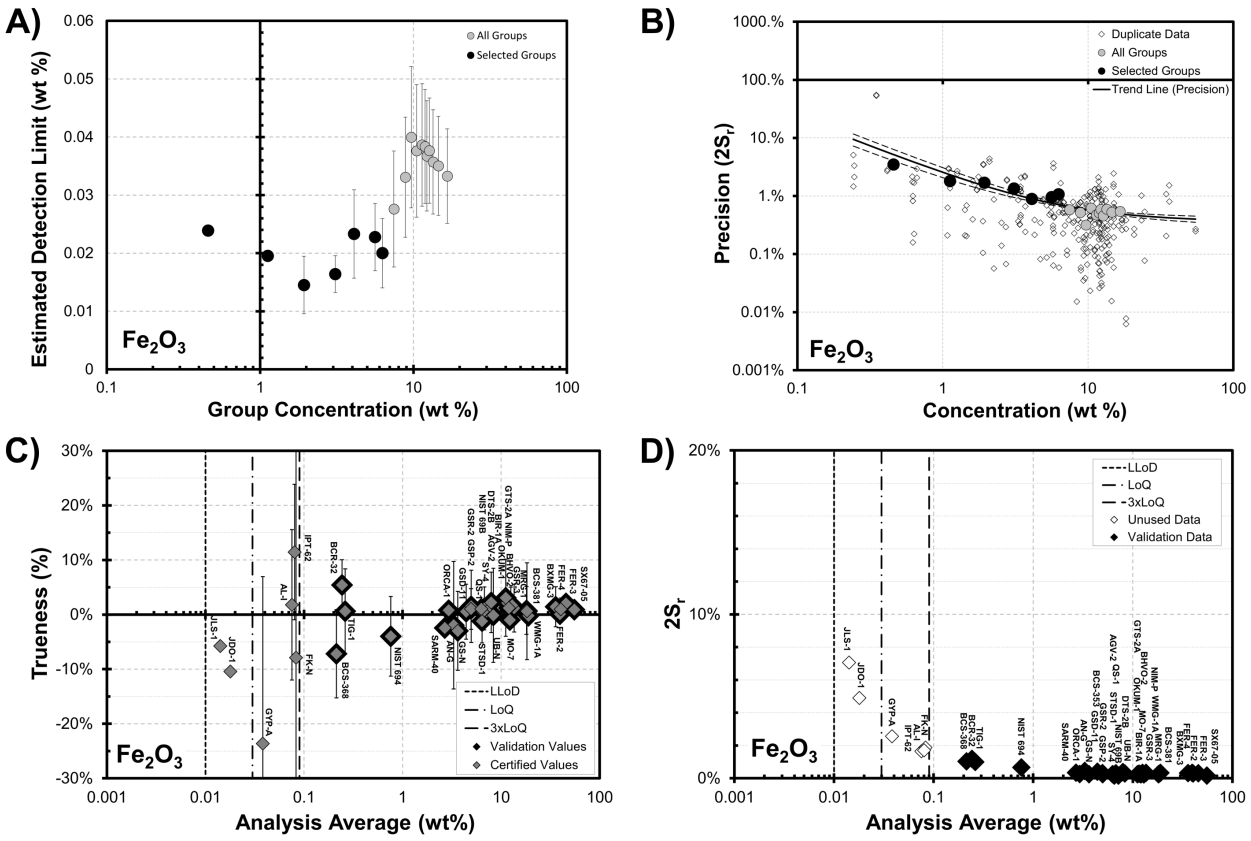


Figure 35.1. Plots summarizing the data used for the estimation of LLoD and optimal precision (Max 2σ) for Fe_2O_3 analyses using test method code XRF-M01. The most reliable estimate of the LLoD and the estimate of the precision of the method was obtained using 7 of the interval concentration groups, which is illustrated in plots **A** and **B**. Plots **C** and **D** show data for the reference materials analyzed by the method. Only those greater than 3× LoQ, but not beyond the scope of the method (i.e., >100 wt %), were used for calculation of accuracy and precision (black diamond symbols). **Abbreviations:** LLoD, lower limit of detection; Max 2 σ, 2σ at maximum concentration; LoQ, limit of quantification.

Table 35.1. Summary of figures of merit obtained for XRF-M01 and XRF-M02 test methods from duplicate analyses.

		2022 LLoD		2022 Precision[a]	
Analyte	**2012 LLoD**	**No. of groups**	**Value ± 2SD**	**No. of groups**	**Value ± 2SD**
XRF-M01 Analytes (wt %)					
Al_2O_3	0.02 ± 0.007	7	0.014 ± 0.011	8	0.4% ± 0.3 %
BaO	0.004 ± 0.0008	10	0.0042 ± 0.0006	16	0.2% ± 2.4 %
CaO	0.006 ± 0.005	9	0.004 ± 0.003	18	0.5% ± 1.0 %
Cr_2O_3	0.002 ± 0.0004	15	0.0015 ± 0.0004	18	0.7% ± 1.8 %
Fe_2O_3	0.01 ± 0.007	7	0.02 ± 0.006	18	0.4% ± 0.8 %
K_2O	0.01 ± 0.0031	8	0.009 ± 0.0026	18	0.2% ± 1.8 %
MgO	0.01 ± 0.004	13	0.0056 ± 0.0021	18	0.3% ± 0.4 %
MnO	0.002 ± 0.0008	17	0.0042 ± 0.0007	18	0.2% ± 0.3 %
Na_2O	0.02 ± 0.0027	15	0.017 ± 0.004	18	0.7% ± 0.6 %
P_2O_5	0.002 ± 0.0005	15	0.00083 ± 0.00014	18	0.8% ± 0.9 %
SiO_2	0.04 ± 0.07	17	0.1 ± 0.17	17	0.3% ± 0.3 %
TiO_2	0.01 ± 0.003	14	0.009 ± 0.004	18	0.2% ± 1.8 %
XRF-M02 Elements (ppm)					
Co	11.2 ± 2.4	16	11.6 ± 1.6	18	0.3% ± 0.6 %
Cu	13.9 ± 2.7	16	16.8 ± 2.9	18	0.9% ± 4.9 %
Ni	8.3 ± 1.1	15	6.8 ± 0.8	18	0.6% ± 2.0 %
Pb	Not available	18	7.6 ± 0.7	18	2.8% ± 2.8 %
Sr	Not available	16	2.87 ± 0.31	18	0.6% ± 0.11 %
V	7.8 ± 0.9	11	11.7 ± 2.1	16	0.4% ± 1.3 %
Zn	5.1 ± 1.2	17	3.5 ± 0.6	18	1.1% ± 0.5 %
Zr	Not available	17	3.2 ± 0.6	18	1.3% ± 0.9 %

[a]***Precision:*** *Optimal 2σ precision achievable by the method based on the regression of the reproducibility of duplicate determinations as a function of concentration.*
Abbreviations: *LLoD, lower limit of detection; SD, standard deviation.*

The upper limits (UL) for the Geo Labs Schedule of Fees and Services (Issue 15) were estimated using a combination of the calibration concentration range and the accuracy test set of CRMs. The highest reasonable concentration value of either the calibration standards or successfully measured reference material was chosen, with a +10% window for extrapolation (Table 35.2 and Table 35.3 provide a summary of the final values).

SUMMARY

The transfer of the XRF-M01 and XRF-M02 analytical application was a learning process with the new spectrometers software, but the fundamental algorithm modules were intact for the required data processing to produce the required calibrations and analytical results. The evaluation process of the new application was informative and provided a detailed analysis of the performance of the test methods and their associated analytical application on the new Zetium® instrument. Based on the analyses used to verify the analytical test methods, several conclusions were reached:

- The new versions of the test methods are accurate over a wide range of concentrations for many elements and yield results that are within accepted published uncertainties for a wide suite of CRMs.
- All figures of merit (LLoD, UL, precision, and accuracy) were confirmed empirically for the total method, including the preparation of samples as fused beads with the new dilution.

Table 35.2. Summary of figures of merit obtained for XRF-M01 test method from the analysis of certified reference materials.

	Al_2O_3	BaO	CaO	Cr_2O_3
Limit of Reporting (LLoR, wt %)	0.02	0.004	0.006	0.002
Limit of Quantification (LoQ, wt %)	0.07	0.013	0.02	0.007
Upper Limit of Validated Range[a] (UL, wt %)	100	1	100	5
Relative Standard Deviation[b] (S_r, %)	0.2	1.5	0.3	1.0
Relative Measurement Precision (%)	± 0.4	± 3	± 0.6	± 2
Method Bias[c] (Weighted Regression, %)	0.6	1.2	-0.3	0.0
Method Trueness[d] (Mean Absolute Trueness, %)	± 1.4	± 3.6	± 1.7	± 5.1

	Fe_2O_3	K_2O	MgO	MnO
Limit of Reporting (LLoR, wt %)	0.01	0.01	0.01	0.002
Limit of Quantification (LoQ, wt %)	0.03	0.03	0.03	0.007
Upper Limit of Validated Range[a] (UL, wt %)	100	20	50	5
Relative Standard Deviation[b] (S_r, %)	0.2	0.2	0.2	1.3
Relative Measurement Precision (%)	± 0.4	± 0.4	± 0.4	± 2.6
Method Bias[c] (Weighted Regression, %)	0.3	-2.9	0.6	1.2
Method Trueness[d] (Mean Absolute Trueness, %)	± 1.6	± 3.6	± 1.7	± 3.0

	Na_2O	P_2O_5	SiO_2	TiO_2
Limit of Reporting (LLoR, wt %)	0.02	0.002	0.04	0.01
Limit of Quantification (LoQ, wt %)	0.07	0.007	0.13	0.03
Upper Limit of Validated Range[a] (UL, wt %)	15	40	100	33
Relative Standard Deviation[b] (S_r, %)	0.3	0.5	0.1	0.3
Relative Measurement Precision (%)	± 0.6	± 1	± 0.2	± 0.6
Method Bias[c] (Weighted Regression, %)	1.7	-3.3	0.4	2.8
Method Trueness[d] (Mean Absolute Trueness, %)	± 2.3	± 3.1	± 0.7	± 2.7

[a]***Validated Range:*** *Defined as the working range in which the method has been validated (LoQ to maximum concentration used in validation statistics or calibration regression). Minimum and maximum values of reference materials used.*

[b]***Relative Standard Deviation (S_r):*** *Defined as the average of the relative standard deviations of all measurements greater than 3 × LoQ (Richardson and Morrison 1995).*

[c]***Method Bias (Weighted Regression):*** *Calculated from the gradient of the linear regression of the measured concentrations against the certified concentrations of the reference materials, with points weighted according to the square root of their variance (Reed 1989; Richardson and Morrison 1995). Bias = (Gradient – 1) × 100 (result in percent).*

[d]***Method Trueness (Mean Absolute Trueness):*** *Defined as the average absolute trueness of the suite of reference materials. Only samples with measured concentrations greater than 3 × LoQ. Absolute Trueness = (│Measured Value – Certified Value│/Certified Value – 1) × 100 (result in percent) (Richardson and Morrison 1995).*

- No changes were made to associated loss-on-ignition methods, therefore no evaluation of the loss-on-ignition methods was required.
- The majority of the analytes yielded LLoD estimates that were the same or better than those obtained using the previous version of the test methods, specifically, Al_2O_3, BaO, CaO, Cr_2O_3, K_2O, MgO, Na_2O, P_2O_5, TiO_2, Co, Ni and Zn. These improvements are the consequence of the greater sensitivity of the new instrument, improved overlap corrections, and difference in dilution (1 g calcined sample with 8 g flux) of the samples, which improves peak resolution.

Table 35.3. Summary of figures of merit obtained for XRF-M02 method from the analysis of certified reference materials.

	Co	Cu	Ni	Pb
Limit of Reporting (LLoR, ppm)	12	60	30	35
Limit of Quantification (LoQ, ppm)	40	200	100	117
Upper Limit of Validated Range[a] (UL, ppm)	5000	15000	15000	6500
Relative Standard Deviation[b] (S_r, %)	2.2	0.5	0.4	0.5
Relative Measurement Precision (%)	± 4.4	± 1	± 0.8	± 1.0
Method Bias[c] (Weighted Regression, %)	-0.1	0.0	0.5	-3.5
Method Trueness[d] (Mean Absolute Trueness, %)	± 8.4	± 0.6	± 1.6	± 3.1

	Sr	V	Zn	Zr
Limit of Reporting (LLoR, ppm)	8	8	40	10
Limit of Quantification (LoQ, ppm)	27	27	133	33
Upper Limit of Validated Range[a] (UL, ppm)	7500	7500	5000	7000
Relative Standard Deviation[b] (S_r, %)	0.4	1.3	0.2	0.5
Relative Measurement Precision (%)	± 0.8	± 2.6	± 0.4	± 1
Method Bias[c] (Weighted Regression, %)	0.0	1.5	0.3	0.6
Method Trueness[d] (Mean Absolute Trueness, %)	± 2.9	± 6.4	± 6.9	± 4.4

[a]***Validated Range:*** *Defined as the working range in which the method has been validated (LoQ to maximum concentration used in validation statistics or calibration regression). Minimum and maximum values of reference materials used.*

[b]***Relative Standard Deviation (S_r):*** *Defined as the average of the relative standard deviations of all measurements greater than 3 × LoQ (Richardson and Morrison 1995).*

[c]***Method Bias (Weighted Regression):*** *Calculated from the gradient of the linear regression of the measured concentrations against the certified concentrations of the reference materials, with points weighted according to the square root of their variance (Reed 1989; Richardson and Morrison 1995). Bias = (Gradient – 1) × 100 (result in percent).*

[d]***Method Trueness (Mean Absolute Trueness):*** *Defined as the average absolute trueness of the suite of reference materials. Only samples with measured concentrations greater than 3 x LoQ. Absolute Trueness = (│Measured Value – Certified Value│/Certified Value – 1) × 100 (result in percent) (Richardson and Morrison 1995).*

- Some of the analytes have slightly degraded LLoDs compared to the previous version of the methods, specifically, Fe_2O_3, MnO, SiO_2, Cu and V. The differences seen with these analytes are reasonable because of the new instrumentation, slight difference in dilution, and lack of suitable materials for evaluation. Few duplicate sample pairs were available or prepared from materials that contained low levels of these analytes. Hence, the LLoDs had to be extrapolated from values that were more than 10 times higher than target or desired values. To compensate for this, the method application counting times have been extended to provide greater precision and accuracy at very low levels. It is anticipated that this will be easier to test and evaluate with the next version of these test methods.
- The previously identified issues with transition metal cross contamination during fusion persists. Consequently, the lower reporting limits for Cu, Ni, Pb and Zn remain at 60 ppm, 30 ppm, 35 ppm, 40 ppm, respectively, despite the estimation of lower values through the duplicate pairs study. The best way to remedy this would be to replace the fluxers, platinum ware and fusion recipes and/or segregate base-metal rich and base-metal poor samples during fusion.

The XRF-M01 and XRF-M02 test methods are as robust on the new instruments using the new application calibration as the previous versions and are fit for purpose. As time and resources permit, improvements or enhancements will be implemented, and evaluation of the methods revisited.

ACKNOWLEDGMENTS

The pandemic situation in 2020–2021 was a major influence on the receipt and installation of the new spectrometers. I would like to thank John Beals, GeoServices Senior Manager, for ensuring that the replacement of the spectrometers continued to move forward and Rick DeBres of Malvern-Panalytical for the extra work and quick response necessary to bring the new spectrometers online as quickly as possible. Natalie Chretien of Geo Labs was key in the preparation of reference materials and samples to complete the verification of the method. Their contribution to the spectrometer replacement allowed me to transfer our methods as quickly as possible.

REFERENCES

Keating, G.L. and Burnham, O.M. 2012. Revision of the calibration for major element analysis of geological samples by wavelength dispersive x-ray fluorescence at the Geoscience Laboratories; *in* Summary of Field Work and Other Activities, 2012, Ontario Geological Survey, Open File Report 6280, p.39-1 to 39-4.

Malvern-PANalytical 2020. PANalytical SuperQ 6.0 manual; Malvern-PANalytical B.V., Almelo, Netherlands.

Reed, B.C. 1989. Linear least-squares fits with errors in both coordinates; American Journal of Physics, v.57, p.642-646.

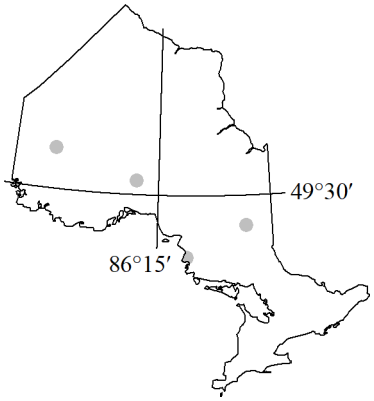
Richardson, J.M. and Morrison, J.L. 1995. Method validation in the Ontario Geoscience Laboratories; Analyst, v.120, p.1519-1526.

Thompson, M. and Howarth, R.J. 1976. Duplicate analysis in geochemical practice. Part I. Theoretical approach and estimation of analytical reproducibility; Analyst, v.101, p.690-698.

Willis, J.P. and Duncan, A.R. 2008. Understanding XRF spectrometry, volume I: Basic concepts and instrumentation; PANalytical B.V., Almelo, Netherlands.

Resident Geologist Program

36. Geochemical Data from the Critical Minerals Mine Waste Sampling Project



G.F. Paju[1]

[1]Resident Geologist Program, Ontario Geological Survey

INTRODUCTION

The Critical Minerals Mine Waste Sampling project was initiated by the Resident Geologist Program (RGP) in 2021 to explore the potential of recovering previously noneconomic and/or undocumented critical minerals from abandoned mine waste sites in Ontario (Azadbakht et al. 2022, p.52-54; Bennett 2022). Additionally, economically viable concentrations of certain minerals have changed with time as high-grade resources have become depleted, resulting in the potential for waste rock to be reprocessed, whether for minerals or building materials.

SAMPLING SITES AND RESULTS

During the 2021 and 2022 field seasons, 5 abandoned mine tailings sites in the Timmins, Sault Ste. Marie, Red Lake and Thunder Bay North RGP districts were sampled (Figure 36.1; Table 36.1). Additional background information about these sites and preliminary results from some of the sites are provided in Bennett (2022). A brief summary for each of the sampled sites is provided. Full details regarding the location of the sample sites at each locality, as well as descriptions of the material sampled, will be provided in the summary publication after the project is complete. Abandoned Mine Identifier (AMIS) data are from Mineral Development and Lands Branch (2022); Ontario Mineral Inventory (formerly Mineral Deposit Inventory (MDI)) numbers are from Ontario Geological Survey (2023b).

All geochemical data reported in this article were obtained from the OGS Geoscience Laboratories in Sudbury using the inductively coupled plasma mass spectrometry (ICP–MS) method designed for soils and unconsolidated materials after a modified aqua regia extraction. Details about the method, including upper reporting limits and lower detection limits for each element, can be found in Ontario Geological Survey (2021, p.18; 2022, p.18). In this article, the threshold grade values for an "Occurrence", as defined by the Ontario Mineral Inventory (OMI) (*see* Ontario Geological Survey 2023a), are used to determine if the results obtained from a mine waste site are of significance (Table 36.2). Complete geochemical results from the 2021 and 2022 sampling programs are provided in Tables 36.3 to 36.7. Geochemical values in bold in Tables 36.6 and 36.7 meet or exceed the "Occurrence" commodity threshold value (*see* Table 36.2) (Ontario Geological Survey 2023a).

Summary of Field Work and Other Activities, 2023,
Ontario Geological Survey, Open File Report 6405, p.36-1 to 36-13.

© King's Printer for Ontario, 2023

Table 36.1. Critical Minerals Mine Waste Sampling project tailings sampling sites details.

Site Name	Resident Geologist District	AMIS Identifier[a]	OMI Number[b]	UTM Zone	Easting[c] (m)	Northing[c] (m)	Commodity[d]
Langmuir Mine	Timmins	10069	MDI42A06SE00006	17	499859	5354094	Ni
Tribag Mine	Sault Ste. Marie	08068	MDI000000001285, MDI41N02SE000034	16	689136	5217719	Cu, Zn, W, Mo
Coppercorp Mine	Sault Ste. Marie	08061	MDI41N02SW00004	16	671177	5209837	Cu, Au, Ag
Tashota-Nipigon Mine	Thunder Bay North	02973	MDI42L04SE00005	16	458055	5543898	Cu, Ag, Bi
South Bay Mine	Red Lake	03892	MDI52N02SE00012	15	522471	5662301	Zn, Cu, Ag, In, Ge, Ga

[a] *Abandoned Mine Identifier (AMIS) data* from *Mineral Development and Lands Branch (2022).*
[b] *Ontario Mineral Inventory (OMI) data* from *Ontario Geological Survey (2023b).*
[c] *Location information provided as Universal Transverse Mercator (UTM) co-ordinates using North American Datum 1983 (NAD83) .*
[d] ***Abbreviations:*** *Ag, silver; Au, gold; Bi, bismuth; Cu, copper; Ga, gallium; Ge, germanium; In, indium; Mo, molybdenum; Ni, nickel; Zn, zinc; W, tungsten.*

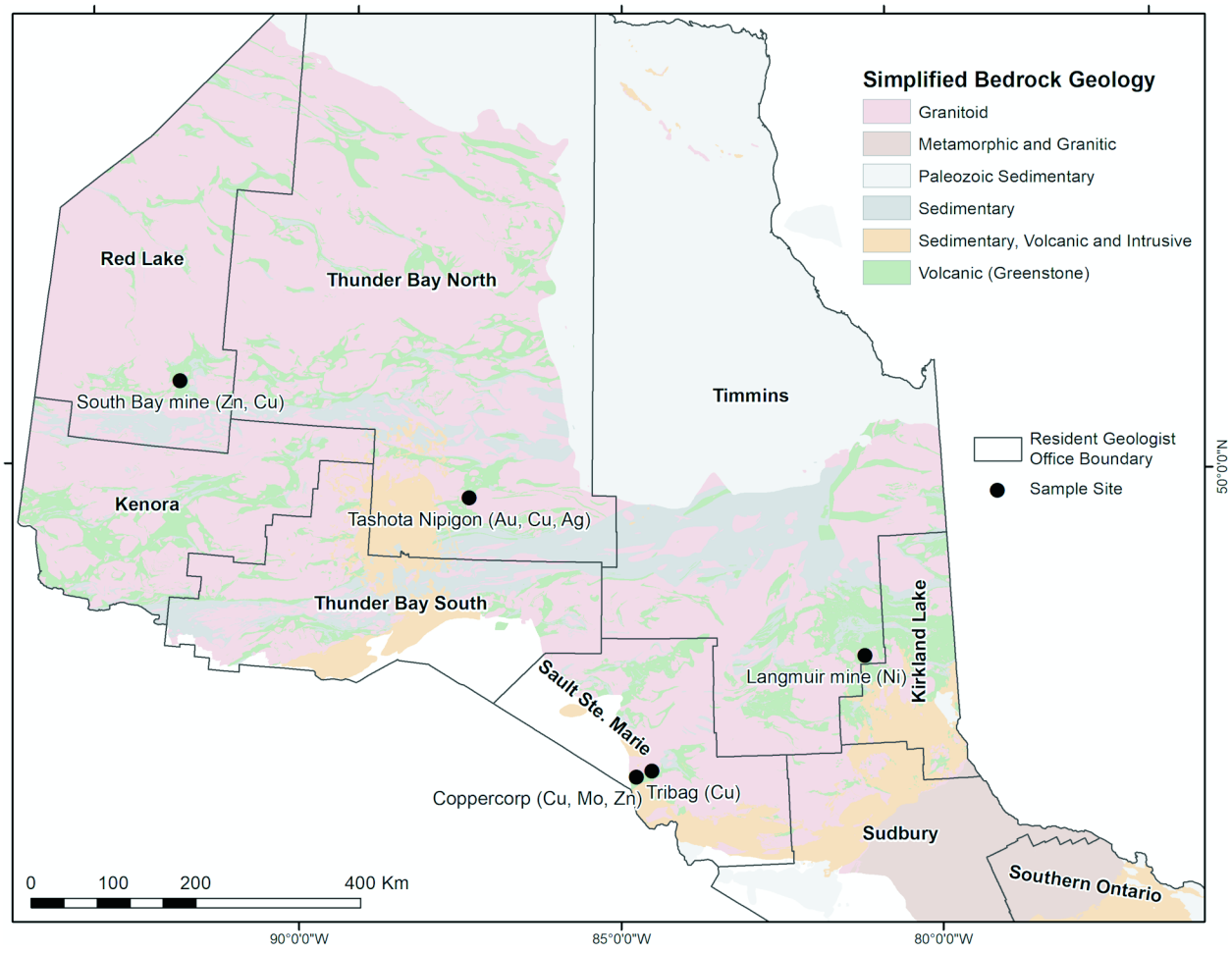


Figure 36.1. Geographic location of Critical Minerals Mine Waste Sampling project tailings sampling sites. Geology *modified from* Ontario Geological Survey (2011).

Langmuir Mine, Timmins District

The Langmuir Mine is located in Langmuir Township, near Timmins (AMIS Identifier 10069; MDI42A06SE00006) and was in production from 1976 to 1992, producing more than 100 000 tons of ore grading 2.2% Ni during operations (*Canadian Mining Journal*, May 21, 2014, www.canadianminingjournal.com/news/nickel-inspiration-to-dewater-former-langmuir-mine). Bennett (2022) gave a full description of this site as well as provided preliminary results for cobalt, copper, nickel and zinc in the tailings. Complete geochemical results for the Langmuir Mine tailings samples are provided in Table 36.3. No elements in the samples from this site exceeded the OMI "Occurrence" threshold values.

Coppercorp Mine, Sault Ste. Marie District

The Coppercorp Mine is located in Ryan Township, approximately 50 km northwest of Sault Ste. Marie (AMIS Identifier 08061, MDI41N02SW00004). It operated from 1965 to 1972 and produced over 10 000 tons of copper (Tortosa 2002). Bennett (2022) gave a full description of this site, as well as provided preliminary results for cobalt, copper, nickel and zinc in the tailings. Complete geochemical results for the Coppercorp Mine tailings samples are provided in Table 36.4. Although some high copper values (up to 1100 ppm Cu) are present (*see* Table 36.4; Bennett 2022), they are all below the OMI "Occurrence" threshold value of 2500 ppm Cu (*see* Tables 36.2 and 36.4). No other elements in the samples from this site exceed the OMI "Occurrence" threshold values.

Tribag Mine, Sault Ste. Marie District

The Tribag Mine is a historical diatreme-hosted porphyry copper mine that operated in the 1960s and 1970s. The site is located in Nicolet Township, approximately 60 km north-northwest of Sault Ste. Marie (AMIS Identifier 08068; MDI000000001285, MDI41N02SE00034). The Tribag Mine produced 1 218 000 tons of copper, grading 1.52% copper (*Northern Ontario Business*, June 10, 2022, www.northernontariobusiness.com/industry-news/mining/exploration-company-hopes-to-find-a-new-batchawana-copper-mine-next-to-an-old-one-5465007), with most of the ore coming from the Breton breccia. The mine closed in the 1970s because of falling copper prices; however, recent exploration has produced positive diamond-drill core assay results (*Northern Ontario Business*, June 10, 2022, www.northernontariobusiness.com/industry-news/mining/exploration-company-hopes-to-find-a-new-batchawana-copper-mine-next-to-an-old-one-5465007). The tailings are also reported to contain a historical tungsten resource (Blecha 1974). Complete geochemical results from the Tribag Mine sampling are provided in Table 36.5. Similar to the Coppercorp Mine tailings, high copper values (up to 1496 ppm Cu) are present, but all are below the OMI "Occurrence" threshold value (*see* Table 36.2).

Tashota-Nipigon Mine, Thunder Bay North District

The Tashota-Nipigon Mine was a historical gold, silver and copper producer located approximately 57 km northwest of Geraldton. Between 1935 and 1938, the Tashota-Nipigon Mine produced 12 356 ounces of gold, 14 527 ounces of silver and 360 306 pounds of copper from 51 250 tons of ore. After mining operations ceased, the site underwent sporadic exploration from the 1960s until the mid 1980s (AMIS Identifier 02973; MDI42L04SE00005) (Mason and White 1986). A total of 9 samples were collected across 2 tailings areas (northern and southern), and complete geochemical results are listed in Table 36.6. As might be expected for a gold deposit, values for both gold and bismuth met or exceeded the OMI "Occurrence" threshold values (*see* Tables 36.6 and 36.2). Notable gold values range from 0.547 to 4.598 ppm Au, and bismuth from 67.45 to 141.64 ppm Bi.

Table 36.2. Grade requirements for mineral occurrences (*from* Ontario Geological Survey 2023a). Silver, gold and lead are the only commodities listed below that are not on Ontario's Critical Minerals list (Ontario 2022).

Commodity	Grade [a,b]
Silver (Ag)	35 g/t (35 ppm)
Gold (Au)	0.5 g/t (0.5 ppm)
Bismuth (Bi)	50 g/t (50 ppm)
Cobalt (Co)	0.02% (200 ppm)
Copper (Cu)	0.25% (2500 ppm)
Indium (In)	5 g/t (5 ppm)
Molybdenum (Mo)	0.08% (800 ppm)
Nickel (Ni)	0.08% (800 ppm)
Lead (Pb)	1.00% (10 000 ppm)
Platinum group elements (PGE)	0.5 g/t (0.5 ppm)
Antimony (Sb)	50 g/t (50 ppm)
Selenium (Se)	0.01% (100 ppm)
Tin (Sn)	0.10% (1000 ppm)
Tellurium (Te)	50 g/t (50 ppm)
Zinc (Zn)	0.50% (5000 ppm)

[a] *Under the grade column, all values listed are an arbitrary one-tenth value of the minimum acceptable economic grade.*
[b] *The threshold values in the grade column were updated and released in April 2023 (Ontario Geological Survey 2023a). These new threshold values were effective immediately. The new threshold values replace those in Wilson et al. (2008, p.81-86, Appendix 3).*

South Bay Mine, Red Lake District

The South Bay Mine is a historical volcanogenic massive sulphide deposit located in Dent Township, approximately 80 km east-northeast of Red Lake, which was mined for zinc, copper and silver from 1971 to 1981 (AMIS Identifier 03892; MDI52N02SE00012). Production numbers during that time were 1 637 948 tons at 11.06% zinc and 1.8% copper (Lichtblau et al. 2015, p.24). The tailings have the potential for zinc, copper and silver. Indium, gallium and germanium may also be present, based on reported mineral occurrences in the vicinity (Lichtblau et al. 2015, p.24). A total of 5 separate areas at this site were sampled, with a total of 16 samples collected in September 2022. The geochemical results are listed in Table 36.7. Of the 5 mine sites examined as part of this study, the South Bay Mine sampling showed the greatest number of commodities (6), including 5 critical minerals, that met or exceeded the OMI "Occurrence" threshold values (*see* Tables 36.2 and 36.7):

- silver ranging from 46.6 to 86.3 ppm Ag
- bismuth ranging from 50.54 to 271.29 ppm Bi
- cobalt ranging from 211.8 to 303.8 ppm Co
- indium ranging from 5.192 to 48.961 ppm In
- selenium above the upper detection limit of the analytical method used at >90 ppm Se
- zinc ranging from 6473 to 28 730 ppm Zn

In addition, arsenic, cadmium, lead and antimony are notably enriched in some samples compared to most rocks.

Table 36.3. Trace element analysis for samples collected from tailings at the Langmuir Mine. The limit of detection (LoD) is listed for each element.

Sample No.	Ag (ppm)	As (ppm)	Au (ppm)	Bi (ppm)	Cd (ppm)	Co (ppm)	Cu (ppm)
LoD	***0.4***	***4***	***0.003***	***0.02***	***0.05***	***0.2***	***2.2***
LANG-0001	<0.4	<4	<0.003	0.19	0.09	15.0	31
LANG-0002	<0.4	<4	<0.003	0.18	0.14	15.0	31
LANG-0003	<0.4	<4	<0.003	0.17	0.11	15.8	31
LANG-0004	<0.4	<4	<0.003	0.18	0.07	15.3	30
LANG-0005	<0.4	<4	<0.003	0.19	0.09	15.6	31
LANG-0006	<0.4	<4	<0.003	0.18	0.11	14.9	30
LANG-0007	<0.4	<4	<0.003	0.19	0.08	16.9	33
LANG-0008	<0.4	<4	<0.003	0.05	0.14	24.9	40
LANG-0009	<0.4	<4	<0.003	0.05	0.05	24.5	41

Sample No.	Hg (ppm)	In (ppm)	Ir (ppm)	Mo (ppm)	Ni (ppm)	Pb (ppm)	Pd (ppm)
LoD	***0.08***	***0.005***	***0.003***	***0.2***	***2***	***0.2***	***0.02***
LANG-0001	<0.08	0.027	<0.003	0.26	46	12.2	<0.02
LANG-0002	<0.08	0.028	<0.003	<0.2	44	12.3	<0.02
LANG-0003	<0.08	0.028	<0.003	0.26	43	10.9	<0.02
LANG-0004	<0.08	0.028	<0.003	0.22	44	11.1	<0.02
LANG-0005	<0.08	0.027	<0.003	0.22	43	11.2	<0.02
LANG-0006	<0.08	0.029	<0.003	0.20	42	10.6	<0.02
LANG-0007	<0.08	0.030	<0.003	0.25	45	12.0	<0.02
LANG-0008	<0.08	0.014	<0.003	1.05	202	2.3	<0.02
LANG-0009	<0.08	<0.005	<0.003	1.02	200	2.8	<0.02

Sample No.	Pt (ppm)	Sb (ppm)	Se (ppm)	Sn (ppm)	Te (ppm)	Tl (ppm)	Zn (ppm)
LoD	***0.005***	***0.02***	***0.2***	***0.06***	***0.04***	***0.004***	***4***
LANG-0001	<0.005	0.12	0.2	0.9	<0.04	0.270	94
LANG-0002	<0.005	0.10	0.3	0.8	<0.04	0.261	72
LANG-0003	<0.005	0.10	0.2	0.8	<0.04	0.258	75
LANG-0004	<0.005	0.09	0.2	0.9	0.04	0.271	72
LANG-0005	<0.005	0.11	0.2	0.9	0.06	0.262	73
LANG-0006	<0.005	0.10	0.2	0.9	<0.04	0.270	70
LANG-0007	<0.005	0.13	0.2	0.9	0.04	0.273	81
LANG-0008	<0.005	0.04	<0.2	0.5	<0.04	0.028	67
LANG-0009	<0.005	3.33	<0.2	65.4	<0.04	0.028	79

*Analyses completed by OGS Geoscience Laboratories in Sudbury, Ontario. All samples were analyzed by inductively coupled plasma mass spectrometry (ICP–MS) after a modified aqua regia extraction designed for soils and unconsolidated materials (*see *Ontario Geological Survey 2021, p.18).*

Abbreviations: *ppm, parts per million; LoD, limit of detection; Ag, silver; As, arsenic; Au, gold; Bi, bismuth; Cd, cadmium; Co, cobalt; Cu, copper; Hg, mercury; In, indium; Ir, iridium; Mo, molybdenum; Ni, nickel; Pb, lead; Pd, palladium; Pt, platinum; Sb, antimony; Se, selenium; Sn, tin; Te, tellurium; Tl, thallium; Zn, zinc.*

Table 36.4. Trace element analysis for samples collected from tailings at the Coppercorp Mine. The limit of detection (LoD) is listed for each element.

Sample No.	Ag (ppm)	As (ppm)	Au (ppm)	Bi (ppm)	Cd (ppm)	Co (ppm)	Cu (ppm)	Hg (ppm)	In (ppm)	Ir (ppm)	Mo (ppm)
LoD	***0.4***	***4***	***0.003***	***0.02***	***0.05***	***0.2***	***2.2***	***0.08***	***0.005***	***0.003***	***0.2***
MTSSSM21001	1.64	<4	0.032	2.27	1.29	31.3	1100	0.10	0.04	<0.003	0.91
MTSSSM21002	0.92	<4	0.06	1.00	0.56	36.0	775	<0.08	0.042	<0.003	0.87
MTSSSM21003	1.42	<4	0.012	1.30	0.78	25.0	976	<0.08	0.037	<0.003	0.99
MTSSSM21004	1.62	5.2	0.017	2.05	1.19	28.6	929	0.10	0.044	<0.003	0.93
MTSSSM21005	2.10	4.1	0.009	2.30	1.06	28.7	896	0.10	0.037	<0.003	0.86
MTSSSM21006	1.18	<4	0.028	1.33	0.82	27.7	597	<0.08	0.036	<0.003	1.12
MTSSSM21007	1.97	<4	0.008	1.61	1.04	29.8	545	0.10	0.042	<0.003	0.88
MTSSSM21008	2.69	<4	0.008	1.37	1.1	27.8	566	0.10	0.036	<0.003	0.94
MTSSSM21009	0.88	4.9	0.012	1.81	1.38	33.2	429	<0.08	0.047	<0.003	1.42
MTSSSM21010	0.87	<4	0.008	1.2	1.30	30.9	420	<0.08	0.045	<0.003	0.95
MTSSSM21011	1.21	<4	0.030	1.63	0.96	27.7	515	0.10	0.039	<0.003	1.21
MTSSSM21012	0.73	4.5	0.009	1.75	1.12	36.4	418	<0.08	0.05	<0.003	1.41
MTSSSM21007 SP	2.02	<4	0.014	1.27	0.94	29.2	525	0.10	0.041	<0.003	0.85

Sample No.	Ni (ppm)	Pb (ppm)	Pd (ppm)	Pt (ppm)	Sb (ppm)	Se (ppm)	Sn (ppm)	Te (ppm)	Tl (ppm)	Zn (ppm)
LoD	***2***	***0.2***	***0.02***	***0.005***	***0.02***	***0.2***	***0.06***	***0.04***	***0.004***	***4***
MTSSSM21001	41	11.7	<0.02	<0.005	1.21	0.2	0.4	<0.04	0.056	142
MTSSSM21002	46	11.3	<0.02	0.007	1.27	<0.2	0.4	<0.04	0.056	166
MTSSSM21003	40	12.8	<0.02	0.006	1.73	0.2	0.3	<0.04	0.054	106
MTSSSM21004	37	13.5	<0.02	0.006	1.57	<0.2	0.5	<0.04	0.054	129
MTSSSM21005	37	12.4	<0.02	0.005	1.39	0.2	0.4	<0.04	0.057	132
MTSSSM21006	39	11.2	<0.02	<0.005	1.57	0.2	0.3	<0.04	0.069	126
MTSSSM21007	38	10.7	<0.02	0.009	1.08	<0.2	0.4	<0.04	0.069	143
MTSSSM21008	38	10.6	<0.02	0.008	1.17	0.2	0.4	<0.04	0.058	135
MTSSSM21009	45	12.6	<0.02	<0.005	1.96	<0.2	0.4	<0.04	0.117	152
MTSSSM21010	39	10.8	<0.02	0.005	1.21	0.2	0.5	<0.04	0.063	145
MTSSSM21011	39	11.5	<0.02	<0.005	1.36	0.2	0.4	<0.04	0.071	129
MTSSSM21012	47	12.4	<0.02	<0.005	2.05	<0.2	0.5	<0.04	0.132	169
MTSSSM21007 SP	37	10.8	<0.02	<0.005	1.17	0.2	0.4	0.04	0.065	136

*Analyses completed by OGS Geoscience Laboratories in Sudbury, Ontario. All samples were analyzed by inductively coupled plasma mass spectrometry (ICP–MS) after a modified aqua regia extraction designed for soils and unconsolidated materials (*see *Ontario Geological Survey 2021, p.18).*

Abbreviations: *ppm, parts per million; LoD, limit of detection; Ag, silver; As, arsenic; Au, gold; Bi, bismuth; Cd, cadmium; Co, cobalt; Cu, copper; Hg, mercury; In, indium; Ir, iridium; Mo, molybdenum; Ni, nickel; Pb, lead; Pd, palladium; Pt, platinum; Sb, antimony; Se, selenium; Sn, tin; Te, tellurium; Tl, thallium; Zn, zinc; SP, sample split (i.e., duplicate analysis).*

Table 36.5. Trace element analysis for samples collected from tailings at the Tribag Mine. The limit of detection (LoD) is listed for each element.

Sample No.	Ag (ppm)	As (ppm)	Au (ppm)	Bi (ppm)	Cd (ppm)	Co (ppm)	Cu (ppm)	Hg (ppm)	In (ppm)	Ir (ppm)	Mo (ppm)
LoD	***0.2***	***0.4***	***0.003***	***0.02***	***0.05***	***0.2***	***0.6***	***0.08***	***0.005***	***0.003***	***0.2***
510-01-001	0.6	26.1	0.008	2.41	0.84	27.7	356.9	0.40	0.052	<0.003	9.4
510-01-002	1.3	42.0	0.010	4.93	1.02	36.9	697.0	0.46	0.087	<0.003	16.4
510-01-003	1.1	34.8	0.010	4.66	1.3	37.2	766.6	0.44	0.081	<0.003	11.0
510-02-001	0.6	21.3	0.004	2.05	0.9	22.9	361.5	0.17	0.053	<0.003	8.6
510-02-002	0.8	38.1	0.008	2.96	0.97	35.2	388.5	0.13	0.069	<0.003	9.5
510-02-003	1.5	96.5	0.008	12.86	1.31	49.5	489.9	0.85	0.124	<0.003	10.4
510-03-001	0.8	39.6	0.009	6.22	0.46	79.3	371.9	0.31	0.070	<0.003	9.9
510-03-002	1.7	101.9	0.012	7.13	1.34	53.8	620.5	0.76	0.138	<0.003	10.2
510-03-003	1.5	56.0	0.010	9.54	1.46	61.7	523.5	0.42	0.108	<0.003	8.9
510-04-001	5.7	272.4	0.067	19.39	4.19	98.0	1830	0.25	0.334	<0.003	25.0
510-04-002	0.6	22.3	0.008	0.52	1.69	20.6	174.4	0.23	0.037	<0.003	5.1
510-04-003	1.1	35.6	0.007	0.92	1.28	17.3	528.7	0.37	0.062	<0.003	9.1
510-04-004	3.0	186.8	0.108	3.43	3.31	90.7	1251.3	0.53	0.221	<0.003	19.3

Sample No.	Ni (ppm)	Pb (ppm)	Pd (ppm)	Pt (ppm)	Sb (ppm)	Se (ppm)	Sn (ppm)	Te (ppm)	Tl (ppm)	Zn (ppm)
LoD	***2***	***0.2***	***0.02***	***0.005***	***0.02***	***0.2***	***0.06***	***0.04***	***0.004***	***4***
510-01-001	29	13.0	<0.02	<0.005	0.93	0.9	0.29	0.38	0.185	117
510-01-002	39	16.2	<0.02	<0.005	1.33	1.5	0.30	0.87	0.218	157
510-01-003	39	19.1	<0.02	<0.005	1.37	1.3	0.40	0.64	0.233	186
510-02-001	28	11.8	<0.02	<0.005	0.89	0.7	0.29	0.33	0.204	144
510-02-002	38	15.7	<0.02	<0.005	1.35	0.9	0.35	0.51	0.244	152
510-02-003	61	32.7	<0.02	<0.005	2.82	1.2	0.48	2.01	0.426	218
510-03-001	48	17.1	<0.02	<0.005	1.71	1.2	0.49	1.11	0.349	85
510-03-002	69	26.4	<0.02	<0.005	3.14	1.2	0.53	0.86	0.454	205
510-03-003	58	29.9	<0.02	<0.005	2.63	1.1	0.73	0.95	0.504	190
510-04-001	120	72.1	<0.02	<0.005	23.32	3.1	0.31	3.58	0.547	611
510-04-002	32	14.4	<0.02	<0.005	1.37	1.2	0.18	0.35	0.223	182
510-04-003	35	25.0	<0.02	<0.005	1.78	1.5	0.23	0.43	0.23	127
510-04-004	79	26.6	<0.02	<0.005	3.98	3.3	0.28	1.08	0.383	476

*Analyses completed by OGS Geoscience Laboratories in Sudbury, Ontario. All samples were analyzed by inductively coupled plasma mass spectrometry (ICP–MS) after a modified aqua regia extraction designed for soils and unconsolidated materials (*see *Ontario Geological Survey 2022, p.18).*

Abbreviations: *ppm, parts per million; LoD, limit of detection; Ag, silver; As, arsenic; Au, gold; Bi, bismuth; Cd, cadmium; Co, cobalt; Cu, copper; Hg, mercury; In, indium; Ir, iridium; Mo, molybdenum; Ni, nickel; Pb, lead; Pd, palladium; Pt, platinum; Sb, antimony; Se, selenium; Sn, tin; Te, tellurium; Tl, thallium; Zn, zinc.*

Table 36.5, ***continued.***

Sample No.	Ag (ppm)	As (ppm)	Au (ppm)	Bi (ppm)	Cd (ppm)	Co (ppm)	Cu (ppm)	Hg (ppm)	In (ppm)	Ir (ppm)	Mo (ppm)
LoD	***0.2***	***0.4***	***0.003***	***0.02***	***0.05***	***0.2***	***0.6***	***0.08***	***0.005***	***0.003***	***0.2***
510-05-001	2.9	79.5	0.020	8.57	1.36	43.3	844.2	0.49	0.176	<0.003	17.2
510-05-002	1.8	58.7	0.018	5.66	1.51	35.4	485.4	0.62	0.128	<0.003	13.2
510-05-003	1.2	26.3	0.008	0.74	1.94	15.5	313.5	0.13	0.072	<0.003	4.1
510-06-001	1.7	102.0	0.024	9.26	0.9	56.7	338.7	0.39	0.127	<0.003	11.2
510-06-002	1.2	59.9	0.009	11.23	0.94	36.1	213.4	0.29	0.101	<0.003	14.7
510-06-003	0.5	17.0	0.005	0.47	0.78	15.6	157.4	0.08	0.038	<0.003	5.4
510-06-004	0.6	18.9	0.004	0.64	1.04	15.5	184.2	0.25	0.040	<0.003	6.7
510-07-001	1.4	41.5	0.012	2.12	1.19	23.4	710.9	0.23	0.076	<0.003	13.5
510-07-002	0.4	13.1	0.003	0.57	1.55	19.0	296.4	<0.08	0.045	<0.003	7.6
510-07-003	0.7	31.0	0.004	1.47	2.09	21.9	300.1	0.18	0.072	<0.003	9.3
510-07-004	0.5	29.0	0.006	0.35	0.93	16.3	412.2	0.13	0.05	<0.003	19.5
510-08-001	1.1	56.1	0.009	16.76	1.27	51.1	542.3	0.26	0.084	<0.003	12.3
510-08-002	0.7	46.7	0.009	3.65	0.88	36.9	444.4	0.28	0.065	<0.003	15.9

Sample No.	Ni (ppm)	Pb (ppm)	Pd (ppm)	Pt (ppm)	Sb (ppm)	Se (ppm)	Sn (ppm)	Te (ppm)	Tl (ppm)	Zn (ppm)
LoD	***2***	***0.2***	***0.02***	***0.005***	***0.02***	***0.2***	***0.06***	***0.04***	***0.004***	***4***
510-05-001	71	62.8	<0.02	<0.005	5.10	1.2	0.52	1.56	0.488	192
510-05-002	60	36.8	<0.02	<0.005	2.34	1.1	0.48	1.08	0.485	203
510-05-003	45	24.4	<0.02	0.005	1.08	0.9	0.44	0.39	0.402	225
510-06-001	75	35.0	<0.02	<0.005	4.69	2.3	0.28	1.97	0.319	154
510-06-002	46	26.2	<0.02	<0.005	2.27	1.7	0.27	1.39	0.306	141
510-06-003	33	11.2	<0.02	<0.005	0.83	1.0	0.17	0.25	0.185	118
510-06-004	33	13.7	<0.02	<0.005	0.69	1.0	0.22	0.31	0.196	122
510-07-001	42	37.7	<0.02	<0.005	2.06	0.9	0.50	0.42	0.393	134
510-07-002	20	13.2	<0.02	<0.005	1.08	0.7	0.35	0.19	0.210	191
510-07-003	40	20.5	<0.02	<0.005	0.92	0.7	0.66	0.26	0.373	254
510-07-004	37	13.6	<0.02	<0.005	0.48	0.7	0.46	0.19	0.309	115
510-08-001	51	28.5	<0.02	<0.005	1.37	1.8	0.42	1.42	0.289	161
510-08-002	42	20.2	<0.02	<0.005	0.94	1.1	0.45	1.14	0.281	128

*Analyses completed by OGS Geoscience Laboratories in Sudbury, Ontario. All samples were analyzed by inductively coupled plasma mass spectrometry (ICP–MS) after a modified aqua regia extraction designed for soils and unconsolidated materials (*see *Ontario Geological Survey 2022, p.18).*

Abbreviations: *ppm, parts per million; LoD, limit of detection; Ag, silver; As, arsenic; Au, gold; Bi, bismuth; Cd, cadmium; Co, cobalt; Cu, copper; Hg, mercury; In, indium; Ir, iridium; Mo, molybdenum; Ni, nickel; Pb, lead; Pd, palladium; Pt, platinum; Sb, antimony; Se, selenium; Sn, tin; Te, tellurium; Tl, thallium; Zn, zinc.*

Table 36.5, *continued*.

Sample No.	Ag (ppm)	As (ppm)	Au (ppm)	Bi (ppm)	Cd (ppm)	Co (ppm)	Cu (ppm)	Hg (ppm)	In (ppm)	Ir (ppm)	Mo (ppm)
LoD	***0.2***	***0.4***	***0.003***	***0.02***	***0.05***	***0.2***	***0.6***	***0.08***	***0.005***	***0.003***	***0.2***
510-09-001	1.3	81.4	0.018	13.85	1.40	59.6	574.6	0.37	0.100	<0.003	21.0
510-09-002	1.4	52.0	0.022	12.74	1.42	47.6	619.8	0.22	0.096	<0.003	12.4
510-10-001	1.1	76.9	0.015	7.61	1.14	103.1	341.9	0.41	0.083	<0.003	10.4
510-10-002	1.2	91.4	0.020	17.32	1.42	75.7	400.5	0.57	0.127	<0.003	13.0
510-10-003	1.2	57.7	0.011	5.64	0.76	56.2	618.8	0.34	0.091	<0.003	18.3
510-11-001	2.6	123	0.022	6.81	1.12	51.7	716.1	0.92	0.157	<0.003	15.8
510-11-002	1.2	28.3	0.007	0.71	2.69	17.1	347.9	0.08	0.071	<0.003	4.6
510-11-003	1.2	45.4	0.010	1.71	1.70	25.7	376.2	0.40	0.095	<0.003	6.9
510-12-001	2.4	88.6	0.026	18.78	0.57	3.3	1324.2	0.59	0.107	<0.003	14.2
510-12-002	1.8	97.0	0.036	20.19	1.79	85.5	1473.7	0.65	0.167	<0.003	14.4
510-12-003	0.9	49.7	0.012	5.66	1.91	48.4	1496.4	0.16	0.083	<0.003	12.7
510-13-001	1.0	51.7	0.009	4.59	1.47	36.4	597.8	0.26	0.084	<0.003	11.6
510-13-002	0.9	62.4	0.012	5.73	1.52	47.5	412.3	0.56	0.080	<0.003	12.2
510-13-003	1.4	29.6	0.010	1.12	1.32	17.0	447.2	0.16	0.057	<0.003	7.2

Sample No.	Ni (ppm)	Pb (ppm)	Pd (ppm)	Pt (ppm)	Sb (ppm)	Se (ppm)	Sn (ppm)	Te (ppm)	Tl (ppm)	Zn (ppm)
LoD	***2***	***0.2***	***0.02***	***0.005***	***0.02***	***0.2***	***0.06***	***0.04***	***0.004***	***4***
510-09-001	47	33.7	<0.02	0.008	2.21	1.8	0.42	1.19	0.283	184
510-09-002	46	32.3	<0.02	<0.005	2.07	1.5	0.37	1.38	0.259	196
510-10-001	48	18.9	<0.02	<0.005	2.09	1.5	0.63	1.10	0.340	147
510-10-002	56	32.1	<0.02	<0.005	2.74	2.2	0.35	3.34	0.229	213
510-10-003	57	30.7	<0.02	<0.005	1.55	1.8	0.33	1.51	0.260	128
510-11-001	74	47.2	<0.02	<0.005	3.11	1.3	0.63	0.88	0.545	188
510-11-002	46	21.3	<0.02	<0.005	1.18	1.1	0.46	0.32	0.366	308
510-11-003	52	22.7	<0.02	<0.005	1.88	1.2	0.5	0.49	0.374	235
510-12-001	13	26.9	<0.02	0.005	3.21	3.1	0.54	1.83	0.323	86
510-12-002	77	40.2	<0.02	<0.005	2.54	3.9	0.43	3.46	0.324	286
510-12-003	59	32.8	<0.02	<0.005	1.98	1.6	0.46	0.98	0.263	325
510-13-001	41	15.9	<0.02	<0.005	3.38	1.3	0.34	1.02	0.237	232
510-13-002	55	21.2	<0.02	<0.005	1.88	1.9	0.41	1.04	0.268	193
510-13-003	37	26.7	<0.02	<0.005	0.85	1.2	0.37	0.46	0.205	179

*Analyses completed by OGS Geoscience Laboratories in Sudbury, Ontario. All samples were analyzed by inductively coupled plasma mass spectrometry (ICP–MS) after a modified aqua regia extraction designed for soils and unconsolidated materials (*see *Ontario Geological Survey 2022, p.18).*

Abbreviations: *ppm, parts per million; LoD, limit of detection; Ag, silver; As, arsenic; Au, gold; Bi, bismuth; Cd, cadmium; Co, cobalt; Cu, copper; Hg, mercury; In, indium; Ir, iridium; Mo, molybdenum; Ni, nickel; Pb, lead; Pd, palladium; Pt, platinum; Sb, antimony; Se, selenium; Sn, tin; Te, tellurium; Tl, thallium; Zn, zinc.*

Table 36.6. Trace element analysis for samples collected from tailings at the Tashota-Nipigon Mine. The limit of detection (LoD) is listed for each element. Numbers in **bold** indicate concentrations above the Ontario Mineral Inventory threshold values listed in Table 36.2.

Sample No.	Ag (ppm)	As (ppm)	Au (ppm)	Bi (ppm)	Cd (ppm)	Co (ppm)	Cu (ppm)	Hg (ppm)	In (ppm)	Ir (ppm)	Mo (ppm)
LoD	***0.2***	***0.4***	***0.003***	***0.02***	***0.05***	***0.2***	***0.6***	***0.08***	***0.005***	***0.003***	***0.2***
22GP-020	1.8	1.5	**1.453**	32.53	<0.05	5.6	72.8	0.14	0.024	<0.003	0.5
22GP-021	0.9	2.9	**0.547**	14.26	<0.05	4.2	38.2	<0.08	0.019	<0.003	0.4
22GP-022	1.1	1.1	**0.924**	25.43	<0.05	5.0	49.8	<0.08	0.020	<0.003	0.6
22GP-023	1.5	2.8	**1.045**	39.37	<0.05	13.0	80.4	0.45	0.031	<0.003	0.8
22GP-024	1.3	1.3	**1.240**	26.68	<0.05	5.1	38.1	0.14	0.024	<0.003	0.6
22GP-025	2.1	2.8	**2.177**	**67.45**	<0.05	16.5	125.6	1.33	0.052	<0.003	1.0
22GP-026	1.8	2.1	**1.723**	48.09	<0.05	10.5	145.4	1.35	0.061	<0.003	0.7
22GP-027	3.9	1.5	**3.950**	**141.64**	<0.05	20.9	115.8	2.28	0.069	<0.003	1.0
22GP-028	3.1	0.9	**4.598**	**95.04**	<0.05	8.7	78.5	2.26	0.044	<0.003	0.7

Sample No.	Ni (ppm)	Pb (ppm)	Pd (ppm)	Pt (ppm)	Sb (ppm)	Se (ppm)	Sn (ppm)	Te (ppm)	Tl (ppm)	Zn (ppm)
LoD	***2***	***0.2***	***0.02***	***0.005***	***0.02***	***0.2***	***0.06***	***0.04***	***0.004***	***4***
22GP-020	7	6.0	<0.02	<0.005	0.17	1.3	0.93	1.70	0.254	37
22GP-021	5	4.9	<0.02	<0.005	0.17	1.1	0.85	0.81	0.277	25
22GP-022	7	5.8	<0.02	<0.005	0.12	1.0	0.9	0.71	0.383	44
22GP-023	15	8.6	<0.02	<0.005	0.20	1.7	1.08	1.41	0.276	40
22GP-024	7	5.6	<0.02	<0.005	0.16	1.5	0.94	1.15	0.282	37
22GP-025	18	6.1	<0.02	0.006	0.20	2.0	1.15	1.90	0.399	47
22GP-026	10	5.0	<0.02	0.006	0.15	1.2	1.09	1.36	0.521	70
22GP-027	25	8.6	<0.02	0.005	0.20	3.7	1.13	3.17	0.425	48
22GP-028	12	6.4	<0.02	<0.005	0.15	2.6	1.02	2.65	0.311	34

*Analyses completed by OGS Geoscience Laboratories in Sudbury, Ontario. All samples were analyzed by inductively coupled plasma mass spectrometry (ICP–MS) after a modified aqua regia extraction designed for soils and unconsolidated materials (*see *Ontario Geological Survey 2022, p.18).*

Abbreviations: *ppm, parts per million; LoD, limit of detection; Ag, silver; As, arsenic; Au, gold; Bi, bismuth; Cd, cadmium; Co, cobalt; Cu, copper; Hg, mercury; In, indium; Ir, iridium; Mo, molybdenum; Ni, nickel; Pb, lead; Pd, palladium; Pt, platinum; Sb, antimony; Se, selenium; Sn, tin; Te, tellurium; Tl, thallium; Zn, zinc.*

Table 36.7. Trace element analysis for samples collected from tailings at the South Bay Mine. The limit of detection (LoD) is listed for each element. Numbers in **bold** indicate concentrations above the Ontario Mineral Inventory threshold values listed in Table 36.2.

Sample No.	Ag (ppm)	As (ppm)	Au (ppm)	Bi (ppm)	Cd (ppm)	Co (ppm)	Cu (ppm)
LoD	***0.2***	***0.4***	***0.003***	***0.02***	***0.05***	***0.2***	***0.6***
2022SB001	1.7	46.3	0.014	2.34	0.60	7.9	89.9
2022SB002	**69.5**	402.5	0.455	48.23	57.31	**255.1**	**2995.2**
2022SB003	**46.9**	568.7	0.317	**72.05**	30.15	**269.1**	1930.9
2022SB004	**48.6**	1594.6	0.348	**146.41**	129.77	**260**	**5836.6**
2022SB005	**46.6**	3996.2	0.348	**271.29**	130.74	**303.8**	**8859.4**
2022SB006	0.9	16.0	0.013	1.43	0.29	10.9	65.7
2022SB007	1.3	64.7	0.016	2.31	0.16	8.4	56.0
2022SB008	28.3	159.1	0.278	34.69	3.71	25.8	381.2
2022SB009	**70.7**	334.2	0.371	43.39	55.85	**211.8**	**6723.6**
2022SB010	33.7	175.1	0.175	26.86	37.03	116.2	**3814.3**
2022SB011	**49.1**	120.3	0.437	**52.91**	4.41	52.4	290.8
2022SB012	**86.3**	328.6	**0.670**	**50.54**	51.01	**220.9**	**2612.7**
2022SB013	**80.2**	451.7	**2.192**	**62.72**	90.12	**238.5**	**4758.7**
2022SB014	32.5	267.8	0.354	**138.48**	0.13	11.8	310.7
2022SB015	26.2	322.5	0.287	**108.31**	2.55	112.6	1550.4
2022SB016	26.0	407.6	0.278	**96.64**	8.54	165.6	1750.0

Sample No.	Hg (ppm)	In (ppm)	Ir (ppm)	Mo (ppm)	Ni (ppm)	Pb (ppm)	Pd (ppm)
LoD	***0.08***	***0.005***	***0.003***	***0.2***	***2***	***0.2***	***0.02***
2022SB001	<0.08	0.403	<0.003	0.4	7	126.6	<0.02
2022SB002	2.20	**5.755**	<0.003	0.9	6	4842.7	<0.02
2022SB003	1.18	4.727	<0.003	1.3	8	34440	<0.02
2022SB004	1.12	**14.337**	<0.003	1.0	7	3180.7	<0.02
2022SB005	1.07	**48.961**	<0.003	1.5	9	2632.1	<0.02
2022SB006	<0.08	0.114	<0.003	0.2	26	90.3	<0.02
2022SB007	<0.08	0.274	<0.003	0.2	23	109.3	<0.02
2022SB008	1.01	2.107	<0.003	0.7	12	2334.6	<0.02
2022SB009	1.27	**9.025**	<0.003	0.8	7	3090.8	<0.02
2022SB010	0.63	4.61	<0.003	0.5	4	1912.8	<0.02
2022SB011	1.41	1.935	<0.003	0.8	11	2846.4	<0.02
2022SB012	2.48	**5.192**	<0.003	1.1	9	4882.7	<0.02
2022SB013	2.25	**9.383**	<0.003	1.1	9	4436.8	<0.02
2022SB014	0.55	2.111	<0.003	1.6	2	1982.7	<0.02
2022SB015	0.48	2.777	<0.003	1.5	5	1653.7	<0.02
2022SB016	0.42	3.671	<0.003	1.4	6	1489.9	<0.02

*Analyses completed by OGS Geoscience Laboratories in Sudbury, Ontario. All samples were analyzed by inductively coupled plasma mass spectrometry (ICP–MS) after a modified aqua regia extraction designed for soils and unconsolidated materials (*see *Ontario Geological Survey 2022, p.18).*

Abbreviations: *ppm, parts per million; LoD, limit of detection; Ag, silver; As, arsenic; Au, gold; Bi, bismuth; Cd, cadmium; Co, cobalt; Cu, copper; Hg, mercury; In, indium; Ir, iridium; Mo, molybdenum; Ni, nickel; Pb, lead; Pd, palladium; Pt, platinum; Sb, antimony; Se, selenium; Sn, tin; Te, tellurium; Tl, thallium; Zn, zinc.*

Table 36.7, *continued*.

Sample No.	Pt (ppm)	Sb (ppm)	Se (ppm)	Sn (ppm)	Te (ppm)	Tl (ppm)	Zn (ppm)
LoD	***0.005***	***0.02***	***0.2***	***0.06***	***0.04***	***0.004***	***4***
2022SB001	<0.005	0.76	5.8	0.58	0.04	0.204	140
2022SB002	<0.005	35.24	59.0	6.08	0.39	1.919	**12435**
2022SB003	<0.005	34.64	**>90**	6.36	0.93	1.654	**6473**
2022SB004	<0.005	49.39	**>90**	6.23	1.80	1.777	**28730**
2022SB005	<0.005	48.76	**>90**	5.07	1.68	2.303	**28394**
2022SB006	<0.005	0.55	1.8	0.67	<0.04	0.240	91
2022SB007	<0.005	0.88	3.3	0.68	0.07	0.225	61
2022SB008	<0.005	13.89	16.8	3.18	0.16	0.479	867
2022SB009	<0.005	37.84	70.7	5.42	0.24	1.365	**12557**
2022SB010	<0.005	25.57	57.0	3.20	0.21	1.004	**8099**
2022SB011	<0.005	13.33	18.7	6.65	0.19	0.644	1012
2022SB012	<0.005	35.53	51.8	12.5	0.27	1.788	**11421**
2022SB013	<0.005	40.88	64.8	10.78	0.34	1.773	**20360**
2022SB014	<0.005	19.46	45.9	5.91	0.67	1.177	130
2022SB015	<0.005	14.92	49.1	4.70	0.66	1.082	674
2022SB016	<0.005	0.76	5.8	0.58	0.04	0.204	140

*Analyses completed by OGS Geoscience Laboratories in Sudbury, Ontario. All samples were analyzed by inductively coupled plasma mass spectrometry (ICP–MS) after a modified aqua regia extraction designed for soils and unconsolidated materials (*see *Ontario Geological Survey 2022, p.18).*

Abbreviations: *ppm, parts per million; LoD, limit of detection; Ag, silver; As, arsenic; Au, gold; Bi, bismuth; Cd, cadmium; Co, cobalt; Cu, copper; Hg, mercury; In, indium; Ir, iridium; Mo, molybdenum; Ni, nickel; Pb, lead; Pd, palladium; Pt, platinum; Sb, antimony; Se, selenium; Sn, tin; Te, tellurium; Tl, thallium; Zn, zinc.*

FUTURE WORK

The next steps for the Critical Minerals Mine Waste Sampling project include expanding the existing geochemical data set to include critical minerals, such as tungsten (e.g., previously reported at Tribag Mine), gallium and germanium (e.g., previously reported at South Bay Mine). The sampling of abandoned gold mine tailing sites for potentially economic concentrations of critical minerals is also being planned, as outlined by Hastie et al. (this volume).

ACKNOWLEDGMENTS

Thank you to all the OGS staff who contributed to their time and expertise to this project. A big thank you to all the RGP staff who, despite the physical challenges of this project persevered; in particular, Ethan Amyotte, Paul Malegus, Sophie Churchley, Edwin Morelli, Barun Maity, Nazha Sabiri and Mark Puumala. Without you this project would not have had the geographic scope that it has had. A special thank you goes to Darla Bennett, who was the RGP lead for this project and who liaised with the rest of the OGS to make sure that this project was a success.

REFERENCES

Azadbakht, Z., Bennett, D., Maity, B.K., Bousquet, P., Daniels, C.M., Hinz, S.L.K., Morelli, E. and Dorland, G. 2022. Report of Activities 2021, Resident Geologist Program, Timmins Regional Resident Geologist Report: Timmins and Sault Ste. Marie Districts; Ontario Geological Survey, Open File Report 6384, 151p.

Bennett, D.J. 2022. Catching it by the tailings: An introduction to the Ontario Geological Survey Critical Minerals mine waste sampling project; *in* Summary of Field Work and Other Activities, 2022, Ontario Geological Survey, Open File Report 6390, p.32-1 to 32-6.

Blecha, M. 1974. Batchawana area—a possible Precambrian porphyry copper district; Canadian Institute of Mining and Metallurgy Bulletin, v.67, no.748, p. 71-76.

Lichtblau, A.F., Ravnaas, C., Storey, C.C., Tims, A., Debicki, R.L., Pettigrew, T.K., Wilson, A.C. and Wetendorf, J. 2015. Report of Activities 2014, Resident Geologist Program, Red Lake Regional Resident Geologist Report: Red Lake and Kenora Districts; Ontario Geological Survey, Open File Report 6301, 83p.

Mason, J. and White, G. 1986. Gold occurrences, prospects and deposits of the Beardmore–Geraldton area, districts of Thunder Bay and Cochrane; Ontario Geological Survey, Open File Report 5630, 680p.

Mineral Development and Lands Branch 2022. Abandoned Mines Information System; Ministry of Northern Development, Mines, Natural Resources and Forestry, online database, April 2022 update, www.hub.geologyontario.mines.gov.on.ca. [accessed November 22, 2023]

Ontario 2022. Ontario's Critical Mineral Strategy: Unlocking the potential to drive economic recovery and prosperity; Ministry of Northern Development, Mines, Natural Resources and Forestry, 53p., www.ontario.ca/page/ontarios-critical-minerals-strategy-2022-2027-unlocking-potential-drive-economic-recovery-prosperity, also available to download: select "Download English PDF". [accessed November 23, 2023]

Ontario Geological Survey 2011. 1:250 000 scale bedrock geology of Ontario; Ontario Geological Survey, Miscellaneous Release—Data 126 – Revision 1.

——— 2021. Geoscience Laboratories 2021 Schedule of Fees and Services, Issue 13, effective April 1, 2021, Ontario Geological Survey, Geoscience Laboratories, 34p.

——— 2022. Geoscience Laboratories 2022 Schedule of Fees and Services, Issue 14, effective April 1, 2022, Ontario Geological Survey, Geoscience Laboratories, 34p.

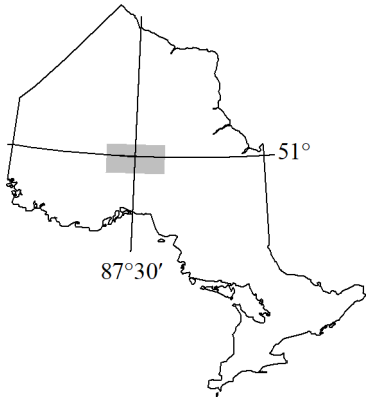
——— 2023a. OMI Definitions and cut-off values; document in Ontario Mineral Inventory, Ontario Geological Survey, online database, April 2023 update, 9p., www.geologyontario.mndm.gov.on.ca/ogsearth.html#mineral-inventory. [accessed October 24, 2023]

——— 2023b. Ontario Mineral Inventory; Ontario Geological Survey, online database, October 2023 update, www.hub.geologyontario.mines.gov.on.ca. [accessed October 13, 2023]

Tortosa, D. 2002. Geological report on the Coppercorp property of Amerigo Resources Ltd., Mamainse Point area, Ontario, prepared for Amerigo Resources Ltd.; Sault Ste. Marie Resident Geologist's Office, Ryan Township, assessment file Ryan-Montreal-0012, AFRI# 20000018747, 61p.

Wilson, A.C., Rowell, D.J., Seim, G.Wm. and Debicki, R.L. 2008. Procedural guidelines for provincially significant mineral potential mineral resource assessments; Ontario Geological Survey, Open File Report 6141, 91p.

37. Geology and Mineral Potential of the Eastern English River Subprovince, Northwestern Ontario: Project Introduction



S.V. Churchley[1]

[1]Resident Geologist Program, Ontario Geological Survey

INTRODUCTION

The understudied English River Subprovince (ERS) has recently drawn more attention as a result of the increased interest in lithium-cesium-tantalum (LCT)-type pegmatites. The ERS has known mineralization linked to its voluminous synorogenic granitoids, and includes rare-element pegmatites, and occurrences of uranium, tungsten and molybdenum (Breaks, Cherry and Janes 1985). Because many of these elements are listed as critical minerals, there has recently been a significant increase in the staking and exploration of the ERS.

Among Archean cratons, the Superior Province is distinct for having large belts of clastic metasedimentary rocks. In Ontario, 2 of these metasedimentary belts are present: the Quetico Subprovince, located south of the Wabigoon Subprovince, and the English River Subprovince, located on the northern boundary of the Winnipeg River and Wabigoon subprovinces (Figure 37.1). Both metasedimentary belts are believed to have formed by deposition of turbidites eroded from adjacent greenstone-granite terranes (predominantly the Uchi Subprovince in the case of the eastern ERS (Corfu, Stott and Breaks 1995; Percival and Easton 2007, p.7-8). Immediately after deposition, the sedimentary rocks underwent a syntectonic high-temperature metamorphism at mid- to lower-crustal levels that reached upper amphibolite and/or granulite facies (e.g., Pan, Heaman and Breaks 1999). This led to migmatization of the metasedimentary rocks at *circa* 2691 Ma, and the formation and emplacement of peraluminous granites at *circa* 2669 to 2650 Ma (Corfu, Stott and Breaks 1995). Because of the known genetic relationship between S-type granitoids and LCT-type pegmatites (*see* for example Černý 1982), the latter are likely to be found in the ERS.

The ERS is an east-striking belt of clastic metasedimentary and plutonic rocks with an average width of 30 km (Breaks 1991). The belt is elongate and extends laterally for over 800 km, from Lake Winnipeg in Manitoba into Ontario where its eastern extent is overlain by Paleozoic sedimentary rocks of the Hudson Bay Lowland (Breaks 1991). The ERS is composed of highly deformed and metamorphosed clastic metasedimentary rocks with minor oxide-facies iron formation (Breaks 1991; Breaks and Bond 1993; Percival and Easton 2007, p.7-8). Somewhat less abundant, but constituting most of the remainder of the ERS, are intrusive rocks with a broad range of ages from 3170 to 2560 Ma (Breaks 1991). Lastly, constituting only approximately 2% of the ERS are metavolcanic rocks (Breaks 1991). In the study area, this includes the largest metavolcanic belt in the ERS: the Melchett Lake greenstone belt (Figure 37.2). The Melchett Lake greenstone belt differs from those in the greenstone-dominated subprovinces in that it is dominated by calc-alkalic felsic to intermediate volcanic rocks (Bond 1979; Bond and Foster 1981a, 1981b; Breaks 1991; Percival and Easton 2007, p.7). Currently, all locations for Ontario Mineral Inventory (Ontario Geological Survey 2023a) records in the eastern ERS occur within and in proximity to the Melchett Lake greenstone belt.

Summary of Field Work and Other Activities, 2023,
Ontario Geological Survey, Open File Report 6405, p.37.1 to 37-7.

© King's Printer for Ontario, 2023

The evolution of the ERS has been divided by Corfu, Stott and Breaks (1995) into 4 stages. The first being deposition of turbidites at 2720 to 2700 Ma during a period of accretion of the Uchi Subprovince to the north, with the Bird River–Separation Lake greenstone belt, the Winnipeg River Subprovince and Wabigoon Subprovince to the south. Erosion from these adjacent subprovinces generated voluminous wackes and mudstones that subsequently were metamorphosed into paragneiss, mica schist, and migmatite. The geochemical and mineralogical composition of the rocks confirms that the provenance of the sediments was derived largely from volcanic and volcaniclastic rocks of the Uchi Subprovince (van de Kamp and Beakhouse 1979; Breaks, Bond and Stott 1978; Corfu, Stott and Breaks 1995; Percival and Easton 2007, p.7). Near the Uchi Subprovince boundary, there is an interfingering, and possibly a tectonic interleaving, of the ERS metasedimentary rocks with the supracrustal rocks of the Uchi Subprovince (Breaks, Bond and Stott 1978; Corfu, Stott and Breaks 1995). This interpretation is consistent with the drill-core intersections described by Debut Diamonds Inc. staff in a 2013 assessment report (Kleinboeck and Lavigne 2013). Drilling conducted near the northeasternmost extent of the ERS intersected highly varied rock types, including iron formations and felsic volcanic rocks interlayered with clastic metasedimentary rocks derived from turbidites. The 3 other evolutionary stages took place from 2720 Ma to *circa* 2660 Ma and included several periods of deformation, metamorphism and emplacement of intrusive suites of which the late peraluminous granites and associated LCT-type pegmatites are the focus of this study.

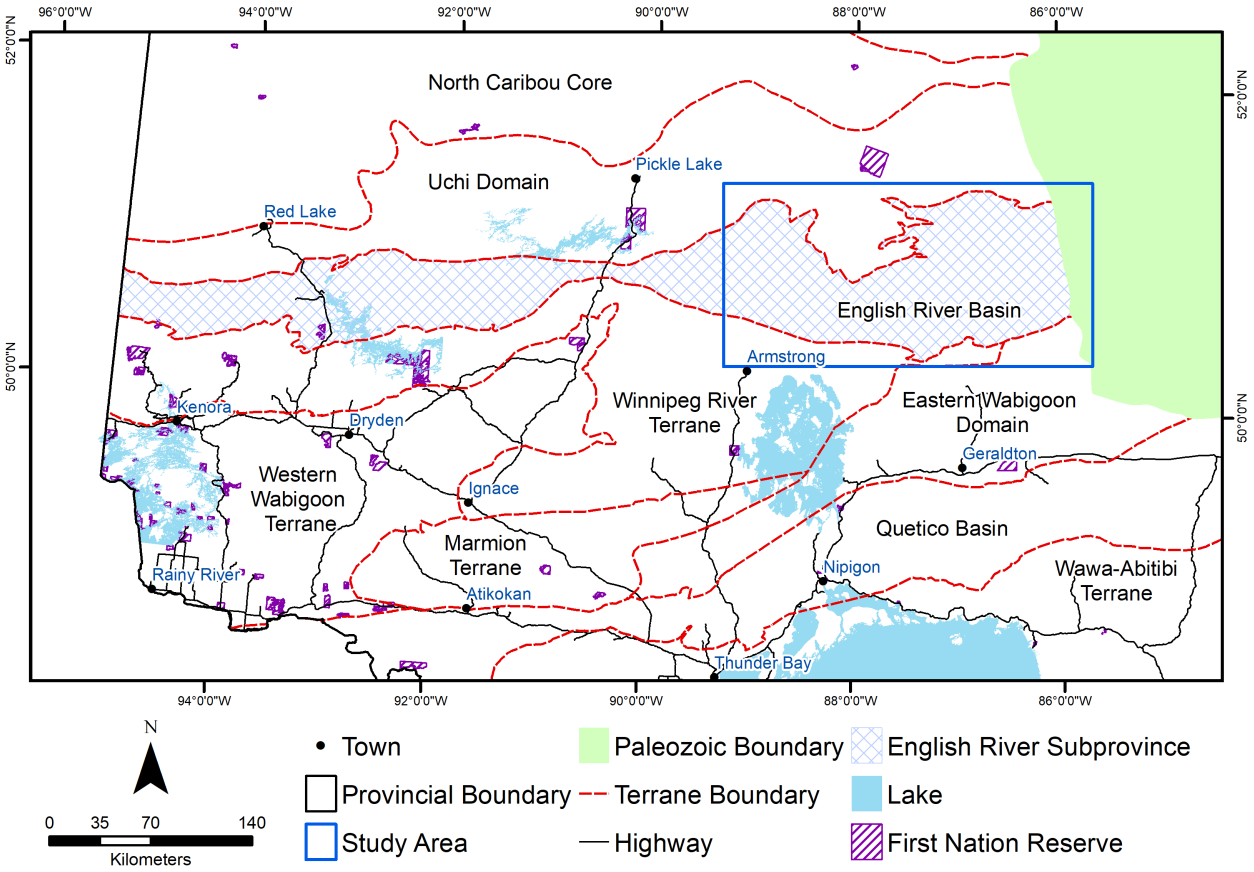


Figure 37.1. Map showing the boundaries of the Archean subprovinces in northwestern Ontario, with the Paleozoic cover in the east. The study area for this project is outlined with the blue rectangle. "North Caribou Core" refers to the core of the North Caribou terrane.

HISTORICAL MAPPING

The most recent and extensive compilation study, which included the eastern ERS, was published by Stott (1984a, 1984b). Smaller scale, and more focussed, studies have since been completed, including mapping in 1993 in the Colpitts–Bury lakes area by Devaney and Nacha (1994). A map of some of the most eastern exposures of the ERS was completed by Thurston and Carter (1969) and, since this work in 1969, no new direct bedrock information has been collected for this area. Furthermore, outcrop data used in making these maps is very sparse and geological contacts are largely inferred in many parts of the eastern ERS. A map for a portion of the northeastern ERS was published recently by Azar and Bellrose (2021), but the geology of the ERS was interpreted only from airborne geophysical and drill-core data.

EXPLORATION HISTORY

Drilling and exploration by companies has been done extensively in the Percy Lake, Durer Lake, Tennent Lake and Stewart Lake areas, primarily for iron. Most of this work was done in the 1950s. Immediately north of these areas, in the Ogoki Lake and northern Durer Lake areas is the Melchett Lake property where drilling has taken place in the 1960s and 1980s. The Melchett Lake greenstone belt is

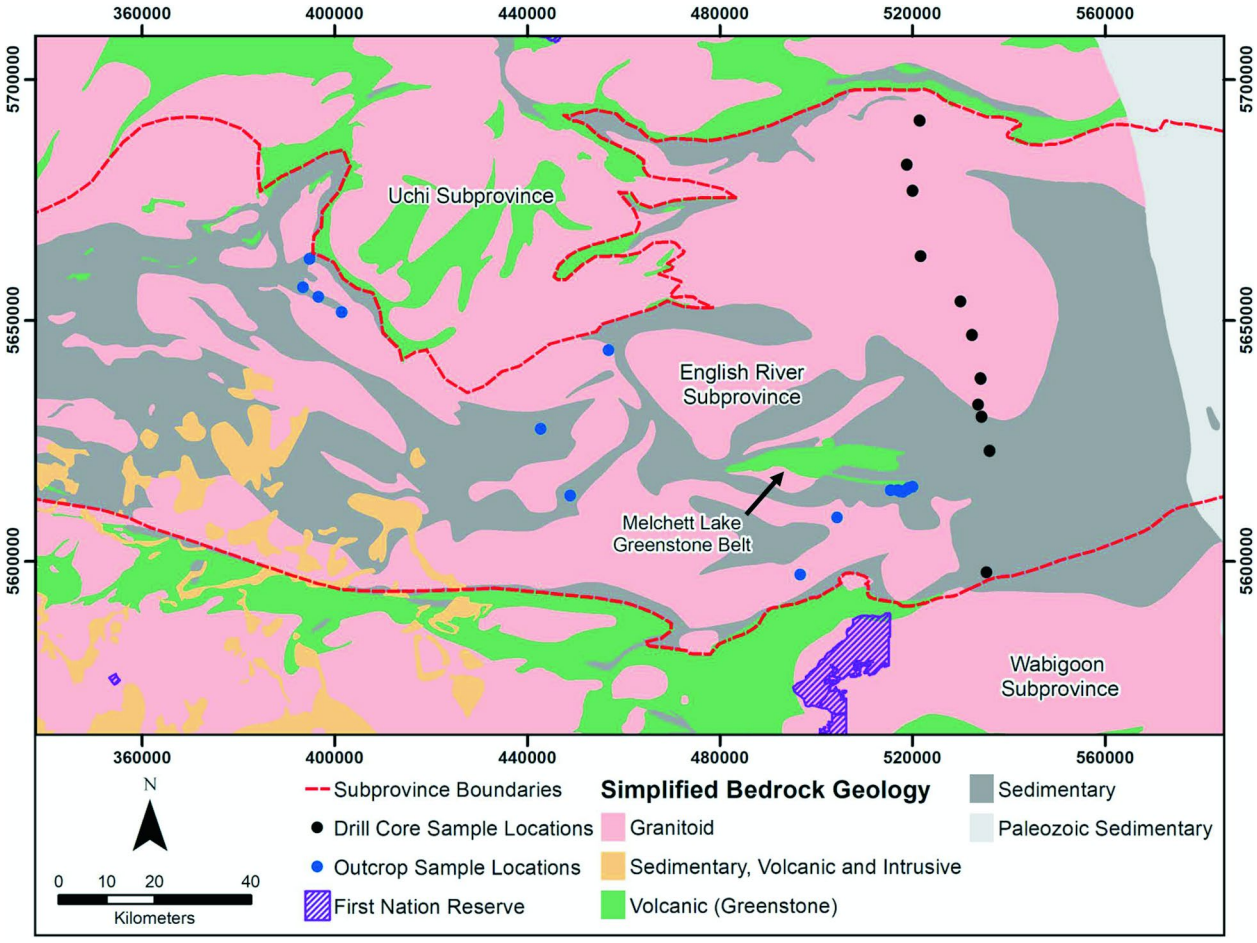


Figure 37.2. Generalized bedrock geology map with 2023 outcrop and drill-core sample locations. Universal Transverse Mercator (UTM) co-ordinates are provided using North American Datum 1983 (NAD83) in Zone 16; regional geology *modified from* Ontario Geological Survey (2011).

a metavolcanic-metasedimentary belt with volcanogenic massive sulphide-style mineralization, including potential for commodities of zinc, lead, copper, silver and gold. Most recently, sporadic drilling to the northeast of Melchett Lake and in the farthest northeastern portion of the eastern ERS was completed by Debut Diamonds Inc. in 2012 for diamond exploration (Kleinboeck and Lavigne 2013).

The eastern ERS overlaps an area that is a potential host to diamond-bearing kimberlite rocks. Several potential kimberlite anomalies were staked in 2010 following the release of a large aeromagnetic survey by the OGS (Ontario Geological Survey 2010), which outlined a total of 101 potential kimberlites. Debut Diamonds Inc. drilled 18 of these targets in 2012. The drilled targets intersected no kimberlites, but almost all anomalies intersected ultramafic intrusive rock, and the identified anomalies were mostly attributed to small pipe-shaped ultramafic intrusions (Kleinboeck and Lavigne 2013). The nature of these intrusions is currently being investigated as part of a Master of Science thesis research project at Lakehead University by S. Killins (P. Hollings, Lakehead University, written communication, 2023). The drilling completed by Debut Diamonds Inc. also indicated a rich variety of rock types in an area where little information exists. Some of the drilling intersected highly metamorphosed metavolcanic and metasedimentary rocks, and oxide-facies iron formation.

PURPOSE

The renewed interest in LCT-type pegmatites makes this the ideal time to investigate further the bedrock geology of the eastern ERS. Information on the eastern ERS is limited because of poor outcrop exposure, as well as limited road access into the area. In addition, much of our knowledge of the eastern ERS is extrapolated from data collected to the west of Armstrong (e.g., Breaks and Bond 1993; Hrabi and Cruden 2006). Metasedimentary subprovinces, such as the ERS in the Superior Province, historically have been understudied and/or under-explored because of a perceived low mineral potential in comparison to the bounding greenstone-dominated subprovinces (Breaks, Cherry and Janes 1985). Therefore, current interest in the geology of metasedimentary and plutonic-dominated terranes, such as the ERS, provides an opportunity to reinvestigate areas that have historically received little attention.

Samples collected for this study will be sent to the OGS Geoscience Laboratories in Sudbury and analyzed for major and trace elements using X-ray fluorescence (XRF) and inductively coupled plasma mass spectrometry (ICP–MS), respectively (Ontario Geological Survey 2023b). Polished sections will be made from collected granitoids and sent to the OGS Geoscience Laboratories to identify the quantity and quality of minerals suitable for potential U/Pb geochronology. Geochemical analysis, coupled with geochronological analyses, will be useful in characterizing the intrusive suites and comparing the data with intrusions of known ages farther to the west. The primary focus of this study will be on the granitoids, especially the younger intrusive rocks, which are recognized to have a higher potential to host mineralization of rare elements (Breaks, Cherry and Janes 1985). This work will help to investigate and further define areas of exploration interest.

PRELIMINARY WORK

During the 2023 field season, staff of the OGS Resident Geologist Program at Thunder Bay North undertook reconnaissance sampling along several major and secondary roads located in the eastern ERS (*see* Figure 37.2). The most common rocks types encountered were paragneiss and migmatized sedimentary rocks (Photo 37.1A), orthogneisses and various felsic intrusive bodies (Photo 37.1B). This is consistent with the results observed in other studies (e.g., Breaks, Bond and Stone 1978), in which the most common rocks observed in both drill core and outcrop include highly metamorphosed metasedimentary rocks, migmatites and gneisses. In addition, 24 bedrock samples were collected and submitted to the OGS Geoscience Laboratories, including 6 samples of pegmatites, 4 granitoids, 5 gneisses and migmatites, and 9 intermediate to ultramafic volcanic and intrusive rocks.

Table 37.1. List of cores, donated by Canada Chrome Corp., from boreholes in the eastern English River Subprovince.

Borehole #	Easting [a] (m)	Northing [a] (m)	Depth From (m)	Depth To (m)
B-2010-1402A	535371	5597716	3.66	8.88
B-2010-2190	536012	5622894	7.16	10.51
B-2010-2210D	536014	5622961	13.26	16.76
B-2010-2380	534335	5629984	10.90	15.47
B-2010-2410D	534325	5630033	12.19	15.79
B-2010-2523-B	533633	5632476	11.89	14.94
B-2010-2526-B	533648	5632509	3.05	15.54
B-2010-2710	534199	5637881	6.10	10.67
B-2010-2750	534149	5637988	4.08	7.62
B-2010-3012-B	532363	5646906	0.15	4.42
B-2010-3026	532336	5647028	1.92	7.71
B-2010-3225-C	529996	5653936	9.42	12.47
B-2010-3227-C	529989	5653970	11.38	14.48
B-2010-3588	521693	5663327	13.75	16.76
B-2010-3589-C	521658	5663364	17.04	20.27
B-2010-4012-C	520038	5676896	9.97	13.96
B-2010-4041-C	520009	5676969	1.89	6.14
B-2010-4190	518793	5682398	13.35	17.92
B-2010-4210	518808	5682308	13.14	18.50
B-2010-4490	521526	5691443	10.88	15.48

[a] *Universal Transverse Mercator (UTM) co-ordinates are provided using North American Datum 1983 (NAD83) in Zone 16.*

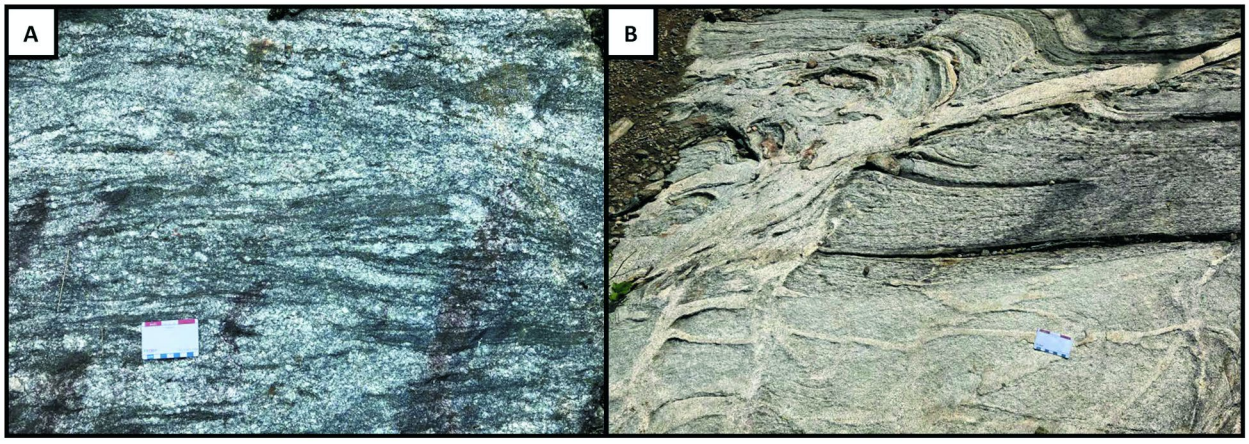


Photo 37.1. Outcrop photos from field work conducted in the English River Subprovince (ERS) in 2023. **A**) Garnet-biotite metatexite (site 23080307: UTM 451803E 5614791N). **B**) Highly metamorphosed metasedimentary rocks crosscut by abundant small felsic pegmatite veins.. These outcrops show some commonly encountered rock types of the ERS and the high degree of metamorphism (site 23080311: UTM 442038E 5627342N). All UTM co-ordinates are provided using NAD83 in Zone 16.

In addition to the field work, the project will also use bedrock samples from drill core that were generously donated to the Ministry of Mines by Canada Chrome Corp. (Table 37.1; *see* Figure 37.2). Among the donated cores, 20 intersected Archean bedrock in the eastern ERS and, therefore, are of particular interest for this study. These cores will be logged and rock types of interest, such as peraluminous granitic rocks and pegmatites, will be sampled for further geochemical and geochronological studies.

FUTURE WORK

Samples collected in the field during the summer of 2023 have been submitted to the Geoscience Laboratories for whole-rock geochemistry. Upon receipt of the results, analysis and interpretation will be used to establish sampling and field work priorities for the 2024 field season. Cutting and sampling of the Canada Chrome Corp. drill core will occur through the fall of 2023. The drill core provided by Debut Diamonds Inc. will also be examined for intersections of felsic intrusive rocks.

ACKNOWLEDGMENTS

Thank you to all Resident Geologist Program staff members who have contributed to this project, including Greg Paju and Anthony Mitchell for their assistance in the field. I would also like to extend thanks to Pete Hollings, Lakehead University, for his assistance in interpretation of the drill core provided by Canada Chrome Corp. Lastly, I would like to extend a thank you to Debut Diamonds Inc. and Canada Chrome Corp., both of which have supported this work through their donations of drill core.

REFERENCES

Azar, B. and Bellrose, J.R. 2021. Precambrian geology of the Makokibatan Lake area, Fort Hope–Miminiska greenstone belt, northwestern Ontario—east sheet; Ontario Geological Survey, Preliminary Map P.3844, scale 1:50 000.

Bond, W.D. 1979. Melchett Lake area, District of Thunder Bay; *in* Summary of Field Work, 1979, Ontario Geological Survey, Miscellaneous Paper 90, p.26-30.

Bond, W.D. and Foster, J.R. 1981a. Precambrian geology of the Melchett Lake area (west part), District of Thunder Bay; Ontario Geological Survey, Preliminary Map P.2392, scale 1:15 840.

——— 1981b. Precambrian geology of the Melchett Lake area (east part), District of Thunder Bay; Ontario Geological Survey, Preliminary Map P.2393, scale 1:15 840.

Breaks, F.W. 1991. English River Subprovince; Chapter 7 *in* Geology of Ontario, Ontario Geological Survey, Special Volume 4, Part 1, p.239-277.

Breaks, F.W. and Bond, W.D. 1993. The English River Subprovince – An Archean gneiss belt: Geology, geochemistry and associated mineralization; Ontario Geological Survey, Open File Report 5846, v.1, p.1-483.

Breaks, F.W., Bond, W.D. and Stone, D. 1978. Preliminary geological synthesis of the English River Subprovince, northwestern Ontario and its bearing upon mineral exploration; Ontario Geological Survey, Miscellaneous Paper 72, 55p.

Breaks, F.W., Cherry M.E. and Janes, D.A. 1985. Metallogeny of Archean granitoid rocks of the English River Subprovince, Superior Province, Ontario, Canada: A review; *in* High Heat Production Granites, Hydrothermal Circulation and Ore Genesis, Institution of Mining and Metallurgy, p.9-31.

Černý, P. 1982. Anatomy and classification of granitic pegmatites; *in* Granitic Pegmatites in Science and Industry, Mineralogical Association of Canada, Short Course Handbook 8, p.1-39.

Corfu, F., Stott, G.M. and Breaks F.W. 1995. U-Pb geochronology and evolution of the English River Subprovince, an Archean low *P*-high *T* metasedimentary belt in the Superior Province; Tectonics, v.14, p.1220-1233.

Devaney, J.R. and Nacha, S. 1994. Precambrian geology, Colpitts–Bury lakes area; Ontario Geological Survey, Open File Map 234, scale 1:20 000.

Hrabi, R.B. and Cruden, A.R. 2006. Structure of the Archean English River Subprovince: Implications for the tectonic evolution of the western Superior Province, Canada; Canadian Journal of Earth Sciences., v.43, p.947-966.

Kleinboeck, J. and Lavigne, M.J. 2013. 2012 Diamond drill program report: Nakina project, Thunder Bay and Porcupine Mining Divisions, Ontario, Canada; unpublished report, Thunder Bay North Resident Geologist's office, assessment file AFRO# 2.54620, 97p.

Ontario Geological Survey 2010. Ontario airborne geophysical surveys, magnetic data, grid and profile data (ASCII and Geosoft® formats) and vector data, Melchett Lake area; Ontario Geological Survey, Geophysical Data Set 1067.

——— 2011. 1:250 000 scale bedrock geology of Ontario; Ontario Geological Survey, Miscellaneous Release—Data 126 – Revision 1.

——— 2023a. Ontario Mineral Inventory; Ontario Geological Survey, online database, September 2023 update, www.hub.geologyontario.mines.gov.on.ca. [accessed October 3, 2023]

——— 2023b. Geoscience Laboratories 2023 Schedule of Fees and Services, Issue 15, effective April 1, 2023; Ontario Geological Survey, Geoscience Laboratories, 36p., www.ontario.ca/page/ontario-geological-survey#section-4, under "Schedule of fees and services", *see* link to download PDF. [accessed November 24, 2023]

Pan, Y., Heaman, L.M. and Breaks, F.W. 1999. Thermo-tectonic evolution of the Umfreville–Conifer Lake granulite zone and the English River–Winnipeg River boundary zone: Preliminary U-Pb geochronological results; in Western Superior Transect Fifth Annual Workshop, Lithoprobe Secretariat, University of British Columbia, Vancouver, British Columbia, Lithoprobe Report No. 70, p.104-108.

Percival, J.A. and Easton, R.M. 2007. Geology of the Canadian Shield in Ontario: An update; Ontario Geological Survey, Open File Report 6196 / Geological Survey of Canada, Open File 5511 / Ontario Power Generation, Report 06819-REP-0120010158-R00, 65p.

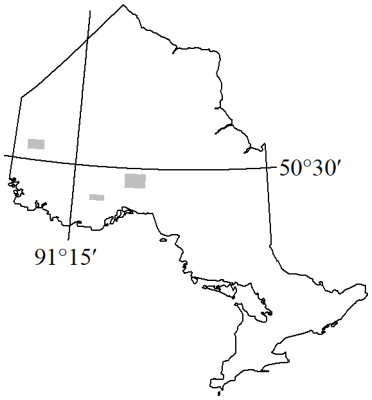
Stott, G.M. 1984a. Mojikit Lake sheet, Thunder Bay District; Ontario Geological Survey, Preliminary Map P.267—Revised, scale 1:126 720.

——— 1984b. Ogoki Lake sheet, Thunder Bay and Cochrane districts; Ontario Geological Survey, Preliminary Map P.274—Revised, scale 1:126 720.

Thurston, P.C. and Carter, M.W. 1969. Operation Fort Hope, Makokibatan–Melchett lakes sheet, districts of Kenora (Patricia Portion), Cochrane and Thunder Bay; Ontario Geological Survey, Preliminary Map P.565, scale 1:126 720.

van de Kamp, P.C. and Beakhouse, G.P. 1979. Paragneisses in the Pakwash Lake area, English River gneiss belt, northwest Ontario; Canadian Journal of Earth Sciences, v.16, p.1753-1763.

38. Characterizing the Geochemistry and Nickel-Copper-Platinum Group Elements Potential of Mafic and Ultramafic Intrusions in Northwestern Ontario



J.R.B. Jonsson[1], P.M. Malegus[1], S.V. Churchley[1] and R.L. Price[1]

[1]Resident Geologist Program, Ontario Geological Survey

INTRODUCTION

Globally, magmatic sulphide deposits host significant resources of nickel, copper, cobalt and platinum group elements (PGE). These deposits occur as concentrations of sulphide minerals hosted within mafic to ultramafic intrusive rocks and are widespread across Ontario, occurring in every Precambrian geologic terrane. Significant magmatic sulphide mineralization in Ontario occurs in Mesoarchean to Neoarchean intrusions of the Superior Province, the Paleoproterozoic Sudbury Igneous Complex, in Mesoproterozoic intrusions related to the Midcontinent Rift and in the Grenville Province. Ontario is home to 10 operating mines in magmatic sulphide deposits: 9 within the Sudbury Igneous Complex and one within the Neoarchean Lac des Iles Complex.

In 1999, Operation Treasure Hunt was initiated by the Ontario Government to stimulate mineral exploration by acquiring new airborne geophysical data, surficial and bedrock geochemical data, and development of new methods. In 2003, following completion of the Operation Treasure Hunt project, the Ontario Geological Survey published a report (Vaillancourt et al. 2003) that assessed 109 mafic to ultramafic intrusions across Ontario. The purpose of this part of Operation Treasure Hunt was to characterize and publish data for intrusions known to be prospective for PGE-dominated magmatic sulphide mineralization. Many of the intrusions studied during Operation Treasure Hunt were host to other economic mineralization (mostly nickel and copper sulphides), including current and past-producing mines, and several of these intrusions are the focus of ongoing mineral exploration.

Despite the work by Vaillancourt et al. (2003), there are hundreds of mafic to ultramafic intrusions in Ontario that have not been systematically assessed for magmatic sulphide mineralization potential. Many of these intrusions have favourable characteristics for potentially containing magmatic sulphide deposits, including geophysical anomalies (e.g., magnetic, conductivity), overburden geochemical anomalies and known sulphide mineralization.

PURPOSE

Evaluating the geochemistry of mafic to ultramafic intrusions can provide insight into the magma history, tectonic setting and potential for economic metal endowment. Factors that may influence metal endowment, that can be determined from the examination of geochemical data, include determining magma source characteristics, the timing of sulphur saturation and the degree of interaction of the magma(s) with their country rocks. Careful evaluation of physical characteristics and whole-rock

Summary of Field Work and Other Activities, 2023,
Ontario Geological Survey, Open File Report 6405, p.38-1 to 38-6.

© King's Printer for Ontario, 2023

geochemistry can inform future mineral exploration and/or the development of models for the emplacement of mafic to ultramafic intrusions and any hosted mineralization.

This study will focus on mafic to ultramafic intrusions that were not evaluated by Vaillancourt et al. (2003) and which, in general, have not been systematically evaluated for magmatic sulphide potential. Many of the intrusions included in this study have been the subject of mineral exploration, although the extensiveness of exploration activities is varied and is limited mainly to sampling of surficial materials, assay analyses and regional-scale geophysical surveys. A minority of the intrusions examined in this study have diamond-drill core available, and a few have publicly available whole-rock geochemical and assay data. Using these existing data, even where limited, will allow this study to focus on intrusions that appear to have favourable characteristics (e.g., geochemistry, lithology, geodynamic setting) for economic mineralization.

Samples collected as part of this study will be analyzed at the Ontario Geological Survey Geoscience Laboratories in Sudbury for a full suite of major and trace elements using X-ray fluorescence (XRF) and inductively coupled plasma mass spectrometry (ICP–MS) following closed-vessel four-acid digestion. All sulphide-bearing samples will also be analyzed for precious metals using lead–fire assay with an ICP–MS finish and for base metals using flame atomic absorption spectrometry following modified aqua regia extraction. More details on analytical methods can be found in Ontario Geological Survey (2023a). To characterize the mineralogy of the samples, polished thin sections will be made of a subset of samples from intrusions that return favourable values.

PRELIMINARY WORK

Initial sample collection and analytical work took place during the 2023 field season. Areas of interest are shown in Figure 38.1, and include the Red Lake, Onaman–Tashota, and Heaven Lake greenstone belts. Sampling in the Red Lake greenstone belt took place in the summer of 2023; whereas drill-core sampling of intrusions in the Onaman–Tashota and Heaven Lake greenstone belts is planned for the winter of 2023–2024, with field sampling planned for the summer of 2024. Despite an initial focus on these areas, work for this study plans to include a range of mafic to ultramafic intrusions across northwest Ontario.

Samples for this project are being collected from outcrop, as well as from drill-core sections stored in Ontario Geological Survey drill-core libraries. The number of samples collected from each intrusion varies based on exposure and size, with a minimum of 6 samples, where possible, collected from each studied intrusion. Sampling is intended to capture the lithological variability of a given intrusion, with a focus on sampling the least altered rocks. Note that all Archean volcanic and intrusive rocks being studied by this project have been metamorphosed to varying degrees (greenschist to amphibolite facies). For brevity, the prefix meta- is implied, but not explicitly used in the subsequent rock descriptions.

Red Lake Greenstone Belt

The Red Lake greenstone belt (Figure 38.2) spans 300 million years of geological history (Mesoarchean to Neoarchean (2.99–2.73 Ga)) and constitutes the western portion of the Uchi Subprovince in Ontario. There are 7 main tectonic assemblages present in the Red Lake greenstone belt, including the volcanic Balmer, Ball, Trout Bay and Confederation assemblages and the sedimentary Slate Bay, Bruce Channel and Huston assemblages (Sanborn-Barrie, Skulski and Parker 2001). Throughout most of Red Lake's history, the area has primarily produced gold, with most of the mineral exploration focussed on gold as well.

Parker (2000) noted the potential for magmatic sulphide deposits containing nickel, copper and PGE mineralization in the Red Lake greenstone belt, but, since then, there has been little, if any, active

exploration for these commodities. Nickel-copper-PGE mineralization is associated with mafic to ultramafic intrusive bodies in the belt, including Ontario Mineral Inventory (OMI) occurrences in the Trout Bay assemblage (e.g., Trout Bay Nickel: MDI52M01SE00192; Gulag: MDI000000002424; and Trout Bay No. 1: MDI52L16NE00029) (Ontario Geological Survey 2023b). Additionally, as part of this study, ultramafic volcanic rocks (komatiites) from the greenstone belt were sampled. Komatiites are abundant throughout the Red Lake greenstone belt and, in many instances, komatiites can host magmatic nickel-copper-PGE deposits (e.g., Lesher and Keays 2002).

In 2023, sampling was limited to the Trout Bay, Ball and Balmer assemblages in the Red Lake greenstone belt, focussing on known mafic to ultramafic intrusions and ultramafic volcanic rocks. Areas sampled include 1) Ball assemblage ultramafic intrusions at Pipestone Bay, 2) Trout Bay assemblage mafic intrusions, 3) mafic intrusions and ultramafic volcanic rocks of unknown tectonic affinity at Golden Arm and Para Lake, 4) Balmer assemblage mafic and ultramafic intrusions and ultramafic volcanic rocks at Middle Narrows, and 5) Balmer assemblage ultramafic intrusions at St. Paul Bay (*see* Figure 38.2 for sample locations). Rock types from the sites that were sampled in 2023 include gabbro, komatiitic basalt, komatiite, serpentinite, peridotite and gabbroic anorthosite.

Heaven Lake Greenstone Belt

The Mesoarchean to Neoarchean Heaven Lake greenstone belt is an up to 5 km wide, northeast-trending greenstone belt located approximately 100 km north of Thunder Bay (*see* Figure 38.1). It is subdivided into the Mesoarchean mafic volcanic rock–dominated Whitton assemblage and the Neoarchean felsic to intermediate volcaniclastic rock–dominated Whistle assemblage (Hart and MacDonald 2000; Tomlinson et al. 2003). The Heaven Lake greenstone belt has undergone limited mineral exploration, mostly targeting volcanogenic massive sulphide mineralization.

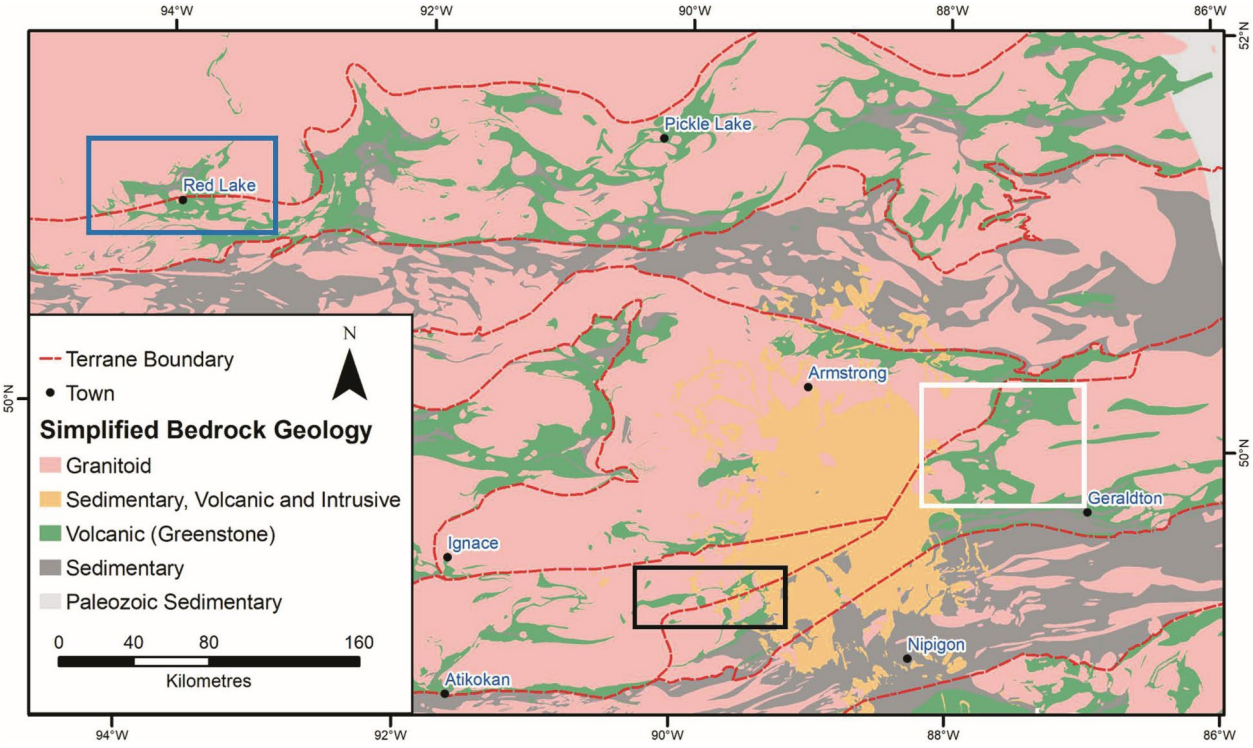


Figure 38.1. Simplified bedrock geology map of northwestern Ontario showing the 3 areas sampled in 2023: Red Lake greenstone belt (outlined in blue); Heaven Lake greenstone belt (outlined in black); and Onaman–Tashota greenstone belt (outlined in white). Regional geology *modified from* Ontario Geological Survey (2011).

The Heaven Lake greenstone belt is interpreted to be part of a mantle plume–derived magmatic province preserved in the Marmion terrane of the Wabigoon Subprovince that also includes the Lumby Lake and Steep Rock greenstone belts (Tomlinson and Condie 2001). Tomlinson et al. (2003) provided Sm/Nd isotopic evidence to show that the parental magma to the Heaven Lake greenstone belt incorporated and/or was partially derived from continental crust. Crustally contaminated mafic to ultramafic rocks that formed in active extensional settings are host to the majority of the world's significant magmatic sulphide systems and, as such, further geochemical characterization and exploration of all of the greenstone belts in the Marmion terrane is warranted.

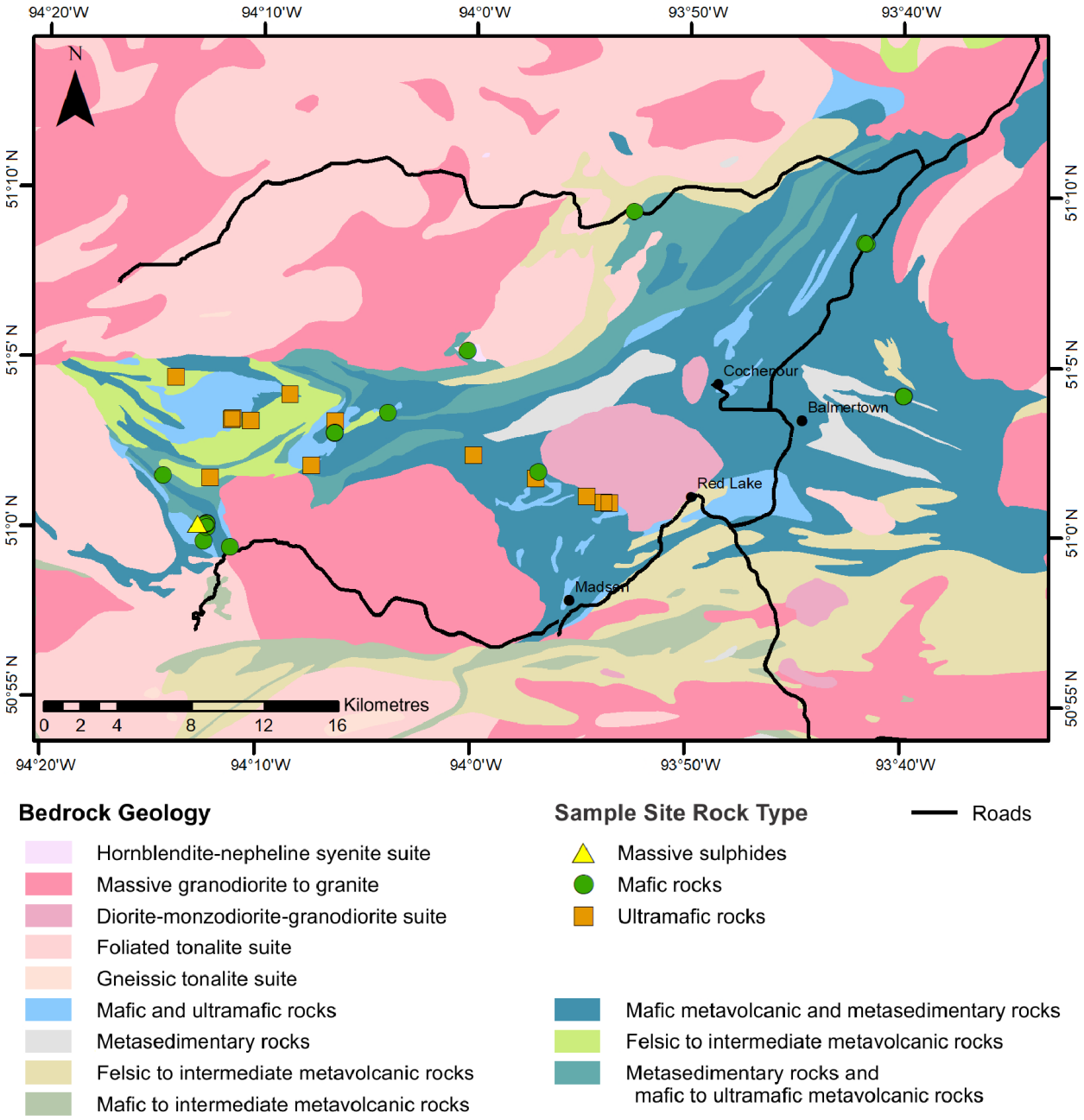


Figure 38.2. Generalized bedrock geology map of the Red Lake greenstone belt showing general sample locations. Bedrock geology *modified from* Ontario Geological Survey (2011).

Of relevance to this study are ultramafic volcanic rocks and mafic to ultramafic intrusive rocks of the Whitton assemblage (for descriptions, *see* Hart and MacDonald 2000). Recent mineral exploration has identified the presence of PGE-enriched magmatic sulphides in a previously unmapped mafic intrusion; however, several known mafic to ultramafic intrusions in the Whitton assemblage have not been systematically explored for magmatic sulphide mineralization. Komatiitic flows and potentially cogenetic ultramafic cumulate rocks also represent targets for potential mineralization.

Onaman–Tashota Greenstone Belt

The Onaman–Tashota greenstone belt consists of Mesoarchean to Neoarchean supracrustal and intrusive rocks in the eastern Wabigoon Subprovince, spanning 80 km from the north to south boundaries of the subprovince (*see* Figure 38.1). The supracrustal rocks are composed predominantly of basaltic and dacitic flows, autobreccia and pyroclastic rocks (Stott et al. 2002). Sedimentary rock units are derived from the underlying volcanic and intrusive rocks and, thus, are typically the youngest supracrustal assemblages in the belt (Stott et al. 2002). In total, 4 episodes of volcanism and 3 main sedimentary episodes are preserved within the stratigraphy of the belt and constitute a total of 13 recognized tectonic assemblages (Stott et al. 2002). Intrusive rocks range from Mesoarchean to Neoarchean in age and felsic to ultramafic in composition, and intruded both the sedimentary and volcanic assemblages of the belt.

Neoarchean mafic to ultramafic intrusions in the Onaman–Tashota greenstone belt have been recognized as potential hosts to nickel-copper-cobalt-PGE deposits, as noted in several exploration recommendations by the Ontario Geological Survey (e.g., Mackasey and Wallace 1978; Amukun 1980; Mason et al. 2001; Cundari 2018). These prior studies proposed further work on the Crooked Green Lake intrusion, the Castlewood Creek intrusion, the Boundary intrusion, the Onaman River intrusion and the Pinel Creek intrusion (Mackasey and Wallace 1978; Mason et al. 2001). Some of the known nickel-copper-cobalt-PGE occurrences in the Onaman–Tashota greenstone belt include the Crooked Green Lake #1 and #2 occurrences (MDI42E13NW00005 and MDI42E13NW00006), the Jacobus Prospect (MDI42E13SE00011) and the Headway A occurrence (MDI000000002987) (Ontario Geological Survey 2023b). The Headway A occurrence and its potential genetic connection to the Final Lake intrusion were featured in Cundari (2018).

FUTURE WORK

Whole-rock geochemical data from the 2023 field season will be analyzed and interpreted prior to the start of the 2024 field season. Additional outcrop and diamond-drill core sampling are planned for the 2024 field season. Areas to be targeted during the 2024 field season include the Birch–Uchi, Obonga and Lumby Lake greenstone belts.

A project update is planned for *Summary of Field Work and Other Activities, 2024* volume. After completion, it is planned that a summary of the results of this study will be published as an OGS Miscellaneous Release—Data (and possibly with an accompanying Open File Report).

ACKNOWLEDGMENTS

The authors would like to thank Robert Cundari and Mark Puumala (Resident Geologist Program (RGP)) for their support and assistance in the conceptualization of this project. Marcus Burnham (Geoscience Laboratories) is acknowledged for his assistance in the selection of analytical methods. Riku Metsaranta (Earth Resources and Geoscience Mapping Section (ERGMS)) and Dorothy Campbell, Therese Pettigrew and Greg Paju (RGP) are recognized for helpful geological discussions and advice in selecting targets. Colleen Kurcinka and Anthony Mitchell (RGP) are thanked for their support in the field.

This article benefitted from reviews by Michael Easton (ERGMS) and Monica Gaiswinkler Easton (Publication Services) and we thank them for it.

REFERENCES

Amukun, S.E. 1980. Geology of the Conglomerate Lake area, District of Thunder Bay; Ontario Geological Survey Report 197, 101p.

Cundari, R. 2018. Copper-nickel-cobalt-platinum group element potential in the Fullerton Lake area: Onaman–Tashota greenstone belt; *in* Ontario Geological Survey, Resident Geologist Program, Recommendations for Exploration 2017–2018, p.70-73.

Hart, T.R. and MacDonald, C.A.M. 2000. Geology of the Heaven Lake greenstone belt, central Wabigoon Subprovince; *in* Summary of Field Work and Other Activities, 2000, Ontario Geological Survey, Open File Report 6032, p17-1 to 17-8.

Lesher, C.M. and Keays, R.R. 2002. Komatiite-associated Ni-Cu-PGE deposits—Geology, mineralogy, geochemistry, and genesis; *in* The Geology, Geochemistry, Mineralogy and Mineral Beneficiation of Platinum-Group Elements, Canadian Institute of Mining, Metallurgy, and Petroleum, Special Volume 54, p.579-617.

Mackasey, W.O. and Wallace, H. 1978. Geology of Elmhirst and Rickaby townships, District of Thunder Bay; Ontario Geological Survey, Geoscience Report 168, 101p.

Mason, J.K., White, G.D., O'Brien, M.S., Komar, C., Stewart, J., Debicki, R. and Drost, A. 2001. Report of Activities 2000, Resident Geologist Program, Thunder Bay North Regional Resident Geologist Report: Thunder Bay North District; Ontario Geological Survey, Open File Report 6048, 56p.

Ontario Geological Survey 2011. 1:250 000 scale bedrock geology of Ontario; Ontario Geological Survey, Miscellaneous Release—Data 126 – Revision 1.

——— 2023a. Geoscience Laboratories 2023 Schedule of Fees and Services, Issue 15, effective April 1, 2023; Ontario Geological Survey, Geoscience Laboratories, 36p., www.ontario.ca/page/ontario-geological-survey#section-4, under "Schedule of fees and services", *see* link to download PDF. [accessed October 20, 2023]

——— 2023b. Ontario Mineral Inventory; Ontario Geological Survey, online database, November 2023 update, www.hub.geologyontario.mines.gov.on.ca. [accessed November 14, 2023]

Parker, J.R. 2000. Nickel-copper-platinum group element sulphide mineralization in the Red Lake greenstone belt: A preliminary report; *in* Summary of Field Work and Other Activities, 2000, Ontario Geological Survey, Open File Report 6032, p.23-1 to 23-14.

Sanborn-Barrie, M., Skulski, T. and Parker, J.[R.] 2001. Three hundred million years of tectonic history recorded by the Red Lake greenstone belt, Ontario; *in* Current Research 2001-C19, Geological Survey of Canada, 32p.

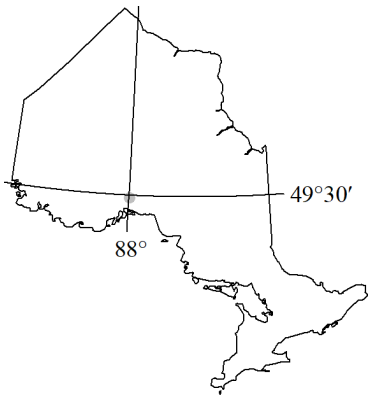
Stott, G.M., Davis, D.W., Parker, J.R., Straub, K.J. and Tomlinson K.Y. 2002. Geology and tectonostratigraphic assemblages, eastern Wabigoon Subprovince, Ontario; Ontario Geological Survey, Preliminary Map P.3449 / Geological Survey of Canada, Open File 4285, scale 1:250 000.

Tomlinson, K.Y. and Condie, K.C. 2001. Archean mantle plumes: Evidence from greenstone belt geochemistry; *in* Mantle Plumes: Their Identification Through Time, Geological Society of America, Special Paper 352, p.341-358.

Tomlinson, K.Y., Davis, D.W., Stone, D. and Hart, T.R. 2003. U–Pb age and Nd isotopic evidence for Archean terrane development and crustal recycling in the south-central Wabigoon Subprovince, Canada; Contributions to Mineralogy and Petrology, v.144, p 684-702.

Vaillancourt, C., Sproule, R.A., MacDonald, C.A. and Lesher, C.M. 2003. Investigation of mafic-ultramafic intrusions in Ontario and implications for platinum group element mineralization: Operation Treasure Hunt; Ontario Geological Survey, Open File Report 6102, 335p.

39. Investigation of Biogeochemical Exploration Techniques to Aid in the Exploration for Lithium-Cesium-Tantalum Pegmatite Dikes: Preliminary Results



E.G. Amyotte[1]

[1]Resident Geologist Program, Ontario Geological Survey

INTRODUCTION

Sampling and chemical analysis of vegetation is widely used as an exploration tool to trace mineralization covered by overburden, but this technique has focussed primarily on the exploration for precious, base and energy metals. Whereas the optimal target vegetation species, uptake characteristics and sample media for the exploration of these metals is relatively well understood, these criteria are not well studied for the biogeochemical exploration of lithium-cesium-tantalum (LCT)-type pegmatites (classification of Černý 1982)

In 2022, the Ontario Geological Survey (OGS) initiated a pilot study to test the feasibility of sampling and analyzing vegetation as an exploration tool using a similar approach to Amyotte et al. (2022) in the Georgia Lake area, which is known to host the most documented LCT-type pegmatite field in Ontario (Pye 1964; Breaks, Selway and Tindle 2008). Regional and property geology and sampling protocols were outlined in Amyotte et al. (2022).

This pilot study involved the collection of 119 vegetation samples from black spruce and grey alder from 2 properties hosting LCT-type pegmatites and their metasedimentary host rocks in the Georgia Lake pegmatite field: 1) Georgia Lake lithium property owned by Rock Tech Lithium Inc. and 2) Jackpot property owned by Imagine Lithium Inc. In preparation for a fall 2023 diamond-drill program, Rock Tech Lithium Inc. is expanding known pegmatite zones at the Georgia Lake lithium property site through geological mapping, sampling and biogeochemical survey (Rock Tech Lithium Inc., news releases, July 3 and September 19, 2023). A National Instrument 43-101 compliant Mineral Resource, published in 2022, outlines an Indicated Resource of 10.60 Mt at 0.88 Li_2O and an Inferred Resource of 4.22 Mt at 1.00% Li_2O for the North Spodumene pegmatite area of the project (Warren et al. 2022). Imagine Lithium Inc. continues to explore on the Jackpot property by field prospecting and diamond drilling (Imagine Lithium Inc., news release, June 20, 2023).

The goal of this study is to determine if the results of trace element analysis of vegetation samples can be used to detect the presence of buried LCT-type pegmatites. The analytical protocol used for the trace element analysis is described in detail in Burnham and Amyotte (this volume). This article summarizes results of this study, which demonstrate the potential of biogeochemical techniques to aid in the exploration for LCT-type pegmatites.

Summary of Field Work and Other Activities, 2023,
Ontario Geological Survey, Open File Report 6405, p.39-1 to 39-8.

© King's Printer for Ontario, 2023

Table 39.1. Metasedimentary whole rock analyses from the Georgia Lake and Jackpot properties. Work was performed at the OGS Geoscience Laboratories. Location information provided as UTM co-ordinates using NAD83 in Zone 16.

Sample ID	Li (ppm)	Cs (ppm)	Ta (ppm)	Easting (m)	Northing (m)
Georgia Lake					
Transect 1					
07082022R025	830.54	226.237	0.514	424548	5477529
07082022R028	323.6	21.626	0.468	424566	5477491
07082022R029	109.95	100.698	0.497	424601	5477427
Transect 2					
07082022R020	1199.33	162.482	0.514	424814	5477676
07082022R021	479.24	17.557	0.429	424786	5477638
Jackpot					
Transect 1					
07062022R001	170.58	15.076	0.496	432481	5461526
07062022R003	279.86	23.062	0.386	432467	5461496
07062022R006	379.29	18.636	0.437	432471	5461407
07062022R010	819.87	41.263	0.447	432499	5461315
Transect 2					
07072022R011	94.24	26.623	0.496	432509	5461552
07072022R012	137	12.997	0.49	432507	5461514
07072022R013	544.9	29.793	0.442	432522	5461482
07072022R016	580.61	17.257	0.394	432544	5461410
07072022R018	1016.77	54.411	0.542	432544	5461359
07072022R019	575.64	21.069	0.466	432525	5461327

RESULTS

Chemistry of the sampled vegetation was performed at the OGS Geoscience Laboratories in Sudbury, Ontario. The results of 3 elements (lithium, cesium and tantalum) are reported using bivariate plots for each vegetation medium along each transect. To assess whether the concentrations are anomalous, they need to be compared to a baseline value (i.e., control). In this study, we define positive anomalous values as those plotting above a specific baseline value. For a given medium (e.g., spruce bark, spruce twigs), the baseline was calculated for each element by calculating the mean concentration of the element measured in vegetation media growing on top of metasedimentary rocks. However, because the host rock (i.e., metasedimentary rocks) was in very close proximity to the pegmatites, host rock samples were affected at varying levels by the metasomatic halo of the pegmatites, as demonstrated by elevated and highly varied lithium and cesium values in the whole rock geochemistry (Table 39.1). This resulted in an overestimation of the baseline values of vegetation media growing on top of metasedimentary rocks. Another parameter to consider is the differential mobility of the elements of interest in the hydrothermal fluids that exsolved from the pegmatites. Of the 3 elements considered, the vegetation baseline of tantalum is likely the most accurate, because it is an immobile element compared to lithium (the most mobile) and cesium. This is confirmed by tantalum concentrations in the host rock (i.e., metasedimentary rocks) that are similar between the 2 examined properties and are comparable to tantalum values commonly seen in metasedimentary rocks in the Quetico Subprovince (M. Duguet, OGS, personal communication, 2023).

Compared to their respective baselines, the bivariant plots show positive anomalies for lithium and tantalum in samples taken above pegmatites compared to those taken above metasedimentary host rocks. Cesium, however, displays patterns that are more difficult to interpret and are likely linked to the metasomatic aureole affecting the host rock and its affect on the calculation of the baselines for the different vegetation media (i.e., overestimation). Of the vegetation media considered in this study,

black spruce twig ends (up to 5 nodes from the start of new growth) appear to have the greatest potential for LCT-type pegmatite exploration.

Georgia Lake Lithium Property

Sampling on the property was limited to 2 transects of 5 samples per vegetation medium (Figure 39.1). These 2 transects run perpendicular to the trend of the pegmatite dikes. Alder leaves were not collected along transect 1 because they had been eaten by insects. Of the 3 elements considered, tantalum is the element that gave the most consistent and reliable results in all media (Figure 39.2). The highest tantalum concentrations were found in vegetation media collected at the apex of the pegmatitic bodies. Of the different vegetation media, the spruce bark above pegmatite gave the least reliable data for tantalum, with all values, except a single value, plotting at the baseline. Regardless of the sampled medium and the location of the sample (i.e., above pegmatite versus above host rock), lithium results are scattered around the calculated baseline. Many data points related to the metasedimentary rocks plot above the baseline; conversely, other data points related to pegmatites plot at the baseline or below. As stated in "Results" , one likely explanation is, that because of the high mobility of the lithium in hydrothermal fluids, the calculated baseline may be an overestimation and may not be appropriate to measure the lithium anomaly. Indeed, the whole rock geochemistry of the metasedimentary rocks sampled along the 2 transects (*see* Table 39.1) generally shows highly varied values for lithium and cesium, whereas tantalum concentrations are less varied. Some of the lithium concentrations are very

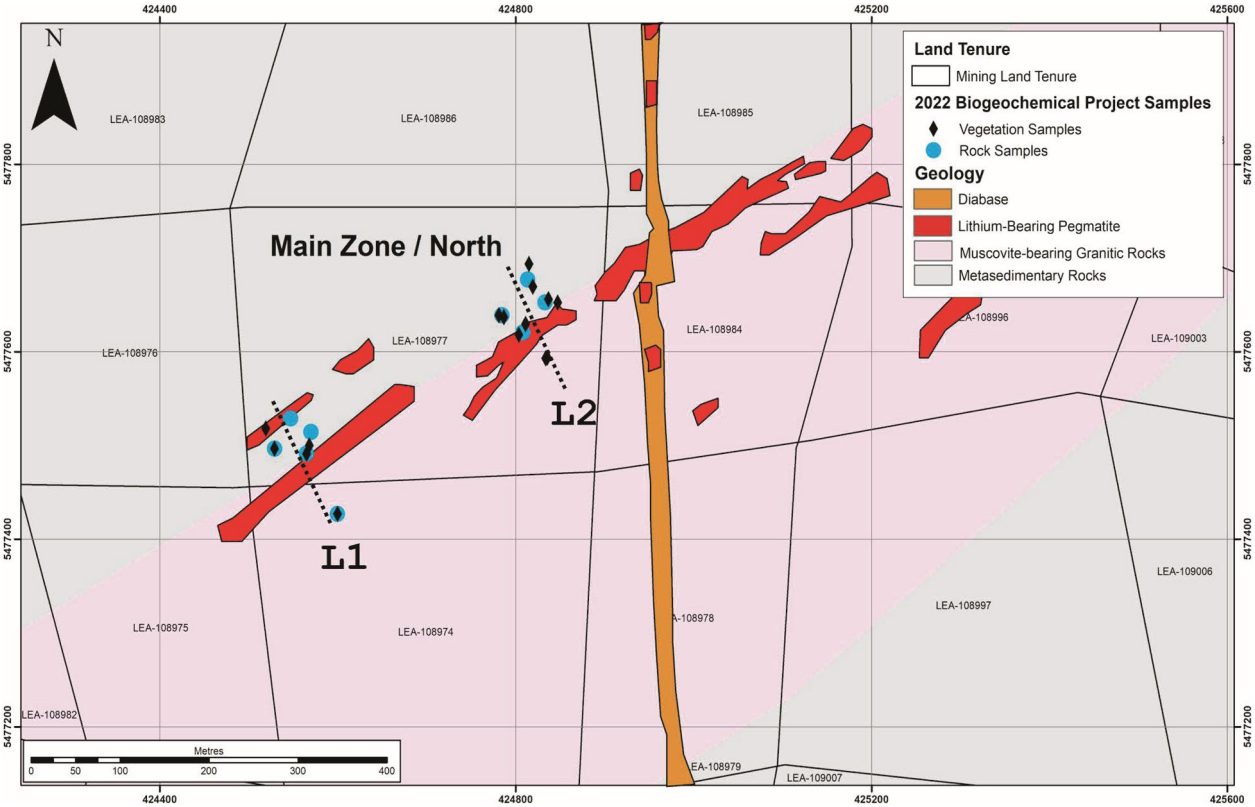


Figure 39.1. Simplified geological map of the Rock Tech Lithium Inc. Georgia Lake lithium property showing bedrock geology overlain by pegmatite dikes (red polygons) and showing the 2022 sampling locations of vegetation (black-filled diamonds) and bedrock samples (blue dots). Label L1 corresponds to Georgia Lake Transect 1; label L2 refers to Georgia Lake Transect 2 in Table 39.1. Bedrock geology *modified from* Ontario Geological Survey (2011); locations of pegmatite dikes *modified from* Selway et al. (2011, p.108). Location information provided as Universal Transverse Mercator (UTM) co-ordinates using North American Datum 1983 (NAD83) in Zone 16.

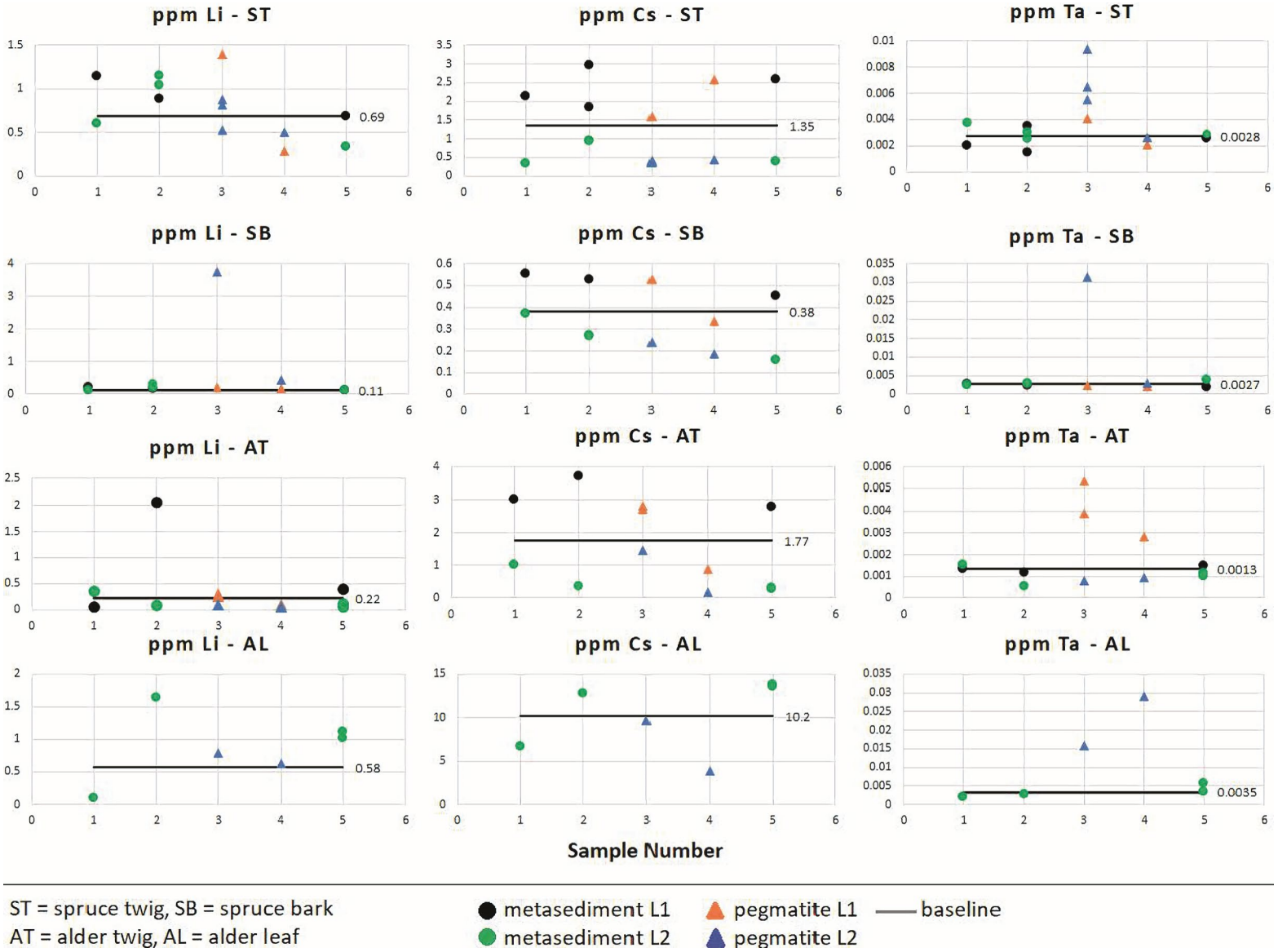


Figure 39.2. Bivariate plots of lithium, cesium and tantalum from selected vegetation media, analyzed using inductively coupled plasma mass spectrometry, from the Georgia Lake lithium property.

elevated (up to 1200 ppm Li). Anomalous concentrations of lithium and cesium in the host rock are reflected in the vegetation media as well. This easily explains the scattering of the data points around the baselines. To eliminate the affect of the metasomatic aureole on the baseline, host rock and associated vegetation sampled farther away from the deposit should be used to calculate a more appropriate baseline. Using the current calculated baselines, cesium values in this data set show significant scatter and cannot be used to detect a buried pegmatite.

Jackpot Property

Similar to the Georgia Lake lithium property, 2 transects were sampled across the strike of the pegmatite dikes (Figure 39.3). Results are shown in Figure 39.4 using bivariate plots and show a good correlation between high tantalum values and pegmatite locations for all vegetation media. Compared to the Georgia Lake property, the lithium baseline is better defined with less scattering of lithium values associated with the metasedimentary rocks (Figure 39.4). However, consistent lithium values above the baseline were observed only in spruce twigs. This contrasts with tantalum in spruce twigs, that appear to be the least reliable vegetation medium. Spruce bark gives more consistently high tantalum results. This was not observed in tantalum results from the Georgia Lake lithium property where spruce twigs had more consistently high tantalum results compared to spruce bark. The reason for this discrepancy requires further investigation. Of the 3 elements, cesium values related to pegmatite show more scattering than lithium or tantalum, although cesium in alder twigs and leaves media sampled on top of pegmatites generally plot above the baseline. This contrasts with the cesium values for vegetation sampled from the Georgia Lake property in which no pattern is discernable.

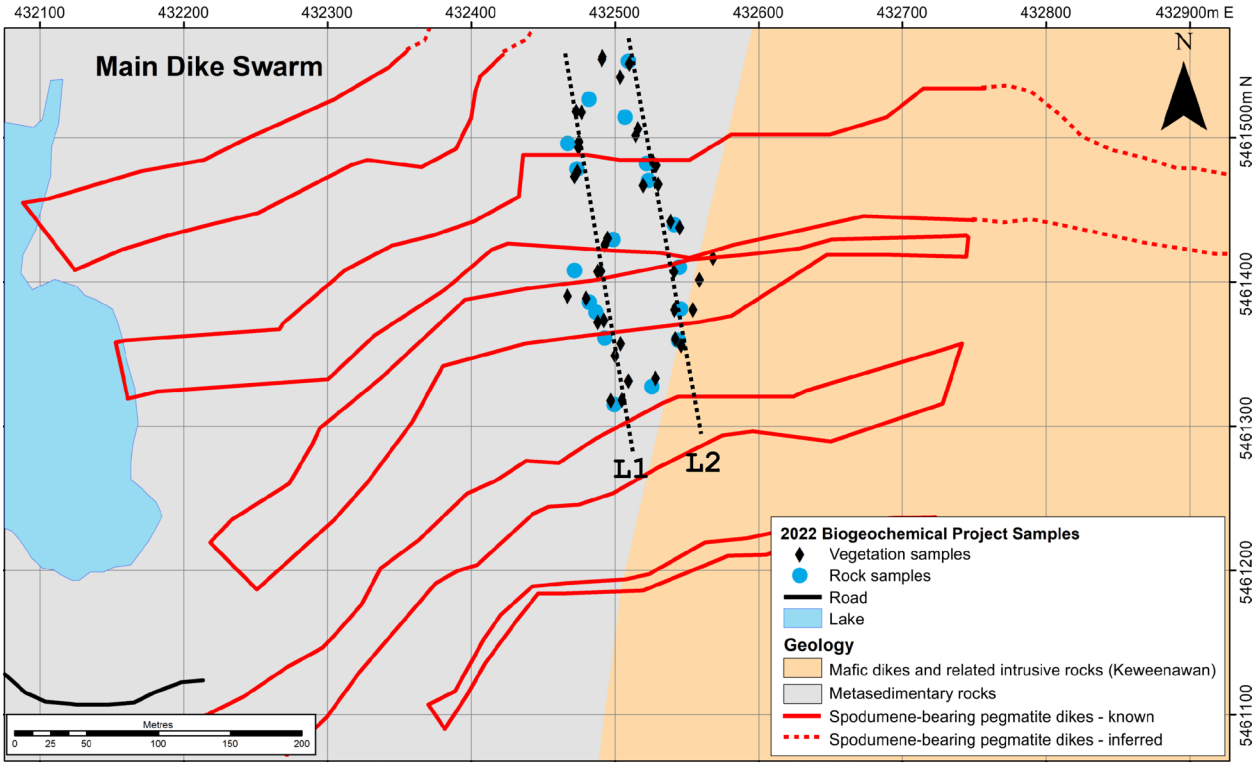


Figure 39.3. Simplified geological map of the Imagine Lithium Inc. Jackpot property showing bedrock geology overlain by pegmatite dikes (red outlines) and showing the 2022 sampling locations of vegetation (black-filled diamonds) and bedrock samples (blue dots). Label L1 corresponds to Jackpot Transect 1; label L2 refers to Jackpot Transect 2 in Table 39.1. Bedrock geology *modified from* Ontario Geological Survey (2011); locations of known and inferred pegmatite dikes *modified from* Imagine Lithium Inc. (Imagine Lithium Inc., news release, March 21, 2022). Location information provided as UTM co-ordinates using NAD83 in Zone 16.

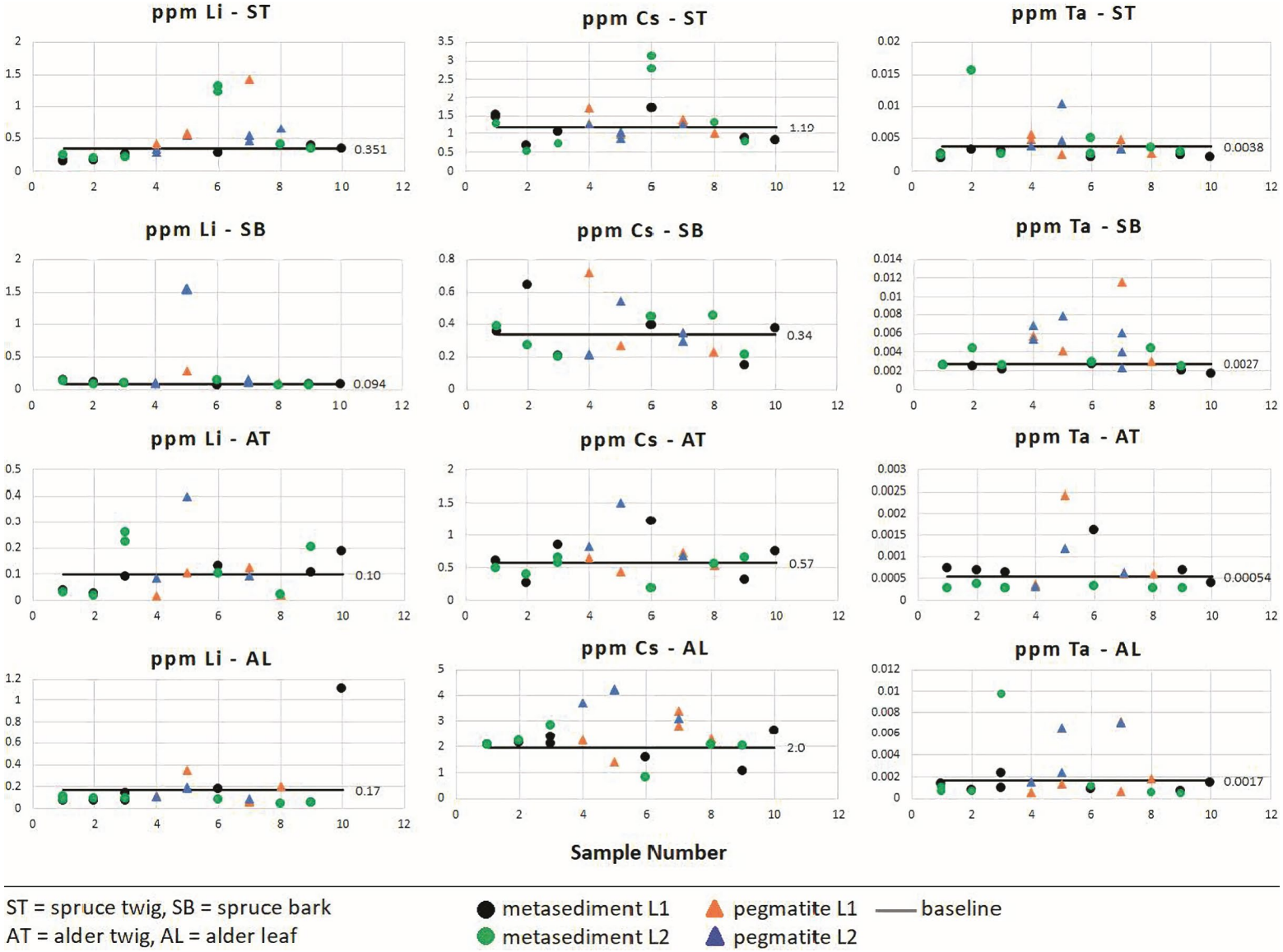


Figure 39.4. Bivariate plots of lithium, cesium and tantalum from selected vegetation media, analyzed using inductively coupled plasma mass spectrometry, from the Jackpot property.

FUTURE WORK

Future biochemical study for the 2024 field season is planned to include resampling of the Jackpot property earlier in the season to determine the effect of seasonal variation on the data. More sampling will also be carried out in areas outside of the metasomatic halo associated with the Jackpot property pegmatites to obtain more appropriate samples to analyze for baseline data. A consideration for future work is to also target a LCT-type pegmatite district hosted by metavolcanic rocks to better understand the influences of different host rocks on the potential of the biochemical method for LCT pegmatite exploration.

ACKNOWLEDGMENTS

Marcus Burnham (Geoscience Laboratories, OGS) is thanked for his continued support and willingness to take on the challenge of revising methods for the analysis of vegetation. Rock Tech Lithium Inc. and Imagine Lithium Inc. are acknowledged for allowing access and sampling on the Georgia Lake Lithium and Jackpot properties. Thunder Bay Resident Geologist Program staff, Sophie Churchley, Greg Paju, Justin Jonsson, Colleen Kurcinka and Sergio Bautista are recognized for their support in field sampling and providing geological expertise on the project. Manuel Duguet (OGS) is thanked for his thorough editing and providing his expertise related to the LCT pegmatite systems and the Georgia Lake pegmatite district to the benefit of this article. Justin Jonsson (OGS) is also acknowledged for editing this article.

REFERENCES

Amyotte, E.G., Kurucz, S.V., Paju, G.F., Jonsson, J.R.B. and Kurcinka, C.E. 2022. Investigation of biogeochemical exploration techniques to aid in the exploration for lithium-cesium-tantalum pegmatite dikes: Project description and preliminary observations; *in* Summary of Field Work and Other Activities, 2022, Ontario Geological Survey, Open File Report 6390, p.31-1 to 31-7.

Breaks, F.W., Selway, J.B. and Tindle, A.G. 2008. The Georgia Lake rare-element pegmatite field and related S-type, peraluminous granites, Quetico Subprovince, north-central Ontario; Ontario Geological Survey, Open File Report 6199, 176p.

Černý, P. 1982. Anatomy and classification of granitic pegmatites; *in* Granitic Pegmatites in Science and Industry, Mineralogical Association of Canada, Short Course Handbook 8, p.1-39.

Ontario Geological Survey 2011. 1:250 000 scale bedrock geology of Ontario; Ontario Geological Survey, Miscellaneous Release—Data 126 – Revision 1.

Pye, E.G. 1965. Geology and lithium deposits of Georgia Lake area, District of Thunder Bay; Ontario Department of Mines, Geological Report 31, 113p.

Selway, J.B., Baker, J.A., Peshkepia, A., Magyarosi, Z. and Dixon, A. 2011. Independent technical report and estimated resources for Georgia Lake lithium property, Beardmore, Ontario, Canada, prepared for Rock Tech Lithium Inc. by Caracle Creek International Consulting Inc.; NI 43-101 Technical Report, filed November 3, 2011 with SEDAR®, *see* www.sedarplus.ca, 328p. [accessed November 17, 2023]

Warren, D., Methven, G., Molavi, M., Nussipakynova, D., Schmitt, R., McIntyre, A., O'Connor, B., Sneyd, A., Murrell, C., Supanz, S. and Schloffer, J. 2022. Georgia Lake Lithium Project Pre-Feasibility Study, Breadmore, Ontario, Canada, prepared for Rock Tech Lithium Inc. by AMC Mining Consultants (Canada) Ltd.; filed November 21, 2022 with SEDAR®, *see* www.sedarplus.ca, 349p. [accessed November 17, 2023]

Index of Authors (with corresponding article numbers)

A

Amyotte, E.G., 32, 39
Atasiei, D., 25

B

Beckett-Brown, C.E., 21, 23
Béland Otis, C., 24
Bennett, D.J. , 3
Biswas, S., 20
Bleeker, W., 14
Brunton, F.R., 25, 26, 29
Burnham, O.M., 19, 32, 33
Burt, A.K., 28, 29

C

Campbell, D.A., 19
Churchley, S.V., 37, 38
Clarke, S.A., 21
Colgrove, L.M., 30
Cormier, R., 4
Crabtree, D.C., 21
Creppin, J.R.H., 7

D

Davis, D.W., 14
Dell, K.M., 30
Duguet, M., 4, 12, 13

E

Easton, R.M., 4, 14, 15, 17, 18
Evangelatos, J., 20

G

Gao, C., 21
Gemmell, T.P., 7
Gordon, C.A., 16
Grant, D., 28

H

Hagedorn, G.W., 21, 23
Hahn, K.E., 27
Handley, L.A., 31
Hastie, E.C.G., 19, 21, 33
Hechler, J.H., 1, 4
Hingst, V.L., 34

J

Jin, J., 25
Jonsson, J.R.B., 38

K

Kalmo, K.J.J., 2
Kamo, S.L., 5, 10, 14
Keating, G.L., 35

L

Launay, G., 11, 13, 21
Levesque, M.D., 3

M

MacDonald, P.J., 9, 10, 19
Malegus, P.M., 10, 19, 38
Marich, A.S., 17, 22
Metsaranta, R.T., 11
Mulligan, R.P.M., 28, 29

P

Paju, G.F., 36
Pelletier, S.G., 6
Perrouty, S., 6
Phillips, A.R., 26
Préfontaine, S., 4, 5
Price, R.L., 38

R

Robichaud, L., 4

T

Tsujita, C.J., 25

V

Vice, L.E.D., 6

W

Walker, J., 8
Wall, C.J., 17

Y

Yeung, K.H., 25, 26, 28, 29

Metric Conversion Table

Conversion from SI to Imperial			Conversion from Imperial to SI		
SI Unit	*Multiplied by*	*Gives*	*Imperial Unit*	*Multiplied by*	*Gives*
		LENGTH			
1 mm	0.039 37	inches	1 inch	**25.4**	mm
1 cm	0.393 70	inches	1 inch	**2.54**	cm
1 m	3.280 84	feet	1 foot	**0.304 8**	m
1 m	0.049 709	chains	1 chain	20.116 8	m
1 km	0.621 371	miles (statute)	1 mile (statute)	**1.609 344**	km
		AREA			
1 cm^2	0.155 0	square inches	1 square inch	**6.451 6**	cm^2
1 m^2	10.763 9	square feet	1 square foot	**0.092 903 04**	m^2
1 km^2	0.386 10	square miles	1 square mile	2.589 988	km^2
1 ha	2.471 054	acres	1 acre	0.404 685 6	ha
		VOLUME			
1 cm^3	0.061 023	cubic inches	1 cubic inch	**16.387 064**	cm^3
1 m^3	35.314 7	cubic feet	1 cubic foot	0.028 316 85	m^3
1 m^3	1.307 951	cubic yards	1 cubic yard	0.764 554 86	m^3
		CAPACITY			
1 L	1.759 755	pints	1 pint	0.568 261	L
1 L	0.879 877	quarts	1 quart	1.136 522	L
1 L	0.219 969	gallons	1 gallon	**4.546 090**	L
		MASS			
1 g	0.035 273 962	ounces (avdp)	1 ounce (avdp)	28.349 523	g
1 g	0.032 150 747	ounces (troy)	1 ounce (troy)	**31.103 476 8**	g
1 kg	2.204 622 6	pounds (avdp)	1 pound (avdp)	**0.453 592 37**	kg
1 kg	0.001 102 3	tons (short)	1 ton(short)	**907.184 74**	kg
1 t	1.102 311 3	tons (short)	1 ton (short)	**0.907 184 74**	t
1 kg	0.000 984 21	tons (long)	1 ton (long)	**1016.046 908 8**	kg
1 t	0.984 206 5	tons (long)	1 ton (long)	**1.016 046 9**	t
		CONCENTRATION			
1 g/t	0.029 166 6	ounce (troy) / ton (short)	1 ounce (troy) / ton (short)	34.285 714 2	g/t
1 g/t	0.583 333 33	pennyweights / ton (short)	1 pennyweight / ton (short)	1.714 285 7	g/t

OTHER USEFUL CONVERSION FACTORS

	Multiplied by	
1 ounce (troy) per ton (short)	31.103 477	grams per ton (short)
1 gram per ton (short)	0.032 151	ounces (troy) per ton (short)
1 ounce (troy) per ton (short)	20.0	pennyweights per ton (short)
1 pennyweight per ton (short)	0.05	ounces (troy) per ton (short)

*Note: Conversion factors in **bold** type are exact. The conversion factors have been taken from or have been derived from factors given in the* Metric Practice Guide for the Canadian Mining and Metallurgical Industries*, published by the Mining Association of Canada in co-operation with the Coal Association of Canada.*

ISSN 0826-9580 (print)
ISBN 978-1-4868-7448-4 (print)

ISSN 1916-6117 (online)
ISBN 978-1-4868-7449-1 (PDF)